DISSECTING THE MOLECULAR BASIS OF

PFCRT–MEDIATED ANTIMALARIAL DRUG RESISTANCE

Stanisław Józef Gabryszewski

Submitted in partial fulfillment of the

requirements for the degree of

Doctor of Philosophy

under the Executive Committee

of the Graduate School of Arts and Sciences

COLUMBIA UNIVERSITY

2016

ABSTRACT

Dissecting the molecular basis of PfCRT-mediated antimalarial drug resistance

Stanisław J. Gabryszewski

The protozoan parasite *Plasmodium falciparum* is responsible for the deadliest form of malaria, which causes 584,000 fatalities annually and whose complications include coma, anemia, respiratory distress, and renal failure. Although malaria eradication efforts were hindered by the rise of chloroquine (CQ) resistance (CQR), CQ continues to be clinically deployed in resistance-free regions. CQR is primarily mediated by mutations in the *P. falciparum chloroquine resistance transporter* (*pfcrt*) gene, which also modulates parasite susceptibility to first-line artemisinin-based combination therapies (ACTs). In certain geographical regions (e.g. Africa), mutant *pfcrt* alleles display considerable fitness costs and have undergone attrition in the absence of CQ pressure. Surveillance of resistant field isolates presently centers on the PfCRT mutation K76T, ubiquitous among CQ-resistant parasites and always accompanied by ≥3 additional mutations. Despite the global adoption of K76T as a molecular marker of CQR, the contributions of this and other mutations to *P. falciparum* drug resistance versus fitness had not been previously defined.

Aims: We aimed to address the following: (1) Do PfCRT mutations beyond PfCRT K76T directly contribute to CQR? (2) Do PfCRT mutations contribute to parasite fitness during the pathogenic asexual blood stage? (3) Are there predictable mutational paths in the evolution of *pfcrt*-mediated drug resistance? (4) How do PfCRT mutations impact current antimalarials, including the first-line ACTs?

Approach: Using zinc finger nucleases, we generated isogenic, *pfcrt*-modified blood-stage *P. falciparum* parasites encoding wild-type (CQ-sensitive) or variant PfCRT haplotypes. Variants included a combinatorial library of alleles harboring 1-4 mutations comprising the simplest CQ-resistant haplotype (Ecu1110). Additional genetic dissections of full-length or partial *pfcrt* alleles encompassed the most common variants found in Africa and Asia, including a unique fitness-neutral mutant allele (Cam734) that has undergone expansion in Southeast Asia. Parasite antimalarial drug susceptibility was determined using IC_{50}-based (cytostatic) assays or parasite survival-based (cytocidal) assays and was combined with data from flow cytometric parasite growth competition assays to computationally model mutant *pfcrt* evolution. To further define the biochemical impacts of PfCRT mutations, our studies leveraged metabolomic, heme fractionation, and drug transport studies.

Results: Key findings emerging from our studies included the following: (1) PfCRT K76T is insufficient for CQR and an inaccessible first mutational step in *pfcrt* evolution; (2) Alongside proliferation rates, parasite resistance gains dictate a constrained *pfcrt* mutational landscape and predict important roles for the active metabolites of CQ and amodiaquine in guiding *pfcrt* evolution; (3) To various degrees, PfCRT polymorphisms beyond K76T increase the potency of both the artemisinin and partner drug components of first-line ACT regimens; (4) Emerging PfCRT mutations (e.g. A144F) directly contribute to the enhanced fitness of *pfcrt* alleles and are necessary for multidrug resistance, independent of K76T.

Conclusions: Our studies uncovered multiple pleiotropic contributions of PfCRT mutations to antimalarial drug resistance, countering earlier dogma that non-K76T mutations are merely compensatory. Evolutionary modeling revealed parasites' ability to navigate constrained mutational landscapes and evolve drug resistance via rare mutational bursts. These results collectively highlight the capacity of PfCRT to acquire novel mutations that successfully balance parasite multidrug resistance with the essential role of PfCRT in maintaining digestive vacuole physiology. Our studies are of direct relevance to the regional recommendations of antimalarials, whose activity is influenced by, and in certain cases enhanced against, *pfcrt*-mutant parasites.

TABLE OF CONTENTS

LIST OF FIGURES AND TABLES

FIGURES

TABLES

ACKNOWLEDGEMENTS

First, I would like to thank my mentor, Dr. David Fidock, for his guidance, support, and the many resources he made available to me to promote my development as an independent researcher. His dedication to his work and the precision with which he executes it are truly admirable, and I will endeavor to emulate these qualities in my future role as a physician-scientist. I suspect that he revels in the fact that I have only further grown in his likeness, as a malariologist-violinist.

I wish to express my utmost gratitude to the members of my Dissertation Committee, for their time and constructive feedback. Thank you to Dr. Jonathan Dworkin, Dr. Steven Spitalnik, and Dr. Matthias Quick, for challenging me to think critically about how I execute, analyze, and communicate my scientific work at each Thesis Committee meeting. I wish also to thank Dr. Myles Akabas from the Albert Einstein College of Medicine for enthusiastically agreeing to serve as a visiting Dissertation Committee member.

I am very appreciative of the time and efforts of all co-authors and collaborators associated with the present work, whose names are listed on the first page of the chapter to which they contributed. The accessibility of many fruitful collaborations with outstanding research groups has been a true asset during my time in the Fidock lab. I am particularly grateful to the following scientists: Dr. Charin Modchang and Dr. Thanat Chookajorn at Mahidol University, for their help with computational modeling; the Roepe lab at Georgetown University, for carrying out

drug transport studies; the Egan lab at the University of Cape Town, for conducting parasite heme fractionation assays; and Dr. Ian Lewis at the University of Calgary as well as Dr. Manuel Llinás at Penn State University, for their assistance with parasite metabolomic profiling.

I am indebted for the crucial financial support from the National Institutes of Health that made my research possible (SJG: F30 AI114070 and T32 GM007367; DAF: R01 AI50234 and AI109023). I am honored and privileged to be the recipient of a Ruth L. Kirschstein National Research Service Award for M.D./Ph.D. trainees.

I also wish to thank all of the Directors and Administrators associated with the following programs at Columbia University: Department of Microbiology & Immunology; Integrated Program in Cell, Molecular, and Biomedical Studies; and the M.D./Ph.D. Program. Their support of my training as a physician-scientist has not gone unnoticed.

I would be remiss without acknowledging the many members of the Fidock lab, past and present, who provided crucial technical assistance and scientific feedback, and who made the lab environment truly invigorating. Many thanks to Tara Abraham, Catie Brownback, Olivia Coburn-Flynn, Dr. Geoffrey Chi-Johnston, Dr. Satish Dhingra, Dr. Eric Ekland, Dr. Brie Falkard, Dr. Nina Gnädig, Dr. Sonia Gulati, Dr. Philipp Henrich, Dr. Bamini Jayabalasingham, Mariana Justino de Almeida, Dr. Santha Kumar, Dr. Andrew Lee, Dr. Becca Lewis, James Muriungi, Dr. Caroline Ng, Dr. Leila Ross, Dr. Daniel Scanfeld, Barbara Stokes, Dr. Judith Straimer, Dr. Manu

Vanaerschot, and Dr. Isabel Veiga, A special thanks goes to Dr. Marcus Lee, whose ingenuity and frequent help with experimental design and troubleshooting played a formative role in my training.

Lastly, I am wholeheartedly grateful for the support I received from my family and friends. Together, we have learned that a good correction factor for my estimated time of arrival from the lab is to multiply the time by three. It is my hope that, through this tangible evidence of my work, I can be redeemed for the hours that have amassed in my second home.

DEDICATION

First, I dedicate this dissertation to the memory of Danuta, my dear grandmother – or Babcia, as I referred to her. When I was two years old, my parents moved to the United States, and Babcia selflessly served as my sole guardian for six years. During this time, she instilled in me a deep appreciation for dedication, humility, and patience, while also encouraging me to learn and to pursue my curiosities. I am certain that, without her care, I would not be the person that I am today.

Second, I dedicate this dissertation to my parents and two sisters. I am grateful to my mother and father, Irena and Józef, for their bold decision to start a new life in the United States and for the sacrifices that they inevitably had to make in order to achieve their goal. I also wish to thank my sisters, Maria and Emilia, for their encouragement and much-appreciated supply of entertainment and good laughs.

Last, but certainly not least, I wish to dedicate this dissertation to my beloved wife, soulmate, and fellow scholar, Carolyn. Standing by my side from the very first day of my M.D./Ph.D. training at Columbia, she has fueled my journey with her unending love and support.

CHAPTER 1: MALARIA BIOLOGY, ANTIMALARIAL DRUG RESISTANCE, AND THE *PLASMODIUM FALCIPARUM* CHLOROQUINE RESISTANCE TRANSPORTER

HISTORY AND BURDEN OF MALARIA

Etiology and phylogeny of malaria, an ancient disease

Malaria predates recorded history and remains a leading infectious scourge. References to malaria abound across vast tracts of time and land and include ancient medical scripts, religious texts, and various bodies of literature.[1] In ancient Mesopotamia, a series of cuneiform writings offered dire warnings about a febrile disease associated with marshy lowlands. The symptoms of this illness were highly evocative of severe malaria:

> *If when it comes over him, his left/right eye makes bobbing movements similar to what a spindle does when it spins and his right/left eye is full of blood, he continually opens his mouth, and he bites his tongue, Lugal-Girra afflicts him.*[2]

In this context, Lugal-Girra is an alternate name for Nergal, the Babylonian god of devastation and pestilence.[2] Intriguingly, depictions of Nergal placed him in the company of fleas and flies,[3] hinting at the future discovery that insects can serve as a vessel of disease. The term "mal'aria" – meaning "bad air" in Italian – is now the sole remnant of the belief that toxic vapors emerging from marshes caused disease. This notion was fundamentally challenged beginning in 1880 with the work of Charles Louis Alphonse Laveran.

Attending to solders suffering from malaria during his time as a military physician in Algeria, the scientifically curious Laveran collected blood samples and closely examined them by light microscopy. To his amazement, in erythrocytes from infected patients, he observed transparent, crescent-shaped organisms that released

motile filaments and bore pigmented granules.[1] Less than two decades following Laveran's landmark discovery of blood-stage malarial parasites, a British physician in the Indian Medical Service, Sir Ronald Ross, clarified the remainder of the parasite life cycle. His painstaking observations included the development of parasites in the mosquito gut, the identification of the mosquito salivary gland as a site of parasite accumulation, and transmission of an avian malarial strain from *Culex* mosquitos to previously healthy birds.[1] Extending Ross's findings, the Italian physician Giovanni Grassi subsequently demonstrated that human malarial species are transmitted by female *Anopheles* mosquitos.[1]

The protozoan parasites first noted by Laveran belong to the genus *Plasmodium*, which require both an invertebrate (i.e. mosquito or sandfly) and a vertebrate (i.e. mammal, bird, or reptile) host.[4] Of the more than 250 existing *Plasmodium* species, five cause human malaria: *P. falciparum*, *P. vivax*, *P. malariae*, *P. ovale* (recognized as a pair of sub-species[5]), and *P. knowlesi*. Macaques serve as the natural reservoir of *P. knowlesi* parasites,[6] and zoonotic infection with other *Plasmodium* species is possible.[7] Interrogations of *Plasmodium* infection *in vivo* have greatly benefited from the availability of rodent-infecting species, which include *P. berghei*, *P. chabaudi*, *P. vinckei*, and *P. yoelii*.[8] A generalized depiction of malarial parasite evolutionary relationships is shown in **Figure 1.1**. Recent advances in molecular diagnostic methods have provided important insights into *Plasmodium* evolutionary phenomena, including host switching (e.g. between bat and rodent species), host restriction (e.g. between human *P. falciparum* and the highly related ape *Laverania* species), and specific transmission histories (e.g. identification of gorilla-specific *P. praefalciparum* as a precursor of human *P. falciparum*).[9,10]

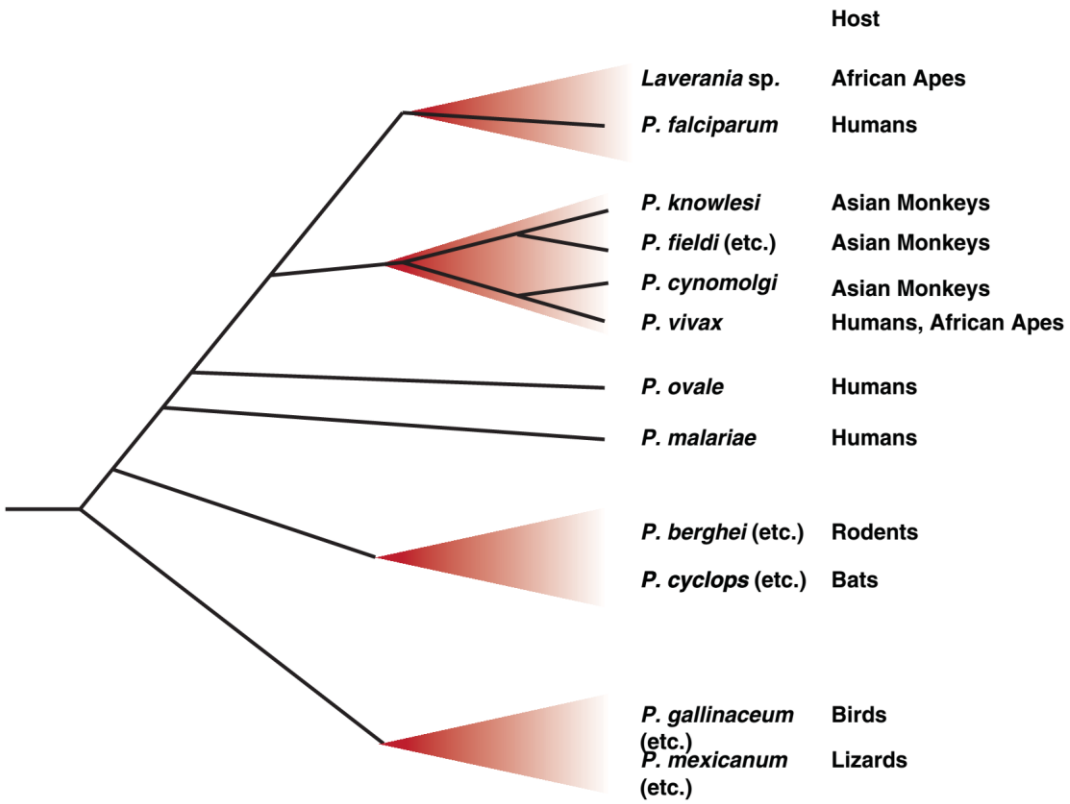

Figure 1.1. Schematic of malarial parasite phylogenetic relationships. Previously inferred molecular phylogenies among *Plasmodium* and related species have been a subject of controversy and can vary substantially depending on the parasite taxa and molecular loci used for analyses.[4] Shown are proposed evolutionary relationships among representative species comprising the genus *Plasmodium* and sub-genus *Laverania*.[9] Several human-infecting *Plasmodium* species (e.g. *P. falciparum* and *P. vivax*) belong to clades that have expanded extensively in the related ape and monkey hosts. Image reproduced with permission from Keeling & Reyner (2015).[9]

Plasmodium species are more broadly classified as *Apicomplexa*, a phylum of obligate intracellular protists bearing (1) an apical complex, used for adhesion and invasion, as well as (2) an apicoplast, an essential organelle derived from the engulfment of a red algal organism.[11] Collectively, apicomplexans are responsible for a diverse set of diseases of humans and animals, in part caused by parasites in the genera *Plasmodium*, *Babesia*, *Cryptosporidium*, *Isospora*, *Toxoplasma*, *Neospora*, *Theileria*, *Sarcocystis*, and *Eimeria*.[4] Comparative studies between *Plasmodium* and related apicomplexan species have identified key differences in parasite genomic structures, metabolism, and host invasion strategies, greatly enhancing our understanding of *Plasmodium* biology and phylogenetic relationships.[12]

Epidemiology and socioeconomic burden of malaria

The global burden of human malaria is disproportionately concentrated in Africa, where up to 90% of the 214 million yearly cases and 438,000 yearly deaths occur.[13] Although the past two decades have witnessed a decline in mortality rates, malaria continues to claim the life of a child every two minutes.[13] Globally, the majority of malarial morbidity is attributable to *P. falciparum*, the most virulent of the causative agents of malaria. The related species *P. vivax* accounts for ~3% of worldwide cases, occurring primarily in Southeast Asia and the Eastern Mediterranean region.[13] Although *P. malariae* and *P. ovale* have achieved global spread, their contributions to the overall burden of malaria are minimal. In recent years, Southeast Asian countries have seen a rise in infections caused by zoonotically transmitted *P. knowlesi* species.[6]

The ecology of mosquito vectors – influenced by mosquito longevity, density, and biting behaviors – has a significant impact on the epidemiology of malaria.[14] In

high-transmission regions with tropical climates, *Anopheles* mosquitos breed extensively, and individuals are bitten multiple times per year.[15] These include sub-Saharan Africa and parts of Oceania, where *P. falciparum* is a common cause of malaria. In contrast, low-transmission regions with cooler climates support significantly lower rates of infection (≤1 bites per year) and are more likely to harbor *P. vivax* parasites, which tolerate cooler climates.[14,15]

In addition to its deleterious impact on human health, malaria also poses a significant socioeconomic burden. Malaria cases cost $300 million per year, an exorbitant expense for malaria-stricken regions whose incomes likely represent a small fraction of the income of a non-malarious country.[13,16] Aside from posing medical costs, malaria inhibits population growth, worker productivity, investment, and foreign trade, collectively hindering economic growth.[16] Consistent with this, retrospective cross-country analyses have revealed that countries with malaria experience slowed economic growth (-1.3% per person per year) as compared to malaria-free regions, even after correcting for possible confounding factors.[16] Thus, in a vicious cycle, poverty sustains malaria, and malaria contributes to further poverty.

Antimalarial eradication and control efforts

The wise adage "hope for the best, prepare for the worst" aids in conceptualizing the deficiencies of previous malaria eradication campaigns, which fell short of anticipating worst-case scenarios. In 1955, following aggressive dichlorodiphenyltrichloroethane (DDT) spraying and an ensuing reduction in malaria transmission in the United States and other regions with temperate climates, the World Health Organization (WHO) inaugurated the Global Malaria Eradication

Program (GMEP).[17] In a plan relying on aggressive DDT spraying, the GMEP aimed to disrupt malaria transmission in malaria-endemic regions.[18] Control efforts also deployed chloroquine (CQ), a gold-standard antimalarial drug at the time, as a means of treatment and disease prevention.[17] Nevertheless, the following two decades saw a rise in DDT and CQ resistance (CQR; see "Antimalarial Drug Resistance" section below) that coincided with financial crises, declining political commitments, inadequate health systems, and lack of agreement on standards for long-term surveillance. Accordingly, the eradication campaign was suspended.[17,18]

Launched in 1998, the Roll Back Malaria Partnership heralded a reprise in political and financial commitment to malaria control. Comprised of politicians, leaders from the private sector and nongovernmental organizations, research scientists, epidemiologists, and economists, the Roll Back Malaria Partnership spearheaded the Global Malaria Action Plan (GMAP).[19] Among the goals articulated by the GMAP for the period 2000-2015 were to reduce global malaria incidence by 75% and to fully provide preventive and therapeutic coverage. Recent (2015) assessments of progress revealed both laudable achievements and an urgent need to expand future efforts. For instance, the majority (54%) of malarious countries achieved the target of 75% reduction in malaria incidence. Less remarkably, despite calls for universal treatment access, only 16% of children aged five or younger received an appropriate first-line antimalarial upon infection with *P. falciparum*.[13] The success of future strategies will hinge upon increased funding, continued political willpower, active engagement with the research community, and improved surveillance measures. Furthermore, as malarious countries achieve milestones on the path to elimination, control efforts will need to account for the changing epidemiology of disease in low-

transmission settings, which may include changes in demographics, rises in imported cases, lesser immunity, and shifts in the predominant infecting *Plasmodium* species.[20]

PARASITE BIOLOGY

Life cycle of human malarial parasites

Plasmodium parasites require two types of hosts for their full development: an invertebrate and a vertebrate. In the case of human malaria, these are female *Anopheles* mosquitos and humans, respectively. The life cycle of human malarial parasites is complex and entails parasite progression through liver and blood stages in the human and sexual development in the mosquito (**Figure 1.2**). As an infected *Anopheles* mosquito probes for blood vessels during a blood meal (**Figure 1.2*A***), it injects ~10-100 motile sporozoites into the human dermis.[21] Initiating the liver stage of infection (**Figure 1.2*B–D***), some of these sporozoites enter the bloodstream, penetrate the liver sinusoids, and invade hepatocytes in a series of traversals that culminate with the infection of a single hepatocyte. Of note, *P. vivax* and *P. ovale* parasites have the capacity to remain dormant in hepatocytes (weeks to ≥1 year) as hypnozoites, which cause the clinical relapses associated with these infections.[14] For all species, over the course of ~5-16 days, actively infected hepatocytes support the development of thousands of merozoites that enter the bloodstream and proceed to infect red blood cells (RBCs).[22]

The ensuing blood stage of the *Plasmodium* life cycle (**Figure 1.2*E–I***) is directly responsible for the clinical course of malaria (see "Clinical manifestations and diagnosis" section below) and will be the focus of subsequent sections of this dissertation.

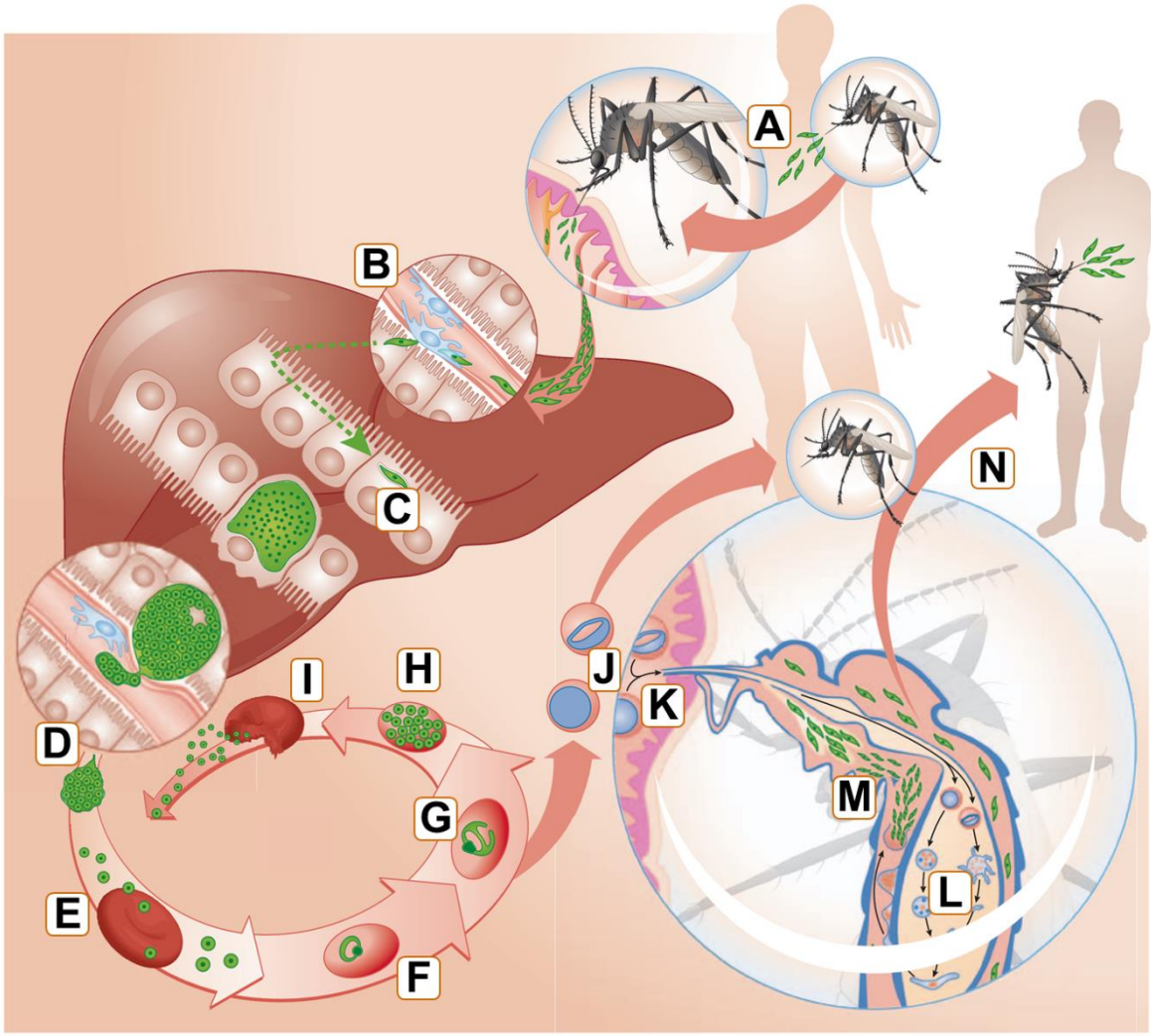

Figure 1.2. The natural life cycle of *Plasmodium* species. (**A**) Transmission of *Plasmodium* from the *Anopheles* mosquito vector to the human host begins via the injection of sporozoites into the dermis during a mosquito blood feed. (**B**) Sporozoites enter the bloodstream and (**C**) migrate to the liver, initiating the asexual liver stage of infection. In the liver, sporozoites traverse multiple hepatocytes and ultimately infect one. In infections with *P. vivax* and *P. ovale*, parasites may remain latent in hepatocytes for an extended period of time as hypnozoites. (**D**) Following growth and replication in the hepatocyte, parasite merozoite forms enter the bloodstream and (**E**) infect erythrocytes, initiating the asexual blood stage of infection. Infected erythrocytes support parasite development into (**F**) ring, (**G**) trophozoite, and (**H**) schizont parasite forms, culminating with the rupture of erythrocytes and release of merozoites that infect new erythrocytes and propagate the blood stage of infection. (**J**) In the blood, a subset of parasites differentiate into sexual gametocyte forms, which are (**K**) transmitted to the mosquito during a subsequent blood feed. (**L**) The sexual stage of *Plasmodium* infection occurs in the mosquito midgut, where fertilized gametes form diploid zygotes. These progress through ookinete and oocyst forms that ultimately (**M**) form and release haploid sporozoites. (**N**) Sporozoites migrate to the salivary glands, where they accumulate until the next blood feed. Image adapted with permission from Portugal *et al*. (2012).[23]

As they mature in host RBCs, parasites progress through ring, trophozoite, and schizont stages, followed by lysis of RBCs and release of 6-30 merozoites that invade new RBCs.[22] Depending on the infecting *Plasmodium* species, the asexual blood stage exhibits one of three possible durations: ~24 hours (*P. knowlesi*), ~48 hours (*P. falciparum*, *P. vivax*, and *P. ovale*), or ~72 hours (*P. malariae*). In the absence of treatment, successive rounds of parasite replication may occur for months, yielding a parasite burden as high as ~10^{12} parasites.[24] Over a period of about two weeks, a small proportion of blood-stage parasites differentiate into sexual gametocytes (**Figure 1.2*J***), which are required for transmission to the mosquito vector.

The *Plasmodium* sexual stage (**Figure 1.2*K–M***) is initiated following a mosquito blood feed and ingestion of male and female gametes. These haploid cells are fertilized in the mosquito midgut, forming the diploid zygote. The zygote matures into an ookinete, which then forms an oocyst beneath the mosquito's gut wall. After 8-15 days, the oocyst bursts, releasing thousands of sporozoites that travel via the hemolymph to the salivary gland. Deposition of these sporozoites into the human dermis in subsequent blood feeds (**Figure 1.2*N***) propagates the parasite life cycle.

Plasmodium morphology

Elucidation of *Plasmodium* morphology enhances our understanding of parasite biology and directly informs disease diagnosis. In 1891, the Russian physician Dmitri Romanowsky found that a mixture of eosin Y and methylene blue differentially stained the nuclei and cytoplasm of blood-stage *Plasmodium* parasites red and blue, respectively.[25] The reproducibility of this stain was subsequently improved by the German chemist Gustav Giemsa, who developed a glycerol-methanol-stabilized

mixture of eosin Y and azure B that would become a mainstay in malarial diagnosis.[25] Beyond aiding with actual identification of *Plasmodium* parasites in patient peripheral blood, microscopic examination of Giemsa-stained blood smears facilitates speciation (**Table 1.1**). As such, it plays an integral role in clinical decision-making and treatment plans. Thin blood smears illustrating representative points in the blood stage of the *P. falciparum* life cycle are shown in **Figure 1.3**.

In addition to light microscopy, several whole cell imaging methods have provided critical insights into the organization of parasite subcellular compartments. Among them are real-time microscopic tracking of fluorescently tagged parasite proteins as well as a variety of electron microscopy (EM)-based techniques, including transmission EM (TEM) of immunolabeled samples and 3D reconstructions of serial thin sections by electron tomography.[26] Collectively, these tools have been particularly effective in clarifying *Plasmodium* ultrastructural architecture during the pathogenic asexual blood stage of infection (**Figure 1.4*A-B***).

In order to simultaneously support their development and avoid phagocytic clearance in the spleen, *P. falciparum* parasites modify the morphology and physiology of their host cell, the RBC. Key alterations include RBC membrane rigidification, orchestration of metabolite partitioning, and formation of membrane knobs that facilitate adhesion of infected RBCs to blood vessel endothelium.[27,28] Essential to these changes is an interplay between the parasite-derived exomembrane system that is found in the host cytoplasm and a set of specialized trafficking pathways that mediate the export of parasite proteins across the parasitophorous vacuole (PV) membrane (PVM), an elastic and protective structure derived from invasion of the host cell.[28,29]

Table 1.1. Morphological features of human blood-stage *Plasmodium* parasites.[a]

	P. falciparum	***P. vivax***	***P. ovale***	***P. malariae***	***P. knowlesi***
RBC size	Normal	Increased	Increased	Normal or decreased	Normal
RBC shape	Distorted by gametocytes; Maurer's spots	May be distorted; Schüffner's dots	Irregular edges; Schüffner's dots	Not distorted; occasional Ziemen's stippling	Not distorted; occasional stippling
Ring	1-2 small chromatin dots; delicate cytoplasm; appliqué forms	Heavy chromatin dot	Heavy chromatin dot	Heavy chromatin dot; occasional accessory dot	Up to three chromatin dots; appliqué forms
Trophozoite	Rare in peripheral blood; compact	Large chromatin mass; ameboid	Compact with large chromatin	Compact; band forms; pigmented	Compact; band forms; pigmented; cytoplasm possibly amoeboid
Schizont	8-24 merozoites; rare in peripheral blood	12-24 merozoites	4-16 merozoites	6-12 merozoites; rosette forms	Up to 16 merozoites
Gametocyte	Crescent-shaped; heavy pigment mass	Round; compact; scattered pigment	Round; compact; scattered pigment	Round; compact; scattered pigment	Round; compact; scattered pigment

[a]Adapted from Roberts & Janovy (2005)[30] and Lee *et al.* (2009).[31] Representative images of *P. falciparum* parasites are shown in **Figure 1.3**.

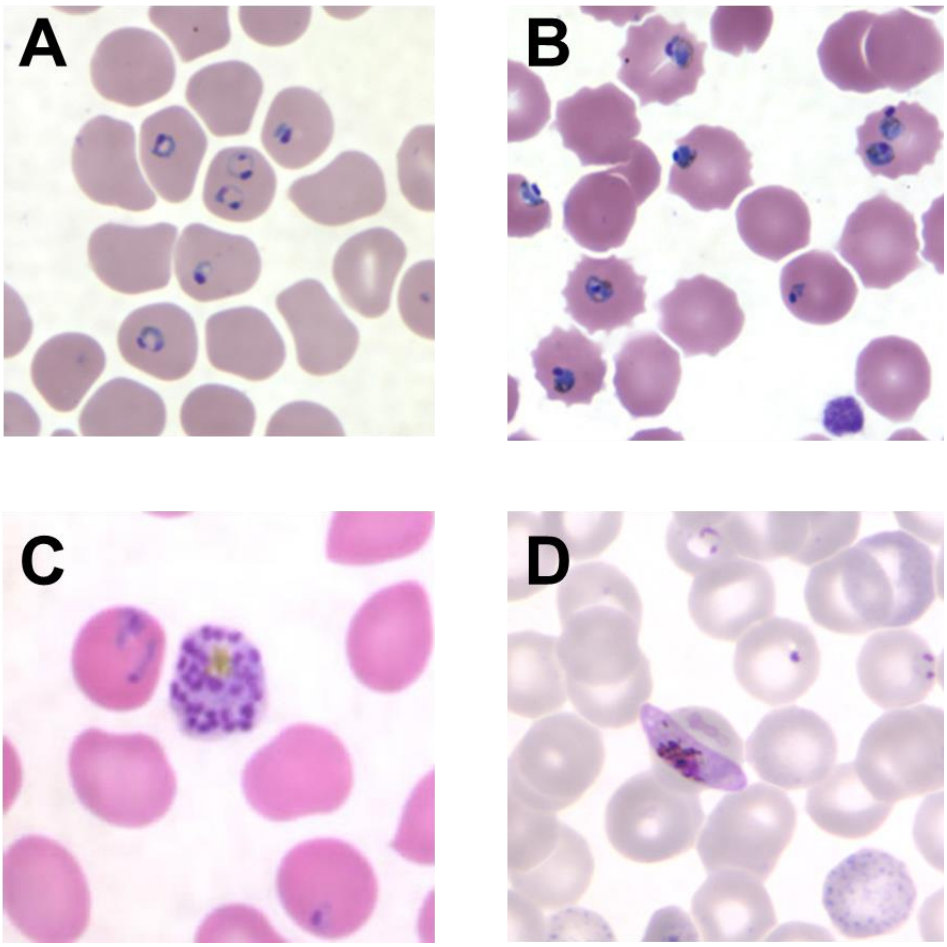

Figure 1.3. Thin blood smears of *P. falciparum* blood-stage parasites. Shown are microscopy images of asexual (**A**) ring, (**B**) trophozoite, (**C**) schizont, and sexual (**D**) gametocyte parasite forms that encompass the blood stage of the *P. falciparum* life cycle. (**A**) Ring forms possess a delicate cytoplasm, thick chromatin dots (1-2), and a diameter approximately one-fifth of the RBC diameter. Infection of RBCs with more than one ring form is common. (**B**) Maturing trophozoites are dense and compact, and occupy an increased proportion of total RBC volume as they develop. They are rarely observed in peripheral blood smears. (**C**) Schizonts harbor 8-24 merozoites situated around a clumped pigment mass and are rarely found in peripheral blood smears. (**D**) Gametocytes are crescent-shaped and distort RBC morphology. The diameter of gametocytes is approximately 1.5× that of RBCs. As compared to microgametocytes (male), macrogametocyte (female) exhibit a darker cytoplasm and more coarse pigmentation. Images reproduced from DPDx, CDC Malaria Image Gallery.[32]

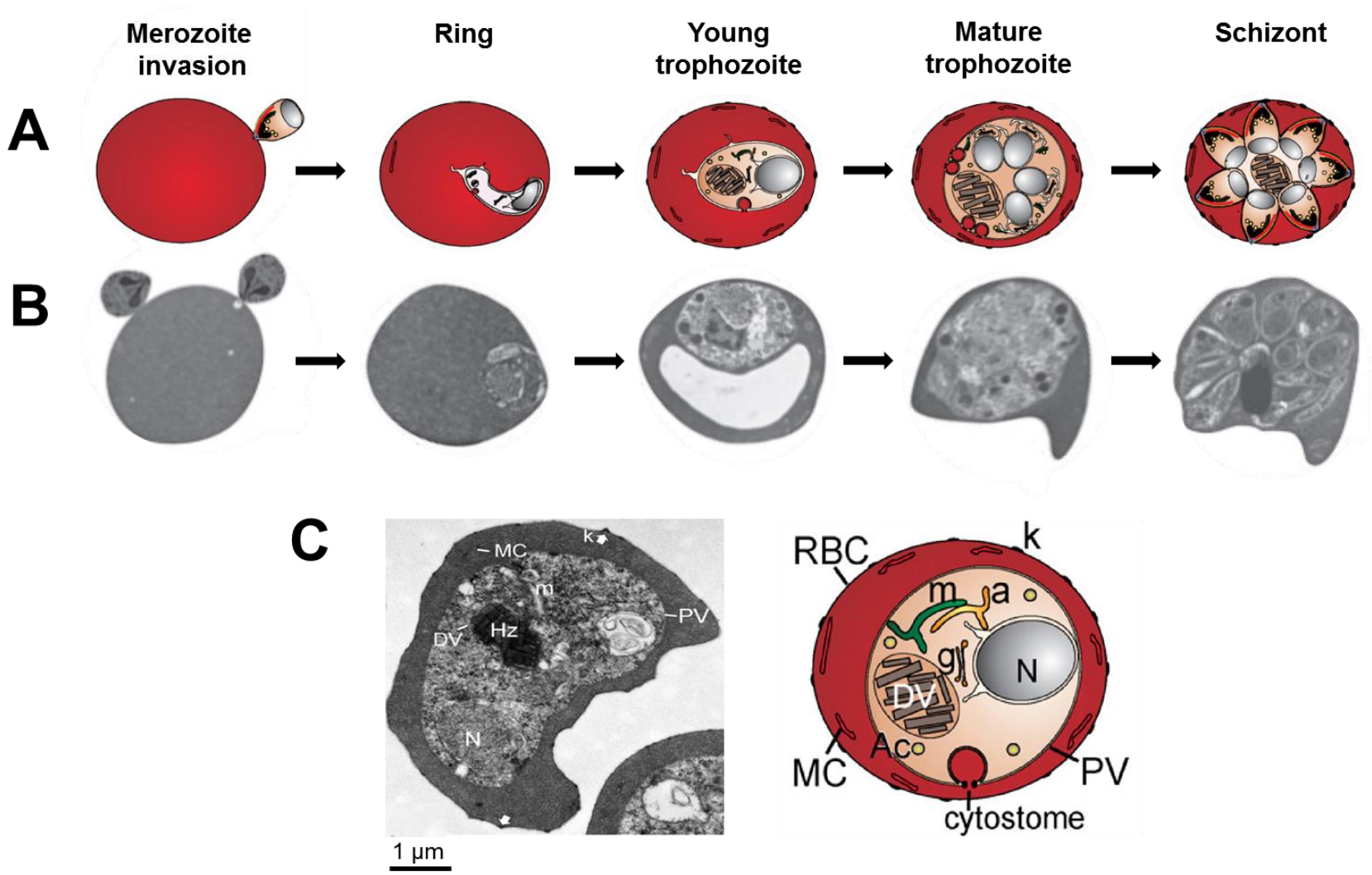

Figure 1.4. (*continued on next page*)

Figure 1.4. Ultrastructural illustrations of *P. falciparum*-infected erythrocytes. Shown are (**A**) schematics and (**B**) thin section TEM images of parasite forms occurring over the course of the *P. falciparum* asexual intraerythrocytic cycle. Following invasion of RBCs by merozoites, parasites progress through ring, trophozoite, and schizont stages, ultimately leading to the release of a new generation of merozoites. (**C**) Ultrastructural illustrations of an infected RBC during the metabolically active trophozoite parasite stage. Images collectively show the presence of the following structures: apicoplast (a), acidocalcisomes (Ac), cytostome, digestive vacuole (DV), Golgi apparatus (g), hemozoin (Hz), knobs (k), Maurer's cleft (MC), mitochondrion (m), nucleus (N), parasitophorous vacuole (PV). Images adapted with permission from Tilley *et al*. (2011)[29] and Hannsen *et al.* (2010).[26]

The capacity of *P. falciparum* to equip a differentiated, compartment-poor cell with an assortment of organelles, trafficking networks, and virulence factors (**Figure 1.4*C***) is a prime example of cellular co-optation and remodeling by a parasitic organism.

Plasmodium metabolism and homeostasis

Publication of the full genome sequence of *P. falciparum* in 2002 provided a valuable lens into the inner workings of human malarial parasites. Harboring over 5,000 genes distributed among 14 chromosomes, the *P. falciparum* genome was reported to encode a higher fraction of immune evasion and cell adhesion proteins than previously sequenced eukaryotic genomes.[33] Additionally, it encoded fewer enzymes and transporters.[33] In light of the unusually high A+T content (>80%) of the *P. falciparum* genome, these predictions came with the caveat that sequence similarity-based genome comparisons will miss sequences that are novel or highly divergent.[33]

It is increasingly apparent that *Plasmodium* parasites have fine-tuned canonical metabolic pathways to meet their specific, stage-dependent growth requirements.[34,35] For example, during the blood stage of infection, central carbon metabolism in non-proliferating gametocytes resembles the citric acid cycle-driven respiration of glucose that is observed in other eukaryotic organisms. In rapidly proliferating asexual blood-stage parasites, however, the majority of parasite biosynthetic intermediates derive from aerobic fermentative glycolysis, reminiscent of the metabolic reprogramming that occurs in cancer cells.[35] Nutrient deprivation is a known stimulus for gametocyte differentiation, corroborating the hypothesis that metabolic cues govern progression through the parasite life cycle, possibly through epigenetic mechanisms.[35]

Recent ^{13}C-based carbon flux analyses performed on blood-stage *Plasmodium* parasites lacking functional pyruvate dehydrogenase (PDH) highlight important nuances in parasite metabolic rewiring. In most eukaryotes, the central metabolic intermediate acetyl-CoA is largely synthesized via the PDH complex in the mitochondria. Interestingly, PDH disruption did not appreciably affect acetyl-CoA synthesis or growth of blood-stage *P. falciparum* parasites.[34] However, it inhibited liver-stage development of the rodent strains *P. berghei* and *P. yoelii* and prevented generation of sporozoites in the mosquito vector for *P. falciparum*, effects attributed to defective fatty acid synthesis.[34,36] This reappropriated role of PDH is consistent with its location in the parasite apicoplast, which plays essential roles in fatty acid, isoprenoid, and heme synthesis.[11]

Plasmodium parasites are equipped to establish and maintain specific physiologic conditions that enable them to progress through their life cycle. During blood-stage infection, parasites facilitate nutrient exchange by inducing an array of external channels with broad solute specificity, termed new permeability pathways (NPPs), that alter (primarily) Na^+ and K^+ ion flow across RBC membranes.[37] Dynamic flux of other ions (e.g. Zn^{2+}) is also known to be indispensable during the blood stage.[38] In the parasite itself, a network of channels and transporters, some still putative, ensure tight control of ion, pH, and volume homeostasis.[37] Previous mathematical modeling suggests that parasites prevent excessive RBC swelling and rupture of deformed RBC membranes by digesting the internal supply of host hemoglobin (Hb) well beyond the levels needed to meet its amino acid requirements (see next section, "Hemoglobin processing in *Plasmodium*").[39,40]

In both their human and mosquito hosts, *Plasmodium* parasites encounter

oxidative insults.[41,42] These are mediated by reactive oxygen (ROS) and nitrogen (RNS) species that are generated, for instance, as a host immune response or by toxic species (e.g. Hb-derived heme).[43] To cope with oxidative stress, parasites are equipped with a specialized system for redox homeostasis, comprised of the thioredoxin reductase-thioredoxin couple, the glutathione reductase-glutathione couple, a set of peroxiredoxins, as well as members of the thioredoxin protein superfamily.[44] Of these, redox state in *Plasmodium* parasites is governed largely by the ratio of the reduced (GSH) and oxidized (GSSG) forms of the tripeptide glutathione, the most abundant redox-active thiol in parasites. Maintenance of a highly reducing environment (>30:1 GSH:GSSG ratio) is important for *Plasmodium* parasites, which actively synthesize GSH to keep up with its constant efflux.[45]

Hemoglobin processing in *Plasmodium*

During their intraerythrocytic growth, *Plasmodium* parasites engulf up to 80% of host Hb through cytostomes and, through vesicular transport, direct it to their digestive vacuole (DV), a lysosome-like organelle with a pH (~5.4) suitable for Hb digestion (**Figure 1.5*A***).[46-49] In addition to providing osmotic stability,[40] processing of host Hb in infected RBCs (**Figure 1.5*B–F***) majorly contributes to the parasite's amino acid pool, which is required for synthesis of parasite proteins.[50] Hb breakdown also unleashes heme (ferrous protoporphyrin X, Fe[II]PIX) (**Figure 1.5*G***). Lacking a heme oxygenase system that is used by many other organisms to dispose of toxic heme species,[49] the parasite detoxifies and incorporates free heme into an inert, crystalline waste product called hemozoin (Hz; **Figure 1.5*H***).

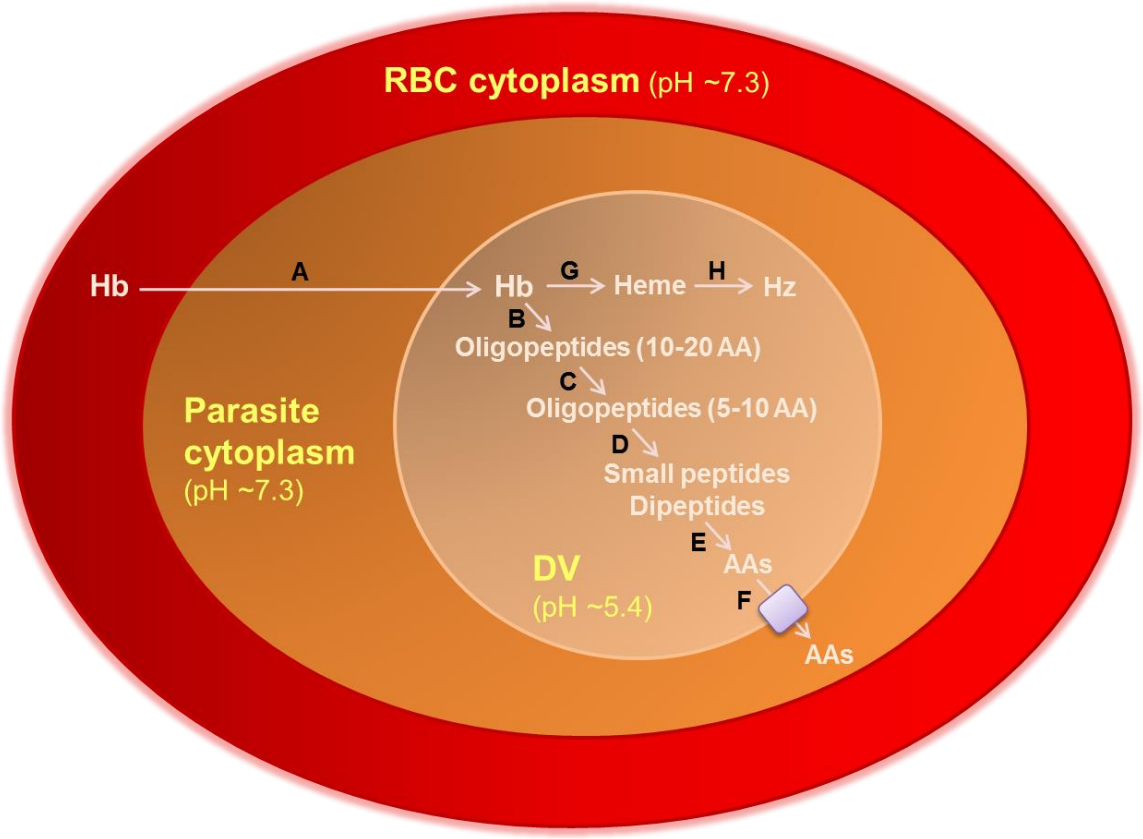

Figure 1.5. Processing of host hemoglobin (Hb) in a *Plasmodium*-infected erythrocyte. (**A**) Following internalization by the parasite's cytostome-vesicle trafficking system, host Hb is directed to the parasite digestive vacuole (DV). There, it undergoes semi-ordered hydrolysis by (**B**) plasmepsins and falcipains, (**C**) falcilysin, (**D**) dipeptidyl amino peptidase 1 (DPAP1), and (**E**) aminopeptidase P (APP), followed by (**F**) export of amino acids (AAs) to the parasite cytoplasm. Small peptides may also be transported to the cytoplasm and undergo processing to AAs by cytosolic aminopeptidases. Breakdown of Hb also releases (**G**) oxidative damage-promoting heme prosthetic groups, which the parasite (**H**) sequesters in an inert crystal structure, hemozoin (Hz).[51,52]

An assortment of parasite proteases with partly overlapping functions is responsible for degrading Hb in the parasite DV, a multi-step process that is critical for parasite survival.[50] In *P. falciparum*, these include aspartic proteases (plasmepsins), cysteine proteases (falcipains), a metalloprotease (falcilysin), at least one dipeptidyl aminopeptidase, and aminopeptidases.[53] In recent investigations performed with *P. falciparum* DV lysates, Chugh *et al.* identified a multi-protein complex consisting of Hb proteases (falcipains, plasmepsins) and a Hz polymerase (heme detoxification protein, HDP).[54] The association of these proteins suggests that the breakdown of Hb in the parasite DV is a concerted process intimately linked to the formation of Hz. This is supported by the observation that falcipain 2 and HDP can efficiently catalyze conversion of Hb to Hz *in vitro*.[54]

The notion that parasites readily sequester chemically labile heme into chemically inert Hz in parallel with Hb degradation is biologically plausible. Detoxification of heme into Hz is essential for parasite survival[55] and is likely supplemented by additional mechanisms, including GSH-mediated and peroxidative degradation.[56,57] As toxic heme (Fe[II]PIX) gets released in the highly acidic DV environment, it is rapidly oxidized to ferric protoporphyrin IX (Fe[III]PIX).[58] Thenceforth, regardless of the oxidative state of the Fe atom (Fe^{2+} or Fe^{3+}), heme has the potential to generate ROS, as per the Fenton or Haber-Weiss chemical reactions.[59] Respectively, these are as follows:

$$Fe^{2+} + H_2O_2 \rightarrow Fe^{3+} + {}^{\cdot}OH + {}^{-}OH$$

$$Fe^{3+} + {}^{\cdot}O_2^{-} \rightarrow Fe^{2+} + O_2$$

As a pro-oxidant, free heme contributes to lipid peroxidation, DNA damage, as well as protein cross-linking and aggregation.[60] A combination of chemical, spectroscopic, and

microscopy methods performed on blood-stage *P. falciparum* trophozoites have shown that parasites harbor ~60% of the total Fe present in infected RBCs, with the vast majority (~90%) concentrated in the parasite DV.[61] Consistent with the essentiality of heme detoxification,[61] ~95% of Hb-derived Fe present in parasites is incorporated into Hz. Importantly, heme prosthetic groups are required by parasites for proper mitochondrial cytochrome function,[49] suggesting an important balance between heme utilization and disposal. Presumably, the parasite's redox defense system (see "*Plasmodium* metabolism and homeostasis" section above) is sufficient to counteract oxidative damage by any residual pro-oxidant heme species.

The mechanism by which heme (Fe[III]PIX) is formed into Hz *in situ* remains unsettled. Using chemical analysis and spectroscopic methods, Slater *et al.* discovered that Hz is nearly identical to *β*-hematin, a synthetic aggregate of Fe[III]PIX.[62] This was corroborated by Raman spectroscopic comparisons of Hz in living parasites, extracted Hz, and synthesized *β*-hematin.[63] Crystallization of head-to-tail dimeric units is thought to underlie the polymerization of heme into Hz (**Figure 1.6**). Specifically, electrostatic interactions between Fe^{3+} of one Fe(III)PIX and a carboxylate group of a second Fe(III)PIX facilitate dimerization, with additional stability provided by hydrogen bonds.[62,64] The head-to-tail dimer can interconvert with monomeric, *μ*-oxo dimeric, and non-crystalline aggregated forms (see **Figure 1.6**), and the extent to which it does so is influenced by ambient pH, ionic composition, and mode of catalysis.[58] Catalysis of Hz polymerization can occur by Hz itself, through the action of the functionally conserved *Plasmodium* protein HDP, and/or via interactions with neutral lipids that were earlier found to associate with Hz in lipid droplets.[65-67] The highly ordered structure of Hz can be appreciated microscopically (**Figure 1.7*A***).

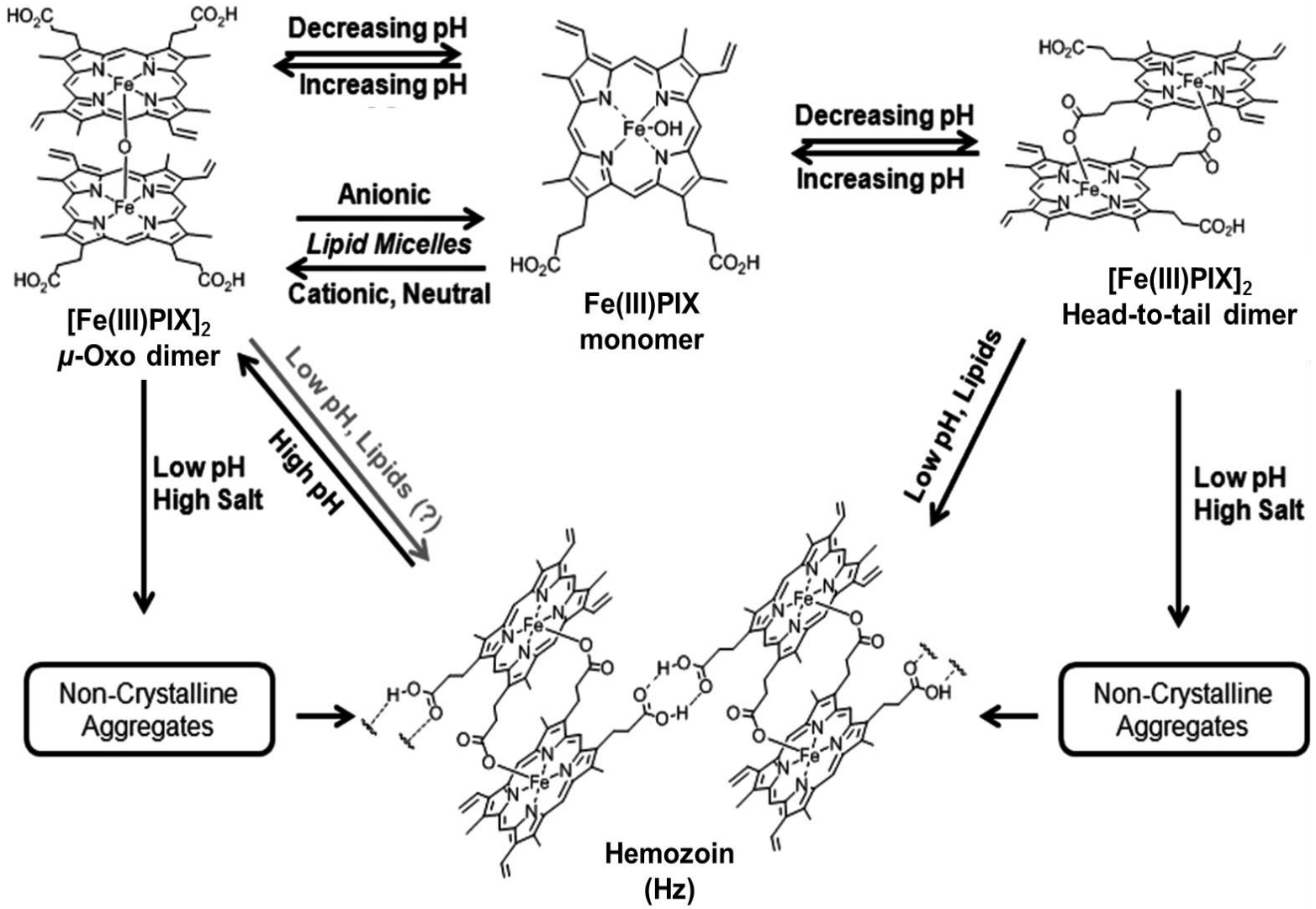

Figure 1.6. *(continued on next page)*

Figure 1.6. Schematic of heme-to-hemozoin polymerization pathways. Shown are observed (black arrows) and hypothetical (gray arrow) pathways leading to the formation of hemozoin (Hz) from heme (ferriprotoporphyrin IX, Fe(III)PIX). The depicted form of the heme monomer is hematin, in which Fe is bound to hydroxide (–OH). Intermediate steps include $[Fe(III)PIX]_2$ dimers and non-crystalline aggregates. The prototypical head-to-tail dimer comprises a Fe^{3+} center of one Fe(III)PIX molecule bonded to a propionate group of a second Fe(III)PIX molecule. The μ-Oxo dimer is composed of oxygen-bridged Fe^{3+} centers of two Fe(III)PIX molecules. The occurrence and directionality of interconversions is influenced by several factors, including solvent type, pH, ionic composition, and presence of lipid catalyst. Image reproduced with permission from Gorka *et al.* (2014).[58]

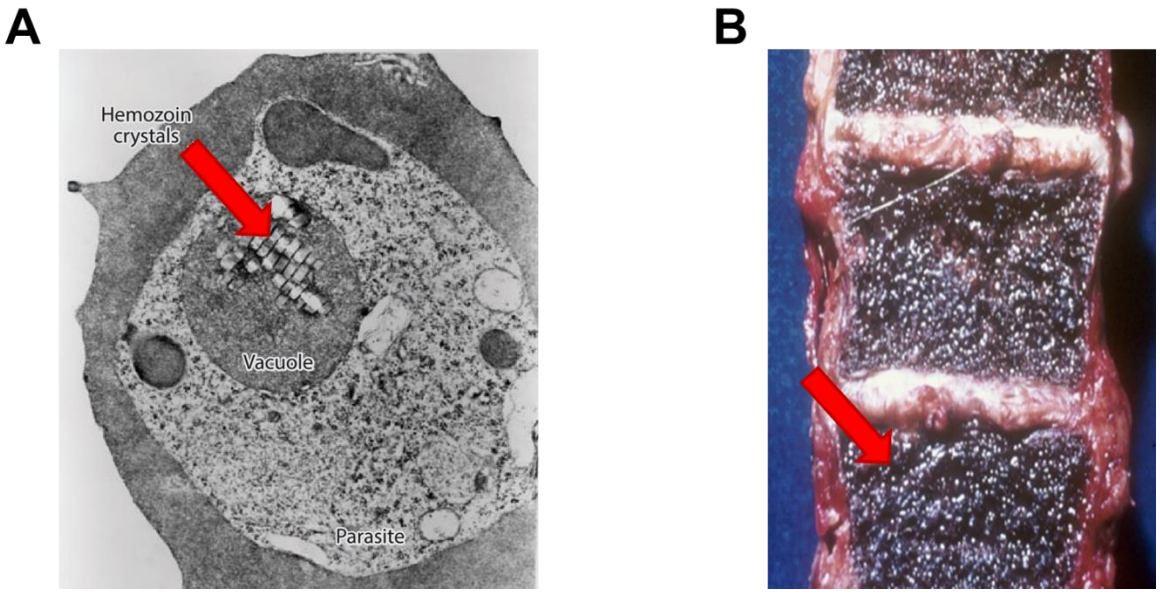

Figure 1.7. Microscopic and gross manifestations of *Plasmodium* malarial pigment. Hemozoin, also known as malarial pigment, can be visualized (**A**) microscopically or (**B**) macroscopically. Shown above are (**A**) an electron micrograph, revealing hemozoin crystals (red arrow) concentrated within the digestive vacuole of a trophozoite, blood-stage *Plasmodium* parasite, and (**B**) a gross specimen of human spine bone marrow from a patient repeatedly infected with *Plasmodium*, with dark pigmentation characteristic of hemozoin (red arrow). Images reproduced with permission from Sigala and Goldberg (2014)[49] and the Institute of Tropical Medicine Antwerp.[68]

Grossly, parasite Hz corresponds to the dark brown pigment that Laveran observed in the 19th century as he examined *Plasmodium*-infected RBCs and that can be found in tissue specimens isolated from infected patients (**Figure 1.7*B***).[1]

Of note, a number of antimalarials from distinct chemical classes access the DV and have been proposed to interfere with parasite heme detoxification and/or require heme for their activity against asexual blood-stage parasites (see **Antimalarial compounds**).[54,55,69-71] Moreover, studies of liver-stage and mosquito-stage parasites suggest a critical role for *de novo* heme synthesis.[72] Complementing host-derived heme in the blood stage, heme during the exoerythrocytic stages is derived through a complex heme biosynthetic pathway with components in the parasite cytosol, mitochondrion, and apicoplast.[49] Given this knowledge, active elucidation of parasite heme metabolism should be a research priority.

MALARIAL DISEASE

Clinical manifestations and diagnosis

Together, human malarial parasites cause a wide spectrum of clinical presentations that span asymptomatic infection through fulminant, possibly lethal, disease. The predominant etiological agents of disease are *P. falciparum* and *P. vivax*. Africa bears the largest global burden of *P. falciparum* malaria, which disproportionately affects the pediatric population.[13] Outside of Africa, adult populations are at higher risk for severe disease, and about half of malaria cases are caused by *P. vivax*.[13] Though not as pathogenic as *P. falciparum*, *P. vivax* may occasionally cause severe disease. Individuals infected with *P. vivax* (but not *P. falciparum*) are prone to disease relapse due to reactivation of hypnozoite parasites from dormancy in the liver (see **Figure 1.2**).

Of note, co-infections consisting of *Plasmodium* and other viral, bacterial, or parasitic pathogens occur among a subset of malaria patients and have various effects on *Plasmodium* replication as well as the pathogenesis, diagnosis, and outcome of disease.[17,73]

Uncomplicated malaria is characterized by a constellation of non-specific clinical symptoms. These include fever (≥40°C), malaise, headache, myalgias, and abdominal discomfort.[14,15,74] Although regularity of disease paroxysms has been previously described as pathognomonic of malarial disease, irregular febrile episodes are common. Reflecting chronic infection in malaria-endemic regions, a palpable spleen may be observed on physical exam.[14] Resolution of uncomplicated malaria is expected (<0.1% mortality rate), provided that parasites are cleared before achieving a high parasitemia (~2% parasitemia, equivalent to ~10^{12} parasites).[14,15] Mortality risk increases substantially with increased blood parasitemia.[15]

A small subset (1-2%) of *Plasmodium* infections progress to severe malaria, which differs between children and adults (**Figure 1.8**).[74] In endemic areas, malarial disease is especially marked among children, who lack robust immunity.[75] However, increased age is an independent risk factor for malaria mortality and is associated with impairments in multiple organ systems.[74,75] Key pediatric complications include cerebral malaria (CM), anemia, and acidosis, all of which suggest a grim clinical outcome.[76] The clinical picture of adult severe malaria is more expansive and includes CM, respiratory distress, jaundice, and acute kidney injury.[74] *Plasmodium* infection of pregnant women may also result in termination of pregnancy or stillbirths.[14] **Table 1.2** summarizes clinical manifestations that are prominent in severe malaria, along with associated prognostic factors.

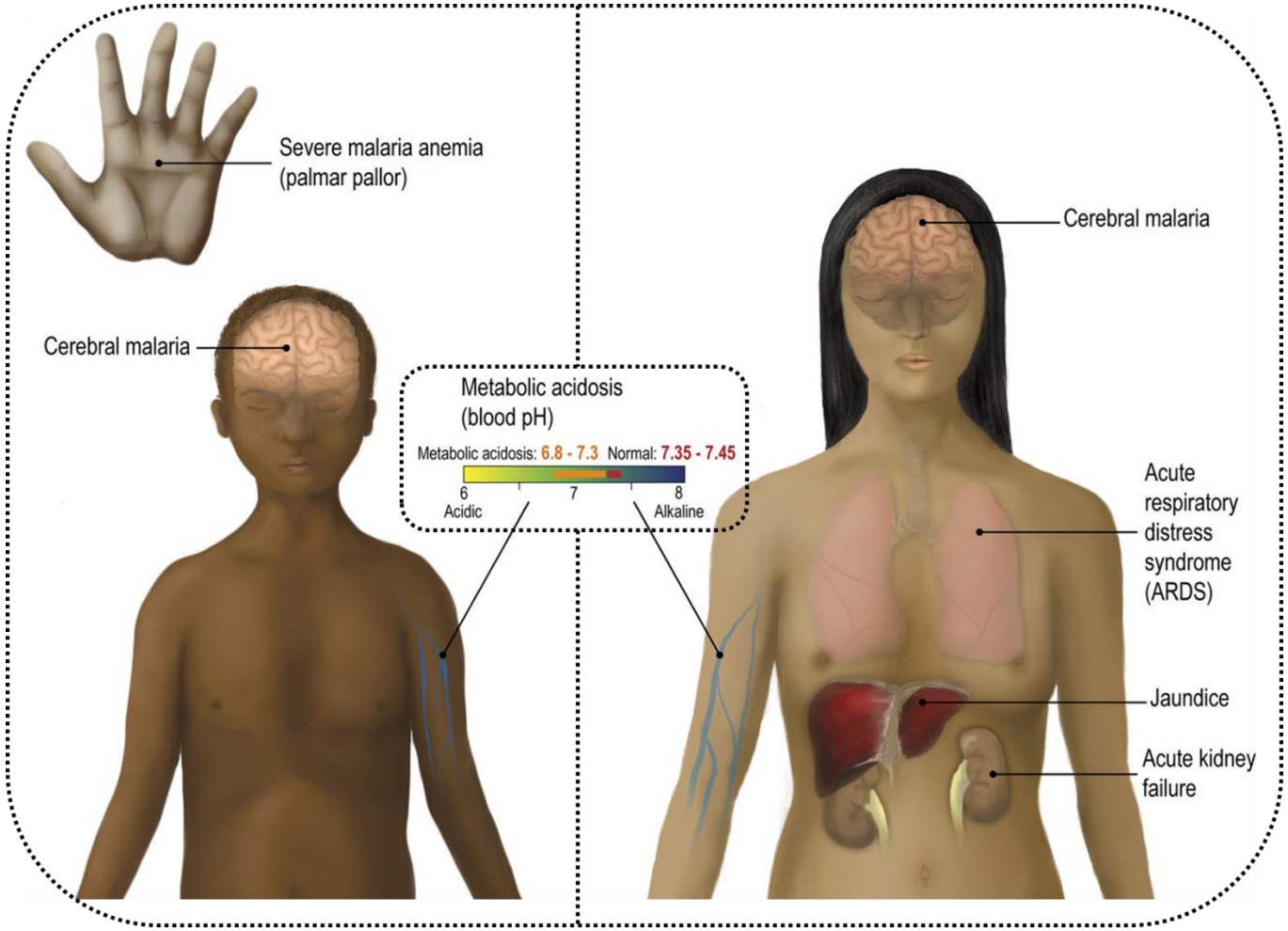

Figure 1.8. Clinical features of severe malaria in children and adults**.** The main manifestations of severe malaria differ between pediatric and adult populations. In children, anemia (pallor), metabolic acidosis, and cerebral malaria are predominant features of severe disease. In adults, metabolic acidosis and cerebral malaria are accompanied by injury to multiple organs, including the liver (jaundice), kidney (acute kidney failure), and lungs (acute respiratory distress syndrome, ARDS). Image adapted with permission from Wassmer *et al*. (2015).[74]

Typified by coma, CM is one of the most important complications of malarial disease, particularly among children aged <5 in sub-Saharan Africa.[13,77] CM is refractory to standard antimalarial treatments, may lead to debilitating neurocognitive impairments, and results in death in up to 20% of cases.[77] Lethality in CM occurs, in part, due to a rapid increase in intracranial pressure.[73] In addition to brain swelling, as detected by neuroimaging, the clinicopathological features of CM (**Figure 1.9**) include characteristic and diagnostically useful retinal changes, termed malarial retinopathy.[73]

In addition to clinical assessment, full malaria diagnosis requires confirmation of infection. The gold standard of parasite identification and classification is analysis of Giemsa-stained thin and thick blood smears by light microscopy. Thick blood smears detect parasites with high sensitivity (0.001% parasitemia), and both thin and thick smears can help to differentiate among various *Plasmodium* species (see **Table 1.1** for key morphological differences).[14] Rapid diagnostic tests (RDTs), have gained traction as another diagnostic tool, particularly in resource-poor settings. RDTs entail the interaction of parasite antigens with antigen-specific antibodies embedded on a dipstick or paper card. One of these antigens, *P. falciparum* Histidine-Rich Protein 2 (PfHRP2) detects infection with sensitivity comparable to light microscopy and, in the absence of a precise determination of parasitemia, serves as an indirect marker of parasite biomass.[78] Of note, quantification of serum PfHRP2 levels can provide important information regarding disease prognosis.[74] Other antigens used in RDTs include lactate dehydrogenase (LDH) and aldolase.[14] PCR-based detection methods are used primarily for surveillance and detection of submicroscopic infections, of particular relevance to malaria elimination efforts.[79]

Table 1.2. Clinical manifestations of severe malarial disease.[a]

Clinical manifestation	Indicator of poor prognosis
Cerebral malaria; seizures	Deep coma; agitation; ↑ convulsions
Acidosis	Arterial pH <7.3; HCO_3^- <15 mM; lactate >5 mM
Normochromic, normocytic anemia	PCV <15%
Renal failure	Anuria; creatinine >265 µM
Pulmonary edema; respiratory distress	Hyperventilation
Hypoglycemia	Glucose <2.2 mM
Systemic inflammation	Shock; hypothermia (<36.5°C); WBC count >12,000/µl; urate >600 µM
Bleeding; coagulopathy	Thrombocyte count <50,000/µl; PT >3 sec; ↑ PTT; FG <200 mg/dL
Muscular weakness; myopathy	↑ CPK; ↑ myoglobin
Hyperparasitemia	$>10^5$ parasites/µl; >20% mature forms; >5% PMNLs with malaria pigment
Jaundice	Total bilirubin >50 µM AST/ALT ratio >3× ULN

[a] ↑, increased; PCV, packed cell volume; PfHRP2, *P. falciparum* Histidine-rich Protein 2; CSF, cerebrospinal fluid; WBC, white blood cell; PT, prothrombin time; PTT, partial thromboplastin time; FG, fibrinogen; CPK, creatinine phosphokinase; PMNLs, polymorphonuclear leukocytes; AST, aspartate transaminase; ALT, alanine transaminase; ULN, upper limit of normal. Adapted from Kasper *et al.* (2015).[14]

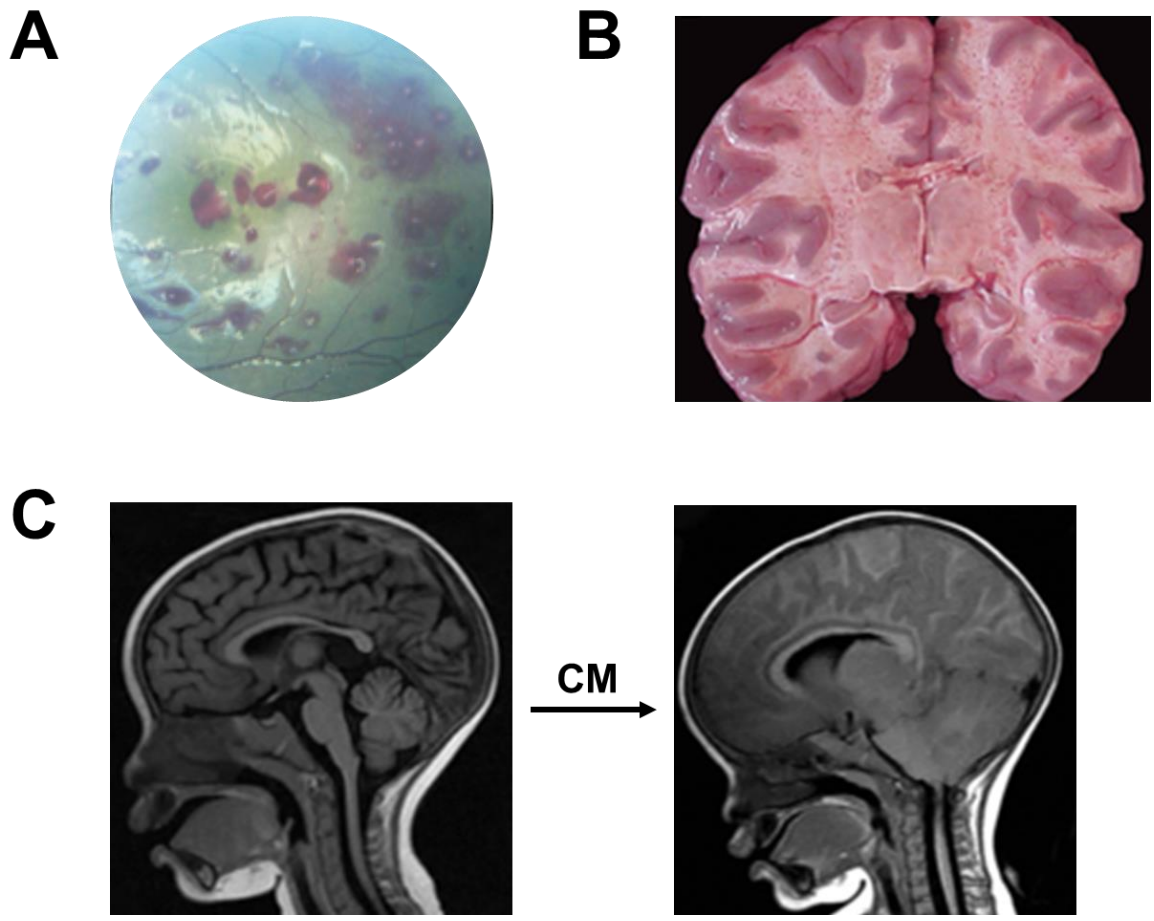

Figure 1.9. Manifestations of cerebral malaria (CM). (**A**) Funduscopic image depicting the white-centered hemorrhages of malarial retinopathy. Additional ocular findings in CM include retinal whitening and discoloration of blood vessels. (**B**) A feature of cerebral cortex pathology in CM is the presence of hemorrhages throughout the white matter. (**C**) Brain swelling in pediatric CM. Shown are representative MRI T2 images depicting the transition from no disease to severe CM. Key changes include flattening of the gyri, narrowing of the sulci, and downward herniation of the cerebellum with resulting crowding of the brainstem. Image reproduced with permission from Taylor and Molyneux (2014).[73]

Pathogenesis and immunity

Malaria pathogenesis is a multifactorial process, and its underlying molecular mechanisms are incompletely understood. Nevertheless, insights from an array of *in vivo* and *in vitro* studies aid in conceptualizing the diverse and complex clinical manifestations of malarial disease. Anemia during blood-stage *Plasmodium* infection arises, in part, from the destruction of RBCs, through both direct lysis and splenic clearance. Release of parasite and host products upon RBC lysis triggers cytokine secretion; clinical consequences include fever and sepsis. Inflammation-induced dyserythropoiesis exacerbates anemia and causes thrombocytopenia. Additionally, utilization of glucose by rapidly proliferating, glycolysis-dependent blood-stage parasites contributes to hypoglycemia and acidosis. This is compounded by reduced delivery of oxygen to host tissues.[14,15,80]

A distinctive property of *P. falciparum* parasites is their ability to sequester in the microvasculature, which helps them avoid immune clearance and prompts endothelial dysfunction (**Figure 1.10**). During each round of their intraerythrocytic life cycle, *P. falciparum* parasites express an antigenically unique form of the *P. falciparum* Erythrocyte Membrane Protein 1 (PfEMP1), an adhesion protein localized to parasite-induced knobs that are present on the RBC surface. Through recombination among ~60 PfEMP1-encoding *var* genes, parasites achieve a wide repertoire of PfEMP1 molecules.[81] These antigenically diverse proteins bind to endothelial receptors with varying affinities and play a key role in parasite immune evasion.[74,81] PfEMP1 may also interact with molecules present on uninfected RBCs, leading to blockage of the microvasculature. The degree of blockage corresponds to prognostic markers of disease, including serum lactate levels and base deficit.[15]

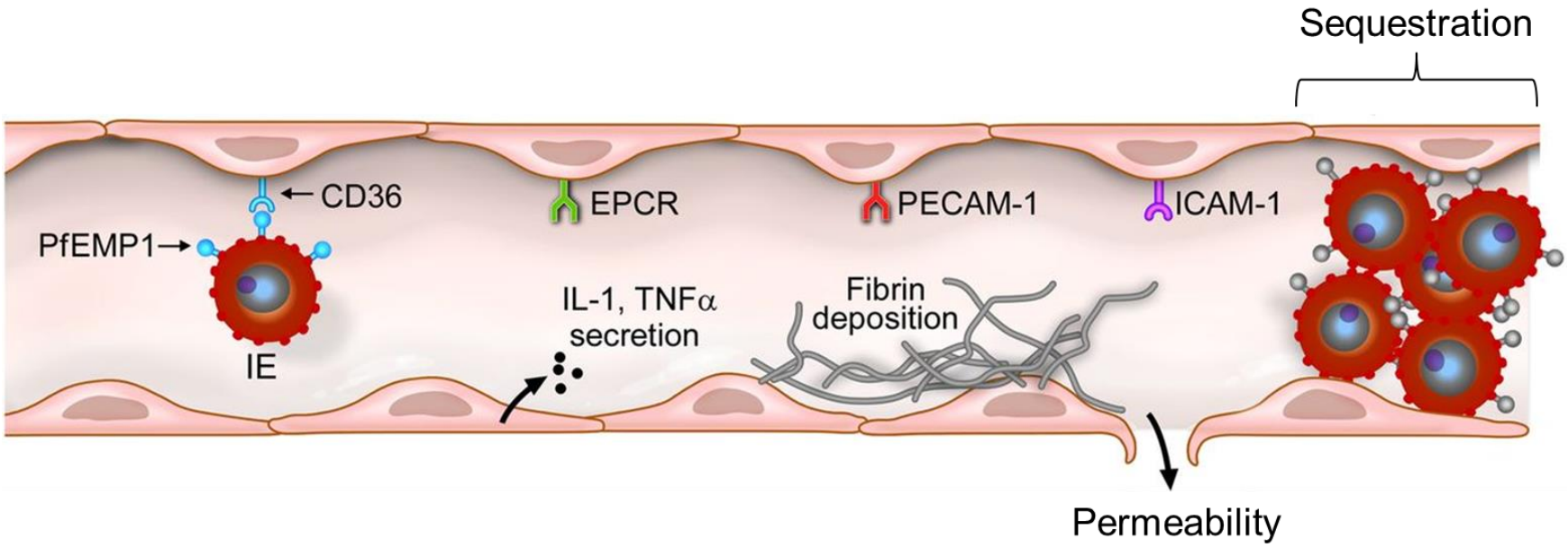

Figure 1.10. Interactions between infected erythrocytes and endothelial cells during *P. falciparum* infection. Shown is a schematic of cellular and molecular events occurring in the microvasculature that contribute to the pathogenesis of *P. falciparum* infection. Found on the surface of an infected RBC is a distinct, parasite-encoded PfEMP1 molecule. In the example above, the PfEMP1 variant is specific for the host endothelial cell receptor CD36. The specific set of receptors expressed by endothelial cells is tissue-dependent. In the placenta and brain, for example, interactions of PfEMP1 variants with the receptors CSA and EPCR, respectively, contribute to the pathogenesis of placental and cerebral malaria. RBC-endothelial cell interactions facilitate sequestration in host tissues, causing a clinical syndrome directly related to the site of sequestration. Ensuing endothelial dysfunction is characterized by alterations in receptor expression, secretion of pro-inflammatory cytokines (e.g. IL-1, TNF-α), fibrin deposition, and increased basement membrane permeability that allows for perivascular infiltration. Image reproduced with permission from Aird *et al*. (2014).[82]

PfEMP1 engagement of endothelial receptors causes secretion of pro-inflammatory cytokines, fibrin deposition, and disruption of the endothelial basement membrane.[82] Inflammation subsequently extends into the surrounding tissue, which is subjected to hypoxia and lactic acidosis caused by microvessel occlusion.[80] Roles for heme species in mediating endothelial dysfunction have also been described. These include direct exposure to heme, as well as indirect effects, such as depletion of nitric oxide (NO), an important mediator of endothelial homeostasis.[80,83]

Depending on the parasite adhesion molecules and the specific host tissues that are involved, the abovementioned cellular and molecular events may produce one or more of the various clinical syndromes of severe malaria (see "Clinical manifestations and diagnosis" section above). Pregnancy-associated malaria, for example, is associated with a PfEMP1 variant that binds to the placental chondroitin sulfate A (CSA) receptor. Another receptor, endothelial protein C receptor (EPCR), has been implicated in the pathogenesis of CM. The levels of EPCR are diminished in CM, and PfEMP1 engagement of EPCR has been proposed to further inhibit the ability of EPCR to regulate the host Protein C cascade, resulting in coagulopathy.[74,82] With regard to pathogenesis, CM manifests itself differently in children and in adults. In children, RBC sequestration occurs either in the presence or absence of vascular pathology and coagulative defects, whereas in adults, intermediate phenotypes may be observed.[73,74] Continued investigation of the pathogenic features that define different subtypes of severe malaria will undoubtedly direct future diagnosis and treatment of this potentially devastating disease.

The pathogenesis and clinical course of malarial disease are greatly influenced by the host immune response. In general, repeated exposure of individuals to

Plasmodium infection in high-transmission, endemic settings such as sub-Saharan Africa confers premunition – protection from disease, but not from infection itself. With time and sustained exposure to infections, protection from parasite replication is also conferred.[15] This effect wanes with reduced exposure.[84] Disease surveillance is therefore called for in low-transmission settings, where disease outbreaks are a threat due to weak immunity.[17]

Aside from the sophisticated immune evasion strategies with which *Plasmodium* parasites are equipped,[81] a number of stage-dependent parasite interactions with the host immune system contribute to malaria pathogenesis. Liver-resident parasites, for instance, temporarily escape sensing by the innate immune system, whereas blood-stage parasites activate innate immunity through the release of stimulatory parasite or host-derived ligands, such as Hz, glycosylphosphatidylinositol (GPI), and uric acid.[85,86] Through its activation of tumor necrosis factor-alpha (TNF-α), which in turn induces activation of a basement membrane-degrading matrix metalloprotease, Hz has been postulated to contribute to loss of endothelial basement membrane integrity.[87]

The humoral and cellular arms of the adaptive immune system are, likewise, important, although their roles are not fully understood.[14] Previous studies have correlated certain antibody class and sub-class profiles with specific transmission settings and disease states.[88] Despite this, the specific correlates for the various degrees of human immunity observed in different transmission settings remain unclear.[84]

A role for dysregulated immune responses in mediating slow acquisition of anti-*Plasmodium* humoral immunity was recently proposed by Ryg-Cornejo *et al.*

based on studies in the *P. berghei* ANKA rodent model. Severe malarial infection inhibited differentiation of T follicular helper (Tfh) cells, which normally induce the establishment of germinal centers that are critical for the development of humoral immunity.[89] This effect was diminished upon blockade of the pro-inflammatory cytokines TNF-α and interferon-gamma (IFN-γ), which confer protection against high parasitemia and, yet, also drive the pathogenesis of severe malaria.[89] The complex interplay between malarial disease and immunity is further highlighted by the ability of human genetic TNF variants to modulate malarial disease susceptibility.[90]

P. falciparum and *P. vivax* possess distinctive biological and molecular features that mediate their different cell tropisms, degrees of virulence, and disease presentations. As compared to infection with *P. falciparum*, *P. vivax* infection is associated with a more benign clinical course, in part due to its preference for reticulocytes and reduced RBC sequestration in host tissues. Still, *P. vivax* instigates profound inflammation, with a pyrogenic threshold lower than *P. falciparum* and the capacity to sustain chronic infections via the hypnozoite stage of its life cycle.[74] Of note, a significant portion of African individuals are null for the Fy^a and Fy^b Duffy antigens that are required for *P. vivax* invasion of RBCs, rendering them resistant to infection.[14] *P. falciparum*, on the other hand, encodes multiple functionally redundant ligands, with the exception of the *P. falciparum* Reticulocyte-binding homolog 5 (PfRh5) protein. PfRh5 is essential for invasion through its interaction with host Basigin (CD147).[91] While some Basigin variants have been documented,[91] other RBC-altering genetic variations play a more pronounced role in protecting individuals from diseases caused by *P. falciparum*. Among them are hemoglobinopathies, thalassemias, and other genetic disorders affecting RBC structure.[92]

Prophylaxis and treatment

In July 2015, the European Medicine Agency's Committee for Medicinal Products for Human Use approved the recombinant *P. falciparum* circumsporozoite (CSP)-based RTS,S/AS01 vaccine, which targets the pre-erythrocytic stages of *P. falciparum*.[93] This vaccine requires four doses and was found to reduce malarial cases by <40% in children aged 5-17 months.[13] Given the enduring challenge of generating a highly immunogenic vaccine capable of halting parasite progression through its biologically complex life cycle, approval of RTS,S/AS01 represents a milestone for malaria vaccine efforts.[94] However, it remains to be seen how the moderate efficacy of RTS,S/AS01, assessed in a controlled trial, will translate into the real-world setting. Presently, vaccination does not play a role in global antimalarial prophylaxis.

Apart from mosquito avoidance and control measures, antimalarial drugs represent the best mode of antimalarial prophylaxis. In this section, general recommendations are considered. Specific regimens and their pharmacology are detailed in the next section (**Antimalarial compounds**). Recommendations for chemoprophylaxis depend on the drug resistance profiles of the relevant geographical region and on the absence of contraindications (**Table 1.3**). As malaria can cause adverse pregnancy outcomes, travel by pregnant women to malaria-endemic regions is discouraged.[95] CQ and mefloquine (MFQ) are appropriate chemoprophylactic agents for pregnant women traveling to areas with CQ-sensitive and CQ-resistant parasites, respectively. These drugs may also be prescribed to infants.[95] Use of primaquine (PMQ) in regions where *P. vivax* is the dominant species is recommended to prevent hypnozoite-mediated relapse of disease. PMQ is also used following travel to an endemic region as a presumptive therapy against *P. vivax* or *P. ovale* hypnozoites.[15,95]

Table 1.3. Antimalarial drugs used for chemoprophylaxis.[a]

Usage	Drug	Contraindications
All areas	Atovaquone-proguanil	Renal impairment; children <5 kg; pregnant women; women with infants <5 kg
	Doxycycline	Children <8 years; pregnant women; significant sun exposure
MFQ-sensitive *P. falciparum*	Mefloquine	MFQ, QN, or QD allergy; psychiatric disorder; seizures; heart conditions
CQ-sensitive *P. falciparum* or *P. vivax*	Chloroquine or Hydroxychloroquine	Known drug hypersensitivity
P. vivax or *P. ovale*	Primaquine	G6PD deficiency (must be checked); pregnant women; breast-fed infants

[a]MFQ, mefloquine; QN, quinine; QD, quinidine; CQ, chloroquine; G6PD, glucose-6-phosphate dehydrogenase. Recommendations may change with time. Adapted from CDC Health Information for International Travel (2016).[95]

Recently, in sub-Saharan Africa, two major intermittent preventive therapy regimens have been implemented, namely sulfadoxine-pyrimethamine (SP) for pregnant women and amodiaquine (AQ)-SP for children aged 3 months – 5 years.[15]

Beyond their role as chemoprophylactic agents, antimalarial drugs serve as the cornerstone of malaria treatment (**Figure 1.4**), chiefly via their action against pathogenic, asexual blood-stage parasites. The first-line artemisinin-based combination therapies (ACTs), which pair two antimalarials with distinct modes of action, are now ubiquitously employed to treat uncomplicated *P. falciparum* infection. While CQ remains the first-line treatment against *P. vivax*, *P. ovale*, *P. malariae*, and *P. knowlesi*, ACTs effectively clear infections caused by these species.[14] Of note, the vast majority of manufactured ACTs is destined for the African continent, where use of ACTs has increased >30-fold in the past decade.[13] In areas with low transmission of *P. falciparum* parasites, a single gametocytocidal dose of PMQ should be administered in conjunction with an ACT.[15]

Treatment of severe malaria requires hospitalization of the infected individual. Patient monitoring should include determination of serum glucose levels, acid-base status, hematocrit, and parasitemia.[14] Parenteral artesunate (AS) is the first-line agent for treatment of severe malaria and has been shown to reduce patient mortality in randomized controlled trials.[15] As needed, patients should also receive glucose for hypoglycemia, packed RBCs for anemia (hematocrit <20%), benzodiazepines for convulsions, and hemodialysis in the case of acute renal failure.[14]

Table 1.4. Antimalarial drugs used for treatment of malaria.[a]

Usage	Drug regimen	Targeted parasite stage(s)	Contraindications
Severe malaria	AS (parenteral)	Blood: asexual, sexual	–
Pf and unknown species first-line; effective against *Pv*, *Po*, *Pm*, and *Pk*; ATM-LUM, AS-AQ, AS-MFQ, or DHA-PPQ for *Pf* in 2nd-3rd trimesters pregnancy	ATM-LUM	Blood: asexual (ATM, LUM), sexual (ATM)	1st trimester pregnancy
	AS-AQ	Blood: asexual (AS, AQ), sexual (AS)	1st trimester pregnancy
	AS-MFQ	Blood: asexual (AS, MFQ), sexual (AS)	1st trimester pregnancy; as for MFQ
	DHA-PPQ	Blood: asexual (DHA, PPQ), sexual (DHA)	1st trimester pregnancy
	AS-SP	Blood: asexual (AS, SP), sexual (AS)	1st trimester pregnancy; known drug hypersensitivity; hepatic or renal impairment
Pv^{CQS}, *Po*, *Pm*, and *Pk* first-line; *Pf*^{CQS}	CQ; hCQ	Blood: asexual	Known drug hypersensitivity
Pf^{CQR}; *Pv*	ATQ-PG	Liver (not hypnozoites); blood: asexual	Renal impairment; children <5 kg; pregnant women; women with infants <5 kg
Pf^{CQR}; *Pv*^{CQR}	DOX	Blood: asexual	Children <8 years; pregnant women; significant sun exposure
	QN	Blood: asexual	Known drug hypersensitivity

(continued)

Table 1.4. *continued*

Usage	Drug regimen	Targeted parasite stage(s)	Contraindications
Pf^{CQR}; *Pv*^{CQR}; *Pf* in 1st trimester pregnancy	QN-CLI	Blood: asexual	As for QN
Pf^{CQR,MFQS}; *Pv*^{CQR}	MFQ	Blood: asexual	Psychiatric disorder; seizures; heart conditions (e.g. conduction abnormalities)
Pv, *Po* radical cure	PMQ	Liver; hypnozoite; blood: sexual only	G6PD deficiency; pregnant women; breast-fed infants

[a]Recommended regimens may change with time. *Plasmodium* drug sensitivity profiles in applicable regions of usage are indicated in superscript. *Pf*, *P. falciparum*; *Pv*, *P. vivax*; *Po*, *P. ovale*; *Pm*, *P. malariae*; *Pk*, *P. knowlesi*; CQR, CQ-resistant; CQS, CQ-sensitive; MFQS, mefloquine-sensitive; AS, artesunate; ATM, artemether; DHA, dihydroartemisinin; LUM, lumefantrine; AQ, amodiaquine; MFQ, mefloquine; PPQ, piperaquine; SP, sulfadoxine-pyrimethamine; CQ, chloroquine; hCQ, hydroxy-CQ; ATQ, atovaquone; PG, proguanil; DOX; doxycycline; QN, quinine; CLI, clindamycin; PMQ, primaquine; G6PD, glucose-6-phosphate dehydrogenase. Adapted from CDC Health Information for International Travel (2016)[95] and WHO Guidelines for the Treatment of Malaria (2015).[96]

ANTIMALARIAL COMPOUNDS

Antimalarial drugs, which comprise distinct chemical classes and modes of action, are central to the prevention, treatment, and global containment of malarial disease. A comprehensive understanding of the pharmacology, molecular targets, and resistance mechanisms associated with these drugs is pertinent to their continued success. A summary of the chemical classifications, pharmacologic properties, and toxicities of clinically employed antimalarial regimens is provided in **Table 1.5**. Chemical structures of representative antimalarial compounds are shown in **Figure 1.11**.

ACTs represent the first-line treatment option for individuals infected with *P. falciparum*, including women during the second and third trimesters of pregnancy.[97] These drugs are also effective in treating non-falciparum infections and should be used when the etiology of malarial infection is unknown.[96] With the aim of rapidly clearing the majority of the parasite biomass and ensuring that remaining parasites do not have an opportunity to expand, ACTs combine a potent but short-lived artemisinin (ART) compound with a much more long-lived partner drug. While the majority of clinically employed antimalarials target the pathogenic asexual blood stage of parasites (see **Table 1.4**), an added benefit of using ARTs is their activity against sexual blood-stage parasites (gametocytes), which decreases parasite transmission.[98] Formulations of ACTs recommended by the WHO include artemether-lumefatrine (ATM-LUM), AS-amodiaquine (AS-AQ), AS-mefloquine (AS-MFQ) dihydroartemisinin-piperaquine (DHA-PPQ), and AS-SP.[96]

Of note, to various degrees, many antimalarial compounds – including ACT component drugs – impact DV physiology and morphology (**Figure 1.12**) and/or require interactions with Hb-derived heme species (e.g. heme, Hz) for their action.[55,58,99,100]

Table 1.5. Pharmacologic properties of antimalarial drugs.[a]

Drug	Class	Pharmacokinetic/pharmacodynamic characteristics						Adverse effects and toxicities
		C_{max} (ng/mL)	T_{max} (h)	$T_{1/2}$ (h)	VD/F (L/kg)	CL/F (L/h/kg)	AUC (ng.h/mL)	
CQ	4-Aminoquinoline	283–1430 (89–220)	2.7–6.9	108–291 (175–290)	31.8–262 (12.6)	0.23–0.80 (0.1–0.16)	8.2E3–1.4E5 (2.3E4–6.4E4)	Pruritis; cardiac abnormalities; retinopathy; myopathy
QN	Quinoline methanol	5.3E3–1.8E4	1.0–5.9	3.21–26	0.45–4.24	1.3E-2–0.3	9.2E3–4.5E6	Hypoglycemia; cinchonism; cardiac abnormalities
AQ	4-Aminoquinoline	5.2–39.3 (161–751)	0.5–2.0 (2.7–45)	3.3–12.4 (90–240)	311–1.0E3 (62–252)	14–57.8 (0.6–0.7)	39–602 (1.5E4–4E4)	Agranulocytosis; hepatotoxicity
PPQ	Bisquinoline	71.6–730	1.48–5.7	324 – 672	529 – 877	0.85 – 1.85	2.4E4 – 5.0E4	Cardiac abnormalities
MFQ	Quinoline methanol	1E3–3.3E3	15–72	194–365	7.87–31.8	1.6E-2–0.2	3.1E5–1.5E6	Neuropsychiatric reactions; convulsions
LUM	Quinoline methanol	4.5E3–2.8E4	2–66	33–275	0.4–8.9	0.08–0.10	2.1E5–2.7E6	Hypersensitivity reactions
PMQ	8-Aminoquinoline	65–295	1.8–4.0	3.5–8.0	2.92–7.94	0.31–1.19	443–2.0E3	Hemolysis in G6PD deficiency
DHA	Endoperoxide	366–698	0.97–2.8	0.85–1.40	1.47–3.59	1.19–2.16	0.84–1.95	Hypersensitivity reactions; reticulocytopenia; neutropenia
AS	Endoperoxide	34–451	0.5–1.4	0.9	0.6–3.4	0.61–15.4	113-419	Hypersensitivity reactions; reticulocytopenia; neutropenia

(continued)

Table 1.5. *continued*

Drug	Class	Pharmacokinetic/pharmacodynamic characteristics						Adverse effects and toxicities
		C_{max} (ng/mL)	T_{max} (h)	$T_{1/2}$ (h)	VD/F (L/kg)	CL/F (L/h/kg)	AUC (ng.h/mL)	
ATM	Endoperoxide	5.2–190	0.5–2.1	0.9–5.2	9.9–144	1.5–41.3	40-385	Hypersensitivity reactions; reticulocytopenia; neutropenia
SDX	Antifolate	5.8E4–2.2E5	3.7–63	98.4–261.6	0.26–0.66	5.8E-4–3.0E-3	1.5E4–6.6E4	Gastrointestinal discomfort; hypersensitivity reactions
PYR	Antifolate	86–860	2.4–41.1	60-450	2.32–7.20	0.34–1.78	2.2E4–1.1E5	Megaloblastic anemia; pancytopenia; lung infiltration
ATQ	Napthoquinone	634–1.3E4	5.1–5.7	29–134	4.7–13	9E-2–0.32	6.4E4–6.6E5	Hypersensitivity reactions; gastrointestinal discomfort
PG	Antifolate	560–751	29–134	8.0–17.6	13.4–22.9	0.71–1.23	7.2E3–1.5E4	Megaloblastic anemia in renal failure
DOX	Tetracycline	3.1E3–6.9E3	1.5–6.0	8.8–22.4	0.75–1.83	29.5–112.0	3.9E4–1.1E5	Renal impairment; photosensitivity; bone growth retardation in young children
CLI	Lincosamide	2.5–14	0.75-3.0	1.9–3.6	49.1–132.6	10.0–26.5	2.5E4–2.7E4	Diarrhea; nausea; pruritis

[a]Pharmacologic data report mean or median (range) values, compiled from studies of drug prophylaxis or treatment of acute malaria. For CQ and AQ, values for the corresponding major *in vivo* metabolites (monodesethyl-CQ and monodesethyl-AQ, respectively) are indicated parenthetically. CQ, chloroquine; QN, quinine; AQ, amodiaquine; PPQ, piperaquine; MFQ, mefloquine; LUM, lumefantrine; PMQ, primaquine; DHA, dihydroartemisinin; AS, artesunate; ATM, artemether; SDX, sulfadoxine; PYR, pyrimethamine; ATQ, atovaquone; PG, proguanil; DOX, doxycycline; CLI, clindamycin; C_{max}, peak serum concentration; T_{max}, time of maximum concentration observed; $T_{1/2}$, half-life; VD/F, volume of distribution; CL/F, clearance; AUC, area under the curve of plasma drug concentration vs. time; G6PD, glucose-6-phosphate dehydrogenase. Adapted from WHO Guidelines for the Treatment of Malaria (2015)[96] and Kasper *et al*. (2015).[14]

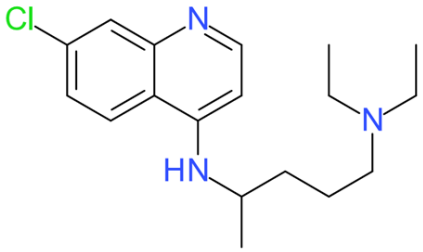

Chloroquine

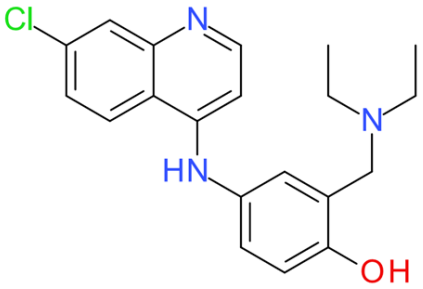

Amodiaquine

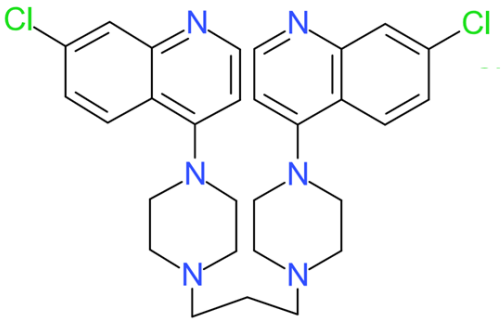

Piperaquine

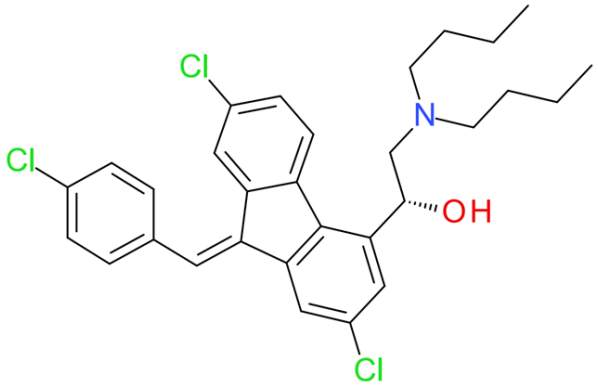

Lumefantrine

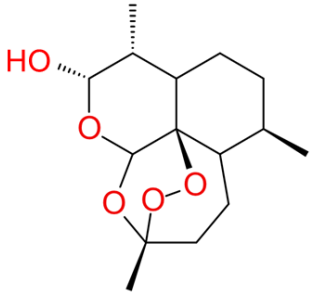

Dihydroartemisinin

Figure 1.11. Chemical structures of representative antimalarial compounds. Shown are chemical structures of the clinically employed antimalarial compounds chloroquine, amodiaquine, piperaquine, lumefantrine, and dihydroartemisinin.

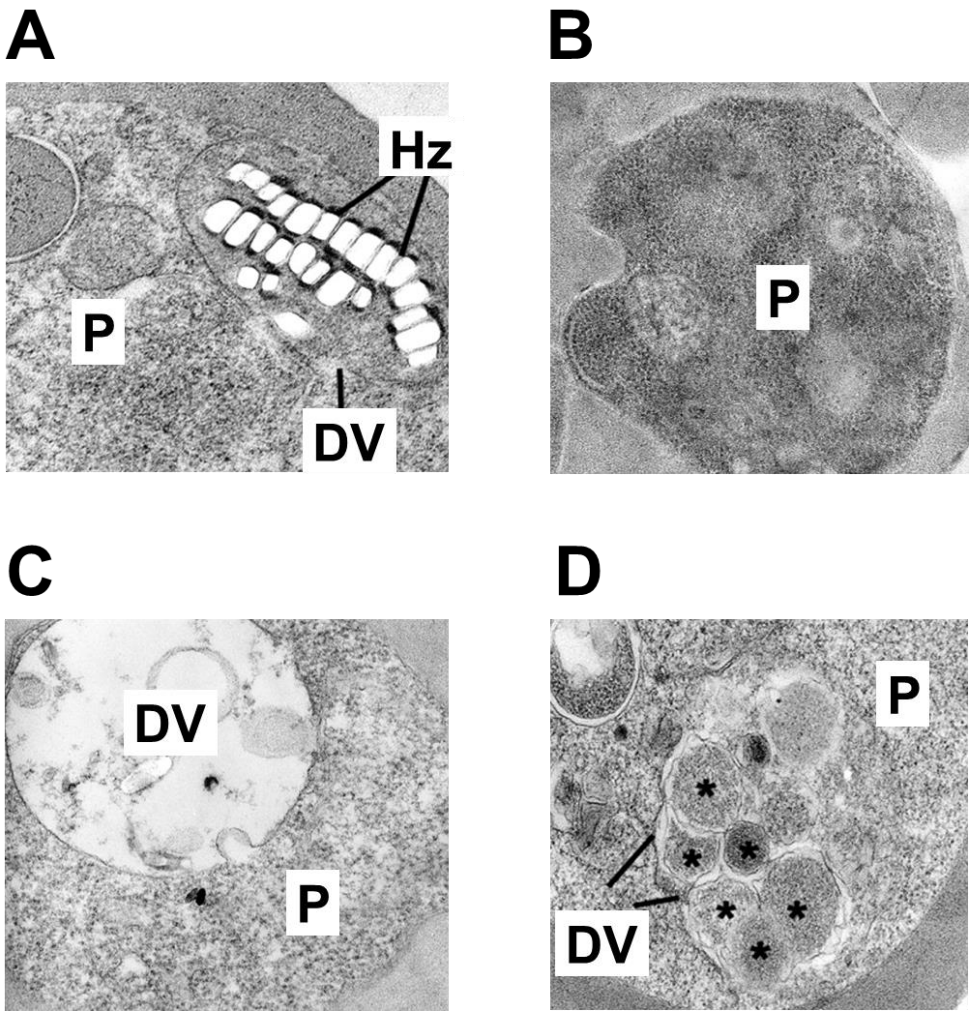

Figure 1.12. Ultrastructural changes of trophozoite blood-stage *P. falciparum* parasites treated with antimalarial drugs. Shown are TEM images of *P. falciparum* blood-stage parasites treated with (**A**) no drug, (**B**) artesunate, (**C**) quinine, or (**D**) piperaquine. (**A**) A normal parasite (P), exhibiting an electron-dense digestive vacuole (DV), where the byproducts of hemoglobin digestion are incorporated into hemozoin (Hz) crystals. (**B**) A parasite treated for 4 h with artesunate, showing amorphous parasite contents with an indistinguishable DV. (**C**) A parasite treated for 8 h with quinine, showing an electron-lucent DV containing very few Hz crystals. (**D**) A parasite treated for 8 hr with piperaquine, showing interrupted DV formation and aggregation of vesicles containing undigested hemoglobin. Adapted with permission from Sachanonta *et al.* (2011).[99]

This clinically important subset of drugs will be emphasized in this dissertation. In addition to ACTs, these drugs include CQ, a relatively safe and inexpensive quinoline-type compound used in the prevention and treatment of infection by CQ-sensitive *Plasmodium* species. The following sub-sections highlight key features of antimalarial drugs, including chemical and pharmacological properties, clinical indications, and insights into mode of action. Specific resistance mechanisms are further discussed in the subsequent section, **Antimalarial drug resistance.**

Quinolines

Following the historic adoption of CQ as a component of malaria control, a number of chemically related compounds surfaced and ultimately strengthened our armamentarium of antimalarial therapies. A common structural feature of these compounds is a quinoline (or quinoline-like) scaffold, which is known to be growth-inhibitory to a variety of pathogens.[101] The consensus regarding the modes of action of different quinoline-type antimalarials is that they interfere with the parasite's heme detoxification system in the DV. Previous studies of quinoline drug–Hz interactions have uncovered key differences that depend on the specific drug and experimental conditions used.[58,102] Ensuring that these interactions are reflective of what occurs *in situ* is, consequently, both a challenge and an impetus for further investigations.

As a whole, the quinoline-type antimalarials have played a laudable role in the treatment and control of malarial disease and continue to retain clinical efficacy, primarily as components of the first-line ACTs. In part due to their ability to target an immutable factor (i.e. heme), the quinolines represent a biologically and chemically

appealing group of compounds. Further dissection of their pharmacological features, cellular action, and molecular basis of resistance is applicable to the design of new quinoline-type compounds exhibiting little to no cross-resistance to our current set of drugs (see "Quinoline-type compounds in development" section).

Chloroquine

Originally named resochin after it was discovered in 1934 by the German scientist Hans Andersag, chloroquine (CQ) resurfaced in 1946 in the United States, where it was rigorously tested and deemed safe and highly effective for clinical use.[95] Chemically, CQ is an alkylated 4-aminoquinoline compound (see **Figure 1.11**). CQ and its hydroxyl analog, hydroxy-CQ (h-CQ), are amphiphilic weak bases that diffuse across cell membranes.[103] CQ possesses two basic groups, a nitrogen within the quinoline ring and a second diethyl-amino nitrogen, with pKa values of 8.1 and 10.2, respectively.[103]

CQ is indicated for prophylaxis against non-falciparum *Plasmodium* species, as well as *P. falciparum* in select, CQ-sensitive regions. The prophylactic weekly doses for children and adults, respectively, are 5 mg/kg (up to 300 mg) and 300 mg. CQ is used to treat *P. falciparum* in areas without CQR, namely parts of Central America, Haiti, the Dominican Republican, and a part of the Middle East.[95] The total standard treatment dose is 25 mg/kg CQ base. Of note, CQ has no activity against liver-stage parasites and is paired with PMQ as a first-line radical therapy against *P. vivax*.[15]

The pharmacokinetics and pharmacodynamics associated with CQ are complex. Following ingestion, CQ is almost fully absorbed in the gastrointestinal tract and undergoes a multiexponential decrease in blood concentration as it gets

distributed throughout multiple body compartments, including melanin-expressing tissues.[96] More than half of drug present in the blood is bound to plasma proteins. Metabolism of CQ occurs in the liver, via CYP2C8, CYP3A4, and CYP2D6 enzymes,[104] which metabolize it to its primary and clinically relevant metabolite, monodesethyl-CQ (md-CQ) as well as a second, minor metabolite, bisdesethyl-CQ (bd-CQ).[105] Blood concentrations of md-CQ may be up to half of the CQ concentration.[106] Importantly, the extent of CQ distribution, not the rate of elimination, governs blood CQ levels (peak: 3-5 hours), which show wide interindividual variability.[96] In a group of Tanzanian individuals who received a standard oral dose of 25 mg/kg CQ base, the range of peak serum concentrations (C_{max}) was 0.8-2.7 μM,[106] with another study reporting >10-fold interindividual differences in CQ and md-CQ levels.[107] As CQ gets released from various tissue stores and eliminated, primarily through the kidney, its elimination half-life ($T_{1/2}$) increases from days to weeks. The terminal $T_{1/2}$ is 1-2 months.

In general, the safety profile of CQ is very favorable. Infrequent side effects include pruritis, headache, hepatitis, and gastrointestinal disturbances. When used chronically, side effects may include retinopathy, myopathy, reduced hearing, photosensitivity, and hair loss. Cardiac side effects, associated with electrocardiographic abnormalities, are rare and primarily an issue in the case of overdose or co-administration with other antiarrhythmic agents. CQ is contraindicated for patients with known hypersensitivity.[96,98]

CQ interferes with the essential process of Hb and heme disposition in asexual blood-stage parasites.[55] After diffusing through multiple cell membranes, CQ reaches the acidic DV, where it gets diprotonated and trapped.[108] The interaction between CQ

and Fe(III)PIX was first observed in aqueous solution,[109] and has since been investigated with various modalities, including resonance Raman spectroscopy of CQ-treated *P. falciparum* trophozoites, which revealed a reduced intensity of bands corresponding to Fe(III)PIX aggregates and no signal for CQ.[110] This was interpreted as π-π binding of CQ to the intersection of dimeric Fe(III)PIX units[110] and is consistent with nuclear magnetic resonance-based studies of Fe(III)PIX monomer-dimer equilibria, which documented a CQ-biased shift favoring the Fe(III)PIX dimer (**Figure 1.13*A***).[111] Suggesting that CQ can also bind to Hz, [^{3}H]-CQ was previously observed to associate with Hz by electron microscope autoradiography.[112] CQ and/or CQ-Fe(III)PIX may directly interfere with the growth of Hz at its crystal face.[58] CQ-induced inhibition of Hz formation was recently associated with cellular redistribution of iron (Fe) content within trophozoite-stage *P. falciparum* (**Figure 1.13*B***).[55]

How exactly CQ kills parasites has not been resolved and likely involves mechanisms beyond the inhibition of Hz formation. This is underscored by the fact that, although CQ and heme interact, the Hz inhibition potency of CQ correlates well with its cytocidal, but not cytostatic, potency against *Plasmodium* parasites.[113] Cytotoxicity may be attributed to a constellation of factors, including an increase in toxic free heme, induction of oxidative damage, formation of toxic heme-CQ complexes, and/or inhibition of one or more uncharacterized physiological processes.[114]

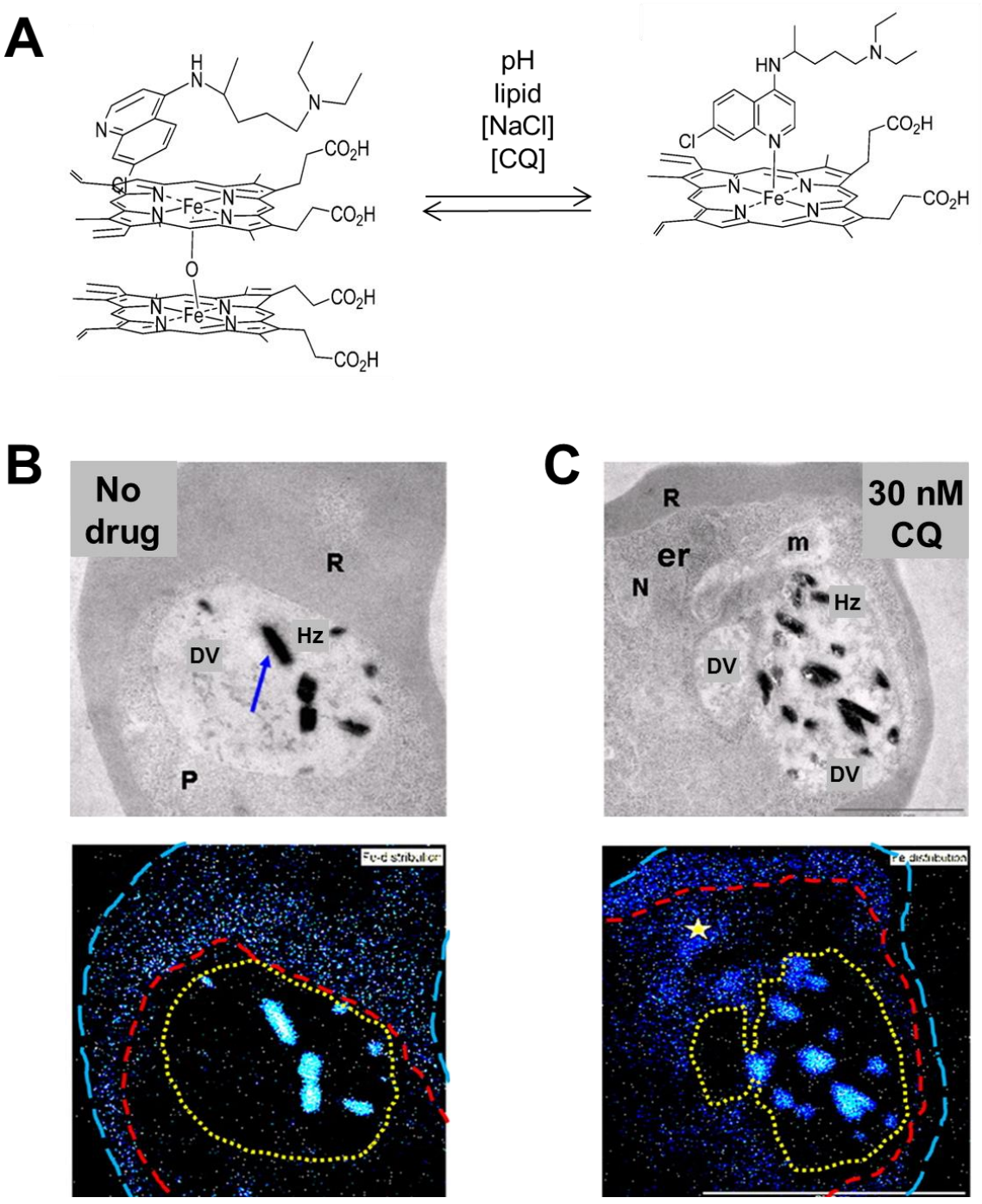

Figure 1.13. (*continued on next page*)

Figure 1.13. Heme-chloroquine (CQ) interactions and effects of CQ on distribution of iron during blood-stage *P. falciparum* infection. (**A**) Schematic of interactions of CQ with monomeric and dimeric forms of heme (Fe[III]PIX). CQ exhibits a preference for the μ-oxo Fe(III)PIX dimer, although changes in composition of the liquid phase can alter this equilibrium. Adapted with permission from Gorka *et* al. (2013).[58] (**B and C**) Iron (Fe) distribution in asexual blood-stage *P. falciparum* trophozoites treated with (**B**) no drug or (**C**) 30 nM CQ. Shown are TEM (top image) and electron spectroscopic imaging (ELI; bottom image) images. Fe distribution (blue dots) was determined by electron energy loss spectroscopy (EELS).[55] Parasite DV, parasite cytosol, and RBC cytosol compartments are represented by dotted/dashed yellow, red, and blue lines, respectively. (**B**) In untreated parasites, Fe is concentrated in hemozoin crystals (blue arrow) in the parasite DV and is also observed throughout the cytoplasm of host RBCs. (**C**) In CQ-treated parasites, iron is found in concentrated foci in the parasite cytosol (see yellow star for example). Fe is also detected in disrupted Hz crystals and the RBC cytosol. In parasites, Fe is present mostly as heme species and, in CQ-treated cells, largely corresponds to the free heme fraction. R, RBC; P, parasite; Hz, hemozoin; DV, digestive vacuole; N, nucleus; er, endoplasmic reticulum; m, mitochondria. Adapted with permission from Combrinck *et al*. (2013).[55]

CQR is common among *P. falciparum* strains throughout the world, with the key exceptions of the Caribbean, Central America, and the Middle East, where CQ use is still appropriate.[95] Interestingly, data from Guinea-Bissau indicates that clinical CQR can be overcome by doubling the standard CQ dose, suggesting that CQR is a saturable process.[115] Most geographical regions in which *P. vivax* is endemic, notably Asia and the Pacific, are now known to harbor CQ-resistant strains.[116] CQR in *P. vivax* is less understood than *P. falciparum* CQR and likely involves distinct mechanisms.[117] The mechanism of *P. falciparum* CQR is discussed in detail in the section "CQ resistance and PfCRT" below. *P. falciparum* CQR occurs at least in part due to the reduced access of CQ to its heme target within the DV.[118] CQ-sensitive *P. falciparum* parasites accumulate significantly more drug than CQ-resistant forms.[119] Mutations in the *P. falciparum chloroquine resistance transporter* (*pfcrt*) gene reduce CQ accumulation and are sufficient to confer parasite CQR.[120] The *P. falciparum multidrug resistance 1* (*pfmdr1*) gene plays a less pronounced, modulatory role in mediating CQR (see "The role of PfMDR1 in antimalarial drug resistance" below).

Quinine

The quinoline methanol (arylaminoalcohol) compound quinine (QN) is the oldest antimalarial drug still used today. QN is one of the active ingredients found in *quina*, the Incan expression for the bark of cinchona trees. Cinchona bark powder was used therapeutically in South America and, later, in Europe prior to the isolation of QN in 1817 by French chemists.[1,98] As the synthesis of QN is challenging, QN and its stereoisomer quinidine (QD) are routinely isolated from botanical sources.[98] Although its use has declined due to the wide deployment of ACTs, QN remains an important

drug for the treatment of CQ-resistant *Plasmodium* infections. Used intravenously, it is also a second-line option for the treatment of severe malaria.[13] Synergistic effects have been documented for QN paired with certain broad-spectrum antibiotics that, like QN, target *Plasmodium* asexual blood stages. These combinations include QN combined with either doxycycline (DOX) or clindamycin (CLI).[121] Of note, QN-CLI is recommended for the treatment of pregnant women with uncomplicated *P. falciparum* during the first trimester of pregnancy.[13]

Upon administration, QN is rapidly absorbed and extensively distributed to various body tissues. QN is metabolized in the liver by multiple enzymes, particularly CYP3A4. Its multiple metabolites include 3-hydroxyquinidine, which has the most antimalarial activity (~10% of QN). In patients not experiencing clinical recovery, the standard dose of QN must be lowered, in part due to the inhibitory effect of malarial disease on QN clearance and distribution to peripheral tissues. The therapeutic index of QN is narrow and may result in hypotension, hypoglycemia, and/or cinchonism, a syndrome characterized by auditory and visual disturbances, headache, gastrointestinal symptoms, and dysphoria. QN increases the cardiac QTc interval, although cardiac side effects are more frequently associated with QD. QN should be avoided in individuals with known hypersensitivity to QN or other alkaloids derived from cinchona plants.[13]

Similar to CQ, QN is thought to interfere with the detoxification of free heme in the parasite DV, consistent with the capacity of QN to inhibit Hz formation[55] and with spectroscopic reports that documented an interaction between QN and Fe(III)PIX.[122] A chemical dissection analysis of QN functional groups revealed that the quinuclidine ring and hydroxyl group of QN were indispensable for its activity and

interaction with Fe(III)PIX.[122] Interestingly, in contrast to CQ (see **Figure 1.13*A***), which shifts the Fe(III)PIX monomer-dimer equilibrium toward dimer formation, QN exhibits a preference for the monomeric form.[58] This observation highlights the existence of distinctions in the activities of different quinoline-type antimalarials.

QN resistance has been detected in multiple geographical regions, including Southeast Asia and the Amazon basin in South America.[123] Despite the shared features in the mechanisms of action of CQ and QN, QN resistance is relatively more complex, involving multiple genetic loci that have parasite strain-specific contributions to resistance. Among known determinants of parasite QN susceptibility are a number of transporters, including PfCRT, PfMDR1, the *P. falciparum* Multidrug Resistance Protein 1 (PfMRP1) transporter, and the *P. falciparum* Sodium-Proton Exchanger (PfNHE).[123,124] The effects of *pfcrt* mutations on QN resistance are allele-specific, parasite genetic background-dependent, and can yield divergent parasite responses to QN as compared to QD.[120,125,126] Amplification and/or mutation of *pfmdr1* has been shown to reduce QN susceptibility.[127,128] Additionally, a novel *P. falciparum* HECT ubiquitin-protein ligase was found to modulate parasite susceptibility to QN and QD in certain parasite genetic backgrounds.[129]

Amodiaquine

Amodiaquine (AQ) is a 4-aminoquinoline compound related to CQ (see **Figure 1.11**). It was developed by Parke-Davis and clinically employed as CQR began to take hold. In the 1960s and 1970, it was distributed in select regions as a medicated salt, supplementing mass drug distribution efforts that largely relied on CQ.[130] Presently, AQ is the partner drug comprising the first-line ACT regimen AS-AQ, which is

indicated for treatment of uncomplicated *Plasmodium* malaria. AQ is also administered in conjunction with SP to very young children in Africa for the purpose of seasonal malaria chemoprevention.[15]

Upon ingestion, AQ is very rapidly absorbed and metabolized by CYP2C8 into its more potent and long-lived metabolite, monodesethyl-AQ (md-AQ). The C_{max} achieved by md-AQ is ~20-fold greater than that of the parent compound. Moreover, the $T_{1/2}$ of md-AQ and AQ are, respectively, ~2 weeks and ~3 hrs. As compared to other ACT regimens, AS-AQ is associated with more frequent gastrointestinal disturbances. AQ is not recommended for prophylaxis, due to the risk of agranulocytosis, hepatitis, and myelotoxicity, which are attributable to the bioactivation of AQ to toxic quinone imine and aldehyde quinone imine metabolites.[131] Additional, rare side effects include cardiac conduction abnormalities, neurological effects, and hypersensitivity reactions. AQ should not be administered to individuals with hepatic impairments or known hypersensitivity.

AQ is thought to interfere with parasite heme detoxification during the asexual blood stage of infection, similar to CQ. This is supported by the observations that, like CQ, AQ forms a dimeric complex with Fe(III)PIX (see **Figure 1.13*A***).[132] In addition, AQ treatment of parasites inhibits the formation of non-toxic Hz with a concomitant increase in toxic free heme.[55] AQ is effective against some CQ-resistant strains, although cross-resistance with CQ does occur and renders it an ineffective therapy in certain geographical regions, including South America. Parasite resistance to AQ is mediated by *pfcrt* and *pfmdr1* alleles, which can interact to yield differential parasite responses to AQ and the related quinoline drug CQ.[133]

Piperaquine

Piperaquine (PPQ) is a bisquinoline compound, characterized by a pair of quinoline groups joined by an aliphatic linker (see **Figure 1.11**). PPQ was first synthesized in the 1960s and was clinically employed soon after throughout China and Indochina due to its potency against CQ-resistant parasites.[134] Currently, PPQ is used only in conjunction with DHA in the first-line ACT formulation DHA-PPQ, used to treat uncomplicated *Plasmodium* infections.

The lipophilic drug PPQ is rapidly absorbed and widely distributed throughout the body, with 99% of drug binding to plasma proteins. A feature of PPQ is its very long $T_{1/2}$ (~1 month). The formulation DHA-PPQ is generally well tolerated. Similar to CQ, PPQ can increase the QT interval on electrocardiography, although adverse cardiac events are improbable. PPQ should be avoided in patients with known hypersensitivity or with QT prolongation.[96,98]

PPQ resistance is actively spreading in Southeast Asia[135-138] and has also been detected in French Guiana, possibly due to inappropriate use by migrant miners.[137] The genetic basis of PPQ resistance is presently undefined and likely multigenic. Novel PfCRT mutations associated with Southeast Asian PPQ-resistant isolates have been reported,[139] but a causal relationship has not been established to date.

In Africa, in recent comparative studies of the efficacy of ACT regimens, DHA-PPQ was found to cure more patients than ATM-LUM and was associated with more long-lived protection from subsequent malarial infection.[140,141] In addition, in a controlled, randomized clinical trial assessing the efficacy of regimens for the prevention of malaria in pregnant African women, DHA-PPQ was found to confer superior protection as compared to SP.[97]

Mefloquine

Mefloquine (MFQ) is a quinoline methanol (arylaminoalcohol). It was discovered as a potent antimalarial as part of a screen of chemical compounds at the Walter Reed Army Institute of Research.[98] MFQ is presently employed for *P. falciparum* prophylaxis and is a partner drug comprising the first-line regimen AS-MFQ, used in MFQ-sensitive areas to treat uncomplicated malaria.

Upon ingestion, MFQ is rapidly absorbed, with significant interindividual variability in the time needed to reach C_{max} (~15-72 hrs). MFQ is metabolized in the liver by CYP3A4, to an inactive metabolite. MFQ is widely distributed to body tissues and permeates the blood-brain barrier, placenta, and mammary glands. ~98% of MFQ is plasma protein-bound. $T_{1/2}$ for MFQ is ~2 weeks. It is excreted primarily by the fecal route. Infrequent side effects associated with MFQ use include hepatitis, gastrointestinal disturbances, and neuropsychiatric abnormalities (e.g. seizures, hallucinations, depression). MFQ should not be administered to individuals with known hypersensitivity, who require fine motor coordination, who are mentally ill, or who have suffered from cerebral malaria.[96,98]

MFQ is a highly effective schizonticide. The mechanism of its action against blood-stage parasites is not entirely clear. MFQ interferes with Hz formation in the parasite DV[55] and is also thought to be active against an as yet unidentified target in the parasite cytosol.[142,143]. Mutations and copy number alterations of the *pfmdr1* locus are implicated in modulating parasite susceptibility to MFQ.[128,144] Amplification of *pfmdr1* is common in Southeast Asia, which harbors MFQ-resistant parasite populations.[145]

Lumefantrine

Lumefantrine (LUM), also known as benflumetol, was discovered as part of a clandestine antimalarial discovery project organized by the Chinese military.[146] Chemically, LUM is an arylaminoalcohol fluorine derivative (see **Figure 1.11**) and shares structural features with the related drugs halofantrine (HF), QN, and MFQ. Clinically, LUM is used solely in combination with an ART compound, namely ATM. ATM-LUM is indicated for the treatment of uncomplicated *Plasmodium* infections. LUM is very lipophilic and ingesting it with fat-rich food enhances its absorbance. LUM undergoes hepatic metabolism by CYP3A4 enzymes to its active metabolite, desbutyl-LUM. Plasma protein binding is 99.7%. Due to the lipophilicity of LUM, wide interindividual variability in LUM C_{max} has been observed (e.g. 4.5-28.3 µg/ml). Its $T_{1/2}$ is 3-5 days. Side effects associated with LUM are rare, although use should be avoided in the case of known hypersensitivity.[96,98]

LUM is thought to interfere with heme detoxification, similar to other quinoline-type compounds. Consistent with this, LUM was found to inhibit Hz formation in drug-treated *P. falciparum* trophozoites.[55] A role for LUM in inhibiting Hz polymerization is further corroborated by the finding that the related drug HF interacts with Fe(III)PIX monomers.[147] Roles for mutations in the parasite *pfcrt* and *pfmdr1* genes in modulating LUM susceptibility have been described (detailed in corresponding sections below). Of note, ATM-LUM is the most widely employed ACT regimen in Africa, and recent clinical studies suggest that LUM efficacy may be compromised.[148,149]

Primaquine

Primaquine (PMQ) is an 8-aminoquinoline compound that was first synthesized by Robert Elderfield of Columbia University.[150] It stands out among presently employed antimalarials due to its ability to target exoerythrocytic stages of *Plasmodium* infection. During the parasite blood stage, PMQ is only active against sexual gametocytes. With the exception of chemoprophylaxis, PMQ should always be used together with another antimalarial compound or regimen that targets the parasite asexual blood stages, such as an ACT or, when applicable, CQ. PMQ represents a powerful tool for control of malaria transmission. It has been recommended that a single, low dose of PMQ be administered to patients in low-transmission settings in order to prevent onward transmission. Furthermore, PMQ is indicated for the radical cure and terminal prophylaxis of infections caused by *P. vivax* and *P. ovale*, which are characterized by a dormant hypnozoite stage that can lead to relapse of malarial disease.[15,96,98]

PMQ is almost fully absorbed from the GI tract and extensively distributed throughout the body, akin to CQ. PMQ achieves peak levels in the blood in 1-4 hrs and is excreted primarily in the urine. Metabolism of PMQ in the liver yields the relatively inactive metabolite carboxy-PMQ as well as reactive metabolites that produce hemolytic anemia in predisposed individuals, including those with glucose-6-phosphate dehydrogenase (G6PD) deficiency. For this reason, screening individuals for G6PD deficiency is a necessity prior to administration of PMQ.

With the exception of hemolysis in predisposed patients, the side effect profile of PMQ is favorable. Patients may experience gastrointestinal discomfort, and cardiac abnormalities are very rare. PMQ should not be administered to patients with known

hypersensitivity or G6PD deficiency. Unless the G6PD status of the embryo is first determined, PMQ should not be used in pregnancy.

Pyronaridine

The Mannich base pyronaridine was developed in China in 1970, at around the same time that LUM was discovered. It was deployed in China for over three decades.[151] PND is a partner drug comprising the ACT formulation AS-PND. This regimen is one of several ACTs (including arterolane-PPQ, ART-PPQ, and ART-napthoquine) that are registered and clinically used but presently not formally endorsed by the WHO.[96] In Cambodia, where the need to adopt new first-line drug combinations is urgent, AS-PND efficacy was unfortunately found to fall below the WHO threshold for medications with long half-lives.[151]

PND is potent against *Plasmodium* asexual blood stages, including those of multidrug-resistant parasites. PND is widely distributed upon absorption and concentrates in erythrocytes. Its $T_{1/2}$ is ~10-13 days. PND is not associated with major side effects, and its toxicity profile is comparable or better than that of CQ, which is well-tolerated. In rodent models, embryotoxicity, but not teratogenicity, has been observed. This warrants clarifying whether PND use should be avoided in pregnancy. Croft *et al.* have recently provided a detailed review of the *in vitro* and *in vivo* pharmacology, toxicology, and clinical features of PND.[152]

The mechanisms of action of PND are thought to overlap with those of other quinoline-type compounds. PND has been reported to interact with hematin and also inhibits GSH-dependent heme degradation.[153,154] Resistance mechanisms for PND

have not yet been defined. The prolonged use of PND as a monotherapy in China suggests that resistance does not evolve easily.[151] A single report in which *ex vivo* PND responses of African parasite isolates were examined suggested that reduced PND susceptibility was associated with the presence of PfCRT mutation K76T.[155]

Artemisinins

ART and its derivatives, collectively called ARTs, are a group of sequiterpene lactone endoperoxide compounds. First extracted from the medicinal sweet wormwood plant *Artemisia annua* by the Chinese chemist Youyou Tu,[156] ART has reduced potency and bioavailability as compared to the several semi-synthetic derivatives that are clinically employed, which include the following: DHA (see **Figure 1.11**), the active *in vivo* metabolite and reduced derivative of ART; ATM, a lipophilic methyl ethyl; and AS, a water-soluble hemisuccinate derivative. ART compounds are active against *Plasmodium* asexual and sexual blood-stage parasites. These compounds are paired with significantly more long-lasting partner drugs in the WHO-sanctioned ACT regimens ATM-LUM, AS-AQ, AS-MFQ, DHA-PPQ, and AS-SP. ACTs are the first-line treatment against uncomplicated *P. falciparum* malaria and are also indicated for women with uncomplicated *P. falciparum* malaria during their second or third trimester of pregnancy. Of note, intravenous AS is the first-line treatment of severe malaria and has been shown to be superior to intravenous QN.[15,96-98]

Relative to other ART compounds, ATM is highly lipophilic, and its otherwise erratic absorption is improved with concurrent ingestion of fatty foods. In contrast, AS is water-soluble, which partly explains the preference for AS in intravenous ART therapy. Following oral administration, the ART derivatives show bioavailability of

≤30% and yield variable degrees of plasma protein binding. Metabolism of the ART parent compounds in the liver produces DHA, which accounts for the majority of antimalarial activity of orally (but not intravenously) administered ART compounds. DHA is extensively distributed, and its T_{max} and $T_{1/2}$ are of a comparable duration (~1-3 hrs). The ARTs are generally well tolerated and rare side effects include gastrointestinal disturbances, dizziness, hepatitis, reticulocytopenia, and neutropenia. ACTs should be avoided in patients with known severe hypersensitivity reactions as well as during the first trimester of pregnancy.

The mechanism of ART action is still elusive, although several important insights have recently emerged. The activity of ARTs depends on the reductive cleavage of the ART-defining endoperoxide bridge.[100] A contributory role for hemoglobinases in ART activation was recently demonstrated by Xie *et al.*, who observed that reduced expression of *P. falciparum* falcipains 2 and 3 conferred ART resistance to early ring-stage parasites.[157] Through various mechanisms, activated ARTs are thought to promote the generation of toxic species, including free heme, whose incorporation into nonreactive Hz is inhibited by ARTs.[54,55]

Alarming evidence that suggested declining clinical efficacy of ARTs in Southeast Asia motivated the identification of mutations in the parasite *kelch13* (*k13*) gene as critical drivers of resistance in this region.[158] A number of distinct K13 mutations have been associated with *in vivo* and *in vitro* indicators of resistance. These are, respectively, delayed parasite clearance from patient blood and enhanced parasite survival in ring-stage survival assays (RSAs) that measure parasite survival following a short-term pulse with 0.7 μM DHA.[158-162] Whole-genome analysis of Cambodian ART-resistant parasite founder populations has revealed an additional

level of genetic complexity, indicating that multiple secondary genetic mediators (including *pfcrt*) equip parasites with a genetic background conducive to the spread of resistance.[159] Of note, an ART-associated K13 mutation (C580Y) was recently identified in Guyana.[163] K13 mutations are also present in low frequencies in African parasites, prompting vigilance and preemptive efforts to characterize the capacity of these parasites to mediate ART resistance.[164]

Other antimalarials in clinical use

Sulfonamide-based antifolates

Sulfadoxine (SDX) is a sulfonamide compound with broad antimicrobial activity. It is often paired with pyrimethamine (PYR) in the synergistic combined therapy SDX-PYR (SP). SDX and PYR inhibit folate synthesis during the asexual blood stage of infection by acting against the dihydropteroate synthase (DHPS) and dihydrofolate reductase (DHFR) enzymes, respectively. Multiple mutations acquired in both of these enzymes confer resistance to these compounds and arise readily when either component is used in isolation. The SP formulation has played an important, albeit temporary, role in the treatment of CQ-resistant *P. falciparum* infections. *P. falciparum* resistance to this regimen quickly developed and spread worldwide (see "Antimalarial drug resistance: a recurrent problem" section below). In the case of PYR resistance, mutations are acquired in a predictable fashion. In Africa, the triple DHFR mutant (N51I C59R S108N), predominates, whereas in Southeast Asia, the quadruple mutant (N51I C59R S108N I164L) is common.[96,98,165]

SP is generally well tolerated, and rare adverse reactions are often due to the sulfonamide component. Rarely, patients may experience rash, Stevens-Johnson

syndrome, leukopenia, thrombocytopenia, and megaloblastic anemia. SP should not be taken by individuals with known hypersensitivity, megaloblastic anemia secondary to folate deficiency, or infants <2 months. Of note, SP increases gametocyte carriage rates.[96,98]

In Africa, SP has been employed for the prevention of malaria in pregnant women and, in conjunction with AQ, as a seasonal chemoprophylactic strategy in infants. The ACT regimen AS-SP is one of the ACT regimens sanctioned for clinical use by the WHO.[96]

Napthoquinone-antifolate combinations

Atovaquone (ATQ) is a ubiquinone-like hydroxynapthoquinone antimicrobial that is paired with proguanil (PG; also known as chloroguanide), a biguanide compound. The combination ATQ-PG is clinically employed for malaria prophylaxis and may also be used in conjunction with AS and PMQ to treat patients in regions where malaria is not endemic (e.g. treatment of travelers).[96]

Before PG is converted by liver CYP enzymes into its active metabolite, cycloguanil, it mediates synergy with ATQ by augmenting the capacity of ATQ to collapse the mitochondrial membrane potential. Specifically, ATQ targets the cytochrome bc_1 complex of the parasite's electron transport chain. This mitochondria-localized system is primarily responsible for regenerating ubiquinone, a cofactor for the essential pyrimidine biosynthesis enzyme dihydroorotate dehydrogenase (DHODH). This is supported by the fact that transgenic expression of a yeast, ubiquinone-independent form of DHODH confers *Plasmodium* ATQ resistance, even though mitochondrial electron transport is inhibited.[166] When metabolized, PG acts to

inhibit the DHFR enzyme that is also inhibited by PYR, although evidence for DHFR-independent mechanisms of toxicity have also been described. ATQ and PG are active against asexual blood-stage as well as liver-stage parasites. However, they do not target the dormant hypnozoite stages of *P. vivax* and *P. ovale*. When used singly, ATQ and PG very readily select for resistant *Plasmodium* parasites. High-level resistance to ATQ is mediated by mutations in the *cytochrome b* (*cytB*) gene. PG is generally not synergistic with ATQ in *cytB*-mutant parasites.[96,98,123,167]

Absorption of ATQ is highly variable, whereas absorption of PG proceeds more readily. Ingestion of ATQ-PG with a fatty meal improves the absorption of drug. Plasma protein binding of ATQ and PG are 99% and 75%, respectively. The $T_{1/2}$ of ATQ is 2-3 days. Metabolism of ATQ is minimal, and it is excreted primarily via the fecal route. ~50% of PG is excreted in the urine. ATQ-PG is generally well-tolerated, and hepatitis, rash, neutropenia, and anemia are among its rare side effects. ATQ-PG should not be given to individuals with known hypersensitivity.[98]

Tetracyclines, lincosamides, and macrolides

A number of broad-spectrum antibiotics have been clinically employed as antimalarial chemotherapies, including the tetracycline compound doxycycline (DOX), the lincosamide compound clindamycin (CLI), and the macrolide compound azithromycin. These compounds are generally paired with another potent antimalarial (e.g. AS or QN). DOX is also used for malaria prophylaxis. QN-CLI is indicated for the treatment of *P. falciparum*-infected women in their first trimester of pregnancy. These antibiotics inhibit prokaryotic protein synthesis, and their antimalarial activity is attributed to activity against the *Plasmodium* apicoplast. Parasite toxicity is manifest

as “delayed death”, whereby the progeny of drug-treated parasites die. Side effects include gastrointestinal disturbances, which may progress to include pseudomembranous colitis. Hypersensitivity reactions may occur, and use in persons with known hypersensitivity should be avoided. DOX should not be used in children <8 years or in pregnant women.[96,98,121,168]

Quinoline-type compounds in development

Despite the wide spread of resistance that cost it its gold-standard status, CQ is regarded as one of the safest, most efficacious antimalarial compounds in the history of malaria prophylaxis and treatment and continues to be used in resistance-free regions. The highly favorable pharmacological profile of CQ has revived interest in developing CQ-like compounds that, through the modification and/or addition of new chemical groups, confer efficacy against both CQ-sensitive and CQ-resistant parasites.

Given the established antimicrobial activity of the quinoline ring that is the hallmark of CQ and related quinoline-containing compounds, a popular strategy employed for the design of new antimalarials has been the conjugation of the quinoline scaffold to a chemically unrelated group. Among the quinoline-conjugated compounds explored to date are quinoline-ART hybrids, quinoline-peroxide hybrids, quinoline hybrids with resistance chemosensitizers, and quinolines conjugated to novel chemical groups with demonstrated antimicrobial activity.[169] Of note, quinoline-based resistance chemosensitizers have previously been shown to interact with Fe(III)PIX and to inhibit parasite formation of Hz. These include the dibemequines, which are known to inhibit PfCRT-mediated CQ transport and which show potency against CQ-

resistant parasites.[170]

Myriad efforts[169-173] have already produced a large collection of compounds that exhibit antiplasmodial activity *in vitro* and *in vivo* and that could be employed in the future to treat drug-resistant strains. The critical role of chemotherapy in the control and treatment of malaria calls for precise characterization of the pharmacology and resistance mechanisms of novel compounds that will inevitably replace ones with waning efficacy.

ANTIMALARIAL DRUG RESISTANCE

Antimalarial drug resistance: a recurrent problem

In the context of *Plasmodium* infection, resistance is the ability of parasites to continue growing in the presence of an appropriately administered drug. Early manifestations of resistance include slowed clearance of parasites from the bloodstream, parasite recrudescence, and increased gametocytemia.[96] In this dissertation, resistance refers to decreased parasite susceptibility to a particular drug, as compared with a fully sensitive parasite line. When applicable, the degree of resistance (e.g. low-level, moderate, high-level, clinical) is emphasized.

A number of distinct factors can promote parasite evolution of drug resistance by yielding sub-therapeutic levels of drug. Among them are drug-drug interactions and interindividual pharmacokinetic and/or pharmacodynamic differences, including reduced rates of absorption, drug metabolism, and/or blood levels of drug. Other contributors include mass drug administrations, counterfeit medications, inappropriate dosing by prescribers, and patient non-compliance.[24,96,174,175] It is noteworthy that a wide range of drug concentrations (~10-1000 nM) for CQ and its

metabolite md-CQ were previously detected in the blood of asymptomatic African patients.[106] The propensity of parasites to develop resistance can also be influenced by non-pharmacological factors, including clonality of infections, parasite biomass, and the parasite's environment within the host (e.g. host genetic predisposition to infection, immunity, nutritional status).[24,176]

Considered to be one of the most powerful drugs used against a major global pathogen, CQ played a seminal role in decreasing malaria morbidity and mortality following its deployment in the mid-20th century.[177] However, the highpoint of CQ efficacy was short-lived. *P. falciparum* CQR was first detected in the late 1950s in South America and Southeast Asia. In the following years, CQR spread throughout these regions and into the Indian subcontinent. CQR was not reported in Africa until the late 1970s, where it spread from east to west. By 1989, CQR had been detected in almost all regions where *P. falciparum* was endemic.[174,177] In the subsequent five years, childhood mortality in sub-Saharan Africa rose markedly, representing a reversal of the downward trend in mortality during the period 1960-1989, when CQ efficacy was still largely retained.[178] Indeed, CQR is thought to be the most important factor that contributed to this setback.[178] The origins and spread of CQR are depicted in **Figure 1.14**.

In response to reports of CQ treatment failure, the affordable and well-tolerated drug regimen SP was briefly employed as a new first-line antimalarial, only to suffer a fate similar to that of CQ (see **Figure 1.14**). SP resistance soon spread to many CQR-endemic regions, and efforts to find replacement medications, including QN and MFQ, further contributed to the development of parasite multidrug

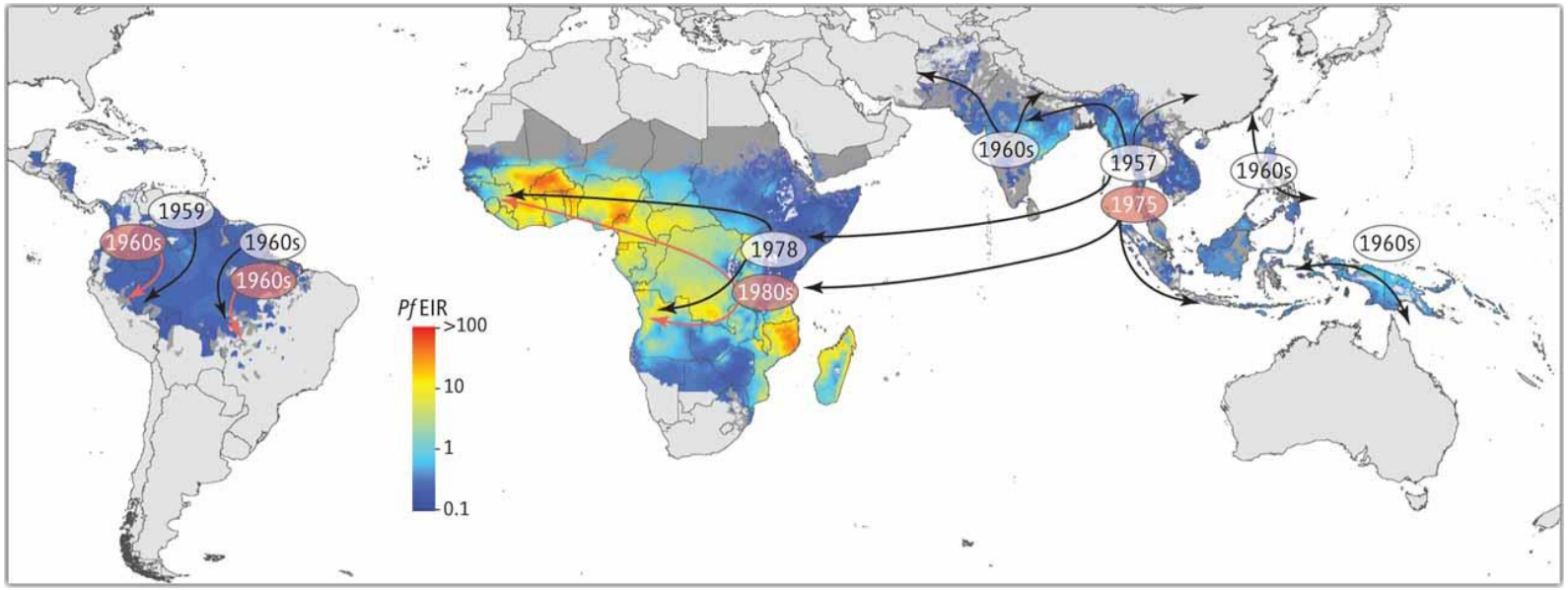

Figure 1.14. Emergence and spread of chloroquine and pyrimethamine resistance. Illustrated are the origins and migration of resistance to the former first-line antimalarials chloroquine (clear ovals and black arrows) and pyrimethamine (tan ovals and arrows). Map colors indicate 2010 *P. falciparum* entomological inoculation rates (*Pf* EIR), which reflect the parasite burden in a particular geographical region. Adapted from Fidock (2013).[179]

resistance, particularly in the low-transmission setting of Southeast Asia, which is now recognized as an epicenter of multidrug-resistant parasites.[180] This is consistent with the low levels of host immunity and preponderance of monoclonal infections that are known to occur in low-transmission areas, an optimal environment for the growth and transmission of drug-resistant parasite strains.

Of note, ART resistance is now present in Southeast Asia and was also recently detected in South America.[163,181] More recently, it has become evident that Southeast Asia harbors parasites resistant to both the short-lived ART and long-lived partner drug components of first-line ACTs. A notable example is DHA-PPQ, which is failing as a therapy in Cambodia.[135] Thus, throughout the globe, *P. falciparum* parasites presently exist that, together, show resistance to each component of the four WHO-recommended regimens AS-AQ, AS-MFQ, DHA-PPQ, and AS-SP.

As for the LUM component of the widely used formulation ATM-LUM, whether overt clinical resistance exists in the field has been debated. Assessing adequate clinical and parasitological responses (ACPRs) in patients from Zaire 28 days following treatment with ATM-LUM or DHA-PPQ, Plucinski *et al.* observed ACPRs of 88% (296/320 patients) and 100%, respectively.[148] This prompted the suggestion that LUM resistance is evolving in this region, which Hamed and Kuhen subsequently challenged, citing the presence of confounding factors (e.g. subtherapeutic dosing, differences in parasite burden).[182] Additional studies focusing on ATM-LUM treatment cases have reported increased rates of parasite recrudescence and decreased *in vitro* LUM susceptibility of parasite isolates derived from recurrent infections.[149,183] In light of these findings, concern regarding the therapeutic efficacy of ATM-LUM, the most commonly used ACT regimen in Africa, is justified.

History shows us that the emergence and spread of antimalarial drug resistance is a recurring problem. As antimalarials are central to the control and treatment of malarial disease, dedicated research should be invested into understanding the ways in which parasites develop resistance, defining the molecular mechanisms of resistance, and formulating appropriate drug regimens with the potential to slow parasite resistance evolution.

CQ resistance and PfCRT

Identification of *pfcrt* as the primary genetic mediator of CQR was a major milestone in the ongoing quest to understand the molecular bases of *P. falciparum* drug resistance. CQR was initially mapped to a segment of the parasite's seventh chromosome through analysis of parasite clones derived from a genetic cross between CQ-sensitive (HB3; Central America) and CQ-resistant (Dd2; Southeast Asia) parasites.[184,185] In a seminal study that pinpointed *pfcrt* as the gene responsible for the CQR phenotype, transgenic expression of *pfcrt* alleles conferred CQR to otherwise CQ-sensitive parasites.[186] The authors observed PfCRT to localize to the parasite DV, where CQ exerts its action, and proposed that CQR occurs via (1) mutant PfCRT-mediated CQ efflux outside of the DV and/or (2) reduced CQ binding to its heme target, through mutant PfCRT-mediated effects on DV physiology.[186]

CQ-resistant parasites are known to accumulate less CQ in their DV than CQ-sensitive parasites.[112,119,187] Accordingly, a long-standing model for CQR has been that CQ-resistant parasites are equipped to reduce CQ access to its heme target in the DV. This model is in line with multiple lines of evidence showing that CQ and heme interact and stall the polymerization of Hz crystals.[55,58,66,188] A direct role for mutant

PfCRT in mediating reduced DV accumulation of CQ was demonstrated using [^{3}H]-CQ accumulation assays performed with *pfcrt*-modified parasite lines bearing an otherwise isogenic background.[120] Of note, subsequent studies revealed that reduced CQ accumulation can only partly account for the mechanism of PfCRT-mediated CQR. In a striking finding, parasites encoding mutant (Dd2) *pfcrt* were fully protected from CQ cytotoxicity, whereas wild-type (HB3) *pfcrt*-expressing parasites showed 50% survival, even though both lines were treated with CQ doses (750 nM and 250 nM CQ, respectively) that yielded equivalent levels of intravacuolar CQ accumulation.[189,190] Mutant PfCRT–CQ interactions are now appreciated to play a predominant role in mediating parasite cytostatic CQR and contribute to the relatively more multigenic basis of cytocidal CQR.[191,192] Elucidation of these complex aspects of parasite CQR is an area of active pursuit.

Using purified plasma membranes isolated from *Pichia pastoris* strains that heterologously expressed PfCRT variants, Zhang *et al.* previously observed the ability of CQ to bind both wild-type (HB3) and mutant (Dd2) PfCRT isoforms (with K_d values of 435 and 385 nM, respectively).[193] In a subsequent study that used reconstituted proteoliposomes harboring wild-type (HB3) or mutant (Dd2 and 7G8) PfCRT isoforms, an interaction was documented between a DV-disposed region of PfCRT helices 9-10 and a perfluorophenylazido biotinylated CQ (AzBCQ) probe.[194] Interestingly, the extent to which pH influenced this interaction was PfCRT isoform-specific. The authors posited that the AzBCQ attachment site positioned the CQ quinoline ring in close proximity to the many transmembrane domain-localized and DV-disposed PfCRT polymorphic residues that are known to be involved in CQR.[194] These findings evoke the possibility that, in addition to interfering with parasite heme detoxification

pathways, CQ may interfere with the as yet unclear native function of PfCRT (see "Insights into PfCRT biological function" section below).

Studies using parasites encoding wild-type and mutant PfCRT isoforms have previously demonstrated that PfCRT mutations can alter the physiology of the parasite DV, eliciting alterations in the pH (pH_{DV}) and volume of the DV.[195-197] A ~0.4-unit reduction in pH_{DV} was ascribed to mutant *pfcrt* alleles by Bennett *et al.*[197] Of note, the equilibria of quinoline drug–heme interactions are highly pH-dependent,[58] suggesting a role for PfCRT mutations in modulating parasite susceptibility to CQ and quinoline compounds beyond their contributions to drug efflux.

Allelic exchange experiments previously showed that, in the context of additional mutations comprising a CQ-resistant isoform of PfCRT, the mutation K76T is indispensable for parasite CQR and the ability of mutant PfCRT to remove CQ from its Fe(III)PIX target in the DV.[126] Clinically, K76T has historically served as a sensitive, although not specific, marker of CQ treatment failure.[198,199] In *Xenopus laevis* oocytes, removal of K76T abrogated mutant PfCRT-mediated CQ transport. By itself, K76T was insufficient to confer CQ transport.[200] As *P. falciparum* PfCRT-mediated CQR is governed by factors beyond drug transport, the sufficiency of K76T for parasite CQR has been unclear. This question was explored in **Chapter 2** of this dissertation. A potential role for K76T in proton transport was suggested in studies heterologously expressing wild-type or mutant (Dd2) PfCRT isoforms in the lysosomal membranes of HEK293 human embryonic kidney cells, both of which induced acidification. Of note, acidification was higher for cells expressing Dd2 PfCRT, and K76T was both necessary and sufficient to confer this phenotype.[201]

How exactly PfCRT mediates CQ transport has been a matter of debate, with

differing hypotheses evoked by distinct experimental systems. A number of groups have advocated for the description of PfCRT as a carrier/pump,[202-204] whereas others have proposed that it functions as a voltage-gated channel.[205,206] An important aspect of parasite DV physiology is maintenance of an electrochemical gradient, which is comprised of the pH and membrane potential differences (ΔpH and Δψ, respectively) across the DV membrane. This gradient is maintained, in part, through the action of a DV H^+-ATPase and a DV H^+-pyrophosphatase.[207] The notion that PfCRT mediates electrochemical gradient-driven transport is supported by several independent heterologous expression studies.[200,201,208-210] Interestingly, as compared to isogenic parasites expressing wild-type (CQ-sensitive) *pfcrt*, mutant (CQ-resistant) *pfcrt*-expressing parasites were previously found to enhance alkalinization of the DV upon treatment with the V-type H^+-ATPase-inhibiting agent concanamycin A, raising the prospect that mutant PfCRT facilitates H^+-coupled drug transport.[211]

A schematic highlighting proposed mechanisms of CQ action and the involvement of mutant PfCRT in mediating CQR is shown in **Figure 1.15**. Of note, the chemical and mode-of-action features of CQ are shared with many first-line antimalarials, and a pleiotropic role for PfCRT mutations in mediating resistance to these agents is becoming increasingly appreciated (see "The pleiotropic role of PfCRT in mediating antimalarial drug resistance" section below). This knowledge calls for continued refinement of our understanding of mechanisms contributing to PfCRT-mediated drug resistance, collectively encompassing drug transport and binding, impacts on Hz polymerization, modulation of parasite physiology, and other as yet unidentified mechanisms.

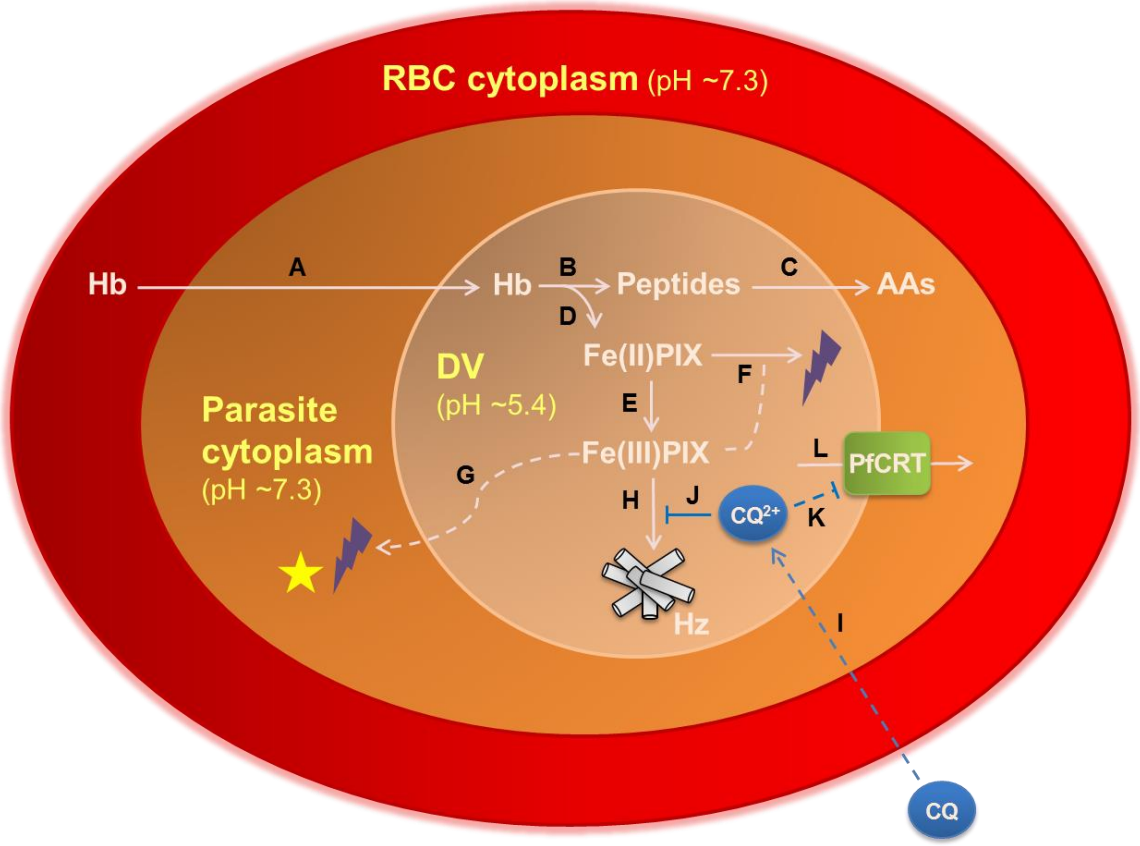

Figure 1.15. Schematic of *P. falciparum* digestive vacuole (DV) physiology, hemoglobin (Hb) processing, and possible modes of chloroquine (CQ) action. (**A**) Parasites import host Hb into the DV, where (**B**) resident proteases digest it into peptides that serve as a source of (**C**) amino acids (AAs) for the generation of new proteins. (**D**) Hb degradation also unleashes heme prosthetic groups in the form of ferrous (Fe^{2+}) protoporphyrin IX (Fe[II]PIX). (**E**) In the DV environment, Fe(II)PIX is rapidly oxidized to ferric (Fe^{3+}) protoporphyrin IX (Fe[III]PIX). (**F**) Through direct and indirect mechanisms, DV-localized Fe(II)PIX and Fe(III)PIX are able to promote oxidative damage (represented by purple lightening bolt). (**G**) Fe(III)PIX may also promote oxidative damage in the parasite cytosol. This is countered by the parasite's redox system (represented by yellow star), in part via glutathione-dependent degradation of free heme. (**H**) Parasites avert heme-mediated toxicity in the DV by transforming it into inert, insoluble hemozoin (Hz) crystals. (**I**) The weak base CQ diffuses into the acidic DV, where it becomes diprotonated (CQ^{2+}) and trapped. (**J**) CQ^{2+} interferes with Hz polymerization and (**K**) may also inhibit PfCRT function. (**L**) Mutant forms of PfCRT mediate CQ resistance, in part by effluxing CQ from the DV.

The pleiotropic role of PfCRT in mediating antimalarial drug resistance

Several antimalarial agents are structurally similar to CQ and are thought to likewise interfere with heme detoxification (see **Antimalarial compounds** section above). Among them are the first-line ACT partner drugs, whose long half-lives effectively render them monotherapies following the rapid clearance of the ART component.[212] Field and *in vitro* studies implicate PfCRT as a modulator of parasite susceptibility to these drugs.[114] For example, a Tanzanian study investigating molecular markers associated with tolerance to the widely used ACT formulation ATM-LUM revealed that mutant PfCRT K76T enhances parasite LUM susceptibility, a finding that was verified in experiments using genetically-modified, isogenic parasites.[213] In contrast, mutant, CQR-conferring PfCRT haplotypes cause reduced susceptibility to AQ, used in the ACT regimen AS-AQ.[214] Although the relationship between parasite susceptibility to PPQ, the partner drug comprising DHA-PPQ, and parasite *pfcrt* genotype is less clear, partial cross-resistance between PPQ and CQ has previously been observed *in vitro*.[215,216] Valderramos *et al.* previously reported that certain mutant *pfcrt* alleles could confer increased PPQ susceptibility in a specific genetic background (D10).[217] In a separate study, one of the genetic changes acquired by CQ-resistant (Dd2) parasites exposed to PPQ pressure was the mutation PfCRT C101F.[218] Interestingly, this mutation was also acquired by an amantadine-pressured CQ-resistant line (FCB), conferring a 2-fold decrease in parasite susceptibility to PPQ.[196]

Additional lines of evidence highlight the ability of *pfcrt* mutations to modulate parasite susceptibility to chemically diverse antimalarial compounds. In experiments performed with genetically modified parasites, Sidhu *et al.* observed *pfcrt*-mediated alterations in parasite susceptibility to QN, MFQ, and ART.[120] Evidence for ongoing

parasite *pfcrt* evolution and acquisition of novel drug resistance phenotypes was recently reported by Pelleau *et al.*, who described the evolution in French Guiana of the novel mutation C350R in the background of the CQ-resistant 7G8 PfCRT haplotype. This mutational event fully abolished CQR and, interestingly, conferred increased PPQ resistance.[137] In a separate study, pressure of CQ-resistant (Dd2) parasites with the thiazepine amide compound IDI-3783 yielded IDI-3783-resistant parasites that acquired the PfCRT mutation Q352R.[219] This mutation was associated with restored CQ sensitivity, highlighting the combination of CQ and IDI-3783 as a parasite "evolutionary trap", a scenario with clear applications for the design of future drug regimens.[219] The recently noted ability of PfCRT to interact with and transport tricyclic compounds in a heterologous expression system further suggests the notion that PfCRT is a pleiotropic multidrug resistance transporter.[220] These observations collectively advocate for the active monitoring of parasite *pfcrt* genotypes, for at least two purposes: to detect existing drug resistance and to guide selection of drug regimens that can preemptively inhibit evolution of additional resistance pathways.

The role of PfMDR1 in antimalarial drug resistance

After *pfcrt*, the most important secondary genetic determinant of parasite susceptibility to CQ and quinoline-type drugs is *pfmdr1*. The parasite *pfmdr1* gene encodes a 162-kDa DV-resident, 12-transmembrane domain protein that shows homology to P-glycoproteins, which mediate multidrug resistance in cancer cells.[221] The native function of PfMDR1 is unclear, although it has been postulated to be involved in the transport of solutes across the DV membrane.[142] Various PfMDR1 mutations, as well as changes in *pfmdr1* copy number, have been associated with

differential parasite responses to a wide array of clinically employed antimalarials. Increased *pfmdr1* copy number is associated with reduced parasite susceptibility to MFQ, QN, LUM, and AS and heightened susceptibility to PPQ.[145,222,223]

The five most common PfMDR1 mutations are N86Y, Y184F, S1034C, N1042D and D1246Y. Studies performed by Veiga *et al.*, in which the *pfmdr1* locus of *P. falciparum* parasites was genetically modified, recently revealed that PfMDR1 N86Y increases parasite resistance to CQ and AQ and increases susceptibility to LUM, MFQ, and DHA.[143] These results are consistent with clinical data that show that AQ-based regimens select for PfMDR1 N86Y, whereas LUM-based regimens select for N86. AQ-based and LUM-based regimens also select for PfMDR1 D1246Y and D1246, respectively.[123] As also seen for *pfcrt* alleles, this highlights that opposite selective forces may operate on the *pfmdr1* locus, providing a rationale for cycling first-line ACT regimens.

Of note, a linkage disequilibrium exists between *pfcrt* and *pfmdr1*,[224,225] and these loci can interact to produce differential parasite drug responses that are genetic background-specific. As an example, analysis of the progeny of a genetic cross between parasites from geographically distinct regions previously highlighted that certain South American *pfcrt* and *pfmdr1* alleles can interact to confer higher levels of AQ resistance as compared to CQR. In contrast, a Southeast Asian *pfcrt* allele yielded greater CQR in the context of different *pfmdr1* alleles.[133] In a recent study in Ghana, significant associations were observed between PfCRT K76T and polymorphisms at PfMDR1 residues 86, 184, and 1034, evoking the suggestion that a synergism between *pfcrt* and *pfmdr1* could explain the unusually slow attrition of mutant *pfcrt*-expressing parasites in Ghana, as compared to other regions in Africa.[226] The ways in which *pfcrt*

and *pfmdr1* interact to confer drug resistance is an area of active investigation. Beyond their role in transport of drugs, *pfmdr1* mutations may have direct impacts on parasite physiology that, in turn, affect *pfcrt*-mediated resistance and/or that offset physiological constraints associated with *pfcrt* mutations.[114]

PfCRT

Insights into PfCRT biological function

The parasite *pfcrt* gene is comprised of 13 exons, which encode a 424-amino acid transmembrane protein that is localized to the parasite DV.[186] The localization and trafficking of PfCRT during the course of the intraerythrocytic life cycle was previously elucidated using live cell imaging of *P. falciparum* parasites expressing inducible GFP-tagged PfCRT. PfCRT-GFP expression was first noted at the membrane of pre-DV compartments in mid-stage rings, which formed the Hz-containing DV in the trophozoite stage. In schizonts, punctate localization of PfCRT-GFP was also noted.[227] Mutational analysis of PfCRT trafficking by Kuhn *et al.* showed that a threonine residue at PfCRT position 416 is critical for sorting of PfCRT to the DV membrane. Additionally, mass spectroscopy revealed that this threonine, as well as a serine at position 411, are phosphoresidues, suggesting that PfCRT sorting and/or function can be modulated by phosphorylation.[228]

Correct processing of host Hb in the DV is required by the parasite, in part to avoid the rapid influx of fluid that would otherwise induce premature cell lysis.[40] Given this, it is conceivable that at least one function of PfCRT entails osmolyte regulation, perhaps through the partitioning of ions across the DV membrane. Consistent with the idea that PfCRT is involved in this vital parasite process is the

knowledge that (1) previous efforts to fully disrupt *pfcrt* did not succeed;[229] (2) mutation or reduced expression of *pfcrt* may promote DV swelling;[196,230] and (3) PfCRT isoforms have differential effects on the acidification of lysosomal or lysosome-like compartments, as discussed in the section above. Earlier studies have implicated roles for PfCRT in the transport of H^+, Cl^-, as well as organic cations (e.g. tetraethylammonium, TEA).[195,201,209,231] Whether these observations translate to the native environment of PfCRT is unclear and poses an experimental challenge.

Another possible function that has been proposed for PfCRT is the transport of amino acids and/or peptides, which are abundantly generated in the DV.[193,209,232-234] Several lines of evidence support this notion. First, mutant isoforms of PfCRT impart a characteristic Hb degradation defect, whereby Hb-derived peptides accumulate in the parasite DV.[232] In addition, drug transport studies performed in *Escherichia coli* or *X. laevis* oocytes have collectively observed that certain charged amino acids and/or peptides can antagonize PfCRT-mediated transport of TEA or CQ, respectively.[200,209] In an independent set of studies using *X. laevis* oocytes, Patzewitz *et al.* demonstrated that mutant PfCRT isoforms are capable of selectively transporting the tripeptide GSH.[234] In light of the suspected role of GSH in heme degradation and the ability of PfCRT isoforms to alter the access of CQ to heme,[56,126] one may postulate that PfCRT is involved in parasite GSH homeostasis. This prospect is in line with the known homology between PfCRT and plastid-localized CRT-like transporters (CLTs), which transport GSH and regulate cytosolic redox potential in *Arabidopsis thaliana*.[235]

Bioinformatic analyses of PfCRT have revealed that it belongs to a superfamily of proteins called the drug/metabolite transporters (DMTs).[233,236] Despite sharing key topological features, members of this superfamily transport a wide range of

substrates, including sugars, ions, weak bases, and organic cations. A number of DMTs, including PfCRT, are thought to have undergone a gene duplication event that resulted in the doubling of an ancestral 5-transmembrane domain protein to one with 10 transmembrane segments.[233,236] Consistent with this, PfCRT is thought to form dimers, and these have been found to occur in the laboratory setting.[194] Residues comprising the transmembrane domains of DMTs are important for substrate specificity and translocation, and submolecular regions spanning a single transmembrane domain can be sufficient to confer substrate specificity.[237]

In the context of drug resistance, it is now appreciated that mutations in PfCRT can confer differential stereospecificities, more than one binding site, and the ability to transport structurally diverse chemical compounds.[125,220,238] Does this pleiotropic property of PfCRT extend to its native function as a putative polyspecific nutrient transporter? Can PfCRT mutations alter the permeability of the DV membrane and promote a leak of one or more endogenous metabolites? Apart from interfering with PfCRT native function, can PfCRT mutations impart novel substrate specificities to PfCRT? Using various experimental systems, pursuit of these outstanding questions will undoubtedly broaden our understanding of PfCRT and will provide novel insights into the druggable features of parasite physiology.

PfCRT polymorphisms

Sequencing of the complete *pfcrt* open reading frame of geographically distinct, CQ-resistant *P. falciparum* isolates has shed light on a general mutational requirement for CQR, namely a non-synonymous mutation at PfCRT residue 76 accompanied by at least three additional non-synonymous mutations. Virtually all CQ-resistant

clinical and laboratory isolates bear the PfCRT mutation K76T, with rare reports of alternative mutations affecting residue 76 (K76A, K76I, and K76N).[114] To date, over 50 distinct PfCRT haplotypes have been reported,[208] although parasite CQ susceptibility data is available for only a fraction of these haplotypes. The highly polymorphic nature of PfCRT haplotypes is highlighted in **Table 1.6** and **Figure 1.16**, which emphasize mutations that will be discussed in subsequent chapters of this dissertation.

PARASITE FITNESS

Parasite determinants of fitness

The fitness of pathogenic organisms refers to their ability to successfully complete their life cycle and generate new progeny. A number of biological factors directly or indirectly impact fitness. In the case of *Plasmodium* parasites, key factors include parasite replication, survival, transmission, vectorial selection, and host vulnerability (**Figure 1.17**). In the laboratory setting, parasite fitness is often quantified using competitive parasite growth assays or by studying a proxy, such as the activity of an essential parasite protein. These approaches are complemented by epidemiological, clinical, and laboratory-based investigations of transmission dynamics, parasite virulence, and determinants of host immunity.[239-241]

The relative fitness differences between *Plasmodium* strains can be gauged via parasite growth rates, as determined *in vitro* or *ex vivo*. These are assessed during the pathogenically relevant setting of asexual blood-stage infection, during which the parasite biomass may reach numbers as high as 10^{12} parasites per

Table 1.6. Representative PfCRT haplotypes.[a]

				Polymorphic PfCRT residue												
PfCRT haplotype	**CQ**	**Region**	**Fitness**	**72**	**74**	**75**	**76**	**144**	**148**	**194**	**220**	**271**	**326**	**333**	**356**	**371**
GC03	S	All	–	C	M	N	K	A	L	I	A	Q	N	T	I	R
Ecu1110	R	SA	↓↓	C	M	N	T	A	L	I	S	Q	D	T	L	R
7G8	R	SA; WP	↓	S	M	N	T	A	L	I	S	Q	D	T	L	R
GB4	R	Af	↓	C	I	E	T	A	L	I	S	E	N	T	I	I
Dd2	R	Af; SeA	↓↓	C	I	E	T	A	L	I	S	E	S	T	T	I
Cam734	R	SeA	–/↑	C	I	D	T	F	I	T	S	E	N	S	I	R

[a]Shown are representative PfCRT haplotypes, which emphasize variants investigated in this dissertation. Polymorphisms shaded in gray differ from those comprising wild-type (GC03; CQ-sensitive) PfCRT. The relative fitness associated with a given PfCRT haplotype, as compared to wild-type (GC03), was inferred from published growth rates determined in isogenic, blood-stage *P. falciparum* parasites.[242,243] ↑ and ↓ indicate increased and decreased parasite fitness, respectively, with the number of arrows representing the degree of difference. –, no change; CQ, chloroquine; S, sensitive; R, resistant; SA, South America; WP, Western Pacific; Af, Africa; SeA, Southeast Asia.

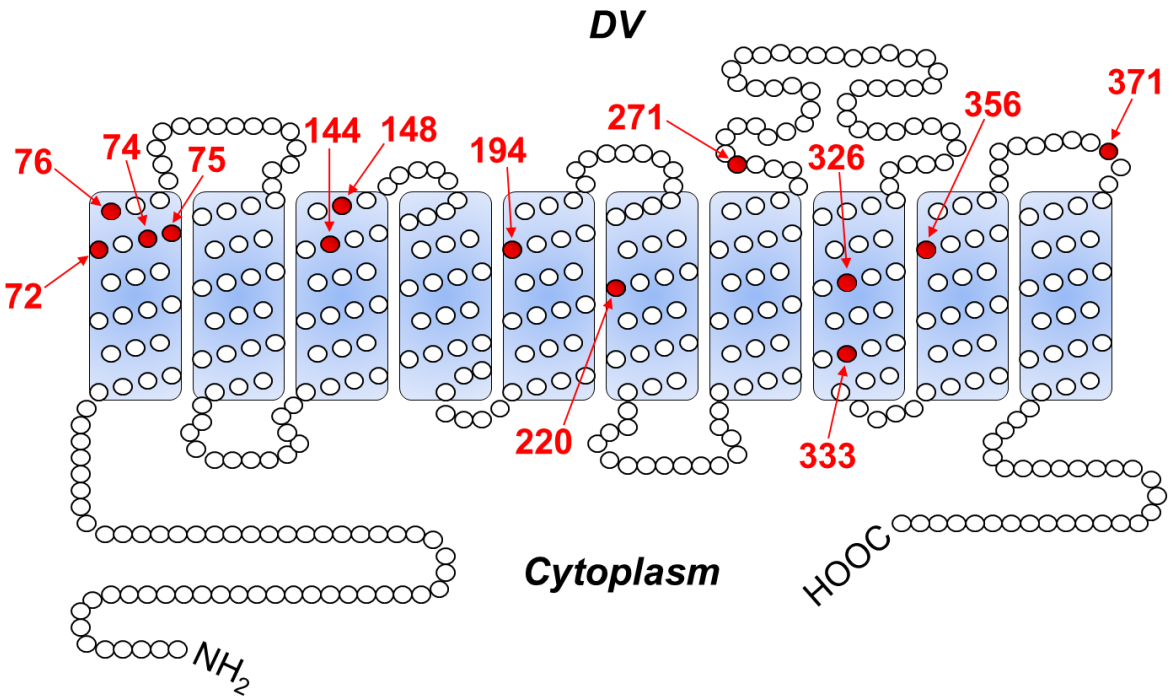

Figure 1.16. Schematic of PfCRT topology. PfCRT is a drug/metabolite transporter with 424 residues and 10 predicted transmembrane domains that span the membrane of the parasite digestive vacuole (DV).[233] N and C termini of the protein are oriented toward the parasite cytoplasm. Representative residues that are mutated among different PfCRT variants are indicated in red. These correspond to PfCRT mutations listed in **Table 1.6**.

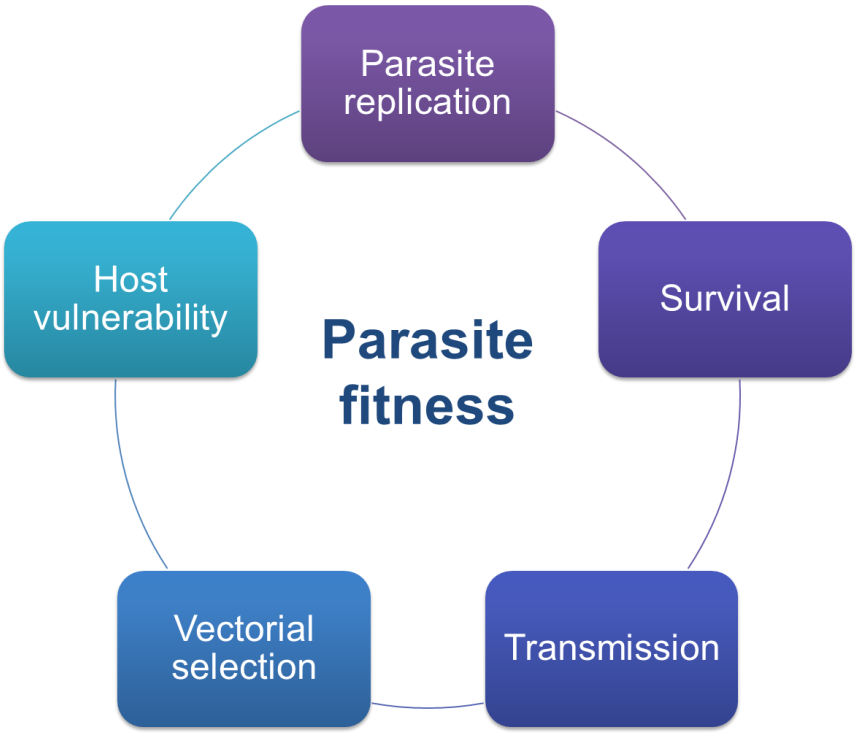

Figure 1.17. Schematic of factors contributing to the fitness of *Plasmodium* parasites. Fitness refers to the ability of organisms to replicate, generate new progeny, and propagate their life cycle. The complex life cycle of *Plasmodium* parasites requires replication in distinct cellular environments. Parasite numbers increase exponentially and directly contribute to malaria pathogenesis during the human blood stage of infection. Before they can be successfully transmitted to the mosquito vector, parasites must withstand host defenses (e.g. antioxidant and immune systems) and survive possible exposure to chemotherapeutics. Parasite fitness is also influenced by the number of gametocytes transmitted to the mosquito vector and their subsequent replicative success. *In vitro* measurements of fitness include biochemical and functional characterizations of essential parasite proteins, assessment of parasite replication in competitive growth assays, and monitoring of specific parasite genotypes via sequencing-based approaches. These are complemented with epidemiological, clinical, and laboratory-based investigations of transmission dynamics, parasite virulence, and host immunity.

host in the absence of drug.[24,123] While it is possible that growth rates in culture might differ from those that would be observed within humans, performing controlled experiments in the setting of the human host is not an option, for obvious reasons. Factors that call for caution in interpreting the results of parasite growth competition experiments include the confounding roles of host immunity, clonality of infections, rates of cross-over, drug levels, vector-specific selection, and modulation of virulence by co-infecting microbes.[240,241,244,245] Despite this, meaningful correlations emerge from comparisons of laboratory-based parasite growth rates and other field-based markers of parasite fitness, as discussed in the next section. Leveraged with focused comparative assessments of parasite growth, the application of whole-genome, transcriptome, and proteome analysis of parasite populations that have been subjected to particular selective forces will collectively aid in identifying parasite-specific signatures of fitness.[244]

PfCRT and the balancing act of parasite drug resistance versus fitness

Parasites evolve resistance to an antimalarial drug by acquiring one or more gene mutations and/or altering gene expression. These changes may interfere with activation of drug, impair drug-target interactions, and/or enhance efflux of drug away from its target site.[240] Particularly for proteins that serve essential functions, as is the case for PfCRT,[229] the fitness of a protein is directly linked to the organism's overall fitness. Consistent with this, the impacts of resistance mutations on protein stability and function evoke the drug resistance mutation-fitness tradeoffs observed for an organism.[246]

The tradeoffs between drug resistance mutations and parasite fitness can be

contextualized by mapping all possible mutational configurations within a gene or genes against the degree of fitness that they confer, collectively referred to as an adaptive landscape.[239] Importantly, the topography of adaptive landscapes is largely influenced by the organism's drug environment.[245] Typically, drug resistance mutations have a deleterious impact on parasite protein function and, consequently, impart a fitness cost. In the absence of drug pressure, these mutations represent low-fitness "valleys" in the parasites' adaptive landscape, and natural selection will act to eliminate them. However, in the scenario of drug pressure, the fitness of parasites is influenced by their ability to survive in the presence of drug, and previously inaccessible mutational paths in the parasite adaptive landscape may become accessible. Sustained drug pressure may facilitate the evolution of additional intragenic or intergenic compensatory mechanisms that reduce fitness costs, further modifying the parasite's adaptive landscape.[240] Of note, mutations may occasionally arise that simultaneously confer drug resistance and impart either no fitness cost or enhanced fitness. In rare instances, this degree of fitness may be comparable to that conferred by the wild-type allele, even in the absence of drug.[240,243,247]

The degree to which mutant resistance alleles are fixed in the population is influenced by their rates of formation, exposure to drug pressure, and relative fitness as compared to other circulating alleles.[240] *De novo* resistance mediated by two major *P. falciparum* drug resistance genes – *dhfr* and *pfcrt* – has been previously estimated to emerge with per-parasite probabilities of 10^{-12} and 10^{-20}, respectively.[24] The discrepancy in these rates can be attributed to the fundamentally distinct modes of resistance conferred by mutations in these genes. Identification of mutational pathways that most readily facilitate the development of resistance is greatly

facilitated by approaches that leverage combinatorial genetic phenotyping of a fitness proxy (e.g. drug resistance in the scenario of drug pressure, growth, protein function) with computational models that simulate drug resistance evolution.[239] This entails generating an allelic panel comprising all possible combinations of mutations that make up a drug resistance allele. Combinatorial genetic strategies were previously applied to model the evolution of *dhfr*-mediated pyrimethamine resistance, which revealed a subset of preferred mutational pathways that correlated with field data.[165,248] Importantly, such studies had not been previously performed for *pfcrt* and form the basis of the work presented in **Chapter 2**.

A wide collection of laboratory and field-based studies provide insights into the influence of drug pressure on the prevalence of *pfcrt* alleles, as well as impacts of *pfcrt* mutations on various aspects of parasite fitness.[114,241] A historic example is the fate of the mutant PfCRT CVIET haplotype (residues 72-76) in Africa. Following its evolution in Asia,[249] this mutant haplotype migrated to the African continent, contributing to the loss of CQ efficacy and resurgence in childhood malaria mortality.[178] However, this devastating trend was reversed when concerted withdrawal of CQ use was implemented in regions of Africa, leading to the rapid attrition of mutant PfCRT, with a concomitant expansion of the fitter, wild-type (CQ-sensitive) CVMNK haplotype.[250-252] This phenomenon has also been observed in a few parts of Asia,[253,254] although these represent exceptions; the CVIET haplotype presently dominates in Asia, despite declined CQ use. In South America[255-257] and elsewhere,[258-260] the SVMNT haplotype has also persisted in the absence of CQ pressure.

Region-specific differences in the prevalence of mutant *pfcrt* alleles can be attributed to a number of factors, including relative growth rates of parasites during

the various stages of their complex life cycle, the extent of drug pressure, and gametocyte carriage rates. As well, regional differences in the extent of parasite transmission have established impacts on host immunity and parasite natural selection, with increased roles for immunity and a higher preponderance of polyclonal infections observed in high-transmission settings, such as Africa.[241,261]

Previous experiments using isogenic asexual blood-stage *P. falciparum* lines engineered to express variant *pfcrt* alleles have collectively shown that, compared to wild-type *pfcrt*, mutant *pfcrt* alleles consistently reduce parasite proliferation, with a single exception (a fitness-enhancing allele identified in Cambodia[262] that is the subject of **Chapter 3** and **Appendix A**).[232,243] This defect in parasite blood-stage fitness was previously associated with defective Hb catabolism, resulting in the abnormal accumulation of Hb-derived peptides in the DV.[232]

Studies in the field setting support the idea that mutant *pfcrt* genotypes negatively impact parasite fitness. In a study in the Gambia, before the start of the high-transmission wet season, wild-type PfCRT-encoding parasites predominated, and mutant PfCRT-encoding parasites only increased in prevalence with drug use.[263] In a separate retrospective study examining associations between *pfcrt* mutational status and the clinical presentation of parasitemic children in Uganda, it was found that the prevalence of mutant *pfcrt* genotypes was lower in febrile children as compared to asymptomatic children.[264] In this region, the widely-used regimen ATM-LUM selects against the mutant *pfcrt* genotype, which can be counteracted by employing the AS-AQ regimen that selects for mutant *pfcrt.*[265] In studies in Zambia, selection against mutant *pfcrt* was also shown to operate at the level of the mosquito vector.[266]

Of note, mutant *pfcrt* alleles may play an important role in facilitating transmission. In Sudan, for example, mutant *pfcrt* genotypes were implicated in facilitating increased gametocyte carriage.[267] This is in line with experiments performed by Ecker *et al.*, which showed that a mutant *pfcrt* allele (7G8) that was transgenically expressed in *P. berghei* enhanced the transmission of CQ-exposed gametocytes to mosquitos.[268] These observations raise the prospect that some mutant *pfcrt* alleles have evolved to offset fitness costs associated with their intraerythrocytic growth by improving transmission to the mosquito vector.

CHAPTER 2: COMBINATORIAL GENETIC MODELING OF *PFCRT*–MEDIATED DRUG RESISTANCE EVOLUTION IN *PLASMODIUM FALCIPARUM*

Stanislaw J. Gabryszewski,[1] Charin Modchang,[3] Lise Musset,[4] Thanat Chookajorn,[5] and David A. Fidock[1,2]

[1]Department of Microbiology and Immunology and [2]Division of Infectious Diseases, Department of Medicine, Columbia University Medical Center, New York, NY, USA; [3]Department of Physics, Faculty of Science, Mahidol University, Bangkok, Thailand; [4]Laboratoire de Parasitologie, WHO Collaborating Center for Surveillance of Anti-Malarial Drug Resistance, Institut Pasteur de la Guyane, Cayenne, French Guiana; [5]Genomics and Evolutionary Medicine Unit, Center of Excellence in Malaria, Faculty of Tropical Medicine, Mahidol University, Bangkok, Thailand

Author contributions: **SJG** and DAF conceived and designed the experiments; **SJG** and LM performed experimental work; **SJG**, CM, TC, and DAF analyzed data; **SJG** and DAF wrote the manuscript.

Note: Portions of this chapter are reproduced from **Gabryszewski SJ**, Modchang C, Musset L, Chookajorn T, and Fidock DA. "Combinatorial genetic modeling of *pfcrt*-mediated drug resistance evolution in *Plasmodium falciparum*." 2016. *Mol Biol Evol.* with permission from the publisher.

ABSTRACT

The emergence of drug resistance continuously threatens global control of infectious diseases, including malaria caused by the protozoan parasite *P. falciparum*. A critical parasite determinant is PfCRT, the primary mediator of CQR and a pleiotropic modulator of susceptibility to first-line ACT partner drugs. Aside from the validated CQR molecular marker K76T, *P. falciparum* parasites have acquired at least three additional *pfcrt* mutations, whose contributions to resistance and fitness have been heretofore unclear. Focusing on the quadruple-mutant Ecuadorian PfCRT haplotype Ecu1110 (K76T/A220S/N326D/I356L), we genetically modified the *pfcrt* locus of isogenic, asexual blood-stage *P. falciparum* parasites using zinc finger nucleases to produce all possible combinations of intermediate *pfcrt* alleles. Our analysis included the related quintuple-mutant PfCRT haplotype 7G8 (Ecu1110+C72S) that is widespread throughout South America and the Western Pacific. Drug susceptibilities and *in vitro* growth profiles of our combinatorial *pfcrt*-modified parasites were used to simulate the mutational trajectories accessible to parasites as they evolved CQR. Our results uncover unique contributions to parasite drug resistance and growth for mutations beyond K76T and predict critical roles for the CQ metabolite md-CQ and the related quinoline-type drug AQ in driving mutant *pfcrt* evolution. Modeling outputs further highlight the influence of parasite proliferation rates alongside gains in drug resistance in dictating successful trajectories. Our findings suggest that *P. falciparum* parasites have navigated constrained *pfcrt* adaptive landscapes by means of probabilistically rare mutational bursts that led to the infrequent emergence of *pfcrt* alleles in the field.

INTRODUCTION

Drug resistance in *Plasmodium* parasites continuously threatens global efforts to control malaria, a leading infectious cause of human morbidity and mortality. Malarial disease is caused by asexual intra-erythrocytic protozoan parasites belonging to the genus *Plasmodium*, with life-threatening cases largely attributed to infection with *Plasmodium falciparum.*[15] Among the most critical parasite determinants of existing and emerging antimalarial drug resistance is the *P. falciparum* Chloroquine Resistance Transporter (PfCRT), a 424-amino acid transmembrane protein with putative involvement in nutrient transport and osmotic balance across the parasite digestive vacuole (DV) membrane.[114,188] Fittingly named for its direct role in conferring resistance to the quinoline-type drug chloroquine (CQ), as validated through genetic linkage[184] and allelic exchange[186] studies, PfCRT has gained recognition as a multidrug resistance transporter with pleiotropic effects on parasite susceptibility to multiple first-line antimalarials.[114,243,269]

Coinciding with the demise of the short-lived Malaria Eradication Program, the arrival of CQ resistance (CQR) heralded a dramatic increase in severe malaria cases.[270] A significant association between CQR and *pfcrt* was observed in microsatellite typing studies of parasites isolated during this period, which detected four distinct geographical origins of CQR, namely Southeast Asia (with subsequent spread into Africa), the Western Pacific, and two foci in South America.[249] Factors that likely sustained sub-therapeutic levels of CQ in the population and thus facilitated the evolution of CQ-resistant *pfcrt* alleles include aggressive deployment of CQ as a monotherapy and unregulated use of prophylactic chloroquinated salts.[130] Despite the setback of resistance to the eradication campaign, CQ played a monumental role in

reducing the global burden of malaria.[271] CQ continues to be employed for the treatment of uncomplicated *P. falciparum* malaria in regions with no or low-level CQR[272] as well as to treat infection with the related malarial parasite *P. vivax*.[273]

Mechanistically, CQ interacts with host hemoglobin-derived heme in the DV, where it inhibits detoxification of heme species that are otherwise toxic to parasites.[55] Mutant PfCRT facilitates CQR by reducing the ability of CQ to access its heme target.[108,274] This is accomplished by mutant PfCRT-mediated CQ efflux out of the DV and may be further attributed to modulation of PfCRT native function.[114,188,275] Chemical and molecular features shared among clinically employed antimalarials, including constituents of the first-line artemisinin-based combination therapies (ACTs), collectively include the presence of a CQ-like structural scaffold, accumulation of drug in the DV, inhibition of heme detoxification, and/or drug activation via heme.[180,276] Consistent with their ability to alter DV physiology, *pfcrt* alleles modulate susceptibility to the first-line ACTs and are selected either for or against depending on the specific drug regimen.[114] This is underscored by a recent meta-analysis of the clinical efficacy of two widely employed ACTs, artesunate-amodiaquine (AS-AQ) and artemether-lumefantrine (ATM-LUM), which revealed a reduction in time to reinfection for parasites encoding mutant PfCRT in patients treated with AS-AQ, and vice versa for ATM-LUM.[265] Monitoring resistance to ACT partner drugs is paramount due to the very short half-lives of artemisinins, which leave their long-acting partner drugs solely responsible for clearing any remaining parasites.[277] Intriguingly, *in vitro* and field studies indicate that *pfcrt* mutations may even modulate parasites' susceptibility to artemisinins themselves.[120,159,278]

Molecular and epidemiological investigations of the effect of drug pressure on

the *pfcrt* locus have historically centered on a single-nucleotide polymorphism (SNP) encoding a lysine-to-threonine substitution (K76T) that is highly prevalent among CQ-resistant parasites.[114] In parasites expressing CQ-resistant *pfcrt* alleles, targeted genetic reversion of PfCRT K76T back to the wild-type residue abolished CQR and its characteristic reversibility by the calcium channel blocker verapamil (VP), in part by enhancing access of CQ to its heme target.[126] In line with these *in vitro* findings, K76T has been associated with *in vivo* CQR and has served as a sensitive, although not highly specific, marker of CQ treatment failure.[198,199], in part due to pre-existing host immunity in areas with high transmission.[279] Mutant *pfcrt*-mediated CQR can also be augmented by secondary factors, including mutant *pfmdr1*.[133,280] Of note, geographically distinct CQ-resistant isolates consistently harbor at least three PfCRT mutations in addition to K76T.[275,281,282] These have been conventionally described as compensatory mutations that arose to preserve the essential function of PfCRT[229], although their precise contributions to parasite drug resistance and fitness have not been defined.

Antimalarial drugs exert selective pressures on multiple facets of the parasite life cycle, which collectively determine parasite fitness.[241,244] Among these are growth of intra-erythrocytic parasites, mosquito transmissibility, and within-host virulence, each of which is influenced by the parasite's *pfcrt* genotype.[114,232,243,263,264,266] A notable example is the mutational status of PfCRT residues 72-76 and its association with the outcome of CQ cessation programs in regions with high-level CQR. In regions in Africa[251,283,284] and Asia[253,254], where the CVIET PfCRT haplotype predominates among CQ-resistant parasites, removal of CQ pressure promoted regional resurgences of CQ-sensitive parasites encoding the fitter, wild-type (CVMNK) PfCRT haplotype. In

contrast, in South America[255-257,285] and in select regions elsewhere[258,260,286,287], the predominant mutant PfCRT haplotype, SVMNT, persists despite a decline in CQ use. The prospect that this haplotype is less deleterious to parasites than CVIET[259] is supported by recent *in vitro* studies, in which isogenic intra-erythrocytic parasites expressing the CVIET-encoding Dd2 *pfcrt* allele demonstrated a higher fitness cost than parasites expressing the SVMNT-encoding 7G8 *pfcrt* allele.[243] Accordingly, as they acquire drug resistance-conferring mutations, parasites traverse discrete adaptive landscapes, defined as an organism's fitness as a function of the mutational events incurred.[288] The ability to ascertain evolutionary histories of *pfcrt* alleles and identify predictable mutational pathways would be of particular relevance to region-specific treatment recommendations, which are routinely informed by *pfcrt* genotypes.

To date, the adaptive landscapes of drug resistance alleles consisting of n mutations have been explored through rigorous combinatorial approaches, in which an experimental proxy for fitness is determined for all 2^n possible mutational intermediates and used to quantify the accessibility of the $n!$ possible stepwise evolutionary trajectories leading to the full-length resistance allele.[239,289] Subsequent comparison of accessible trajectories can illuminate preferred mutational pathways and uncover epistatic interactions between mutant residues that may constrain the evolutionary potential of a gene of interest.[290,291] For *Plasmodium*, such combinatorial analyses have not previously been performed for PfCRT and have been limited to heterologous expression studies that explored the mutational acquisition of dihydrofolate reductase (DHFR)-mediated antifolate resistance.[165,248,292,293]

The feasibility of mapping mutational trajectories accessible to *P. falciparum* parasites is greatly facilitated by recent advances in genome editing strategies.[294] In

the present study, we utilized *pfcrt*-specific zinc finger nucleases (ZFNs) to conduct a combinatorial genetic dissection of the CQ-resistant South American *pfcrt* allele Ecu1110 during the pathogenically relevant parasite asexual blood stage. Consisting of the fewest number of mutations observed in a CQ-resistant parasite, the Ecu1110 PfCRT haplotype (K76T, A220S, N326D, I356L) is closely related to the highly prevalent 7G8 haplotype, which differs by the presence of a single additional mutation (C72S). Here, we profiled the drug susceptibility and *in vitro* growth of isogenic parasites expressing all possible *pfcrt* alleles spanning the evolutionary transition from CQ-sensitive (wild-type) to CQ-resistant (Ecu1110), as well as the CQ-resistant *pfcrt* allele 7G8. These experimentally derived genotype-phenotype relationships were subsequently applied to an evolutionary model in order to probe the adaptive landscape of parasites as they acquire drug resistance. This is the first combinatorial description of the trade-offs experienced by *P. falciparum* parasites as they acquire mutations in the *pfcrt* gene, a core determinant of antimalarial drug resistance.

METHODS

Parasite cultivation

P. falciparum-infected human erythrocytes were cultured at 4% hematocrit in 0.5% Albumax II (Invitrogen)-supplemented RPMI-1640 culture medium[160] at 37°C, 5% O_2 / 5% CO_2 / 90% N_2.

Allelic replacement plasmids, parasite transfections, and verification of genetic editing.

To construct donor plasmids for ZFN-based allelic replacement of *pfcrt*, we used previously generated plasmids that encode an assortment of *pfcrt* alleles (GC03, 7G8, Ecu1110, as well as all allelic permutations of Ecu1110 *pfcrt* mutations) as templates for PCR amplification of *pfcrt* exons 2 through 13 with primers p1 + p2 (see **Table 2.1** for primer details). Amplicons were subsequently cloned into the p*crt*^{Dd2}-h*dhfr* donor plasmid backbone[295] via SalI and NcoI restriction sites. The plasmid pZFN^{crt}-*bsd*, which encodes *pfcrt*-specific ZFNs, has been described previously.[295] The composition of donor and ZFN-encoding plasmids is further detailed in **Figure 2.1**.

To genetically modify the *pfcrt* locus of 7G8 parasites, parasites were electroporated with 40 µg purified donor plasmid (p*crt*-h*dhfr*), as detailed elsewhere,[167] and subsequently pressured with 2.5 nM WR99210 (Jacobus Pharmaceuticals). Donor plasmid-enriched parasites were electroporated with 40 µg pZFN^{crt}-*bsd* and pressured with 2.5 nM WR99210 and 2 µg/ml Blasticidin HCl (Invitrogen) for six consecutive days, followed by pressure with 2.5 nM WR99210.

Table 2.1. Primers used in this study.[a]

Primer	Oligonucleotide sequence (5' → 3')	Description	Lab name
p1	AACCATGGATTTATTGTGTAATAATTGAATCGACG	NcoI-*pfcrt* exon 13 R	p1640
p2	CCCTTGTCGACCTTAACAGATGGCTC	SalI-*pfcrt* intron1-exon 2 F	p3519
p3	TCAAACATGACAAGGGAAATAGT	*pfcrt* exon 5 F	p2427
p4	CCAAGAATAAACATGCGAAACC	*pfcrt* exon 7 R	p3806
p5	CTTGAATTCGACCTTAACAGATGGCTCAC	*pfcrt* exon 2 F	p3264
p6	CTTATCGATAAGCAGAAGAACATATTAATAGGAATACTTAATTG	*pfcrt* exon 3 R	p3265
p7	CTTGGGCCCAAGTTGTACTGCTTCTAAGC	*pfcrt* gDNA 5′ UTR F	p3404
p8	CTCGAGATGGTTGGTTCGCTAAACTGC	h*DHFR* F	p3315
p9	TTGACCCTTATATATTCCACCCA	*pfcrt* gDNA 3′ UTR R	p3403
p10	GAGGCGCCTATTTCAAAAATCTTAGCATAAGGATT	*pbcrt* 3′ UTR R	p1644
p11	CATACTTCTTTATAACTTTATGTGACATTTAC	*pbcrt* 3′ UTR R GSP RT-PCR	p4397
p12	CCGTTAATAATAAATACACGCAG	*pfcrt* 5′ UTR F RT-PCR	p4396
p13	GTGACATTTACAAAAATCATTTCCATG	*pbcrt* 3′ UTR R RT-PCR	p4413

[a]Nucleotides corresponding to restriction sites are underlined. F, forward; R, reverse; gDNA, genomic DNA; *pbcrt, P. berghei chloroquine resistance transporter*; UTR, untranslated region; GSP, gene-specific primer.

Bulk cultures of recombinant parasites were subjected to direct blood PCR analysis (2 μl packed red blood cells per 20 μl 1× KAPA Blood Mix B PCR reaction; KAPA Biosystems) to assess for allelic exchange at the *pfcrt* locus. PCR-based screening for genetic editing is further detailed in **Figure 2.1**. Genetically-edited bulk cultures were cloned by limiting dilution.[296] For each recombinant *pfcrt* allele, a minimum of two parasite clones demonstrating appropriate genetic editing by PCR (**Figure 2.1**) were selected for further analysis. Sequence integrity was verified upon initial isolation of parasite clones and during the course of drug susceptibility and *in vitro* growth assays by PCR-amplifying the genetically modified *pfcrt* locus with primers p10 + p7 and sequencing with primers p3 and p4. All clones were additionally subjected to RT-PCR to verify the sequence of *pfcrt* transcripts. Briefly, parasite pellets were resuspended in 1 ml TRI Reagent (MRC) and subjected to extraction with chloroform, as detailed elsewhere.[297] The upper aqueous phase was transferred to a new Eppendorf tube, mixed with an equal volume of 70% ethanol, and transferred to a RNeasy Mini spin column to isolate RNA, as per manufacturer's instructions (Qiagen). RNA was subsequently DNAse-treated with RQ1 DNAse (Promega), and ~100 ng was used as a template for first-strand cDNA synthesis with gene-specific primer p11 (*pbcrt* 3′ UTR reverse) using the SuperScript III First-Strand Synthesis System for RT-PCR (Invitrogen). The *pfcrt* locus was subsequently PCR-amplified from cDNA using primers p12 + p13 and sequenced with primers p3 and p4. All primer details are found in **Table 2.1**.

Quantification of PfCRT protein expression

Following two synchronizations with 5% sorbitol, trophozoite-stage parasites were lysed with 0.1% saponin. Protein lysates were washed with PBS and resuspended in RIPA lysis buffer (Boston BioProducts) supplemented with Halt Protease Inhibitor Cocktail (ThermoFisher Scientific). Proteins extracted from ~10^7 parasites were subsequently incubated at 65°C for 10 min in sample buffer, electrophoretically separated on a 4-12% Criterion XT Bis-Tris Gel (BioRad), and transferred onto a PVDF membrane (Millipore). Membranes were incubated with rabbit polyclonal anti-PfCRT[186] or anti-PfERD2 (MRA-1; MR4, BEI Resources, NIAID, NIH) primary antibodies, followed by anti-rabbit horseradish peroxidase-conjugated secondary antibody. Protein was visualized by chemiluminescence and quantified using Image Studio software (LI-COR). Levels of PfCRT protein were normalized to those of the PfERD2 loading control and expressed relative to isogenic parasites encoding the wild-type *pfcrt* allele ($7G8^{GC03}$) for a total of three independent protein harvests. Data are summarized in **Table 2.2**.

Drug susceptibility assays

To assess *in vitro* drug susceptibility, parasites were dispensed into 96-well plates containing a two-fold dilution series of CQ ± 0.8 µM VP, md-CQ, md-AQ, LUM, or AS, pre-aliquoted with a BioTek Precision Pipetting System. Parasites were incubated at 2% final hematocrit in culture medium containing 50 mM HEPES. After 72 h, parasites were stained with SYBR Green I and MitoTracker Deep Red, and growth was determined using an Accuri C6 flow cytometer.[168] Drug inhibitory concentrations that cause 50% (IC_{50}) or 90% (IC_{90}) inhibition of parasite growth were

Table 2.2. PfCRT protein expression levels in *pfcrt*-modified and reference parasite lines.[a]

Line			Line			Line		
$7G8^{GC03}$	mean	1.00 ± 0.2	$7G8^{EcuAD}$	mean	0.97 ± 0.40	$7G8^{7G8}$	mean	0.76 ± 0.19
	n	3		*n*	3		*n*	3
	P	–		*P*	0.90		*P*	0.40
$7G8^{EcuA}$	mean	0.98 ± 0.07	$7G8^{EcuACD}$	mean	0.71 ± 0.32	7G8	mean	0.76 ± 0.27
	n	3		*n*	3		*n*	3
	P	0.90		*P*	0.70		*P*	0.70
$7G8^{EcuAC}$	mean	1.16 ± 0.21	$7G8^{EcuABCD}$	mean	0.87 ± 0.19			
	n	3		*n*	3			
	P	0.70		*P*	0.70			

[a]PfCRT protein expression was evaluated for parasite lines exhibiting significant differences in chloroquine IC_{50} values (**Table 2.5**) and/or *in vitro* growth rates (**Table 2.9**) as compared to the recombinant reference line $7G8^{GC03}$, which encodes the wild-type *pfcrt* allele. Protein lysates from three independent cultures of doubly sorbitol-synchronized, trophozoite-stage parasites were subjected to SDS-PAGE, probed with rabbit anti-PfCRT or anti-ERD2 antibodies, and quantified by densitometry. For each parasite strain, signals of PfCRT protein bands were normalized to those of the loading control (PfERD2) and are expressed above as mean ± SEM values, relative to the $7G8^{GC03}$ parasite line. *n*, number of independent protein harvests; *P, P* value, as determined in a non-parametric Mann-Whitney *U* test versus the comparator line $7G8^{GC03}$. Of note, PfCRT protein levels showed no significant correlation with either degree of CQR (R^2=0.23, *P*=0.34) or *in vitro* parasite growth (R^2=0.003, *P*=0.92).

calculated as previously described.[217] Reversibility of CQR by 0.8 μM VP is expressed as the CQ RMI, equivalent to the quotient of the CQ+VP IC_{50} divided by the CQ IC_{50}.[298] Statistical significance was determined via non-parametric Mann-Whitney *U* tests using GraphPad Prism 6 software.

In vitro growth assays

In vitro fitness of recombinant and reference parasite lines was assessed in 1:1 co-culture assays with the fluorescent reporter line NF54^{eGFP} (R^{GFP}). To generate R^{GFP}, a cassette encoding the eGFP fluorescence probe flanked by 5′ hsp70 and 3′ hsp86 UTRs was genomically integrated into CQ-sensitive (wild-type *pfcrt*) NF54-*attB* parasites via *attB*×*attP*-based recombination catalyzed by the mycobacteriophage Bxb1 integrase.[296] The robustness of this fluorescence reporter line was recently validated in *in vitro* fitness studies conducted in blood-stage parasites.[299] Assays were initiated by preparing co-cultures consisting of R^{GFP} (GFP^+) and a single *pfcrt*-modified test line ($GFP^–$) in a 1:1 ratio with respect to final parasitemia of each line. Using flow cytometric detection of eGFP, expressed by the reporter line, as well as the far-red fluorescent dye SYTO61, which facilitates differentiation between uninfected and infected red blood cells,[300] the $GFP^–$ proportion of parasites was monitored for 10 generations and used to derive the per-generation selection coefficient (*s*) for each test strain. Statistical significance was assessed via two-way ANOVA with Sidak's post-hoc test using GraphPad Prism 6 software.

Parasite growth was determined every third day for 10 generations, and the parasitemia of each co-culture was maintained between 0.3% and 8%. For each co-culture, the frequencies at generation *t* of the test allele ($GFP^–$) and the reporter allele

(GFP$^+$) are represented as p_t and q_t, respectively. The relative fitness (ω) of the test allele is equivalent to e^m, where m corresponds to the slope of the graph of $\ln(p_t/q_t)$ versus t as per the relationship $\ln(p_t/q_t) = \ln(p_0/q_0) + t\ln(\omega)$, which holds true for haploid organisms.[301] The relative fitness for each test strain was normalized to that of the 7G8^{GC03} parasite line, which encodes the wild-type (GC03) *pfcrt* allele, yielding the normalized relative fitness (ω'). The per-generation selection coefficient (s) for each test strain was then computed as per the relationship $\omega' = 1 + s$.[247] Statistical significance was assessed via two-way ANOVA with Sidak's post-hoc test using GraphPad Prism 6 software. *In vitro* growth data are summarized in **Table 2.9**.

Modeling of *pfcrt* evolutionary trajectories

In our mutational model, the total fitness associated with each *pfcrt* allele (f_T) was derived from the relationship $f_T = af_D + (1-a)f_G$, where f_D is the fitness index attributable to drug resistance, f_G is the fitness index attributable to parasite growth in the absence of drug, and a is the drug pressure coefficient (range for each parameter: 0 to 1). The f_D index is equivalent to the IC_{50} value for a parasite line, normalized to the highest IC_{50} value observed among all combinatorial lines for a given drug. Similarly, the f_G index is equivalent to the relative *in vitro* growth (ω') of a parasite line in the absence of drug, normalized to the highest observed ω' value. Thus, in the case of full drug pressure (a=1), the highest f_T value is ascribed to the *pfcrt* allele that confers the highest degree of resistance, whereas in the completely drug-free environment (a=0), the highest f_T value is shown by the *pfcrt* allele that confers maximum parasite growth.

We adapted previously established methods[165,248,302] to explore seven distinct

mutational scenarios that lead to the evolution of Ecu1110 *pfcrt* from the GC03 (wild-type) *pfcrt* allele. These mutational scenarios are as follows: 0→1→2→3→4; 0→1→2→4; 0→1→3→4; 0→2→3→4; 0→1→4; 0→2→4; and 0→3→4, where each number corresponds to the number of total mutations acquired. For all hypothetical *pfcrt* alleles comprising each mutational scenario, adaptive landscapes were generated by random sampling of f_D and f_G values from normal distributions based on *pfcrt* allele-specific means and SEMs. To examine the role of drug pressure on mutational pathway accessibility, the drug pressure coefficient a was varied from 0 to 1, in increments of 0.1. We note that f_T and the experimentally derived growth selection coefficient s were in agreement (R^2=0.974) for growth experiments performed with 7.5 nM CQ (a=0.04). Evolutionary excursions along each landscape were then simulated by randomly choosing one or more mutations, depending on the mutational scenario. The probability of a new mutant allele occurring is equal to the total fitness difference (Δf_T) between the new allele and the precursor allele. In our simulations, a uniform random number (r) was selected. The new allele was accepted only if $r<\Delta f_T$. A new mutant was only accepted if its f_T value was larger than that of its precursor allele. To calculate pathway probabilities, we simulated 10^4 normal-distributed adaptive landscapes and explored each with 10^5 independent iterations. The pathway probability was then calculated from the formula $P_i = N_i / N_{total}$, where P_i is the probability that parasites evolve along pathway i, N_i is the number of times that the simulations achieve the Ecu_{ABCD} allele by traversing pathway i, and N_{total} is the total number of runs (N_{total}=10^9 in our analysis). All simulations were performed using MATLAB software.

RESULTS

Generation of a combinatorial panel of *pfcrt* alleles in isogenic *P. falciparum* parasites

Surveys of PfCRT haplotypes in geographically distinct CQ-resistant isolates of *P. falciparum* indicate that CQR requires at least four mutations, namely K76T and at least three accompanying non-synonymous mutations.[114] While this suggests that CQ-resistant parasites necessitate compensatory mutations to maintain PfCRT function, several key questions remain unanswered: Which SNPs directly influence drug resistance, which neutralize fitness costs, and which contribute in both regards? Are there predictable mutational trajectories in the evolution of PfCRT-mediated drug resistance? To address these questions, our study centered on the CQ-resistant Ecuadorian *pfcrt* allele Ecu1110,[186] which harbors four mutations and is therefore amenable to a comprehensive dissection of the genetic determinants of parasite drug resistance and fitness.

To perform a combinatorial analysis of *pfcrt*, we used ZFNs (**Figure 2.1**) to genetically engineer a series of intra-erythrocytic parasites encoding all 16 combinations of the four mutations that comprise the Ecu1110 allele. These are K76T, A220S, N326D, and I356L, which we respectively refer to as Ecu_A, Ecu_B, Ecu_C, and Ecu_D, with the quadruple-SNP Ecu1110 haplotype represented as Ecu_{ABCD} (**Table 2.3**). Due to the slow growth of the Ecu1110 parasite strain in culture, we chose to introduce the full set of combinatorial alleles into the South American recipient strain 7G8. This line is derived from a Brazilian clinical isolate[303] and was recently used with success to modify the parasite *pfcrt* locus in ZFN-based studies.[137]

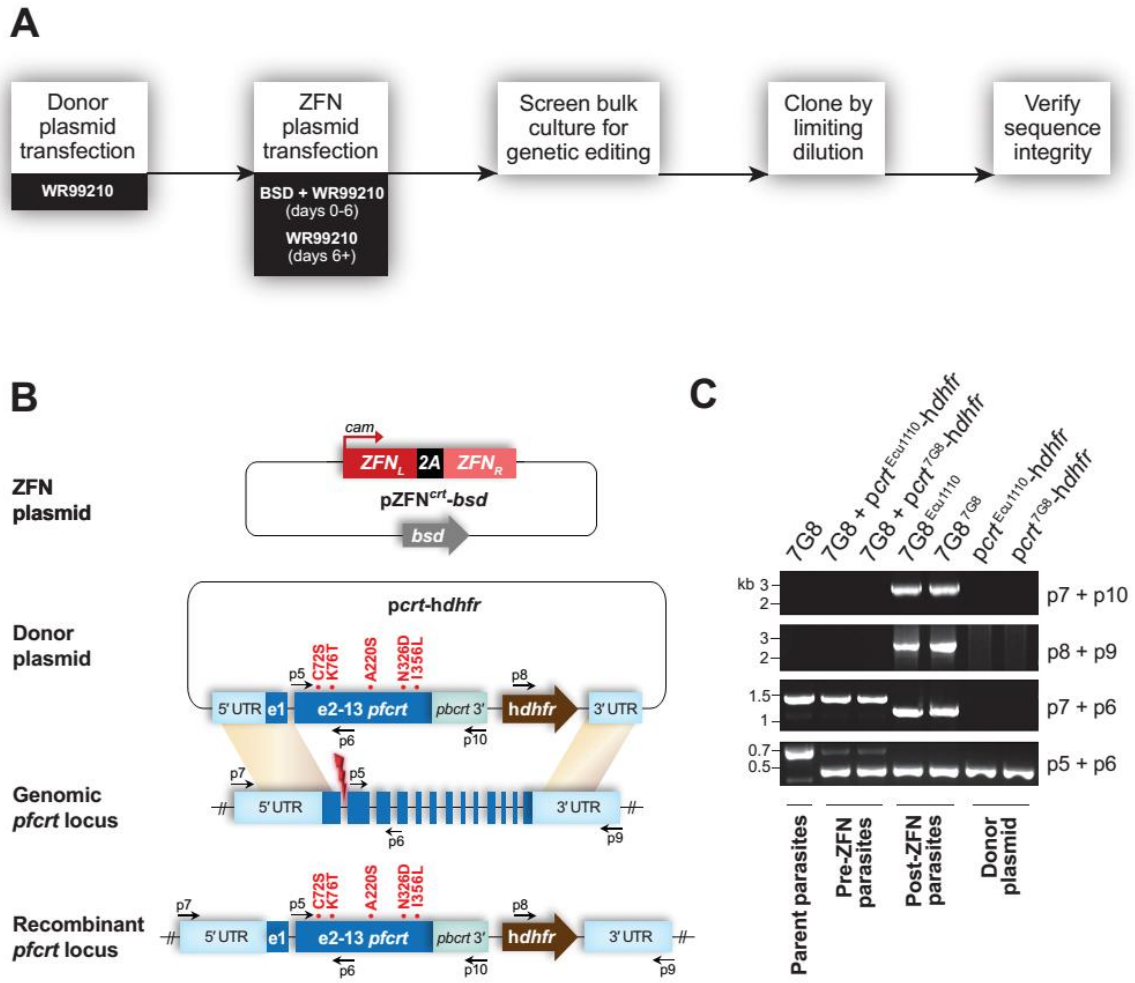

Figure 2.1. Zinc finger nuclease (ZFN)-mediated genomic modification of the *pfcrt* locus. Shown are schematics of the (**A**) parasite genome editing workflow and (**B**) *pfcrt* allelic replacement strategy. Briefly, parasites were transfected with a donor template plasmid (p*crt*-h*dhfr*) comprising a compacted *pfcrt* coding sequence with mutations of interest (indicated in red), an adjacent *P. berghei crt* (*pbcrt*) 3′ UTR element, the human *dhfr* (h*dhfr*) selection cassette, as well as flanking left (~0.4 kb upstream of the intron 1-exon 2 boundary) and right (~1 kb native 3′ UTR) homology regions. A complete list of PfCRT haplotypes included in this study is found in **Table 2.3**. Parasites were subsequently transfected with pZFN^{crt}-*bsd*, which encodes the *blasticidin S deaminase* (*bsd*) selection cassette and facilitates 2A peptide-linked co-expression of ZFN monomers (ZFN_L and ZFN_R) via the *calmodulin* (*cam*) promoter. These ZFNs introduce a double-stranded DNA break in the intron 1-exon 2 boundary of *pfcrt* (indicated by red bolt). Homology-directed DNA repair yields the recombinant *pfcrt* locus, which is amenable to PCR-based screening due to the absence of *pfcrt* introns 2 through 12. Recombinant parasites were cloned by limiting dilution and sequenced at the DNA and RNA levels. (**C**) PCR-based verification of representative ZFN-edited (7G8^{Ecu1110} and 7G8^{7G8}) parasites. Controls include parental parasites (7G8), unedited donor plasmid-enriched parasites (7G8 + p*crt*-h*dhfr*), and the donor plasmid alone (pcrt-h*dhfr*). Primer (p) locations are illustrated in panel **B**. ZFN-edited lines showed the expected band sizes of 0.4 kb (p5+p6), 1.2 kb (p7+p6), 2.5 kb (p8+p9), and 2.7 kb (p7+p10).

Table 2.3. Summary of PfCRT haplotypes.[a]

	PfCRT residue				
PfCRT haplotype	**72**	**76**	**220**	**326**	**356**
GC03 (WT)	C	K	A	N	I
Ecu_A	C	T	A	N	I
Ecu_B	C	K	S	N	I
Ecu_C	C	K	A	D	I
Ecu_D	C	K	A	N	L
Ecu_{AB}	C	T	S	N	I
Ecu_{AC}	C	T	A	D	I
Ecu_{AD}	C	T	A	N	L
Ecu_{BC}	C	K	S	D	I
Ecu_{BD}	C	K	S	N	L
Ecu_{CD}	C	K	A	D	L
Ecu_{ABC}	C	T	S	D	I
Ecu_{ABD}	C	T	S	N	L
Ecu_{ACD}	C	T	A	D	L
Ecu_{BCD}	C	K	S	D	L
Ecu1110 (Ecu_{ABCD})	C	T	S	D	L
7G8	S	T	S	D	L

[a]Mutations different from the GC03 (wild-type) PfCRT haplotype are indicated in gray. DNA substitutions encoding each PfCRT mutation are as follows: C72S: TGT→AGT; K76T: AAA→ACA; A220S: GCC→TCC; N326D: AAC→GAC; I356L: ATA→TTA.

The highly prevalent, quintuple-SNP 7G8 PfCRT haplotype is distinguished from Ecu1110 PfCRT by one additional mutation (C72S; see **Table 2.3**) and was included in our allelic panel. This parasite line, $7G8^{7G8}$ (recombinant *pfcrt* allele indicated in superscript), served as a control for ZFN-based modification of *pfcrt* and was comparable to genetically unedited 7G8 parasites with regard to CQ susceptibility and growth rates.

Our ZFN-based genetic engineering strategy is depicted in **Figure 2.1*A***. Briefly, we constructed a donor plasmid for each combinatorial *pfcrt* allele (see **Table 2.3**), which was transfected into 7G8 recipient parasites. Donor plasmid-enriched parasites were subsequently transfected with a plasmid encoding *pfcrt*-specific ZFNs that were previously validated.[295] Homology-directed repair of DNA breaks catalyzed by these ZFNs yielded the recombinant *pfcrt* locus (**Figure 2.1*B***). For each recombinant line, two individual clones were isolated for subsequent analysis. Genetic editing of the *pfcrt* locus was evaluated by diagnostic PCRs (**Figure 2.1*C***), followed by sequencing of parasite gDNA and cDNA using primers listed in **Table 2.1**. Additionally, *pfcrt* sequence integrity was monitored in all recombinant parasite lines throughout the duration of all assays. Phenotypic differences between parasite strains were not attributable to levels of PfCRT expression (see **Table 2.2**).

Effect of *pfcrt* combinatorial alleles on parasite CQ susceptibility

To evaluate the contribution of PfCRT mutations to parasite resistance to CQ and its primary active metabolite, md-CQ, we subjected our panel of *pfcrt*-modified isogenic parasite lines to flow cytometry-based drug susceptibility assays and determined drug concentrations that cause 50% (IC_{50}) and 90% (IC_{90}) inhibition of parasite growth. We

also analyzed the genetically unmodified reference lines GC03, Ecu1110, and 7G8 (corresponding PfCRT haplotypes listed in **Table 2.3**). Antimalarial IC_{50} and IC_{90} values are summarized in **Table 2.4** and **Table 2.5**, respectively. For all strains tested, drug responses were compared against those of isogenic $7G8^{GC03}$ parasites, which encode the wild-type (GC03) *pfcrt* allele.

Our drug susceptibility findings for CQ (**Figure 2.2*A***) and md-CQ (**Figure 2.2*B***) revealed that the CQR-associated mutation K76T is insufficient for parasite CQR. Intriguingly, as compared to $7G8^{GC03}$ parasites, $7G8^{EcuA}$ parasites exhibited significant md-CQ hypersensitivity (mean IC_{50} values of 20.9 and 15.1 nM, respectively; **Table 2.4**), highlighting a critical role for mutations beyond K76T in conferring CQR. This is further corroborated by the md-CQ responses of multiple lines with PfCRT haplotypes lacking K76T ($7G8^{EcuC}$, $7G8^{EcuD}$, $7G8^{EcuBC}$, $7G8^{EcuCD}$, $7G8^{EcuBCD}$), which showed modest (1.5 to 2.5-fold) yet significant elevations in md-CQ IC_{50} as compared to $7G8^{GC03}$ parasites (**Figure 2.2*B*; Table 2.4**). The reduced md-CQ susceptibility of these lines was accentuated at the IC_{90} level (**Table 2.5**).

To dissect the impact of specific SNPs on parasite drug resistance, we compared the drug responses of PfCRT haplotype pairs differing at only one residue. For every combinatorial PfCRT haplotype, we determined the successive contribution of each Ecu1110 PfCRT-specific SNP to CQ and md-CQ resistance (**Table 2.6**). We considered all instances in which mutational acquisition conferred a significant change in CQ or md-CQ IC_{50} values as compared to the precursor PfCRT haplotype. Invariably, in all such instances, Ecu_C N326D served to increase drug resistance. Ecu_D I356L similarly conferred increased drug resistance, with one exception ($Ecu_C \rightarrow Ecu_{CD}$; see **Table 2.6**), whereby it decreased md-CQ resistance.

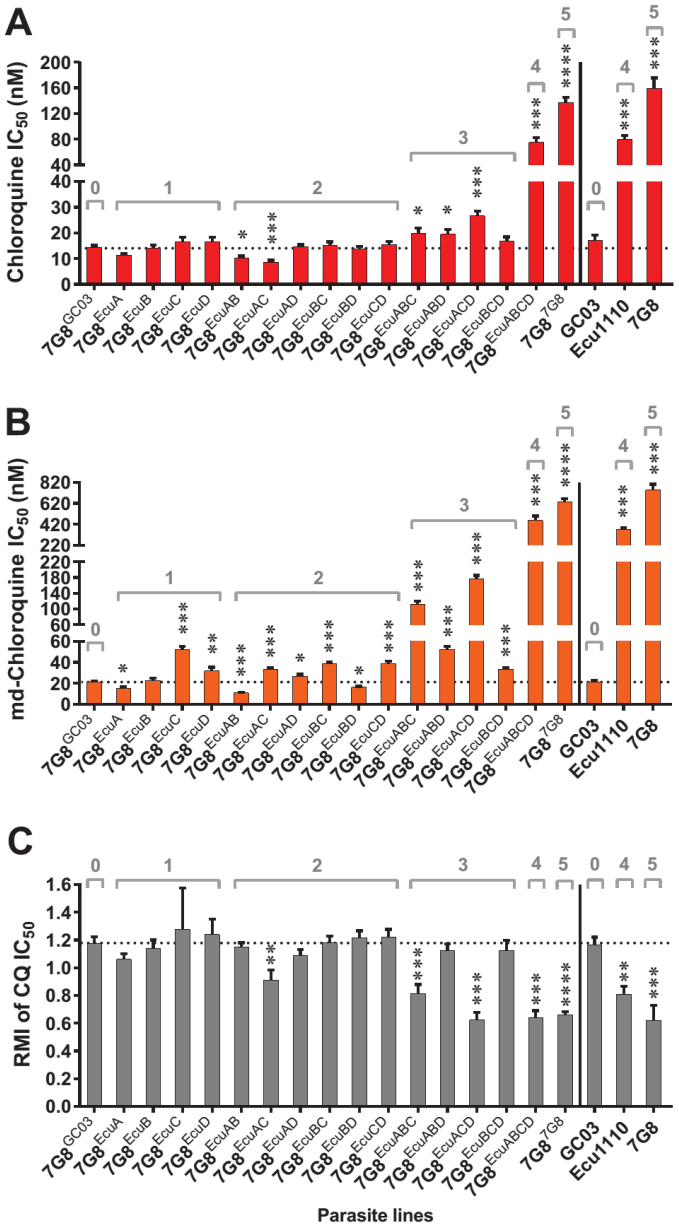

Figure 2.2. Chloroquine resistance profiles of *pfcrt*-modified and reference parasite lines. Parasite growth inhibition was determined by flow cytometry after 72 h exposure to serial dilutions of (**A**) chloroquine (CQ), (**B**) monodesethyl-chloroquine (md-CQ), or (**C**) CQ in the presence or absence of 0.8 μM verapamil (VP). Bar graphs represent (**A** and **B**) mean ± SEM IC_{50} values or (**C**) mean ± SEM CQ response modification index (RMI) values, equivalent to (IC_{50} for CQ+VP) ÷ (IC_{50} for CQ only). Results encompass 5 to 15 independent assays conducted in duplicate. Statistical differences were determined via non-parametric Mann-Whitney *U* tests, using the mean IC_{50} value of wild-type *pfcrt*-expressing $7G8^{GC03}$ parasites (dotted black line) as the comparator. The total number of *pfcrt* mutations encoded by parasite lines is indicated in gray. When applicable, the y-axis was split to illustrate subtle, statistically significant differences in IC_{50} values. IC_{50}, IC_{90}, and CQ RMI values are summarized along with corresponding statistical tests in **Table 2.4**, **Table 2.5**, and **Table 2.7,** respectively. **P*<0.05; ***P*<0.01; ****P*<0.001. *****P*<0.0001.

Table 2.4. Antimalarial IC_{50} values of *pfcrt*-modified and reference parasite lines.[a]

Line		CQ IC_{50}	CQ+VP IC_{50}	md-CQ IC_{50}	md-AQ IC_{50}	LUM IC_{50}	AS IC_{50}
7G8^{GC03}	IC_{50}	14.2 ± 0.9	16.5 ± 0.9	20.9 ± 1.0	18.1 ± 1.0	0.90 ± 0.10	1.32 ± 0.08
	n	15	15	15	15	13	17
	P	–	–	–	–	–	–
7G8^{EcuA}	IC_{50}	11.3 ± 0.7	11.8 ± 0.5	15.1 ± 1.6	20.8 ± 0.9	0.68 ± 0.10	0.83 ± 0.09
	n	5	5	5	5	6	6
	P	0.076	**0.010**	**0.010**	0.22	0.27	**0.0026**
7G8^{EcuB}	IC_{50}	13.9 ± 1.4	15.5 ± 1.0	22.5 ± 2.2	20.2 ± 1.7	1.12 ± 0.12	1.38 ± 0.16
	n	5	5	5	5	6	6
	P	0.72	0.63	0.56	0.26	0.20	0.61
7G8^{EcuC}	IC_{50}	16.6 ± 1.6	20.8 ± 0.6	52.1 ± 3.2	26.1 ± 0.8	0.94 ± 0.11	1.39 ± 0.12
	n	5	5	5	5	6	6
	P	0.17	**0.015**	**0.0001**	**0.0003**	0.78	0.93
7G8^{EcuD}	IC_{50}	16.5 ± 1.8	19.4 ± 0.9	31.6 ± 3.8	19.1 ± 1.4	1.31 ± 0.20	1.43 ± 0.17
	n	5	5	5	5	6	6
	P	0.17	0.098	**0.0037**	0.67	**0.044**	0.44
7G8^{EcuAB}	IC_{50}	10.2 ± 0.8	11.8 ± 1.2	10.8 ± 0.8	17.9 ± 1.1	0.86 ± 0.11	0.80 ± 0.07
	n	5	5	5	5	4	5
	P	**0.010**	**0.014**	**0.0001**	0.82	0.93	**0.0009**
7G8^{EcuAC}	IC_{50}	8.7 ± 0.6	8.0 ± 0.8	33.2 ± 1.9	24.6 ± 2.6	0.62 ± 0.09	0.64 ± 0.06
	n	5	5	5	5	4	5
	P	**0.0001**	**0.0001**	**0.0003**	**0.042**	0.056	**< 0.0001**
7G8^{EcuAD}	IC_{50}	14.6 ± 0.9	15.9 ± 1.1	26.7 ± 1.8	24.0 ± 1.4	0.71 ± 0.07	1.19 ± 0.12
	n	5	5	5	5	4	5
	P	0.40	0.82	**0.011**	**0.0077**	0.30	0.32
7G8^{EcuBC}	IC_{50}	15.2 ± 1.3	17.9 ± 1.4	38.3 ± 1.9	27.1 ± 2.4	0.80 ± 0.11	1.30 ± 0.15
	n	5	5	5	5	4	5
	P	0.31	0.44	**0.0001**	**0.0005**	0.84	0.80

(continued)

Table 2.4. *continued*

Line		CQ IC_{50}	CQ+VP IC_{50}	md-CQ IC_{50}	md-AQ IC_{50}	LUM IC_{50}	AS IC_{50}
7G8^{EcuBD}	IC_{50}	13.8 ± 0.9	16.9 ± 1.5	16.1 ± 1.0	20.0 ± 0.9	1.20 ± 0.13	1.34 ± 0.13
	n	5	5	5	5	4	5
	P	0.80	0.73	**0.024**	0.55	0.16	0.82
7G8^{EcuCD}	IC_{50}	15.4 ± 1.3	18.8 ± 1.7	38.9 ± 1.9	28.0 ± 3.1	0.75 ± 0.07	1.30 ± 0.13
	n	5	5	5	5	4	5
	P	0.27	0.31	**0.0001**	**0.0015**	0.64	0.97
7G8^{EcuABC}	IC_{50}	19.8 ± 2.1	16.0 ± 1.9	111 ± 8.6	44.6 ± 5.5	0.44 ± 0.07	0.68 ± 0.06
	n	5	5	5	5	4	6
	P	**0.020**	0.82	**0.0001**	**0.0001**	**0.010**	**< 0.0001**
7G8^{EcuABD}	IC_{50}	19.4 ± 1.9	21.7 ± 2.1	52.4 ± 2.7	23.8 ± 1.0	0.69 ± 0.10	1.44 ± 0.10
	n	5	5	5	5	4	6
	P	**0.019**	**0.042**	**0.0001**	**0.0054**	0.60	0.60
7G8^{EcuACD}	IC_{50}	26.7 ± 1.9	16.9 ± 2.4	176 ± 9.9	60.8 ± 2.5	0.62 ± 0.04	0.98 ± 0.07
	n	5	5	5	5	4	6
	P	**0.0005**	0.95	**0.0001**	**0.0001**	0.12	**0.037**
7G8^{EcuBCD}	IC_{50}	16.7 ± 1.9	18.7 ± 2.4	33.4 ± 1.6	25.2 ± 1.1	0.78 ± 0.11	1.63 ± 0.10
	n	5	5	5	5	4	6
	P	0.20	0.50	**0.0005**	**0.0005**	0.76	**0.019**
7G8^{EcuABCD}	IC_{50}	75.2 ± 7.5	46.9 ± 2.7	455 ± 44.3	113 ± 6.1	0.81 ± 0.14	0.79 ± 0.09
	n	5	5	5	5	6	6
	P	**0.0001**	**0.0001**	**0.0001**	**0.0001**	0.65	**0.0013**
7G8^{7G8}	IC_{50}	137 ± 7.7	89.4 ± 5.1	634 ± 30.1	154 ± 5.8	0.64 ± 0.06	0.89 ± 0.05
	n	15	15	15	15	13	17
	P	**< 0.0001**	**< 0.0001**	**< 0.0001**	**< 0.0001**	**0.023**	**< 0.0001**
GC03	IC_{50}	17.0 ± 2.2	19.9 ± 2.7	20.9 ± 1.6	19.2 ± 1.7	1.99 ± 0.10	1.44 ± 0.10
	n	5	5	5	5	4	6
	P	0.23	0.27	0.93	0.57	**0.0008**	0.40

(continued)

Table 2.4. *continued*

Line		CQ IC_{50}	CQ+VP IC_{50}	md-CQ IC_{50}	md-AQ IC_{50}	LUM IC_{50}	AS IC_{50}
Ecu1110	IC_{50}	79.3 ± 6.5	64.4 ±7.6	370 ± 15.0	86.1 ± 4.0	1.22 ± 0.21	0.96 ± 0.08
	n	5	5	5	5	4	6
	P	**0.0001**	**0.0001**	**0.0001**	**0.0001**	0.26	**0.038**
7G8	IC_{50}	160 ± 16.1	102 ± 9.1	749 ± 54.4	174 ± 10.2	0.54 ± 0.07	0.69 ± 0.08
	n	5	5	5	5	6	6
	P	**0.0001**	**0.0001**	**0.0001**	**0.0001**	**0.0087**	**0.0001**

[a]IC_{50} values (nM) indicate the mean IC_{50} ± SEM, as determined in 4 to 17 independent assays. CQ + VP assays were performed with 0.8 µM VP. CQ, chloroquine; VP, verapamil; md-CQ, monodesethyl-chloroquine; md-AQ, monodesethyl-amodiaquine; LUM, lumefantrine; AS, artesunate; *n*, number of assays; *P, P* value, as determined in a non-parametric Mann-Whitney *U* test versus the wild-type *pfcrt*-encoding parasite line $7G8^{GC03}$. *P* values <0.05 are indicated in **bold** and shaded in grey.

Table 2.5. Antimalarial IC_{90} values of *pfcrt*-modified and reference parasite lines.[a]

Line		CQ IC_{90}	CQ+VP IC_{90}	md-CQ IC_{90}	md-AQ IC_{90}	LUM IC_{90}	AS IC_{90}
$7G8^{GC03}$	IC_{90}	25.4 ± 1.8	31.9 ± 2.2	40.5 ± 2.7	29.1 ± 1.3	3.77 ± 0.20	3.71 ± 0.18
	n	15	15	15	15	14	17
	P	–	–	–	–	–	–
$7G8^{EcuA}$	IC_{90}	25.6 ± 2.8	27.7 ± 1.1	39.5 ± 4.8	33.9 ± 4.4	3.21 ± 0.41	2.60 ± 0.34
	n	5	5	5	5	6	6
	P	0.93	0.41	0.95	0.40	0.11	**0.0095**
$7G8^{EcuB}$	IC_{90}	27.1 ± 1.8	29.3 ± 0.3	44.5 ± 5.1	33.2 ± 3.8	3.92 ± 0.28	3.56 ± 0.47
	n	5	5	5	5	6	6
	P	0.45	0.92	0.61	0.40	0.66	0.99
$7G8^{EcuC}$	IC_{90}	30.8 ± 1.5	36.8 ± 2.8	111 ± 7.3	50.6 ± 5.5	3.87 ± 0.27	3.64 ± 0.40
	n	5	5	5	5	6	6
	P	0.066	**0.042**	**0.0001**	**0.0005**	0.84	0.91
$7G8^{EcuD}$	IC_{90}	30.5 ± 2.1	30.7 ± 0.4	56.4 ± 3.8	32.4 ± 3.0	4.81 ± 0.73	3.92 ± 0.51
	n	5	5	5	5	6	6
	P	0.14	0.23	**0.015**	0.36	0.27	0.55
$7G8^{EcuAB}$	IC_{90}	21.5 ± 3.2	27.1 ± 3.9	29.5 ± 2.9	31.9 ± 2.4	2.97 ± 0.46	2.22 ± 0.19
	n	5	5	5	5	4	5
	P	0.25	0.18	**0.014**	0.44	0.082	**0.0003**
$7G8^{EcuAC}$	IC_{90}	25.3 ± 2.1	25.3 ± 1.1	111 ± 9.4	57.0 ± 3.0	2.77 ± 0.39	2.60 ± 0.82
	n	5	5	5	5	4	5
	P	0.93	**0.024**	**0.0001**	**0.0001**	**0.043**	**0.046**
$7G8^{EcuAD}$	IC_{90}	29.2 ± 1	33.5 ± 2.6	57.8 ± 4.4	33.5 ± 2.7	3.96 ± 0.26	3.29 ± 0.32
	n	5	5	5	5	4	5
	P	0.20	0.23	**0.008**	0.080	0.80	0.44
$7G8^{EcuBC}$	IC_{90}	31.4 ± 2.3	38.5 ± 3.8	91 ± 10.3	43.1 ± 4.3	4.30 ± 0.32	3.32 ± 0.32
	n	5	5	5	5	4	5
	P	0.081	0.14	**0.0003**	**0.0009**	0.10	0.26

(continued)

Table 2.5. *continued*

Line		CQ IC_{90}	CQ+VP IC_{90}	md-CQ IC_{90}	md-AQ IC_{90}	LUM IC_{90}	AS IC_{90}
7G8^{EcuBD}	IC_{90}	27.7 ± 0.9	32.2 ± 3.7	36.1 ± 3.1	30.7 ± 1.1	4.66 ± 0.28	3.58 ± 0.15
	n	5	5	5	5	4	5
	P	0.44	0.80	0.46	0.31	**0.046**	0.75
7G8^{EcuCD}	IC_{90}	31.5 ± 2.3	38.6 ± 2.9	79.3 ± 7.9	40.2 ± 5.3	4.36 ± 0.65	3.65 ± 0.25
	n	5	5	5	5	4	5
	P	0.12	0.17	**0.0001**	**0.0037**	0.44	0.93
7G8^{EcuABC}	IC_{90}	45.2 ± 6.2	47.1 ± 3.8	377 ± 58.7	117 ± 13.0	1.96 ± 0.15	2.17 ± 0.31
	n	5	5	5	5	4	6
	P	**0.0054**	**0.0077**	**0.0001**	**0.0001**	**0.0007**	**0.0012**
7G8^{EcuABD}	IC_{90}	40.7 ± 4.7	47.1 ± 6.5	125 ± 9.1	47.4 ± 4.3	3.57 ± 0.21	3.26 ± 0.22
	n	5	5	5	5	4	6
	P	**0.0054**	**0.011**	**0.0001**	**0.0005**	0.53	0.22
7G8^{EcuACD}	IC_{90}	70.8 ± 9.1	52.9 ± 5.2	475 ± 25.6	130 ± 13.2	2.40 ± 0.15	2.34 ± 0.17
	n	5	5	5	5	4	6
	P	**0.0001**	**0.0025**	**0.0001**	**0.0001**	**0.0046**	**0.0001**
7G8^{EcuBCD}	IC_{90}	35.7 ± 3.7	42.0 ± 5.6	85.5 ± 12.4	51.3 ± 2.8	3.61 ± 0.15	3.77 ± 0.22
	n	5	5	5	5	4	6
	P	**0.033**	**0.019**	**0.0003**	**0.0003**	0.56	0.85
7G8^{EcuABCD}	IC_{90}	170 ± 21.9	115 ± 3.6	1005 ± 64.0	245 ± 28.0	3.36 ± 0.41	2.84 ± 0.47
	n	5	5	5	5	6	6
	P	**0.0001**	**0.0001**	**0.0001**	**0.0001**	0.47	0.090
7G8^{7G8}	IC_{90}	289 ± 17.3	212 ± 11.2	1392 ± 88.1	282 ± 14.8	3.42 ± 0.30	2.60 ± 0.17
	n	15	15	15	15	14	17
	P	**< 0.0001**	**< 0.0001**	**< 0.0001**	**< 0.0001**	0.12	**< 0.0001**
GC03	IC_{90}	30.3 ± 3.3	39.6 ± 5.4	45.1 ± 4.5	27.3 ± 1.3	8.27 ± 0.11	4.51 ± 0.25
	n	5	5	5	5	4	6
	P	0.20	0.27	0.35	0.45	**0.0007**	**0.029**

(continued)

Table 2.5. *continued*

Line		CQ IC_{90}	CQ+VP IC_{90}	md-CQ IC_{90}	md-AQ IC_{90}	LUM IC_{90}	AS IC_{90}
Ecu1110	IC_{90}	187 ± 20.5	164 ± 19.4	881 ± 28.6	167 ± 14.1	5.49 ± 0.98	3.29 ± 0.38
	n	5	5	5	5	4	6
	P	**0.0001**	**0.0001**	**0.0001**	**0.0001**	0.061	0.46
7G8	IC_{90}	309 ± 40.5	226 ± 9.0	1509 ± 160	312 ± 32.8	2.22 ± 0.16	2.46 ± 0.48
	n	5	5	5	5	6	6
	P	**0.0001**	**0.0001**	**0.0001**	**0.0001**	**0.0002**	**0.023**

[a]IC_{90} values (nM) indicate the mean IC_{90} ± SEM, as determined in 4 to 17 independent assays. CQ + VP assays were performed with 0.8 μM VP. CQ, chloroquine; VP, verapamil; md-CQ, monodesethyl-chloroquine; md-AQ, monodesethyl-amodiaquine; LUM, lumefantrine; AS, artesunate; *n*, number of assays; *P, P* value, as determined in a non-parametric Mann-Whitney *U* test versus the wild-type *pfcrt*-encoding parasite line $7G8^{GC03}$. *P* values <0.05 are indicated in **bold** and shaded in grey.

Table 2.6. Successive contributions of Ecu1110 PfCRT mutations to CQ resistance.[a]

Preceding haplotype		+ K76T (Ecu_A)	+ A220S (Ecu_B)	+ N326D (Ecu_C)	+ I356L (Ecu_D)
GC03 (WT)	Succeeding haplotype	Ecu_A	Ecu_B	Ecu_C	Ecu_D
	CQ IC_{50}	ns	ns	ns	ns
	md-CQ IC_{50}	↓ (*)	ns	↑ (***)	↑ (**)
Ecu_A	Succeeding haplotype		Ecu_{AB}	Ecu_{AC}	Ecu_{AD}
	CQ IC_{50}	–	ns	ns	↑ (*)
	md-CQ IC_{50}		↓ (*)	↑ (**)	↑ (**)
Ecu_B	Succeeding haplotype	Ecu_{AB}		Ecu_{BC}	Ecu_{BD}
	CQ IC_{50}	↓ (*)	–	ns	ns
	md-CQ IC_{50}	↓ (**)		↑ (**)	ns
Ecu_C	Succeeding haplotype	Ecu_{AC}	Ecu_{BC}		Ecu_{CD}
	CQ IC_{50}	↓ (**)	ns	–	ns
	md-CQ IC_{50}	↓ (**)	↓ (*)		↓ (*)
Ecu_D	Succeeding haplotype	Ecu_{AD}	Ecu_{BD}	Ecu_{CD}	
	CQ IC_{50}	ns	ns	ns	–
	md-CQ IC_{50}	ns	↓ (**)	ns	
Ecu_{AB}	Succeeding haplotype			Ecu_{ABC}	Ecu_{ABD}
	CQ IC_{50}	–	–	↑ (**)	↑ (**)
	md-CQ IC_{50}			↑ (**)	↑ (**)
Ecu_{AC}	Succeeding haplotype		Ecu_{ABC}		Ecu_{ACD}
	CQ IC_{50}	–	↑ (**)	–	↑ (**)
	md-CQ IC_{50}		↑ (**)		↑ (**)
Ecu_{AD}	Succeeding haplotype		Ecu_{ABD}	Ecu_{ACD}	
	CQ IC_{50}	–	ns	↑ (**)	–
	md-CQ IC_{50}		↑ (**)	↑ (**)	

(continued)

Table 2.6. *continued*

Preceding haplotype		+ K76T (Ecu_A)	+ A220S (Ecu_B)	+ N326D (Ecu_C)	+ I356L (Ecu_D)
Ecu_{BC}	Succeeding haplotype	Ecu_{ABC}			Ecu_{BCD}
	CQ IC_{50}	ns	–	–	ns
	md-CQ IC_{50}	↑ (**)			ns
Ecu_{BD}	Succeeding haplotype	Ecu_{ABD}		Ecu_{BCD}	
	CQ IC_{50}	↑ (*)	–	ns	–
	md-CQ IC_{50}	↑ (**)		↑ (**)	
Ecu_{CD}	Succeeding haplotype	Ecu_{ACD}	Ecu_{BCD}		
	CQ IC_{50}	↑ (**)	ns	–	–
	md-CQ IC_{50}	↑ (**)	ns		
Ecu_{ABC}	Succeeding haplotype				Ecu_{ABCD}
	CQ IC_{50}	–	–	–	↑ (**)
	md-CQ IC_{50}				↑ (**)
Ecu_{ABD}	Succeeding haplotype			Ecu_{ABCD}	
	CQ IC_{50}	–	–	↑ (**)	–
	md-CQ IC_{50}			↑ (**)	
Ecu_{ACD}	Succeeding haplotype		Ecu_{ABCD}		
	CQ IC_{50}	–	↑ (**)	–	–
	md-CQ IC_{50}		↑ (**)		
Ecu_{BCD}	Succeeding haplotype	Ecu_{ABCD}			
	CQ IC_{50}	↑ (**)	–	–	–
	md-CQ IC_{50}	↑ (**)			

[a]Chloroquine (CQ) and monodesethyl-chloroquine (md-CQ) IC_{50} values (**Table 2.4**) were subjected to non-parametric Mann-Whitney *U* tests to determine whether acquisition of the indicated Ecu1110 PfCRT mutation by a precursor PfCRT haplotype caused a significant increase (↑) or decrease (↓) in the IC_{50} value of the succeeding haplotype. Significant (P<0.05) differences are shaded in grey. PfCRT haplotypes are detailed in **Table 2.3**. WT, wild-type; *, P<0.05; **, P<0.01; ***, P<0.001.

In contrast, Ecu$_B$ A220S only increased resistance in the context of triple-SNP PfCRT haplotypes, while conferring decreased md-CQ resistance for double-SNP haplotypes. The mutational milieu was likewise important for Ecu$_A$ K76T, which decreased drug resistance for haplotypes leading up to the triple-SNP stage, at which point it conferred increased resistance. In addition, as compared to Ecu$_{ABCD}$, we observed significantly increased CQ (**Figure 2.2*A***; $P<0.001$) and md-CQ (**Figure 2.2*B***; $P<0.01$) IC_{50} values for 7G8 PfCRT, indicating a direct role for C72S, the sole distinction between these two haplotypes (see **Table 2.3**).

A characteristic trait of in vitro parasite CQR is its reversibility by VP, which was previously linked to the parasite *pfcrt* locus via quantitative trait loci mapping.[280] To examine the roles of specific *pfcrt* mutations on VP reversibility of CQR, we assessed parasite susceptibility to CQ in the presence or absence of 0.8 μM VP and computed the CQ response modification index (RMI), defined as the ratio between the IC_{50} for CQ plus VP and the IC_{50} for CQ alone (**Figure 2.2*C***; **Table 2.7**). Consistent with published VP reversibility profiles,[133] Ecu1110 and 7G8 reference parasites exhibited comparable VP chemosensitization of CQR (1.5 to 1.9-fold reductions in CQ RMI relative to the CQ-sensitive line GC03). This finding was recapitulated by isogenic parasites expressing the corresponding *pfcrt* alleles (1.7 to 1.8-fold reductions in CQ RMI for $7G8^{EcuABCD}$ and $7G8^{7G8}$ relative to $7G8^{GC03}$). Moreover, we noted direct roles for K76T and N326D in the VP reversibility effect, as the mutational acquisition of Ecu$_A$ K76T by the Ecu$_{BCD}$ PfCRT haplotype and the acquisition of Ecu$_C$ N326D by the Ecu$_{ABD}$ haplotype both conferred VP-reversible CQR to parasites encoding the resulting Ecu$_{ABCD}$ haplotype ($P<0.01$ for both trajectories).

Table 2.7. Verapamil-mediated CQ resistance reversibility of *pfcrt*-modified and reference parasite lines.[a]

Line			Line			Line		
	RMI	1.18 ± 0.05		RMI	1.09 ± 0.04		RMI	1.13 ± 0.07
7G8^{GC03}	*n*	15	7G8^{EcuAD}	*n*	5	7G8^{EcuBCD}	*n*	5
	P	–		*P*	0.60		*P*	0.82
	RMI	1.06 ± 0.04		RMI	1.18 ± 0.05		RMI	0.64 ± 0.05
7G8^{EcuA}	*n*	5	7G8^{EcuBC}	*n*	5	7G8^{EcuABCD}	*n*	5
	P	0.11		*P*	0.92		*P*	**0.0001**
	RMI	1.14 ± 0.06		RMI	1.22 ± 0.05		RMI	0.70 ± 0.02
7G8^{EcuB}	*n*	5	7G8^{EcuBD}	*n*	5	7G8^{7G8}	*n*	15
	P	0.38		*P*	0.60		*P*	**< 0.0001**
	RMI	1.28 ± 0.13		RMI	1.22 ± 0.06		RMI	1.17 ± 0.05
7G8^{EcuC}	*n*	5	7G8^{EcuCD}	*n*	5	GC03	*n*	5
	P	0.82		*P*	0.69		*P*	0.85
	RMI	1.24 ± 0.11		RMI	0.81 ± 0.07		RMI	0.81 ± 0.06
7G8^{EcuD}	*n*	5	7G8^{EcuABC}	*n*	5	Ecu1110	*n*	5
	P	0.92		*P*	**0.0002**		*P*	**0.0015**
	RMI	1.15 ± 0.03		RMI	1.12 ± 0.05		RMI	0.62 ± 0.05
7G8^{EcuAB}	*n*	5	7G8^{EcuABD}	*n*	5	7G8	*n*	5
	P	0.85		*P*	0.48		*P*	**0.0001**
	RMI	0.91 ± 0.07		RMI	0.62 ± 0.06			
7G8^{EcuAC}	*n*	5	7G8^{EcuACD}	*n*	5			
	P	**0.0086**		*P*	**0.0001**			

[a]Reversibility of chloroquine (CQ) resistance by 0.8 µM verapamil (VP) is indicated as the CQ response modification index (RMI), equivalent to (IC_{50} for CQ+VP) ÷ (IC_{50} for CQ only). Shown are mean RMI ± SEM values, as determined in 5 to 15 independent assays. *n*, number of assays; *P, P* value, as determined in a non-parametric Mann-Whitney *U* test versus the parasite line 7G8^{GC03}. *P* values <0.05 are indicated in **bold** and shaded in grey.

Effect of *pfcrt* combinatorial alleles on parasite susceptibility to ACT component drugs

In view of the role of PfCRT as a determinant of parasite multidrug resistance,[114] we investigated the influence of combinatorial PfCRT haplotypes on parasite susceptibility to the artemisinin compound AS and the ACT partner drugs AQ and LUM (**Figure 2.3**), which comprise the widely used ACT formulations AS-AQ and ATM-LUM.[180] The quinoline-type antimalarial AQ is of particular interest due to its historical use in regions with parasites harboring the Ecu1110 and 7G8 *pfcrt* alleles.[259] Focusing on the clinically relevant metabolite of AQ, md-AQ, we observed substantial overlap between parasites' susceptibility to md-AQ (**Figure 2.3*A***; **Table 2.4**) and md-CQ (**Figure 2.2*B***; **Table 2.4**). This is consistent with cross-resistance between CQ and AQ that is mediated in part by PfCRT variants.[114] Similar to our results for CQ, K76T was insufficient to confer md-AQ resistance (**Figure 2.3*A***; **Table 2.4**). Of note, an important role in mediating md-AQ resistance was uncovered for Ecu_C N326D, as acquisition of N326D by any PfCRT haplotype lacking this mutation consistently conferred elevated md-AQ IC_{50} and/or IC_{90} values (**Tables 2.4–2.5**). As $7G8^{7G8}$ parasites showed significantly higher md-AQ IC_{50} values than $7G8^{EcuABCD}$ parasites ($P<0.01$), we also identified a contributory role for PfCRT C72S in md-AQ resistance.

Treatment of parasite lines with the arylaminoalcohol drug LUM yielded more subtle differences in drug responses (**Figure 2.3*B***; **Table 2.4**). Compared to the $7G8^{GC03}$ line, we observed a modest (1.4-fold), although significant, increase in LUM susceptibility for $7G8^{7G8}$ parasites, in line with previous reports that CQ-resistant PfCRT haplotypes confer increased LUM susceptibility.[213] We attribute the

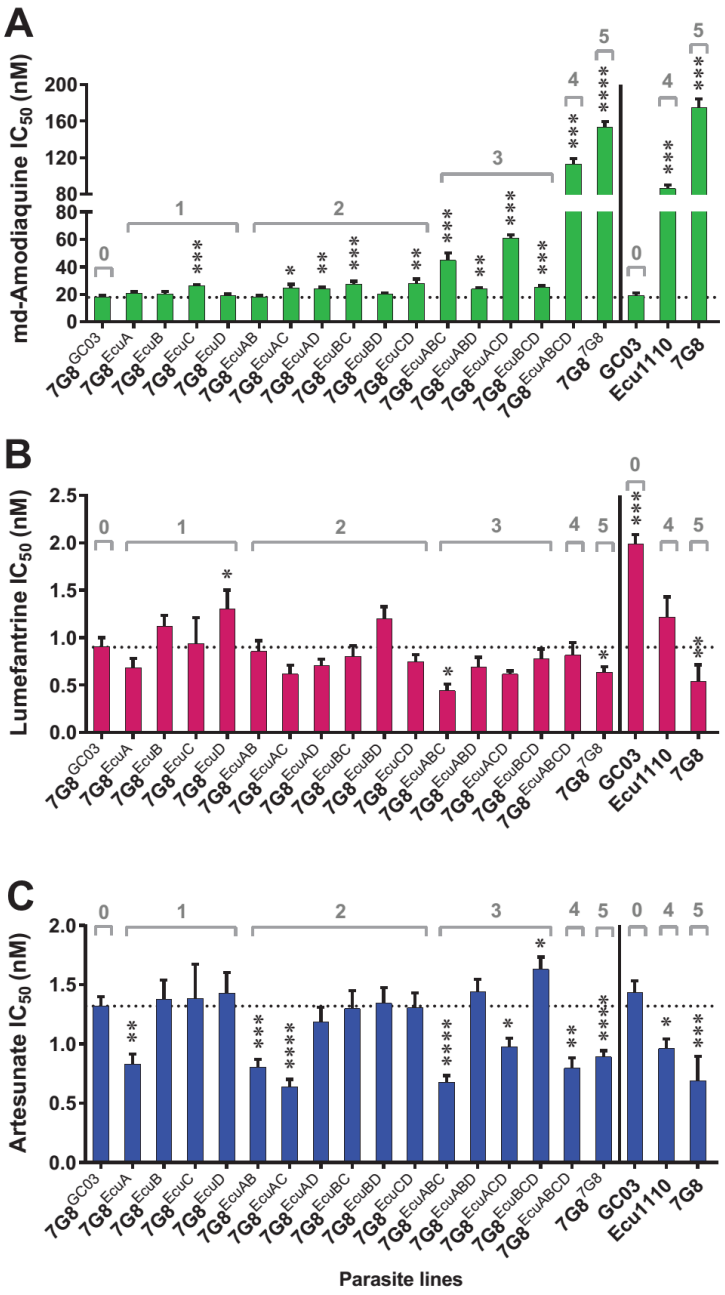

Figure 2.3. Susceptibility of *pfcrt*-modified and reference parasite lines to first-line antimalarial compounds monodesethyl-amodiaquine (md-AQ), lumefantrine (LUM), and artesunate (AS). Parasite growth inhibition was determined by flow cytometry after 72 h exposure to serial dilutions of (**A**) md-AQ, (**B**) LUM, or (**C**) AS. Bar graphs indicate mean IC_{50} values ± SEM, as determined in 4 to 17 independent assays conducted in duplicate. Statistical differences were determined via non-parametric Mann-Whitney *U* tests, using the mean IC_{50} value of wild-type *pfcrt*-expressing $7G8^{GC03}$ parasites (dotted black line) as the comparator. The total number of *pfcrt* mutations encoded by parasite lines is indicated in gray. When applicable, the y-axis was split to illustrate subtle, statistically significant differences in IC_{50} values. IC_{50} and IC_{90} values, numbers of assays, and corresponding statistical tests are summarized in **Tables 2.4**-**2.5**. **P*<0.05; ***P*<0.01; ****P*<0.001. *****P*<0.0001.

constricted range of observed LUM IC_{50} values to the high sensitivity of the 7G8 genetic background to LUM at baseline.[243] Our LUM susceptibility findings nevertheless illustrate that *pfcrt* mutations exert opposing forces on parasite LUM resistance (e.g. $7G8^{EcuABC}$ and $7G8^{EcuD}$ respectively showed elevated and reduced LUM IC_{50} values, as compared to $7G8^{GC03}$; **Figure 2.3*B*; Table 2.4**).

Consistent with previous *in vitro* investigations,[120] our collection of combinatorial *pfcrt* alleles modulated parasite susceptibility to the artemisinin compound AS (**Figure 2.3*C*; Table 2.4**). As anticipated, full-length mutant *pfcrt* alleles significantly increased AS sensitivity (1.5 to 1.7-fold decrease in AS IC_{50} for $7G8^{EcuABCD}$ and $7G8^{7G8}$ as compared to $7G8^{GC03}$). Interestingly, K76T was sufficient to confer increased parasite AS sensitivity (1.6-fold decrease in AS IC_{50} for $7G8^{EcuA}$ versus $7G8^{GC03}$). Additionally, increased parasite AS resistance was afforded upon acquisition of Ecu_D I356L, with two distinct mutational trajectories (Ecu_{AB}→Ecu_{ABD} and Ecu_{AC}→Ecu_{ACD}; **Figure 2.3*C*; Table 2.4**) conferring significant elevations in AS IC_{50} values ($P<0.01$ and $P<0.05$, respectively).

Effect of *pfcrt* combinatorial alleles on *in vitro* parasite growth

As organisms acquire mutations in response to drug pressure, they experience fitness constraints that affect the course of their adaptive evolution. Accordingly, we evaluated the impact of our set of combinatorial *pfcrt* alleles on the *in vitro* growth of intra-erythrocytic parasites, which serves as a proxy for fitness.[239,240] To initiate the growth assays, we seeded co-cultures with equal (1:1) proportions of CQ-sensitive (wild-type *pfcrt*) GFP-positive (GFP^+) reporter parasites and *pfcrt*-modified GFP-negative (GFP^-) test parasites. Co-cultures were established in the absence or

presence of a sub-lethal dose of CQ (7.5 nM; 0.5×CQ IC_{50} of CQ-sensitive reporter line). Using flow cytometry, we regularly determined the proportion of co-culture expressing the test *pfcrt* allele (GFP^- parasite population). The relative proportions of parasite populations were recorded every third day for 10 generations (**Figure 2.4*A***), natural log-transformed (**Figure 2.4*B***), and subjected to a linear regression analysis.[239,243] To quantify parasite fitness costs, we derived the relative fitness (ω) of a given parasite line as compared to isogenic, wild-type *pfcrt*-expressing parasites ($7G8^{GC03}$) in the absence of drug pressure and computed the per-generation selection coefficient (s) for each line as per the relationship $s=\omega'-1$. Thus, as compared to the wild-type *pfcrt* allele, $s=0$, $s>0$, and $s<0$ signify alleles that are selectively neutral, advantageous, and disadvantageous, respectively.

As compared to the $7G8^{GC03}$ parasite line, our isogenic, *pfcrt*-modified parasites exhibited various degrees of *in vitro* fitness (range of mean s values: -0.26 to 0.11), with the majority of *pfcrt* alleles conferring comparable ($s=0$) or inferior ($s<0$) relative fitness (**Figure 2.5**; **Table 2.8**). A notable exception was the Ecu_{AD} haplotype, which demonstrated significantly enhanced relative fitness ($s=0.07$ to 0.11, i.e. 7% to 11% growth advantage per parasite generation). Although we did not observe a selective advantage for any *pfcrt* alleles in the presence of 7.5 nM CQ, this sub-therapeutic CQ concentration had a significantly deleterious impact on the growth of parasites encoding haplotypes Ecu_A, Ecu_C, and Ecu_{AB} (**Figure 2.5**; **Table 2.8**). Notably, in this genetic background, PfCRT K76T was insufficient for CQ resistance and had a deleterious impact on parasite growth that was exacerbated by CQ. Interestingly, expression of the full-length Ecu1110 PfCRT haplotype in the Ecu1110 genetic background was associated with a significant reduction in growth

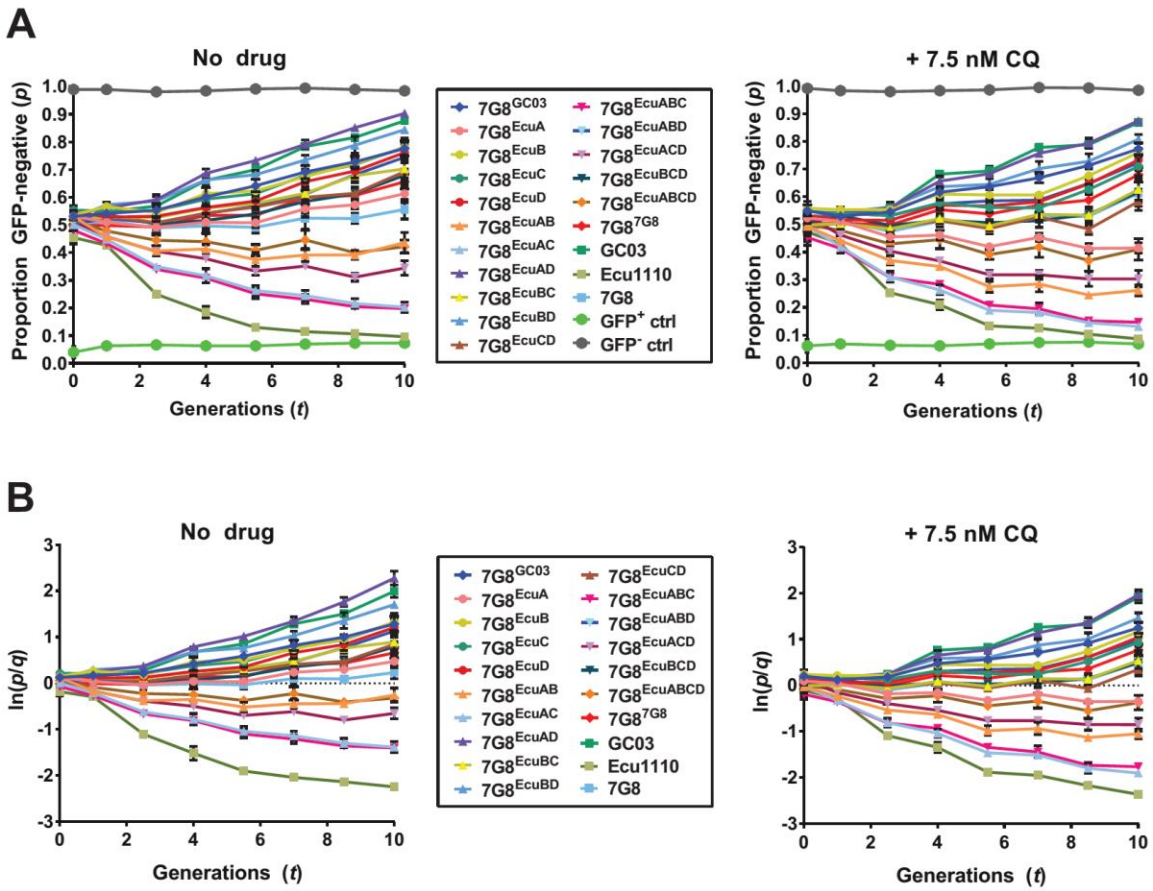

Figure 2.4. *In vitro* asexual blood stage growth data for *pfcrt*-modified and reference parasites. Co-cultures consisting of equal proportions of a single GFP-negative (GFP^-) test line and a GFP-positive (GFP^+) reporter line (R^{GFP}) were initiated at day 0 and monitored by flow cytometry for 10 parasite generations. Three independent assays were conducted in duplicate in the absence or presence of a sub-lethal dose of CQ (7.5 nM; 0.5×CQ IC_{50} of the CQ-sensitive R^{GFP} line). (**A**) Plots of mean ± SEM proportions of the GFP^- test (*pfcrt*-modified or reference) line (*p*) as a function of time (*t*, equivalent to number of parasite generations). GFP^+ (R^{GFP} only) and GFP^- ($7G8^{7G8}$ only) controls were included and showed levels of fluorescence that were consistent across time. (**B**) Plots of mean ± SEM natural log-transformed ratios of the GFP^- test line to the GFP^+ reporter line at time *t* (p_t/q_t) for each co-culture. These parameters were used to derive the *in vitro* growth selection coefficients of test lines (see **Figure 2.5**).

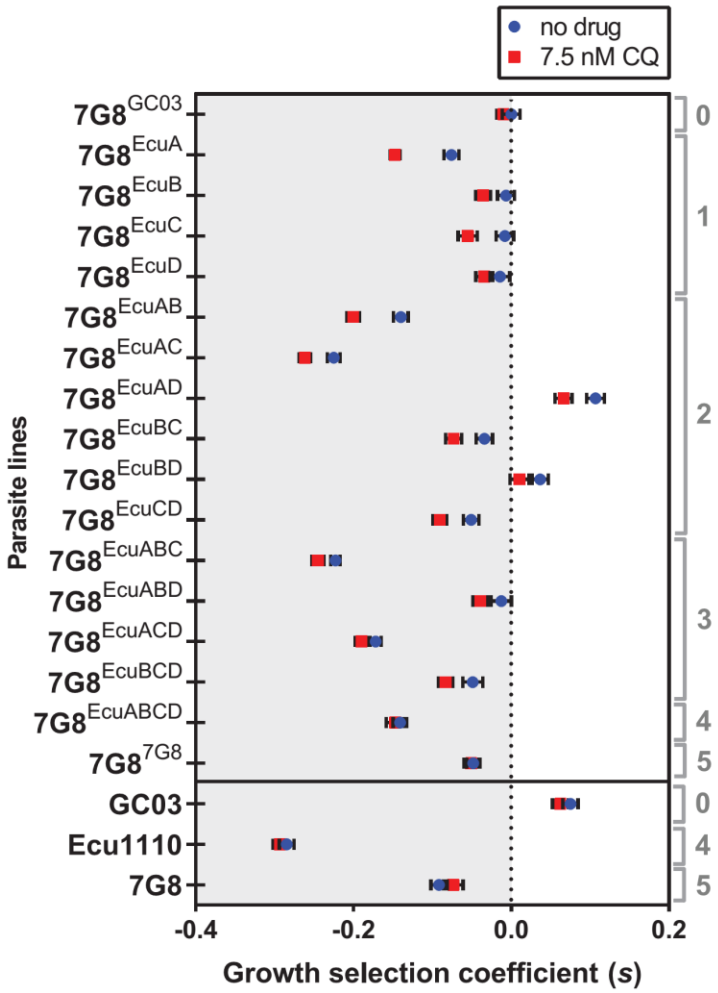

Figure 2.5. *In vitro* growth of *pfcrt*-modified and reference parasite lines. To assess parasite *in vitro* growth, co-cultures initially consisting of a 1:1 ratio of a single GFP^{-} test (recombinant or reference) line and a GFP^{+} reporter line (R^{GFP}) were monitored by flow cytometry for 10 generations. Three independent assays were conducted in duplicate in the absence or presence of a sub-lethal dose of chloroquine (CQ; 7.5 nM, equivalent to 0.5×CQ IC$_{50}$ of CQ-sensitive R^{GFP} line). The per-generation selection coefficient (*s*) for each test strain was derived from parasite growth curves (see **Figure 2.4**). Shown are mean ± SEM *s* values for lines subjected to no drug or 7.5 nM CQ. The total number of *pfcrt* mutations encoded by parasite lines is indicated in gray. Mean *s* values, as well as results of inter-strain and intra-strain statistical tests are summarized in **Table 2.8**.

Table 2.8. *In vitro* growth selection coefficients of *pfcrt*-modified and reference parasite lines.[a]

Line		No drug	7.5 nM CQ	Line		No drug	7.5 nM CQ	Line		No drug	7.5 nM CQ
7G8^{GC03}	*s*	0.00 ± 0.011	-0.01 ± 0.008	7G8^{EcuAD}	*s*	0.11 ± 0.011	0.07 ± 0.011	7G8^{EcuBCD}	*s*	-0.05 ± 0.013	-0.08 ± 0.009
	P_1	–	–		P_1	**< 0.0001**	**< 0.0001**		P_1	**0.011**	**< 0.0001**
	P_2	> 0.99			P_2	0.081			P_2	0.26	
7G8^{EcuA}	*s*	-0.08 ± 0.010	-0.15 ± 0.006	7G8^{EcuBC}	*s*	-0.03 ± 0.010	-0.07 ± 0.010	7G8^{EcuABCD}	*s*	-0.14 ± 0.009	-0.15 ± 0.011
	P_1	**< 0.0001**	**< 0.0001**		P_1	0.2563	**0.0002**		P_1	**< 0.0001**	**< 0.0001**
	P_2	**< 0.0001**			P_2	0.11			P_2	> 0.99	
7G8^{EcuB}	*s*	-0.01 ± 0.011	-0.04 ± 0.009	7G8^{EcuBD}	*s*	0.04 ± 0.010	0.01 ± 0.012	7G8^{7G8}	*s*	-0.05 ± 0.009	-0.05 ± 0.009
	P_1	> 0.99	0.74		P_1	0.17	0.95		P_1	**0.013**	0.069
	P_2	0.56			P_2	0.73			P_2	> 0.99	
7G8^{EcuC}	*s*	-0.01 ± 0.011	-0.06 ± 0.012	7G8^{EcuCD}	*s*	-0.05 ± 0.010	-0.09 ± 0.009	GC03	*s*	0.07 ± 0.010	0.06 ± 0.010
	P_1	> 0.99	**0.026**		P_1	**0.0064**	**< 0.0001**		P_1	**< 0.0001**	**< 0.0001**
	P_2	**0.018**			P_2	0.095			P_2	0.99	
7G8^{EcuD}	*s*	-0.01 ± 0.012	-0.03 ± 0.011	7G8^{EcuABC}	*s*	-0.22 ± 0.006	-0.25 ± 0.007	Ecu1110	*s*	-0.28 ± 0.009	-0.29 ± 0.009
	P_1	0.99	0.81		P_1	**< 0.0001**	**< 0.0001**		P_1	**< 0.0001**	**< 0.0001**
	P_2	0.96			P_2	0.91			P_2	> 0.99	
7G8^{EcuAB}	*s*	-0.14 ± 0.009	-0.20 ± 0.008	7G8^{EcuABD}	*s*	-0.01 ± 0.013	-0.04 ± 0.010	7G8	*s*	-0.09 ± 0.010	-0.07 ± 0.012
	P_1	**< 0.0001**	**< 0.0001**		P_1	0.99	0.52		P_1	**< 0.0001**	**0.0002**
	P_2	**0.0005**			P_2	0.72			P_2	0.99	
7G8^{EcuAC}	*s*	-0.23 ± 0.008	-0.26 ± 0.007	7G8^{EcuACD}	*s*	-0.17 ± 0.007	-0.19 ± 0.008				
	P_1	**< 0.0001**	**< 0.0001**		P_1	**< 0.0001**	**< 0.0001**				
	P_2	0.17			P_2	0.99					

[a]Parasite *in vitro* growth was evaluated in the absence or presence of a sub-lethal dose of CQ (7.5 nM; 0.5×CQ IC_{50} of the CQ-sensitive reference line 7G8^{GC03}) and normalized against 7G8^{GC03} in the absence of drug pressure (6 total replicates per condition). The per-generation selection coefficient (indicated above as *s* ± SEM) was derived from the relative fitness index (ω') as per the relationship $s = \omega' - 1$, such that $s<0$ and $s>0$ respectively indicate growth inferior or superior to the 7G8^{GC03} parasite line, which encodes wild-type *pfcrt*. CQ, chloroquine; P_1, *P* value for inter-strain comparisons, determined versus the parasite line 7G8^{GC03} using two-way ANOVA with Sidak's post-hoc test; P_2, *P* value for intra-strain comparisons, determined for a given parasite strain in the absence versus presence of 7.5 nM CQ using two-way ANOVA with Sidak's post-hoc test. *P* values <0.05 are indicated in **bold** and shaded in grey.

as compared to the 7G8 background (14% per-generation growth disadvantage for Ecu1110 versus $7G8^{Ecu1110}$ parasites, regardless of CQ pressure; $P<0.0001$). This suggests the presence of additional fitness-enhancing genetic factors in the 7G8 genetic background.

We further examined the specific contribution of PfCRT SNPs to parasite growth by identifying all instances in which mutational acquisition conferred a significant change in growth as compared to the precursor PfCRT haplotype (**Table 2.9**). In all such cases, K76T, A220S, and N326D (Ecu_A, Ecu_B, and Ecu_C, respectively) had a deleterious impact on parasite growth, with a single exception for Ecu_A K76T (increased growth for $Ecu_D \rightarrow Ecu_{AD}$; see **Table 2.9**). In contrast, Ecu_D I356L consistently increased *in vitro* growth. Additionally, as compared to Ecu_{ABCD}, 7G8 PfCRT conferred enhanced *in vitro* growth (10% growth advantage per generation for $7G8^{7G8}$ versus $7G8^{EcuABCD}$ parasites, regardless of CQ pressure; $P<0.0001$). Thus, in this genetic background, the 7G8 hallmark mutation C72S (see **Table 2.3**) positively contributed to both parasite drug resistance and growth rate.

Modeling the evolution of *pfcrt*-mediated CQR

The course of *P. falciparum* drug resistance evolution is shaped by the adaptive landscapes parasites traverse as they acquire drug resistance mutations. To further explore *pfcrt* adaptive landscapes, we employed a modified computational model based on previously established algorithms.[165,248,302] Briefly, experimentally derived drug resistance and growth data for isogenic parasites encoding all *pfcrt* alleles spanning the transition from CQ-sensitive (wild-type; GC03) to CQ-resistant (Ecu1110) were used to simulate adaptive landscapes, and the mutational pathway

Table 2.9. Successive contributions of Ecu1110 PfCRT mutations to *in vitro* parasite growth.[a]

Preceding haplotype		+ K76T (Ecu_A)	+ A220S (Ecu_B)	+ N326D (Ecu_C)	+ I356L (Ecu_D)
GC03 (WT)	Succeeding haplotype	Ecu_A	Ecu_B	Ecu_C	Ecu_D
	No drug	↓ (****)	ns	ns	ns
	7.5 nM CQ	↓ (****)	ns	ns	ns
Ecu_A	Succeeding haplotype		Ecu_{AB}	Ecu_{AC}	Ecu_{AD}
	No drug	–	↓ (**)	↓ (****)	↑ (****)
	7.5 nM CQ		↓ (*)	↓ (****)	↑ (****)
Ecu_B	Succeeding haplotype	Ecu_{AB}		Ecu_{BC}	Ecu_{BD}
	No drug	↓ (****)	–	ns	ns
	7.5 nM CQ	↓ (****)		ns	ns
Ecu_C	Succeeding haplotype	Ecu_{AC}	Ecu_{BC}		Ecu_{CD}
	No drug	↓ (****)	ns	–	ns
	7.5 nM CQ	↓ (****)	ns		ns
Ecu_D	Succeeding haplotype	Ecu_{AD}	Ecu_{BD}	Ecu_{CD}	
	No drug	↑ (****)	ns	ns	–
	7.5 nM CQ	↑ (****)	ns	↓ (*)	
Ecu_{AB}	Succeeding haplotype			Ecu_{ABC}	Ecu_{ABD}
	No drug	–	–	↓ (****)	↑ (****)
	7.5 nM CQ			ns	↑ (****)
Ecu_{AC}	Succeeding haplotype		Ecu_{ABC}		Ecu_{ACD}
	No drug	–	ns	–	↑ (*)
	7.5 nM CQ		ns		↑ (***)
Ecu_{AD}	Succeeding haplotype		Ecu_{ABD}	Ecu_{ACD}	
	No drug	–	↓ (****)	↓ (****)	–
	7.5 nM CQ		↓ (****)	↓ (****)	

(continued)

Table 2.9. *continued*

Preceding haplotype		+ K76T (Ecu_A)	+ A220S (Ecu_B)	+ N326D (Ecu_C)	+ I356L (Ecu_D)
	Succeeding haplotype	Ecu_{ABC}			Ecu_{BCD}
Ecu_{BC}	No drug	↓ (****)	–	–	ns
	7.5 nM CQ	↓ (****)			ns
	Succeeding haplotype	Ecu_{ABD}		Ecu_{BCD}	
Ecu_{BD}	No drug	ns	–	↓ (****)	–
	7.5 nM CQ	ns		↓ (****)	
	Succeeding haplotype	Ecu_{ACD}	Ecu_{BCD}		
Ecu_{CD}	No drug	↓ (****)	ns	–	–
	7.5 nM CQ	↓ (****)	ns		
	Succeeding haplotype				Ecu_{ABCD}
Ecu_{ABC}	No drug	–	–	–	↑ (****)
	7.5 nM CQ				↑ (****)
	Succeeding haplotype			Ecu_{ABCD}	
Ecu_{ABD}	No drug	–	–	↓ (****)	–
	7.5 nM CQ			↓ (****)	
	Succeeding haplotype		Ecu_{ABCD}		
Ecu_{ACD}	No drug	–	ns	–	–
	7.5 nM CQ		ns		
	Succeeding haplotype	Ecu_{ABCD}			
Ecu_{BCD}	No drug	↓ (****)	–	–	–
	7.5 nM CQ	↓ (**)			

[a]*In vitro* parasite growth selection coefficient values (**Table 2.8**) were analyzed by two-way ANOVA with Sidak's post-hoc test to determine whether acquisition of the indicated Ecu1110 PfCRT mutation by a precursor PfCRT haplotype resulted in a significant increase (↑) or decrease (↓) in the per-generation selection coefficient (*s*) of the succeeding PfCRT haplotype. Significant (P<0.05) differences are shaded in grey. PfCRT haplotypes are detailed in **Table 2.3**. CQ, chloroquine; WT, wild-type; *, P<0.05; **, P<0.01; ***, P<0.001; ****, P<0.0001.

accessibility was subsequently determined for each landscape. Pathways were deemed accessible only if each mutational step led to a progressive increase in the total fitness (f_T) of parasites. In our evolutionary model, f_T is comprised of normalized parasite growth (f_G) and drug resistance (f_D) indices as per the relationship $f_T = af_D + (1-a)f_G$, where f_D represents normalized IC_{50} values, f_G represents normalized relative *in vitro* growth values (ω) in the absence of drug, and the drug pressure coefficient a represents drug inhibitory level. In our simulations, f_D and f_G indices were generated from normal distributions based on the means and SEMs of *pfcrt* allele-specific IC_{50} and ω' values, respectively. Our model considers the role of drug pressure in facilitating CQR evolution via the drug pressure coefficient a (range: 0 to 1). Thus, selection is based solely on parasite growth rates for a=0 and on parasite drug resistance for a=1. Inspection of the parasite growth index (f_G) plotted as a function of the drug resistance index (f_D) based on simulations performed for CQ and md-CQ (**Figure 2.6**) revealed comparable trade-off profiles for the parent drug and its active metabolite, with no significant correlation observed between f_G and f_D, as per Pearson's correlation analysis (CQ: R^2=0.057, P=0.37; md-CQ: R^2=0.15, P=0.13).

Evolutionary modeling was first performed to determine the realization probabilities for the mutational pathways (p) leading from wild-type to the full-length Ecu1110 *pfcrt* allele via sequential acquisition of single mutations (0→1→2→3→4; **Figure 2.7*A***). Modeling was performed for a range of drug pressure scenarios by varying the coefficient a from 0 to 1 in 0.1 increments. For every a value, each of 10^4 adaptive landscapes was subjected to 10^5 evolutionary excursions (10^9 total excursions), and mutational pathway realization probabilities were

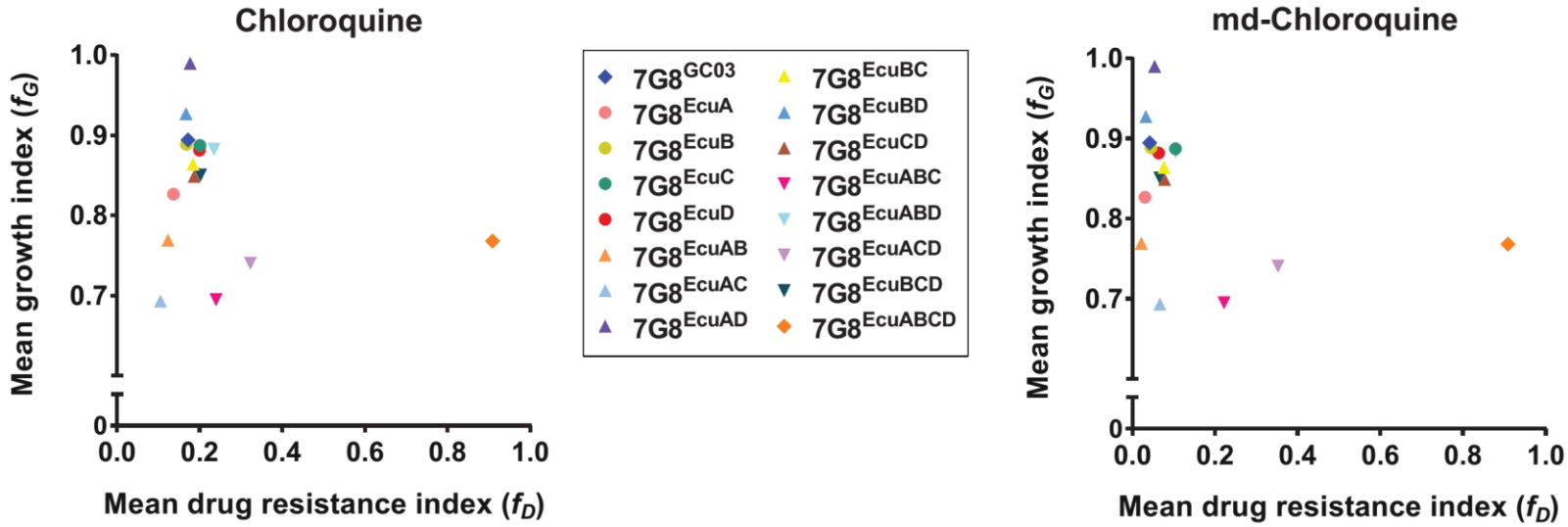

Figure 2.6. Trade-offs between parasite *in vitro* growth and drug resistance. For each *pfcrt*-modified strain, relative growth (f_G) in the absence of drug pressure was plotted as a function of the parasite's relative resistance (f_D) to chloroquine or monodesethyl-chloroquine. Calculation of f_G and f_D is detailed in **Methods.**

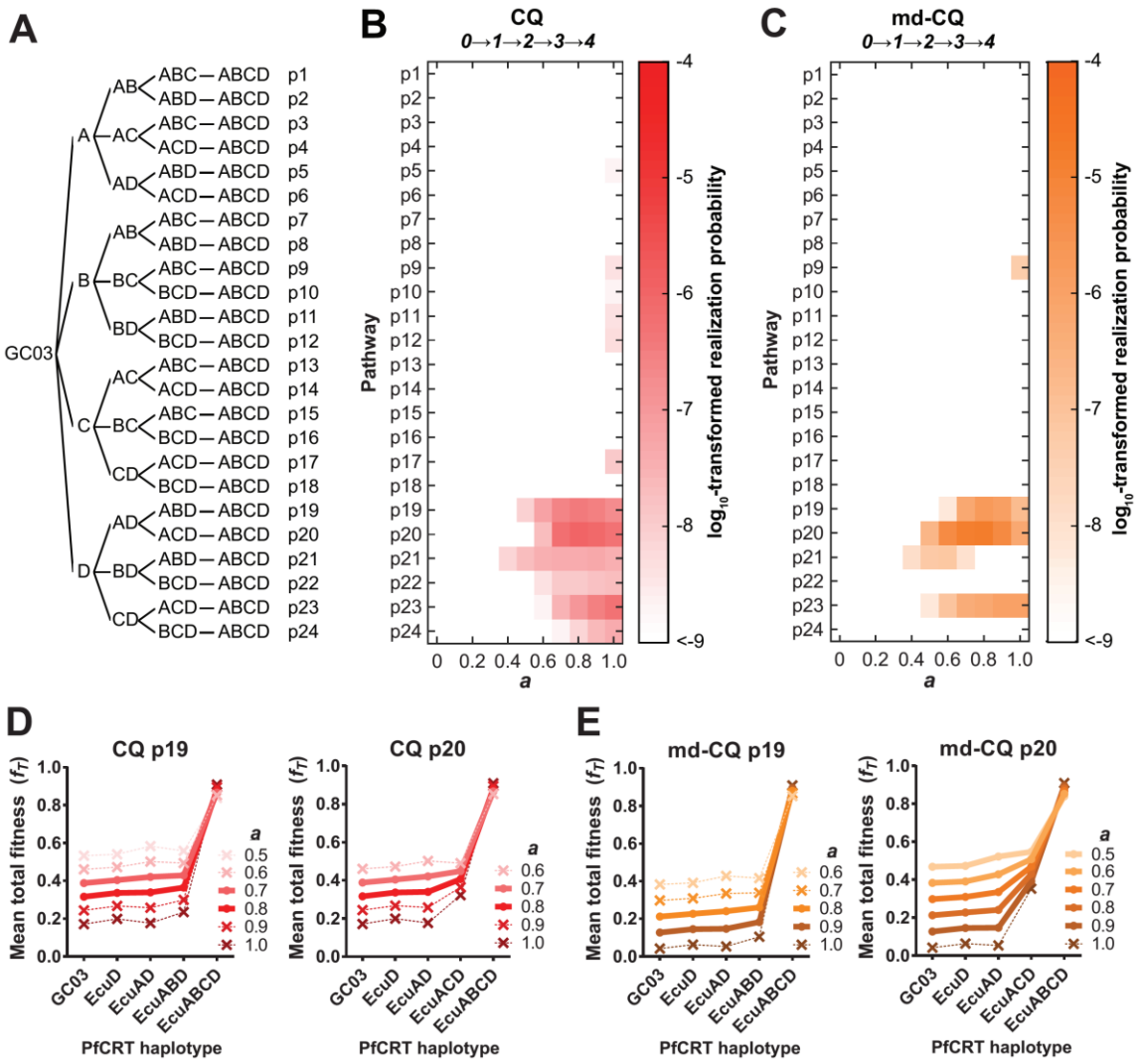

Figure 2.7. Modeling of chloroquine (CQ) and monodesethyl-chloroquine (md-CQ)-directed *pfcrt* evolution. (**A**) Schematic of the 24 theoretical pathways (p1 to p24) leading from wild-type (GC03) to Ecu1110 (ABCD) PfCRT via the sequential (0→1→2→3→4) acquisition of single mutations A, B, C, and D (K76T, A220S, N326D, and I356L, respectively). (**B** and **C**) Accessibility of mutational pathways for (**B**) CQ-directed and (**C**) md-CQ-directed evolutionary modeling. Adaptive landscapes were simulated based on experimentally derived parasite drug resistance and growth indices and used to quantify the realization probability for a given mutational pathway. Simulations explored the effect of drug pressure (*a*), from *a*=0 (i.e. growth rates fully dictate trajectory) through *a*=1 (i.e. parasite resistance fully dictates trajectory). Heat map color intensity corresponds to $\log_{10}$-transformed pathway realization probability. (**D** and **E**) Adaptive landscapes illustrating the interplay of total parasite fitness (f_T), mutations acquired, and extent of drug pressure (*a*). With regard to the total realization probability for all *a* values, the top two realized (**D**) CQ-directed and (**E**) md-CQ-directed mutational pathways are p19 and p20. Shown are trajectories for each of these mutational pathways based on mean f_T values, which encompass the complete set of simulated adaptive landscapes for each drug. Accessible (i.e. f_T increases progressively) and inaccessible (i.e. f_T valleys are present) trajectories are indicated by thick lines/circles and dotted lines/crosses, respectively. Plots of representative accessible mutational trajectories are shown in **Figure 2.8**.

recorded for modeling based on CQ (**Figure 2.7*B***) and md-CQ (**Figure 2.7*C***) data. The i^{th} pathway absolute realization probability (P_i) was calculated from the formula N_i / N_{total}, where N_i is the number of times that the simulations achieve the Ecu_{ABCD} allele by traversing pathway i, and N_{total} is the total number of runs. Pathway realization probabilities for evolutionary modeling of CQ and md-CQ resistance are reported in **Table 2.10** and **Table 2.11**, respectively. For both drugs, p20 (see **Figure 2.7*A***) showed the maximum realization probability, with a >10-fold increase in predictive ability for the active metabolite as compared to the parent drug (9.43×10^{-7} for CQ versus 1.39×10^{-5} for md-CQ). Highlighting the important interaction between parasite resistance (f_D) and growth (f_G) in dictating drug resistance evolution, the highest realization probabilities in both cases occurred for simulations in which total parasite fitness (f_T) was informed by both f_D and f_G indices (a=0.8).

Based on total pathway realization probabilities for both CQ and md-CQ modeling, the top two Ecu1110 *pfcrt* evolutionary pathways were p20 and p19 (**Tables 2.10–2.11**), which feature Ecu_D I356L as the first mutation acquired (see **Figure 2.7*A***). Remarkably, although accessible trajectories were observed for both pathways for a wide range of drug pressure scenarios (**Figure 2.8**), many excursions through these pathways were inaccessible due to the existence of adaptive valleys (i.e. f_T not progressively increasing), as highlighted by plots of mean f_T values encompassing all adaptive landscapes generated in our analysis for both CQ (**Figure 2.7*D***) and md-CQ (**Figure 2.7*E***) modeling. Our data show that, out of 10^9 total excursions simulated for each a value for the 0→1→2→3→4 mutational scenario, CQ-directed and md-CQ-directed evolution of the full-length Ecu1110 *pfcrt* allele were respectively supported by $\leq9.4\times10^2$ and $\leq1.4\times10^4$ excursions, with no

Table 2.10. Mutational pathway realization probabilities for CQ evolutionary modeling.[a]

	Mutational scenario: 0 → 1 → 2 → 3 → 4											
Pathway	***a* = 0**	***a* = 0.1**	***a* = 0.2**	***a* = 0.3**	***a* = 0.4**	***a* = 0.5**	***a* = 0.6**	***a* = 0.7**	***a* = 0.8**	***a* = 0.9**	***a* = 1.0**	**Total**
p1	0	0	0	0	0	0	0	0	0	0	0	0
p2	0	0	0	0	0	0	0	0	0	0	0	0
p3	0	0	0	0	0	0	0	0	0	0	0	0
p4	0	0	0	0	0	0	0	0	0	0	0	0
p5	0	0	0	0	0	0	0	0	0	0	2.0E-09	2.0E-09
p6	0	0	0	0	0	0	0	0	0	0	1.0E-09	1.0E-09
p7	0	0	0	0	0	0	0	0	0	0	0	0
p8	0	0	0	0	0	0	0	0	0	0	0	0
p9	0	0	0	0	0	0	0	0	0	0	4.0E-09	4.0E-09
p10	0	0	0	0	0	0	0	0	0	0	2.0E-09	2.0E-09
p11	0	0	0	0	0	0	0	0	1.0E-09	1.0E-09	4.0E-09	6.0E-09
p12	0	0	0	0	0	0	0	0	0	0	5.0E-09	5.0E-09
p13	0	0	0	0	0	0	0	0	0	0	0	0
p14	0	0	0	0	0	0	0	0	0	0	0	0
p15	0	0	0	0	0	0	0	0	0	0	0	0
p16	0	0	0	0	0	0	0	0	0	0	0	0
p17	0	0	0	0	0	0	0	0	0	0	1.1E-08	1.1E-08
p18	0	0	0	0	0	0	0	0	0	1.0E-09	0	1.0E-09
p19	0	0	0	0	0	8.0E-09	5.6E-08	2.4E-07	3.7E-07	3.0E-07	1.7E-07	1.1E-06
p20	0	0	0	0	0	0	2.1E-08	5.5E-07	9.4E-07	8.1E-07	5.0E-07	2.8E-06
p21	0	0	0	1.0E-09	7.0E-09	2.1E-08	3.2E-08	3.7E-08	4.3E-08	4.6E-08	3.4E-08	2.2E-07
p22	0	0	0	0	0	1.0E-09	4.0E-09	1.1E-08	1.2E-08	1.5E-08	1.8E-08	6.1E-08
p23	0	0	0	0	0	0	2.0E-09	2.8E-08	9.3E-08	2.7E-07	4.9E-07	8.8E-07
p24	0	0	0	0	0	0	0	2.0E-09	7.0E-09	2.5E-08	4.2E-08	7.6E-08
p1-p24	***0***	***0***	***0***	***1.0E-09***	***7.0E-09***	***3.0E-08***	***1.2E-07***	***8.7E-07***	***1.5E-06***	***1.5E-06***	***1.3E-06***	***5.2E-06***

(continued)

Table 2.10. *continued*

Mutational scenario: 0 → 1 → 2 → 4												
Pathway	***a* = 0**	***a* = 0.1**	***a* = 0.2**	***a* = 0.3**	***a* = 0.4**	***a* = 0.5**	***a* = 0.6**	***a* = 0.7**	***a* = 0.8**	***a* = 0.9**	***a* = 1.0**	**Total**
p25	0	0	0	0	0	0	0	0	0	0	1.0E-09	1.0E-09
p26	0	0	0	0	0	0	0	0	0	0	0	0
p27	0	0	0	0	0	0	0	0	0	0	0	0
p28	0	0	0	0	0	0	0	0	0	0	0	0
p29	0	0	0	0	0	0	0	0	0	6.0E-09	1.4E-07	1.5E-07
p30	0	0	0	0	0	0	0	0	0	4.7E-08	1.7E-07	2.2E-07
p31	0	0	0	0	0	0	0	0	0	0	0	0
p32	0	0	0	0	0	0	0	0	0	0	1.9E-08	1.9E-08
p33	0	0	0	0	0	0	0	0	0	8.0E-09	1.1E-07	1.1E-07
p34	0	0	7.0E-09	2.0E-06	7.5E-06	1.8E-05	2.7E-05	2.9E-05	1.9E-05	1.1E-05	4.3E-06	1.2E-04
p35	0	0	1.4E-07	7.2E-07	1.5E-06	2.1E-06	2.1E-06	2.0E-06	1.6E-06	1.2E-06	8.2E-07	1.2E-05
p36	0	0	0	0	0	1.7E-08	1.4E-07	7.1E-07	1.7E-06	3.1E-06	4.0E-06	9.6E-06
p25-p36	***0***	***0***	***1.5E-07***	***2.7E-06***	***9.0E-06***	***2.0E-05***	***2.9E-05***	***3.2E-05***	***2.2E-05***	***1.5E-05***	***9.6E-06***	***1.4E-04***
Mutational scenario: 0 → 1 → 3 → 4												
Pathway	***a* = 0**	***a* = 0.1**	***a* = 0.2**	***a* = 0.3**	***a* = 0.4**	***a* = 0.5**	***a* = 0.6**	***a* = 0.7**	***a* = 0.8**	***a* = 0.9**	***a* = 1.0**	**Total**
p37	0	0	0	0	0	0	0	0	3.7E-08	2.8E-07	1.5E-06	1.9E-06
p38	0	0	0	0	0	0	0	0	2.7E-08	2.8E-07	1.3E-06	1.6E-06
p39	0	0	0	0	0	0	0	0	6.9E-08	5.1E-07	2.5E-06	3.1E-06
p40	0	0	0	0	0	0	0	2.1E-08	9.5E-07	9.4E-06	3.8E-05	4.8E-05
p41	0	0	0	0	0	0	1.4E-08	2.8E-07	3.1E-06	1.3E-05	3.4E-05	5.1E-05
p42	0	0	0	0	0	0	3.0E-09	1.0E-07	1.1E-06	5.0E-06	1.3E-05	2.0E-05
p43	0	0	0	0	0	0	0	2.5E-07	7.2E-06	5.7E-05	2.1E-04	2.8E-04
p44	0	0	0	0	0	0	9.9E-08	8.6E-06	8.1E-05	3.0E-04	7.0E-04	1.1E-03
p45	0	0	0	0	0	0	9.2E-08	1.4E-06	6.7E-06	2.1E-05	4.8E-05	7.7E-05
p46	0	0	5.5E-08	3.2E-07	2.0E-06	6.5E-06	2.0E-05	5.2E-05	1.1E-04	2.1E-04	3.3E-04	7.2E-04
p47	0	0	0	0	0	5.7E-07	1.6E-05	9.3E-05	2.9E-04	6.7E-04	1.2E-03	2.3E-03
p48	0	0	0	0	1.0E-09	2.1E-07	1.7E-06	7.3E-06	2.0E-05	4.7E-05	9.2E-05	1.7E-04
p37-p48	***0***	***0***	***5.5E-08***	***3.2E-07***	***2.0E-06***	***7.3E-06***	***3.8E-05***	***1.6E-04***	***5.2E-04***	***1.3E-03***	***2.7E-03***	***4.8E-03***

(continued)

Table 2.10. *continued*

Mutational scenario: 0 → 2 → 3 → 4												
Pathway	***a* = 0**	***a* = 0.1**	***a* = 0.2**	***a* = 0.3**	***a* = 0.4**	***a* = 0.5**	***a* = 0.6**	***a* = 0.7**	***a* = 0.8**	***a* = 0.9**	***a* = 1.0**	**Total**
p49	0	0	0	0	0	0	0	0	0	0	1.4E-07	1.4E-07
p50	0	0	0	0	0	0	0	0	0	0	1.5E-07	1.5E-07
p51	0	0	0	0	0	0	0	0	0	0	0	0
p52	0	0	0	0	0	0	0	0	0	0	0	0
p53	0	0	0	0	0	0	0	0	0	0	4.7E-07	4.7E-07
p54	0	0	0	0	0	0	0	0	0	3.5E-08	1.0E-06	1.1E-06
p55	0	0	0	0	0	0	0	0	1.9E-08	1.2E-06	9.8E-06	1.1E-05
p56	0	0	0	0	0	0	0	0	2.5E-08	3.5E-07	2.8E-06	3.2E-06
p57	0	0	0	0	0	0	3.0E-09	1.9E-07	1.2E-06	7.7E-06	2.4E-05	3.3E-05
p58	0	0	0	0	0	0	0	2.7E-08	3.6E-07	3.1E-06	1.2E-05	1.5E-05
p59	0	0	0	0	0	1.0E-08	6.5E-08	1.0E-06	9.1E-06	5.5E-05	1.9E-04	2.6E-04
p60	0	0	0	0	0	1.0E-09	2.1E-08	2.9E-07	1.4E-06	7.3E-06	2.5E-05	3.4E-05
p49-p60	***0***	***0***	***0***	***0***	***0***	***1.1E-08***	***8.9E-08***	***1.5E-06***	***1.2E-05***	***7.5E-05***	***2.7E-04***	***3.6E-04***
Mutational scenario: 0 → 1 → 4												
Pathway	***a* = 0**	***a* = 0.1**	***a* = 0.2**	***a* = 0.3**	***a* = 0.4**	***a* = 0.5**	***a* = 0.6**	***a* = 0.7**	***a* = 0.8**	***a* = 0.9**	***a* = 1.0**	**Total**
p61	0	0	0	0	0	0	0	0	4.5E-08	1.6E-06	1.6E-05	1.7E-05
p62	0	0	1.2E-07	2.9E-07	4.4E-07	1.5E-06	9.9E-06	3.0E-05	1.3E-04	3.6E-04	8.6E-04	1.4E-03
p63	0	2.0E-09	4.1E-06	1.7E-05	4.1E-05	1.5E-04	4.6E-04	1.1E-03	2.4E-03	4.8E-03	7.9E-03	1.7E-02
p64	0	7.0E-09	1.3E-05	6.1E-05	2.1E-04	6.2E-04	1.5E-03	3.2E-03	5.9E-03	9.6E-03	1.4E-02	3.5E-02
p61-p64	***0***	***9.0E-09***	***1.7E-05***	***7.8E-05***	***2.5E-04***	***7.7E-04***	***2.0E-03***	***4.3E-03***	***8.4E-03***	***1.5E-02***	***2.3E-02***	***5.3E-02***
Mutational scenario: 0 → 2 → 4												
Pathway	***a* = 0**	***a* = 0.1**	***a* = 0.2**	***a* = 0.3**	***a* = 0.4**	***a* = 0.5**	***a* = 0.6**	***a* = 0.7**	***a* = 0.8**	***a* = 0.9**	***a* = 1.0**	**Total**
p65	0	0	0	0	0	0	0	0	0	0	1.9E-06	1.9E-06
p66	0	0	0	0	0	0	0	0	0	0	0	0
p67	0	0	0	0	0	0	0	0	0	3.7E-07	7.1E-06	7.4E-06
p68	0	0	0	0	0	0	0	0	2.1E-06	3.6E-05	2.9E-04	3.2E-04
p69	0	0	0	0	0	0	7.6E-07	2.4E-06	3.2E-05	1.6E-04	4.9E-04	6.8E-04
p70	0	0	0	1.4E-07	0	8.0E-07	3.1E-06	2.0E-05	1.5E-04	6.7E-04	2.0E-03	2.8E-03
p65-p70	***0***	***0***	***0***	***1.4E-07***	***0***	***8.0E-07***	***3.9E-06***	***2.2E-05***	***1.8E-04***	***8.7E-04***	***2.8E-03***	***3.8E-03***

(continued)

Table 2.10. *continued*

	Mutational scenario: 0 → 3 → 4											
Pathway	***a* = 0**	***a* = 0.1**	***a* = 0.2**	***a* = 0.3**	***a* = 0.4**	***a* = 0.5**	***a* = 0.6**	***a* = 0.7**	***a* = 0.8**	***a* = 0.9**	***a* = 1.0**	**Total**
p71	0	0	0	0	0	0	2.4E-05	1.5E-03	9.5E-03	2.5E-02	4.5E-02	8.1E-02
p72	0	0	0	0	3.7E-07	1.2E-04	2.6E-03	1.2E-02	2.3E-02	3.3E-02	4.2E-02	1.1E-01
p73	0	0	0	0	0	2.9E-04	7.4E-03	2.4E-02	4.2E-02	6.4E-02	8.8E-02	2.3E-01
p74	0	0	0	0	1.9E-06	2.8E-04	2.3E-03	5.5E-03	9.9E-03	1.5E-02	2.2E-02	5.5E-02
p71-p74	***0***	***0***	***0***	***0***	***2.3E-06***	***6.9E-04***	***1.2E-02***	***4.3E-02***	***8.4E-02***	***1.4E-01***	***2.0E-01***	***4.8E-01***

[a]Adaptive landscapes were generated for seven distinct mutational scenarios and subjected to evolutionary excursions to determine the realization probability for a given mutational pathway (p). Excursions were performed for a range of drug pressure scenarios, with the drug pressure coefficient (*a*) varying from 0 (no pressure) to 1 (full pressure). For each mutational pathway, we report individual realization probabilities for each *a* value, as well as the total pathway realization probability for all *a* values. The highest total realization probabilities (top three probabilities for four-step and three-step mutational scenarios and top two probabilities for two-step scenarios) are underlined. We also report the sum of realization probabilities for the full set of pathways comprising a mutational scenario, shown in ***bolded italics***. Schematics of mutational pathways are collectively illustrated in **Figure 2.7** (***A***), **Figure 2.9** (***A***, ***D***, ***G***), and **Figure 2.10** (***A***, ***D***, ***G***).

Table 2.11. Mutational pathway realization probabilities for md-CQ evolutionary modeling.[a]

	Mutational scenario: 0 → 1 → 2 → 3 → 4											
Pathway	***a* = 0**	***a* = 0.1**	***a* = 0.2**	***a* = 0.3**	***a* = 0.4**	***a* = 0.5**	***a* = 0.6**	***a* = 0.7**	***a* = 0.8**	***a* = 0.9**	***a* = 1.0**	**Total**
p1	0	0	0	0	0	0	0	0	0	0	0	0
p2	0	0	0	0	0	0	0	0	0	0	0	0
p3	0	0	0	0	0	0	0	0	0	0	0	0
p4	0	0	0	0	0	0	0	0	0	0	0	0
p5	0	0	0	0	0	0	0	0	0	0	0	0
p6	0	0	0	0	0	0	0	0	0	0	0	0
p7	0	0	0	0	0	0	0	0	0	0	0	0
p8	0	0	0	0	0	0	0	0	0	0	0	0
p9	0	0	0	0	0	0	0	0	0	0	5.0E-08	5.0E-08
p10	0	0	0	0	0	0	0	0	0	0	0	0
p11	0	0	0	0	0	0	0	0	0	0	0	0
p12	0	0	0	0	0	0	0	0	0	0	0	0
p13	0	0	0	0	0	0	0	0	0	0	0	0
p14	0	0	0	0	0	0	0	0	0	0	0	0
p15	0	0	0	0	0	0	0	0	0	0	0	0
p16	0	0	0	0	0	0	0	0	0	0	0	0
p17	0	0	0	0	0	0	0	0	0	0	0	0
p18	0	0	0	0	0	0	0	0	0	0	0	0
p19	0	0	0	0	0	0	6.0E-09	5.9E-07	1.9E-06	1.2E-06	1.5E-07	3.8E-06
p20	0	0	0	0	0	2.1E-07	4.9E-06	1.3E-05	1.4E-05	5.7E-06	6.3E-07	3.8E-05
p21	0	0	0	1.0E-09	1.1E-08	5.8E-08	6.9E-08	1.0E-08	0	0	0	1.5E-07
p22	0	0	0	0	0	0	1.0E-09	0	0	0	0	1.0E-09
p23	0	0	0	0	1.0E-09	6.0E-09	8.1E-08	4.2E-07	6.5E-07	9.8E-07	1.1E-06	3.2E-06
p24	0	0	0	0	0	0	0	1.0E-09	0	0	0	1.0E-09
p1-p24	***0***	***0***	***0***	***1.0E-09***	***1.2E-08***	***2.7E-07***	***5.1E-06***	***1.4E-05***	***1.7E-05***	***7.9E-06***	***1.9E-06***	***4.5E-05***

(continued)

Table 2.11. *continued*

Mutational scenario: 0 → 1 → 2 → 4												
Pathway	***a* = 0**	***a* = 0.1**	***a* = 0.2**	***a* = 0.3**	***a* = 0.4**	***a* = 0.5**	***a* = 0.6**	***a* = 0.7**	***a* = 0.8**	***a* = 0.9**	***a* = 1.0**	**Total**
p25	0	0	0	0	0	0	0	0	0	0	0	0
p26	0	0	0	0	0	0	0	0	0	0	1.0E-08	1.0E-08
p27	0	0	0	0	0	0	0	0	0	0	1.9E-08	1.9E-08
p28	0	0	0	0	0	0	0	0	0	0	0	0
p29	0	0	0	0	0	0	0	0	0	0	4.6E-07	4.6E-07
p30	0	0	0	0	0	0	0	0	0	0	0	0
p31	0	0	0	0	0	0	0	0	0	0	0	0
p32	0	0	0	0	0	0	0	0	0	0	0	0
p33	0	0	0	0	0	0	0	0	0	0	0	0
p34	0	0	2.0E-07	5.3E-06	1.8E-05	4.3E-05	9.3E-05	1.3E-04	1.0E-04	3.6E-05	3.3E-06	4.3E-04
p35	0	0	5.1E-07	2.0E-06	3.8E-06	5.0E-06	3.0E-06	4.5E-07	9.0E-09	0	0	1.5E-05
p36	0	0	0	1.0E-09	6.0E-09	8.4E-08	9.9E-07	3.7E-06	4.9E-06	6.0E-06	6.3E-06	2.2E-05
p25-p36	***0***	***0***	***7.1E-07***	***7.3E-06***	***2.2E-05***	***4.8E-05***	***9.7E-05***	***1.3E-04***	***1.0E-04***	***4.2E-05***	***1.0E-05***	***4.7E-04***
Mutational scenario: 0 → 1 → 3 → 4												
Pathway	***a* = 0**	***a* = 0.1**	***a* = 0.2**	***a* = 0.3**	***a* = 0.4**	***a* = 0.5**	***a* = 0.6**	***a* = 0.7**	***a* = 0.8**	***a* = 0.9**	***a* = 1.0**	**Total**
p37	0	0	0	0	0	0	0	0	0	0	2.0E-07	2.0E-07
p38	0	0	0	0	0	0	0	0	0	0	6.6E-08	6.6E-08
p39	0	0	0	0	0	0	0	0	0	0	2.5E-07	2.5E-07
p40	0	0	0	0	0	0	9.0E-09	2.7E-08	6.0E-08	2.0E-06	3.8E-05	4.0E-05
p41	0	0	0	0	0	3.0E-09	1.6E-08	1.8E-08	3.4E-08	7.9E-07	1.4E-05	1.5E-05
p42	0	0	0	0	0	0	0	0	0	1.8E-07	4.3E-06	4.5E-06
p43	0	0	0	0	0	0	4.1E-06	1.7E-04	8.3E-04	2.2E-03	4.3E-03	7.5E-03
p44	0	0	0	0	0	8.0E-06	1.6E-04	7.3E-04	2.0E-03	4.2E-03	7.3E-03	1.5E-02
p45	0	0	0	0	0	0	0	0	0	0	0	0
p46	0	0	1.2E-07	1.1E-06	4.9E-06	1.8E-05	6.0E-05	1.5E-04	2.8E-04	4.5E-04	6.7E-04	1.6E-03
p47	0	0	0	1.4E-08	9.4E-06	6.4E-05	2.5E-04	6.8E-04	1.3E-03	2.2E-03	3.4E-03	7.9E-03
p48	0	0	0	0	1.8E-08	2.3E-08	1.6E-07	1.1E-06	6.2E-06	2.3E-05	6.5E-05	9.6E-05
p37-p48	***0***	***0***	***1.2E-07***	***1.1E-06***	***1.4E-05***	***9.0E-05***	***4.7E-04***	***1.7E-03***	***4.4E-03***	***9.1E-03***	***1.6E-02***	***3.2E-02***

(continued)

Table 2.11. *continued*

Mutational scenario: 0 → 2 → 3 → 4												
Pathway	***a* = 0**	***a* = 0.1**	***a* = 0.2**	***a* = 0.3**	***a* = 0.4**	***a* = 0.5**	***a* = 0.6**	***a* = 0.7**	***a* = 0.8**	***a* = 0.9**	***a* = 1.0**	**Total**
p49	0	0	0	0	0	0	0	0	0	0	0	0
p50	0	0	0	0	0	0	0	0	0	0	0	0
p51	0	0	0	0	0	0	0	0	0	0	5.4E-04	5.4E-04
p52	0	0	0	0	0	0	0	0	0	0	8.0E-04	8.0E-04
p53	0	0	0	0	0	0	0	0	0	1.4E-05	4.4E-04	4.6E-04
p54	0	0	0	0	0	0	0	0	1.0E-08	7.2E-05	1.8E-03	1.9E-03
p55	0	0	0	0	0	0	0	2.9E-07	4.8E-05	1.4E-03	3.5E-03	4.9E-03
p56	0	0	0	0	0	0	0	0	5.0E-09	2.3E-07	1.1E-06	1.3E-06
p57	0	0	0	0	1.0E-09	1.0E-08	1.5E-07	1.5E-06	1.4E-05	1.4E-06	2.0E-09	1.7E-05
p58	0	0	0	0	0	0	0	8.4E-08	3.3E-06	5.4E-07	1.0E-09	4.0E-06
p59	0	0	0	0	3.0E-08	2.0E-07	3.5E-06	5.4E-05	8.3E-04	2.7E-03	4.0E-03	7.6E-03
p60	0	0	0	0	0	0	1.4E-08	6.0E-08	3.4E-07	4.3E-07	3.6E-07	1.2E-06
p49-p60	***0***	***0***	***0***	***0***	***3.1E-08***	***2.1E-07***	***3.7E-06***	***5.6E-05***	***9.0E-04***	***4.2E-03***	***1.1E-02***	***1.6E-02***
Mutational scenario: 0 → 1 → 4												
Pathway	***a* = 0**	***a* = 0.1**	***a* = 0.2**	***a* = 0.3**	***a* = 0.4**	***a* = 0.5**	***a* = 0.6**	***a* = 0.7**	***a* = 0.8**	***a* = 0.9**	***a* = 1.0**	**Total**
p61	0	0	0	0	0	0	0	0	0	0	1.3E-06	1.3E-06
p62	0	0	3.4E-07	2.0E-07	8.0E-07	3.0E-07	9.1E-07	2.6E-07	2.0E-06	2.3E-05	3.0E-04	3.2E-04
p63	0	1.0E-08	1.6E-05	6.3E-05	2.3E-04	7.7E-04	2.7E-03	7.5E-03	1.7E-02	2.9E-02	4.3E-02	1.0E-01
p64	0	3.0E-09	3.0E-05	1.3E-04	3.9E-04	1.1E-03	3.0E-03	6.0E-03	9.5E-03	1.4E-02	1.8E-02	5.2E-02
p61-p64	***0***	***1.3E-08***	***4.6E-05***	***1.9E-04***	***6.2E-04***	***1.9E-03***	***5.7E-03***	***1.4E-02***	***2.7E-02***	***4.3E-02***	***6.1E-02***	***1.5E-01***
Mutational scenario: 0 → 2 → 4												
Pathway	***a* = 0**	***a* = 0.1**	***a* = 0.2**	***a* = 0.3**	***a* = 0.4**	***a* = 0.5**	***a* = 0.6**	***a* = 0.7**	***a* = 0.8**	***a* = 0.9**	***a* = 1.0**	**Total**
p65	0	0	0	0	0	0	0	0	0	0	0	0
p66	0	0	0	0	0	0	0	0	0	0	4.4E-03	4.4E-03
p67	0	0	0	0	0	0	0	0	9.4E-07	4.1E-04	9.3E-03	9.7E-03
p68	0	0	0	0	0	0	0	4.4E-06	7.1E-04	1.4E-02	2.9E-02	4.4E-02
p69	0	0	0	0	0	6.E-07	4.8E-06	5.2E-05	3.3E-04	2.4E-05	2.6E-07	4.1E-04
p70	0	0	0	0	0	3.2E-06	3.5E-05	5.2E-04	6.1E-03	1.7E-02	2.2E-02	4.5E-02
p65-p70	***0***	***0***	***0***	***0***	***0***	***3.8E-06***	***4.0E-05***	***5.8E-04***	***7.1E-03***	***3.1E-02***	***6.5E-02***	***1.0E-01***

(continued)

Table 2.11. *continued*

	Mutational scenario: 0 → 3 → 4											
Pathway	***a* = 0**	***a* = 0.1**	***a* = 0.2**	***a* = 0.3**	***a* = 0.4**	***a* = 0.5**	***a* = 0.6**	***a* = 0.7**	***a* = 0.8**	***a* = 0.9**	***a* = 1.0**	**Total**
p71	0	0	0	0	0	3.6E-04	1.3E-02	3.3E-02	5.9E-02	8.9E-02	1.2E-01	3.2E-01
p72	0	0	0	0	5.6E-05	5.5E-03	1.5E-02	2.2E-02	3.0E-02	4.0E-02	5.1E-02	1.6E-01
p73	0	0	0	0	2.4E-03	2.3E-02	4.3E-02	6.8E-02	9.8E-02	1.3E-01	1.7E-01	5.4E-01
p74	0	0	0	6.8E-08	4.0E-05	1.6E-04	7.0E-04	2.8E-03	7.4E-03	1.4E-02	2.1E-02	4.6E-02
p71-p74	***0***	***0***	***0***	***6.8E-08***	***2.5E-03***	***2.9E-02***	***7.2E-02***	***1.3E-01***	***1.9E-01***	***2.7E-01***	***3.6E-01***	***1.1E+00***

[a]Adaptive landscapes were generated for seven distinct mutational scenarios and subjected to evolutionary excursions to determine the realization probability for a given mutational pathway (p). Excursions were performed for a range of drug pressure scenarios, with the drug pressure coefficient (*a*) varying from 0 (no pressure) to 1 (full pressure). For each mutational pathway, we report individual realization probabilities for each *a* value, as well as the total pathway realization probability for all *a* values. The highest total realization probabilities (top three probabilities for four-step and three-step mutational scenarios and top two probabilities for two-step scenarios) are underlined. We also report the sum of realization probabilities for the full set of pathways comprising a mutational scenario, shown in ***bolded italics***. Schematics of mutational pathways are collectively illustrated in **Figure 2.7** (***A***), **Figure 2.9** (***A***, ***D***, ***G***), and **Figure 2.10** (***A***, ***D***, ***G***).

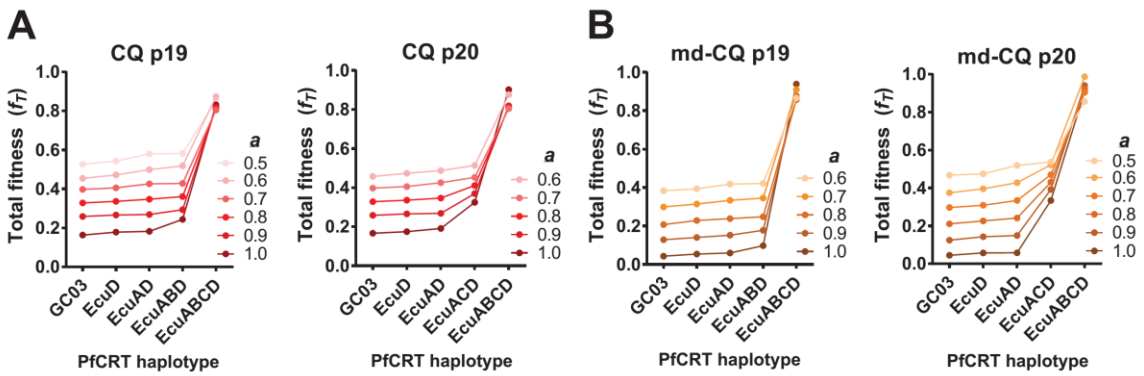

Figure 2.8. Representative accessible (**A**) chloroquine (CQ)-directed and (**B**) monodesethyl-chloroquine (md-CQ)-directed *pfcrt* mutational trajectories. Shown are trajectories for the top two pathways (p19 and p20) for the 0→1→2→3→4 mutational scenario. The higher the drug pressure coefficient *a*, the greater the impact of drug resistance (and the lower the contribution of parasite growth) on the total fitness index, f_T. Corresponding trajectories encompassing the complete set of simulated adaptive landscapes (based on mean f_T values) are shown in **Figure 2.7*D*** and **Figure 2.7*E*** for CQ and md-CQ, respectively.

appreciable effect on total parasite fitness (f_T) until the three-SNP intermediate (Ecu_{ABD} or Ecu_{ACD}).

In the scenario of CQR evolution via sequential acquisition of single mutations (0→1→2→3→4), three distinct mutational intermediates spanned the transition from wild-type to Ecu1110 *pfcrt*. Given the apparent adaptive constraints associated with this evolutionary course, we next explored trajectories in which up to three mutations were acquired simultaneously, thus requiring fewer intermediates. These scenarios could occur with pre-existing alleles and/or with pressure from other antimalarials. Evolutionary modeling was performed as for the 0→1→2→3→4 mutational scenario, with 10^9 total evolutionary excursions examined for various drug pressure scenarios (range of *a* values: 0 to 1). Results for CQ and md-CQ mutational pathways requiring either two (0→1→2→4; 0→1→3→4; or 0→2→3→4) or one (0→1→4; 0→2→4; or 0→3→4) intermediate steps are illustrated in **Figure 2.9** and **Figure 2.10**, respectively. Pathway probabilities are listed in **Tables 2.10–2.11**. Consistent with our results for the 0→1→2→3→4 mutational scenario, the top realized pathways overwhelmingly featured initial acquisition of Ecu_D I356L and/or Ecu_C N326D. Notably, for both CQ and md-CQ modeling, mutational sequences 0→1→3→4 and 0→3→4 yielded realization probabilities up to ~10^5-fold greater than those for the 0→1→2→3→4 scenario (e.g. compare total probabilities for p1-24 and p71-p74 in **Tables 2.10–2.11**). This suggests the possibility that rare bursts of multiple mutations facilitated the emergence of CQR-conferring *pfcrt* alleles.

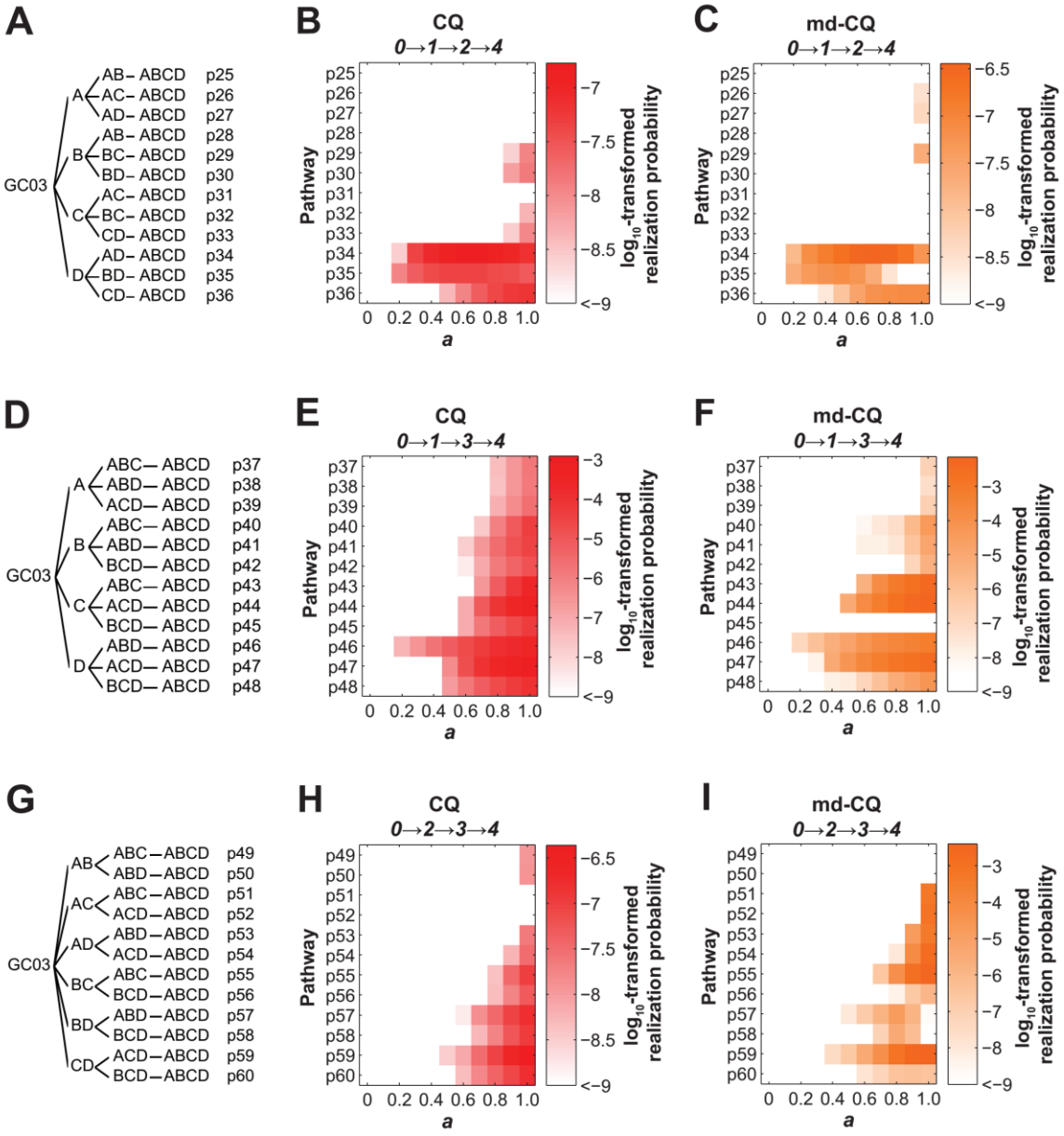

Figure 2.9. Modeling of chloroquine (CQ) and monodesethyl-chloroquine (md-CQ)-directed Ecu1110 *pfcrt* evolution via two mutational intermediate steps. (**A**) Schematic of the 12 theoretical pathways (p25 to p36) in the 0→1→2→4 mutational scenario, leading from wild-type (GC03) to Ecu1110 (ABCD) PfCRT. A, B, C, and D correspond to mutations K76T, A220S, N326D, and I356L, respectively. (**B** and **C**) Accessibility of mutational pathways p25 to p36 as informed by (**B**) CQ and (**C**) md-CQ data. Color map intensity corresponds to $\log_{10}$-transformed pathway realization probability. Simulations explored the combined effect of drug resistance and growth rates by modulating the coefficient *a*, varied from *a*=0 (no drug pressure, full contribution of growth rates) through *a*=1 (full drug pressure, no contribution of growth rates). (**D**) Schematic of the 12 theoretical pathways (p37 to p48) in the 0→1→3→4 mutational scenario. (**E** and **F**) Accessibility of mutational pathways p37 to p48 for (**E**) CQ and (**F**) md-CQ. (**G**) Schematic of the 12 theoretical pathways (p49 to p60) in the 0→2→3→4 mutational scenario. (**H** and **I**) Accessibility of mutational pathways p49 to p60 for (**H**) CQ and (**I**) md-CQ.

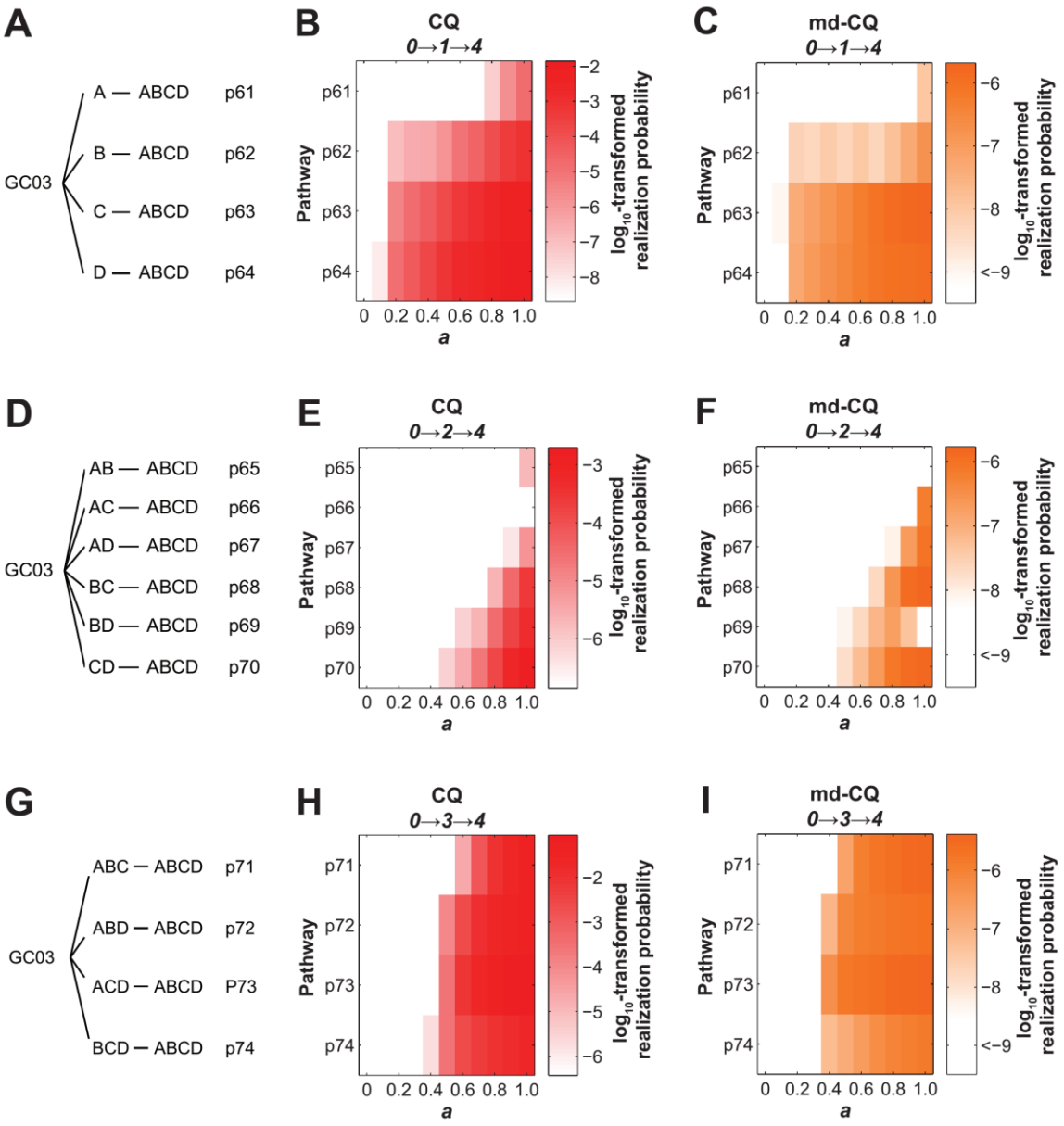

Figure 2.10. Modeling of chloroquine (CQ) and monodesethyl-chloroquine (md-CQ)-directed Ecu1110 *pfcrt* evolution via one mutational intermediate step. (**A**) Schematic of the four theoretical pathways (p61 to p64) in the 0→1→4 mutational scenario, leading from wild-type (GC03) to Ecu1110 (ABCD) PfCRT. A, B, C, and D correspond to mutations K76T, A220S, N326D, and I356L, respectively. (**B** and **C**) Accessibility of mutational pathways p61 to p64 as informed by (**B**) CQ and (**C**) md-CQ data and determined via computational modeling. Color map intensity corresponds to $\log_{10}$-transformed pathway realization probability. Simulations explored the effect of drug pressure (*a*), from *a*=0 (no pressure) through *a*=1 (full pressure). (**D**) Schematic of the six theoretical pathways (p65 to p70) in the 0→2→4 mutational scenario. (**E** and **F**) Accessibility of mutational pathways p65 to p70 for (**E**) CQ and (**F**) md-CQ. (**G**) Schematic of the four theoretical pathways (p71 to p74) in the 0→3→4 mutational scenario. (**H** and **I**) Accessibility of mutational pathways p71 to p74 for (**H**) CQ and (**I**) md-CQ.

Modeling of md-AQ-directed *pfcrt* evolution

Given the known cross-resistance between CQ and AQ and the historical use of AQ in South America, where the Ecu1110 and 7G8 PfCRT haplotypes are common (see **Discussion**), we also explored the impact of AQ drug pressure on Ecu1110 *pfcrt* evolution. Similar to the CQ and md-CQ evolutionary modeling, we performed evolutionary modeling for md-AQ, the primary active metabolite of AQ. Our results are shown in **Figure 2.11** for a range of mutational scenarios, with pathway probabilities detailed in **Table 2.12**. Indicating extensive overlap between CQ and AQ in directing *pfcrt* evolution, the majority (77.8%) of top pathways based on md-AQ modeling (see **Table 2.12**) coincided with top pathways as identified by md-CQ modeling (see **Table 2.11**). A role for md-AQ in aiding *pfcrt* evolution is further evident from comparisons of total realization probabilities associated with different quinoline-type drugs (**Table 2.13**). As compared to CQ and md-CQ, md-AQ-directed *pfcrt* evolution yielded, respectively, upwards of >10-fold and >100-fold increases in accessibility for the sequential, single-step mutational scenario (0→1→2→3→4; see p23 in **Table 2.13**). Similar to CQ and md-CQ, for scenarios in which mutational intermediates were skipped due to simultaneous acquisition of more than one mutation, md-AQ-directed evolution was comparably associated with a substantial increase in pathway accessibility (e.g. compare p23 and p73 in **Table 2.13** and compare total probabilities for p1-24 and p71-p74 in **Table 2.12**).

It is noteworthy that the CQR-conferring 7G8 *pfcrt* allele remains the most prevalent allele in South America, despite declines in CQ and AQ use in this region.[257,259] As 7G8 *pfcrt* is distinguished from the Ecu1110 *pfcrt* allele by the presence of a single additional mutation (C72S), our modeling of Ecu1110 *pfcrt*

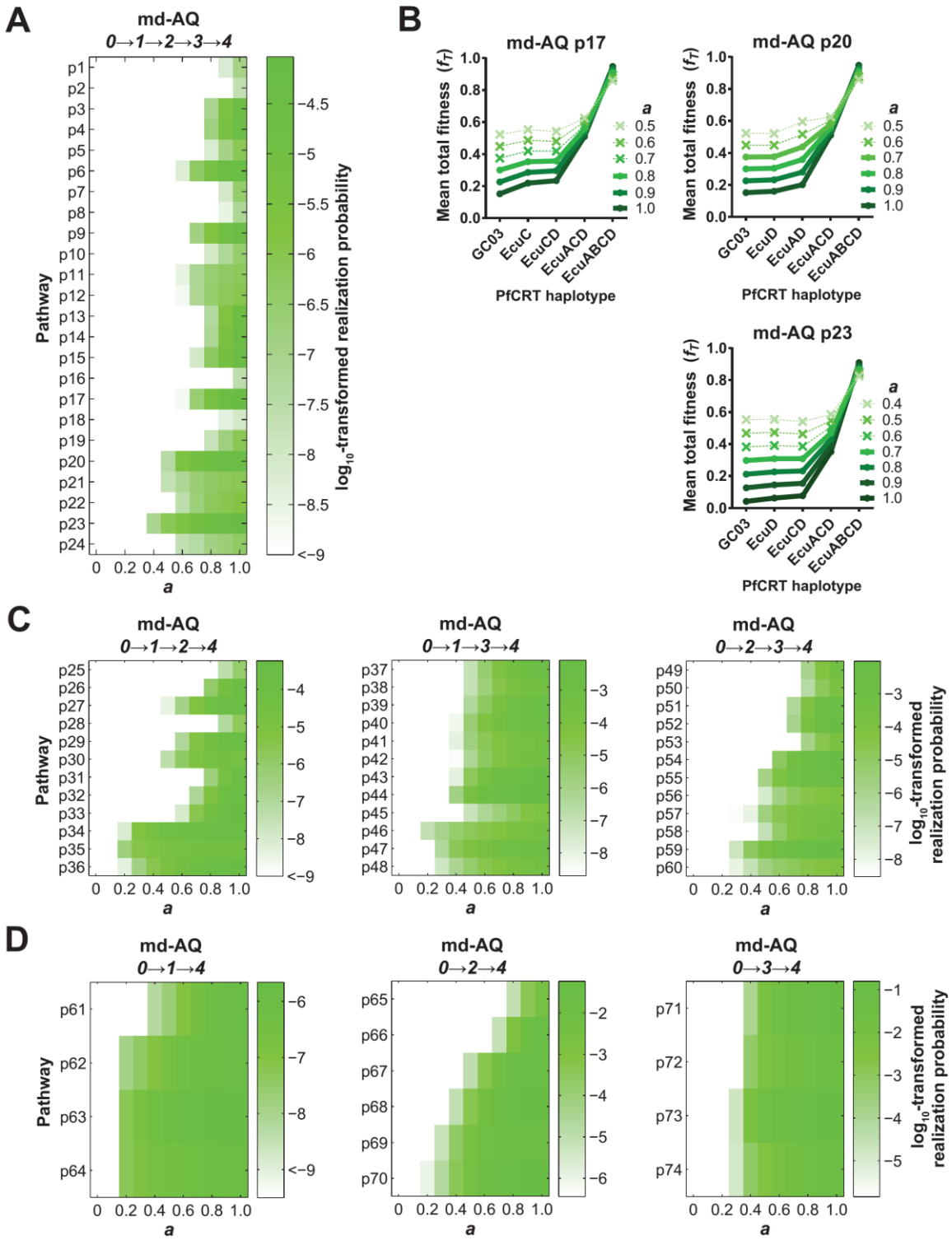

Figure 2.11. (*continued on next page*)

Figure 2.11. Modeling of monodesethyl-amodiaquine (md-AQ)-directed evolution of Ecu1110 *pfcrt*. (**A**) Mutational pathway accessibility for the 0→1→2→3→4 scenario, as informed by md-AQ data and determined via computational modeling. Color map intensity corresponds to $\log_{10}$-transformed pathway realization probability. Simulations explored the effect of drug pressure (*a*), from *a*=0 (no pressure) through *a*=1 (full pressure). (**B**) Adaptive landscapes illustrating the interplay of total parasite fitness (f_T), mutations acquired, and extent of drug pressure (*a*) for the top three realized md-AQ-directed mutational pathways (p17, p20, p23) for the 0→1→2→3→4 scenario. Shown are trajectories based on mean f_T values, which encompass the complete set of simulated adaptive landscapes. Accessible (i.e. f_T increases progressively) and inaccessible (i.e. f_T valleys are present) trajectories are indicated by thick lines/circles and dotted lines/crosses, respectively. (**C**) Accessibility of pathways requiring two mutational intermediate steps in md-AQ-directed evolution of Ecu1110 *pfcrt*. (**D**) Accessibility of pathways requiring a single mutational intermediate step in md-AQ-directed evolution of Ecu1110 *pfcrt*. Schematics of the theoretical mutational pathways for all mutational scenarios are collectively illustrated in **Figure 2.7** (***A***), **Figure 2.9** (***A***, ***D***, ***G***), and **Figure 2.10** (***A***, ***D***, ***G***).

Table 2.12. Mutational pathway realization probabilities for md-AQ evolutionary modeling.[a]

	Mutational scenario: 0 → 1 → 2 → 3 → 4											
Pathway	***a* = 0**	***a* = 0.1**	***a* = 0.2**	***a* = 0.3**	***a* = 0.4**	***a* = 0.5**	***a* = 0.6**	***a* = 0.7**	***a* = 0.8**	***a* = 0.9**	***a* = 1.0**	**Total**
p1	0	0	0	0	0	0	0	0	0	6.0E-09	1.2E-07	1.3E-07
p2	0	0	0	0	0	0	0	0	0	0	2.2E-08	2.2E-08
p3	0	0	0	0	0	0	0	0	7.9E-08	2.9E-06	2.3E-05	2.6E-05
p4	0	0	0	0	0	0	0	0	1.6E-07	4.6E-06	3.5E-05	4.0E-05
p5	0	0	0	0	0	0	0	0	7.0E-09	1.1E-07	8.4E-07	9.5E-07
p6	0	0	0	0	0	0	5.0E-09	4.8E-07	6.1E-06	2.7E-05	5.5E-05	8.9E-05
p7	0	0	0	0	0	0	0	0	0	9.0E-09	3.5E-07	3.6E-07
p8	0	0	0	0	0	0	0	0	0	3.0E-09	6.7E-08	7.0E-08
p9	0	0	0	0	0	0	0	1.4E-07	2.0E-06	1.2E-05	3.6E-05	5.0E-05
p10	0	0	0	0	0	0	0	0	9.0E-09	5.1E-08	3.1E-07	3.7E-07
p11	0	0	0	0	0	0	3.0E-09	7.0E-08	2.7E-07	4.8E-07	6.6E-07	1.5E-06
p12	0	0	0	0	0	0	2.0E-09	6.1E-08	3.2E-07	6.5E-07	9.4E-07	2.0E-06
p13	0	0	0	0	0	0	0	0	4.4E-08	1.9E-06	2.0E-05	2.2E-05
p14	0	0	0	0	0	0	0	0	6.6E-08	3.2E-06	3.1E-05	3.4E-05
p15	0	0	0	0	0	0	0	1.0E-08	5.3E-07	6.4E-06	3.2E-05	3.9E-05
p16	0	0	0	0	0	0	0	0	0	1.0E-09	2.6E-08	2.7E-08
p17	0	0	0	0	0	0	2.0E-09	2.9E-07	5.3E-06	3.0E-05	9.3E-05	1.3E-04
p18	0	0	0	0	0	0	0	0	0	4.0E-09	1.0E-08	1.4E-08
p19	0	0	0	0	0	0	0	1.0E-09	1.7E-08	1.5E-07	8.0E-07	9.7E-07
p20	0	0	0	0	0	3.9E-08	2.6E-06	9.8E-06	2.0E-05	3.3E-05	4.5E-05	1.1E-04
p21	0	0	0	1.0E-09	1.0E-09	1.8E-08	6.1E-08	2.4E-07	4.5E-07	7.0E-07	8.3E-07	2.3E-06
p22	0	0	0	0	0	0	2.7E-08	2.0E-07	5.6E-07	9.3E-07	1.3E-06	3.0E-06
p23	0	0	0	1.0E-09	7.4E-08	7.6E-07	3.1E-06	9.1E-06	2.1E-05	4.2E-05	7.5E-05	1.5E-04
p24	0	0	0	0	0	0	2.1E-08	3.7E-08	1.3E-07	2.5E-07	4.8E-07	9.2E-07
p1-p24	***0***	***0***	***0***	***2.0E-09***	***7.5E-08***	***8.2E-07***	***5.8E-06***	***2.0E-05***	***5.7E-05***	***1.7E-04***	***4.5E-04***	***7.0E-04***

(continued)

Table 2.12. *continued*

Mutational scenario: 0 → 1 → 2 → 4												
Pathway	***a* = 0**	***a* = 0.1**	***a* = 0.2**	***a* = 0.3**	***a* = 0.4**	***a* = 0.5**	***a* = 0.6**	***a* = 0.7**	***a* = 0.8**	***a* = 0.9**	***a* = 1.0**	**Total**
p25	0	0	0	0	0	0	0	0	0	4.7E-08	8.0E-07	8.4E-07
p26	0	0	0	0	0	0	0	0	1.0E-06	3.0E-05	2.0E-04	2.3E-04
p27	0	0	0	0	0	4.0E-09	2.5E-07	6.7E-06	5.6E-05	1.9E-04	3.2E-04	5.7E-04
p28	0	0	0	0	0	0	0	0	0	8.3E-08	2.1E-06	2.2E-06
p29	0	0	0	0	0	1.0E-09	9.9E-08	4.2E-06	3.7E-05	1.4E-04	3.4E-04	5.2E-04
p30	0	0	0	0	0	4.7E-08	1.2E-06	9.4E-06	2.2E-05	2.6E-05	2.6E-05	8.5E-05
p31	0	0	0	0	0	0	0	0	4.7E-07	2.2E-05	1.8E-04	2.1E-04
p32	0	0	0	0	0	0	0	1.5E-07	9.1E-06	9.0E-05	3.3E-04	4.2E-04
p33	0	0	0	0	0	0	1.2E-08	2.9E-06	4.5E-05	2.3E-04	5.9E-04	8.7E-04
p34	0	0	8.0E-09	6.6E-06	2.4E-05	5.3E-05	9.0E-05	1.3E-04	1.8E-04	2.2E-04	2.6E-04	9.7E-04
p35	0	0	5.0E-07	3.7E-06	9.3E-06	1.7E-05	2.4E-05	3.1E-05	3.5E-05	3.5E-05	3.6E-05	1.9E-04
p36	0	0	5.0E-09	2.8E-07	2.8E-06	1.3E-05	3.9E-05	8.7E-05	1.7E-04	2.9E-04	4.6E-04	1.1E-03
p25-p36	***0***	***0***	***5.1E-07***	***1.1E-05***	***3.6E-05***	***8.3E-05***	***1.5E-04***	***2.7E-04***	***5.6E-04***	***1.3E-03***	***2.7E-03***	***5.2E-03***
Mutational scenario: 0 → 1 → 3 → 4												
Pathway	***a* = 0**	***a* = 0.1**	***a* = 0.2**	***a* = 0.3**	***a* = 0.4**	***a* = 0.5**	***a* = 0.6**	***a* = 0.7**	***a* = 0.8**	***a* = 0.9**	***a* = 1.0**	**Total**
p37	0	0	0	0	0	1.0E-07	4.4E-06	6.9E-05	3.9E-04	1.2E-03	2.5E-03	4.2E-03
p38	0	0	0	0	0	1.1E-07	2.4E-06	2.5E-05	1.0E-04	2.4E-04	3.9E-04	7.5E-04
p39	0	0	0	0	0	3.9E-07	9.0E-06	1.1E-04	5.7E-04	1.6E-03	3.3E-03	5.6E-03
p40	0	0	0	0	6.0E-09	3.5E-06	5.8E-05	2.9E-04	7.1E-04	1.3E-03	2.1E-03	4.4E-03
p41	0	0	0	0	1.1E-08	1.7E-06	1.6E-05	5.6E-05	1.2E-04	2.0E-04	3.0E-04	7.0E-04
p42	0	0	0	0	3.0E-09	5.9E-07	9.3E-06	5.0E-05	1.4E-04	2.7E-04	4.5E-04	9.2E-04
p43	0	0	0	0	1.3E-08	1.3E-05	2.0E-04	8.4E-04	2.0E-03	3.6E-03	5.7E-03	1.2E-02
p44	0	0	0	0	1.6E-06	1.8E-04	8.5E-04	2.0E-03	3.6E-03	5.7E-03	8.4E-03	2.1E-02
p45	0	0	0	0	2.0E-09	8.6E-08	5.8E-07	2.5E-06	9.0E-06	2.8E-05	7.4E-05	1.1E-04
p46	0	0	1.4E-07	9.6E-07	4.1E-06	1.2E-05	2.7E-05	5.5E-05	9.6E-05	1.6E-04	2.5E-04	6.1E-04
p47	0	0	0	4.5E-07	1.7E-05	6.6E-05	1.6E-04	3.3E-04	6.1E-04	1.1E-03	1.6E-03	3.9E-03
p48	0	0	0	4.8E-08	7.5E-07	4.5E-06	1.8E-05	4.9E-05	1.1E-04	2.0E-04	3.4E-04	7.2E-04
p37-p48	***0***	***0***	***1.4E-07***	***1.5E-06***	***2.3E-05***	***2.8E-04***	***1.4E-03***	***3.9E-03***	***8.5E-03***	***1.6E-02***	***2.5E-02***	***5.5E-02***

(continued)

Table 2.12. *continued*

Mutational scenario: 0 → 2 → 3 → 4												
Pathway	***a* = 0**	***a* = 0.1**	***a* = 0.2**	***a* = 0.3**	***a* = 0.4**	***a* = 0.5**	***a* = 0.6**	***a* = 0.7**	***a* = 0.8**	***a* = 0.9**	***a* = 1.0**	**Total**
p49	0	0	0	0	0	0	0	0	1.1E-06	5.6E-05	5.1E-04	5.7E-04
p50	0	0	0	0	0	0	0	0	4.0E-07	1.7E-05	1.3E-04	1.5E-04
p51	0	0	0	0	0	0	0	6.1E-07	1.0E-04	1.4E-03	4.4E-03	5.8E-03
p52	0	0	0	0	0	0	0	1.3E-06	1.7E-04	2.0E-03	6.3E-03	8.5E-03
p53	0	0	0	0	0	0	0	3.0E-09	1.5E-06	2.7E-05	1.3E-04	1.6E-04
p54	0	0	0	0	0	0	1.2E-05	3.9E-04	2.1E-03	4.7E-03	6.4E-03	1.4E-02
p55	0	0	0	0	0	1.4E-06	9.0E-05	7.0E-04	1.9E-03	3.7E-03	6.0E-03	1.2E-02
p56	0	0	0	0	0	4.0E-08	1.7E-06	1.1E-05	3.1E-05	5.9E-05	9.8E-05	2.0E-04
p57	0	0	0	4.0E-09	1.5E-08	2.1E-06	2.3E-05	8.4E-05	1.6E-04	2.6E-04	3.5E-04	8.8E-04
p58	0	0	0	0	0	1.4E-07	8.1E-06	7.1E-05	2.0E-04	3.4E-04	4.9E-04	1.1E-03
p59	0	0	0	1.0E-07	1.3E-05	2.0E-04	8.7E-04	2.1E-03	3.9E-03	6.4E-03	9.7E-03	2.3E-02
p60	0	0	0	1.4E-08	1.6E-07	1.7E-06	6.9E-06	1.7E-05	3.3E-05	5.5E-05	8.8E-05	2.0E-04
p49-p60	***0***	***0***	***0***	***1.2E-07***	***1.3E-05***	***2.1E-04***	***1.0E-03***	***3.4E-03***	***8.6E-03***	***1.9E-02***	***3.5E-02***	***6.7E-02***
Mutational scenario: 0 → 1 → 4												
Pathway	***a* = 0**	***a* = 0.1**	***a* = 0.2**	***a* = 0.3**	***a* = 0.4**	***a* = 0.5**	***a* = 0.6**	***a* = 0.7**	***a* = 0.8**	***a* = 0.9**	***a* = 1.0**	**Total**
p61	0	0	0	0	4.0E-07	4.8E-06	9.3E-05	9.0E-04	4.0E-03	9.7E-03	1.8E-02	3.2E-02
p62	0	0	1.5E-06	1.2E-05	8.7E-05	4.4E-04	1.8E-03	4.4E-03	7.8E-03	1.1E-02	1.5E-02	4.0E-02
p63	0	0	3.0E-05	2.8E-04	1.4E-03	4.8E-03	1.1E-02	1.9E-02	2.8E-02	3.8E-02	4.8E-02	1.5E-01
p64	0	1.0E-09	3.4E-05	1.7E-04	4.8E-04	9.9E-04	1.7E-03	2.8E-03	4.3E-03	6.3E-03	8.4E-03	2.5E-02
p61-p64	***0***	***1.0E-09***	***6.6E-05***	***4.6E-04***	***2.0E-03***	***6.2E-03***	***1.5E-02***	***2.7E-02***	***4.4E-02***	***6.5E-02***	***8.9E-02***	***2.5E-01***
Mutational scenario: 0 → 2 → 4												
Pathway	***a* = 0**	***a* = 0.1**	***a* = 0.2**	***a* = 0.3**	***a* = 0.4**	***a* = 0.5**	***a* = 0.6**	***a* = 0.7**	***a* = 0.8**	***a* = 0.9**	***a* = 1.0**	**Total**
p65	0	0	0	0	0	0	0	0	1.1E-05	4.2E-04	3.3E-03	3.7E-03
p66	0	0	0	0	0	0	0	7.3E-06	1.2E-03	1.3E-02	3.6E-02	5.0E-02
p67	0	0	0	0	0	1.2E-05	5.0E-04	5.4E-03	2.0E-02	3.2E-02	3.7E-02	9.4E-02
p68	0	0	0	0	9.1E-06	4.5E-04	5.0E-03	1.7E-02	2.9E-02	4.1E-02	5.4E-02	1.5E-01
p69	0	0	3.6E-07	7.0E-06	2.2E-04	2.0E-03	6.8E-03	1.0E-02	1.1E-02	1.2E-02	1.3E-02	5.5E-02
p70	0	0	1.0E-06	1.9E-05	4.3E-04	3.4E-03	1.1E-02	2.1E-02	3.1E-02	4.4E-02	5.9E-02	1.7E-01
p65-p70	***0***	***0***	***1.4E-06***	***2.6E-05***	***6.6E-04***	***5.9E-03***	***2.3E-02***	***5.3E-02***	***9.2E-02***	***1.4E-01***	***2.0E-01***	***5.2E-01***

(continued)

Table 2.12. *continued*

	Mutational scenario: 0 → 3 → 4											
Pathway	***a* = 0**	***a* = 0.1**	***a* = 0.2**	***a* = 0.3**	***a* = 0.4**	***a* = 0.5**	***a* = 0.6**	***a* = 0.7**	***a* = 0.8**	***a* = 0.9**	***a* = 1.0**	**Total**
p71	0	0	0	0	1.2E-04	5.0E-03	2.0E-02	4.0E-02	6.4E-02	9.3E-02	1.3E-01	3.5E-01
p72	0	0	0	1.5E-06	5.9E-04	4.8E-03	9.7E-03	1.5E-02	2.1E-02	2.8E-02	3.6E-02	1.1E-01
p73	0	0	0	1.6E-05	6.0E-03	2.3E-02	4.2E-02	6.4E-02	9.1E-02	1.2E-01	1.6E-01	5.1E-01
p74	0	0	0	1.5E-05	7.1E-04	3.0E-03	7.6E-03	1.4E-02	2.2E-02	3.2E-02	4.4E-02	1.2E-01
p71-p74	***0***	***0***	***0***	***3.3E-05***	***7.4E-03***	***3.6E-02***	***7.9E-02***	***1.3E-01***	***2.0E-01***	***2.7E-01***	***3.7E-01***	***1.1E+00***

[a]Adaptive landscapes were generated for seven distinct mutational scenarios and subjected to evolutionary excursions to determine the realization probability for a given mutational pathway (p). Excursions were performed for a range of drug pressure scenarios, with the drug pressure coefficient (*a*) varying from 0 (no pressure) to 1 (full pressure). For each mutational pathway, we report individual realization probabilities for each *a* value, as well as the total pathway realization probability for all *a* values. The highest total realization probabilities (top three probabilities for four-step and three-step mutational scenarios and top two probabilities for two-step scenarios) are underlined. We also report the sum of realization probabilities for the full set of pathways comprising a mutational scenario, shown in ***bolded italics***. Schematics of mutational pathways are collectively illustrated in **Figure 2.7** (***A***), **Figure 2.9** (***A***, ***D***, ***G***), and **Figure 2.10** (***A***, ***D***, ***G***).

Table 2.13. Representative *pfcrt* mutational trajectories accessible to quinoline drug resistance evolution.[a]

	Mutational intermediates					Total realization probability		
Pathway	**0**	**1**	**2**	**3**	**4**	**CQ**	**md-CQ**	**md-AQ**
p20	WT	D	AD	ACD	ABCD	2.8×10^{-6}	3.8×10^{-5}	1.1×10^{-4}
p23	WT	D	CD	ACD	ABCD	8.8×10^{-7}	3.2×10^{-6}	1.5×10^{-4}
p47	WT	D	–	ACD	ABCD	2.3×10^{-3}	7.9×10^{-3}	3.9×10^{-3}
p73	WT	–	–	ACD	ABCD	2.3×10^{-1}	5.4×10^{-1}	5.1×10^{-1}

[a]Total realization probabilities for the collectively most accessible mutational pathways (p) identified in modeling of CQ, md-CQ, and md-AQ resistance evolution (see **Tables 2.10**–**2.12**). Shown are the two most accessible pathways for the 0→1→2→3→4 mutational scenario, as well as the most accessible pathways for the 0→1→3→4 and 0→3→4 scenarios. PfCRT haplotypes are listed in **Table 2.3**. 0-4, number of mutations comprising the given PfCRT haplotype; –, skipped mutational intermediate; CQ, chloroquine; md-CQ, monodesethyl-chloroquine; md-AQ, monodesethyl-amodiaquine; WT, wild-type (GC03); D, EcuD; AD, EcuAD; ACD, EcuACD; ABCD, EcuABCD (Ecu1110).

evolution may be used to draw inferences about the evolution of the highly prevalent 7G8 allele. Collectively, our data indicate that, in the 7G8 genetic background, PfCRT C72S confers increased parasite resistance to the quinoline compounds CQ, md-CQ, and md-AQ, while simultaneously enhancing parasite growth. Thus, we postulate that the top mutational pathways identified for the evolution of Ecu1110 *pfcrt* also represent mutational paths leading to the evolution of 7G8 *pfcrt*.

DISCUSSION

In this study, we harnessed ZFN-based combinatorial genetics and computational evolutionary modeling to probe the evolutionary trajectories accessible to parasites as they acquire mutations in the *pfcrt* gene, the primary determinant of CQR and a key modulator of susceptibility to several currently deployed antimalarials.[114] Our simulations revealed pronounced biological constraints associated with the evolution of Ecu1110 *pfcrt*, a prototypical CQ-resistant allele comprised of four mutations, the smallest number required for resistance.[186] Among the pathways based on the sequential accumulation of single mutations leading to the Ecu1110 allele, the maximum realization probabilities for CQ and md-CQ resistance were, respectively, ~5×10^{-7} and ~10^{-6} (see **Tables 2.10–2.11**). In comparison, earlier modeling of pyrimethamine resistance evolution mediated by the sequential gain of up to four mutations in the *pfdhfr* gene (**Table 2.14**) showed a maximum realization probability of ~3×10^{-4}.[302] These findings are consistent with historical records showing that the evolution of drug-resistant forms of *pfcrt* in natural parasite populations occurred more rarely than for mutant *pfdhfr*.[304]

Our modeling of *pfcrt* evolution uncovered multiple adaptive valleys (see **Figure 2.7*D*** and **Figure 2.7*E***) associated with the sequential acquisition of single mutations, such that the gain of a subsequent mutation generally constrained resistance evolution by reducing the total parasite fitness (f_T). We consequently examined scenarios in which two or more mutations were acquired simultaneously. This analysis revealed pathways with vast increases in accessibility (up to a maximum total realization probability of ~2×10^{-1} and ~5×10^{-1} for CQ and md-CQ, respectively; see **Tables 2.10–2.11**). As the fixation of *pfcrt* alleles bearing one to

Table 2.14. Comparison of combinatorial genetic studies modeling *Plasmodium* drug resistance gene evolution.

	Lozovsky *et al.* (*PNAS*, 2009)	**Brown *et al.*** (*Mol Biol Evol*, 2010)	**Kümpornsin, Modchang *et al*.** (*Mol Biol Evol*, 2014)	**This study**
Gene (mutations)	*pfdhfr* (4 mutations)	*pfdhfr* (4 mutations)	*pfdhfr* (4 mutations); *pfgch1* (gene amplification)[d]	*pfcrt* (4 mutations)
Drug(s)	pyrimethamine	pyrimethamine	pyrimethamine	chloroquine; monodesethyl-chloroquine; monodesethyl-amodiaquine
Experimental organism	*E. coli*	*S. cerevisiae*	*E. coli*	*P. falciparum*
Evolutionary excursions	10^7	10^9	10^6	10^9
Range of realization probabilities of top three pathways	0.11 – 0.55[a]	*(i.)* 0.13 – 0.27[b,c] *(ii.)* 0.19 – 0.40[a,c]	0 – 1.5E-05	CQ: 1.7E-07 – 5.0E-07[f] md-CQ: 1.5E-07 – 1.1E-06[f] md-AQ: 5.5E-05 – 9.3E-05[f]
Sum of realization probabilities of top three pathways	0.88[a]	*(i.)* 0.52[b] *(ii.)* 0.85[a]	2.0E-05[e]	CQ: 1.2E-06[f] md-CQ: 1.9E-06[f] md-AQ: 2.2E-04[f]

[a]Based on correlated fixation probability model, which assumes that the probability of fixation of a beneficial mutation is positively correlated with the magnitude of its effect.

[b]Based on equal fixation probability model, which assumes that all beneficial mutations (mutations that increase IC_{50}) fix with equal probability.

[c]Note that the top three pathways identified in this study differed depending on the choice of probability model.

[d]This study employed an evolutionary model modified from Lozovsky *et al.* (*PNAS*, 2009) to explore the interplay of *pfdhfr1* and *pfgch1* in directing pyrimethamine resistance evolution. To assess the effect of *pfgch1* amplification, the authors calculated absolute probabilities.

[e]Maximum absolute probabilities observed for mutational scenario of *pfgch1* amplification.

[f]Values shown are for the scenario of step-wise acquisition of single mutations (0→1→2→3→4) for a=1.0. CQ, chloroquine; md-CQ, monodesethyl-chloroquine; md-AQ, monodesethyl-amodiaquine.

three mutations has not been documented in the field, we hypothesize that *pfcrt*-mediated CQR arose through mutational bursts with brief periods of intervening growth, whereby one or more mutations were acquired and expanded during a short time window prior to the acquisition of additional mutations. Based on our combined IC_{50} and growth data, the most likely scenario would be the near-simultaneous emergence of three to four mutations. While this would be an exceptionally infrequent event, we note that several months of intermittent *in vitro* pressure of a CQ-resistant *P. falciparum* strain (K1) with the antimalarial halofantrine selected for a *pfcrt* variant with three additional point mutations.[305]

Mathematical modeling of the acquisition of multiple mutations in response to selective pressure has previously shown that the temporality of mutational events, population size, and duration of evolution might jointly facilitate the emergence of mutations with a frequency significantly greater than the cumulative product of single-mutation rates,[306] previously estimated to be ~10^{-9} for *P. falciparum*.[307,308] In the absence of evidence for hypermutator *P. falciparum* lineages,[307,309] the emergence of Ecu1110 *pfcrt* in the low-transmission setting of South America can be attributed to the convergence of multiple factors, including the extent of drug pressure on parasite populations, monoclonality of infections, rate of genetic exchange between strains during sexual stage development in the mosquito vector, and host immunity.[240] Of note, our model did not specifically investigate mutational reversion and conversion events,[310] which could overcome suboptimal peaks in the *pfcrt* adaptive landscape. Additional *pfcrt* mutations might also have been acquired via meiotic recombination between intermediate alleles in *P. falciparum* sexual stages.

Our analysis of the Ecu1110 and 7G8 *pfcrt* allelic variants leads us to speculate

on the evolution of the Dd2 allele, which carries eight point mutations and dominates in Southeast Asia. This allele, or a similar isoform, earlier spread from Asia into Africa, resulting in the widespread loss of CQ efficacy.[311] We postulate that the Dd2 allele occurred via one or more major bursts of multiple mutations in a very limited number of parasites that spread under selective CQ pressure. Resultant population bottlenecks would have consequently diminished the effective population size, reduced competition with fitter wild-type parasites, and enabled mutant parasites to traverse fitness valleys toward high-level resistance.[246] We note that the Dd2 allele, while more CQ-resistant than the 7G8 allele, demonstrates a significant fitness cost.[232,243] Evidence of ongoing selection is provided by the emergence in Cambodia of the Cam734 *pfcrt* allele that harbors nine mutations (of which five are not found in Dd2) and that, while less CQ-resistant than Dd2, confers a level of parasite fitness comparable to the wild-type allele.[243]

Prior combinatorial modeling of *pfdhfr* evolution in yeast has shown that *in vitro* growth rates can serve as a robust assessment of organismal fitness.[248] In the absence of a comprehensive way to account for all biological characteristics that impact fitness during the complex *Plasmodium* life cycle, we quantified the parasite growth index (f_G) associated with specific *pfcrt* mutations. Our analysis was performed within the pathogenically relevant setting of asexual blood stage infection, during which parasite numbers can rapidly increase and be exposed to drug pressure. The critical role of the f_G parameter and its interplay with parasite drug resistance (f_D) is demonstrated by the modulation of evolutionary pathway accessibilities by the drug pressure coefficient a, which governed the relative influence of f_G and f_D in dictating *pfcrt* evolution (see **Figure 2.7**). Our study illuminates mutational determinants of

asexual blood-stage parasite fitness. Most notably, Ecu$_D$ I356L consistently contributed to enhanced *in vitro* parasite growth and was the most accessible primary mutational step in our CQ and md-CQ evolutionary excursions. Interestingly, this mutation also increased AS IC_{50} values (see **Figure 2.3C**), evoking the recent association of the I356T mutation in Southeast Asia with *k13*-mutant artemisinin-resistant parasite populations.[159]

Recent studies with *P. falciparum* parasites differing in their *pfcrt* allele have found that CQR-conferring PfCRT isoforms cause the accumulation of high levels of hemoglobin-derived peptides in the parasite DV, which was associated with a deleterious impact on parasite growth.[232] Future studies with our combinatorial *pfcrt* variants can be used to address the impact of specific mutations on hemoglobin digestion. Given that the evolution of *pfcrt*-mediated CQR also required successful transmission of variant PfCRT isoforms to the mosquito vector, examining the effect of specific *pfcrt* mutations on transmission is equally merited. This is of interest in light of rodent malaria studies that demonstrated a transmission advantage associated with the expression of the 7G8 *pfcrt* allele in CQ-treated gametocytes.[268]

Our genetic dissection recalls important insights from recent studies of CQ transport mediated by PfCRT isoforms heterologously expressed in either *X. laevis* or *S. cerevisiae*.[208,312] In agreement with both studies, we observed Ecu$_A$ K76T to be insufficient for CQR and uncovered direct contributions to CQR by additional PfCRT mutations, in particular Ecu$_C$ N326D. Crystallographic insights, presently lacking for PfCRT or its homologs, indicate that even seemingly conservative substitutions (e.g. isoleucine to leucine, as in I356L) can significantly impact a protein's structure and function.[313] In addition to PfCRT I356L, the apparent need for mutational acquisition

of basic, polar, and acidic side chains at residues 76, 220, and 326, respectively, suggests specific electrostatic and conformational requirements for PfCRT-mediated CQR. Our findings clarify previous discussions about the role of non-K76T mutations, which have been surmised to solely compensate for a loss of native PfCRT function.[170,314,315] Of note, *in vitro* and field-based studies have also observed that parasites harboring the conventional CQR marker K76T can acquire novel PfCRT mutations (e.g. C101F or C350R) that abolish resistance to CQ (Eastman et al. 2011; Pelleau et al. 2015),[137,218] emphasizing the need for caution in interpreting the CQ susceptibility status of isolates based on incomplete *pfcrt* genotypes.

Interestingly, as compared to Ecu1110 PfCRT, which lacks the C72S mutation, 7G8 PfCRT conferred decreased rates of CQ transport,[208,312] yet increased the degrees of CQR and *in vitro* growth in *P. falciparum*. It is noteworthy that, in studies of isogenic parasite lines encoding variant PfCRT haplotypes from the Philippines (PH1 and PH2) that likewise only differ at residue 72, C72S conferred increased parasite CQR, yet in that case reduced parasite growth.[243] Collectively, these findings underscore the impact of the overall mutational milieu on the roles of specific *pfcrt* mutations. Furthermore, they raise the prospect that certain mutations may alleviate CQ-mediated inhibition of native PfCRT function without having a direct impact on drug transport.

In selecting the geographically related 7G8 parasite genetic background[303] for our combinatorial analysis, we aimed to single out the specific contributions of and interactions between *pfcrt* mutations in the evolution of the quintuple-SNP 7G8 *pfcrt* allele that is widespread throughout South America. Of note, we did not observe desired allelic replacement events in our initial efforts to engineer *pfcrt* alleles

(namely Ecu_A and Ecu_{ABCD}) in GC03 (CQ-sensitive) parasites, which were derived from an earlier genetic cross between HB3 (CQ-sensitive) and Dd2 (CQ-resistant) parasites.[316] Consistent with this, previous allelic exchange studies have unmasked the incompatibility of *pfcrt* alleles with certain genetic backgrounds.[217] As point mutations in the gene encoding the DV-resident *P. falciparum* multidrug resistance 1 (PfMDR1) transporter have previously been found to modulate *pfcrt*-mediated CQR in some parasite strains,[317] we speculate that *pfmdr1* may serve as a secondary genetic determinant of CQR evolution. It is conceivable that *pfmdr1* mutations might modulate the accessibility of *pfcrt* mutational trajectories, akin to the recently documented capacity of the GTP cyclohydrolase 1 (*gch1*) gene to enhance the accessibility of *pfdhfr* mutational trajectories in the evolution of pyrimethamine resistance.[302] It remains to be determined whether PfMDR1 mutations S1034C and D1246Y,[318] present in 7G8 but not Ecu1110 parasites, might partly account for the different *in vitro* growth rates observed between parasites encoding identical (Ecu1110) *pfcrt* alleles in these two genetic backgrounds. With the availability of validated genetic engineering strategies targeting both *pfmdr1*[143] and *pfcrt*, further exploration of the epistatic interactions between these two critical drug resistance loci is now possible.

In our analysis, the Ecu1110 PfCRT haplotype was identified as an accessible mutational precursor of the quintuple-SNP 7G8 haplotype, which was relatively more CQ-resistant and less deleterious to parasite growth. Our data support the rise of the 7G8 PfCRT haplotype in multiple geographical loci, where the Ecu1110-type haplotype has also been documented albeit at far lower frequencies,[257,319] as well as the ultimate success of the 7G8 PfCRT haplotype in spreading across vast tracts of

the malaria-endemic world.[259] To date, 7G8 *pfcrt* is at or near fixation in South America[256,257] and the Western Pacific[320] and has been identified in some surveys of parasites from Africa, the Indian subcontinent, and Southeast Asia.[260,287,321,322] Notably, prior CQ and AQ use has been documented in each of these geographical regions, leading to the earlier conjecture that AQ might have driven the selection for 7G8 *pfcrt*.[133,323] Considering inter-individual variability in peak blood CQ concentration achieved in response to the standard CQ dose of 25 mg/kg,[105] the long terminal elimination half-life of CQ,[324] as well as the deployment of prophylactic chloroquinated and/or amodiaquinated salts,[130] we posit that the evolution of mutant *pfcrt* was likely facilitated by sustained sub-therapeutic drug concentrations in these populations. It is notable that in our delineation of *pfcrt* mutational pathways, md-CQ, the active metabolite of CQ, was associated with a higher pathway predictive ability. A comparison of the pharmacology of CQ and md-CQ in the setting of the parasite DV will be essential to contextualizing these differences. To our knowledge, the accumulation of md-CQ in the parasite DV of CQ-resistant versus CQ-sensitive strains has yet to be explored.

Beyond CQR, our results also corroborate the pleiotropic role of PfCRT in modulating responses to critical first-line ACT component drugs and shed light on opposing selective pressures exerted by these compounds. Notably, parasites encoding 7G8 *pfcrt* exhibited high-level cross-resistance between CQ and md-AQ (the active metabolite of AQ), whereas their susceptibility to both AS and LUM was significantly increased as compared to wild-type *pfcrt*-expressing parasites. Accordingly, sole use of the ACT formulation AS-AQ in geographical regions where the 7G8 PfCRT haplotype is established should be avoided. A contributory role for AQ in facilitating

pfcrt evolution of the drug-resistant Ecu1110 and 7G8 alleles is further supported by the shared subset of mutational trajectories that were favored by CQ and AQ in our analysis.

Our combinatorial evolutionary modeling sheds light on the capacity of *P. falciparum* parasites to produce and sustain rare bursts of mutational events. In part due to selective pressures from one or more antimalarial agents acting upon an immutable host factor (e.g. heme), such mutational events were likely responsible for generating stably persisting drug-resistant *pfcrt* alleles that ultimately caused the global loss of CQ efficacy. Of particular concern is the recent emergence of artemisinin resistance in Southeast Asia, driven largely by *k13* gene point mutations that arose in genetically distinct parasite subpopulations.[158,160,161,325] Clonal expansions of *k13*-mutant parasites suggest the selection of several favorable genetic backgrounds, resulting in population bottlenecks that might have facilitated parasite progression via fitness valleys.[159] More recently, PPQ resistance in Southeast Asia is now leading to treatment failures with the first-line regimen DHA-PPQ.[135,138,139] The genetic basis of PPQ resistance is presently elusive, partly because of clonal subpopulation structures that hinder initial genome-wide association studies to pinpoint causal resistance determinants. Genetic and drug susceptibility profiling of newly resistant strains can also inform the selection of drug regimens that exert opposing selective pressures as a means to constrain the evolution of multidrug-resistant parasites. Given the central role of chemotherapy in alleviating the worldwide burden of malaria, leveraging genomic surveillance of malarial parasites with evolutionary and population genetic principles will facilitate detection of selection signatures that could compromise the efficacy of our present arsenal of antimalarial drugs.

CHAPTER 3: EVOLUTION OF FITNESS COST-NEUTRAL MUTANT PFCRT CONFERRING *PLASMODIUM FALCIPARUM* 4-AMINOQUINOLINE DRUG RESISTANCE IS ACCOMPANIED BY ALTERED DIGESTIVE VACUOLE PHYSIOLOGY AND REDUCED METABOLIC STRESS

Stanislaw J. Gabryszewski,[1] Satish K. Dhingra,[1] Jill M. Combrinck,[3] Ian A. Lewis,[5] Paul S. Callaghan,[6] Matthew R. Hassett,[6] Amila Siriwardana,[6] Lise Musset,[7] Peter J. Smith,[3] Manuel Llinás,[8] Timothy J. Egan,[4] Paul D. Roepe,[6] David A. Fidock[1,2]

[1]Department of Microbiology and Immunology and [2]Division of Infectious Diseases, Department of Medicine, Columbia University Medical Center, New York, NY, USA; [3]Division of Pharmacology, Department of Medicine, and [4]Department of Chemistry, University of Cape Town, Cape Town, South Africa; [5]Department of Biological Sciences, University of Calgary, Calgary, AB, Canada; [6]Departments of Chemistry and Biochemistry and Cellular & Molecular Biology, Georgetown University, Washington, DC, USA; [7]Laboratoire de Parasitologie, WHO Collaborating Center for Surveillance of Anti-Malarial Drug Resistance, Institut Pasteur de la Guyane, Cayenne, French Guiana; [8]Departments of Biochemistry & Molecular Biology and Chemistry, Center for Malaria Research and Center for Infectious Diseases Dynamics, Pennsylvania State University, University Park, PA.

Author contributions: **SJG** and DAF conceived and designed the experiments; **SJG**, SKD, JMC, PJS, PSC, MRH, AS, LM, and IAL performed experimental work; **SJG**, JMC, IAL, ML, TJE, PDR, and DAF analyzed data; **SJG** and DAF wrote the manuscript.

Note: The work presented herein represents a manuscript prepared for publication.

ABSTRACT

Southeast Asia is an epicenter of multidrug-resistant *Plasmodium falciparum* strains. Selective pressures on the subcontinent have recurrently produced several allelic variants of parasite drug resistance genes, including the *P. falciparum chloroquine resistance transporter* (*pfcrt*). Despite significant reductions in the deployment of the 4-aminoquinoline drug chloroquine (CQ), which selected for the mutant *pfcrt* alleles that halted CQ efficacy decades ago, the parasite *pfcrt* locus is continuously evolving. This is highlighted by the emergence and expansion of a highly mutated allele, Cam734 *pfcrt*, which has evolved the unique ability to confer parasite CQ resistance without an associated fitness cost. In the present study, we used *pfcrt*-specific zinc finger nucleases to genetically dissect this allele in the pathogenic setting of asexual blood-stage infection. Comparative analysis of the drug resistance and growth profiles of isogenic parasites encoding full-length or partial Cam734, Dd2 (the most common Southeast Asian variant), and wild-type *pfcrt* alleles revealed previously unknown roles of PfCRT mutations in modulating parasite susceptibility to multiple antimalarial therapeutic agents, including the rare A144F mutation that has not been observed beyond Southeast Asia and that proved essential for Cam734-mediated CQ resistance. These studies were leveraged with biochemical approaches that collectively uncovered distinct effects of mutant Cam734 and Dd2 PfCRT isoforms on parasite CQ transport and cellular metabolism, including hemoglobin catabolism and disposition of heme. Our studies provide important insights into the complex molecular basis of PfCRT-mediated antimalarial drug resistance, of relevance to global health efforts aiming to characterize novel alleles that may undermine the efficacy of first-line antimalarial drug regimens.

INTRODUCTION

Human malaria remains a leading global health scourge in part due to multidrug resistance mechanisms evolved by *Plasmodium falciparum*, the protozoan species responsible for the most severe forms of disease.[15] Artemisinin-based combination therapies (ACTs) are the current first-line means of controlling malarial infections, including ones dominated with drug-resistant strains that arose during previous selective sweeps resulting from the global use of chloroquine (CQ) and sulfadoxine-pyrimethamine.[181,249,326] The 4-aminoquinoline compound CQ was especially pivotal earlier in reducing mortality rates.[327] However, the multi-focal emergence and spread of CQ resistance (CQR) contributed to stalled control measures and substantial increases in malaria-associated hospitalizations and deaths.[270] Nevertheless, owing to its safety, affordability, and established efficacy against non-resistant parasites, CQ continues to be deployed in regions that are free of CQR or harbor CQ-sensitive *P. vivax*.[114] Interestingly, studies of infections with CQ-resistant *P. falciparum* strains in Guinea-Bissau recently revealed a ~5-fold increase in CQ efficacy upon doubling the standard dose in children aged <5 years, the age demographic at highest risk for malaria mortality.[115] These findings coincide with a reprise in efforts to delineate the molecular basis of resistance to antimalarials bearing the hallmark CQ-type quinoline moiety.[328]

Genetic linkage and allelic replacement studies have previously identified *pfcrt* variants as the primary determinant of CQR.[120,186] These findings are supported by evidence of directional selection for mutant *pfcrt* alleles in *P. falciparum* parasite populations exposed to extensive CQ pressure.[329] A secondary, strain-dependent contribution to CQR has also been noted for the *P. falciparum multidrug resistance 1*

(*pfmdr1*) gene.[128,143,330] Among CQ-resistant field isolates, PfCRT isoforms are comprised of geographically distinct clusters of single-nucleotide polymorphisms (SNPs), namely K76T and 3 to 8 additional point mutations. PfCRT K76T is a critical, albeit insufficient, determinant of parasite *in vitro* CQR.[242] This mutation also predicts *in vivo* CQ treatment failure with high sensitivity but lower specificity.[198] At the cellular level, PfCRT is a multi-pass transporter embedded in the parasite digestive vacuole (DV) membrane, with enigmatic functions that may include transport of ions and/or peptides.[188,201,209,235] In the absence of PfCRT structural information, mutational approaches have led studies into the effect of specific PfCRT mutations on drug transport and parasite growth.[208,242,312]

Point mutations in PfCRT have also been associated with altered parasite susceptibility to ACT component drugs, namely artemisinins and their partner drugs (including amodiaquine, lumefantrine, and piperaquine).[149,159,213,218,323] This is of particular relevance given reports of emerging clinical resistance to these first-line agents.[135,331] To various degrees, these compounds interfere with or are otherwise impacted by parasite-mediated catabolism of host hemoglobin (Hb), which supplies parasites with amino acids and helps maintain intracellular osmolarity.[49,54,55,100] This catabolic process produces ferriprotoporphyrin IX heme, which in its reactive free form can exert lethal oxidative damage to the parasite.[59] For quinoline-based antimalarials, drug-heme interactions in the DV cause toxicity by preventing incorporation of ferriprotoporphyrin IX heme dimers (ß-hematin) into the non-reactive hemozoin (Hz) crystals that account for >95% of total heme.[58,61] Consistent with this inhibition of ß-hematin mineralization, CQ treatment of drug-sensitive D10 parasites was recently observed by transmission electron microscopy to disrupt the highly

ordered fringe pattern of Hz crystals.[55]

Cell fractionation methods in *P. falciparum* have further demonstrated that, upon CQ treatment, the proportion of total heme present as Hz significantly diminishes, whereas the proportion corresponding to free heme increases.[55] These responses are dose-dependent and inversely proportional to parasite survival.[55] Prior to accessing its heme target, the weak base and lipophilic drug CQ traverses multiple lipid bilayers and accumulates in the acidic DV via weak-base trapping.[203] CQR-promoting PfCRT isoforms transport CQ out of the DV, consequently restricting CQ-heme contacts and allowing Hz formation to proceed.[114,188] Of note, the mutational status of *pfcrt* impacts DV volume and pH, both of which influence Hz formation kinetics.[195] Interestingly, recent metabolomic analyses of CQ-resistant versus CQ-sensitive *P. falciparum* strains detected a link between mutant *pfcrt*-mediated CQR and the elevated accumulation of peptides derived from Hb digestion.[232] Given the reduced growth of CQ-resistant parasites (expressing the Dd2 or 7G8 mutant *pfcrt* alleles) relative to isogenic parasites encoding wild-type *pfcrt*, defective Hb degradation was postulated as a cellular basis for the reduced fitness associated with mutant *pfcrt.*[232] Reduced fitness of these mutant alleles was confirmed in *in vitro* studies.[232,243] and was observed at a population level in Africa, whereby removal of CQ pressure led to the attrition of mutant *pfcrt*-expressing parasites in favor of wild-type, CQ-sensitive strains.[263,332]

A pathogen's fitness refers to its capacity to support infection and generate new progeny. For *P. falciparum* parasites, fitness is influenced in part by growth of pathogenic asexual blood-stage parasites, selection, mosquito-human transmission, and selection within the mosquito vector.[232,263,266] In general, these factors are

impaired in parasites expressing mutant, CQR-associated PfCRT isoforms.[114,241] To date, over 50 distinct PfCRT haplotypes have been recorded.[208] Of these, the Asian haplotype Dd2 (M74I/N75E/K76T/A220S/Q271E/N326S/I356T/R371I, thought to have disseminated throughout Africa) and the South American/Oceanian haplotype 7G8 (C72S/K76T/A220S/N326D/I356L) account for the vast majority of global mutational patterns, with additional isoforms harboring four or more SNPs and resembling either the Dd2 (e.g. the six-SNP African variant GB4) or 7G8 (e.g. the four-SNP South American variant Ecu1110) PfCRT haplotype.[114] Recent modeling in *P. falciparum* suggests that *pfcrt* evolution occurred via punctuated periods of mutation too brief to allow fixation of partial (i.e. bearing 1-3 SNPs) resistance alleles, shedding light on physiologic constraints that explain the rarity of mutant *pfcrt* emergence in the field.[242] Intriguingly, studies from Cambodia, an epicenter of multidrug resistance in *P. falciparum*, also revealed a highly polymorphic CQR-conferring *pfcrt* allele, Cam734.[262] Cam734 *pfcrt* encodes nine mutations (see **Table 3.1**), five of which (N75D, A144F, L148I, I194T, T333S) are not found in the predominant Southeast Asian CQ-resistant allele, Dd2 *pfcrt.*[208] After Dd2, Cam734 *pfcrt* represents the second most common allele in Southeast Asia[159] and, unlike other CQR-associated isoforms, supports parasite growth comparable to isogenic parasites encoding the CQ-sensitive, wild-type *pfcrt* allele.[243]

The emerging Cam734 PfCRT isoform presents an opportunity to explore *P. falciparum* genetic determinants that concurrently confer drug resistance and fully neutralize fitness costs, a unique feature not associated with other mutant PfCRT variants. Herein, we leveraged drug resistance versus growth profiling of isogenic, *pfcrt*-modified asexual blood-stage parasites. These studies were combined with

biochemical approaches – including metabolomic, heme fractionation, and drug transport studies – in order to address the following questions: (1) To what extent do the rare mutations present in Cam734 PfCRT directly impact parasite resistance to clinically employed antimalarials? (2) Which mutations are compensatory and thus serve to preserve PfCRT function? (3) Mechanistically, how does mutant Cam734 PfCRT confer CQR without an accompanying fitness cost? Results provided herein broaden our present understanding of the mechanistic basis of CQR and inform field efforts that evaluate *pfcrt* genotypes as a tool to predict the drug susceptibility status of clinical isolates.

Table 3.1. Summary of PfCRT haplotypes.[a]

	PfCRT residue											
PfCRT haplotype	**74**	**75**	**76**	**144**	**148**	**194**	**220**	**271**	**326**	**333**	**356**	**371**
GC03 (wild-type)	M	N	K	A	L	I	A	Q	N	T	I	R
Dd2	I	E	T	A	L	I	S	E	S	T	T	I
Cam734	I	D	T	F	I	T	S	E	N	S	I	R
Cam734 D75N	I	N	T	F	I	T	S	E	N	S	I	R
Cam734 F144A	I	D	T	A	I	T	S	E	N	S	I	R
Cam734 I148L	I	D	T	F	L	T	S	E	N	S	I	R
Cam734 T194I	I	D	T	F	I	I	S	E	N	S	I	R
Cam734 S333T	I	D	T	F	I	T	S	E	N	T	I	R

[a]Mutations distinct from the GC03 (wild-type) PfCRT haplotype are shaded, with Cam734 PfCRT-specific mutations indicated in dark gray and all other mutations indicated in light gray. DNA substitutions encoding each PfCRT mutation are as follows: M74I: ATG→ATT; N75D: AAT→GAT; N75E: AAT→GAA; K76T: AAA→ACA; A144F: GCC→TTC; L148I: CTT→ATT; I194T: ATA→ACA; A2220S: GCC→TCC; Q271E: CAA→GAA; N326S: AAC→AGC; T333S: ACC→AGC; I356T: ATA→ACA; R371I: AGA→ATA.

METHODS

Parasite cultivation

Human RBCs (Interstate Blood Bank) harboring *P. falciparum* asexual blood-stage parasites were cultured at 2-4% hematocrit in RPMI-1640-based malaria cell culture medium supplemented with 0.5% Albumax II (Invitrogen).[167] Cultures were incubated at 37°C, 5% O_2 / 5% CO_2 / 90% N_2.

Genetic modification of the parasite *pfcrt* locus

Previously generated plasmids collectively encoding a set of full-length (e.g. Cam734) or back-mutated (e.g. Cam734 F144A) *pfcrt* alleles were used as templates for PCR amplification of *pfcrt* exons 2 through 13 with primers p1 + p2 (see **Table 3.2** for all primer details). To generate *pfcrt* donor plasmids, these amplicons were cloned into the p*crt*^{Dd2}-h*dhfr* donor plasmid backbone[295] using NcoI and SalI restriction sites.

A schematic of our genetic engineering strategy is shown in **Figure 3.1*A***. Briefly, GC03 parasites were transfected with 40 µg donor plasmid (p*crt*-h*dhfr*) and subjected to pressure with 2.5 nM WR99210 (Jacobus Pharmaceuticals). Donor plasmid-enriched parasites were subsequently transfected with 40 µg pZFN^{crt}-*bsd* and pressured with 2.5 nM WR99210 and 2 µg/ml Blasticidin HCl (Invitrogen) for six days, followed by prolonged pressure with 2.5 nM WR99210. To screen for desired genetic modification events (see **Figure 3.1*B***), recombinant parasites were analyzed by direct blood PCR (KAPA Biosystems), as earlier described.[242] Bulk cultures demonstrating evidence of genetic editing were cloned by limiting dilution[333] and two parasite clones per successful editing were selected for further analysis

Table 3.2. Primers used in this study.[a]

Primer	Oligonucleotide sequence (5' → 3')	Description	Lab name
p1	AACCATGGATTTATTGTGTAATAATTGAATCGACG	NcoI-*pfcrt* exon 13 R	p1640
p2	CCCTTGTCGACCTTAACAGATGGCTC	SalI-*pfcrt* intron1-exon 2 F	p3519
p3	TCAAACATGACAAGGGAAATAGT	*pfcrt* exon 5 F	p2427
p4	CCAAGAATAAACATGCGAAACC	*pfcrt* exon 7 R	p3806
p5	CTTGAATTCGACCTTAACAGATGGCTCAC	*pfcrt* exon 2 F	p3264
p6	CTTATCGATAAGCAGAAGAACATATTAATAGGAATACTTAATTG	*pfcrt* exon 3 R	p3265
p7	CTTGGGCCCAAGTTGTACTGCTTCTAAGC	*pfcrt* gDNA 5′ UTR F	p3404
p8	CTCGAGATGGTTGGTTCGCTAAACTGC	h*DHFR* F	p3315
p9	TTGACCCTTATATATTCCACCCA	*pfcrt* gDNA 3′ UTR R	p3403
p10	GAGGCGCCTATTTCAAAAATCTTAGCATAAGGATT	*pbcrt* 3′ UTR R	p1644

[a]Nucleotides corresponding to restriction sites are underlined. F, forward; R, reverse; gDNA, genomic DNA; *pbcrt, P. berghei chloroquine resistance transporter*; UTR, untranslated region.

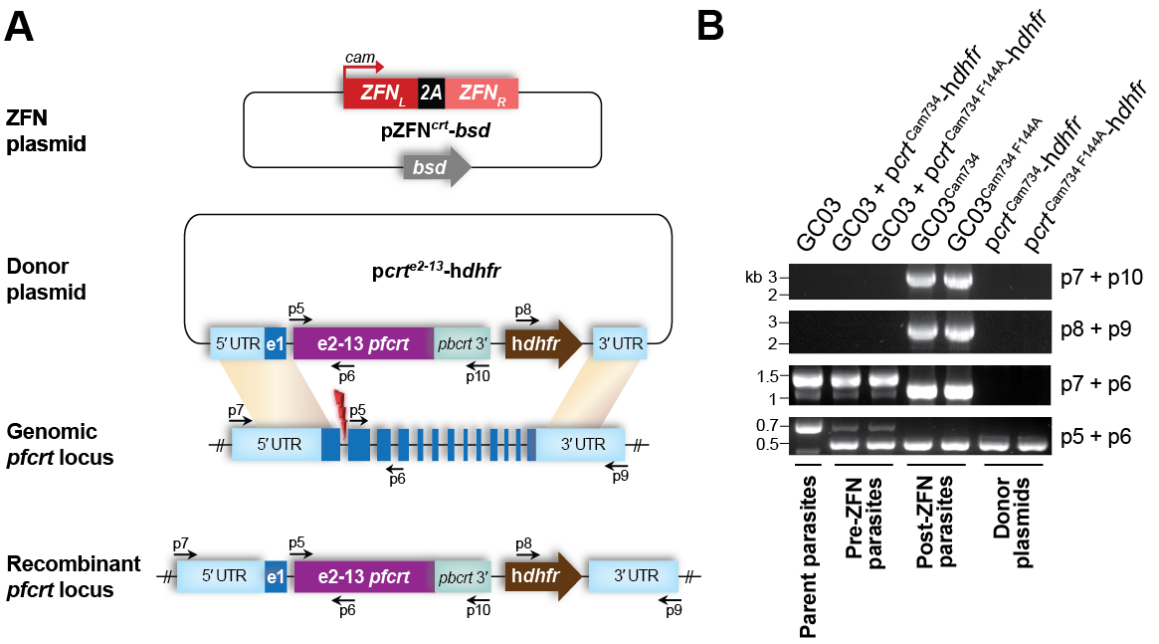

Figure 3.1. Genetic modification of the *pfcrt* locus via zinc finger nucleases (ZFNs). (**A**) Genetic engineering strategy. Briefly, parasites were transfected with a donor template plasmid (p*crt*-h*dhfr*) with the coding region corresponding to exons 2 to 13 (e2-13) of a *pfcrt* allele of interest (indicated in purple; see **Table 3.1** for full list of *pfcrt* alleles). Donor plasmids also include the following: a *P. berghei crt* (*pbcrt*) 3′ UTR sequence, a human *dhfr* (h*dhfr*) selection cassette, and flanking left (~0.4 kb upstream of the intron 1-exon 2 boundary) and right (~1 kb native 3′ UTR) homology regions.[295] Donor plasmid-enriched parasites were transfected with pZFN^{crt}-*bsd*, which encodes a pair of *pfcrt*-specific ZFNs (ZFN$_L$ and ZFN$_R$) via the *calmodulin* (*cam*) promoter and includes the *blasticidin S deaminase* (*bsd*) selection cassette. Operating as an obligate heterodimer, ZFN$_L$ and ZFN$_R$ catalyze a double-stranded DNA break in the *pfcrt* intron 1-exon 2 region (indicated with a red bolt). Recombinant parasites that were successfully generated via DNA repair mechanisms encode *pfcrt* e2-13 bearing mutations of interest. Recombinant parasites were cloned by limiting dilution, genetic editing was verified by diagnostic PCR (see **Figure 3.1*B***), and sequence integrity was verified at the DNA and RNA levels. (**B**) Diagnostic PCRs of representative recombinant parasites encoding full-length (GC03^{Cam734}) and back-mutated (GC03$^{Cam734\ F144A}$) *pfcrt* alleles. Controls include genetically unedited parental parasites (GC03), unedited donor plasmid-enriched parasites (GC03 + either p*crt*^{Cam734}-h*dhfr* or p*crt*$^{Cam734\ F144A}$-h*dhfr*) and donor plasmids alone (p*crt*^{Cam734}-h*dhfr* or p*crt*$^{Cam734\ F144A}$-h*dhfr*). Primer (p) locations are illustrated in **Figure 3.1*A***. PCR amplicons for ZFN-edited lines demonstrated the expected sizes of 0.4 kb (p5+p6), 1.2 kb (p7+p6), 2.5 kb (p8+p9), and 2.7 kb (p7+p10).

To verify sequence integrity of parasite clones, the *pfcrt* locus was PCR-amplified using primers p10 + p7 and subsequently sequenced with primers p3 and p4. Sequence integrity was also verified at the transcript level by RT-PCR, as previously described.[242] The previously generated[295] $GC03^{GC03}$ and $GC03^{Dd2}$ lines as well as the unedited GC03 parental line were also included in subsequent analyses.

Drug susceptibility assays

Drug inhibitory concentrations that result in 50% (IC_{50}) or 90% (IC_{90}) growth inhibition were determined for a panel of drugs (CQ ± 0.8 µM verapamil [VP], monodesethyl-CQ, monodesethyl-amodiaquine, quinine, piperaquine, lumefantrine, artesunate, and pyronaridine), as previously described.[217] Using an Accuri C6 flow cytometer, growth of parasites after 72 h exposure to drug was quantified via SYBR Green I and MitoTracker Deep Red staining. Reversibility of CQR by 0.8 µM VP was expressed as the CQ response modification index (RMI), equivalent to the quotient of the CQ+VP IC_{50} divided by the CQ IC_{50}.[298] Statistical significance was determined via non-parametric Mann-Whitney *U* tests using GraphPad Prism 6 software.

In vitro growth assays and derivation of growth selection coefficients

As a proxy for *in vitro* fitness, growth of parasite lines was assessed in 1:1 co-culture assays with the fluorescent reporter line $NF54^{eGFP}$, using previously described methods.[242] Briefly, 1:1 co-cultures consisting of the reporter line (GFP^+) and a single *pfcrt*-modified test line (GFP^-) were grown for 10 generations, and parasitemias were maintained between 0.3% and 8%. The GFP^- proportion of parasites was determined every third day by flow cytometric detection of GFP and the far-red fluorescent dye

SYTO61, which identifies infected RBCs (iRBCs).

The ratio of the frequencies of the GFP$^-$ test strain (p_t) and the GFP$^+$ reporter strain (q_t) at time t was natural log-transformed and used to calculate the fitness (ω) of the test allele as per $\ln\left(\frac{p_t}{q_t}\right) = \ln\left(\frac{p_0}{q_0}\right) + t\ln(\omega)$.[242] The relative fitness for each test strain was normalized to that of the GC03^{Cam734} parasite line, which encodes the full-length Cam734 *pfcrt* allele, and was expressed as the normalized relative fitness (ω'). The per-generation selection coefficient (s) for each test strain was subsequently computed as per the relationship $s = \omega' - 1$.[247] Statistical significance was assessed via two-way ANOVA with Sidak's post-hoc test using GraphPad Prism 6 software.

Metabolite extraction and mass spectrometric analysis

All parasite culturing, metabolite extraction, mass spectrometry data acquisition, and data analyses were conducted using previously established methods.[232] Briefly, after double synchronization with 5% sorbitol, late-stage (~36-42 h) *P. falciparum* trophozoites were magnetically purified using CS columns and a SuperMACS magnetic separator (Miltneyi Biotec). Eluted iRBCs were resuspended at 0.4% hematocrit and allowed to recover for 2 h at 37°C in a tissue culture incubator. Following recovery, cells were rapidly cooled to 4°C and pelleted by centrifugation at 2,000×g for 5 min. Media was then aspirated away from the iRBC pellets, and metabolites were extracted by resuspending cells in cold (4°C) 90% methanol, homogenized by vortexing, and centrifuged at 10,000×g for 5 min at 4°C. The supernatant metabolite extracts were harvested and stored at -80°C until metabolomic analysis. Just prior to analysis, samples were dried under a stream of N_2 and were resuspended at a 4:1 dilution (relative to the original iRBC pellet volume)

in HPLC-grade water. High-resolution mass spectrometry data were acquired on a Thermo Fisher Exactive Mass spectrometer in negative mode using 25 min reverse phase gradients using ion-pairing chromatography.[232] Metabolites were identified using the known chromatographic retention times of standards, and metabolite signals were quantified using MAVEN.[232] To allow for more direct metabolite-to-metabolite comparison of phenotypes, raw mass spectrometry signals were expressed as *z*-scores. Briefly, for each metabolite, the mean expected signal ($\bar{x}$) was defined as the mean intensity observed in the control line ($GC03^{Dd2}$). Likewise, the standard deviation (s) for each metabolite signal was calculated from signals observed in the $GC03^{Dd2}$ line (deduced from 4 replicates acquired from 3 independent harvests). The *z*-score (z_i) for each observed signal (x_i) was then computed as per the relationship $z_i = [x_i - \bar{x}]/s$ and plotted according to metabolite class. For summary statistics, *z*-scores were calculated from the signals observed for each compound class. These classes were comprised of metabolites that are directly associated with a metabolic pathway (e.g. TCA metabolism included TCA intermediates as well as the TCA-associated amino acid glutamate). *P* values were computed by one-way ANOVA. All data analyses and statistical test were conducted using custom in-house software written in the R statistical software environment.

Heme fractionation experiments

The heme fraction profiles of *pfcrt*-modified $GC03^{GC03}$, $GC03^{Dd2}$, and $GC03^{Cam734}$ parasites were determined following recently published protocols.[334] First, parasite growth in response to CQ was determined using the lactate dehydrogenase assay.[335] Heme fractionation assays were then initiated by incubating sorbitol-synchronized,

early ring-stage parasites in the absence or presence of CQ in multiples (0.5×, 1×, 2×, 2.5×, and 3×) of the biological CQ IC_{50}. After 32 h, iRBCs were treated with 1% saponin to release mature trophozoites, followed by hypotonic lysis and centrifugation. Supernatants were treated with 2% SDS and 2.5% pyridine, yielding the Hb fraction. Pellets were treated with 2% SDS and 2.5% pyridine, sonicated, and centrifuged, and supernatants were removed to isolate the free heme fraction. The remaining pellets were solubilized in 2% SDS and 0.1 M NaOH, sonicated, neutralized with HCl, and treated with 2% SDS and 2.5% pyridine to generate the Hz fraction. For each fraction, the UV-visible spectrum of heme present as a heme-pyridine complex was measured with a multi-well plate reader (Spectramax 340 PC, Molecular Devices). The abundance of Hb, free heme, and Hz species was reported as a percent and as an absolute amount of heme Fe per cell. Cells were quantified using flow cytometry, as previously described.[334] Statistical significance was assessed via unpaired *t* tests with Welch's correction using GraphPad Prism 6 software.

Yeast drug transport assays

Cultivation, transfection, and quantitative growth rate analysis of *Saccharomyces cerevisiae* yeast strains was performed following previously detailed protocols.[208,281] Briefly, CH1305 yeast strains were transfected with either pYES2 (blank vector) or pYES2-derived plasmids encoding galactose/raffinose-inducible, codon-optimized PfCRT isoforms GC03 (HB3; wild-type), Cam734, Cam738, or Dd2. Quantitative assessment of yeast growth, a validated proxy for CQ transport,[336] was done in PfCRT-inducing (galactose/raffinose) or PfCRT-noninducing (glucose) conditions, with a starting cell density (OD_{600}) of 0.1. Yeast growth ± 5 mM CQ was measured in

triplicate with a Tecan GENios microplate reader following established parameters.[208] PfCRT protein expression of yeast lines was evaluated using Western blot analysis.

Comparison of protein levels of yeast-expressed PfCRT isoforms

Protein extracts from yeast strains harboring V5-tagged PfCRT isoforms or empty vector were prepared and subjected to Western blot analysis, as in previous studies.[336] Briefly, total protein in the yeast crude membrane fraction was quantified using the amido black assay. 7 μg total protein was subsequently incubated at 65°C for 5 min, electrophoretically separated on a 12% SDS-PAGE gel, and transferred onto a PVDF membrane. Membranes were incubated with horseradish peroxidase-conjugated anti-V5-antibodies, and the 51.8-kDa PfCRT-V5 protein was detected by chemiluminescence using Amersham Hyperfilm ECL.

Spinning disk confocal microscopy (SDCM)

Measurements of parasite digestive vacuole (DV) volumes, data acquisition, deconvolution, and 3D restoration were performed as previously described[191,195,337] using a customized Perkin-Elmer spinning disk confocal microscope. Images were acquired with a 491 nm laser line at 200 ms exposure and 35% laser power. For CQ treatment, cultures were treated for 30 min in malaria culture media with 0.5% Albumax containing two times the 50% lethal dose of CQ (2× CQ $LD_{50,}$ corresponding to 200 nM for $GC03^{GC03}$ and $GC03^{Cam734\ F144A}$; 1.2 μM for $GC03^{Cam734}$; and 2.2 μM for $GC03^{Dd2}$, as determined using established protocols.[338] These concentrations collectively span the range of 12×–18× CQ IC_{50}). Cells were mounted onto a coverslip in HBSS containing the same concentration of CQ, and images were obtained.

Single-cell photometry (SCP)

SCP experiments were done as previously detailed[197,339] using a custom system comprised of a Nikon Diaphot microscope, a Photometrics Sensys 12-bit CCD camera, associated optics, custom perfusion cells, and custom dynamic thresholding software. Parasite cultures were treated for 30 min with media with 0.5% Albumax and a concentration of CQ corresponding to 2× CQ LD_{50} of each line (as detailed for SDCM experiments above). To measure pH, parasites were perfused with Hanks' balanced salt solution (HBSS) with the same CQ concentration, followed by calibration solutions.

RESULTS

Generation of isogenic parasites encoding full-length or back-mutated Cam734 *pfcrt* alleles

To dissect the contributions of the rare mutations comprising Cam734 PfCRT to parasite drug resistance and fitness, we utilized a recently established[295] gene editing approach (**Figure 3.1**) with *pfcrt*-specific zinc finger nucleases (ZFNs). Starting with the GC03 strain, a CQ-sensitive progeny of the HB3×Dd2 genetic cross,[184] we engineered isogenic parasites encoding full-length Cam734 *pfcrt* (GC03^{Cam734}; PfCRT haplotype of recombinant lines listed in superscript) as well as partial Cam734-like isoforms containing "back-to-wild-type" mutations at PfCRT residues 75, 144, 148, 194, and 333 (see **Table 3.1**). Our parasite panel also included the GC03^{GC03} and GC03^{Dd2} lines, which encode the wild-type GC03 (CQ-sensitive) and mutant Dd2 (CQ-resistant) haplotypes, respectively (see **Table 3.1**). For each recombinant line, two independent clones were selected, and *pfcrt* sequence integrity was verified using sequencing primers listed in **Table 3.2**. Recombinant parasite design and validation is further detailed in **Figure 3.1** and **Methods**.

Cam734 *pfcrt*-defining mutations impact parasite responses to CQ

We examined the roles of Cam734 PfCRT-constituent mutations in mediating CQR by assessing the responses of recombinant, *pfcrt*-modified parasites, along with genetically unmodified GC03 and Dd2 strains (see **Table 3.1**), to CQ and its clinically relevant metabolite, monodesethyl-CQ (md-CQ). The latter compound was included in our analysis as it shows a greater distinction between CQ-sensitive and CQ-

resistant lines and may have been the primary evolutionary selective agent.[120,242] Using 72 h flow cytometry-based drug susceptibility assays, we determined antimalarial drug concentrations that result in 50% (IC_{50}) and 90% (IC_{90}) inhibition of parasite proliferation (**Table 3.3**). For all drug susceptibility results, statistical comparisons were performed against $GC03^{Cam734}$ parasites, which encode full-length Cam734 *pfcrt*. We note that, in our analysis, recombinant GC03 parasites encoding the major Southeast Asian *pfcrt* variants Cam734 and Dd2 conferred moderate (~5-fold and ~14-fold) and high-level (~26-fold and ~43-fold) increases in CQ and md-CQ IC_{50} values, respectively, when compared to CQ-sensitive $GC03^{GC03}$ parasites (**Table 3.3**). This is consistent with earlier *P. falciparum* drug susceptibility studies.[243]

CQ (**Figure 3.2*A***; **Table 3.3**) and md-CQ (**Figure 3.2*B***; **Table 3.3**) susceptibility profiles revealed direct roles for multiple Cam734 PfCRT-defining mutations in conferring CQR. Among these, PfCRT A144F was indispensable for CQ and md-CQ resistance (compare $GC03^{Cam734}$ with the $GC03^{Cam734\ F144A}$ line). The Cam734 F144A PfCRT haplotype (see **Table 3.1**) is equivalent to Cam738 PfCRT, which, like Cam734, was initially documented in Cambodia but, in contrast, did not achieve wide regional spread.[262] Notably, although this haplotype harbors K76T and ≥3 additional mutations, its mutational configuration is nevertheless insufficient for CQR (see **Figure 3.2*A*** and **Table 3.3**). This underscores the notion of K76T as an insufficient predictor of CQR status and supports the fact that CQR can be abolished through the acquisition of additional PfCRT substitutions (e.g. C101F, L272F, C350R), even when K76T is present.[137,196,199,208]

Our analysis also found contributory roles for PfCRT mutations N75D, L148I, and T333S in conferring parasite resistance to CQ (**Figure 3.2*A***; **Table 3.3**) as well as

Table 3.3. Antimalarial IC_{50} and IC_{90} values of *pfcrt*-modified and reference parasite lines.[a]

		GC03^{Cam734} back-mutants								
	GC03^{Cam734}	**D75N**	**F144A**	**I148L**	**T194I**	**S333T**	**GC03^{GC03}**	**GC03^{Dd2}**	**GC03**	**Dd2**
CQ IC_{50}	73.4 ± 5.2	42.8 ± 4.7	11.4 ± 1.1	34.2 ± 3.3	56.1 ± 3.7	38.4 ± 4.5	14.0 ± 1.6	189 ± 19.2	11.8 ± 0.7	217 ± 16.7
n	12	6	6	5	5	6	10	10	5	5
P	–	**0.002**	**0.0001**	**0.0006**	0.06	**0.0008**	**< 0.0001**	**< 0.0001**	**0.0003**	**0.0003**
CQ IC_{90}	148 ± 10.1	91.4 ± 9.0	27.8 ± 2.2	87.2 ± 3.9	114 ± 7.1	81 ± 9.3	23.1 ± 2.1	329 ± 25.6	20.9 ± 2.2	412 ± 30
n	12	6	6	5	5	6	10	9	5	5
P	–	**0.002**	**0.0001**	**0.0003**	0.08	**0.0004**	**< 0.0001**	**< 0.0001**	**0.0003**	**0.0003**
CQ+VP IC_{50}	40.5 ± 4.0	41.1 ± 8.4	10.8 ± 2.6	31.2 ± 1.9	33.2 ± 3.0	23.4 ± 6.0	18.0 ± 2.1	29.2 ± 4.6	14.8 ± 2.9	68.7 ± 10.2
n	12	6	6	5	5	6	10	10	5	5
P	–	0.75	**0.002**	0.08	0.15	**0.024**	**0.0011**	**0.05**	**0.006**	**0.027**
CQ+VP IC_{90}	103 ± 9.2	86.4 ± 16.5	30.8 ± 7.8	89.8 ± 9.7	88.3 ± 7.9	63.6 ± 15.7	31.9 ± 4.5	110 ± 13.7	23.2 ± 4.5	156 ± 14.1
n	12	6	6	5	5	6	10	10	5	5
P	–	0.58	**0.0013**	0.15	0.12	**0.032**	**0.0002**	0.67	**0.002**	**0.020**
md-CQ IC_{50}	489 ± 36.1	320 ± 26.5	31.9 ± 3.5	131 ± 17.7	404 ± 15.2	317 ± 27.2	18.6 ± 0.8	804 ± 60.2	20.4 ± 1.6	948 ± 83.2
n	12	6	6	5	5	6	10	10	5	5
P	–	**0.003**	**0.0001**	**0.0003**	0.10	**0.007**	**< 0.0001**	**< 0.0001**	**0.0003**	**0.0003**
md-CQ IC_{90}	925 ± 66.7	653 ± 74.5	104 ± 4.6	301 ± 34.6	823 ± 38.1	650 ± 68.1	34.6 ± 1.6	1582 ± 94	36.9 ± 4.0	1522 ± 100
n	12	6	6	5	5	6	10	10	5	5
P	–	**0.007**	**0.0001**	**0.0003**	0.18	**0.007**	**< 0.0001**	**< 0.0001**	**0.0003**	**0.002**
md-AQ IC_{50}	61.1 ± 3.1	40.9 ± 2.1	15.2 ± 1.6	27.0 ± 1.0	50.9 ± 3.1	42.5 ± 3.8	14.6 ± 1.3	58.8 ± 3.7	13.8 ± 1.5	66.9 ± 7.4
n	12	6	6	5	5	6	10	10	5	5
P	–	**0.0004**	**0.0001**	**0.0003**	0.08	**0.003**	**< 0.0001**	0.75	**0.0003**	0.57
md-AQ IC_{90}	107 ± 4.4	67.9 ± 6.0	24.8 ± 2.3	52.4 ± 2.4	92.0 ± 9.0	72.9 ± 8.2	21.4 ± 2.2	105 ± 7.1	20.1 ± 3.3	111 ± 5.5
n	12	6	6	5	5	6	10	10	5	5
P	–	**0.0008**	**0.0001**	**0.0003**	0.08	**0.003**	**< 0.0001**	0.53	**0.0003**	0.57

(continued)

Table 3.3. *continued*

		GC03^{Cam734} back-mutants								
	GC03^{Cam734}	**D75N**	**F144A**	**I148L**	**T194I**	**S333T**	**GC03^{GC03}**	**GC03^{Dd2}**	**GC03**	**Dd2**
QN IC_{50}	37.2 ± 4.2	39.7 ± 5.8	23.9 ± 2.3	26.8 ± 3.4	36.4 ± 1.8	37.4 ± 4.8	55.1 ± 4.6	39.3 ± 4.2	65.4 ± 11.5	91.7 ± 11.7
n	10	6	6	5	3	6	10	10	3	3
P	–	0.71	**0.011**	0.10	0.81	0.86	**0.0052**	0.52	**0.028**	**0.007**
QN IC_{90}	144 ±11.0	114 ± 13.1	77.9 ± 6.7	120 ±15.8	114 ± 12.4	108 ± 10.0	171 ± 6.5	157 ± 11.6	173 ± 6.3	290 ± 52.5
n	10	6	6	5	3	6	10	10	3	3
P	–	0.11	**0.001**	0.20	0.24	0.07	0.09	0.43	0.16	**0.014**
PPQ IC_{50}	9.1 ± 0.6	11.9 ±1.2	11.1 ± 0.6	14.1 ± 1.5	9.8 ± 1.2	9.8 ± 0.5	11.1 ± 0.5	13.3 ± 1.1	10.4 ± 0.6	12.2 ± 0.7
n	8	6	6	3	3	6	8	8	3	3
P	–	0.11	0.08	**0.049**	0.38	0.49	0.10	**0.007**	0.50	**0.049**
PPQ IC_{90}	21.4 ± 1.9	25.0 ± 1.2	26.6 ± 0.6	28.6 ± 1.2	21.3 ± 3.2	22.0 ± 1.7	20.4 ± 1.8	27.9 ± 2.7	17.1 ± 2.2	25.9 ± 1.2
n	8	6	6	3	3	6	8	8	3	3
P	–	0.28	0.08	**0.049**	0.67	> 0.99	0.70	0.07	0.17	0.28
LUM IC_{50}	1.03 ± 0.07	1.30 ± 0.14	1.07 ± 0.04	1.09 ± 0.07	1.37 ± 0.21	1.32 ± 0.10	2.13 ± 0.13	1.08 ± 0.10	2.08 ± 0.07	1.07 ± 0.03
n	6	5	5	2	2	5	6	6	3	2
P	–	0.13	0.65	0.64	0.14	0.052	**0.002**	0.91	**0.024**	0.86
LUM IC_{90}	4.63 ± 0.37	4.94 ± 0.41	4.42 ± 0.21	4.60 ± 0.05	4.98 ± 0.56	5.40 ± 0.58	7.56 ± 0.47	5.73 ± 0.81	8.33 ± 0.31	6.52 ± 0.57
n	6	5	5	2	2	5	6	6	3	2
P	–	0.77	0.87	0.64	0.43	0.42	**0.004**	0.42	**0.024**	0.14
AS IC_{50}	0.67 ± 0.08	0.84 ± 0.12	0.52 ± 0.07	0.86 ± 0.05	0.83 ± 0.16	0.73 ± 0.08	1.17 ± 0.13	0.73 ± 0.11	0.90 ± 0.01	1.83 ± 0.21
n	7	5	5	7	2	5	7	7	3	6
P	–	0.29	0.20	0.18	0.39	0.56	**0.007**	0.56	0.18	**0.0012**
AS IC_{90}	2.31 ± 0.36	2.33 ± 0.29	1.94 ± 0.08	3.37 ± 0.33	2.24 ± 0.03	2.31 ± 0.11	3.57 ± 0.35	2.53 ± 0.45	2.83 ± 0.29	4.03 ± 0.41
n	7	5	5	7	2	5	7	7	3	6
P	–	0.55	0.50	0.053	0.50	0.36	**0.018**	0.31	0.18	**0.022**

(*continued*)

Table 3.3. *continued*

		GC03^{Cam734} back-mutants								
	GC03^{Cam734}	**D75N**	**F144A**	**I148L**	**T194I**	**S333T**	**GC03^{GC03}**	**GC03^{Dd2}**	**GC03**	**Dd2**
PND IC_{50}	5.0 ± 0.3	6.2 ± 0.3	5.9 ± 0.3	5.0 ± 0.4	5.6 ± 0.8	5.9 ± 0.3	6.5 ± 0.2	5.3 ± 0.5	5.8 ± 0.4	5.7 ± 0.7
n	8	4	4	3	3	4	6	6	5	3
P	–	0.073	0.15	0.78	0.50	0.15	**0.008**	0.41	0.17	0.19
PND IC_{90}	7.9 ± 0.4	8.7 ± 0.1	8.7 ± 0.1	8.4 ± 0.6	8.8 ± 0.3	8.7 ± 0.1	9.7 ± 0.6	9.1 ± 0.6	8.7 ± 0.1	8.7 ± 0.1
n	8	4	4	3	3	4	6	6	5	3
P	–	0.28	0.28	0.50	0.28	0.48	**0.011**	0.34	0.18	0.19

[a]IC_{50} and IC_{90} values (nM) indicate the mean ± SEM, as determined in 2 to 12 independent assays performed in duplicate. CQ + VP assays were performed with 0.8 µM VP. CQ, chloroquine; VP, verapamil; md-CQ, monodesethyl-chloroquine; md-AQ, monodesethyl-amodiaquine; QN, quinine; PPQ, piperaquine; LUM, lumefantrine; AS, artesunate; PND, pyronaridine; *n*, number of assays; *P* values were determined in a non-parametric Mann-Whitney *U* test versus the parasite line GC03^{Cam734}. *P* values <0.05 are indicated in **bold** and shaded in gray.

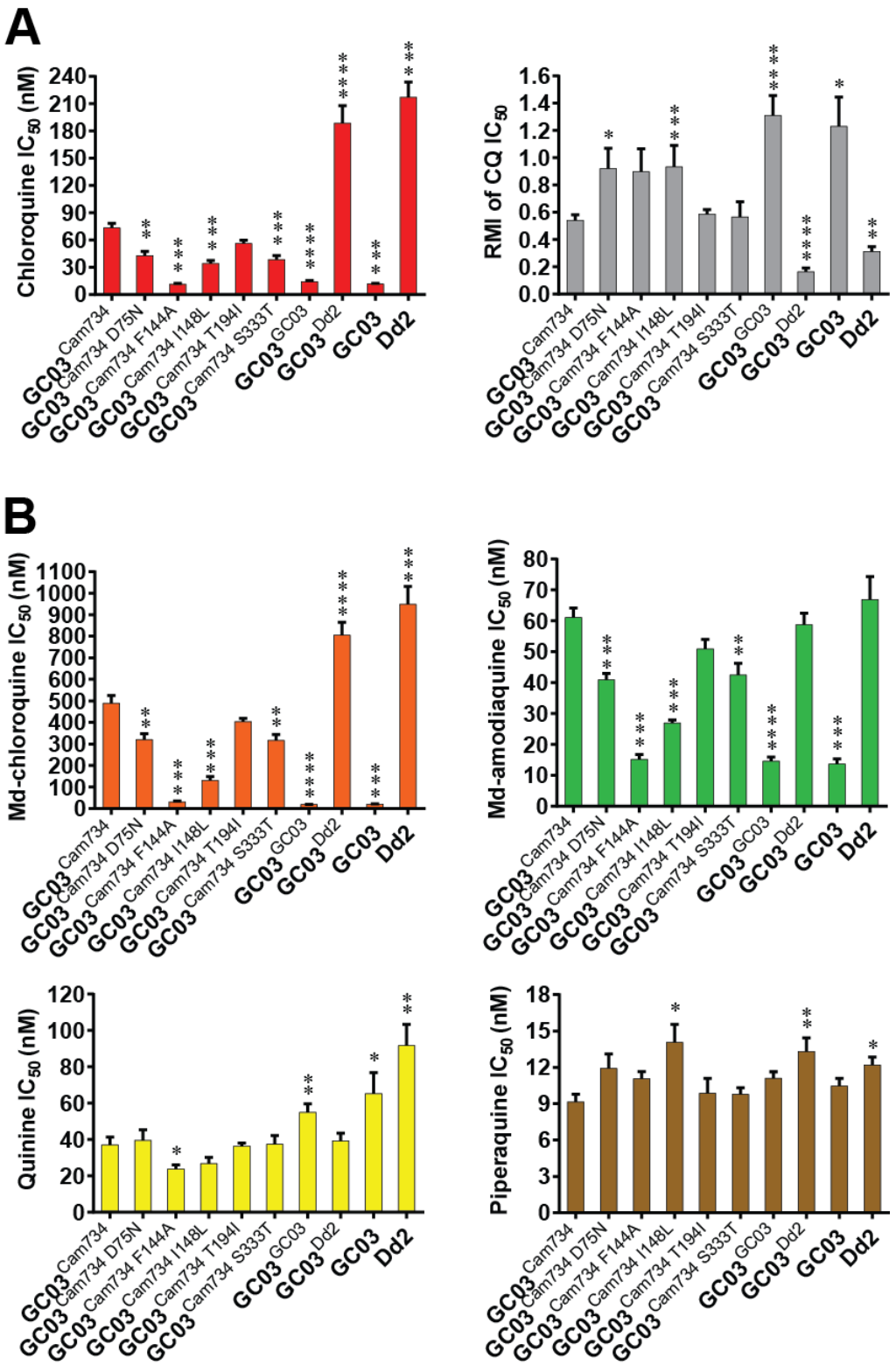

Figure 3.2. *(continued on next page)*

Figure 3.2. Drug resistance profiles of *pfcrt*-modified and reference parasite lines. (**A**) Parasite chloroquine (CQ) responses and verapamil (VP) reversibility of CQ resistance. Briefly, flow cytometry was used to assess growth of parasites following 72 h exposure to the indicated antimalarial drugs. Bar graphs correspond to mean ± SEM IC_{50} or response modification index (RMI) values. The RMI of CQ IC_{50} is equivalent to (IC_{50} for CQ + VP) ÷ (IC_{50} for CQ only), as detailed in **Methods**. (**B**) Parasite responses to monodesethyl (md)-chloroquine, md-amodiaquine, quinine, and piperaquine. Bar graphs indicate mean ± SEM IC_{50} values. Results encompass 3 to 12 independent assays conducted in duplicate. Statistical differences were determined via non-parametric Mann-Whitney *U* tests, using the mean IC_{50} value of Cam734 *pfcrt*-expressing $GC03^{Cam734}$ parasites as the comparator. Antimalarial drug susceptibility and CQ RMI data are summarized along with corresponding statistical tests in **Table 3.3** and **Table 3.4**, respectively. **P*<0.05; ***P*<0.01; ****P*<0.001. *****P*<0.0001.

md-CQ (**Figure 3.2*B*; Table 3.3**), as parasite lines encoding back-mutations at each of the corresponding PfCRT residues demonstrated significant reductions in resistance (range of 1.5 to 3.7-fold reductions in CQ or md-CQ IC_{50} values for $GC03^{Cam734\ D75N}$, $GC03^{Cam734\ I148L}$, and $GC03^{Cam734\ S333T}$ as compared to $GC03^{Cam734}$ parasites). Thus, to various degrees, N75D, A144F, L148I, and T333S directly contribute to CQR and are not merely compensatory in terms of restoring function or fitness to mutant PfCRT isoforms. Only the I194T mutation was found to not significantly contribute to CQR.

A defining molecular feature of *P. falciparum* CQR is resistance reversal by the calcium channel blocker verapamil (VP).[126] The extent to which VP modifies CQR, referred to as the CQ response modification index (RMI), is PfCRT isoform-specific and is calculated by dividing the IC_{50} value for CQ in the presence of 0.8 μM VP by the IC_{50} value for CQ alone.[298] Our CQR reversibility results are depicted in **Figure 3.2*A*** and **Table 3.4**. Consistent with previous studies,[243] isogenic parasites expressing PfCRT variants Cam734 ($GC03^{Cam734}$) and Dd2 ($GC03^{Dd2}$) exhibited moderate and high-level CQR reversibility (2.4-fold and 8.1-fold reductions in the CQ RMI, respectively, versus the $GC03^{GC03}$ line that showed no CQR reversibility). Among the recombinant lines encoding partial, back-to-wild-type Cam734 PfCRT haplotypes, $GC03^{Cam734\ D75N}$ and $GC03^{Cam734\ I148L}$ parasites exhibited statistically significant increases in CQ RMI values as compared to $GC03^{Cam734}$ parasites, highlighting critical roles for mutations N75D and L148I in the VP reversibility effect. These findings uncover a novel role for PfCRT residue 148 in mediating VP reversal of CQR and align with previous studies that implicate mutation at residue 75 in mediating this reversal phenotype.[133,243]

Table 3.4. Verapamil-mediated CQ resistance reversibility of *pfcrt*-modified and reference parasite lines.[a]

Line			Line			Line		
GC03^{Cam734}	RMI	0.54 ± 0.04	GC03$^{Cam734\ T194I}$	RMI	0.59 ± 0.03	GC03	RMI	1.2 ± 0.21
	n	12		*n*	5		*n*	5
	P	–		*P*	0.63		*P*	**0.025**
GC03$^{Cam734\ D75N}$	RMI	0.92 ± 0.15	GC03$^{Cam734\ S333T}$	RMI	0.57 ± 0.11	Dd2	RMI	0.31 ± 0.04
	n	6		*n*	6		*n*	5
	P	**0.020**		*P*	0.84		*P*	**0.0048**
GC03$^{Cam734\ F144A}$	RMI	0.90 ± 0.17	GC03^{GC03}	RMI	1.3 ± 0.15			
	n	6		*n*	10			
	P	0.13		*P*	**< 0.0001**			
GC03$^{Cam734\ I148L}$	RMI	0.93 ± 0.07	GC03^{Dd2}	RMI	0.16 ± 0.03			
	n	5		*n*	10			
	P	**0.0002**		*P*	**< 0.0001**			

[a]Reversibility of chloroquine (CQ) resistance by 0.8 µM verapamil (VP) is indicated as the CQ response modification index (RMI), equivalent to (IC_{50} for CQ+VP) ÷ (IC_{50} for CQ only). Shown are mean RMI ± SEM values, as determined in 5 to 12 independent assays. *n*, number of assays. *P* values were determined in a non-parametric Mann-Whitney *U* test versus the parasite line GC03^{Cam734}. *P* values <0.05 are indicated in **bold** and shaded in gray.

Cam734 *pfcrt*-defining mutations impact parasite responses to clinically important antimalarials

As PfCRT variants can modulate parasite susceptibility to a host of antimalarials,[114] we also assessed the effects of Cam734 PfCRT-constituent mutations on parasite responses to clinically employed antimalarials beyond CQ (**Figure 3.2** and **Figure 3.3**). We explored the following: (1) ACT partner drugs, including monodesethyl-amodiaquine (md-AQ, the active metabolite of AQ), lumefantrine (LUM), piperaquine (PPQ), and pyronaridine (PND); (2) the ACT artemisinin derivative artesunate (AS); and (3) quinine (QN), a second-line agent used to treat severe malaria. In keeping with known cross-resistance relationships between CQ and AQ,[114] we observed significant reductions in md-AQ resistance (**Figure 3.2*B*; Table 3.3**) among parasites harboring reversions of mutations N75D, A144F, L148I, and T333S (range of 1.4 to 4.0-fold reductions in md-AQ IC_{50} values for $GC03^{Cam734\ D75N}$, $GC03^{Cam734\ F144A}$, $GC03^{Cam734\ I148L}$, and $GC03^{Cam734\ S333T}$ as compared to $GC03^{Cam734}$ parasites). Reversion of PfCRT mutation A144F back to wild-type (compare $GC03^{Cam734\ F144A}$ with $GC03^{Cam734}$) was likewise associated with a significant (~1.6-fold) reduction in QN IC_{50} (**Figure 3.2*B*; Table 3.3**), emphasizing A144F as a critical determinant of parasite resistance to multiple quinoline-type antimalarials. We further detected a modest (~1.5-fold), statistically significant increase in PPQ IC_{50} for the $GC03^{Cam734\ I148L}$ line, as compared to $GC03^{Cam734}$. This highlights the capacity of *pfcrt* mutations to impact parasite PPQ resistance, a rising problem in Southeast Asia with a presently unclear genetic basis.[135,136,138] As compared to wild-type (GC03) *pfcrt*, full-length Cam734 sensitized parasites to LUM, AS, and PND, and this phenotype was not modulated by any of the Cam734-constituent mutations studied herein (**Figure 3.3**; **Table 3.3**).

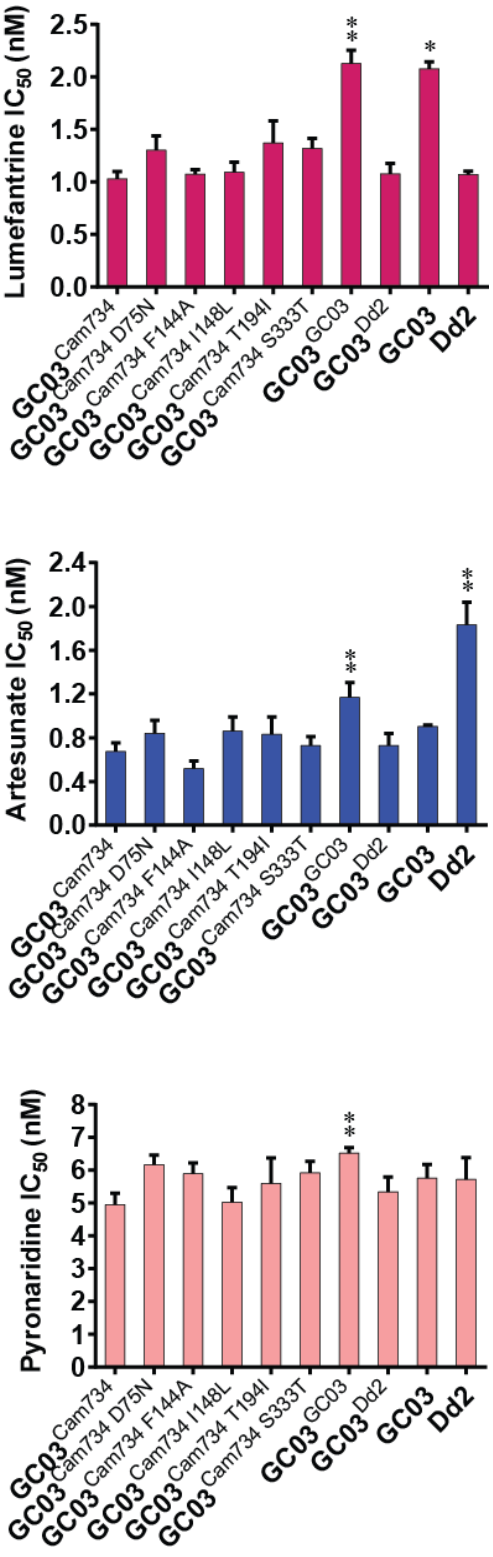

Figure 3.3. *(continued on next page)*

Figure 3.3. Parasite responses to lumefantrine, artesunate, and pyronaridine. Following 72 h exposure of parasites to the indicated antimalarial drugs, parasite growth was assessed using flow cytometry. Bar graphs correspond to mean ± SEM IC_{50} values. Results encompass 2 to 12 independent assays conducted in duplicate. Statistical differences were determined via non-parametric Mann-Whitney *U* tests, using the mean IC_{50} value of Cam734 *pfcrt*-expressing $GC03^{Cam734}$ parasites as the comparator. IC_{50} and IC_{90} values are summarized along with corresponding statistical tests in **Table 3.3**. **P*<0.05; ***P*<0.01; ****P*<0.001. *****P*<0.0001.

Cam734 *pfcrt*-defining mutations offset parasite fitness costs *in vitro*

Previous efforts to disrupt the *pfcrt* gene demonstrated that it is essential for survival of blood-stage *P. falciparum* parasites.[229] Furthermore, *pfcrt* mutations can be deleterious to parasite growth,[242,243] a measurable phenotype that serves as a proxy for fitness and reflects parasite functional requirements.[239] To evaluate the contributions of Cam734 *pfcrt*-constituent SNPs to parasite growth, we used previously established co-culture methods[242,299] to determine the relative growth rates of our isogenic, *pfcrt*-modified parasites. Briefly, this entailed setting up 1:1 co-cultures consisting of equal proportions of a CQ-sensitive, wild-type *pfcrt*-expressing GFP-positive (GFP^+) reporter line and a *pfcrt*-modified GFP-negative (GFP^-) test line (see **Methods**). To assess the impact of a sub-therapeutic dose of CQ on parasite growth, experiments were performed in the absence or presence of 7.5 nM CQ (~0.5× CQ IC_{50} of CQ-sensitive $GC03^{GC03}$ parasites). These co-cultures were monitored for 10 generations, with the GFP^- proportion of co-culture determined every third day by flow cytometry (**Figure 3.4**). As detailed in **Methods**, these data were used to derive the per-generation selection coefficient (s) of each test line (**Figure 3.5**; **Table 3.5**). The s parameter serves as a proxy for the degree of fitness of a given parasite line, as compared to $GC03^{Cam734}$ parasites, which encode the full-length Cam734 *pfcrt* allele ($s=0$, $s>0$, and $s<0$ indicate fitness levels equal, greater than, or less than that of $GC03^{Cam734}$ parasites).

As determined in our *in vitro* growth assays (**Figure 3.5**; **Table 3.5**), the growth rate of parasites encoding Cam734 *pfcrt* was markedly increased relative to isogenic parasites encoding mutant Dd2 *pfcrt* ($s=-0.25$ for $GC03^{Dd2}$ versus $GC03^{Cam734}$) and was more comparable to growth of parasites encoding wild-type GC03 *pfcrt* ($s=0.06$ for

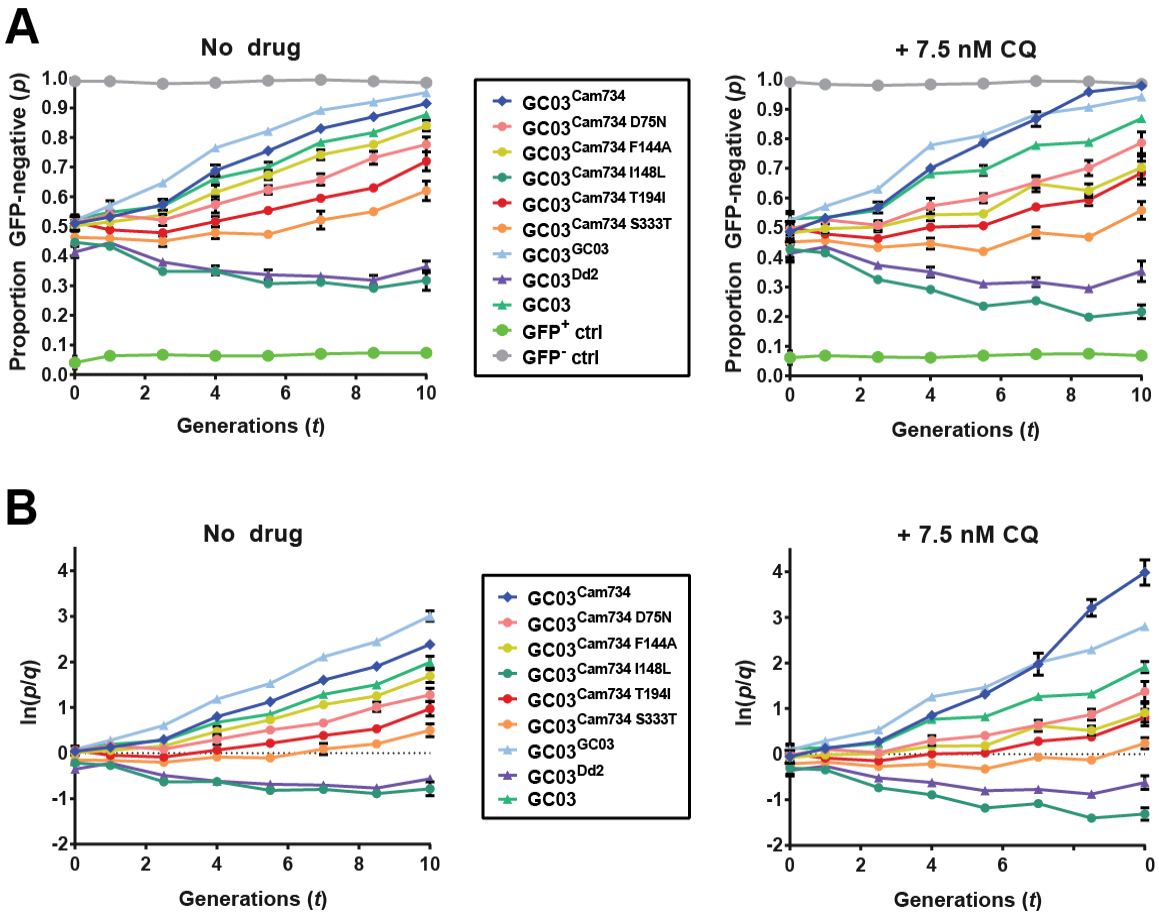

Figure 3.4. *In vitro* growth plots of *pfcrt*-modified and reference parasites. Co-cultures consisting of 1:1 proportions of a single GFP-negative (GFP^-) test line and a GFP-positive (GFP^+) reporter line were seeded at day 0 and regularly monitored by flow cytometry for 10 parasite generations (see **Methods**). Three independent assays were conducted in duplicate in the absence or presence of a sub-lethal dose of chloroquine (CQ; 7.5 nM, equivalent to ~0.5× CQ IC_{50} of the CQ-sensitive line $GC03^{GC03}$). (**A**) Plots of the mean ± SEM proportion of GFP^- test lines (*p*) as a function of number of parasite generations (*t*). GFP^+ (reporter line only) and GFP^- ($GC03^{GC03}$ only) control (ctrl) lines exhibited steady fluorescence levels over the duration of the experiment. (**B**) Plots of mean ± SEM natural log (ln)-transformed ratios of the proportion of a GFP^- test line to the GFP^+ reporter line at time *t* (p_t/q_t). This parameter was used to derive *in vitro* growth selection coefficients (*s*).

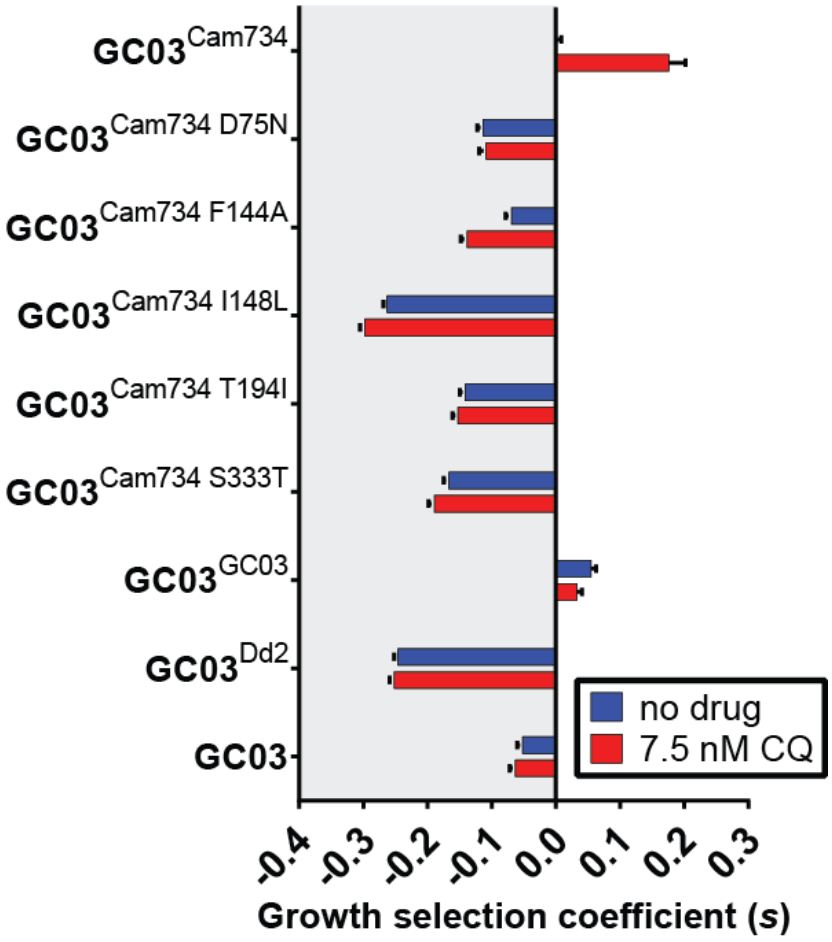

Figure 3.5. *In vitro* growth profiles of *pfcrt*-modified and reference parasite lines. Briefly, co-cultures initially consisting of a 1:1 ratio of a GFP$^-$ test strain and a GFP$^+$ reporter strain were monitored by flow cytometry for 10 generations (see **Methods** and **Figure 3.4**), and the per-generation selection coefficient (*s*) for each test strain was derived from parasite growth curves. Bar graphs correspond to mean ± SEM *s* values for parasites subjected to no drug or 7.5 nM chloroquine (CQ). A summary of *s* values and inter-strain and intra-strain statistical tests is provided in **Table 3.5**.

Table 3.5. *In vitro* growth selection coefficients of *pfcrt*-modified and reference parasite lines.[a]

Line		No drug	7.5 nM CQ	Line		No drug	7.5 nM CQ
GC03^{Cam734}	*s*	0.00 ± 0.008	0.18 ± 0.026	GC03$^{Cam734\ S333T}$	*s*	-0.17 ± 0.008	-0.19 ± 0.009
	P_1	–	–		P_1	**< 0.0001**	**< 0.0001**
	P_2	**< 0.0001**			P_2	0.69	
GC03$^{Cam734\ D75N}$	*s*	-0.11 ± 0.009	-0.11 ± 0.011	GC03^{GC03}	*s*	0.06 ± 0.007	0.03 ± 0.008
	P_1	**< 0.0001**	**< 0.0001**		P_1	**0.002**	**< 0.0001**
	P_2	> 0.99			P_2	0.71	
GC03$^{Cam734\ F144A}$	*s*	-0.07 ± 0.009	-0.14 ± 0.010	GC03^{Dd2}	*s*	-0.25 ± 0.006	-0.25 ± 0.007
	P_1	**< 0.0001**	**< 0.0001**		P_1	**< 0.0001**	**< 0.0001**
	P_2	**< 0.0001**			P_2	> 0.99	
GC03$^{Cam734\ I148L}$	*s*	-0.26 ± 0.006	-0.30 ± 0.007	GC03	*s*	-0.05 ± 0.009	-0.06 ± 0.009
	P_1	**< 0.0001**	**< 0.0001**		P_1	**0.0047**	**< 0.0001**
	P_2	0.15			P_2	0.99	
GC03$^{Cam734\ T194I}$	*s*	-0.14 ± 0.009	-0.15 ± 0.009				
	P_1	**< 0.0001**	**< 0.0001**				
	P_2	0.99					

[a]Parasite *in vitro* growth was evaluated in the absence or presence of a sub-lethal dose of CQ (7.5 nM; ~0.5×CQ IC_{50} of the CQ-sensitive line GC03^{GC03}) and normalized against GC03^{Cam734} in the absence of drug pressure (6 replicates per condition). The per-generation selection coefficient (indicated above as *s* ± SEM) was derived from the relative fitness index (ω') as per the relationship $s = \omega' - 1$, such that $s<0$ and $s>0$ respectively indicate growth inferior or superior to that of the GC03^{Cam734} parasite line, which encodes the full-length Cam734 *pfcrt* allele. CQ, chloroquine; P_1, *P* value for inter-strain comparisons, determined versus the parasite line GC03^{Cam734} using two-way ANOVA with Sidak's post-hoc test; P_2, *P* value for intra-strain comparisons, determined for a given parasite strain in the absence versus presence of 7.5 nM CQ using two-way ANOVA with Sidak's post-hoc test. *P* values <0.05 are indicated in **bold** and shaded in gray.

GC03^{GC03} versus GC03^{Cam734}). These findings agree with earlier studies of isogenic, *pfcrt*-modified lines constructed via an independent allelic exchange strategy.[243] Remarkably, growth of GC03^{Cam734} parasites was significantly enhanced (~1.2-fold; **Figure 3.5**; **Table 3.5**) by the presence of a sub-lethal dose of CQ (7.5 nM), surpassing the growth rates of all other parasite lines, including those expressing GC03 *pfcrt*. Our results further demonstrate that the Cam734 PfCRT-constituent mutations N75D, A144F, L148I, I194T, and T333S distinctly contribute to the growth of asexual blood-stage parasites expressing full-length Cam734 PfCRT, as the corresponding partial, back-mutant haplotypes conferred significantly decreased relative growth rates (*s* value range of -0.07 to -0.30 for GC03$^{Cam734\ D75N}$, GC03$^{Cam734\ F144A}$, GC03$^{Cam734\ I148L}$, GC03$^{Cam734\ T194I}$, and GC03$^{Cam734\ S333T}$; see **Table 3.5**).

Among the back-mutant parasites, the most deleterious growth was observed for parasites expressing Cam734 I148L PfCRT, which was reminiscent of the growth phenotype of the Dd2 PfCRT isoform that is known to substantially impair parasite fitness (compare GC03$^{Cam734\ I148L}$ versus GC03^{Dd2}; **Figure 3.5**; **Table 3.5**). Considering our dissection of the roles of Cam734 PfCRT mutations in parasite CQ susceptibility and growth, our results suggest that PfCRT I194T is a critical compensatory mutation, while mutations N75D, A144F, I148L, and S333T play dual roles, directly contributing to CQR and compensating for associated fitness costs.

Cam734 *pfcrt* affects parasite hemoglobin processing and central carbon metabolism

The catabolism of host-derived Hb is an essential parasite process that liberates two major products: (1) free heme that is subsequently incorporated into crystalline Hz

and (2) free Hb-derived peptides that ultimately contribute to the parasite's nutrient pool.[340] Recent studies have shown that peptides derived from either α or β chains of Hb can accumulate up to 32-fold within isogenic parasites expressing CQ-resistant (Dd2 and 7G8) *pfcrt* alleles as compared to CQ-sensitive (wild-type) *pfcrt*-expressing parasites.[232] The accumulation of Hb-derived peptides in parasites expressing PfCRT variants was subsequently linked to impaired Hb catabolism and a consequent defect in their *in vitro* fitness, as measured by growth rate analysis.[232] Given the unique capacity of mutant Cam734 PfCRT to neutralize fitness costs that are typically associated with CQ-resistant PfCRT isoforms, we proceeded to examine whether Cam734 PfCRT mitigates the accumulation of Hb-derived peptides.

To test this, we measured endogenous metabolite levels in isogenic lines encoding the CQ-resistant *pfcrt* alleles Cam734 and Dd2 ($GC03^{Cam734}$ and $GC03^{Dd2}$). Briefly, red blood cells (RBCs) harboring late-stage (~36-42 h) trophozoites were magnetically purified, metabolites were extracted, and extracts were analyzed using established mass spectrometry-based metabolomic methods.[232] Results of our metabolomic analysis are depicted in **Figure 3.6** for individual metabolites and **Figure 3.7** for compound classes. Metabolite signal intensities and *z*-scores are reported in **Table 3.6** and **Table 3.7**, respectively. Our results show that the CQ-resistant *pfcrt* alleles Cam734 and Dd2 conferred comparably accumulated levels of Hb-derived peptides (P=0.33; see **Figure 3.7** and **Table 3.7**), which have previously been shown to accumulate in the $GC03^{Dd2}$ line.[232] As perturbations in Hb metabolism are generally associated with a fitness cost, the similarity in peptide levels between $GC03^{Cam734}$ and $GC03^{Dd2}$ parasites indicates that Cam734 PfCRT promotes parasite growth through mechanisms other than changes in peptide accumulation.

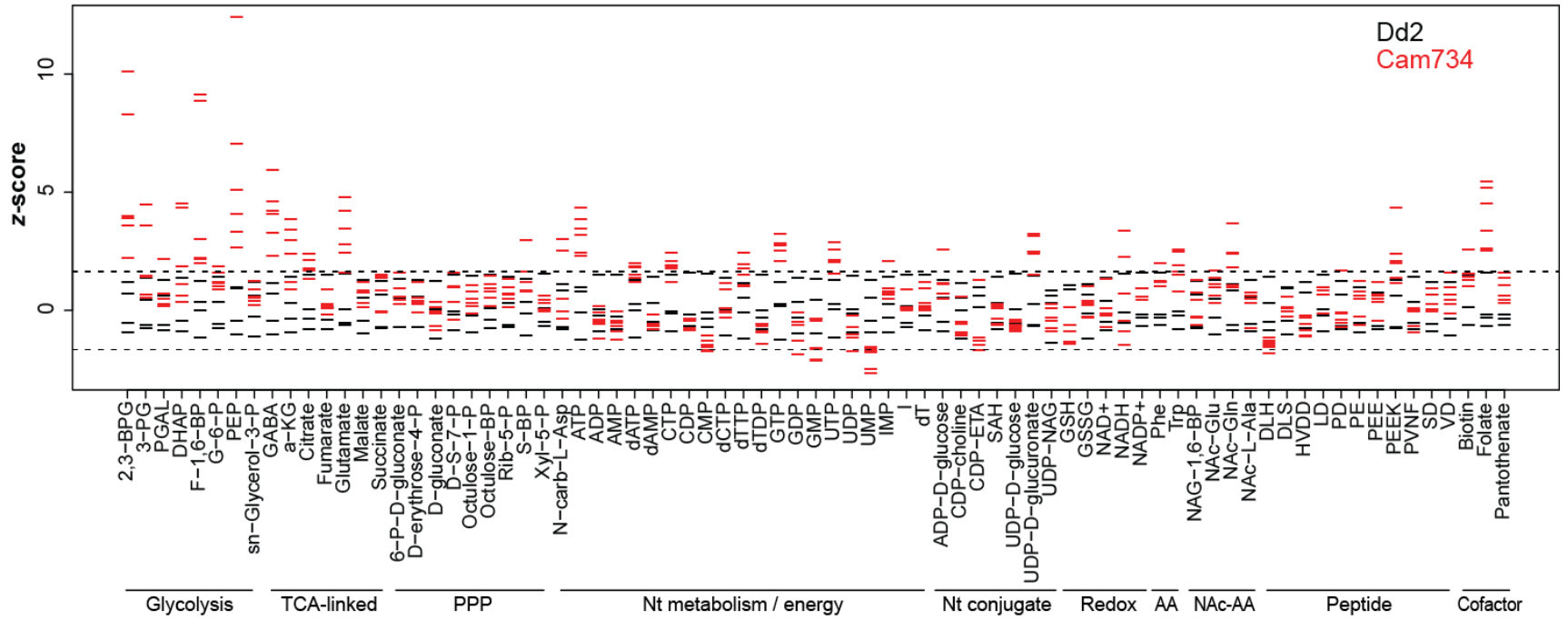

Figure 3.6. Individual metabolite profiles of isogenic, mutant *pfcrt*-expressing parasites. Metabolite extracts derived from tightly-synchronized trophozoite-stage isogenic (GC03) parasites encoding either Dd2 or Cam734 *pfcrt* were analyzed by mass spectrometry. Metabolite signals were converted to *z*-scores. Each bar shows the *z*-score for an experimental replicate obtained for GC03^{Dd2} (black) or GC03^{Cam734} (red) parasites. Dashed lines represent lower (5%) and upper (95%) boundaries for the normal distribution, as defined for GC03^{Dd2} parasites. Values outside this range in the GC03^{Cam734} samples differ significantly from the isogenic GC03^{Dd2} line. Metabolites were harvested on three independent occasions (*n*=4 to 6 total replicates per parasite strain). Metabolite *z*-scores, *P* values, and full names of individual metabolites are detailed in **Table 3.7**. TCA, tricarboxylic acid; PPP, pentose phosphate pathway; Nt, nucleotide; AA, amino acid; NAc, N-Acetylated. Mass spectrometric analysis by I. Lewis.

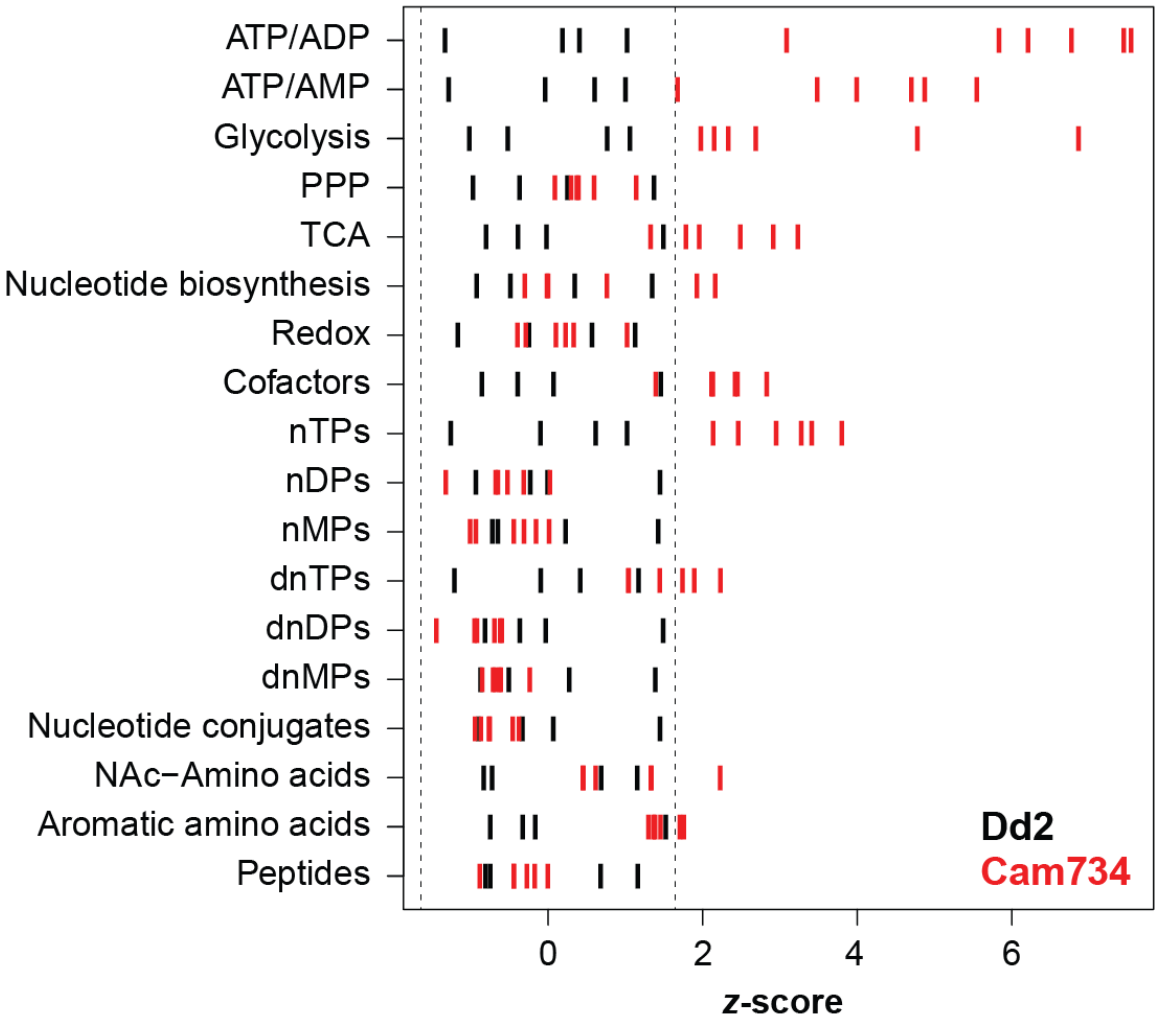

Figure 3.7. Metabolomic profiles of isogenic, mutant *pfcrt*-expressing parasites. Metabolite extracts derived from tightly-synchronized trophozoite-stage isogenic (GC03) parasites encoding either Dd2 or Cam734 *pfcrt* were analyzed by mass spectrometry. For each metabolite class, individual metabolite signals were averaged and expressed as *z*-scores (detailed in **Methods**), allowing for comparisons across distinct metabolite classes. Dashed lines represent lower (5%) and upper (95%) boundaries for the normal distribution, as defined for GC03^{Dd2} (black) parasites. Values outside this range in the GC03^{Cam734} (red) samples differ significantly from the isogenic GC03^{Dd2} line. Metabolites were harvested on three independent occasions (n=4-6 total replicates per parasite strain). Compound class abbreviations, *z*-scores, and *P* values are presented in **Table 3.7**. Mass spectrometric analysis by I. Lewis.

Table 3.6. Metabolite mass spectrometry signal intensities.[a]

		GC03^{Dd2}				GC03^{Cam734}					
Class	**Compound**	***r1***	***r2***	***r3***	***r4***	***r1***	***r2***	***r3***	***r4***	***r5***	***r6***
Glyc	2,3-bisphosphoglycerate (2,3-BPG)	1.82 E+06	2.04 E+06	1.75 E+06	2.13 E+06	2.62 E+06	2.61 E+06	2.55 E+06	2.31 E+06	3.38 E+06	3.70 E+06
	3-phosphoglycerate (3-PG)	1.67 E+05	3.27 E+05	1.75 E+05	2.56 E+05	2.62 E+05	2.74 E+05	3.33 E+05	3.31 E+05	4.95 E+05	5.62 E+05
	D-glyceraldehdye-3-phosphate (PGAL)	9.98 E+03	1.38 E+04	1.04 E+04	1.26 E+04	1.24 E+04	1.19 E+04	1.28 E+04	1.20 E+04	1.18 E+04	1.55 E+04
	Dihydroxy-acetone-phosphate (DHAP)	3.30 E+03	4.87 E+03	2.88 E+03	3.99 E+03	3.96 E+03	4.62 E+03	4.20 E+03	5.30 E+03	7.42 E+03	7.60 E+03
	Fructose-1,6-bisphosphate (F-1,6-BP)	6.46 E+05	6.81 E+05	5.40 E+05	7.63 E+05	8.52 E+05	8.30 E+05	8.48 E+05	9.27 E+05	1.47 E+06	1.49 E+06
	Glucose-6-phosphate (G-6-P)	1.48 E+06	2.01 E+06	1.42 E+06	1.73 E+06	1.87 E+06	1.94 E+06	1.95 E+06	2.07 E+06	1.90 E+06	2.14 E+06
	Phosphoenolpyruvate (PEP)	2.78 E+06	3.13 E+06	2.65 E+06	3.13 E+06	4.16 E+06	3.90 E+06	3.72 E+06	3.55 E+06	4.64 E+06	5.96 E+06
	sn-Glycerol-3-phosphate (sn-Glycerol-3-P)	6.77 E+05	8.99 E+05	5.45 E+05	8.09 E+05	9.08 E+05	7.81 E+05	7.50 E+05	8.00 E+05	8.03 E+05	8.55 E+05
TCA	4-aminobutyrate (GABA)	3.98 E+05	4.30 E+05	3.86 E+05	4.21 E+05	4.91 E+05	4.73 E+05	5.27 E+05	5.00 E+05	4.53 E+05	4.89 E+05
	α-ketoglutarate (α-KG)	1.72 E+04	2.05 E+04	1.87 E+04	2.34 E+04	2.61 E+04	2.77 E+04	2.28 E+04	2.20 E+04	3.01 E+04	2.89 E+04
	Citrate	6.36 E+04	9.01 E+04	6.86 E+04	7.32 E+04	8.77 E+04	9.69 E+04	9.31 E+04	1.00 E+05	1.00 E+05	9.19 E+04
	Fumarate	4.23 E+04	9.85 E+04	3.08 E+04	5.83 E+04	5.64 E+04	4.94 E+04	5.91 E+04	6.24 E+04	5.72 E+04	8.04 E+04
	Glutamate	7.30 E+05	8.25 E+05	6.94 E+05	6.87 E+05	9.04 E+05	8.27 E+05	9.95 E+05	9.45 E+05	8.82 E+05	1.03 E+06
	Malate	5.87 E+04	9.15 E+04	4.88 E+04	7.68 E+04	8.26 E+04	8.11 E+04	6.91 E+04	8.13 E+04	7.29 E+04	8.99 E+04
	Succinate	6.76 E+04	1.03 E+05	6.78 E+04	9.28 E+04	7.99 E+04	7.95 E+04	1.06 E+05	9.64 E+04	1.07 E+05	1.08 E+05

(*continued*)

Table 3.6. *continued*

Class	Compound	GC03^{Dd2} r1	GC03^{Dd2} r2	GC03^{Dd2} r3	GC03^{Dd2} r4	GC03^{Cam734} r1	GC03^{Cam734} r2	GC03^{Cam734} r3	GC03^{Cam734} r4	GC03^{Cam734} r5	GC03^{Cam734} r6
PPP	6-phospho-D-gluconate (6-P-D-gluconate)	1.46 E+05	2.80 E+05	1.47 E+05	2.30 E+05	2.10 E+05	2.12 E+05	2.23 E+05	2.54 E+05	2.32 E+05	2.99 E+05
	D-erythrose-4-phosphate (D-erythrose-4-P)	4.78 E+04	7.30 E+04	4.80 E+04	6.41 E+04	6.14 E+04	6.36 E+04	6.20 E+04	6.00 E+04	5.58 E+04	7.20 E+04
	D-gluconate	2.65 E+05	3.07 E+05	1.90 E+05	2.48 E+05	2.44 E+05	2.07 E+05	2.14 E+05	2.40 E+05	2.54 E+05	2.64 E+05
	D-sedoheptulose-7-phosphate (D-S-7-P)	6.23 E+04	9.54 E+04	4.92 E+04	6.47 E+04	9.70 E+04	8.47 E+04	8.54 E+04	8.48 E+04	5.83 E+04	7.27 E+04
	Octulose-1-phosphate (Octulose-1-P)	1.02 E+04	1.34 E+04	7.49 E+03	9.22 E+03	1.06 E+04	9.54 E+03	1.11 E+04	1.03 E+04	1.19 E+04	1.24 E+04
	Octulose-bisphosphate (Octulose-BP)	3.34 E+04	4.81 E+04	3.08 E+04	3.72 E+04	4.07 E+04	3.80 E+04	4.37 E+04	4.25 E+04	4.51 E+04	4.78 E+04
	Ribose-5-phosphate (Rib-5-P)	2.74 E+04	4.79 E+04	2.67 E+04	3.69 E+04	4.07 E+04	3.86 E+04	4.67 E+04	4.33 E+04	3.49 E+04	4.01 E+04
	Sedoheptulose bisphosphate (S-BP)	6.62 E+04	9.16 E+04	4.98 E+04	7.45 E+04	8.28 E+04	8.33 E+04	8.28 E+04	8.96 E+04	9.74 E+04	1.20 E+05
	Xylulose-5-phosphate (Xyl-5-P)	2.20 E+04	4.06 E+04	2.06 E+04	2.73 E+04	2.71 E+04	2.61 E+04	3.25 E+04	3.09 E+04	2.96 E+04	2.71 E+04
Nt met	N-Carbamoyl-L-aspartate (N-carb-L-Asp)	5.73 E+04	5.37 E+04	2.96 E+04	3.14 E+04	8.55 E+04	7.80 E+04	3.66 E+04	4.09 E+04	4.10 E+04	4.83 E+04
	ATP	1.22 E+07	1.59 E+07	1.41 E+07	1.56 E+07	1.97 E+07	1.82 E+07	2.16 E+07	2.08 E+07	1.84 E+07	2.01 E+07
	ADP	1.68 E+06	2.50 E+06	1.90 E+06	2.01 E+06	1.81 E+06	1.57 E+06	1.85 E+06	1.95 E+06	2.04 E+06	1.79 E+06
	AMP	1.72 E+05	3.21 E+05	2.22 E+05	2.07 E+05	1.68 E+05	1.44 E+05	1.81 E+05	1.90 E+05	2.22 E+05	1.94 E+05
	dATP	1.44 E+05	3.31 E+05	2.32 E+05	2.50 E+05	3.47 E+05	3.22 E+05	3.70 E+05	3.74 E+05	3.35 E+05	3.84 E+05
	dAMP	1.95 E+03	5.41 E+03	3.71 E+03	2.51 E+03	2.24 E+03	1.98 E+03	2.32 E+03	2.35 E+03	2.92 E+03	2.20 E+03
	CTP	1.09 E+05	1.83 E+05	1.35 E+05	1.33 E+05	2.13 E+05	1.96 E+05	1.95 E+05	2.01 E+05	1.93 E+05	1.74 E+05

(*continued*)

Table 3.6. *continued*

Class	Compound	GC03^{Dd2} r1	GC03^{Dd2} r2	GC03^{Dd2} r3	GC03^{Dd2} r4	GC03^{Cam734} r1	GC03^{Cam734} r2	GC03^{Cam734} r3	GC03^{Cam734} r4	GC03^{Cam734} r5	GC03^{Cam734} r6
Nt met *(cont.)*	CDP	4.06 E+04	7.67 E+04	4.83 E+04	4.56 E+04	4.38 E+04	3.75 E+04	4.40 E+04	4.54 E+04	4.55 E+04	3.88 E+04
	CMP	4.37 E+04	6.70 E+04	3.97 E+04	4.71 E+04	2.90 E+04	2.70 E+04	3.51 E+04	3.24 E+04	3.03 E+04	2.76 E+04
	dCTP	1.75 E+04	3.40 E+04	2.53 E+04	2.50 E+04	2.53 E+04	2.28 E+04	3.07 E+04	3.25 E+04	2.43 E+04	2.41 E+04
	dTTP	4.43 E+05	1.01 E+06	7.09 E+05	8.56 E+05	1.09 E+06	9.90 E+05	1.32 E+06	1.20 E+06	9.74 E+05	1.15 E+06
	dTDP	3.23 E+04	6.07 E+04	3.78 E+04	4.20 E+04	3.10 E+04	2.46 E+04	3.38 E+04	3.50 E+04	3.47 E+04	3.06 E+04
	GTP	1.16 E+05	2.40 E+05	1.92 E+05	1.87 E+05	3.23 E+05	2.85 E+05	3.44 E+05	3.24 E+05	3.20 E+05	3.07 E+05
	GDP	7.44 E+04	1.10 E+05	9.48 E+04	8.41 E+04	8.00 E+04	6.98 E+04	8.76 E+04	7.98 E+04	8.16 E+04	6.07 E+04
	GMP	2.37 E+05	4.22 E+05	2.86 E+05	3.53 E+05	1.45 E+05	1.47 E+05	2.81 E+05	2.86 E+05	1.88 E+05	1.82 E+05
	UTP	1.16 E+06	2.39 E+06	1.77 E+06	1.88 E+06	2.83 E+06	2.54 E+06	2.83 E+06	2.77 E+06	3.04 E+06	3.21 E+06
	UDP	2.62 E+05	4.42 E+05	3.24 E+05	3.36 E+05	2.47 E+05	2.05 E+05	2.57 E+05	2.55 E+05	3.16 E+05	2.78 E+05
	UMP	2.41 E+05	3.93 E+05	2.74 E+05	3.40 E+05	1.24 E+05	1.36 E+05	1.93 E+05	1.98 E+05	1.83 E+05	1.87 E+05
	IMP	6.69 E+05	9.34 E+05	5.66 E+05	7.57 E+05	7.91 E+05	8.31 E+05	8.19 E+05	8.59 E+05	8.38 E+05	1.04 E+06
	Inosine (I)	1.60 E+04	3.52 E+04	1.72 E+04	2.36 E+04	2.22 E+04	2.29 E+04	2.22 E+04	2.33 E+04	2.33 E+04	3.00 E+04
	Thymidine (dT)	9.60 E+02	5.27 E+03	2.09 E+03	2.54 E+03	2.72 E+03	4.74 E+03	2.56 E+03	2.85 E+03	3.11 E+03	4.20 E+03

(*continued*)

Table 3.6. *continued*

Class	Compound	GC03^{Dd2} r1	GC03^{Dd2} r2	GC03^{Dd2} r3	GC03^{Dd2} r4	GC03^{Cam734} r1	GC03^{Cam734} r2	GC03^{Cam734} r3	GC03^{Cam734} r4	GC03^{Cam734} r5	GC03^{Cam734} r6
Nt conj	ADP-D-glucose	8.51 E+04	1.08 E+05	8.00 E+04	9.81 E+04	1.00 E+05	9.73 E+04	1.00 E+05	1.06 E+05	1.05 E+05	1.23 E+05
	CDP-choline	1.33 E+04	1.54 E+04	1.11 E+04	1.43 E+04	1.24 E+04	1.22 E+04	1.15 E+04	1.16 E+04	1.14 E+04	1.44 E+04
	CDP-ethanolamine (CDP-ETA)	7.43 E+05	7.81 E+05	6.27 E+05	8.07 E+05	6.29 E+05	6.41 E+05	5.98 E+05	6.17 E+05	6.30 E+05	8.34 E+05
	S-Adenosyl-L-homocysteine (SAH)	9.54 E+04	2.36 E+05	1.12 E+05	1.67 E+05	1.24 E+05	1.09 E+05	1.51 E+05	1.56 E+05	1.07 E+05	1.63 E+05
	UDP-D-glucose	1.18 E+07	5.44 E+06	5.20 E+06	7.17 E+06	5.91 E+06	5.17 E+06	4.32 E+06	4.66 E+06	4.87 E+06	5.53 E+06
	UDP-D-glucuronate	2.04 E+05	3.00 E+05	2.02 E+05	2.46 E+05	3.44 E+05	3.02 E+05	3.83 E+05	3.47 E+05	3.47 E+05	3.78 E+05
	UDP-N-acetyl-glucosamine (UDP-NAG)	3.57 E+06	3.69 E+06	2.43 E+06	3.40 E+06	3.04 E+06	2.78 E+06	2.96 E+06	3.26 E+06	2.70 E+06	3.37 E+06
Redox	Glutathione (GSH)	2.44 E+04	5.43 E+04	1.94 E+04	5.07 E+04	1.15 E+04	9.87 E+03	1.95 E+04	2.45 E+04	2.46 E+04	3.73 E+04
	Glutathione disulfide (GSSG)	9.60 E+06	1.25 E+07	7.12 E+06	1.15 E+07	9.26 E+06	9.20 E+06	1.07 E+07	1.09 E+07	1.04 E+07	1.23 E+07
	NAD+	1.82 E+06	2.73 E+06	1.65 E+06	2.26 E+06	1.99 E+06	1.72 E+06	2.00 E+06	2.10 E+06	1.95 E+06	2.69 E+06
	NADH	8.08 E+03	8.09 E+03	8.75 E+03	1.11 E+04	8.23 E+03	6.73 E+03	7.56 E+03	9.86 E+03	1.21 E+04	1.37 E+04
	NADP+	3.54 E+05	5.18 E+05	3.23 E+05	3.64 E+05	4.20 E+05	4.30 E+05	4.63 E+05	4.63 E+05	4.29 E+05	4.60 E+05
AA	Phenylalanine (Phe)	3.91 E+05	5.10 E+05	4.07 E+05	4.15 E+05	4.92 E+05	4.91 E+05	5.34 E+05	4.81 E+05	4.89 E+05	4.91 E+05
	Tryptophan (Trp)	4.22 E+05	5.14 E+05	4.45 E+05	4.52 E+05	5.19 E+05	5.56 E+05	4.85 E+05	5.29 E+05	5.53 E+05	5.13 E+05
NAc AA	N-Acetyl-glucosamine-1,6-bisphosphate (NAG-1,6-BP)	1.65 E+04	2.80 E+04	1.64 E+04	2.45 E+04	1.92 E+04	1.71 E+04	1.88 E+04	2.33 E+04	2.50 E+04	2.81 E+04
	N-Acetyl-glutamate (NAc-Glu)	8.99 E+03	1.54 E+04	6.17 E+03	1.22 E+04	1.27 E+04	1.57 E+04	1.14 E+04	1.47 E+04	1.41 E+04	1.68 E+04

(*continued*)

Table 3.6. *continued*

Class	Compound	GC03^{Dd2}				GC03^{Cam734}					
		r1	***r2***	***r3***	***r4***	***r1***	***r2***	***r3***	***r4***	***r5***	***r6***
NAc AA *(cont.)*	N-Acetyl-glutamine (NAc-Gln)	2.18 E+04	3.39 E+04	2.32 E+04	3.24 E+04	3.38 E+04	3.32 E+04	3.83 E+04	4.21 E+04	4.23 E+04	5.00 E+04
	N-Acetyl-L-alanine (NAc-L-Ala)	3.03 E+03	4.01 E+03	2.76 E+03	4.60 E+03	4.15 E+03	3.77 E+03	3.91 E+03	4.16 E+03	2.88 E+03	4.05 E+03
Peptide	DLH	2.28 E+06	4.34 E+06	2.60 E+06	3.34 E+06	1.77 E+06	1.69 E+06	1.87 E+06	1.99 E+06	1.38 E+06	1.64 E+06
	DLS	1.35 E+06	2.26 E+06	1.62 E+06	2.27 E+06	1.88 E+06	1.81 E+06	1.70 E+06	1.86 E+06	1.81 E+06	2.09 E+06
	HVDD	2.31 E+06	3.48 E+06	2.30 E+06	3.21 E+06	2.61 E+06	2.57 E+06	2.09 E+06	2.24 E+06	2.12 E+06	2.40 E+06
	LD	2.63 E+05	4.32 E+05	1.57 E+05	2.30 E+05	3.74 E+05	3.74 E+05	3.38 E+05	3.54 E+05	2.43 E+05	3.35 E+05
	PD	2.60 E+06	3.21 E+06	2.52 E+06	3.49 E+06	2.58 E+06	2.71 E+06	2.66 E+06	2.85 E+06	2.87 E+06	3.70 E+06
	PE	3.30 E+06	4.02 E+06	3.11 E+06	4.02 E+06	3.95 E+06	3.44 E+06	3.80 E+06	3.86 E+06	3.27 E+06	4.15 E+06
	PEE	1.87 E+06	2.74 E+06	1.80 E+06	2.54 E+06	2.42 E+06	2.36 E+06	2.48 E+06	2.76 E+06	1.98 E+06	2.50 E+06
	PEEK	1.89 E+05	2.21 E+05	1.88 E+05	2.37 E+05	2.64 E+05	2.57 E+05	2.40 E+05	2.55 E+05	2.34 E+05	3.12 E+05
	PVNF	1.36 E+06	2.34 E+06	1.49 E+06	1.88 E+06	1.70 E+06	1.72 E+06	1.73 E+06	1.75 E+06	1.31 E+06	1.42 E+06
	SD	1.72 E+05	2.40 E+05	1.60 E+05	2.20 E+05	1.96 E+05	1.95 E+05	2.04 E+05	2.19 E+05	1.92 E+05	2.30 E+05
	VD	4.51 E+04	5.93 E+04	3.87 E+04	5.45 E+04	5.74 E+04	5.26 E+04	5.47 E+04	5.10 E+04	4.74 E+04	6.32 E+04
Cofactor	Biotin	2.58 E+04	3.93 E+04	3.06 E+04	2.57 E+04	3.96 E+04	4.60 E+04	3.88 E+04	3.96 E+04	3.80 E+04	3.61 E+04
	Folate	1.27 E+05	1.23 E+05	1.49 E+05	1.29 E+05	1.60 E+05	1.61 E+05	1.83 E+05	1.94 E+05	1.91 E+05	1.70 E+05
	Pantothenate	8.66 E+04	1.65 E+05	9.53 E+04	1.03 E+05	1.66 E+05	1.57 E+05	1.31 E+05	1.46 E+05	1.24 E+05	1.20 E+05

[a]Mass spectrometric signal intensities for metabolites derived from trophozoite-stage isogenic (GC03) parasites encoding either Dd2 or Cam734 *pfcrt*. Metabolites were harvested on three independent occasions, yielding 4 and 6 individual replicates (r) for the $GC03^{Dd2}$ and $GC03^{Cam734}$ strains, respectively. Glyc, glycolysis; TCA, tricarboxylic acid cycle; PPP, pentose phosphate pathway; Nt met, nucleotide metabolism and energy; Nt conj, nucleotide conjugate; AA, amino acid; NAc AA, N-acetylated amino acid.

Table 3.7. Metabolite *z*-scores and *P* values.[a]

Compound class or compound	GC03^{Dd2}				GC03^{Cam734}						
	r1	***r2***	***r3***	***r4***	***r1***	***r2***	***r3***	***r4***	***r5***	***r6***	***P***
Compound classes											
ATP/ADP	0.12	-1.40	0.34	0.95	6.14	7.38	7.47	5.77	3.02	6.70	0.0002
ATP/AMP	0.53	-1.36	-0.11	0.93	4.63	5.48	4.80	3.92	1.61	3.41	0.0011
Glycolysis	-0.59	0.99	-1.09	0.70	2.62	2.26	2.08	1.90	4.71	6.79	0.0133
Pentose phosphate pathway (PPP)	-0.44	1.30	-1.04	0.18	0.30	0.02	0.23	0.53	0.32	1.07	0.3740
Tricarboxylic acid (TCA) cycle	-0.46	1.42	-0.87	-0.09	1.89	1.26	2.84	2.42	1.71	3.16	0.0035
Nucleotide biosynthesis	0.27	1.28	-0.99	-0.56	2.09	1.85	-0.37	-0.08	-0.07	0.69	0.3360
Redox	-0.32	1.06	-1.24	0.50	-0.36	-0.47	0.16	0.26	0.03	0.95	0.8439
Cofactors	-0.93	1.39	0.00	-0.46	2.38	2.35	2.06	2.76	2.04	1.32	0.0017
Nucleoside triphosphates (nTPs)	-1.33	0.95	-0.17	0.55	2.88	2.06	3.73	3.34	2.39	3.21	0.0004
Nucleoside diphosphates (nDPs)	-1.00	1.38	-0.30	-0.08	-0.72	-1.39	-0.59	-0.39	-0.05	-0.75	0.1939
Nucleoside monophosphates (nMPs)	-0.79	1.35	-0.72	0.15	-1.08	-1.00	-0.38	-0.23	-0.51	-0.06	0.2602
Deoxynucleoside triphosphates (dnTPs)	-1.28	1.10	-0.16	0.35	1.38	0.97	2.16	1.82	0.97	1.67	0.0123
Deoxynucleoside diphosphates (dnDPs)	-0.89	1.42	-0.44	-0.10	-0.99	-1.51	-0.76	-0.67	-0.69	-1.02	0.0586
Deoxynucleoside monophosphates (dnMPs)	-0.94	1.32	0.21	-0.58	-0.76	-0.92	-0.70	-0.68	-0.31	-0.78	0.1290
Nucleotide conjugates	1.38	-0.40	-0.97	0.00	-0.53	-0.84	-1.01	-0.82	-0.94	-0.45	0.1006
N-Acetyl (NAc)-Amino Acids	-0.79	1.08	-0.90	0.62	0.39	0.38	0.54	1.26	1.27	2.16	0.0974
Aromatic amino acids	-0.82	1.45	-0.40	-0.24	1.31	1.69	1.38	1.29	1.64	1.23	0.0081
Peptides	-0.88	1.09	-0.82	0.61	-0.34	-0.51	-0.51	-0.24	-0.95	-0.07	0.3296
Individual compounds											
2,3-bisphosphoglycerate (2,3-BPG)	-0.66	0.60	-1.02	1.08	3.89	3.81	3.49	2.11	8.19	10.0	0.0123
3-phosphoglycerate (3-PG)	-0.85	1.27	-0.75	0.33	0.41	0.57	1.35	1.33	3.50	4.39	0.0708
D-glyceraldehdye-3-phosphate (PGAL)	-0.95	1.16	-0.71	0.50	0.38	0.11	0.61	0.16	0.08	2.08	0.3372
Dihydroxy-acetone-phosphate (DHAP)	-0.53	1.28	-1.01	0.26	0.23	0.99	0.50	1.77	4.22	4.42	0.0844
Fructose-1,6-bisphosphate (F-1,6-BP)	-0.13	0.25	-1.27	1.14	2.11	1.87	2.07	2.92	8.77	9.04	0.0389
Glucose-6-phosphate (G-6-P)	-0.68	1.30	-0.88	0.25	0.78	1.03	1.07	1.50	0.91	1.77	0.0279
Phosphoenolpyruvate (PEP)	-0.57	0.85	-1.12	0.84	4.99	3.95	3.23	2.54	6.95	12.3	0.0168
sn-Glycerol-3-phosphate (sn-Glycerol-3-P)	-0.36	1.08	-1.21	0.50	1.14	0.31	0.12	0.44	0.46	0.79	0.2500
4-aminobutyrate (GABA)	-0.53	1.04	-1.12	0.61	4.08	3.15	5.84	4.52	2.20	3.97	0.0007

(*continued*)

Table 3.7. *continued*

Compound class or compound	GC03^{Dd2}				GC03^{Cam734}						P
	r1	*r2*	*r3*	*r4*	*r1*	*r2*	*r3*	*r4*	*r5*	*r6*	
Individual compounds *(cont.)*											
α-ketoglutarate (α-KG)	-1.03	0.20	-0.46	1.30	2.29	2.87	1.07	0.76	3.76	3.32	0.0128
Citrate	-0.90	1.41	-0.46	-0.06	1.20	2.00	1.67	2.28	2.30	1.56	0.0037
Fumarate	-0.51	1.39	-0.90	0.03	-0.04	-0.27	0.05	0.17	-0.01	0.77	0.8015
Glutamate	-0.06	1.43	-0.62	-0.75	2.69	1.47	4.11	3.34	2.33	4.68	0.0026
Malate	-0.54	1.19	-1.06	0.42	0.72	0.64	0.01	0.65	0.21	1.10	0.2466
Succinate	-0.85	1.13	-0.84	0.55	-0.16	-0.19	1.28	0.75	1.31	1.41	0.2177
6-phospho-D-gluconate (6-P-D-gluconate)	-0.84	1.20	-0.81	0.44	0.14	0.17	0.34	0.81	0.47	1.48	0.2634
D-erythrose-4-phosphate (D-erythrose-4-P)	-0.84	1.18	-0.82	0.47	0.25	0.43	0.30	0.14	-0.19	1.10	0.4755
D-gluconate	0.25	1.12	-1.29	-0.08	-0.17	-0.94	-0.79	-0.25	0.04	0.25	0.5188
D-sedoheptulose-7-phosphate (D-S-7-P)	-0.29	1.41	-0.96	-0.16	1.49	0.86	0.90	0.87	-0.49	0.25	0.2548
Octulose-1-phosphate (Octulose-1-P)	0.06	1.34	-1.04	-0.35	0.22	-0.22	0.39	0.08	0.71	0.94	0.4555
Octulose-bisphosphate (Octulose-BP)	-0.52	1.41	-0.87	-0.02	0.44	0.08	0.83	0.67	1.01	1.36	0.1475
Ribose-5-phosphate (Rib-5-P)	-0.74	1.32	-0.81	0.22	0.60	0.39	1.20	0.86	0.01	0.54	0.2147
Sedoheptulose bisphosphate (S-BP)	-0.25	1.21	-1.19	0.23	0.70	0.73	0.71	1.09	1.54	2.87	0.0611
Xylulose-5-phosphate (Xyl-5-P)	-0.62	1.42	-0.77	-0.03	-0.06	-0.17	0.53	0.35	0.22	-0.06	0.7547
N-Carbamoyl-L-aspartate (N-carb-L-Asp)	0.98	0.74	-0.92	-0.80	2.93	2.41	-0.44	-0.14	-0.14	0.37	0.3538
ATP	-1.33	0.86	-0.21	0.68	3.10	2.21	4.22	3.75	2.33	3.34	0.0005
ADP	-0.99	1.38	-0.34	-0.04	-0.61	-1.32	-0.50	-0.20	0.06	-0.66	0.2779
AMP	-0.91	1.42	-0.14	-0.37	-0.98	-1.36	-0.77	-0.63	-0.14	-0.57	0.1374
dATP	-1.24	1.19	-0.09	0.14	1.40	1.07	1.70	1.75	1.25	1.88	0.0077
dAMP	-0.94	1.32	0.21	-0.58	-0.76	-0.92	-0.70	-0.68	-0.31	-0.78	0.1290
CTP	-1.01	1.38	-0.15	-0.22	2.34	1.80	1.77	1.95	1.69	1.09	0.0041
CDP	-0.75	1.47	-0.28	-0.44	-0.55	-0.94	-0.54	-0.46	-0.45	-0.86	0.1603
CMP	-0.47	1.45	-0.80	-0.19	-1.67	-1.84	-1.17	-1.40	-1.57	-1.80	0.0053
dCTP	-1.17	1.27	-0.03	-0.07	-0.02	-0.40	0.77	1.05	-0.17	-0.20	0.7377
dTTP	-1.29	1.06	-0.19	0.42	1.40	0.97	2.34	1.85	0.91	1.64	0.0137
dTDP	-0.89	1.42	-0.44	-0.10	-0.99	-1.51	-0.76	-0.67	-0.69	-1.02	0.0586
GTP	-1.33	1.10	0.16	0.07	2.70	1.97	3.12	2.74	2.65	2.40	0.0004
GDP	-1.07	1.26	0.25	-0.44	-0.71	-1.37	-0.21	-0.72	-0.60	-1.97	0.1049

(*continued*)

Table 3.7. *continued*

Compound class or compound	GC03^{Dd2}				GC03^{Cam734}						*P*
	r1	***r2***	***r3***	***r4***	***r1***	***r2***	***r3***	***r4***	***r5***	***r6***	
Individual compounds *(cont.)*											
GMP	-1.09	1.21	-0.47	0.35	-2.22	-2.20	-0.54	-0.47	-1.69	-1.76	0.0302
UTP	-1.27	1.17	-0.07	0.16	2.02	1.45	2.02	1.91	2.45	2.78	0.0018
UDP	-1.06	1.35	-0.22	-0.07	-1.26	-1.82	-1.11	-1.15	-0.33	-0.83	0.0493
UMP	-1.05	1.19	-0.56	0.41	-2.76	-2.60	-1.75	-1.67	-1.89	-1.84	0.0020
IMP	-0.40	1.30	-1.06	0.16	0.38	0.64	0.56	0.82	0.68	1.96	0.1246
Inosine (I)	-0.80	1.39	-0.66	0.07	-0.09	0.00	-0.09	0.03	0.03	0.80	0.7990
Thymidine (dT)	-0.96	1.40	-0.34	-0.09	0.00	1.11	-0.09	0.08	0.22	0.81	0.4704
ADP-D-glucose	-0.61	1.19	-1.01	0.43	0.59	0.37	0.62	1.03	1.02	2.44	0.1028
CDP-choline	-0.12	1.03	-1.33	0.41	-0.62	-0.70	-1.07	-1.04	-1.17	0.48	0.2084
CDP-ethanolamine (CDP-ETA)	0.04	0.53	-1.42	0.85	-1.39	-1.25	-1.78	-1.55	-1.38	1.19	0.1743
S-Adenosyl-L-homocysteine (SAH)	-0.90	1.32	-0.64	0.22	-0.45	-0.69	-0.03	0.06	-0.72	0.17	0.5489
UDP-D-glucose	1.44	-0.64	-0.72	-0.08	-0.49	-0.73	-1.01	-0.90	-0.83	-0.61	0.0988
UDP-D-glucuronate	-0.74	1.35	-0.78	0.17	2.31	1.38	3.14	2.36	2.36	3.04	0.0014
UDP-N-acetyl-glucosamine (UDP-NAG)	0.52	0.72	-1.47	0.22	-0.42	-0.85	-0.55	-0.02	-1.00	0.18	0.3623
Glutathione (GSH)	-0.72	0.96	-1.00	0.76	-1.44	-1.53	-0.99	-0.71	-0.71	0.01	0.1044
Glutathione disulfide (GSSG)	-0.24	0.98	-1.29	0.56	-0.39	-0.41	0.22	0.30	0.09	0.90	0.8073
NAD+	-0.61	1.27	-0.97	0.30	-0.26	-0.81	-0.23	-0.04	-0.33	1.20	0.8858
NADH	-0.65	-0.64	-0.18	1.46	-0.54	-1.59	-1.01	0.59	2.14	3.28	0.6599
NADP+	-0.41	1.47	-0.76	-0.30	0.35	0.46	0.84	0.84	0.45	0.81	0.1675
Phenylalanine (Phe)	-0.74	1.47	-0.44	-0.29	1.14	1.10	1.90	0.92	1.08	1.11	0.0237
Tryptophan (Trp)	-0.92	1.42	-0.34	-0.15	1.54	2.47	0.67	1.79	2.39	1.39	0.0115
N-Acetyl-glucosamine-1,6-bisphosphate (NAG-1,6-BP)	-0.83	1.14	-0.85	0.54	-0.37	-0.74	-0.43	0.33	0.63	1.16	0.8618
N-Acetyl-glutamate (NAc-Glu)	-0.42	1.18	-1.13	0.38	0.52	1.28	0.18	1.01	0.87	1.56	0.0913
N-Acetyl-glutamine (NAc-Gln)	-0.97	0.98	-0.75	0.73	0.96	0.86	1.69	2.30	2.34	3.57	0.0172
N-Acetyl-L-alanine (NAc-L-Ala)	-0.67	0.48	-0.98	1.17	0.65	0.20	0.36	0.66	-0.84	0.53	0.6121
DLH	-0.94	1.31	-0.59	0.22	-1.50	-1.59	-1.40	-1.26	-1.93	-1.64	0.0055
DLS	-1.13	0.83	-0.56	0.86	0.02	-0.15	-0.37	-0.03	-0.14	0.47	0.9380
HVDD	-0.84	1.07	-0.86	0.63	-0.35	-0.43	-1.22	-0.96	-1.15	-0.70	0.1046

(*continued*)

Table 3.7. *continued*

Compound class or compound	GC03^{Dd2}				GC03^{Cam734}						*P*
	r1	***r2***	***r3***	***r4***	***r1***	***r2***	***r3***	***r4***	***r5***	***r6***	
Individual compounds *(cont.)*											
LD	-0.07	1.39	-0.97	-0.35	0.89	0.89	0.57	0.72	-0.24	0.55	0.2448
PD	-0.75	0.54	-0.92	1.13	-0.80	-0.52	-0.63	-0.22	-0.19	1.58	0.8335
PE	-0.65	0.86	-1.06	0.85	0.70	-0.37	0.39	0.52	-0.71	1.13	0.6127
PEE	-0.78	1.07	-0.92	0.63	0.39	0.25	0.51	1.10	-0.54	0.56	0.4524
PEEK	-0.81	0.51	-0.85	1.16	2.28	1.98	1.26	1.90	1.03	4.23	0.0169
PVNF	-0.92	1.29	-0.63	0.26	-0.15	-0.12	-0.09	-0.03	-1.04	-0.78	0.4389
SD	-0.69	1.10	-0.99	0.58	-0.05	-0.08	0.16	0.54	-0.14	0.84	0.6428
VD	-0.46	1.07	-1.16	0.55	0.87	0.35	0.57	0.17	-0.22	1.50	0.3111
Biotin	-0.71	1.40	0.03	-0.73	1.46	2.46	1.32	1.46	1.20	0.90	0.0156
Folate	-0.42	-0.77	1.47	-0.27	2.43	2.49	4.42	5.36	5.07	3.25	0.0011
Pantothenate	-0.72	1.47	-0.48	-0.27	1.48	1.25	0.53	0.94	0.32	0.20	0.1372

[a]Metabolite compound classes and individual metabolite *z*-scores (see **Methods** for *z*-score derivation). *P* values were determined using one-way ANOVA. Corresponding metabolite signal intensities are reported in **Table 3.6**. Metabolites were harvested on three independent occasions, yielding 4 and 6 individual replicates (r) for the GC03^{Dd2} and GC03^{Cam734} strains, respectively. *P* values <0.05 are shaded in gray.

Intriguingly, a survey of the metabolomes of GC03^{Cam734} and GC03^{Dd2} parasites revealed several distinguishing metabolic phenotypes. Most significantly, ATP/ADP and ATP/AMP ratios were significantly higher in GC03^{Cam734} parasites than in GC03^{Dd2} parasites (P=0.0002 and P=0.0001, respectively; see **Figure 3.7** and **Table 3.7**). Low ATP/AMP ratios are a classic marker of metabolic stress[341] and the relatively higher ratios seen in GC03^{Cam734} parasites are consistent with their increased *in vitro* growth rate as compared with GC03^{Dd2} (see **Figure 3.5**). GC03^{Cam734} parasites also exhibited significantly increased levels of glycolytic and tricarboxylic acid (TCA) cycle-associated metabolites (P=0.003 and P=0.01, respectively; see **Figure 3.7** and **Table 3.7**), suggesting differences in central carbon processing as a metabolic compensatory mechanism associated with the Cam734 *pfcrt* allele.[342] Collectively, these findings indicate that parasites encoding Cam734 and Dd2 PfCRT both suffer from impaired parasite Hb catabolism, but that the metabolic impact of these changes is more severe for lines encoding Dd2 PfCRT.

Distribution of heme species in isogenic *pfcrt*-modified parasites

CQ treatment of *P. falciparum* parasites affects their disposition of heme species, namely free heme, Hz, and Hb. In a dose-dependent manner, CQ causes a decrease in the formation of non-toxic Hz crystals, an increase in toxic free heme, and an accompanying reduction in parasite survival.[55] To date, the profiles of heme fractions had only been explored in CQ-sensitive (D10, NF54, D6) parasites.[334,343] Given the central role of *pfcrt* in dictating parasite responses to CQ, we examined the composition of heme species in CQ-treated and untreated isogenic parasites encoding the CQ-sensitive (wild-type) *pfcrt* allele GC03 and the CQ-resistant (mutant) *pfcrt*

alleles Cam734 and Dd2. Our heme fractionation assay entailed treatment of synchronous, early ring-stage parasites with CQ in multiples (range of 0× to 3×) of parasite line-specific CQ IC_{50} values. After 32 h, trophozoite-stage parasites were subjected to a series of cellular fractionation steps. The abundance of heme present as Hb, free heme, or Hz was subsequently determined spectrophotometrically and reported both as a percentage of total heme (**Figure 3.8**) and as an amount of heme iron (Fe) per cell (**Figure 3.9**).

Our results demonstrate that parasite exposure to CQ caused a dose-dependent increase in free heme for all *pfcrt*-modified parasite lines (**Figure 3.8*A*** and **Figure 3.9*A***). Considering all CQ treatments, maximal mean free heme Fe concentrations of 10.5, 12.6, and 19.3 femtograms (fg) per cell were observed in $GC03^{Cam734}$, $GC03^{Dd2}$, and $GC03^{GC03}$ parasites (**Figure 3.9*A***), respectively. The difference between $GC03^{Cam734}$ and $GC03^{GC03}$ parasites achieved statistical significance (P=0.02 by unpaired t test with Welch's correction). Inversely correlating with free heme profiles, Hz profiles of *pfcrt*-modified parasites showed comparable, CQ dose-dependent decreases in Hz (**Figure 3.8*B*** and **Figure 3.9*B***).

We note that $GC03^{GC03}$ parasites showed a higher, statistically significant level of heme at baseline (i.e. in the absence of CQ) as compared to $GC03^{Dd2}$ and $GC03^{Cam734}$ parasites (P=0.004 and P=0.0012, respectively, by unpaired t tests with Welch's correction), although the lowest level of Hz achieved in all three CQ-treated strains was comparable (**Figure 3.8*B***). The reason for this difference in baseline free heme is not yet known. We hypothesize that free heme in untreated parasites is sequestered, possibly through association with neutral lipids in the DV.[65] The baseline difference between wild-type and mutant *pfcrt*-expressing parasites may be attributed to the

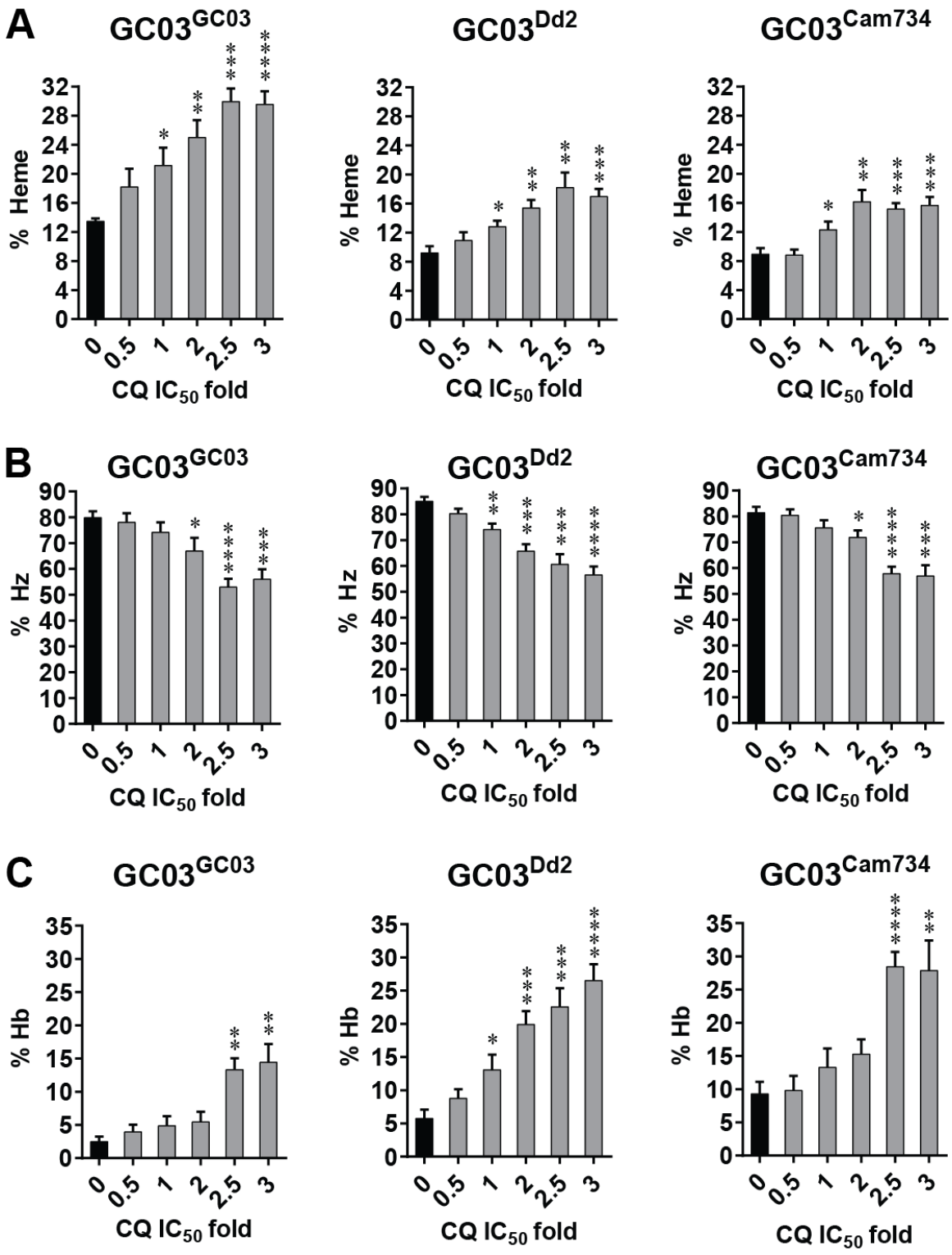

Figure 3.8. *(continued on next page)*

Figure 3.8. Distribution of heme species in control and chloroquine (CQ)-treated *pfcrt*-modified parasite lines. The percent of total heme present as (**A**) free heme, (**B**) hemozoin (Hz), and (**C**) hemoglobin (Hb) was measured spectrophotometrically in isogenic parasites expressing the wild-type (CQ-sensitive) GC03 *pfcrt* allele or mutant (CQ-resistant) Dd2 and Cam734 *pfcrt* alleles. Prior to heme fractionation, synchronous parasites were exposed for 32 h to multiples of line-specific CQ IC_{50} values (1× CQ IC_{50} of 19.5 nM, 187 nM, and 90.9 nM for $GC03^{GC03}$, $GC03^{Dd2}$, and $GC03^{Cam734}$, respectively). Bar graphs indicate mean ± SEM percentage values for 5 to 10 independent replicates. For each parasite line, values obtained for CQ-treated samples (gray bars) were compared against the untreated control (black bars), and statistical significance was determined via unpaired *t* tests with Welch's correction. Absolute concentrations of heme species are depicted in **Figure 3.9**. **P*<0.05; ***P*<0.01; ****P*<0.001; *****P*<0.0001. Experiments performed by Egan laboratory.

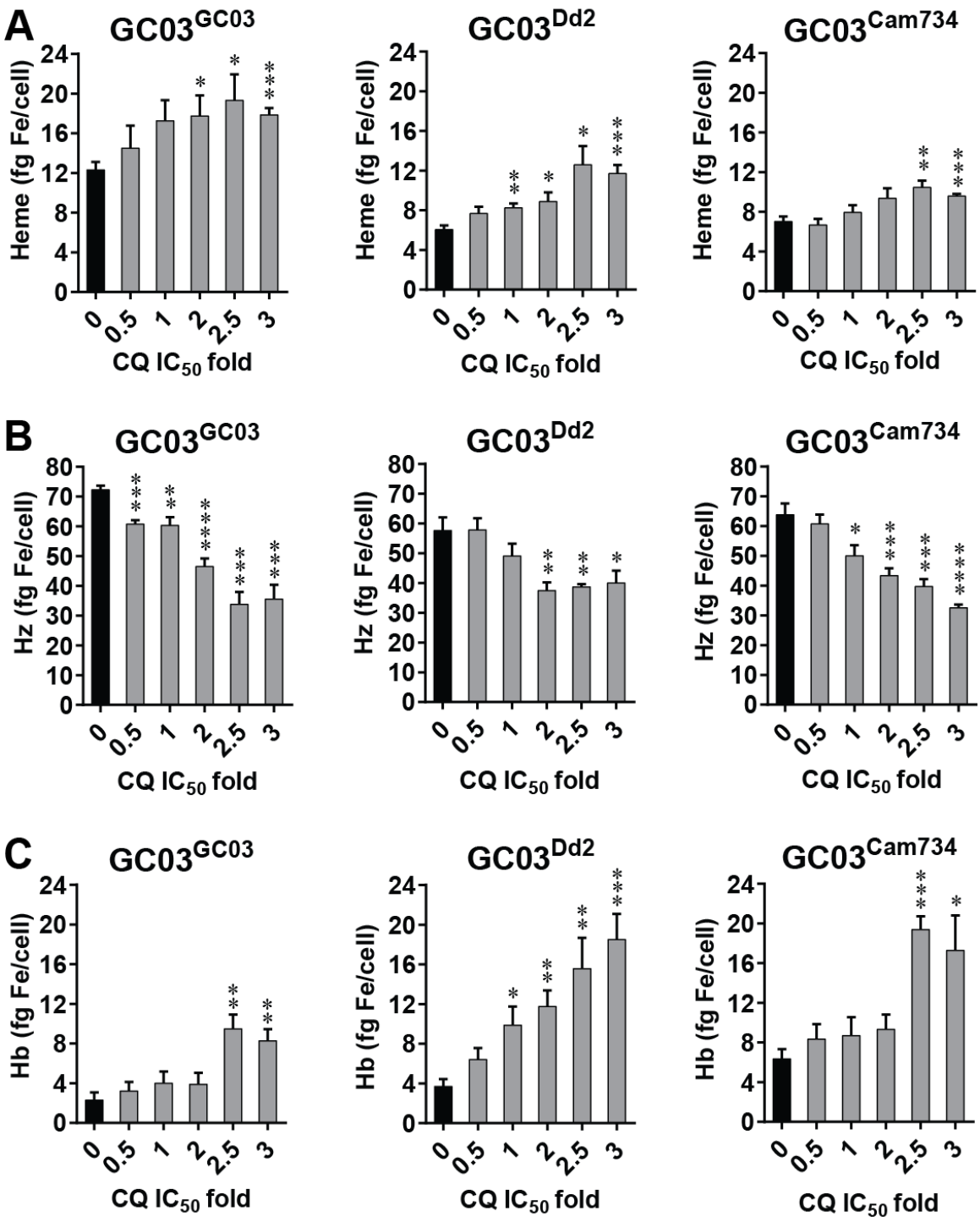

Figure 3.9. *(continued on next page)*

Figure 3.9. Absolute concentrations of heme species in control and chloroquine (CQ)-treated *pfcrt*-modified parasite lines. The amount (in femtograms, fg) of heme Fe per cell present as (**A**) free heme, (**B**) hemozoin (Hz), or (**C**) hemoglobin (Hb) was measured spectrophotometrically in isogenic parasites expressing the wild-type (CQ-sensitive) GC03 *pfcrt* allele or mutant (CQ-resistant) Dd2 and Cam734 *pfcrt* alleles. Prior to heme fractionation, synchronous parasites were exposed for 32 h to CQ concentrations corresponding to line-specific CQ IC_{50} folds (1× CQ IC_{50} values of 19.5 nM, 187 nM, and 90.9 nM for $GC03^{GC03}$, $GC03^{Dd2}$, and $GC03^{Cam734}$, respectively. In absolute values, 0.5× CQ IC_{50} for $GC03^{Cam734}$ is equivalent to 2.3× the CQ IC_{50} for $GC03^{GC03}$ and 0.25× the CQ IC_{50} for $GC03^{Dd2}$). Bar graphs indicate mean ± SEM percentage values for 5 to 8 technically independent replicates. For each parasite line, values obtained for CQ-treated samples (gray bars) were compared against the untreated control (black bars), and statistical significance was determined via unpaired *t* tests with Welch's correction. **P*<0.05; ***P*<0.01; ****P*<0.001; *****P*<0.0001. Experiments performed by Egan laboratory.

larger DV of GC03^{Dd2} and GC03^{Cam734} lines, as compared to GC03^{GC03} parasites (see **Table 3.8**), resulting in a lower lipid to aqueous volume ratio. A fixed lipid-aqueous portioning coefficient and consequent fixed ratio of lipid to aqueous heme concentration would yield an increased quantity of aqueous free heme (volume × concentration), which in turn is mostly incorporated into Hz.

Several notable differences were observed among the Hb profiles of *pfcrt*-modified lines (**Figure 3.8*C*** and **Figure 3.9*C***). First, isogenic parasites encoding mutant *pfcrt* alleles Cam734 and Dd2 exhibited higher concentrations of Hb as compared to wild-type (GC03) *pfcrt*-expressing parasites (mean Hb-specific heme Fe concentrations of 6.3, 3.7, and 2.3 fg per cell, respectively; **Figure 3.9*C***), with the difference between GC03^{GC03} and GC03^{Cam734} lines achieving statistical significance (P=0.006 by unpaired t test with Welch's correction). Consistent with previous findings,[55] CQ-sensitive GC03^{GC03} parasites (**Figure 3.8*C*** and **Figure 3.9*C***) showed a significant elevation in Hb species that did not occur until 2.5× CQ IC_{50}. A comparable delay in Hb digestion until 2.5× CQ IC_{50} was observed for Cam734 *pfcrt*-expressing GC03^{Cam734} parasites, contrasting with the profile of Dd2 *pfcrt*-expressing GC03^{Dd2} parasites, which showed elevations in Hb species at a lower (1×) CQ IC_{50} fold (**Figure 3.8*C*** and **Figure 3.9*C***). The increase in Hb observed for GC03^{Dd2} parasites coincided with a statistically significant increase in free heme at 1× CQ IC_{50} (see **Figure 3.8*A***). This is consistent with previous studies of CQ-treated parasites, in which increases in undigested Hb were found to follow significant increases in free heme.[55] This suggests a secondary mechanism of CQ action, whereby Hb degradation at higher CQ concentrations is inhibited, possibly through a physiologic effect of elevated CQ on the activity of DV-resident hemoglobinases. Alternatively, elevated concentrations of free

heme in aqueous environments have been shown to form heme aggregates capable of disrupting lipid bilayers and triggering membrane disorder, which in turn could disrupt Hb transport and metabolism.[344]

For each *pfcrt*-modified line, we also compared the CQ dose dependence of parasite free heme fractions versus parasite growth (**Figure 3.10**). Interestingly, for each line, the free heme concentration curve crossed the parasite growth curve at approximately the same mid-point (IC_{50} value), indicating that the inverse relationship between CQ action on free heme levels and growth inhibition that was previously established for parasite lines encoding wild-type *pfcrt*[334] is preserved among lines encoding CQ-resistant *pfcrt* alleles. These data reinforce the conception that CQ-mediated growth inhibition results from this drug's inhibition of parasite-mediated inactivation of reactive heme via its incorporation into chemically inert Hz.

Cam734 PfCRT confers membrane potential-sensitive CQ transport

A key feature of CQR in *P. falciparum* parasites is the ability of mutant PfCRT to efflux CQ from the parasite DV, in turn reducing CQ access to heme. Measurement of drug transport is experimentally challenging in *Plasmodium* parasites due to the presence of multiple membrane-bound intracellular compartments. Accordingly, we evaluated CQ transport mediated by Cam734 PfCRT using a recently optimized *S. cerevisiae* galactose-inducible PfCRT expression system.[208] Yeast-expressed PfCRT isoforms localize largely to the cell membrane and mediate transport of CQ from the external medium (low pH, positive membrane potential [Ψ]) to the yeast cytosol (high pH, negative Ψ), recapitulating the electrochemical gradient-driven transport of CQ from the parasite DV (low pH, positive Ψ) to the parasite

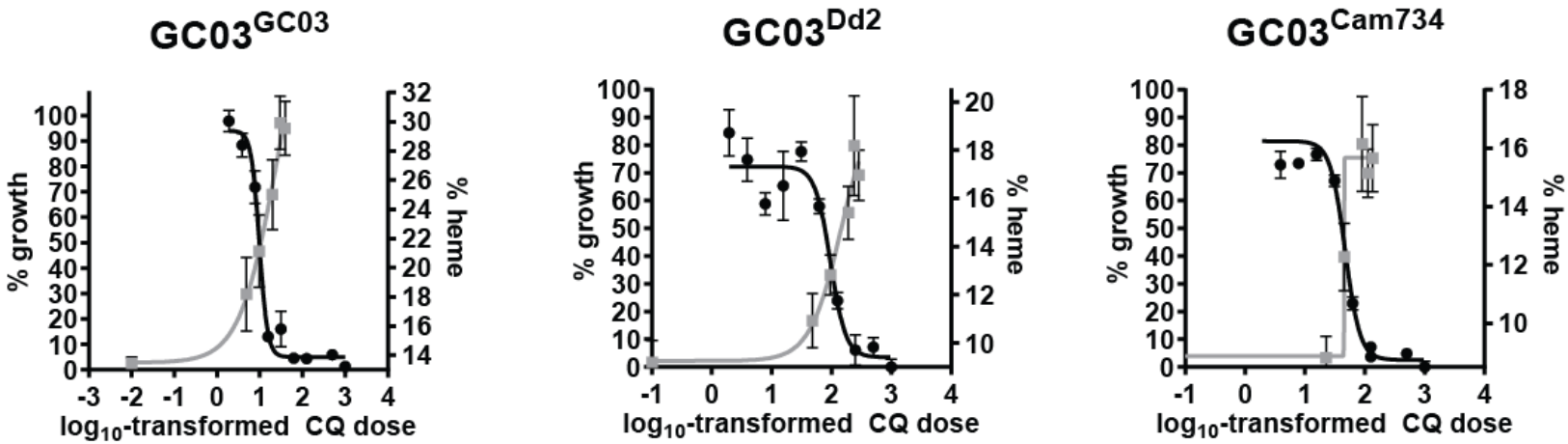

Figure 3.10. Survival and percentage free heme as a function of chloroquine (CQ) concentration for *pfcrt*-modified parasites. Shown are curves of parasite growth (black curve) and of the percentage of heme species present as free heme (gray curve), graphed as a function of the $\log_{10}$-transformed CQ concentration (in nM). Plotted points and error bars correspond to mean ± SEM measurements made in parasite growth assays (*n*=8-10) or heme fractionation assays (*n*=5-10), as detailed in **Methods**. Experiments performed by Egan laboratory.

cytosol (high pH, negative Ψ).[336] Of note, at baseline, the yeast cell membrane possesses a high ΔpH and a low Δψ. By increasing the pH of the external medium ($pH_{external}$), the cell membrane ΔpH can be experimentally lowered, yielding a compensatory potassium channel-dependent increase in Δψ.[336] In this system, at higher Δψ, CQ transport by CQ-resistant PfCRT isoforms is more pronounced as compared to the basal level of transport mediated by the CQ-sensitive GC03 (wild-type; equivalent to HB3) PfCRT isoform.[208,281] Earlier studies have validated that growth rates of PfCRT-expressing yeast serve as a proxy for CQ transport.[281]

Using quantitative growth rate analyses, we examined the effect of varying external pH (and hence the Δψ) in yeast strains expressing PfCRT isoforms GC03, Cam734, Cam738 (Cam734 F144A), or Dd2 (see **Table 3.1** for haplotypes). Growth was assessed in the presence of 5 mM CQ, a concentration required for this drug to exert differential growth inhibitory activity on yeast strains expressing various PfCRT isoforms.[208] As a negative control, we also included yeast harboring no PfCRT (vector control). To examine the effect of Δψ on transport, we assessed growth over a range of $pH_{external}$ values (range of 7.20 [low Δψ] to 7.45 [high Δψ]; **Figure 3.11*A***). Intriguingly, in low Δψ conditions, growth of yeast expressing Cam734 PfCRT was comparable to that of yeast expressing the CQ-sensitive GC03 PfCRT isoform (**Figure 3.12**). However, when the Δψ was clamped to higher values, Cam734 PfCRT conferred a CQR-associated delayed growth phenotype that was intermediate to that of GC03 (wild-type) and Dd2 PfCRT (**Figure 3.12**). Of note, the growth phenotype associated with the Cam738 isoform (lacking the Cam734 mutation A144F) was intermediate to that of empty vector and wild-type PfCRT. This provides evidence that the A144F

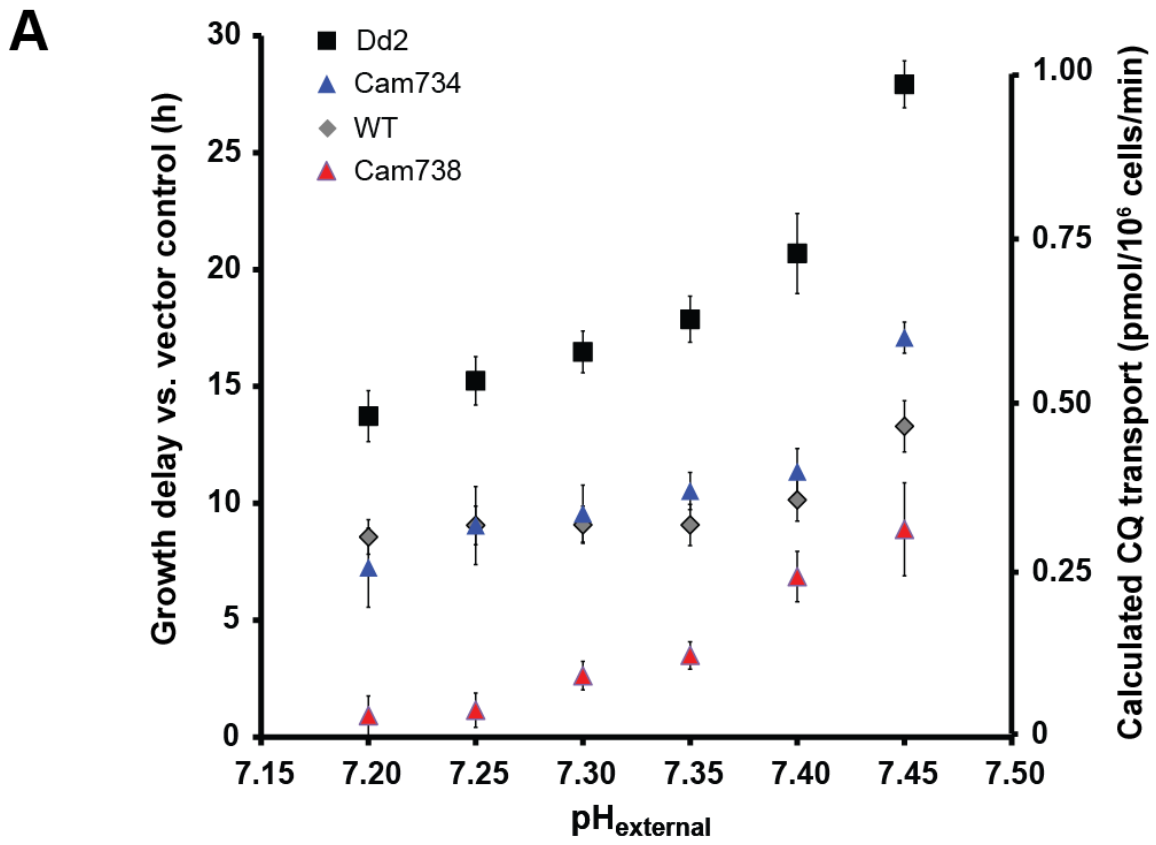

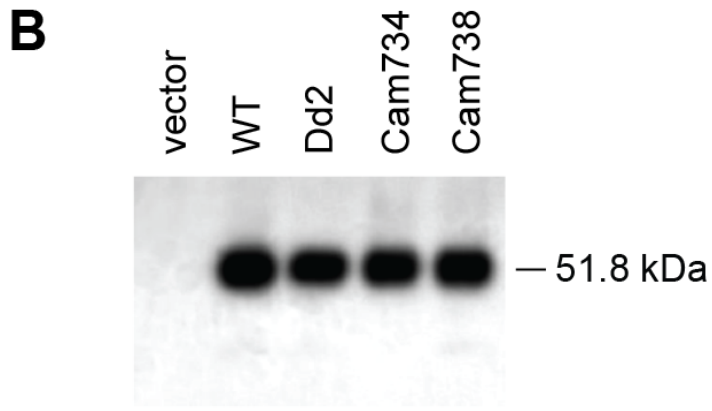

Figure 3.11. *(continued on next page)*

Figure 3.11. Membrane potential ($\Delta\psi$) dependence of PfCRT-mediated yeast growth delay and PfCRT isoform expression. (**A**) Growth delay of yeast lines encoding wild-type (gray diamonds), Dd2 (black squares), Cam734 (blue triangles), or Cam738 (Cam734 F144A; red triangles) PfCRT (tagged to a V5 epitope at its C terminus[281]) was measured in the presence of 5 mM CQ and normalized to growth of yeast harboring empty vector (see **Methods**). Growth was examined for a range (7.20 to 7.45) of $pH_{external}$ values. Through compensatory mechanisms, the yeast $\Delta\psi$ increases with increased $pH_{external}$. CQ transport rates were calculated as previously described.[281] Error bars indicate the SEM for at least three independent yeast clones analyzed in triplicate. (**B**) Yeast protein extracts were subjected to Western blot analysis with anti-V5 antibodies, as described in **Methods**. Briefly, total protein concentrations in the yeast crude membrane fractions were quantified using an amido black assay and 7.0 µg protein was electrophoretically separated and transferred onto a PVDF membrane. Levels of the 51.8-kDa PfCRT-V5 protein were comparable for all PfCRT isoforms (GC03, Dd2, Cam734, Cam738). A yeast strain harboring an empty vector was included in the analysis as a negative control. Experiments performed by Roepe laboratory.

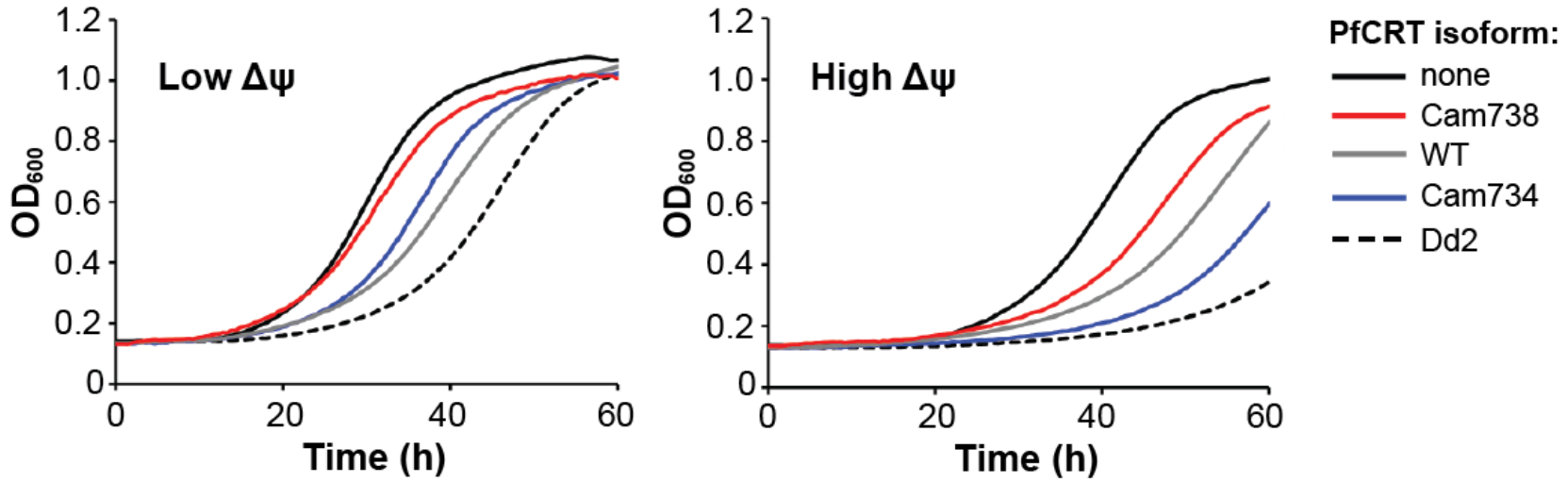

Figure 3.12. Effect of membrane potential (Δψ) on chloroquine (CQ)-induced growth inhibition of yeast expressing PfCRT isoforms. Growth (measured as OD_{600}) of yeast harboring no (empty vector; solid black line), wild-type (WT; GC03/HB3; gray line), Cam734 (blue line), Cam738 (Cam734 F144A; red line) or Dd2 (dashed black line) PfCRT was assessed in the presence of 5 mM CQ in low-Δψ (left panel; $pH_{external}$ 7.20) or high-Δψ (right panel; $pH_{external}$ 7.45) conditions, as detailed in **Methods**. Increased growth inhibition correlates with increased CQ accumulation in the yeast cytosol and reflects increased CQ resistance.[281] Δψ increases with increased $pH_{external}$ due to compensatory mechanisms that maintain the cell membrane electrochemical gradient. Growth of yeast lines over the $pH_{external}$ range of 7.20 – 7.45 is surveyed in **Figure 3.11*A*.** Experiments performed by Roepe laboratory.

mutation is critical for drug transport mediated by the Cam734 isoform and is consistent with our drug assay data that showed a CQR phenotype for parasites expressing Cam734 *pfcrt*, but not Cam738 *pfcrt* (see **Figure 3.2*A***). These PfCRT-specific phenotypes were not attributable to differences in protein expression, as comparable protein expression of PfCRT variants was observed upon galactose induction of yeast (**Figure 3.11*B***).

We have observed that Cam734 is significantly potentiated by $\Delta\psi$, resembling a CQ-sensitive PfCRT isoform at low $\Delta\psi$ and a mutant, CQ-resistant PfCRT isoform at high $\Delta\psi$. This unique plasticity in mediating drug transport may underlie the improved asexual blood-stage fitness associated with the Cam734 PfCRT isoform, as compared with Dd2 (see **Figure 3.5**), whereby Cam734-defining mutations confer drug transport only in certain $\Delta\psi$ DV conditions. We also note that CQ transport, as assessed in heterologous expression systems, may only partially account for *in vitro* parasite CQR. This is highlighted by the earlier observation that the CQ-resistant Ecu1110 PfCRT variant confers lower parasite CQR, but higher CQ transport, than the related 7G8 PfCRT variant.[242,312,345] Thus, the possibility also exists that Cam734 facilitates CQR in part by alleviating CQ-mediated inhibition of an endogenous PfCRT function. Continued elucidation of the elusive function of PfCRT will assist in clarifying these distinctions.

Differential effects of PfCRT isoforms on parasite digestive vacuole pH and volume

Investigations utilizing the entrapment of a dextran-conjugated NERF to probe the pH and volume of the parasite DV have previously documented the ability of PfCRT

mutations to alter DV physiology.[195,197,345] Using similar methods (see **Methods**), we determined the DV pH and volume in isogenic parasites encoding GC03, Dd2, Cam734, and Cam738 (Cam734 F144A) PfCRT, in the presence or absence of CQ concentrations corresponding to 2× CQ 50% lethal dose (LD_{50}; see **Methods**). From smallest to largest DV volume as well as from most alkaline to most acidic DV pH, the order of parasite lines was found to be as follows: $GC03^{GC03}$, $GC03^{Cam734\ F144A}$, $GC03^{Cam734}$, and $GC03^{Dd2}$ (**Table 3.8**). This order was preserved upon a brief (30 min) addition of CQ, which consistently increased DV volume (by 13% to 33%). As the composition of the DV environment governs the degree of heme-to-Hz conversion,[58] one might envisage that, compared to Dd2 PfCRT, the reduced DV size and more wild-type (GC03) PfCRT-like like DV pH associated with the Cam734 isoform may play a role in neutralizing fitness costs typically associated with mutant PfCRT variants.

Table 3.8. Digestive vacuole volume size and pH of *pfcrt*-modified lines.[a]

	DV volume size ± SEM (μm^3)			pH ± SEM	
Line	**No drug**	**CQ**	**% increase**	**No drug**	**CQ**
GC03^{GC03}	1.92 ± 0.04	2.16 ± 0.72	13%	5.74 ± 0.01	5.70 ± 0.01
GC03^{Cam734}	2.52 ± 0.03	3.10 ± 0.17	23%	5.55 ± 0.02	5.54 ± 0.01
GC03$^{Cam734\ F144A}$	2.34 ± 0.02	2.75 ± 0.21	17%	5.61 ± 0.02	5.61 ± 0.01
GC03^{Dd2}	2.79 ± 0.05	3.72 ± 0.13	33%	5.24 ± 0.01	5.28 ± 0.02

[a]For the indicated isogenic, *pfcrt*-modified lines, digestive vacuole (DV) volume size and pH were determined using spinning disk confocal microscopy and single-cell photometry, respectively. Measurements were made following 30 min exposure to no drug or 2× CQ LD_{50}. Results are reported as mean ± SEM DV volume size (μm^3) or pH, as determined for ≥20 parasites, beginning in each case with tightly synchronized young trophozoites. DV volume values for CQ-treated parasites were compared against those of untreated controls to determine the percent increase in size. Experiments performed by Roepe laboratory.

DISCUSSION

To ensure successful progression through their life cycle, drug-resistant *P. falciparum* parasites must balance the acquisition of drug resistance with the maintenance of essential physiological processes. Focusing on the pathogenic intraerythrocytic stages of parasite growth, we explored herein how novel mutations comprising the unusually polymorphic Cam734 PfCRT variant contribute to this complex relationship. Our analysis of the drug responses and growth rates of isogenic, *pfcrt*-modified lines reveals that multiple PfCRT mutations possess dual roles, contributing to both quinoline resistance and parasite proliferation. This was most notable for the A144F mutation that is unique to Cam734 PfCRT, which proved to be indispensable for parasite resistance to multiple quinoline-type compounds, including CQ, QN, and the first-line ACT partner drug AQ. This phenotype is reminiscent of earlier work, in which back-mutation of K76T ablated CQ resistance and nearly halved the degree of parasite resistance to QN.[126] Of note, CQ-sensitive parasites encoding Cam734 F144A PfCRT (i.e. Cam738; see **Table 3.1**) retained K76T as well as 7 other mutations, thus meeting the canonical mutational criteria for a CQ-resistant haplotype.[114] A clinical correlation that agrees with the notion that mutations beyond K76T can profoundly alter parasite drug responses is the fact that K76T predicts clinical CQR with good sensitivity, but only moderate specificity.[198,199]

In light of the previously documented impacts of CQ on parasite heme disposition (reduced Hz, increased free heme) and the ability of PfCRT mutations to regulate the access of CQ to its heme target in the DV,[55,58,126] we used our isogenic parasite lines to explore the role of PfCRT in the critical process of heme detoxification. An interesting difference noted between isogenic lines encoding

Cam734 and Dd2 PfCRT was the wild-type (GC03)-like propensity of Cam734 PfCRT to delay Hb digestion until higher CQ IC_{50} folds, as compared to Dd2 (see **Figure 3.8*C***). Our observed elevation of Hb species with increased CQ dose recalls prior studies that showed an increase in undigested Hb following CQ treatment, in part by inhibiting vesicular trafficking of host RBC Hb to the DV.[346,347] We predict that future PfCRT-focused experiments will provide important insights into the mechanisms by which various clinically important antimalarials (e.g. AQ, LUM, AS) induce increased heme levels,[55] akin to CQ, and yet retain potency against both CQ-sensitive and CQ-resistant strains.

Our metabolomics analysis (see **Figure 3.7**) and total hemoglobin quantification (see **Figure 3.8*C*** and **Figure 3.9*C***) clearly show that $GC03^{Cam734}$ parasites exhibit major changes in the Hb digestion pathway. Given that these changes are normally associated with impaired fitness,[232] our results raise an obvious question: does Cam734 PfCRT impart a metabolic compensatory mechanism that allows these parasites to circumvent the normally deleterious effects of altered Hb digestion? Previous heterologous expression studies using *Xenopus laevis* oocytes have reported the ability of PfCRT mutations to selectively confer transport of the tripeptide glutathione.[234] However, we saw no significant differences in glutathione or any other redox-associated metabolites (see **Figure 3.6** and **Table 3.7**) between isogenic lines encoding Cam734 or Dd2 PfCRT, suggesting that major redox-related metabolic changes are unlikely to account for the improved fitness associated with the Cam734 *pfcrt* allele. In contrast, we observed striking differences in ATP/AMP ratios and central carbon metabolism between lines encoding Cam734 and Dd2 PfCRT (see **Figure 3.7**), suggesting changes in energy metabolism as a physiologically

compensatory mechanism.

Recent evolutionary genetic studies of the adaptive landscapes (i.e. mutational paths and their accompanying fitness costs) associated with drug resistance-conferring mutations in parasite *dihydrofolate reductase* (*dhfr*) and *pfcrt* genes highlight key points that can be used to hypothesize how Cam734 *pfcrt* evolved: (1) forward *pfcrt* evolution is a physiologically constrained process that is consistent with the rarity of *pfcrt* alleles bearing three or fewer polymorphisms; (2) forward and reverse gene evolution are associated with distinct adaptive landscapes; and (3) adaptive landscapes can be substantially modified by their drug environment.[242,245,348,349] The spread of CQR in Asia as well as in Africa has long been attributed to a single (Dd2 or Dd2-like) *pfcrt* allele.[249] Of note, Cam734 shares four of the eight mutations comprising both the eight-amino acid Dd2 variant (see **Table 3.1**) and the related 6-amino acid variant GB4 (equivalent to Dd2 S326N T356I) that is also seen in Southeast Asia (Gabryszewski *et al.*, manuscript in preparation). We posit that, faced with high CQ pressure, parasites underwent mutational bursts (as previously suggested[242]) that led to the evolution of Dd2 *pfcrt*. With reduced CQ pressure, a "reverse" evolutionary process might have led to the loss of some mutations and eventual acquisition of novel ones, as in the case of Cam734 *pfcrt*.

In their report documenting Cam734 *pfcrt* in Cambodia, Durrand *et al.* also reported the related allele Cam738 (Cam734 F144A).[262] We posit that Cam738 served as a mutational precursor of the more evolutionarily successful Cam734 allele. This is supported by the inferior growth of isogenic parasites expressing Cam738 *pfcrt* as compared with Cam734 *pfcrt,* in the absence or presence of CQ or other quinoline drugs (see **Figure 3.2** and **Figure 3.5**). Of note, selective forces favoring mutation of

PfCRT residue 144 are apparent in Asia, in some cases requiring two nucleotide substitutions. For example, in the Philippines and in China, PfCRT haplotypes have been detected that, respectively, harbor the mutations A144T and A144Y.[350,351] Interestingly, addition of A144Y to the CQ-resistant Dd2 PfCRT isoform was previously found to abrogate CQ transport in *S. cerevisiae*.[208]

With sustained exposure to drug selective forces, parasites may evolve intergenic and/or intragenic compensatory changes that allow them to persist even in the absence of drug pressure.[240] The Cam734-defining compensatory mutations identified in our analysis reveal an intragenic basis for the enhanced fitness of this CQ-resistant allele, which could explain its continued presence in Southeast Asia despite the lack of CQ use for several decades to treat *P. falciparum* malaria. The degree to which secondary genetic factors also play a role is presently unclear. We note that our *pfcrt*-modified lines were generated in GC03 parasites, a clone of the HB3 (Central America) × Dd2 (Asia) genetic cross.[185] These parasites encode the HB3 *pfmdr1* haplotype, which differs from Dd2 PfMDR1 at three distinct residues (86, 184, 1042).[142] A recent study has shown that the PfMDR1 N86Y mutation (present in Dd2 parasites) augments the degree of CQR imparted by mutant Dd2 PfCRT.[143] We have recently observed that, as compared to GC03 parasites (see **Figure 3.2*A***), expression of Cam734 *pfcrt* in the Dd2 genetic background results in higher, Dd2-like levels of CQR (unpublished data). This is consistent with a prior transfection-based study that highlighted the importance of parasite genetic background in dictating the level to which mutant *pfcrt* alleles can mediate CQR.[217]

The notion that additional genetic changes are required to produce high-level CQR in parasites encoding Cam734 PfCRT evokes a previous finding that mutant

PfCRT-encoding parasites exhibit increased expression of proteins involved in pH regulation, including a V-type H^+ pyrophosphatase.[352] Our observation that, compared with Dd2, Cam734 PfCRT required a higher $\Delta\psi$ to manifest increased growth in the presence of CQ (consistent with elevated drug transport; see **Figure 3.12**) suggests that high-level Cam734 PfCRT-mediated drug resistance may be potentiated by parasite proteins that govern the $\Delta\psi$ across the DV membrane. We speculate that this plasticity in drug transport might be a reflection of the balance that Cam734 PfCRT has achieved in mediating resistance while also avoiding fitness costs. Future genetic dissections of *pfcrt* alleles, as well as candidate secondary genetic modulators (e.g. *pfmdr1*), are possible with the recent advent of efficient parasite genome editing tools.[143,353] Leveraging these approaches with analysis of parasite whole-genome sequences will aid in deciphering the genetic complexities that underlie new and emerging multidrug resistance phenotypes.

CHAPTER 4: REDEFINING THE GEOGRAPHIC LANDSCAPE OF MUTANT PFCRT AND ITS PLEIOTROPIC IMPACT ON *PLASMODIUM FALCIPARUM* MULTIDRUG RESISTANCE AND FITNESS

Stanislaw J. Gabryszewski,[1] Satish K. Dhingra,[1] Philipp P. Henrich,[1] David A. Fidock[1,2]

[1]Department of Microbiology and Immunology and [2]Division of Infectious Diseases, Department of Medicine, Columbia University Medical Center, New York, NY, USA

Author contributions: **SJG** and DAF conceived and designed the experiments; **SJG** and SKD performed experimental work; **SJG**, PPH, and DAF analyzed data; **SJG** and DAF wrote the manuscript.

Note: The work presented herein represents a manuscript in preparation.

ABSTRACT

Just a few geographical origins fully account for the historic emergence of chloroquine (CQ) resistance (CQR)-conferring variants of the *Plasmodium falciparum* Chloroquine Resistance Transporter (PfCRT), whose spread undermined the global gold-standard status of CQ. One of these variants evolved in Southeast Asia and eventually spread into and throughout Africa, where it contributed to stalled control efforts and a resurgence in malarial mortality. This PfCRT variant has been widely assumed to be the eight-amino acid Dd2 isoform (M74I/N75E/K76T/A220S/Q271E/N326S/I356T/R371I), which spread widely throughout Southeast Asia. In the context of higher parasite transmission and declining CQ use, wild-type PfCRT has re-emerged to become the most common PfCRT haplotype in Africa, followed by the six-amino acid GB4 variant (Dd2 S326N T356I) that was either the original haplotype that arrived from Asia or that has since emerged in Africa as *pfcrt* mutations were divested. To better understand these regional differences in allele prevalence, we genetically modified the *pfcrt* locus of asexual blood-stage *P. falciparum* parasites using zinc finger nucleases and generated a panel of isogenic parasites encoding all PfCRT haplotypes spanning the mutational interval between GB4 and Dd2, which differ at PfCRT residues 326 and/or 356. We explored the recent association of PfCRT mutations N326S and I356T with artemisinin resistance by generating our allelic panel in parasites either sensitive (wild-type K13) or resistant (R539T K13) to artemisinin. Phenotypic analysis of the drug susceptibility profile, degree of stage-specific survival following brief exposure to drug pulses, and growth kinetics of these lines revealed unique and complex impacts of PfCRT mutations on both drug resistance and fitness. Our data support the evidence that PfCRT mutations can

confer the properties of a multidrug resistance transporter, constrained by fitness costs imposed by its essential role in regulating digestive vacuole physiology. Comprehensive characterization of PfCRT variants that arose in response to global CQ pressure and that are now subjected to complex, region-specific selective forces are of direct relevance to the regional recommendations of antimalarials, whose activity is influenced by and, in certain cases, enhanced against PfCRT variants.

INTRODUCTION

The pathogenesis of human malaria is initiated by intraerythrocytic *Plasmodium* parasites, with *Plasmodium falciparum* causing the most severe and lethal disease. Recent reductions in the global incidence of malaria can be attributed in large part to the global deployment of artemisinin-based combination therapies (ACTs) to treat asexual blood stage infections, combined with vector control strategies.[13] ACTs consist of a fast-acting, albeit rapidly eliminated, artemisinin (ART) compound paired with a long-lived partner drug that is required to clear residual parasite biomass. Worryingly, emerging resistance to ACTs is now a reality, in part due to mismatched pharmacokinetic profiles of ACT components and parasite evolution of multidrug resistance.[123] The untimely rise and dispersal of chloroquine (CQ) and sulfadoxine-pyrimethamine resistance during past malaria control campaigns underscores the pressing need to identify and characterize novel drug resistance mechanisms before they render current drugs widely ineffective.[17]

Artemether-lumefantrine (ATM-LUM), artesunate-amodiaquine (AS-AQ), and dihydroartemisinin-piperaquine (DHA-PPQ) are the three most widely used ACTs worldwide. The structural hallmark of the core ART component (ATM, AS, DHA) is an endoperoxide bridge that, upon cleavage by heme, provokes oxidative stress.[100] First reported in Western Cambodia and now increasingly observed in neighboring countries,[181,354] the clinical indicator of waning ART efficacy is delayed parasite clearance from patient blood.[354] This phenotype tracks with mutations in the parasite *kelch13* (*k13*) gene[158] that are sufficient to confer parasite ART resistance *in vitro*,[160] which manifests as an increase in survival of ring-stage parasites to a brief, pharmacologically relevant pulse of the ART metabolite DHA.[162,355] Although ACTs

are widely used beyond Asia and *k13* mutations are infrequently detected among African parasite isolates,[356,357] so far only Southeast Asian parasites have experienced demonstrable selective pressures on the *k13* locus.[164] The spread of ART resistance in Southeast Asia has been attributed in part to the acquisition of secondary resistance determinants, including mutations in parasite genes encoding Apicoplast ribosomal protein S10 (ArpS10), Ferredoxin (Fd), *P. falciparum* Multidrug Resistance 2 Transporter (PfMDR2), and *P. falciparum* Chloroquine Resistance Transporter (PfCRT).[159] Of these, *pfcrt* mutations are known to modulate parasite ART susceptibility *in vitro*.[120,242] However, their effects on parasite DHA survival, the *in vitro* correlate of clinical ART resistance, had not been explored. Interestingly, Miotto *et al.* recently identified PfCRT N326S and I356T as mutations common among ART-resistant founder parasite populations.[159]

The recent evolution of resistance to first-line ACT partner drugs poses an additional layer of urgency. Reports from Southeast Asia now indicate rapidly emerging resistance to the bisquinoline compound PPQ.[135,136,138,358] Analogous to the ring-stage survival assay (RSA) for *in vitro* detection of ART resistance, a PPQ survival assay (PSA) was recently developed, whereby parasite survival is evaluated following two days of exposure to a pharmacologically relevant PPQ dose.[139] The genetic basis of resistance to PPQ has yet to be elucidated, although variations in genes affecting parasite digestive vacuole (DV) physiology and hemoglobin (Hb) processing, including *pfcrt* and the gene encoding the *P. falciparum* Multidrug Resistance 1 Transporter (PfMDR1), are speculated to be of importance.[139,223] Modulation of blood-stage parasite PPQ susceptibility by PfCRT mutations in certain genetic backgrounds is supported by at least four independent *in vitro*

studies.[137,196,217,218] As well, the mutational status of *pfcrt* and *pfmdr1* is known to impact the efficacy of the aryl-aminoalcohol compound LUM[143,148,213,359] and the quinoline compound AQ.[133,143,149] In the case of *pfcrt*, ATM-LUM and AS-AQ select for wild-type and mutant *pfcrt* alleles, respectively.[149] Selection of wild-type *pfcrt* was also previously reported for DHA-PPQ,[360] although the precise impact of PPQ on the *pfcrt* locus is less clear.[183] Evidence for ACT regimen-dependent selection of PfCRT variants corroborates recent descriptions of PfCRT as a pleiotropic mediator of multidrug resistance.[114,220,242]

As its name suggests, PfCRT was initially designated as the primary mediator of resistance to chloroquine (CQ). Following its historic contribution to malaria control efforts, CQ ultimately lost its status as a gold-standard antimalarial during the second half of the 20th century due to the multi-focal emergence and spread of chloroquine resistance (CQR).[249,271] Despite this, CQ continues to be used to treat *P. falciparum* infections in resistance-free regions and remains a first-line treatment of non-falciparum malaria.[32] Upon accumulating in the parasite digestive vacuole (DV), CQ interferes with parasite detoxification of heme, a potentially toxic byproduct of Hb digestion.[55] PfCRT mutations mediate CQR by conferring restricted access of CQ to its heme target,[188] of relevance given the centrality of Hb catabolism and heme detoxification to the modes of action and/or resistance of a wide array of antimalarials.[55,58,100,276] Consistently accompanied by ≥3 PfCRT single-nucleotide polymorphisms (SNPs), PfCRT K76T is necessary, but insufficient, for parasite CQR and serves as a sensitive, but not specific, marker of CQ treatment failure.[114,198,242] Recent studies have begun to uncover distinct roles for mutations beyond K76T in contributing to – and, in some instances, fully abolishing – parasite CQR, while also

altering responses to other drugs.[137,196,242,243]

In this study, we investigated the geographic distribution of *pfcrt* alleles and determined their impact on asexual blood-stage parasite drug resistance and fitness. Specifically, we explored the PfCRT haplotypes present in Asia (eight-SNP variant Dd2) and Africa (six-SNP variant GB4), which differ at PfCRT residues 326 and 356. Of note, Dd2 PfCRT harbors N326S and I356T, the ART resistance-associated PfCRT mutations reported by Miotto *et al.* that are common among Southeast Asian parasite isolates.[159] We evaluated the impact of these mutations on parasite proliferation and antimalarial drug responses using isogenic blood-stage parasites encoding GB4 PfCRT, Dd2 PfCRT, or intermediate PfCRT haplotypes encoding Dd2 S326N or Dd2 T356I PfCRT. Our analysis included a *k13*-mutant genetic background (R539T K13) permissive for enhanced ring-stage parasite DHA survival, which was used to explore the capacity of PfCRT mutations to modulate this ART resistance phenotype. Our findings redefine the global distribution of *pfcrt* alleles and their historical dissemination and provide new insights into the contributions of PfCRT mutations to the complex balance of parasite drug resistance and fitness.

METHODS

Parasite cultivation and genetic modification

Unless stated otherwise, *P. falciparum*-infected human erythrocytes were cultured at 4% hematocrit in RPMI-1640 culture medium supplemented with 0.5% Albumax II (Invitrogen). Cultures were incubated at 37°C, 5% O_2 / 5% CO_2 / 90% N_2.

To genetically modify the *pfcrt* locus of Dd2 or Dd2$_{R539T}$ parasites (**Figure 4.1**), a set of p*crt*-h*dhfr* donor plasmids encoding variant *pfcrt* alleles was prepared. This set included the previously generated plasmids p*crt*^{GC03}-h*dhfr* and p*crt*^{Dd2}-h*dhfr* (*pfcrt* allele listed in superscript; see **Table 4.1**). Site-directed mutagenesis (SDM)[361] with *Pfu*Turbo Polymerase (Agilent) and primer pairs p1+p2 and p3+p4 was used to introduce PfCRT back-to-wildtype S326N and/or T356I reversions into the donor template p*crt*^{Dd2}-h*dhfr*, generating the additional donor plasmids p*crt*$^{Dd2\ S326N}$-h*dhfr*, p*crt*$^{Dd2\ T356I}$-h*dhfr*, and , p*crt*^{GB4}-h*dhfr*.

Briefly, Dd2 or Dd2$_{R539T}$ parasites (≥4% parasitemia, mostly ring-stage) were transformed with 40 µg donor plasmid (p*crt*-h*dhfr*) and pressured with 2.5 nM WR99210 (Jacobus Pharmaceuticals). Parasites enriched with the p*crt*-h*dhfr* plasmid were similarly transformed with pZFN^{crt}-*bsd* and pressured with 2.5 nM WR99210 + 2 µg/ml Blasticidin HCl (Invitrogen) for six days, followed by continuous pressure with 2.5 nM WR99210. As detailed elsewhere,[242] blood PCR reactions (KAPA Biosystems) were used to assess for successful allelic replacement in bulk cultures and in cloned recombinant parasites. Parasites were cloned by limiting dilution following established protocols.[296] The full-length *pfcrt* gene was PCR-amplified with primer pair p9+p12 and sequenced with primers p5 and p6 to verify sequence integrity (see **Table 4.2** for primer list).

Table 4.1. PfCRT and K13 haplotypes of recombinant isogenic parasite lines.[a]

	PfCRT								K13
Parasite line	**74**	**75**	**76**	**220**	**271**	**326**	**356**	**371**	**539**
$Dd2^{GC03}$	M	N	K	A	Q	N	I	R	R
$Dd2^{Dd2}$	I	E	T	S	E	S	T	I	R
$Dd2^{Dd2\ S326N}$	I	E	T	S	E	N	T	I	R
$Dd2^{Dd2\ T356I}$	I	E	T	S	E	S	I	I	R
$Dd2^{GB4}$ ($Dd2^{Dd2\ S326N\ T356I}$)	I	E	T	S	E	N	I	I	R
$Dd2_{R539T}{}^{GC03}$	M	N	K	A	Q	N	I	R	T
$Dd2_{R539T}{}^{Dd2}$	I	E	T	S	E	S	T	I	T
$Dd2_{R539T}{}^{Dd2\ S326N}$	I	E	T	S	E	N	T	I	T
$Dd2_{R539T}{}^{Dd2\ T356I}$	I	E	T	S	E	S	I	I	T
$Dd2_{R539T}{}^{GB4}$ ($Dd2_{R539T}{}^{Dd2\ S326N\ T356I}$)	I	E	T	S	E	N	I	I	T

[a]The mutational status of PfCRT and K13 is summarized for all recombinant parasite lines generated in this study. Mutations are shaded in gray. The PfCRT haplotype encoded by Dd2 (wild-type K13) and $Dd2_{R539T}$ (mutant R539T K13) parasites is indicated in superscript, with GC03 designating the wild-type PfCRT haplotype.

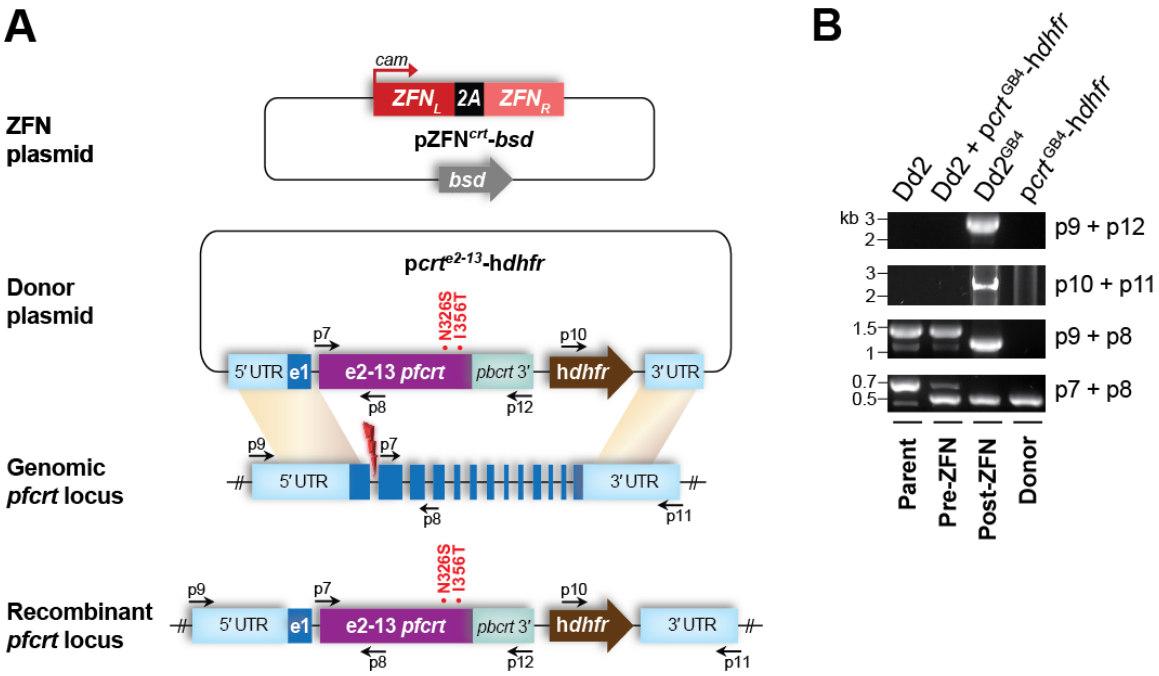

Figure 4.1. Parasite allelic modification of *pfcrt* and validation of genetic editing. (**A**) Zinc finger nuclease (ZFN)-based genetic engineering strategy. As detailed in **Methods**, parasites were first enriched with a donor plasmid (p*crt*-h*dhfr*) that encodes *pfcrt* exons 2-13 (e2-13) and includes mutations of interest (indicated in purple). A comprehensive list of PfCRT haplotypes that were introduced into Dd2 or Dd2$_{R539T}$ parasites is found in **Table 4.1**. The p*crt*-h*dhfr* plasmid also comprises the following elements: *P. berghei crt* (*pbcrt*) 3′ UTR, human *dhfr* (h*dhfr*) selection cassette, as well as *pfcrt-hdhfr*-flanking homology regions (~0.4 kb upstream of the intron 1-exon 2 boundary and ~1 kb native 3′ UTR downstream of *hdhfr*). Parasites were subsequently transfected with pZFN^{crt}-*bsd*. This plasmid facilitates *calmodulin* (*cam*) promoter-driven expression of a pair of *pfcrt*-targeting ZFNs (ZFN$_L$ and ZFN$_R$) and includes the *blasticidin S deaminase* (*bsd*) selection cassette. Following ZFN-catalyzed introduction of a double-stranded break in *pfcrt* (indicated with lightening bolt), parasites that employ the p*crt*-h*dhfr* plasmid as a donor template incorporate mutations of interest through homologous recombination-based mechanisms. (**B**) Blood PCR-based verification of *pfcrt* allelic exchange. Shown are representative results for Dd2 parasites into which the full-length GB4 *pfcrt* allele was introduced (Dd2^{GB4}) as well as controls, namely genetically unedited parental parasites (Dd2), unedited donor plasmid-enriched parasites (Dd2 + p*crt*^{GB4}-h*dhfr*), and the sole donor plasmid (p*crt*^{GB4}-h*dhfr*). All appropriately edited lines showed the expected DNA band migration patterns: 0.4 kb (p7+p8), 1.2 kb (p9+p8), 2.5 kb (p10+p11), and 2.7 kb (p9+p12). Primer (p) locations are illustrated in **Figure 4.1*A***.

Table 4.2. Primers used in this study.[a]

Primer	Oligonucleotide sequence (5' → 3')	Description	Lab name
p1	CCTTCGCATTGTTTTCCTTCTTTAACATTTGTGATAATTTAATAACCAGC	SDM PfCRT S326N F	p1765
p2	GCTGGTTATTAAATTATCACAAATGTTAAAGAAGGAAAACAATGCGAAGG	SDM PfCRT S326N F	p1766
p3	GTTAGTTGTATACAAGGTCCAGCAATAGCAATTGCTTATTAC	SDM PfCRT T356I F	p5633
p4	GTAATAAGCAATTGCTATTGCTGGACCTTGTATACAACTAAC	SDM PfCRT T356I R	p5634
p5	TCAAACATGACAAGGGAAATAGT	*pfcrt* exon 5 F	p2427
p6	CCAAGAATAAACATGCGAAACC	*pfcrt* exon 7 R	p3806
p7	CTTGAATTCGACCTTAACAGATGGCTCAC	*pfcrt* exon 2 F	p3264
p8	CTTATCGATAAGCAGAAGAACATATTAATAGGAATACTTAATTG	*pfcrt* exon 3 R	p3265
p9	CTTGGGCCCAAGTTGTACTGCTTCTAAGC	*pfcrt* gDNA 5′ UTR F	p3404
p10	CTCGAGATGGTTGGTTCGCTAAACTGC	h*DHFR* F	p3315
p11	TTGACCCTTATATATTCCACCCA	*pfcrt* gDNA 3′ UTR R	p3403
p12	GAGGCGCCTATTTCAAAAATCTTAGCATAAGGATT	*pbcrt* 3′ UTR R	p1644

[a]SDM, site-directed mutagenesis; F, forward; R, reverse; gDNA, genomic DNA; *pbcrt, P. berghei chloroquine resistance transporter*; UTR, untranslated region.

Drug susceptibility assays

The concentrations of antimalarial drugs that were 50% and 90% growth-inhibitory (i.e. IC_{50} and IC_{90}) to asexual blood-stage parasites were determined using a flow cytometry-based assay that detects parasite nuclei and mitochondria using SYBR Green I and MitoTracker Deep Red, respectively.[242] Parasites were subjected to two-fold serial dilutions of drug, and parasite growth was determined with an Accuri C6 flow cytometer after 72 h. Our antimalarial drug panel included CQ ± 0.8 μM verapamil (VP), monodesethyl-CQ, monodesethyl-AQ, LUM, AS, PPQ, pyronaridine (PND), and quinine (QN). To determine verapamil (VP)-mediated reversibility of CQR, the CQ+VP IC_{50} value was divided by the CQ IC_{50} value, yielding the CQ response modification index (RMI).[298] Statistical significance was determined via non-parametric Mann-Whitney *U* tests using GraphPad Prism 6 software.

In vitro growth assays

Growth of asexual blood-stage parasites was assessed *in vitro* using a previously described method that employs flow cytometric detection of GFP and the far-red fluorescent dye SYTO61.[242] Briefly, 1:1 co-cultures were established with a GFP-positive (GFP^+) fluorescent reporter line (R^{GFP}) and a single GFP-negative (GFP^-) *pfcrt*-modified test line. R^{GFP} in these assays corresponds to the previously generated CQ-resistant $Dd2^{BiP\text{-}eGFP}$ line. This line uses a BiP promoter to drive enhanced GFP (eGFP) expression and has a genetic background comparable to that of our *pfcrt*-modified test lines.[299] Using flow cytometry, we determined the proportion of GFP^- parasites (corresponding to the *pfcrt*-modified test line) every three days for 20 days (i.e. 10 parasite generations). Cultures were regularly monitored and diluted such

that parasitemia never exceeded 8%.

The frequencies of the GFP$^-$ test line and the GFP$^+$ reporter line at time t are referred to as p_t and q_t, respectively. As previously detailed, the fitness (ω) associated with a particular test line was derived from the natural log-transformed ratio p_t/q_t and normalized to isogenic parasites encoding the wild-type (GC03) *pfcrt* allele in the Dd2 genetic background (Dd2^{GC03}), yielding the relative fitness (ω') metric. The *in vitro* growth selection coefficient (s) for each test strain was derived from the relationship $s = \omega' - 1$.[242] Statistical significance was assessed via two-way ANOVA with Sidak's post-hoc test using GraphPad Prism 6 software.

DHA and PPQ survival assays

Stage-specific survival assays were conducted following published protocols, with minor modifications.[139,160,355] Briefly, 15 ml of parasite culture was synchronized with 5% sorbitol and cultivated through the mature schizont stage (≥0.5% schizont parasitemia). Cultures were heparinized for 30 min at 37°C in RPMI-1640 medium containing 15 U/ml sodium heparin (Millipore), with occasional mild vortexing. Parasites were subsequently subjected to a gradient of 75% Percoll (Sigma-Aldrich) and centrifuged at 3400 rpm for 15 min. The schizont fraction was washed with RPMI-1640 medium and incubated with human RBCs for 3 h to initiate a new asexual blood-stage cycle, followed by synchronization with 5% sorbitol to eliminate non-ring parasite forms. Serial dilutions of DHA or PPQ were pre-aliquoted into 96-well plates using a BioTek Precision Pipetting System. Parasite cultures at early-ring (t=0–3 hpi) or mid-trophozoite (t=18–21 h post-invasion) stages were added to plates containing drug dilutions, to 200 µl final volume, 0.5% parasitemia, 2% hematocrit. Duplicate

wells were included for each parasite line and drug concentration. Vehicle controls for DHA and PPQ survival assays were DMSO and 0.5% lactic acid, respectively. For DHA survival assays, parasites were incubated in drug for 3 h. For PPQ survival assays, parasites were incubated through the 48 hpi timepoint. Following drug incubation, parasites were washed three times with RPMI-1640 medium and grown in fresh medium until the assay endpoint of 72 h. Parasitemia was assessed by flow cytometry, which correlated with microscopic assessment of parasitemia. Parasite survival is equivalent to parasitemia in the presence of drug divided by the parasitemia in the vehicle control well, expressed as a percentage.

RESULTS AND DISCUSSION

Distribution of *pfcrt* alleles in Africa and Southeast Asia

Together, Africa and Southeast Asia account for the vast majority of the global burden of malaria. Using the MalariaGEN Pf3k database of *P. falciparum* whole genome sequences that encompass these regions,[159] we assessed the geographic distribution of allelic *pfcrt* variants (**Figure 4.2**). In Africa, wild-type (GC03) PfCRT comprised 75% of the total haplotypes. Of the mutant PfCRT haplotypes in this region, GB4 was the most common (47% of mutant haplotypes; 12% of total haplotypes), followed by Dd2 S326N (28% of mutants; 7% of total). The remaining portion of mutant haplotypes (25% of mutants; 6% of total) was comprised of various, polymorphic haplotypes, with the GB4 S220A PfCRT variant being most common. In contrast, in Southeast Asia, the wild-type PfCRT haplotype comprised only 8% of the total haplotypes. Dd2 was the most common mutant haplotype (57% of mutants; 52% of total), followed by Cam734 (15% of mutants; 14% of total), GB4 (13% of mutants; 12% of total), and other mutant haplotypes (14% of mutants; 15% of total).

Several striking features emerge from this data. First, the predominant *pfcrt* allele in Africa is not the 8-amino acid variant Dd2, the first mutant *pfcrt* allele that was discovered through the analysis of the HB3×Dd2 genetic cross.[185] It is also not the 7-amino acid variant Dd2 T356I, which lacks the I356T mutation. Both the Dd2 and Dd2 T356I alleles were originally observed in Asian and African parasites available at the time that *pfcrt* was reported (2000), and it has been frequently assumed that Dd2 was the original allele that spread from Asia to Africa, which caused a devastating loss of CQ efficacy and increase in malaria mortality.[186,249,270] It is now evident that a 6-amino acid variant (represented by the strain GB4 from Gabon) and

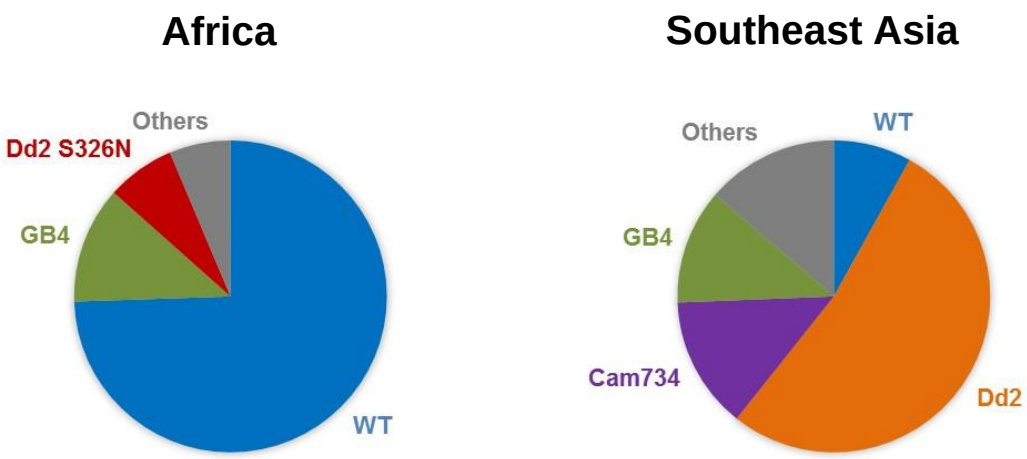

Figure 4.2. Predominant *pfcrt* alleles are distinct in Africa and Asia. Pie charts illustrate the regional proportion of the indicated haplotypes, as estimated based on whole genome sequences present in the MalariaGEN Pf3k database.[159] Pie chart sections correspond to the following haplotype proportions: Africa – WT 75%; GB4 12%; Dd2 S326N 7%; Others 6%; Southeast Asia – wild-type (WT) 8%; Dd2 52%; Cam734 14%; GB4 12%; Others 14%. The mutational composition of the WT (GC03), Dd2, GB4, and Dd2 S326N PfCRT haplotypes is shown in **Table 4.1**. Cam734 PfCRT consists of the following mutations: M74I, N75D, K76T, A144F, L148I, I194T, A220S, Q271E, T333S.

a 7-amino acid variant that has not yet been described in any culture-adapted strain (referred here to as Dd2 S326N) are the predominant mutant PfCRT variants in Africa. Interestingly, the GB4 variant is quite abundant in Southeast Asia. Further studies with isolates collected over time will be required to identify whether GB4 was the original allele that spread from Asia into Africa, or whether both continents have seen a progressive loss of PfCRT mutations, starting from the 8-amino acid or 7-amino acid variants. These observations were only made possible with the recent report of 1,500 and 1,000 *P. falciparum* genomes from Africa and Asia, respectively, highlighting the value of large-scale genome studies.[164]

Generation of isogenic parasites encoding variant *pfcrt* and *k13* alleles

Herein, we aimed to characterize the most prevalent mutant PfCRT haplotypes in Africa and Southeast Asia (GB4 and Dd2, respectively), in relation to wild-type (GC03) PfCRT. The mutational composition of these haplotypes is similar, with Dd2 PfCRT harboring two mutations (N326S and I356T) on top of the six mutations (M74I, N75E, K76T, A220S, Q271E, R371I) it shares with the GB4 isoform (**Table 4.1**). To define cellular features associated with the GB4 and Dd2 PfCRT haplotypes that may provide a basis for their regional distributions, and to dissect the roles of PfCRT S326N and T356I in parasite drug resistance versus fitness, we genetically modified the *pfcrt* locus of *P. falciparum* asexual blood-stage parasites. Using an established zinc finger nuclease (ZFN)-based approach (**Figure 4.1**), we generated isogenic parasites varying only by the *pfcrt* allele that they express. The *pfcrt* sequence of these parasite lines was verified using primers listed in **Table 4.2**. Our PfCRT haplotype panel included full-length GC03 (wild-type), GB4, and Dd2 PfCRT as well

intermediates spanning the mutational interval between GB4 and Dd2, namely Dd2 S326N and Dd2 T356I PfCRT (see **Table 4.1**). Of note, inclusion of the Dd2 S326N PfCRT haplotype in our analysis allowed us to characterize the second most common mutant PfCRT haplotype in Africa (see **Figure 4.2**). To explore the recently reported association of PfCRT mutations N326S and I356T with ART-resistant founder parasite populations,[159] we generated this panel of PfCRT haplotypes in two separate parasite backgrounds, namely Dd2 and $Dd2_{R539T}$, which encode wild-type and mutant R539T K13, respectively (see **Table 4.1**). The latter strain is equivalent to $Dd2^{R539T}$, a published *k13*-modified line that exhibited one of the highest levels of ART resistance in the Dd2 background.[160]

CQ responses of *pfcrt*-modified lines

Mutant forms of PfCRT are most extensively recognized for their ability to confer CQR. To assess whether variants in our panel of *pfcrt* alleles have an impact on parasite CQ responses, we subjected asexual blood-stage parasites to flow cytometry-based drug susceptibility assays and determined 50% and 90% growth-inhibitory antimalarial drug concentrations (IC_{50} and IC_{90}, respectively; **Table 4.3**). For CQ (**Figure 4.3*A***) and its main *in vivo* metabolite, monodesethyl-CQ (md-CQ; **Figure 4.3*B***), mutant PfCRT isoforms Dd2, Dd2 S326N, Dd2 T356I, and GB4 each conferred statistically significant increases in drug IC_{50} values as compared with the GC03 (wild-type) isoform ($P<0.002$ in all instances). Among the mutant isoforms, the highest and lowest levels of resistance to CQ and md-CQ were conferred, respectively, by Dd2 and GB4 PfCRT (**Figure 4.3**; **Table 4.3**). The reduced level of resistance associated with GB4 PfCRT (~1.6-fold

Table 4.3. Antimalarial IC_{50} and IC_{90} values of *pfcrt*-modified parasite lines.[a]

	***pfcrt* allele in Dd2 background**					***pfcrt* allele in Dd2$_{R539T}$ background**				
	Dd2	**Dd2 S326N**	**Dd2 T356I**	**GB4**	**GC03**	**Dd2**	**Dd2 S326N**	**Dd2 T356I**	**GB4**	**GC03**
CQ IC_{50}	161 ± 10.1	134 ± 10.5	144 ± 10.1	102 ± 10.8	11.9 ± 0.4	152 ± 10.8	131 ± 14.6	132 ± 12.9	92.5 ± 8.8	12.9 ± 0.5
n	7	7	5	4	8	7	6	5	4	7
P	–	0.53	0.97	**0.009**	**<0.0001**	0.99	0.43	0.57	**0.0011**	**<0.0001**
CQ IC_{90}	261 ± 12.0	231 ± 9.9	268 ± 27.6	204 ± 18.1	18.8 ± 1.7	277 ± 24.4	255 ± 17.8	263 ± 26.9	199 ± 13.3	24.9 ± 0.7
n	7	7	5	4	8	7	6	5	4	7
P	–	0.92	>0.99	0.43	**<0.0001**	>0.99	>0.99	>0.99	0.32	**<0.0001**
CQ+VP IC_{50}	32.5 ± 4.1	26.6 ± 4.6	22.5 ± 5.8	30.7 ± 8.9	13.3 ± 0.8	23.8 ± 6.1	26.6 ± 4.7	19.0 ± 6.8	23.9 ± 4.7	13.2 ± 0.6
n	6	6	5	3	7	6	5	5	3	6
P	–	0.99	0.88	>0.99	0.07	0.93	>0.99	0.57	0.98	0.09
CQ+VP IC_{90}	80.2 ± 7.2	62.3 ± 0.9	79.5 ± 8.7	66.6 ± 11.6	24.7 ± 1.7	78.8 ± 13.2	72.1 ± 12.8	71.7 ± 13.8	59.3 ± 8.11	26.4 ± 1.1
n	6	5	5	3	7	6	5	5	3	6
P	–	0.90	>0.99	>0.99	**0.0005**	>0.99	>0.99	>0.99	0.90	**0.0014**
md-CQ IC_{50}	845 ± 44	703 ± 80	744 ± 69	537 ± 66	21.2 ± 0.8	720 ± 29	608 ± 56	602 ± 47	426 ± 53	21.0 ± 2.4
n	7	7	5	4	7	7	6	5	4	6
P	–	0.48	0.92	**0.006**	**<0.0001**	0.65	**0.03**	**0.04**	**<0.0001**	**<0.0001**
md-CQ IC_{90}	1527 ± 68	1309 ±83	1428 ± 58	828 ± 74	48.3 ± 1.7	1334 ± 134	1144 ± 137	1186 ± 109	742 ± 103	48.1 ± 3.3
n	7	7	5	4	7	7	6	5	4	6
P	–	0.69	>0.99	**0.0002**	**<0.0001**	0.82	0.08	0.22	**<0.0001**	**<0.0001**
md-AQ IC_{50}	90.7 ± 6.2	45.3 ± 2.9	71.5 ± 7.7	44.4 ± 6.8	23.7 ± 1.7	79.1 ± 3.8	46.5 ± 2.2	69.5 ± 2.2	43.5 ± 5.8	27.1 ± 1.9
n	7	7	5	4	7	7	6	5	4	6
P	–	**<0.0001**	0.07	**<0.0001**	**<0.0001**	0.54	**<0.0001**	**0.03**	**<0.0001**	**<0.0001**
md-AQ IC_{90}	163 ± 8.7	88.9 ± 4.6	117 ± 13.8	79.7 ± 8.5	37.7 ± 2.7	131 ± 11.3	80.2 ± 6.6	122 ± 9.9	64.1 ± 12.3	36.7 ± 3.2
n	7	6	5	3	6	7	6	5	3	6
P	–	**<0.0001**	**0.013**	**<0.0001**	**<0.0001**	0.13	**<0.0001**	**0.04**	**<0.0001**	**<0.0001**

(continued)

Table 4.3. *continued*

	***pfcrt* allele in Dd2 background**					***pfcrt* allele in Dd2$_{R539T}$ background**				
	Dd2	**Dd2 S326N**	**Dd2 T356I**	**GB4**	**GC03**	**Dd2**	**Dd2 S326N**	**Dd2 T356I**	**GB4**	**GC03**
QN IC_{50}	139 ± 22.5	134 ± 21.1	118 ± 15.6	128 ± 19.7	96.9 ± 8.2	98.1 ± 16.2	120 ± 15.0	103 ± 8.6	126 ± 43.0	83.7 ± 6.6
n	4	7	5	4	6	4	4	4	4	4
P	–	>0.99	0.98	>0.99	0.85	0.92	>0.99	0.96	>0.99	0.67
QN IC_{90}	355 ± 19	393 ± 58	363 ± 4	587 ± 169	318 ± 68	390 ± 25	436 ± 50	408 ± 59	399 ± 96	296 ± 42
n	4	7	5	4	6	4	4	4	4	4
P	–	>0.99	>0.99	0.50	>0.99	>0.99	>0.99	>0.99	>0.99	>0.99
PPQ IC_{50}	1.3 ± 0.1	1.2 ± 0.1	1.3 ± 0.1	1.4 ± 0.1	1.0 ± 0.1	1.2 ± 0.1	1.0 ± 0.1	1.0 ± 0.1	1.3 ± 0.1	0.9 ± 0.1
n	6	7	5	4	8	6	5	5	4	6
P	–	>0.99	>0.99	>0.99	0.55	>0.99	0.51	0.66	>0.99	0.09
PPQ IC_{90}	3.0 ± 0.2	2.5 ± 0.3	3.0 ± 0.1	3.0 ± 0.5	2.3 ± 0.3	2.6 ± 0.2	2.0 ± 0.1	2.6 ± 0.3	2.5 ± 0.3	1.8 ± 0.1
n	6	7	5	4	8	6	5	5	4	6
P	–	0.88	>0.99	>0.99	0.47	0.20	0.99	0.97	0.07	0.96
LUM IC_{50}	1.1 ± 0.1	1.2 ± 0.2	1.0 ± 0.04	1.6 ± 0.5	2.0 ± 0.2	1.0 ± 0.2	1.2 ± 0.2	1.1 ± 0.2	1.1 ± 0.04	1.9 ± 0.4
n	4	7	4	3	6	4	4	4	3	4
P	–	>0.99	>0.99	0.91	0.12	>0.99	>0.99	>0.99	>0.99	0.40
LUM IC_{90}	11.2 ± 1.1	8.9 ± 1.1	13.2 ± 1.3	16.0 ± 5.6	12.2 ± 1.2	9.1 ± 1.4	8.7 ± 1.4	7.0 ± 0.6	12.0 ± 7.1	9.2 ± 0.7
n	4	7	4	3	6	4	4	4	3	4
P	–	>0.99	>0.99	0.92	>0.99	>0.99	>0.99	0.94	>0.99	>0.99
AS IC_{50}	2.3 ± 0.2	2.2 ± 0.3	2.5 ± 0.2	1.8 ± 0.2	2.3 ± 0.2	2.3 ± 0.3	2.5 ± 0.3	2.2 ± 0.2	1.7 ± 0.3	3.0 ± 0.2
n	7	9	6	5	10	7	6	6	5	6
P	–	>0.99	>0.99	0.93	>0.99	>0.99	>0.99	>0.99	0.83	0.77
AS IC_{90}	4.1 ± 0.3	4.7 ± 0.6	5.5 ± 0.7	4.2 ± 0.8	4.9 ± 0.5	4.6 ± 0.6	4.9 ± 0.6	5.0 ± 0.6	3.7 ± 1.0	5.7 ± 0.9
n	7	7	6	3	8	7	6	6	3	7
P	–	>0.99	0.86	>0.99	>0.99	>0.99	>0.99	>0.99	>0.99	0.65

(continued)

Table 4.3. *continued*

	***pfcrt* allele in Dd2 background**					***pfcrt* allele in Dd2$_{R539T}$ background**				
	Dd2	**Dd2 S326N**	**Dd2 T356I**	**GB4**	**GC03**	**Dd2**	**Dd2 S326N**	**Dd2 T356I**	**GB4**	**GC03**
PND IC_{50}	11.7 ± 2.1	10.8 ± 1.0	12.6 ± 1.5	10.2 ± 1.1	9.3 ± 1.6	11.8 ± 1.5	14.2 ± 1.3	13.6 ± 1.8	8.2 ± 3.0	14.0 ± 1.9
n	5	6	5	3	7	5	4	5	3	5
P	–	>0.99	>0.99	>0.99	0.99	>0.99	>0.99	>0.99	0.96	>0.99
PND IC_{90}	19.5 ± 4.1	17.0 ± 0.5	21.7 ± 3.5	17.8 ± 0.7	13.9 ± 2.4	20.1 ± 3.1	21.7 ± 4.0	21.0 ± 3.3	14.5 ± 5.6	19.3 ± 3.2
n	5	6	5	3	7	5	4	5	3	5
P	–	>0.99	>0.99	>0.99	0.94	>0.99	>0.99	>0.99	>0.99	>0.99

[a]IC_{50} and IC_{90} values (nM) indicate the mean ± SEM, as determined in 3 to 10 independent assays. CQ + VP assays were performed with 0.8 μM VP. CQ, chloroquine; VP, verapamil; md-CQ, monodesethyl-chloroquine; md-AQ, monodesethyl-amodiaquine; QN, quinine; PPQ, piperaquine; LUM, lumefantrine; AS, artesunate; PND, pyronaridine; *n*, number of assays. Statistical significance was determined via one-way ANOVA with Tukey's multiple comparisons test. *P* values (in **bold** and shaded in gray if <0.05) are reported for comparisons with the parasite line Dd2^{Dd2}.

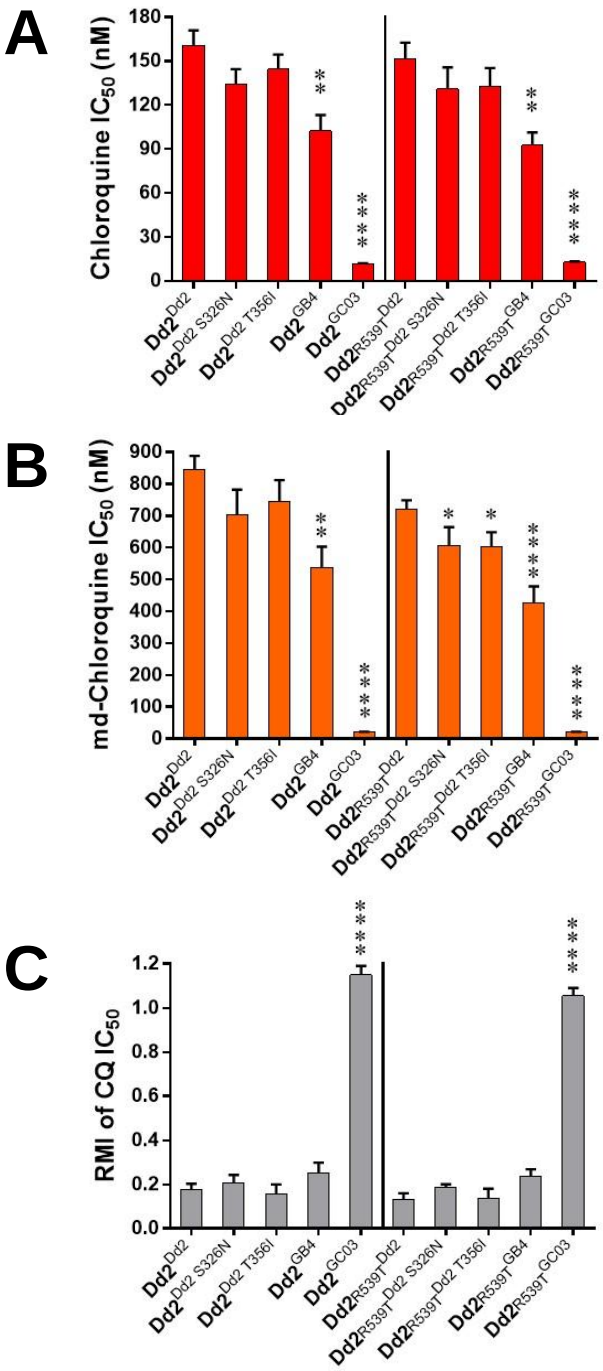

Figure 4.3. Chloroquine responses of *pfcrt*-modified lines. (**A** and **B**) Parasite susceptibilities to (**A**) chloroquine (CQ) and (**B**) monodesethyl (md)-CQ were assessed by flow cytometry following exposure to the indicated drug for 72 h. Bar graphs correspond to mean ± SEM IC_{50} values. (**C**) Verapamil (VP)-mediated reversibility of CQ resistance. Parasite IC_{50} values for CQ + 800 nM VP and CQ alone were determined as described for CQ and md-CQ. The quotient of these values yielded the CQ response modification index (RMI). Bar graphs correspond to mean ± SEM RMI values. For all panels, results reflect 4 independent assays, conducted in duplicate. **P*<0.05; ***P*<0.01; *****P*<0.0001.

reduction versus Dd2 PfCRT for CQ and md-CQ) was significant in both the Dd2 and $Dd2_{R539T}$ parasite genetic backgrounds ($P<0.01$). Additionally, PfCRT haplotypes Dd2 S326N and Dd2 T356I conferred a slight reduction in parasite CQ and md-CQ resistance, as compared with Dd2 PfCRT, achieving statistical significance in the $Dd2_{R539T}$ background for md-CQ ($P<0.05$; **Figure 4.3*B*; Table 4.3**).

Laboratory studies of CQ-resistant parasites have previously identified chemosensitization by the calcium channel blocker verapamil (VP) as a defining feature of parasite CQR. VP reversibility of CQR is reported as the CQ response modification index (RMI), i.e. the IC_{50} value for CQ plus 800 nM VP divided by the IC_{50} value for CQ alone.[298] Comparison of RMI values among our *pfcrt*-modified lines (**Figure 4.3*C*; Table 4.4**) showed that Dd2 PfCRT confers a significant degree of CQR reversibility, consistent with previous studies.[120] RMI values associated with the Dd2, Dd2 S326N, Dd2 T356I, and GB4 isoforms (**Figure 4.3*C***) were comparably reduced as compared to isogenic parasites expressing the wild-type (GC03) isoform, which did not confer chemosensitization. As anticipated, none of the CQ responses that were evaluated were altered by mutation of the *k13* locus ($P>0.05$ for all pairwise comparisons of *pfcrt*-matched parasites in Dd2 versus $Dd2_{R539T}$ backgrounds).

Given the similarity in mutational composition of GB4 and Dd2 PfCRT (see **Table 4.1**) and the physiological constraints known to be associated with *de novo* evolution of *pfcrt* alleles,[242] it is plausible that these isoforms share a common mutational trajectory. Our CQ susceptibility findings suggest that GB4 PfCRT may indeed be a mutational precursor of Dd2 PfCRT, at least in the setting of drug pressure.

Table 4.4. Verapamil-mediated CQ resistance reversibility of *pfcrt*-modified parasite lines.[a]

	***pfcrt* allele in Dd2 background**					***pfcrt* allele in Dd2$_{R539T}$ background**				
	Dd2	**Dd2 S326N**	**Dd2 T356I**	**GB4**	**GC03**	**Dd2**	**Dd2 S326N**	**Dd2 T356I**	**GB4**	**GC03**
RMI	0.17 ± 0.03	0.21 ± 0.04	0.16 ± 0.04	0.25 ± 0.05	1.2 ± 0.04	0.13 ± 0.03	0.19 ± 0.01	0.14 ± 0.09	0.24 ± 0.04	1.1 ± 0.04
n	7	7	5	4	8	7	6	5	4	7
P	–	>0.99	>0.99	0.92	**<0.0001**	>0.99	>0.99	>0.99	0.99	**<0.0001**

[a]Reversibility of chloroquine (CQ) resistance by 0.8 µM verapamil (VP) is indicated as the CQ response modification index (RMI), equivalent to (IC_{50} for CQ+VP) ÷ (IC_{50} for CQ only). Shown are mean RMI ± SEM values, as determined in 4 to 8 independent assays. *n*, number of assays. *P* values were determined in a non-parametric Mann-Whitney *U* test versus the parasite line GC03^{Cam734}. *P* values <0.05 are indicated in **bold** and shaded in gray.

Susceptibility of *pfcrt*-modified lines to clinically employed antimalarials

PfCRT isoforms are increasingly noted to function as modulators of parasite susceptibility to multiple antimalarials beyond CQ, including first-line ACT components. We therefore examined the drug susceptibility profiles of our isogenic, *pfcrt*-modified lines to a panel of clinically important drugs (**Figure 4.4**; **Table 4.3**). Among these are the ACT artemisinin compound AS, various ACT partner drugs (LUM; PPQ; the AQ *in vivo* metabolite monodesethyl-AQ; and pyronaridine, PND), and the quinoline-type drug quinine (QN). Consistent with the known cross-resistance between CQ and AQ,[114] all mutant *pfcrt* alleles heightened parasite resistance to md-AQ, as compared with wild-type (GC03) *pfcrt*, with Dd2 *pfcrt* conferring the highest level of md-AQ resistance (**Figure 4.4**; **Table 4.3**). Interestingly, an important contributory role was identified for PfCRT mutation N326S; mutant PfCRT haplotypes bearing S326N reversions (i.e. Dd2 S326N and GB4; see **Table 4.1**) conferred a marked, statistically significant ($P<0.0001$) reduction in md-AQ resistance relative to the Dd2 isoform (**Figure 4.4**; **Table 4.3**). The notion that PfCRT residue 326 is a key mediator of AQ resistance agrees with a recent report that described mutation N326D, found among South American and Western Pacific parasite isolates, as a direct contributor to md-AQ resistance.[242] We note that no statistically significant differences were observed among parasite lines for the compounds LUM, AS, PPQ, PND, and QN (**Figure 4.4**; **Table 4.3**).

Of note, AQ is the partner drug in the ACT regimen AS-AQ that is widely used for treatment and prevention of malaria in Africa. AQ also comprises the formulation AQ-sulfadoxine-pyrimethamine, which is administered prophylactically to young children in some areas of sub-Saharan Africa during months of high transmission.

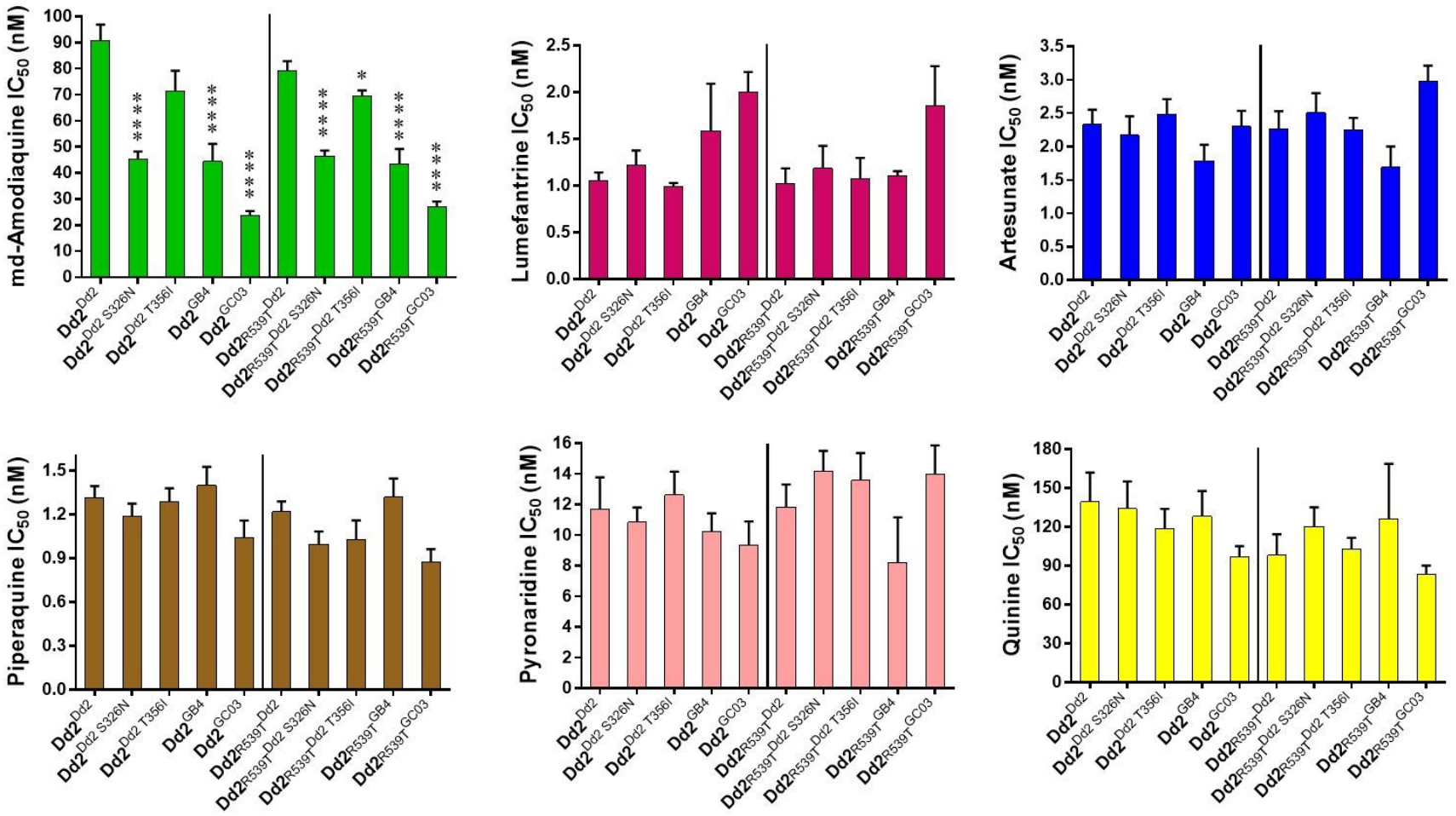

Figure 4.4. Responses of *pfcrt*-modified lines to various clinically employed antimalarial drugs. Parasite susceptibilities to monodesethyl (md)-amodiaquine, lumefantrine, artesunate, piperaquine, pyronaridine, and quinine were assessed by flow cytometry following exposure to the indicated drug for 72 h. Bar graphs correspond to mean ± SEM IC_{50} values. **P*<0.05; *****P*<0.0001.

Recent clinical studies by Yeka *et al.* documented a lower incidence of parasite recrudescence following treatment with AS-AQ as compared to ATM-LUM, the two most widely deployed regimens that are known to select for mutant and wild-type *pfcrt*-expressing parasites, respectively.[149] Based on the wide prevalence of the wild-type *pfcrt* allele in Africa and the paucity of *pfcrt* alleles that conferred a high degree of AQ resistance in our study, continued use of AQ-based regimens in Africa seems justified. A meta-analysis of worldwide AS-AQ efficacy sheds light on a distinct situation in Asia, where the Dd2 *pfcrt* allele is widely prevalent and where the risk of parasite recrudescence following AS-AQ treatment is significantly (7-fold) higher as compared to Africa.[362] Given this data, it is possible that only certain AQ resistance-conferring *pfcrt* alleles (e.g. Dd2) are able to confer the minimum degree of AQ resistance necessary to sustain resistant parasite populations, whereas other mutant *pfcrt* alleles (e.g. GB4, Dd2 S326N) are more rapidly cleared and, in the context of appropriate dosing, pose less of a threat.

Survival of *k13*-mutant, *pfcrt*-modified lines exposed to DHA

Although our drug susceptibility assays did not reveal significant shifts in AS IC_{50} values among parasite lines, the utility of IC_{50}-based studies for the detection of clinical ART resistance is limited. A more powerful metric is parasite survival following drug pulses that mimic its pharmacology *in vivo*. For ART compounds, reduced DHA susceptibility of early ring-stage (0-3 h) parasites in RSAs conducted *in vitro* correlates with ART resistance in the clinical setting, defined as slower rates of parasite clearance.[162,355,363] This phenotype has been associated with mutations in the parasite *k13* gene, which is sufficient to mediate enhanced parasite survival following

exposure to DHA *in vitro* in RSAs.[158,160]

In the present study, we interrogated the effect of variant *pfcrt* allele expression on parasite DHA survival during the ring and trophozoite parasite intraerythrocytic stages. Our inquiry was motivated by several lines of evidence implicating a possible role for PfCRT in modulating parasite ART responses: (1) Disposition of heme, the putative ART activator, is affected by parasite *pfcrt* genotypes;[55,232]; (2) In addition to their activity against ring-stage parasites, ARTs are potent against trophozoites, during which both PfCRT and heme are highly abundant;[114,157] (3) A multigenic basis of ART resistance was recently revealed by whole genome analyses, which identified an association between ART resistance and PfCRT mutations N326S and I356T;[159] (4) In some genetic backgrounds, PfCRT mutations can modulate asexual blood-stage parasite susceptibility to ART compounds.[120,242] To probe the capacity of PfCRT mutations to modulate the parasite's ability to survive DHA pressure, we employed the *k13*-mutant $Dd2_{R539T}$ genetic background (see **Table 4.1**), which bears a R539T K13 mutation that confers *in vitro* RSA survival to DHA.

While DHA-based survival assays are routinely performed on early-ring (0–3 h) stage parasites with 700 nM DHA, we aimed to consider the possibility that PfCRT mutations may modulate ART resistance at sub-physiologic levels of DHA and that this effect may be restricted to a specific stage of the parasite intraerythrocytic life cycle. Accordingly, we evaluated the survival of early ring (0–3 h) and mid-trophozoite (28–31 h) *P. falciparum* blood-stage parasites following exposure to a wide range of DHA concentrations (1.4–700 nM). Results for ring-stage DHA survival assays (**Figure 4.5*A***) showed that varying the *pfcrt* allele expressed at this stage had no

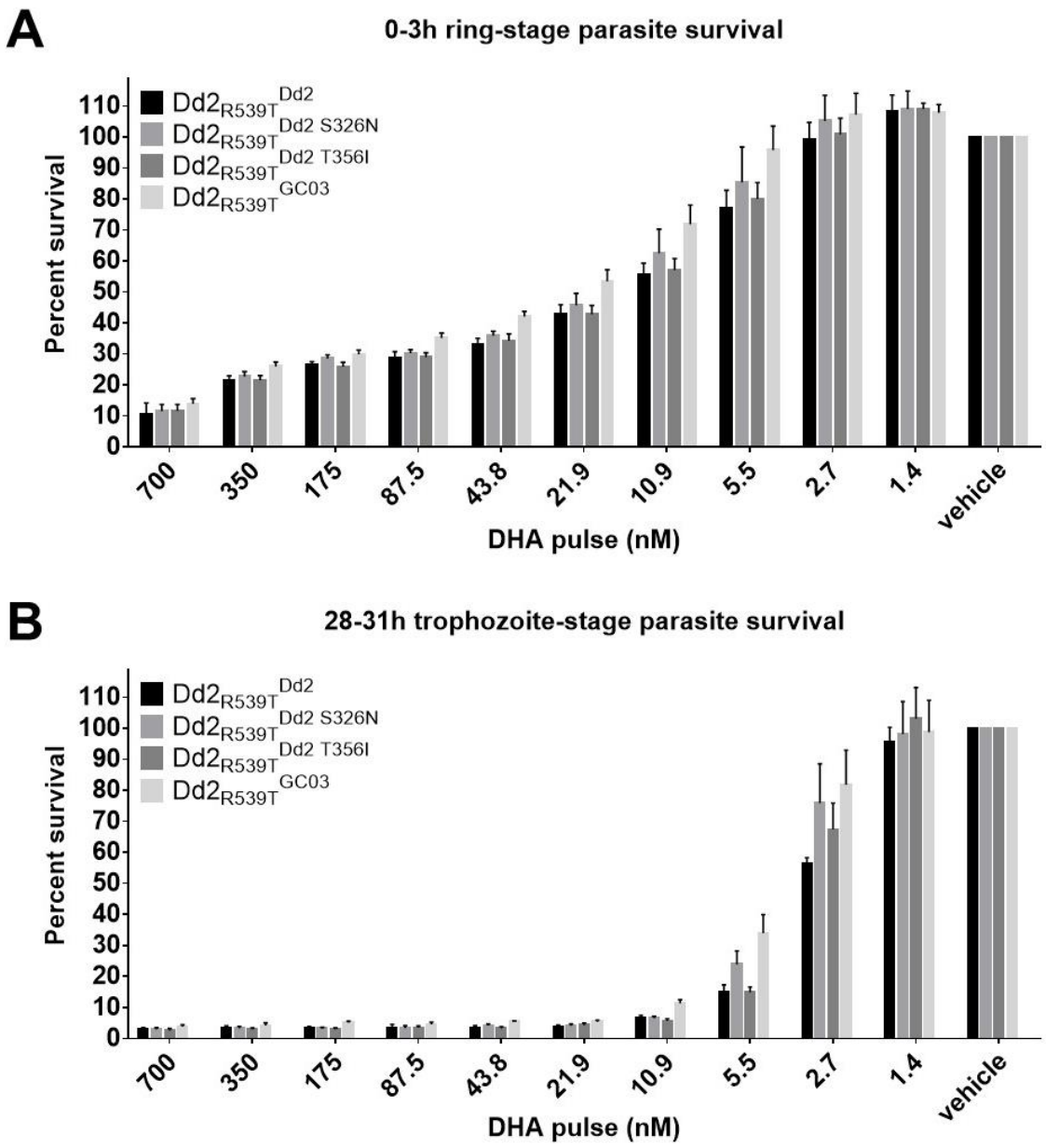

Figure 4.5. Dihydroartemisinin (DHA) survival of *k13*-mutant, *pfcrt*-modified lines. Tightly synchronized parasites at the (**A**) early ring (0-3 hours post-invasion, hpi) or (**B**) mid-trophozoite (28-31 hpi) developmental stage were exposed to a three-hour pulse of DHA at the indicated concentrations. Parasite viability was determined by flow cytometry at 72 hpi. Bar graphs correspond to the mean ± SEM percentage DHA survival, equivalent to the parasitemia of DHA-treated parasites divided by the parasitemia of vehicle control (DMSO)-treated parasites. Data represent three independent experiments, conducted in duplicate.

discernible effect on parasite survival for any concentration examined. In contrast, in trophozoite-stage DHA survival assays (**Figure 4.5*B***), significant differences in parasite survival were observed at the sub-physiologic concentration of 5.5 nM DHA. Specifically, parasites encoding wild-type (GC03) PfCRT exhibited significantly increased protection from DHA toxicity as compared to parasites encoding either Dd2 or Dd2 T356I PfCRT (P=0.004 and P=0.02, respectively, as determined by ANOVA with Sidak's post-hoc comparison). Interestingly, PfCRT Dd2 S326N was associated with increased parasite survival as compared to the Dd2 haplotype, a difference that was significant at 2.7 nM DHA (P=0.005 by ANOVA with Sidak's post-hoc comparison). We note that, compared to ring-stage parasites, all parasites at this stage were considerably more susceptible to DHA exposure (e.g. compare parasite survival for 700 nM DHA in **Figure 4.5*A*** and for 5.5–10.9 nM DHA in **Figure 4.5*B***, which show comparable survival rates). This can be attributed to the higher levels of activating heme that results from increased Hb catabolism in trophozoites. Additional experiments are underway to explore the impact of the GB4 PfCRT isoform on parasite DHA survival.

These findings contribute to our presently incomplete understanding of ART action and the possible involvement of PfCRT, particularly during the parasite trophozoite stage. An aspect of ART toxicity to *Plasmodium* parasites is thought to involve the induction of oxidative stress, as suggested by previous real-time studies of parasite glutathione (GSH)-dependent redox state.[363] Given the prospect that GSH is potentially one of the substrates of PfCRT,[209,364] it is plausible that variant forms of PfCRT may help the parasite avert oxidative damage, perhaps through PfCRT-mediated transport of GSH into the parasite DV, where GSH can degrade toxic

heme.[59,154] Whether through this or a GSH-independent mechanism, PfCRT variants can influence parasite disposition of free heme (see **Chapter 3**), whose putative activation of ART activator is thought to account for >65% of the activity of ARTs during the trophozoite stage.[100,157]

The trophozoite stage-specific findings that Dd2 S326N and Dd2 T356I PfCRT conferred either increased or no change in parasite DHA survival as compared to Dd2 PfCRT (see **Figure 4.5*B***) may appear counterintuitive in light of the recent association of mutations N326S and I356T with ART-resistant founder populations.[159] An explanation for these results is that, rather than contributing directly to protection from ACT toxicity, the presence of PfCRT mutations N326S and/or I356T provides a parasite genetic background that is conducive to the acquisition of additional ART resistance-conferring mutations and that aids in minimizing associated fitness costs.

Survival of *k13*-mutant, *pfcrt*-modified lines exposed to PPQ

Similar to ART resistance, IC_{50}-based drug susceptibility studies appear insufficient to reveal parasite resistance to the first-line ACT partner drug PPQ. This is apparent from *ex vivo* analyses of recrudescent parasites derived from DHA-PPQ treatment failures, which show a wide range of PPQ IC_{50} values that overlap with IC_{50} values of non-resistant isolates.[139] The molecular basis of PPQ resistance is likely multigenic and is clinically paramount in the context of DHA-PPQ resistance that is spreading throughout Cambodia as well as surrounding regions in Southeast Asia.[365] Recent studies of PPQ-resistant parasites have highlighted the effectiveness of *in vitro* PPQ-based parasite survival assays in uncovering resistance phenotypes that correlate with *in vivo* parasite recrudescence. In these assays, parasites are subjected to 200

nM PPQ for 48 h. The basis for a much longer duration of drug exposure as compared to DHA-based assays is the relatively more prolonged half-life of PPQ in the blood following treatment.[139,366] Parasite survival is then assessed at the 72 h endpoint.

Similar to our DHA-based survival assays, we subjected *pfcrt*-modified $Dd2_{R539T}$ parasites to serial dilutions of PPQ. To probe for stage-specific effects, we first treated parasites with PPQ at either the early-ring stage (t=0–3 hours post-invasion, hpi) or mid-trophozoite stage (t=28–31 hpi). Parasites were incubated with PPQ through the 48 hpi timepoint, and parasite viability was assessed by flow cytometry at 72 h. Results for PPQ survival assays initiated during the early ring stage (**Figure 4.6*A***) showed comparable degrees of sensitivity of *pfcrt*-modified parasites to concentrations substantially lower than 200 nM PPQ, the physiologic dose used to detect clinically relevant PPQ resistance. Intriguingly, for PPQ survival assays initiated during the mid-trophozoite stage (**Figure 4.6*B***), differential, *pfcrt* allele-specific PPQ responses were especially marked for parasites treated with 12.5 nM PPQ. As compared to isogenic parasites encoding Dd2 PfCRT, parasites encoding Dd2 S326N, Dd2 T356I, and GC03 (wild-type) PfCRT haplotypes showed significant differences in parasite survival (P=0.003, P=0.04, and P<0.0001, respectively, as determined by ANOVA and Sidak's post-hoc test). Of note, GC03 PfCRT did not protect against PPQ action, whereas PPQ mutant PfCRT haplotypes (especially Dd2 T356I; see **Figure 4.6*B***) provided protection. Additional experiments are underway to explore the impact of the GB4 PfCRT isoform on parasite PPQ survival.

The apparent modulatory capacity of PfCRT residue 356 that we observed in our trophozoite-stage PPQ survival assays (see **Figure 4.6*B***) adds to a growing body of evidence that certain PfCRT mutations can alter the susceptibility of parasites to

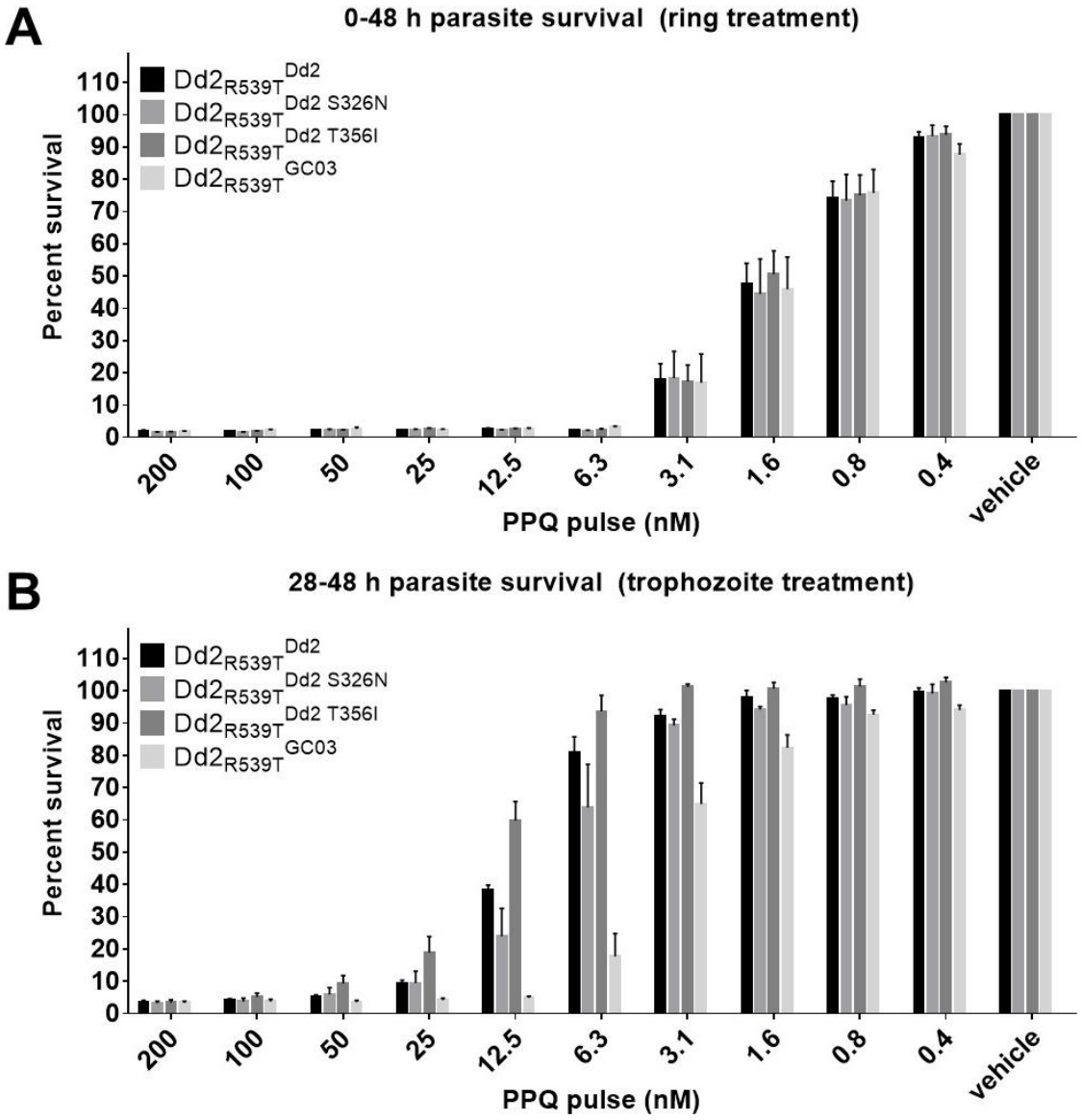

Figure 4.6. Piperaquine (PPQ) survival of *k13*-mutant, *pfcrt*-modified lines. Tightly synchronized parasites in the (**A**) early ring (0-3 hours post-invasion, hpi) or (**B**) mid-trophozoite (28-31 hpi) developmental stage were incubated at the indicated doses of PPQ until 48 hpi, after which drug was washed out. Parasite viability was determined by flow cytometry at 72 hpi. Bar graphs correspond to the mean ± SEM percentage PPQ survival, equivalent to the parasitemia of PPQ-treated parasites divided by the parasitemia of vehicle control (5% lactic acid)-treated parasites. Data represent three independent experiments, conducted in duplicate.

PPQ.[137,217,218] For example, Pellau *et al.* recently demonstrated that the novel French Guianese PfCRT mutation C350R conferred decreased parasite susceptibility to PPQ.[137] Interestingly, based on bioinformatic analysis, residues 326-356 are predicted to span PfCRT residues present within the ninth transmembrane domain of PfCRT. This domain is thought to have roles in substrate binding and/or translocation.[233] Of note is a recent report by Duru *et al.* of at least two distinct mutations spanning this region of PfCRT among PPQ-resistant clinical isolates from Southeast Asia.[139] Collectively, these observations suggest that PfCRT might be one factor involved in PPQ resistance, with probable contributions from additional genetic loci. Furthermore, they emphasize the need to swiftly delineate molecular markers that will aid in containing the spread of PPQ resistance in Southeast Asia.

In vitro growth of *pfcrt*-modified lines

Plasmodium fitness is a multifaceted property that reflects parasites' reproductive success over multiple rounds of infection. A critical aspect of and proxy for parasite fitness is the growth of pathogenic asexual blood-stage parasites, which may reach a biomass as high as 10^{12} parasites per infected individual.[239,367] Previous analyses of isogenic parasites expressing variant *pfcrt* alleles have shed light on their ability to influence parasite growth rates and have aided in inferring how they spread globally.[242,243] Herein, we used an established[242] flow cytometery-based co-culture assay that compares growth of GFP-negative (GFP^-) *pfcrt*-modified test lines with that of a GFP-positive (GFP^+) reporter line. The GFP^- proportion of co-culture was regularly determined for a period of 10 parasite generations and used to derive the per-generation selection coefficient (s) associated with a given *pfcrt* allele. This

parameter was used as a reflection of asexual blood-stage fitness, with s=0, s>0, and s<0 indicating fitness equal, greater than, and less than that of $Dd2^{GC03}$ parasites (i.e. parasites encoding wild-type alleles at both the *pfcrt* and *k13* loci).

Our results revealed key differences in the fitness costs associated with mutant *pfcrt* alleles (**Figure 4.7**; **Table 4.5**). In general, among *pfcrt*-matched lines, parasites harboring mutant K13 R539T (i.e. $Dd2_{R539T}$) showed a more pronounced, statistically significant growth defect as compared to parasites with wild-type K13 (i.e. Dd2), with the exception of lines encoding either GB4 or Dd2 T356I PfCRT (no significant difference in Dd2 versus $Dd2_{R539T}$ backgrounds; **Figure 4.7**; **Table 4.5**). In both the Dd2 and $Dd2_{R539T}$ genetic backgrounds, Dd2 and Dd2 T356I PfCRT isoforms conferred a notable fitness cost (range of mean s values: -0.16 to -0.24; **Figure 4.7**; **Table 4.5**). Interestingly, PfCRT isoforms Dd2 S326N and GB4, predominant in Africa (see **Figure 4.2**), were associated with a less severe fitness cost (range of mean s values: -0.09 to -0.04; **Table 4.5**). Earlier studies with isogenic, *pfcrt*-modified parasites support the notion that Dd2 PfCRT confers a substantial fitness cost to parasites, as compared with other variant haplotypes.[243] Our present observations hint at the prospect that parasite populations expressing a markedly unfit PfCRT haplotype are able to persist in Southeast Asia, but not Africa. These differences could be attributed to one or more of the following factors: (1) the specific drug regimens used, their pharmacokinetic disposition in local populations, and the selective forces that these drugs exert on the parasite *pfcrt* locus; (2) *pfcrt* allele-specific differences in parasite transmission to the mosquito vector; (3) a higher level of transmission in Africa than in Southeast Asia, which translates to increased immune protection as well as a higher degree of allelic competition, facilitating the attrition of unfit alleles.

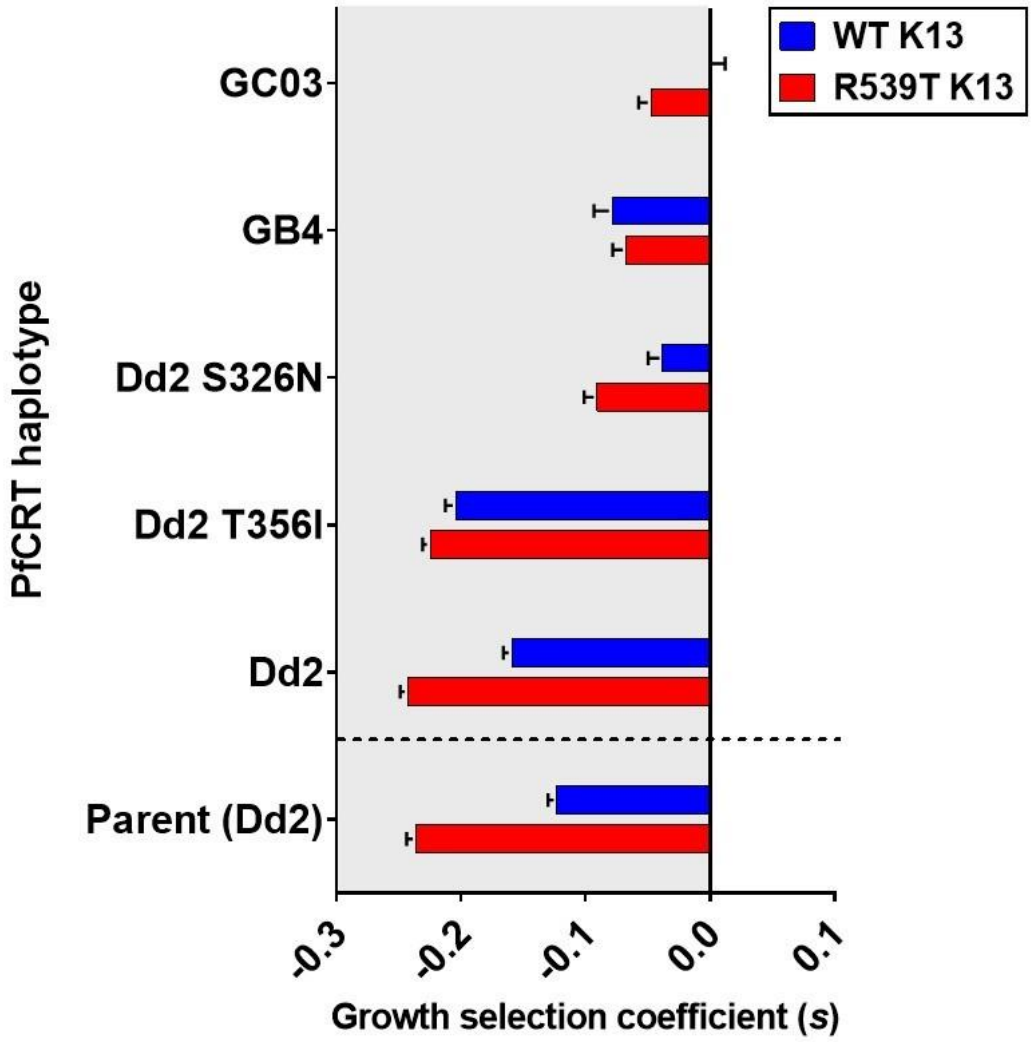

Figure 4.7. *In vitro* growth characteristics of *pfcrt*-modified and reference parasite lines. Briefly, 1:1 co-cultures consisting of a GFP^{-} test strain and a GFP^{+} reporter strain were initiated at day 0 and monitored by flow cytometry for 10 generations, as described in **Methods**. The per-generation selection coefficient (*s*) for each test strain reflects parasite growth as compared to $Dd2^{GC03}$ parasites, which encode the wild-type (GC03) *pfcrt* allele (i.e. *s*=0 for $Dd2^{GC03}$). Bar graphs correspond to mean ± SEM *s* values (detailed in **Table 4.5**), as determined in three independent assays, conducted in duplicate.

Table 4.5. *In vitro* growth selection coefficients of *pfcrt*-modified and reference parasite lines.[a]

	Dd2 parent	**Dd2 recombinants**				
pfcrt allele	**Dd2**	**Dd2**	**Dd2 S326N**	**Dd2 T356I**	**GB4**	**GC03**
s	-0.12 ± 0.007	-0.16 ± 0.007	-0.04 ± 0.011	-0.20 ± 0.009	-0.08 ± 0.014	0.00 ± 0.012
P_1	**<0.0001**	**<0.0001**	**0.03**	**<0.0001**	**<0.0001**	–
	$Dd2_{R539T}$ parent	**$Dd2_{R539T}$ recombinants**				
pfcrt allele	**Dd2**	**Dd2**	**Dd2 S326N**	**Dd2 T356I**	**GB4**	**GC03**
s	-0.24 ± 0.007	-0.24 ± 0.006	-0.09 ± 0.010	-0.22 ± 0.006	-0.07 ± 0.011	-0.05 ± 0.010
P_1	**<0.0001**	**<0.0001**	**0.01**	**<0.0001**	0.54	–
P_2	**<0.0001**	**<0.0001**	**0.002**	0.57	0.96	**<0.0001**

[a]Growth selection coefficients (*s*) of recombinant and parental parasite lines were determined as detailed in **Methods** and normalized against the $Dd2^{GC03}$ line, which encodes the wild-type (GC03) *pfcrt* allele. $s<0$ and $s>0$ indicate growth inferior or superior to that of the $Dd2^{GC03}$ line, respectively. Listed are mean *s* ± SEM values, which encompass three independent experiments performed in duplicate ($n=6$ total replicates per line). Statistical comparisons were done using two-way ANOVA with Sidak's post-hoc test. P_1 indicates the statistical significance for *pfcrt*-variant lines as compared to otherwise isogenic parasites encoding GC03 *pfcrt* (either $Dd2^{GC03}$ or $Dd2_{R539T}^{GC03}$). P_2 indicates the statistical significance observed between *pfcrt*-matched lines in the Dd2 (wild-type K13) versus $Dd2_{R539T}$ (mutant K13) genetic backgrounds. *P* values <0.05 are indicated in **bold** and shaded in gray.

Discussion

In this work, we studied the major PfCRT haplotypes in Africa and Southeast Asia (GB4 and Dd2, respectively) as a means of genetically dissecting the widely referred to "African/Asian" Dd2 PfCRT variant. Focusing on PfCRT mutations beyond the predominant and well-characterized molecular marker K76T, we investigated the pleiotropic roles of PfCRT amino acid positions 326 and 356, which define the majority of variant PfCRT haplotypes circulating in either Africa or Asia.

Our findings illuminate the capacity of PfCRT mutations to alter parasite responses to distinct classes of antimalarials. Among these classes of compounds are several first-line ACTs, whose efficacy is compromised in select geographical regions. The observation that PfCRT mutations can modulate the cytocidal activity of DHA, albeit in a stage-specific manner and only at low nanomolar concentrations, should serve as a stimulus for further investigation of other candidate genetic determinants of ART resistance (e.g. *fd*, *pfmdr2*). It is conceivable that these may amplify *pfcrt*-mediated reductions in parasite susceptibility.

In light of our finding of PfCRT-mediated modulation of ART susceptibility, our data indicates that varying selective forces may be inherent to a single ACT formulation; for example, in our survival assays, DHA and PPQ selected for K76 and K76T, respectively. Likewise, opposing selective forces may be exerted by the long-lived partner drugs comprising distinct ACT formulations. Consistent with this, we documented the ability of PfCRT mutations to modulate parasite AQ and PPQ susceptibility in *pfcrt* allele-specific ways. Our results support the practice of antimalarial regimen cycling and active monitoring of *pfcrt* genotypes. Of note, the finding that PfCRT Dd2 T356I can decrease parasite susceptibility to PPQ calls

attention to the mounting problem of resistance to this drug, and suggests that characterization of PfCRT mutations emerging in settings with PPQ resistance should be prioritized. Additional experiments, currently underway, will reveal whether the presence of PfCRT I356T in the GB4 haplotype likewise increases parasite PPQ resistance.

Our work adds to a growing collection of studies of drug transport, drug susceptibility of isogenic parasite strains, and *pfcrt* allele prevalence in the field, which collectively support the notion of PfCRT as a pleiomorphic mediator of parasite multidrug resistance.[120,137,208,213,220] As malaria control efforts intensify in the coming years, their success will depend, in part, on the precise definition and monitoring of markers of parasite multidrug resistance.

CHAPTER 5: CONCLUSIONS & FUTURE DIRECTIONS

DISSECTING THE POLYMORPHIC *PFCRT* GENE, ONE (OR MORE THAN ONE) SNP AT A TIME

In 2012, Straimer *et al.* established a zinc finger nuclease (ZFN)-based gene editing system tailored to the parasite *P. falciparum chloroquine resistance transporter* (*pfcrt*) gene.[295] This system has served as an incredibly powerful tool for ascertaining the effects of *pfcrt* single nucleotide polymorphisms (SNPs) on the biology and drug responses of pathogenic asexual blood-stage *P. falciparum* parasites. The ZFN strategy promotes targeted incorporation of mutations through the introduction of a double-stranded DNA (dsDNA) break at a defined site in the parasite genome.[295] Mutations are subsequently captured as parasites repair the dsDNA break through non-crossover-based pathways.[353] In contrast, earlier *pfcrt* allelic exchange strategies relied on infrequent, stochastic crossover events that facilitated capture of entire episomes and led to concatamerization.[120,217,243] These methods were associated with lower gene editing efficiency and required extended periods of drug selection.

Great strides have been made in the four years since the establishment of a ZFN-based system for *pfcrt* genetic editing. Once a drawn-out process that took months and, in some cases, more than one year, parasite genetic editing can now be performed over the course of several weeks. Editing efficiencies approaching 100% were observed for a number of the *pfcrt*-modified recombinant lines described in this dissertation. At present, a large compendium of recombinant parasites is at our disposal, encompassing various partial and full-length *pfcrt* alleles expressed in one or more distinct genetic backgrounds. To date, at least 55 recombinant, *pfcrt*-modified lines have been generated and cloned (A. Lee and S. Dhingra, personal

communication), 35 of which are characterized in **Chapters 2-4** of this dissertation.

Of note, success of genetic editing was partly dependent on the genetic background of parasites. For example, in our initial attempt to engineer a panel of combinatorial PfCRT haplotypes based on the Ecuadorian Ecu1110 variant (see **Chapter 2**), the GC03 (CQ-sensitive) genetic background was not receptive to allelic exchange with certain haplotypes, such as Ecu_A (i.e. K76T; wild-type at all other residues). It is likely that some mutant *pfcrt* alleles are associated with physiological constraints that render them incompatible with particular genetic backgrounds. Such incompatibilities have been observed in previous allelic exchange experiments and may be attributable to complex interactions between *pfcrt* and secondary genetic loci, such as the *P. falciparum multidrug resistance 1* (*pfmdr1*) gene.[217] Consistent with this, recent transcriptome comparisons of *P. falciparum* lines bearing different variants and/or levels of *pfcrt* and *pfmdr1* revealed tight associations in the levels of transcripts expressed by these genes.[368]

Deployment of parasite *pfcrt* genetic editing approaches in future investigations will be key to delineating the putative roles of *pfcrt* mutations in driving resistance to our first-line antimalarials. A notable example is PPQ resistance, whose spread in Southeast Asia is coinciding with the rise of novel mutations in *pfcrt*.[139] Additionally, as chloroquine (CQ) remains a first-line drug for the treatment of infection with *P. vivax,* elucidation of the presently unclear mechanisms of *P. vivax* CQ resistance (CQR) is warranted. Application of the ZFN-based system to probe the capacity of *P. vivax chloroquine resistance transporter* (*pvcrt*) gene mutations to confer CQR is presently underway in our laboratory (D. Fidock, personal communication).

Site-specific endonuclease-based genetic editing systems, including ZFNs and the more recently developed CRISPR-Cas9 system, have revolutionized our ability to manipulate multiple parasite genetic loci. This will allow for discernment of potential epistatic interactions between *pfcrt* and known (e.g. *pfmdr1*) as well as candidate (e.g. *ferredoxin, fd*; *P. falciparum multidrug resistance 2*, *pfmdr2*) genetic loci implicated in modulating parasite susceptibility to various antimalarial compounds.[127,159] As *Plasmodium* parasites continue to evolve genetically complex resistance mechanisms, the efficacy of present and future antimalarials will hinge upon our ability to identify and characterize candidate drug resistance mutations. This will require leveraging data from large-scale genome-wide association studies (GWAS) with targeted dissections of gene-specific impacts on parasite drug resistance and fitness.

DISTINCT ROLES OF PFCRT MUTATIONS IN *P. FALCIPARUM* DRUG RESISTANCE AND FITNESS

The investigations described herein provide critical insights into the roles of PfCRT mutations in the fine balance between drug resistance and fitness maintained by *P. falciparum* parasites during their asexual blood stage (**Table 5.1**). Importantly, our results shed light on distinct contributions of PfCRT mutations beyond the well-characterized CQR-associated mutation K76T. A popular dogma in earlier descriptions of PfCRT mutations has been that PfCRT K76T serves as the central mediator of CQR, with additional mutations playing compensatory roles (i.e. offsetting associated fitness costs).[170,369,370] However, several lines of evidence counter this dogma.

Table 5.1. Summary of effects of PfCRT mutations on drug resistance and fitness of asexual blood-stage *P. falciparum*.[a]

PfCRT mutation	Parent haplotype	Background	CQR	Fitness	Additional notes
C72S	7G8	7G8	↑	↑	AQR^{CQR}
N75D	Cam734	GC03	↑	↑	↑ CQR^{VPR}; ↑ AQR
K76T	Ecu1110	7G8	↑ > ↓	↓ >> ↑	↑ CQR^{VPR}; AQR^{CQR}; ↓ ASR
A144F	Cam734	GC03	↑	↑	↑ AQR; ↑ QNR
L148I	Cam734	GC03	↑	↑	↑ CQR^{VPR}; ↑ AQR; ↓ PPQR
I194T	Cam734	GC03	–	↑	–
A220S	Ecu1110	7G8	↑ > ↓	↓ or ↑	AQR^{CQR}
N326D	Ecu1110	7G8	↑	↓	↑ CQR^{VPR}; AQR^{CQR}; ↑ AQR
N326S	Dd2	Dd2	–	↓	↑ AQR
T333S	Cam734	GC03	↑	↑	↑ AQR
I356L	Ecu1110	7G8	↑ >> ↓	↑ >> ↓	AQR^{CQR}
I356T	Dd2	Dd2	–	–	↓ PPQR

[a]This table summarizes results presented in **Chapters 2-4** of this dissertation. Future investigations, in mutational contexts and/or genetic backgrounds not examined herein, may ascribe additional phenotypes to PfCRT mutations. For each PfCRT mutation, the parent haplotype context and genetic background in which it was studied are indicated. Mutational composition of PfCRT haplotypes is detailed in **Table 1.6**. ↑ and ↓ represent increases and decreases, respectively. The degree to which phenotypic changes were noted is indicated by > (i.e. more than) and >> (*i.e.* substantially more than), with – indicating absence of evidence. Resistance encompasses results from either cytostatic (IC_{50}-based) or cytocidal (parasite survival-based) assays and indicates relative changes in resistance, which don't necessarily correspond to clinical resistance. Fitness reflects parasite growth *in vitro*, in the absence of drug. CQR, chloroquine resistance; AQR, amodiaquine resistance; AQR^{CQR}, AQR–CQR cross-resistance; CQR^{VPR} verapamil reversibility (VPR) of CQR; ASR, artesunate resistance; QNR, quinine resistance; PPQR, piperaquine resistance.

First, consistent with findings gleaned from heterologous drug transport studies,[208,312] we observed that PfCRT K76T is insufficient to confer CQR in asexual blood-stage parasites, the biological setting in which CQ is chiefly active against *Plasmodium.* In fact, certain non-K76T mutations (e.g. N326D) could confer statistically significant increases in parasite resistance to the active metabolite of CQ, monodesethyl-CQ (md-CQ). Of note, mutation of PfCRT 326 (e.g. N326D, N326S) was associated with increased parasite drug resistance to quinoline-type drugs and consistently had a deleterious impact on asexual blood-stage parasite fitness (see **Table 5.1**), indicating that this non-K76T mutation is not compensatory. This is consistent with the recent report of reduced CQR and increased proliferation of recombinant parasites that initially encoded PH1 PfCRT (K76, A144T, L160Y, N326D) but lost the N326D mutation during long-term culture.[243] In the genetic dissection of Cam734 *pfcrt* (see **Chapter 3**), of the five novel mutations examined, only PfCRT I194T was associated with a purely compensatory role (i.e. improved parasite growth), whereas the remaining four mutations improved parasite growth and directly contributed to parasite CQR (see **Table 5.1**). We also noted an exception to the rule of thumb that parasite CQR requires K76T in the presence of ≥3 additional mutations; removal of the A144F mutation from Cam734 PfCRT (i.e. Cam734 F144A) yielded CQ-sensitive parasites that nevertheless harbored K76T and seven additional PfCRT mutations.

Our results indicate that the key CQR-associated mutation K76T confers CQR only in certain mutational contexts, with direct contributions from other mutations, some of which also offset fitness costs. How the various full-length and partial *pfcrt* alleles decribed herein impact parasite fitness is presently unclear, in large part due to the enigmatic biological function of PfCRT. New perspectives in this regard will be

facilitated through functional characterizations of the recombinant lines harboring these alleles, using metabolomics and other approaches.[232] While peak expression of mutant PfCRT occurs in hemozoin (Hz)-rich trophozoites, PfCRT is also found within rings and schizonts and, when mutated, is able to confer CQR at these stages.[337] Spinning disk confocal microscopy-based methods have been established that could evaluate whether any of the PfCRT isoforms studied herein have an impact on the various stages of the parasite blood-stage lifecycle, at baseline or in the presence of CQ.[337] Interestingly, earlier work, in which a mutant (7G8) *pfcrt* allele was integrated into the genome of the rodent malaria species *P. berghei*, documented the ability of mutant PfCRT to enhance parasite infectivity to mosquitos in the presence of CQ.[268] Since transmission is an important element of parasite fitness, another critical question worth exploring is whether the various *pfcrt* alleles studied herein have discernable impacts on transmission of gametocytes to the mosquito vector.

We note that, with the exception of parasite survival assays performed in **Chapter 4**, the 50% growth-inhibitory concentration (IC_{50}) to a given drug was largely used as a metric of parasite resistance throughout our studies. In focusing on parasite growth inhibition in our analyses, we characterized the cytostatic effects of antimalarial drugs. While cytostatic, IC_{50}-based assays are routinely performed to profile parasite drug response, cytocidal, 50% lethal dose (LD_{50})-based assays more exclusively reveal drug concentrations required to kill parasites. It is known that (1) PfCRT mediates both cytostatic and cytocidal CQR; (2) Cytocidal CQ concentrations can be up to 100× higher than concentrations required for a cytostatic effect; and (3) The fold-increase in CQR between a resistant and susceptible line is decreased for cytocidal resistance as compared with cytostatic resistance.[371] These features were

recapitulated in a preliminary analysis of the cytocidal effects of CQ on a subset of our isogenic, *pfcrt*-modified lines from the Ecu1110 *pfcrt* genetic dissection study (see **Chapter 2**). Our results collectively underscore the utility of relative drug resistance relationships in defining the impacts of *pfcrt* SNPs. Future work will be needed to delineate the complex pharmacology of these drugs and to define how exactly *in vitro* metrics of resistance reflect what occurs *in vivo*.

Apart from CQ, a number of other clinically employed antimalarials included in our analysis were associated with varied parasite responses attributable to *pfcrt* SNPs (see **Table 5.1**). These included monodesethyl-amodiaquine (md-AQ; the active metabolite of AQ), quinine (QN), piperaquine (PPQ), lumefantrine (LUM), and the artemisinin (ART) compound artesunate (AS). As was the case for CQ, differences in parasite susceptibilities conferred by these mutations were often mutational milieu-dependent. With reduced deployment of CQ due to widespread CQR, these and future antimalarial compounds will have an increased role in dictating which *pfcrt* genotypes persist and what *pfcrt* mutations may arise in a particular geographical region. The identification of molecular markers reflecting the ever-changing landscape of global antimalarials will necessitate continued monitoring of the full-length sequence of the parasite *pfcrt* gene, complemented with whole-genome surveillance.

INSIGHTS INTO PFCRT FUNCTION AND DRUG RESISTANCE MECHANISMS

Our understanding of the molecular basis of CQR was greatly propelled in 2000 by Fidock *et al.*, who identified PfCRT as a central mediator of resistance.[186] Ensuing

studies have provided important insights into the impacts of PfCRT mutations on parasite CQ responses, CQ accumulation, drug transport, and digestive vacuole (DV) physiology, although many questions still remain.[188] The results presented in **Chapters 2-4** add to this growing body of knowledge.

An important aspect of CQ action is interference with parasite heme detoxification, causing disrupted Hz formation, with a concomitant increase in heme.[55] Prior to our study of the heme disposition in isogenic, *pfcrt*-modified parasites (see **Chapter 3**), the capacity of PfCRT mutations to alter parasite heme disposition had not been explored. For lines encoding both CQ-sensitive and CQ-resistant variants of PfCRT, we observed a clear relationship between rise in free heme concentration and extent of parasite growth inhibition. Interestingly, mutant PfCRT-encoding lines showed higher levels of undigested hemoglobin as compared with isogenic parasites encoding wildtype PfCRT. In addition to CQ, a number of clinically important drugs (e.g. AQ, LUM, QN, AS) are also known to perturb parasite heme detoxification pathways.[55] Their inclusion in future characterizations of *pfcrt*-modified lines may uncover mechanistic bases that underlie the various degrees of potency of these drugs against both CQ-sensitive and CQ-resistant parasites.

Intriguingly, in our analysis of recombinant lines bearing only a single PfCRT mutation, we found that the PfCRT K76T mutation confers hypersensitivity to CQ and, even more notably, to its active metabolite, md-CQ. Induction of a similar CQ hypersensitivity by PfCRT mutations C101F and L272F was recently described by Pulcini *et al.*[196] Lone expression of K76T may increase the potency of CQ through changes in the physiology of the DV, which may in turn affect CQ partitioning and its interactions with Hz. An additional mechanism may be the impact of this mutation

on PfCRT native function in the absence of compensatory mutations, rendering parasites hypersensitive to exogenous sources of stress. DV volume and pH studies, such as those applied in studies described in **Chapter 3**, would clarify if lone expression of K76T imparts significant alterations to DV physiology.

Comparison of parasite CQ IC_{50} values (see **Chapters 2-4**) with published PfCRT CQ transport activities, assessed in heterologous expression systems, highlights important correlations between these two metrics. In all studies, K76T was insufficient for CQR, and distinct contributions to CQR were noted for non-K76T mutations, such as N326D.[208,312] Of the three-SNP PfCRT isoforms characterized in drug transport studies in *Xenopus laevis* oocytes, Ecu_{ACD} conferred the highest level of CQR, consistent with our data;[312] however, the increase in CQ transport associated with the Ecu_{ACD}→Ecu_{ABCD} trajectory was substantial (>2-fold) in our studies, but very subtle in the drug transport studies. A notable disparity concerns PfCRT C72S, the single distinction between Ecu1110 and 7G8 PfCRT, which consistently reduced drug transport rates, yet increased CQR in our parasite-based studies (see **Figure 2.2**).[208,312]

CQ interference with PfCRT function is suggested by the earlier observation of CQ–PfCRT binding.[193] We believe that future investigations should leverage phenotyping of *pfcrt*-modified parasites with investigation of PfCRT binding to and transport of drug – not just CQ, but also its active metabolite, md-CQ. As seen in **Chapter 2**, md-CQ played a more marked role than CQ in uncovering certain parasite CQ responses and in dictating parasite traversal through *pfcrt* mutational landscapes (see **Figure 2.7**). In the absence of a crystal structure of PfCRT, a combined genetic-chemical dissection would also clarify roles of PfCRT mutations in drug binding and conferral of parasite CQR. Akin to analysis performed by Lakshmanan *et al.*, this

would entail subjecting a panel of *pfcrt*-modified parasite lines described in our studies to a series of CQ-like compounds with altered chemical groups.[126] Insights from such a study would also provide insights about *pfcrt* mutational changes that could compromise the efficacy of novel quinoline-like compounds.

PfCRT is a drug/metabolite transporter (DMT) that is thought to encode 10 transmembrane domains.[233] The majority of the mutations studied herein are predicted to occur within these domains, which are collectively implicated in binding, translocation, and discrimination between substrates.[233] Interestingly, PfCRT transmembrane domains 3 and 8, the predicted locations of PfCRT amino acids 144 and 326, are associated with substrate specificity. In our studies, mutations N326D and N326S always had a deleterious impact on parasite growth, raising the possibility that they impair the transport of a native substrate. Interestingly, the mutation A144F enhanced parasite growth in the context of the mutant Cam734 PfCRT isoform, which was associated with enhanced energy utilization as compared to the less fit Dd2 isoform (see **Chapter 3**). In addition to challenging the dogma that PfCRT variants confer a parasite fitness cost-associated Hb degradation defect, our results suggest that future metabolomic comparisons of parasites encoding various PfCRT isoforms should include metabolites beyond peptides. It is tempting to speculate that the Cam734 PfCRT isoform may have evolved mutations that, together, confer a moderate degree of CQ transport and simultaneously accentuate the transport of one or more vital endogenous substrates. We also note that the threonine of PfCRT I194T falls within a putative helix packing motif (GxxxxT) that may be important for PfCRT homodimerization.[233] How the various amino acid substitutions studied herein may impact the post-translational modifications, stability, and substrate recognition of

PfCRT should be explored in future work.

In a recent heterologous expression study of PfCRT transport performed in *E. coli*, Juge *et al.* reported the ability of PfCRT isoforms to mobilize organic cations, basic amino acids, and polyamines in an electrochemical gradient-dependent manner.[209] As His-tagged *E. coli* YbeL proteins were required at the N and C termini of PfCRT in order to achieve expression, the direct implications of these studies in terms of elucidating native PfCRT function are unclear. Nevertheless, these results present the intriguing possibility of PfCRT as a polyspecific substrate/multidrug resistance transporter, with transport capacities that are refashioned depending on its mutational composition. This is supported by previous reports that have either demonstrated or suggested roles for PfCRT in the transport of ions, peptides, and chemically distinct compounds.[200,201,211,220,232-234,238,372]

As efforts to elucidate PfCRT native function continue to be pursued, an important question emerges: Might PfCRT be a modulator of parasite redox state? Earlier studies have documented widespread oxidation of parasite proteins in response to CQ.[373] Of note, altering the redox state of parasites can affect their response to CQ; inducers of oxidative stress increase CQ susceptibility, and vice versa.[374,375] Patzewitz *et al.* have raised the possibility that PfCRT transports glutathione (GSH), which is involved in degrading toxic heme.[154] More recently, modulation of CQ-induced oxidative stress by *pfcrt* alleles was observed in preliminary studies using isogenic *pfcrt*-modified lines that encode sensors of GSH-specific redox state in the parasite cytosol (F. Mohring and K. Becker, personal communication). The possibility that PfCRT modulates redox state is further corroborated by a string of digestive vacuole (DV)-localized PfCRT amino acids that

show homology to redox-active Fur superfamily proteins, whose functions include redox sensing.[376,377]

Compared to quinoline resistance, the role of the *pfcrt* locus in conferring ART resistance is less clear. In **Chapter 4**, we have seen evidence that PfCRT isoforms can differentially protect parasites from the cytocidal action of dihydroartemisinin (DHA), the active metabolite of ART. Of note, this modulatory effect was only observed during the parasite trophozoite stage, when both PfCRT and the ART activator heme are highly abundant. An important aspect of ART action is interference with the parasite's GSH-dependent degradation of toxic heme.[378] We hypothesize that PfCRT mutations may affect this process, particularly during the trophozoite stage, when the role of *kelch13* (*k13*) mutations in conferring ART resistance is less marked. Particularly in Southeast Asia, *P. falciparum* parasites are equipped with multidrug resistance mechanisms that are already compromising their susceptibility to first-line ARTs and several ACT partner drugs. Efforts to prevent their spread are contingent upon our ability to define the multigenic basis of resistance, which includes complex and still undefined contributions from the *pfcrt* locus.

EVOLUTION OF *PFCRT* ALLELES

The analysis of various, geographically-distinct *pfcrt* alleles presented in **Chapters 2-4** lends itself to an overarching question: How did these alleles evolve? Microsatellite and *pfcrt* genotyping data suggest that CQR emerged in a few geographically separate foci – in South America, Asia (with subsequent spread to Africa), and Oceania.[249,350] In **Chapter 2**, we designed a combinatorially complete panel of *pfcrt* alleles, expressed in otherwise isogenic asexual blood-stage *P. falciparum* parasites, in order to explore

the mutational paths accessible to parasite drug resistance evolution. Our results revealed a significantly constrained adaptive landscape in the evolution of *pfcrt*-mediated CQR, providing a molecular basis for the infrequent occurrence of variant *pfcrt* alleles in the field, despite the long-standing use of CQ. Consistent with this, antimalarial drugs that have a non-*pfcrt* genetic basis of drug resistance (e.g. atovaquone, pyrimethamine) are known to yield resistant parasites with much higher frequencies.[24] This may be, in part, due to the fact that CQ and other quinoline-type compounds target heme, an immutable host factor.

In South America and Oceania, the mutant *pfcrt* allele 7G8 is at or near fixation.[24,256,257,320] In **Chapter 2**, we showed that the 7G8 allele conferred a significantly higher level of CQR and asexual blood-stage parasite fitness, as compared with Ecu1110 *pfcrt*. This data supports the evolutionary success of quadruple-SNP Ecu1110 *pfcrt* and, to a much higher extent, quintuple-SNP 7G8 *pfcrt*. These two alleles have been documented to co-occur in several independent geographical regions (e.g. parts of South America, Africa, and Southeast Asia), with 7G8 *pfcrt* dominating in each case.[259] Of note, our data highlighted the capacity of AQ to drive *pfcrt* evolution, consistent with the use of AQ in many of the regions where the Ecu1110 and 7G8 haplotypes have been observed.[259] Evidence for ongoing evolution of *pfcrt* in South America is supported by the recent emergence of an isoform which bears the mutation C350R in the background of 7G8 PfCRT and which completely abolishes CQR (see **Appendix B**).[137]

The three most common Asian PfCRT variants – GB4, Dd2, and Cam734 – are substantially more polymorphic (6-9 SNPs; see **Table 1.6**) than the variants observed in South America and Oceania. As a result, they were only subjected to partial genetic

dissections. Suggesting that *pfcrt* evolution is operating in Southeast Asia, Cam734 PfCRT presently represents about one-fifth of the circulating PfCRT variants in this region, whereas it had not been detected in earlier (2002) characterizations of the origins of PfCRT variants (see **Chapter 3** and **Appendix A**).[243,249,262] There is presently no evidence that partial *pfcrt* alleles bearing ≤3 SNPs can be sustained in the field setting. Extrapolating from our findings in **Chapter 2**, we thus postulate that the initial steps involved in the evolution of Cam734 (as well GB4 and Dd2 PfCRT) likely involved one or more major bursts of multiple mutations in a very short period of time and in a very limited number of parasites. The bottleneck exerted by drug pressure would have reduced competition with fitter, wild-type *pfcrt*-expressing parasites, allowing mutant parasites to expand.

In their report of the existence of Cam734 *pfcrt* among CQ-resistant parasite isolates in Cambodia, Durrand *et al.* also reported a related allele, Cam738 (equivalent to Cam734 F144A), which we found to confer parasite susceptibility to quinoline-type drugs and which imparted a significant fitness cost. Thus, Cam738 is a candidate mutational precursor of Cam734, and the A144F mutation that was acquired to yield the Cam734 allele may have been selected for by one or more quinoline-type compounds (e.g. CQ, AQ, or QN). The enhanced quinoline resistance and fitness phenotypes that we observed for Cam734 *pfcrt*, as compared with the Cam738 allele, correctly predict the virtual absence of Cam738 *pfcrt* in Southeast Asia (as assessed by accessing the recent MalariaGEN Pf3k database of *P. falciparum* whole-genome sequences).[159] The absence of a Cam734 *pfcrt*-associated fitness cost, an anomaly for a mutant *pfcrt* allele, calls for vigilance and careful characterization of drug regimens that may select for this allele and/or promote its further evolution.

It is possible that cytocidal-based assays (e.g. DHA and PPQ survival assays) will reveal Cam734 *pfcrt*-specific responses that were not apparent in our IC_{50}-based assays.

Previous analysis by Wootton *et al.* of the *pfcrt* coding region of CQ-resistant parasite isolates from Africa and Asia revealed a PfCRT haplotype consisting of 6-8 mutations with very similar flanking microsatellite haplotypes, suggesting a common origin for these CQ-resistant alleles.[249] These PfCRT mutations correspond to the GB4-to-Dd2 PfCRT mutational spectrum that we investigated in **Chapter 4**. Of note, African CQ-resistant isolates in the study of Wootton *et al.*, as well as another independent study, often exhibited the Dd2 T356I PfCRT haplotype (see **Table 1.6**).[186,249] However, in our studies (see **Chapter 4**), we found the 6-SNP GB4 and 7-SNP PfCRT S326N haplotypes to be the most common variants in Africa, suggestive of regional evolution. Significant directional selection of *pfcrt* alleles has also been seen in regions of Africa where CQ pressure was withdrawn, leading to the attrition of mutant *pfcrt*-expressing parasites and concomitant resurgence in the wild-type *pfcrt* allele, which now predominates in Africa.[332]

In contrast, despite the significant fitness cost associated with the Dd2 *pfcrt* allele that we have consistently observed *in vitro* (see **Chapter 3** and **Appendix A**), Dd2 *pfcrt* remains the most common allele in Southeast Asia. This may be due to a presently unclear drug selective pressure and may be further attributable to the lower degree of parasite transmission in Asia as compared with Africa. Interestingly, in a recent analysis of blood specimens collected from two African patients infected with *P. falciparum*, Gadalla *et al.* noted wild-type–mutant hybrid PfCRT haplotypes.[379] While this report did not address the biological significance of this finding, it did

suggest that intragenic recombination is in effect in the high-transmission setting of Africa. In addition to intragenic recombination and parasite clonality, factors that can influence the ability of parasites to evolve drug resistance include genetic changes at secondary loci that contribute to resistance and/or compensate for reduced fitness, gene amplification events, as well as population genetic-specific differences (e.g. immunity) that have an impact on parasite sequence diversity. Whole-genome sequencing approaches aid in discerning each of these factors, which are expected to differ substantially between Africa and Asia.[380,381]

While it has been suggested that Dd2 *pfcrt* was the ancestral precursor of variant alleles in Asia and Africa,[249] it is also possible that a less polymorphic precursor (e.g. 6-SNP variant GB4) occurred first, spread to both regions, and evolved into the Dd2 *pfcrt* allele in Southeast Asia in the presence of selective pressure. This would be consistent with our preliminary evidence that the GB4 *pfcrt* allele confers a level of parasite fitness more comparable to that of the fit, wild-type *pfcrt* allele than that of Dd2 *pfcrt* (see **Chapter 4**). A limitation of our study is that the genetic background of our *pfcrt*-modified lines, Dd2, is of Asian origin. Additional analysis in African-background parasites might reveal different phenotypes.

Are forward (i.e. wild-type to mutant) and reverse (i.e. mutant to wild-type) evolutionary processes distinct? A recent combinatorial study of a four-SNP *P. vivax dihydrofolate reductase* (*dhfr*) allelic variant, expressed in yeast, emphasized that they are not; upon encountering a fitness valley associated with an intermediate *dhfr* allele, organisms were no longer able to continue mutational trajectories leading to the wild-type allele, despite the absence of drug pressure and the fact that the wild-type allele represented a higher level of fitness.[349] Accordingly, in the absence of drug

pressure, restoration of drug susceptibility is more likely to occur via expansion of populations encoding the fitter, wild-type allele or through compensatory mutations at novel sites within the genome.[349] A secondary genetic locus that might have epistatic effects on *pfcrt* evolution is *pfmdr1*.[143,226] It would be interesting to explore whether certain *pfmdr1* mutations either block or facilitate progression of parasite *pfcrt* evolution. Our understanding of parasite adaptive landscapes would undoubtedly be broadened through genetic combinatorial experiments examining region-matched *pfcrt* and *pfmdr1* allelic combinations. The genetic tools for carrying out such analyses are now at our disposal.[143,295]

As the progression of organisms through adaptive landscapes is known to be intricately influenced by their drug environment,[245] additional genetic combinatorial experiments conducted in a wide range of drug concentrations as well as in the presence of drug combinations could provide additional insights into parasite *pfcrt* adaptive landscapes. A complementary experimental approach that should be employed in future studies is *in vitro* selection of drug resistance. Specifically, one or more *P. falciparum* isogenic lines encoding a *pfcrt* allele of interest would be subjected to drug pressure, and subsequent sequencing of resistant parasites would either recapitulate anticipated mutational trajectories or identify novel ones. We note that the ability to induce mutation of the *pfcrt* locus *in vitro* was previously demonstrated for the drug halofantrine (HF), which caused the K1 (CQ-resistant) parasite line to acquire three novel *pfcrt* mutations.[305]

As present first-line antimalarials show signs of reduced clinical efficacy and ultimately become replaced with new regimens, and as malaria control efforts escalate to include elimination, regional dynamics of *P. falciparum* infection will inevitably

undergo profound changes. These factors will reshape the adaptive landscapes accessible to parasites in their evolution of high-level drug resistance, requiring updated resistance markers and refined molecular rationales for new drug design. The use of *in vitro* approaches to dissect parasite adaptive landscapes may uncover new, accessible mutational paths and fitness valleys that could be exploited for these purposes.

THE RELEVANCE OF PFCRT MUTATIONS TO DRUG RESISTANCE SURVEILLANCE

Following the global rise and spread of *P. falciparum* resistance to CQ and its replacement drug regimen, sulfadoxine-pyrimethamine, the adoption of ART-based combination therapies (ACTs) ushered in an era of new drug selective forces, new parasite resistance mechanisms, and new molecular markers of resistance. Identification of resistance markers will be greatly facilitated by analysis of whole parasite genome sequences, complemented with *in vitro* genetic editing studies. This has already revealed *k13* as a key genetic mediator of ART resistance.[181] In addition to the ARTs, our present arsenal of antimalarial compounds includes a number of quinoline-type drugs and, in some regions, even CQ itself. Thus, in addition to defining novel genetic loci involved in mediating parasite drug resistance, careful assessment of *pfcrt* genotypes should be continued in both the laboratory and the field.

The most commonly employed ACT in Africa is artemether (ATM)-LUM. Analysis of recurrent infections following ATM-LUM treatment in Burkina Faso showed a preponderance of parasites encoding wild-type K76 PfCRT.[360] This finding

was recapitulated in a more recent randomized clinical trial in Uganda.[149] Of note, a 16% higher risk of recurrent malaria was documented in patients receiving ATM-LUM, as compared to the second ACT regimen AS-AQ, which selects for mutant PfCRT K76T.[149] In Burkina Faso, selection of K76 was also reported for the ACT regimen DHA-PPQ.[360] However, this is not supported by other reports from Africa, which did not observe a clear relationship between PfCRT residue 76 and altered PPQ susceptibility.[382,383]

In Asia, a dire situation exists in Cambodia, where treatment failures are increasingly noted for the first-line regimen DHA-PPQ.[135] Interestingly, comparison of the whole-genome sequences with *in vitro* PPQ survival of parasites derived from cases of DHA-PPQ treatment failure by Duru *et al.* revealed an increased proportion of PfCRT mutations H97Y, M343L, and G353V among PPQ-resistant parasites (each in the background of Dd2 PfCRT, the most common mutant haplotype in Asia).[139] Given the ambiguous relationship between PPQ susceptibility and PfCRT residue 76 that is often assessed in isolation, as well as the knowledge that non-K76T PfCRT mutations can modulate parasite PPQ susceptibility,[137,196,218] it is very possible that the novel mutations reported by Duru *et al.* are driving DHA-PPQ resistance in Southeast Asia. Generation and analysis of isogenic, *pfcrt*-modified lines encoding these mutations will help to establish whether they have a causal role in mediating parasite PPQ resistance and should be prioritized.

The reduced efficacy of AS-AQ in Asia is also worth noting. A recent meta-analysis documented a seven-fold higher rate of parasite recrudescence following AS-AQ treatment in Asia as compared to Africa.[362] In a randomized trial conducted in Myanmar, AS-AQ was significantly associated with recrudescence of *P. falciparum*

infections as compared to ATM-LUM, AS-mefloquine (MFQ), and DHA-PPQ.[384] The work presented herein identified a strong link between parasite susceptibility to the clinically relevant *in vivo* metabolite of AQ, md-AQ, and the mutational status of PfCRT residue 326, with both the South American/Western Pacific mutation N326D and the African mutation N326S conferring increased md-AQ resistance (see **Chapter 2** and **Chapter 4**). This begs the question: Could mutant PfCRT 326 be employed as an important marker of reduced parasite AQ susceptibility? Monitoring of the mutational status of PfCRT 326 would, for example, distinguish between the related mutant PfCRT Dd2 and GB4 haplotypes that are both present in Southeast Asia and that differ at PfCRT residues 326 and 356 (see **Chapter 4**). The declining utility of the conventional resistance marker K76T calls for continued characterization of non-K76T mutations, including mutations emerging in regions with documented resistance.[137,199,208] Identification of new resistance markers would inform region-specific treatment recommendations and possibly shed light on new "evolutionary trap" drug cycling regimens that, like AS-AQ and ATM-LUM (which select for K76T and K76, respectively), could be used to slow the expansion of resistant parasite populations.

The emergence of *P. falciparum* resistance to first-line antimalarial regimens serves as a clear impetus for the development of new drug regimens, some of which include drugs bearing the CQ-like quinoline scaffold.[328] The discovery of novel compounds with antiplasmodial activity and identification of potential genetic resistance markers is facilitated through high-throughput screens (HTSs) driven by public-private partnerships, including the Medicines for Malaria Venture (MMV).[385] Importantly, compounds with a high propensity to promote novel mechanisms of

parasite drug resistance and/or that show cross-resistance with current antimalarials must be deprioritized. Related to this effort, Chugh *et al.* evaluated the capacity of a panel of sensitive and multidrug-resistant *P. falciparum* strains to deconvolute cross-resistance signals when treated with a series of novel 1,2,4-oxadiazole compounds.[386] Characterization of three such compounds revealed that they were inactive against mutant *pfcrt*-expressing drug-resistant strains. Of note, resistance was associated with inhibition of the Hb-degrading cysteine protease Falcipain 2 and with little to no verapamil reversibility, features distinct from CQR and yet still implicating a role for mutant PfCRT-mediated alterations in Hb processing.[386] In earlier work, using a HTS and genome-wide association study, Yuan *et al.* demonstrated that the differential susceptibilities of *P. falciparum* parasites to a set of 32 potent and chemically diverse compounds could be vastly accounted for by variation at just three genetic loci, one of which was *pfcrt*.[387] While *pfcrt*-mediated resistance mechanisms chiefly affect drugs active against asexual blood-stage parasites, intriguing reports from *S. cerevisiae* and *X. laevis* oocyte heterologous expression studies collectively suggest the ability of certain PfCRT isoforms to transport gametocytocidal compounds, namely primaquine and methylene blue.[208,220]

Containment of the clinical burden and spread of malaria suffered a setback with the rise and spread of CQR. Despite this, CQ remains central to the treatment of infections caused by multiple *Plasmodium* species. Parasite CQR can be overcome by augmenting the standard drug dosage, is amenable to chemosensitization by certain resistance-reversing compounds, and shares resistance mechanism with a number of antimalarial drugs that are clinically employed or in development.[114,275] Furthermore, playing either a partial or no role in CQR, a number of PfCRT

mutations, some of which await characterization, are subjected to various selective forces exerted by first-line ACT component drugs. Decades after the disappointing suspension of the Global Malaria Eradication Program, the prospect of malaria eradication has resurfaced as a public health goal, with significantly higher involvement of the research community. Continued vector control, treatment with potent antimalarial drugs, and implementation of aggressive surveillance measures informed by genomic and genetic approaches will collectively ensure that this goal is achievable.

REFERENCES

1. Sherman, I.W. *Twelve diseases that changed our world*, ix, 219 p. (ASM Press, Washington, DC, 2007).

2. Scurlock, J.A. & Andersen, B.R. *Diagnoses in Assyrian and Babylonian medicine: ancient sources, translations, and modern medical analyses*, xxiii, 879 p. (University of Illinois Press, Urbana, 2005).

3. Greenberg, B. & Kunich, J.C. *Entomology and the law: flies as forensic indicators*, xiii, 306 p. (Cambridge University Press, Cambridge, 2002).

4. Carlton, J.M., Perkins, S.L. & Deitsch, K.W. *Malaria parasites: comparative genomics, evolution and molecular biology*, x, 280 p. (Caister Academic Press, Norfolk, UK, 2013).

5. Sutherland, C.J. *et al.* Two nonrecombining sympatric forms of the human malaria parasite *Plasmodium ovale* occur globally. *J Infect Dis* **201**, 1544-50 (2010).

6. Collins, W.E. & Barnwell, J.W. *Plasmodium knowlesi*: finally being recognized. *J Infect Dis* **199**, 1107-8 (2009).

7. Ramasamy, R. Zoonotic malaria - global overview and research and policy needs. *Front Public Health* **2**, 123 (2014).

8. Schofield, L. & Grau, G.E. Immunological processes in malaria pathogenesis. *Nat Rev Immunol* **5**, 722-35 (2005).

9. Keeling, P.J. & Rayner, J.C. The origins of malaria: there are more things in heaven and earth. *Parasitology* **142 Suppl 1**, S16-25 (2015).

10. Liu, W. *et al.* Origin of the human malaria parasite *Plasmodium falciparum* in gorillas. *Nature* **467**, 420-5 (2010).

11. Foth, B.J. & McFadden, G.I. The apicoplast: a plastid in *Plasmodium falciparum* and other Apicomplexan parasites. *Int Rev Cytol* **224**, 57-110 (2003).

12. Arisue, N. & Hashimoto, T. Phylogeny and evolution of apicoplasts and apicomplexan parasites. *Parasitol Int* **64**, 254-9 (2015).

13. World Health Organization. World Malaria Report 2015.

14. Kasper, D.L. *Harrison's Principles of Internal Medicine*. (McGraw Hill Education, New York, 2015).

15. White, N.J. *et al.* Malaria. *Lancet* **383**, 723-35 (2014).

16. Sachs, J. & Malaney, P. The economic and social burden of malaria. *Nature* **415**, 680-5 (2002).

17. Greenwood, B.M. *et al.* Malaria: progress, perils, and prospects for eradication. *J Clin Invest* **118**, 1266-76 (2008).

18. Najera, J.A., Gonzalez-Silva, M. & Alonso, P.L. Some lessons for the future from the Global Malaria Eradication Programme (1955-1969). *PLoS Med* **8**, e1000412 (2011).

19. Roll Back Malaria. Global Malaria Action Plan. 2016.

20. Cotter, C. *et al.* The changing epidemiology of malaria elimination: new strategies for new challenges. *Lancet* **382**, 900-11 (2013).

21. Prudencio, M., Rodriguez, A. & Mota, M.M. The silent path to thousands of merozoites: the *Plasmodium* liver stage. *Nat Rev Microbiol* **4**, 849-56 (2006).

22. Su, X., Hayton, K. & Wellems, T.E. Genetic linkage and association analyses for trait mapping in *Plasmodium falciparum*. *Nat Rev Genet* **8**, 497-506 (2007).

23. Portugal, S., Drakesmith, H. & Mota, M.M. Superinfection in malaria: *Plasmodium* shows its iron will. *EMBO Rep* **12**, 1233-42 (2011).

24. White, N.J. Antimalarial drug resistance. *J Clin Invest* **113**, 1084-92 (2004).

25. Fleischer, B. Editorial: 100 years ago: Giemsa's solution for staining of plasmodia. *Trop Med Int Health* **9**, 755-6 (2004).

26. Hanssen, E., Goldie, K.N. & Tilley, L. Ultrastructure of the asexual blood stages of *Plasmodium falciparum*. *Methods Cell Biol* **96**, 93-116 (2010).

27. Glenister, F.K., Coppel, R.L., Cowman, A.F., Mohandas, N. & Cooke, B.M. Contribution of parasite proteins to altered mechanical properties of malaria-infected red blood cells. *Blood* **99**, 1060-3 (2002).

28. Goldberg, D.E. & Cowman, A.F. Moving in and renovating: exporting proteins from *Plasmodium* into host erythrocytes. *Nat Rev Microbiol* **8**, 617-21 (2010).

29. Tilley, L., Dixon, M.W. & Kirk, K. The *Plasmodium falciparum*-infected red blood cell. *Int J Biochem Cell Biol* **43**, 839-42 (2011).

30. Roberts, L.S. & Janovy, J. *Foundations of Parasitology*, xvii, 702 p. (McGraw-Hill, Boston, 2005).

31. Lee, K.S., Cox-Singh, J. & Singh, B. Morphological features and differential counts of *Plasmodium knowlesi* parasites in naturally acquired human infections. *Malar J* **8**, 73 (2009).

32. Centers for Disease Control and Prevention. DPDx Malaria Image Gallery. 2016.

33. Gardner, M.J. *et al.* Genome sequence of the human malaria parasite *Plasmodium falciparum*. *Nature* **419**, 498-511 (2002).

34. Cobbold, S.A. *et al.* Kinetic flux profiling elucidates two independent acetyl-CoA biosynthetic pathways in *Plasmodium falciparum*. *J Biol Chem* **288**, 36338-50 (2013).

35. Salcedo-Sora, J.E., Caamano-Gutierrez, E., Ward, S.A. & Biagini, G.A. The proliferating cell hypothesis: a metabolic framework for *Plasmodium* growth and development. *Trends Parasitol* **30**, 170-5 (2014).

36. Shears, M.J., Botte, C.Y. & McFadden, G.I. Fatty acid metabolism in the *Plasmodium* apicoplast: Drugs, doubts and knockouts. *Mol Biochem Parasitol* **199**, 34-50 (2015).

37. Kirk, K. Ion Regulation in the Malaria Parasite. *Annu Rev Microbiol* **69**, 341-59 (2015).

38. Marvin, R.G. *et al.* Fluxes in "free" and total zinc are essential for progression of intraerythrocytic stages of *Plasmodium falciparum*. *Chem Biol* **19**, 731-41 (2012).

39. Lew, V.L., Macdonald, L., Ginsburg, H., Krugliak, M. & Tiffert, T. Excess haemoglobin digestion by malaria parasites: a strategy to prevent premature host cell lysis. *Blood Cells Mol Dis* **32**, 353-9 (2004).

40. Mauritz, J.M. *et al.* The homeostasis of *Plasmodium falciparum*-infected red blood cells. *PLoS Comput Biol* **5**, e1000339 (2009).

41. Molina-Cruz, A. *et al.* Reactive oxygen species modulate *Anopheles gambiae* immunity against bacteria and *Plasmodium*. *J Biol Chem* **283**, 3217-23 (2008).

42. Pabon, A., Carmona, J., Burgos, L.C. & Blair, S. Oxidative stress in patients with non-complicated malaria. *Clin Biochem* **36**, 71-8 (2003).

43. Mohring, F., Pretzel, J., Jortzik, E. & Becker, K. The redox systems of *Plasmodium falciparum* and *Plasmodium vivax*: comparison, in silico analyses and inhibitor studies. *Curr Med Chem* **21**, 1728-56 (2014).

44. Jortzik, E. & Becker, K. Thioredoxin and glutathione systems in *Plasmodium falciparum*. *Int J Med Microbiol* **302**, 187-94 (2012).

45. Muller, S. Role and Regulation of Glutathione Metabolism in *Plasmodium falciparum*. *Molecules* **20**, 10511-34 (2015).

46. Abdel-Muhsin, A.M. *et al.* Evolution of drug-resistance genes in *Plasmodium falciparum* in an area of seasonal malaria transmission in Eastern Sudan. *J Infect Dis* **189**, 1239-44 (2004).

47. Milani, K.J., Schneider, T.G. & Taraschi, T.F. Defining the morphology and mechanism of the hemoglobin transport pathway in *Plasmodium falciparum*-infected erythrocytes. *Eukaryot Cell* **14**, 415-26 (2015).

48. Rudzinska, M.A., Trager, W. & Bray, R.S. Pinocytotic uptake and the digestion of hemoglobin in malaria parasites. *J Protozool* **12**, 563-76 (1965).

49. Sigala, P.A. & Goldberg, D.E. The peculiarities and paradoxes of *Plasmodium* heme metabolism. *Annu Rev Microbiol* **68**, 259-78 (2014).

50. Liu, J., Istvan, E.S., Gluzman, I.Y., Gross, J. & Goldberg, D.E. *Plasmodium falciparum* ensures its amino acid supply with multiple acquisition pathways and redundant proteolytic enzyme systems. *Proc Natl Acad Sci U S A* **103**, 8840-5 (2006).

51. Goldberg, D.E. Hemoglobin degradation. *Curr Top Microbiol Immunol* **295**, 275-91 (2005).

52. Wunderlich, J., Rohrbach, P. & Dalton, J.P. The malaria digestive vacuole. *Front Biosci (Schol Ed)* **4**, 1424-48 (2012).

53. van Dooren, G.G., Kennedy, A.T. & McFadden, G.I. The use and abuse of heme in apicomplexan parasites. *Antioxid Redox Signal* **17**, 634-56 (2012).

54. Chugh, M. *et al.* Protein complex directs hemoglobin-to-hemozoin formation in *Plasmodium falciparum*. *Proc Natl Acad Sci U S A* **110**, 5392-7 (2013).

55. Combrinck, J.M. *et al.* Insights into the role of heme in the mechanism of action of antimalarials. *ACS Chem Biol* **8**, 133-7 (2013).

56. Atamna, H. & Ginsburg, H. Heme degradation in the presence of glutathione. A proposed mechanism to account for the high levels of non-heme iron found in the membranes of hemoglobinopathic red blood cells. *J Biol Chem* **270**, 24876-83 (1995).

57. Loria, P., Miller, S., Foley, M. & Tilley, L. Inhibition of the peroxidative degradation of haem as the basis of action of chloroquine and other quinoline antimalarials. *Biochem J* **339 (Pt 2)**, 363-70 (1999).

58. Gorka, A.P., de Dios, A. & Roepe, P.D. Quinoline drug-heme interactions and implications for antimalarial cytostatic versus cytocidal activities. *J Med Chem* **56**, 5231-46 (2013).

59. Lehane, A.M., McDevitt, C.A., Kirk, K. & Fidock, D.A. Degrees of chloroquine resistance in *Plasmodium* - is the redox system involved? *Int J Parasitol Drugs Drug Resist* **2**, 47-57 (2012).

60. Kumar, S. & Bandyopadhyay, U. Free heme toxicity and its detoxification systems in human. *Toxicol Lett* **157**, 175-88 (2005).

61. Egan, T.J. *et al.* Fate of haem iron in the malaria parasite *Plasmodium falciparum*. *Biochem J* **365**, 343-7 (2002).

62. Slater, A.F. *et al.* An iron-carboxylate bond links the heme units of malaria pigment. *Proc Natl Acad Sci U S A* **88**, 325-9 (1991).

63. Frosch, T. *et al.* In situ localization and structural analysis of the malaria pigment hemozoin. *J Phys Chem B* **111**, 11047-56 (2007).

64. Pagola, S., Stephens, P.W., Bohle, D.S., Kosar, A.D. & Madsen, S.K. The structure of malaria pigment beta-haematin. *Nature* **404**, 307-10 (2000).

65. Pisciotta, J.M. *et al.* The role of neutral lipid nanospheres in *Plasmodium falciparum* haem crystallization. *Biochem J* **402**, 197-204 (2007).

66. Egan, T.J. Recent advances in understanding the mechanism of hemozoin (malaria pigment) formation. *J Inorg Biochem* **102**, 1288-99 (2008).

67. Jani, D. *et al.* HDP-a novel heme detoxification protein from the malaria parasite. *PLoS Pathog* **4**, e1000053 (2008).

68. Institute of Tropical Medicine Antwerp. Illustrated Lecture Notes on Tropical Medicine. 2016.

69. Bray, P.G., Mungthin, M., Ridley, R.G. & Ward, S.A. Access to hematin: the basis of chloroquine resistance. *Mol Pharmacol* **54**, 170-9 (1998).

70. Klonis, N. *et al.* Artemisinin activity against *Plasmodium falciparum* requires hemoglobin uptake and digestion. *Proc Natl Acad Sci U S A* **108**, 11405-10 (2011).

71. Mungthin, M., Bray, P.G., Ridley, R.G. & Ward, S.A. Central role of hemoglobin degradation in mechanisms of action of 4-aminoquinolines, quinoline methanols, and phenanthrene methanols. *Antimicrob Agents Chemother* **42**, 2973-7 (1998).

72. Nagaraj, V.A. *et al.* Malaria parasite-synthesized heme is essential in the mosquito and liver stages and complements host heme in the blood stages of infection. *PLoS Pathog* **9**, e1003522 (2013).

73. Taylor, T.E. & Molyneux, M.E. The pathogenesis of pediatric cerebral malaria: eye exams, autopsies, and neuroimaging. *Ann N Y Acad Sci* **1342**, 44-52 (2015).

74. Wassmer, S.C. *et al.* Investigating the Pathogenesis of Severe Malaria: A Multidisciplinary and Cross-Geographical Approach. *Am J Trop Med Hyg* **93**, 42-56 (2015).

75. Dondorp, A.M. *et al.* The relationship between age and the manifestations of and mortality associated with severe malaria. *Clin Infect Dis* **47**, 151-7 (2008).

76. von Seidlein, L. *et al.* Predicting the clinical outcome of severe falciparum malaria in African children: findings from a large randomized trial. *Clin Infect Dis* **54**, 1080-90 (2012).

77. Sahu, P.K. *et al.* Pathogenesis of cerebral malaria: new diagnostic tools, biomarkers, and therapeutic approaches. *Front Cell Infect Microbiol* **5**, 75 (2015).

78. Manning, L. & Davis, T.M. The mechanistic, diagnostic and prognostic utility of biomarkers in severe malaria. *Biomark Med* **7**, 363-80 (2013).

79. Zimmerman, P.A. & Howes, R.E. Malaria diagnosis for malaria elimination. *Curr Opin Infect Dis* **28**, 446-54 (2015).

80. Miller, L.H., Ackerman, H.C., Su, X.Z. & Wellems, T.E. Malaria biology and disease pathogenesis: insights for new treatments. *Nat Med* **19**, 156-67 (2013).

81. Kirkman, L.A. & Deitsch, K.W. Antigenic variation and the generation of diversity in malaria parasites. *Curr Opin Microbiol* **15**, 456-62 (2012).

82. Aird, W.C., Mosnier, L.O. & Fairhurst, R.M. *Plasmodium falciparum* picks (on) EPCR. *Blood* **123**, 163-7 (2014).

83. Ferreira, A., Balla, J., Jeney, V., Balla, G. & Soares, M.P. A central role for free heme in the pathogenesis of severe malaria: the missing link? *J Mol Med (Berl)* **86**, 1097-111 (2008).

84. Langhorne, J., Ndungu, F.M., Sponaas, A.M. & Marsh, K. Immunity to malaria: more questions than answers. *Nat Immunol* **9**, 725-32 (2008).

85. Coban, C., Ishii, K.J., Horii, T. & Akira, S. Manipulation of host innate immune responses by the malaria parasite. *Trends Microbiol* **15**, 271-8 (2007).

86. Gallego-Delgado, J., Ty, M., Orengo, J.M., van de Hoef, D. & Rodriguez, A. A surprising role for uric acid: the inflammatory malaria response. *Curr Rheumatol Rep* **16**, 401 (2014).

87. Prato, M., Giribaldi, G., Polimeni, M., Gallo, V. & Arese, P. Phagocytosis of hemozoin enhances matrix metalloproteinase-9 activity and TNF-alpha production in human monocytes: role of matrix metalloproteinases in the pathogenesis of falciparum malaria. *J Immunol* **175**, 6436-42 (2005).

88. Leoratti, F.M. *et al.* Pattern of humoral immune response to *Plasmodium falciparum* blood stages in individuals presenting different clinical expressions of malaria. *Malar J* **7**, 186 (2008).

89. Ryg-Cornejo, V. *et al.* Severe Malaria Infections Impair Germinal Center Responses by Inhibiting T Follicular Helper Cell Differentiation. *Cell Rep* **14**, 68-81 (2016).

90. McGuire, W., Hill, A.V., Allsopp, C.E., Greenwood, B.M. & Kwiatkowski, D. Variation in the TNF-alpha promoter region associated with susceptibility to cerebral malaria. *Nature* **371**, 508-10 (1994).

91. Crosnier, C. *et al.* Basigin is a receptor essential for erythrocyte invasion by *Plasmodium falciparum*. *Nature* **480**, 534-7 (2011).

92. Williams, T.N. Human red blood cell polymorphisms and malaria. *Curr Opin Microbiol* **9**, 388-94 (2006).

93. Miura, K. Progress and prospects for blood-stage malaria vaccines. *Expert Rev Vaccines*, 1-17 (2016).

94. Hoffman, S.L., Vekemans, J., Richie, T.L. & Duffy, P.E. The March Toward Malaria Vaccines. *Am J Prev Med* **49**, S319-33 (2015).

95. Centers for Disease Control and Prevention. Health Information for International Travel: Malaria. 2016.

96. World Health Organization. Guidelines for the treatment of malaria (2015).

97. Kakuru, A. *et al.* Dihydroartemisinin-Piperaquine for the Prevention of Malaria in Pregnancy. *N Engl J Med* **374**, 928-39 (2016).

98. Goodman, L.S., Brunton, L.L., Chabner, B. & Knollmann, B.r.C. *Goodman & Gilman's Pharmacological Basis of Therapeutics*, 2084 p. (McGraw-Hill, New York, 2011).

99. Sachanonta, N. *et al.* Ultrastructural and real-time microscopic changes in *P. falciparum*-infected red blood cells following treatment with antimalarial drugs. *Ultrastruct Pathol* **35**, 214-25 (2011).

100. Klonis, N., Creek, D.J. & Tilley, L. Iron and heme metabolism in *Plasmodium falciparum* and the mechanism of action of artemisinins. *Curr Opin Microbiol* **16**, 722-7 (2013).

101. Marella, A. *et al.* Quinoline: A versatile heterocyclic. *Saudi Pharm J* **21**, 1-12 (2013).

102. Kadish, K.M., Smith, K.M. & Guilard, R. *Handbook of porphyrin science: with applications to chemistry, physics, materials science, engineering, biology and medicine*

(World Scientific, London, 2010).

103. Krishna, S. & White, N.J. Pharmacokinetics of quinine, chloroquine and amodiaquine. Clinical implications. *Clin Pharmacokinet* **30**, 263-99 (1996).

104. Projean, D. *et al. In vitro* metabolism of chloroquine: identification of CYP2C8, CYP3A4, and CYP2D6 as the main isoforms catalyzing N-desethylchloroquine formation. *Drug Metab Dispos* **31**, 748-54 (2003).

105. Ducharme, J. & Farinotti, R. Clinical pharmacokinetics and metabolism of chloroquine. Focus on recent advancements. *Clin Pharmacokinet* **31**, 257-74 (1996).

106. Hellgren, U. *et al.* Response of *Plasmodium falciparum* to chloroquine treatment: relation to whole blood concentrations of chloroquine and desethylchloroquine. *Bull World Health Organ* **67**, 197-202 (1989).

107. Hellgren, U., Alvan, G. & Jerling, M. On the question of interindividual variations in chloroquine concentrations. *Eur J Clin Pharmacol* **45**, 383-5 (1993).

108. Roepe, P.D. Molecular and physiologic basis of quinoline drug resistance in *Plasmodium falciparum* malaria. *Future Microbiol* **4**, 441-55 (2009).

109. Cohen, S.N., Phifer, K.O. & Yielding, K.L. Complex Formation between Chloroquine and Ferrihaemic Acid in Vitro, and Its Effect on the Antimalarial Action of Chloroquine. *Nature* **202**, 805-6 (1964).

110. Webster, G.T., Tilley, L., Deed, S., McNaughton, D. & Wood, B.R. Resonance Raman spectroscopy can detect structural changes in haemozoin (malaria pigment) following incubation with chloroquine in infected erythrocytes. *FEBS Lett* **582**, 1087-92 (2008).

111. Casabianca, L.B. *et al.* Quinine and chloroquine differentially perturb heme monomer-dimer equilibrium. *Inorg Chem* **47**, 6077-81 (2008).

112. Sullivan, D.J., Jr., Gluzman, I.Y., Russell, D.G. & Goldberg, D.E. On the molecular mechanism of chloroquine's antimalarial action. *Proc Natl Acad Sci U S A* **93**, 11865-70 (1996).

113. Gorka, A.P., Jacobs, L.M. & Roepe, P.D. Cytostatic versus cytocidal profiling of quinoline drug combinations via modified fixed-ratio isobologram analysis. *Malar J* **12**, 332 (2013).

114. Ecker, A., Lehane, A.M., Clain, J. & Fidock, D.A. PfCRT and its role in antimalarial drug resistance. *Trends Parasitol* **28**, 504-14 (2012).

115. Ursing, J., Rombo, L., Bergqvist, Y., Rodrigues, A. & Kofoed, P.E. High-Dose Chloroquine for Treatment of Chloroquine-Resistant *Plasmodium falciparum* Malaria. *J Infect Dis* **213**, 1315-21 (2016).

116. Price, R.N. *et al.* Global extent of chloroquine-resistant *Plasmodium vivax*: a systematic review and meta-analysis. *Lancet Infect Dis* **14**, 982-91 (2014).

117. Nomura, T. *et al.* Evidence for different mechanisms of chloroquine resistance in 2 *Plasmodium* species that cause human malaria. *J Infect Dis* **183**, 1653-61 (2001).

118. Bray, P.G. *et al.* PfCRT and the trans-vacuolar proton electrochemical gradient: regulating the access of chloroquine to ferriprotoporphyrin IX. *Mol Microbiol* **62**, 238-51 (2006).

119. Fitch, C.D. Chloroquine resistance in malaria: a deficiency of chloroquine binding. *Proc Natl Acad Sci U S A* **64**, 1181-7 (1969).

120. Sidhu, A.B., Verdier-Pinard, D. & Fidock, D.A. Chloroquine resistance in *Plasmodium falciparum* malaria parasites conferred by *pfcrt* mutations. *Science* **298**, 210-3 (2002).

121. Gaillard, T., Dormoi, J., Madamet, M. & Pradines, B. Macrolides and associated antibiotics based on similar mechanism of action like lincosamides in malaria. *Malar J* **15**, 85 (2016).

122. Alumasa, J.N. *et al.* The hydroxyl functionality and a rigid proximal N are required for forming a novel non-covalent quinine-heme complex. *J Inorg Biochem* **105**, 467-75 (2011).

123. Cui, L., Mharakurwa, S., Ndiaye, D., Rathod, P.K. & Rosenthal, P.J. Antimalarial Drug Resistance: Literature Review and Activities and Findings of the ICEMR Network. *Am J Trop Med Hyg* **93**, 57-68 (2015).

124. Nkrumah, L.J. *et al.* Probing the multifactorial basis of *Plasmodium falciparum* quinine resistance: evidence for a strain-specific contribution of the sodium-proton exchanger PfNHE. *Mol Biochem Parasitol* **165**, 122-31 (2009).

125. Cooper, R.A. *et al.* Alternative mutations at position 76 of the vacuolar transmembrane protein PfCRT are associated with chloroquine resistance and unique stereospecific quinine and quinidine responses in *Plasmodium falciparum*. *Mol Pharmacol* **61**, 35-42 (2002).

126. Lakshmanan, V. *et al.* A critical role for PfCRT K76T in *Plasmodium falciparum* verapamil-reversible chloroquine resistance. *EMBO J* **24**, 2294-305 (2005).

127. Duraisingh, M.T. & Cowman, A.F. Contribution of the *pfmdr1* gene to antimalarial drug-resistance. *Acta Trop* **94**, 181-90 (2005).

128. Sidhu, A.B., Valderramos, S.G. & Fidock, D.A. *pfmdr1* mutations contribute to quinine resistance and enhance mefloquine and artemisinin sensitivity in *Plasmodium falciparum*. *Mol Microbiol* **57**, 913-26 (2005).

129. Sanchez, C.P. *et al.* A HECT Ubiquitin-Protein Ligase as a Novel Candidate Gene for Altered Quinine and Quinidine Responses in *Plasmodium falciparum*. *PLoS Genet* **10**, e1004382 (2014).

130. Payne, D. Did medicated salt hasten the spread of chloroquine resistance in *Plasmodium falciparum*? *Parasitol Today* **4**, 112-5 (1988).

131. Ongarora, D.S. *et al.* Antimalarial benzoheterocyclic 4-aminoquinolines: Structure-activity relationship, *in vivo* evaluation, mechanistic and bioactivation studies. *Bioorg Med Chem* **23**, 5419-32 (2015).

132. de Dios, A.C., Casabianca, L.B., Kosar, A. & Roepe, P.D. Structure of the amodiaquine-FPIX mu oxo dimer solution complex at atomic resolution. *Inorg Chem* **43**, 8078-84 (2004).

133. Sa, J.M. *et al.* Geographic patterns of *Plasmodium falciparum* drug resistance distinguished by differential responses to amodiaquine and chloroquine. *Proc Natl Acad Sci U S A* **106**, 18883-9 (2009).

134. Davis, T.M., Hung, T.Y., Sim, I.K., Karunajeewa, H.A. & Ilett, K.F. Piperaquine: a resurgent antimalarial drug. *Drugs* **65**, 75-87 (2005).

135. Amaratunga, C. *et al.* Dihydroartemisinin-piperaquine resistance in *Plasmodium falciparum* malaria in Cambodia: a multisite prospective cohort study. *Lancet Infect Dis* **16**, 357-65 (2016).

136. Leang, R. *et al.* Evidence of *Plasmodium falciparum* Malaria Multidrug Resistance to Artemisinin and Piperaquine in Western Cambodia: Dihydroartemisinin-Piperaquine Open-Label Multicenter Clinical Assessment. *Antimicrob Agents Chemother* **59**, 4719-26 (2015).

137. Pelleau, S. *et al.* Adaptive evolution of malaria parasites in French Guiana: Reversal of chloroquine resistance by acquisition of a mutation in *pfcrt*. *Proc Natl Acad Sci U S A* **112**, 11672-7 (2015).

138. Saunders, D.L. *et al.* Dihydroartemisinin-piperaquine failure in Cambodia. *N Engl J Med* **371**, 484-5 (2014).

139. Duru, V. *et al. Plasmodium falciparum* dihydroartemisinin-piperaquine failures in Cambodia are associated with mutant K13 parasites presenting high survival rates in novel piperaquine *in vitro* assays: retrospective and prospective investigations. *BMC Med* **13**, 305 (2015).

140. Wanzira, H. *et al.* Longitudinal outcomes in a cohort of Ugandan children randomized to artemether-lumefantrine versus dihydroartemisinin-piperaquine for the treatment of malaria. *Clin Infect Dis* **59**, 509-16 (2014).

141. Zani, B., Gathu, M., Donegan, S., Olliaro, P.L. & Sinclair, D. Dihydroartemisinin-piperaquine for treating uncomplicated *Plasmodium falciparum* malaria. *Cochrane Database Syst Rev* **1**, CD010927 (2014).

142. Rohrbach, P. *et al.* Genetic linkage of *pfmdr1* with food vacuolar solute import in *Plasmodium falciparum*. *EMBO J* **25**, 3000-11 (2006).

143. Veiga, M.I. *et al.* Globally prevalent PfMDR1 mutations modulate *Plasmodium falciparum* susceptibility to artemisinin-based combination therapies. *Nat Commun* **7**, 11553 (2016).

144. Preechapornkul, P. *et al. Plasmodium falciparum pfmdr1* amplification, mefloquine resistance, and parasite fitness. *Antimicrob Agents Chemother* **53**, 1509-15 (2009).

145. Price, R.N. *et al.* Mefloquine resistance in *Plasmodium falciparum* and increased *pfmdr1* gene copy number. *Lancet* **364**, 438-47 (2004).

146. Cui, L. & Su, X.Z. Discovery, mechanisms of action and combination therapy of artemisinin. *Expert Rev Anti Infect Ther* **7**, 999-1013 (2009).

147. de Villiers, K.A., Marques, H.M. & Egan, T.J. The crystal structure of halofantrine-

ferriprotoporphyrin IX and the mechanism of action of arylmethanol antimalarials. *J Inorg Biochem* **102**, 1660-7 (2008).

148. Plucinski, M.M. *et al.* Efficacy of artemether-lumefantrine and dihydroartemisinin-piperaquine for treatment of uncomplicated malaria in children in Zaire and Uige Provinces, angola. *Antimicrob Agents Chemother* **59**, 437-43 (2015).

149. Yeka, A. *et al.* Artesunate/Amodiaquine Versus Artemether/Lumefantrine for the Treatment of Uncomplicated Malaria in Uganda: A Randomized Trial. *J Infect Dis* **213**, 1134-42 (2016).

150. Edgcomb, J.H. *et al.* Primaquine, SN 13272, a new curative agent in vivax malaria; a preliminary report. *J Natl Malar Soc* **9**, 285-92 (1950).

151. Leang, R. *et al.* Efficacy and safety of pyronaridine-artesunate for the treatment of uncomplicated *Plasmodium falciparum* malaria in western Cambodia. *Antimicrob Agents Chemother* (2016).

152. Croft, S.L. *et al.* Review of pyronaridine anti-malarial properties and product characteristics. *Malar J* **11**, 270 (2012).

153. Auparakkitanon, S., Chapoomram, S., Kuaha, K., Chirachariyavej, T. & Wilairat, P. Targeting of hematin by the antimalarial pyronaridine. *Antimicrob Agents Chemother* **50**, 2197-200 (2006).

154. Famin, O., Krugliak, M. & Ginsburg, H. Kinetics of inhibition of glutathione-mediated degradation of ferriprotoporphyrin IX by antimalarial drugs. *Biochem Pharmacol* **58**, 59-68 (1999).

155. Madamet, M. *et al.* The *Plasmodium falciparum* chloroquine resistance transporter is associated with the *ex vivo P. falciparum* African parasite response to pyronaridine. *Parasit Vectors* **9**, 77 (2016).

156. Nobel Media AB. The Nobel Prize in Physiology or Medicine 2015.

157. Xie, S.C. *et al.* Haemoglobin degradation underpins the sensitivity of early ring stage *Plasmodium falciparum* to artemisinins. *J Cell Sci* **129**, 406-16 (2016).

158. Ariey, F. *et al.* A molecular marker of artemisinin-resistant *Plasmodium falciparum* malaria. *Nature* **505**, 50-5 (2014).

159. Miotto, O. *et al.* Genetic architecture of artemisinin-resistant *Plasmodium falciparum*. *Nat Genet* **47**, 226-34 (2015).

160. Straimer, J. *et al.* Drug resistance. K13-propeller mutations confer artemisinin resistance in *Plasmodium falciparum* clinical isolates. *Science* **347**, 428-31 (2015).

161. Takala-Harrison, S. *et al.* Independent emergence of artemisinin resistance mutations among *Plasmodium falciparum* in Southeast Asia. *J Infect Dis* **211**, 670-9 (2015).

162. Witkowski, B. *et al.* Novel phenotypic assays for the detection of artemisinin-resistant *Plasmodium falciparum* malaria in Cambodia: in-vitro and ex-vivo drug-response studies. *Lancet Infect Dis* **13**, 1043-9 (2013).

163. Chenet, S.M. *et al.* Independent Emergence of the *Plasmodium falciparum* Kelch Propeller Domain Mutant Allele C580Y in Guyana. *J Infect Dis* **213**, 1472-5 (2016).

164. Malaria, G.E.N.P.f.C.P. Genomic epidemiology of artemisinin resistant malaria. *Elife* **5**(2016).

165. Lozovsky, E.R. *et al.* Stepwise acquisition of pyrimethamine resistance in the malaria parasite. *Proc Natl Acad Sci U S A* **106**, 12025-30 (2009).

166. Painter, H.J., Morrisey, J.M., Mather, M.W. & Vaidya, A.B. Specific role of mitochondrial electron transport in blood-stage *Plasmodium falciparum*. *Nature* **446**, 88-91 (2007).

167. Fidock, D.A., Nomura, T. & Wellems, T.E. Cycloguanil and its parent compound proguanil demonstrate distinct activities against *Plasmodium falciparum* malaria parasites transformed with human dihydrofolate reductase. *Mol Pharmacol* **54**, 1140-7 (1998).

168. Ekland, E.H., Schneider, J. & Fidock, D.A. Identifying apicoplast-targeting antimalarials using high-throughput compatible approaches. *FASEB J* **25**, 3583-93 (2011).

169. Vandekerckhove, S. & D'Hooghe, M. Quinoline-based antimalarial hybrid compounds. *Bioorg Med Chem* **23**, 5098-119 (2015).

170. Egan, T.J. & Kuter, D. Dual-functioning antimalarials that inhibit the chloroquine-resistance transporter. *Future Microbiol* **8**, 475-89 (2013).

171. Mushtaque, M. & Shahjahan. Reemergence of chloroquine (CQ) analogs as multi-targeting antimalarial agents: A review. *Eur J Med Chem* **90**, 280-95 (2015).

172. Peyton, D.H. Reversed chloroquine molecules as a strategy to overcome resistance in malaria. *Curr Top Med Chem* **12**, 400-7 (2012).

173. Raj, R. *et al.* Discovery of highly selective 7-chloroquinoline-thiohydantoins with potent antimalarial activity. *Eur J Med Chem* **84**, 425-32 (2014).

174. D'Alessandro, U. & Buttiens, H. History and importance of antimalarial drug resistance. *Trop Med Int Health* **6**, 845-8 (2001).

175. von Seidlein, L. & Greenwood, B.M. Mass administrations of antimalarial drugs. *Trends Parasitol* **19**, 452-60 (2003).

176. Ekland, E.H. & Fidock, D.A. *In vitro* evaluations of antimalarial drugs and their relevance to clinical outcomes. *Int J Parasitol* **38**, 743-7 (2008).

177. Wellems, T.E. & Plowe, C.V. Chloroquine-resistant malaria. *J Infect Dis* **184**, 770-6 (2001).

178. Snow, R.W., Trape, J.F. & Marsh, K. The past, present and future of childhood malaria mortality in Africa. *Trends Parasitol* **17**, 593-7 (2001).

179. Fidock, D.A. Microbiology. Eliminating malaria. *Science* **340**, 1531-3 (2013).

180. Eastman, R.T. & Fidock, D.A. Artemisinin-based combination therapies: a vital tool in efforts to eliminate malaria. *Nat Rev Microbiol* **7**, 864-74 (2009).

181. Fairhurst, R.M. Understanding artemisinin-resistant malaria: what a difference a year makes. *Curr Opin Infect Dis* **28**, 417-25 (2015).

182. Hamed, K. & Kuhen, K. No robust evidence of lumefantrine resistance. *Antimicrob Agents Chemother* **59**, 5865-6 (2015).

183. Tumwebaze, P. *et al.* Impact of antimalarial treatment and chemoprevention on the drug sensitivity of malaria parasites isolated from Ugandan children. *Antimicrob Agents Chemother* **59**, 3018-30 (2015).

184. Su, X., Kirkman, L.A., Fujioka, H. & Wellems, T.E. Complex polymorphisms in an approximately 330 kDa protein are linked to chloroquine-resistant *P. falciparum* in Southeast Asia and Africa. *Cell* **91**, 593-603 (1997).

185. Wellems, T.E., Walker-Jonah, A. & Panton, L.J. Genetic mapping of the chloroquine-resistance locus on *Plasmodium falciparum* chromosome 7. *Proc Natl Acad Sci U S A* **88**, 3382-6 (1991).

186. Fidock, D.A. *et al.* Mutations in the *P. falciparum* digestive vacuole transmembrane protein PfCRT and evidence for their role in chloroquine resistance. *Mol Cell* **6**, 861-71 (2000).

187. Krogstad, D.J. *et al.* Efflux of chloroquine from *Plasmodium falciparum*: mechanism of chloroquine resistance. *Science* **238**, 1283-5 (1987).

188. Roepe, P.D. PfCRT-mediated drug transport in malarial parasites. *Biochemistry* **50**, 163-71 (2011).

189. Cabrera, M., Paguio, M.F., Xie, C. & Roepe, P.D. Reduced digestive vacuolar accumulation of chloroquine is not linked to resistance to chloroquine toxicity. *Biochemistry* **48**, 11152-4 (2009).

190. Gligorijevic, B., Purdy, K., Elliott, D.A., Cooper, R.A. & Roepe, P.D. Stage independent chloroquine resistance and chloroquine toxicity revealed via spinning disk confocal microscopy. *Mol Biochem Parasitol* **159**, 7-23 (2008).

191. Gaviria, D. *et al.* A process similar to autophagy is associated with cytocidal chloroquine resistance in *Plasmodium falciparum*. *PLoS One* **8**, e79059 (2013).

192. Roepe, P.D. To kill or not to kill, that is the question: cytocidal antimalarial drug resistance. *Trends Parasitol* **30**, 130-5 (2014).

193. Zhang, H., Paguio, M. & Roepe, P.D. The antimalarial drug resistance protein *Plasmodium falciparum* chloroquine resistance transporter binds chloroquine. *Biochemistry* **43**, 8290-6 (2004).

194. Lekostaj, J.K., Natarajan, J.K., Paguio, M.F., Wolf, C. & Roepe, P.D. Photoaffinity labeling of the *Plasmodium falciparum* chloroquine resistance transporter with a novel perfluorophenylazido chloroquine. *Biochemistry* **47**, 10394-406 (2008).

195. Gligorijevic, B., Bennett, T., McAllister, R., Urbach, J.S. & Roepe, P.D. Spinning disk confocal microscopy of live, intraerythrocytic malarial parasites. 2. Altered vacuolar volume regulation in drug resistant malaria. *Biochemistry* **45**, 12411-23 (2006).

196. Pulcini, S. *et al.* Mutations in the *Plasmodium falciparum* chloroquine resistance transporter, PfCRT, enlarge the parasite's food vacuole and alter drug sensitivities. *Sci Rep* **5**, 14552 (2015).

197. Bennett, T.N. *et al.* Drug resistance-associated PfCRT mutations confer decreased *Plasmodium falciparum* digestive vacuolar pH. *Mol Biochem Parasitol* **133**, 99-114 (2004).

198. Djimde, A. *et al.* A molecular marker for chloroquine-resistant falciparum malaria. *N Engl J Med* **344**, 257-63 (2001).

199. Goswami, D. *et al.* PfCRT mutant haplotypes may not correspond with chloroquine resistance. *J Infect Dev Ctries* **8**, 768-73 (2014).

200. Martin, R.E. *et al.* Chloroquine transport via the malaria parasite's chloroquine resistance transporter. *Science* **325**, 1680-2 (2009).

201. Reeves, D.C. *et al.* Chloroquine-resistant isoforms of the *Plasmodium falciparum* chloroquine resistance transporter acidify lysosomal pH in HEK293 cells more than chloroquine-sensitive isoforms. *Mol Biochem Parasitol* **150**, 288-99 (2006).

202. Chinappi, M., Via, A., Marcatili, P. & Tramontano, A. On the mechanism of chloroquine resistance in *Plasmodium falciparum*. *PLoS One* **5**, e14064 (2010).

203. Papakrivos, J., Sa, J.M. & Wellems, T.E. Functional characterization of the *Plasmodium falciparum* chloroquine-resistance transporter (PfCRT) in transformed *Dictyostelium discoideum* vesicles. *PLoS One* **7**, e39569 (2012).

204. Sanchez, C.P. *et al.* Differences in trans-stimulated chloroquine efflux kinetics are linked to PfCRT in *Plasmodium falciparum*. *Mol Microbiol* **64**, 407-20 (2007).

205. Bray, P.G. *et al.* Defining the role of PfCRT in *Plasmodium falciparum* chloroquine resistance. *Mol Microbiol* **56**, 323-33 (2005).

206. Paguio, M.F., Cabrera, M. & Roepe, P.D. Chloroquine transport in *Plasmodium falciparum*. 2. Analysis of PfCRT-mediated drug transport using proteoliposomes and a fluorescent chloroquine probe. *Biochemistry* **48**, 9482-91 (2009).

207. Saliba, K.J. *et al.* Acidification of the malaria parasite's digestive vacuole by a H+-ATPase and a H+-pyrophosphatase. *J Biol Chem* **278**, 5605-12 (2003).

208. Callaghan, P.S., Hassett, M.R. & Roepe, P.D. Functional Comparison of 45 Naturally Occurring Isoforms of the *Plasmodium falciparum* Chloroquine Resistance Transporter (PfCRT). *Biochemistry* **54**, 5083-94 (2015).

209. Juge, N. *et al. Plasmodium falciparum* chloroquine resistance transporter is a H+-coupled polyspecific nutrient and drug exporter. *Proc Natl Acad Sci U S A* **112**, 3356-61 (2015).

210. Naude, B., Brzostowski, J.A., Kimmel, A.R. & Wellems, T.E. *Dictyostelium discoideum* expresses a malaria chloroquine resistance mechanism upon transfection with mutant, but not wild-type, *Plasmodium falciparum* transporter PfCRT. *J Biol Chem* **280**, 25596-603 (2005).

211. Lehane, A.M. & Kirk, K. Chloroquine resistance-conferring mutations in *pfcrt* give rise to

a chloroquine-associated H+ leak from the malaria parasite's digestive vacuole. *Antimicrob Agents Chemother* **52**, 4374-80 (2008).

212. Dondorp, A.M. *et al.* The threat of artemisinin-resistant malaria. *N Engl J Med* **365**, 1073-5 (2011).

213. Sisowath, C. *et al. In vivo* selection of *Plasmodium falciparum* parasites carrying the chloroquine-susceptible *pfcrt* K76 allele after treatment with artemether-lumefantrine in Africa. *J Infect Dis* **199**, 750-7 (2009).

214. Folarin, O.A. *et al. In vitro* amodiaquine resistance and its association with mutations in *pfcrt* and *pfmdr1* genes of *Plasmodium falciparum* isolates from Nigeria. *Acta Trop* **120**, 224-30 (2011).

215. Muangnoicharoen, S., Johnson, D.J., Looareesuwan, S., Krudsood, S. & Ward, S.A. Role of known molecular markers of resistance in the antimalarial potency of piperaquine and dihydroartemisinin *in vitro*. *Antimicrob Agents Chemother* **53**, 1362-6 (2009).

216. Hao, M. *et al. In vitro* sensitivities of *Plasmodium falciparum* isolates from the China-Myanmar border to piperaquine and association with polymorphisms in candidate genes. *Antimicrob Agents Chemother* **57**, 1723-9 (2013).

217. Valderramos, S.G. *et al.* Identification of a mutant PfCRT-mediated chloroquine tolerance phenotype in *Plasmodium falciparum*. *PLoS Pathog* **6**, e1000887 (2010).

218. Eastman, R.T., Dharia, N.V., Winzeler, E.A. & Fidock, D.A. Piperaquine resistance is associated with a copy number variation on chromosome 5 in drug-pressured *Plasmodium falciparum* parasites. *Antimicrob Agents Chemother* **55**, 3908-16 (2011).

219. Lukens, A.K. *et al.* Harnessing evolutionary fitness in *Plasmodium falciparum* for drug discovery and suppressing resistance. *Proc Natl Acad Sci U S A* **111**, 799-804 (2014).

220. van Schalkwyk, D.A. *et al.* Verapamil-Sensitive Transport of Quinacrine and Methylene Blue via the *Plasmodium falciparum* Chloroquine Resistance Transporter Reduces the Parasite's Susceptibility to these Tricyclic Drugs. *J Infect Dis* **213**, 800-10 (2016).

221. Valderramos, S.G. & Fidock, D.A. Transporters involved in resistance to antimalarial drugs. *Trends Pharmacol Sci* **27**, 594-601 (2006).

222. Sidhu, A.B. *et al.* Decreasing *pfmdr1* copy number in *Plasmodium falciparum* malaria heightens susceptibility to mefloquine, lumefantrine, halofantrine, quinine, and artemisinin. *J Infect Dis* **194**, 528-35 (2006).

223. Veiga, M.I. *et al. pfmdr1* amplification is related to increased *Plasmodium falciparum in vitro* sensitivity to the bisquinoline piperaquine. *Antimicrob Agents Chemother* **56**, 3615-9 (2012).

224. Duraisingh, M.T. *et al.* Linkage disequilibrium between two chromosomally distinct loci associated with increased resistance to chloroquine in *Plasmodium falciparum*. *Parasitology* **121 (Pt 1)**, 1-7 (2000).

225. Mu, J. *et al.* Multiple transporters associated with malaria parasite responses to chloroquine and quinine. *Mol Microbiol* **49**, 977-89 (2003).

226. Asare, K.K. *et al.* Synergism between *pfcrt* and *pfmdr1* genes could account for the slow recovery of chloroquine sensitive *Plasmodium falciparum* strains in Ghana after chloroquine withdrawal. *J Infect Public Health* (2016).

227. Ehlgen, F., Pham, J.S., de Koning-Ward, T., Cowman, A.F. & Ralph, S.A. Investigation of the *Plasmodium falciparum* food vacuole through inducible expression of the chloroquine resistance transporter (PfCRT). *PLoS One* **7**, e38781 (2012).

228. Kuhn, Y. *et al.* Trafficking of the phosphoprotein PfCRT to the digestive vacuolar membrane in *Plasmodium falciparum*. *Traffic* **11**, 236-49 (2010).

229. Waller, K.L. *et al.* Chloroquine resistance modulated *in vitro* by expression levels of the *Plasmodium falciparum* chloroquine resistance transporter. *J Biol Chem* **278**, 33593-601 (2003).

230. Garg, A. *et al.* Targeting protein translation, RNA splicing, and degradation by morpholino-based conjugates in *Plasmodium falciparum*. *Proc Natl Acad Sci U S A* **112**, 11935-40 (2015).

231. Lehane, A.M., Hayward, R., Saliba, K.J. & Kirk, K. A verapamil-sensitive chloroquine-associated H+ leak from the digestive vacuole in chloroquine-resistant malaria parasites. *J Cell Sci* **121**, 1624-32 (2008).

232. Lewis, I.A. *et al.* Metabolic QTL Analysis Links Chloroquine Resistance in *Plasmodium falciparum* to Impaired Hemoglobin Catabolism. *PLoS Genet* **10**, e1004085 (2014).

233. Martin, R.E. & Kirk, K. The malaria parasite's chloroquine resistance transporter is a member of the drug/metabolite transporter superfamily. *Mol Biol Evol* **21**, 1938-49 (2004).

234. Patzewitz, E.M. *et al.* Glutathione transport: a new role for PfCRT in chloroquine resistance. *Antioxid Redox Signal* **19**, 683-95 (2013).

235. Maughan, S.C. *et al.* Plant homologs of the *Plasmodium falciparum* chloroquine-resistance transporter, PfCRT, are required for glutathione homeostasis and stress responses. *Proc Natl Acad Sci U S A* **107**, 2331-6 (2010).

236. Tran, C.V. & Saier, M.H., Jr. The principal chloroquine resistance protein of *Plasmodium falciparum* is a member of the drug/metabolite transporter superfamily. *Microbiology* **150**, 1-3 (2004).

237. Aoki, K., Ishida, N. & Kawakita, M. Substrate recognition by nucleotide sugar transporters: further characterization of substrate recognition regions by analyses of UDP-galactose/CMP-sialic acid transporter chimeras and biochemical analysis of the substrate specificity of parental and chimeric transporters. *J Biol Chem* **278**, 22887-93 (2003).

238. Bellanca, S. *et al.* Multiple drugs compete for transport via the *Plasmodium falciparum* chloroquine resistance transporter at distinct but interdependent sites. *J Biol Chem* **289**, 36336-51 (2014).

239. Hartl, D.L. What can we learn from fitness landscapes? *Curr Opin Microbiol* **21**, 51-7 (2014).

240. Hughes, D. & Andersson, D.I. Evolutionary consequences of drug resistance: shared principles across diverse targets and organisms. *Nat Rev Genet* **16**, 459-71 (2015).

241. Rosenthal, P.J. The interplay between drug resistance and fitness in malaria parasites. *Mol Microbiol* **89**, 1025-38 (2013).

242. Gabryszewski, S.J., Modchang, C., Musset, L., Chookajorn, T. & Fidock, D.A. Combinatorial Genetic Modeling of *pfcrt*-Mediated Drug Resistance Evolution in *Plasmodium falciparum*. *Mol Biol Evol* **33**, 1554-70 (2016).

243. Petersen, I. *et al.* Balancing drug resistance and growth rates via compensatory mutations in the *Plasmodium falciparum* chloroquine resistance transporter. *Mol Microbiol* **97**, 381-95 (2015).

244. Mackinnon, M.J. & Marsh, K. The selection landscape of malaria parasites. *Science* **328**, 866-71 (2010).

245. Ogbunugafor, C.B., Wylie, C.S., Diakite, I., Weinreich, D.M. & Hartl, D.L. Adaptive Landscape by Environment Interactions Dictate Evolutionary Dynamics in Models of Drug Resistance. *PLoS Comput Biol* **12**, e1004710 (2016).

246. DePristo, M.A., Weinreich, D.M. & Hartl, D.L. Missense meanderings in sequence space: a biophysical view of protein evolution. *Nat Rev Genet* **6**, 678-87 (2005).

247. Baker, S. *et al.* Fitness benefits in fluoroquinolone-resistant *Salmonella* Typhi in the absence of antimicrobial pressure. *Elife* **2**, e01229 (2013).

248. Brown, K.M. *et al.* Compensatory mutations restore fitness during the evolution of dihydrofolate reductase. *Mol Biol Evol* **27**, 2682-90 (2010).

249. Wootton, J.C. *et al.* Genetic diversity and chloroquine selective sweeps in *Plasmodium falciparum*. *Nature* **418**, 320-3 (2002).

250. Kublin, J.G. *et al.* Reemergence of chloroquine-sensitive *Plasmodium falciparum* malaria after cessation of chloroquine use in Malawi. *J Infect Dis* **187**, 1870-5 (2003).

251. Laufer, M.K. *et al.* Return of chloroquine-susceptible falciparum malaria in Malawi was a reexpansion of diverse susceptible parasites. *J Infect Dis* **202**, 801-8 (2010).

252. Mita, T. *et al.* Expansion of wild type allele rather than back mutation in *pfcrt* explains the recent recovery of chloroquine sensitivity of *Plasmodium falciparum* in Malawi. *Mol Biochem Parasitol* **135**, 159-63 (2004).

253. Chen, N. *et al.* No genetic bottleneck in *Plasmodium falciparum* wild-type *pfcrt* alleles reemerging in Hainan Island, China, following high-level chloroquine resistance. *Antimicrob Agents Chemother* **52**, 345-7 (2008).

254. Wang, X. *et al.* Decreased prevalence of the *Plasmodium falciparum* chloroquine resistance transporter 76T marker associated with cessation of chloroquine use against *P. falciparum* malaria in Hainan, People's Republic of China. *Am J Trop Med Hyg* **72**, 410-4 (2005).

255. Gama, B.E. *et al.* Chloroquine and sulphadoxine-pyrimethamine sensitivity of

Plasmodium falciparum parasites in a Brazilian endemic area. *Malar J* **8**, 156 (2009).

256. Griffing, S. *et al. pfmdr1* amplification and fixation of *pfcrt* chloroquine resistance alleles in *Plasmodium falciparum* in Venezuela. *Antimicrob Agents Chemother* **54**, 1572-9 (2010).

257. Vieira, P.P. *et al. pfcrt* Polymorphism and the spread of chloroquine resistance in *Plasmodium falciparum* populations across the Amazon Basin. *J Infect Dis* **190**, 417-24 (2004).

258. Mallick, P.K. *et al.* Mutant *pfcrt* "SVMNT" haplotype and wild type *pfmdr1* "N86" are endemic in *Plasmodium vivax* dominated areas of India under high chloroquine exposure. *Malar J* **11**, 16 (2012).

259. Sa, J.M. & Twu, O. Protecting the malaria drug arsenal: halting the rise and spread of amodiaquine resistance by monitoring the PfCRT SVMNT type. *Malar J* **9**, 374 (2010).

260. Tan, L.L., Lau, T.Y., Timothy, W. & Prabakaran, D. Full-length sequence analysis of chloroquine resistance transporter gene in *Plasmodium falciparum* isolates from Sabah, Malaysia. *ScientificWorldJournal* **2014**, 935846 (2014).

261. Walliker, D., Hunt, P. & Babiker, H. Fitness of drug-resistant malaria parasites. *Acta Trop* **94**, 251-9 (2005).

262. Durrand, V. *et al.* Variations in the sequence and expression of the *Plasmodium falciparum* chloroquine resistance transporter (PfCRT) and their relationship to chloroquine resistance *in vitro*. *Mol Biochem Parasitol* **136**, 273-85 (2004).

263. Ord, R. *et al.* Seasonal carriage of *pfcrt* and *pfmdr1* alleles in Gambian *Plasmodium falciparum* imply reduced fitness of chloroquine-resistant parasites. *J Infect Dis* **196**, 1613-9 (2007).

264. Tukwasibwe, S. *et al.* Differential prevalence of transporter polymorphisms in symptomatic and asymptomatic falciparum malaria infections in Uganda. *J Infect Dis* **210**, 154-7 (2014).

265. Venkatesan, M. *et al.* Polymorphisms in *Plasmodium falciparum Chloroquine Resistance Transporter* and *Multidrug Resistance 1* Genes: Parasite Risk Factors that Affect Treatment Outcomes for *P. falciparum* Malaria after Artemether-Lumefantrine and Artesunate-Amodiaquine. *Am J Trop Med Hyg* **91**, 833-43 (2014).

266. Mharakurwa, S., Sialumano, M., Liu, K., Scott, A. & Thuma, P. Selection for chloroquine-sensitive *Plasmodium falciparum* by wild *Anopheles arabiensis* in Southern Zambia. *Malar J* **12**, 453 (2013).

267. Osman, M.E., Mockenhaupt, F.P., Bienzle, U., Elbashir, M.I. & Giha, H.A. Field-based evidence for linkage of mutations associated with chloroquine (*pfcrt*/*pfmdr1*) and sulfadoxine-pyrimethamine (*pfdhfr*/*pfdhps*) resistance and for the fitness cost of multiple mutations in *P. falciparum*. *Infect Genet Evol* **7**, 52-9 (2007).

268. Ecker, A., Lakshmanan, V., Sinnis, P., Coppens, I. & Fidock, D.A. Evidence that mutant PfCRT facilitates the transmission to mosquitoes of chloroquine-treated *Plasmodium* gametocytes. *J Infect Dis* **203**, 228-36 (2011).

269. Park, D.J. *et al.* Sequence-based association and selection scans identify drug resistance loci in the *Plasmodium falciparum* malaria parasite. *Proc Natl Acad Sci U S A* **109**, 13052-7 (2012).

270. Trape, J.F. The public health impact of chloroquine resistance in Africa. *Am J Trop Med Hyg* **64**, 12-7 (2001).

271. Wellems, T.E. *Plasmodium* chloroquine resistance and the search for a replacement antimalarial drug. *Science* **298**, 124-6 (2002).

272. Okech, B.A. *et al.* Therapeutic efficacy of chloroquine for the treatment of uncomplicated *Plasmodium falciparum* in Haiti after many decades of its use. *Am J Trop Med Hyg* **92**, 541-5 (2015).

273. Amaratunga, C. *et al.* Chloroquine remains effective for treating *Plasmodium vivax* malaria in Pursat Province, Western Cambodia. *Antimicrob Agents Chemother* **58**, 6270-2 (2014).

274. Fitch, C.D. Ferriprotoporphyrin IX, phospholipids, and the antimalarial actions of quinoline drugs. *Life Sci* **74**, 1957-72 (2004).

275. Summers, R.L., Nash, M.N. & Martin, R.E. Know your enemy: understanding the role of PfCRT in drug resistance could lead to new antimalarial tactics. *Cell Mol Life Sci* **69**, 1967-95 (2012).

276. Hawley, S.R. *et al.* Relationship between antimalarial drug activity, accumulation, and inhibition of heme polymerization in *Plasmodium falciparum in vitro*. *Antimicrob Agents Chemother* **42**, 682-6 (1998).

277. White, N.J. Qinghaosu (artemisinin): the price of success. *Science* **320**, 330-4 (2008).

278. Henriques, G. *et al.* Directional selection at the *pfmdr1*, *pfcrt*, *pfubp1* and *pfap2mu* loci of *Plasmodium falciparum* in Kenyan children treated with ACT. *J Infect Dis* **210**, 2001-8 (2014).

279. Djimde, A.A. *et al.* Clearance of drug-resistant parasites as a model for protective immunity in *Plasmodium falciparum* malaria. *Am J Trop Med Hyg* **69**, 558-63 (2003).

280. Patel, J.J. *et al.* Chloroquine susceptibility and reversibility in a *Plasmodium falciparum* genetic cross. *Mol Microbiol* **78**, 770-87 (2010).

281. Baro, N.K., Callaghan, P.S. & Roepe, P.D. Function of resistance conferring *Plasmodium falciparum* chloroquine resistance transporter isoforms. *Biochemistry* **52**, 4242-9 (2013).

282. Ecker, A., Lewis, R.E., Ekland, E.H., Jayabalasingham, B. & Fidock, D.A. Tricks in *Plasmodium*'s molecular repertoire--escaping 3'UTR excision-based conditional silencing of the chloroquine resistance transporter gene. *Int J Parasitol* **42**, 969-74 (2012).

283. Mekonnen, S.K. *et al.* Return of chloroquine-sensitive *Plasmodium falciparum* parasites and emergence of chloroquine-resistant *Plasmodium vivax* in Ethiopia. *Malar J* **13**, 244 (2014).

284. Mwai, L. *et al.* Chloroquine resistance before and after its withdrawal in Kenya. *Malar J*

8, 106 (2009).

285. Adhin, M.R., Labadie-Bracho, M. & Bretas, G. Molecular surveillance as monitoring tool for drug-resistant *Plasmodium falciparum* in Suriname. *Am J Trop Med Hyg* **89**, 311-6 (2013).

286. de Almeida, A., Arez, A.P., Cravo, P.V. & do Rosario, V.E. Analysis of genetic mutations associated with anti-malarial drug resistance in *Plasmodium falciparum* from the Democratic Republic of East Timor. *Malar J* **8**, 59 (2009).

287. Khattak, A.A. *et al.* A comprehensive survey of polymorphisms conferring anti-malarial resistance in *Plasmodium falciparum* across Pakistan. *Malar J* **12**, 300 (2013).

288. Olson-Manning, C.F., Wagner, M.R. & Mitchell-Olds, T. Adaptive evolution: evaluating empirical support for theoretical predictions. *Nat Rev Genet* **13**, 867-77 (2012).

289. Poelwijk, F.J., Kiviet, D.J., Weinreich, D.M. & Tans, S.J. Empirical fitness landscapes reveal accessible evolutionary paths. *Nature* **445**, 383-6 (2007).

290. Kogenaru, M., de Vos, M.G. & Tans, S.J. Revealing evolutionary pathways by fitness landscape reconstruction. *Crit Rev Biochem Mol Biol* **44**, 169-74 (2009).

291. Weinreich, D.M., Delaney, N.F., Depristo, M.A. & Hartl, D.L. Darwinian evolution can follow only very few mutational paths to fitter proteins. *Science* **312**, 111-4 (2006).

292. Costanzo, M.S., Brown, K.M. & Hartl, D.L. Fitness trade-offs in the evolution of dihydrofolate reductase and drug resistance in *Plasmodium falciparum*. *PLoS One* **6**, e19636 (2011).

293. Jiang, P.P., Corbett-Detig, R.B., Hartl, D.L. & Lozovsky, E.R. Accessible mutational trajectories for the evolution of pyrimethamine resistance in the malaria parasite *Plasmodium vivax*. *J Mol Evol* **77**, 81-91 (2013).

294. de Koning-Ward, T.F., Gilson, P.R. & Crabb, B.S. Advances in molecular genetic systems in malaria. *Nat Rev Microbiol* **13**, 373-87 (2015).

295. Straimer, J. *et al.* Site-specific genome editing in *Plasmodium falciparum* using engineered zinc-finger nucleases. *Nat Methods* **9**, 993-8 (2012).

296. Adjalley, S.H., Lee, M.C. & Fidock, D.A. A method for rapid genetic integration into *Plasmodium falciparum* utilizing mycobacteriophage Bxb1 integrase. *Methods Mol Biol* **634**, 87-100 (2010).

297. Rio, D.C., Ares, M., Jr., Hannon, G.J. & Nilsen, T.W. Purification of RNA using TRIzol (TRI reagent). *Cold Spring Harb Protoc* (2010).

298. Mehlotra, R.K. *et al.* Evolution of a unique *Plasmodium falciparum* chloroquine-resistance phenotype in association with *pfcrt* polymorphism in Papua New Guinea and South America. *Proc Natl Acad Sci U S A* **98**, 12689-94 (2001).

299. Baragana, B. *et al.* A novel multiple-stage antimalarial agent that inhibits protein synthesis. *Nature* **522**, 315-20 (2015).

300. Fu, Y., Tilley, L., Kenny, S. & Klonis, N. Dual labeling with a far red probe permits analysis of growth and oxidative stress in *P. falciparum*-infected erythrocytes. *Cytometry A* **77**, 253-63 (2010).

301. Hartl, D.L. & Clark, A.G. *Principles of population genetics*, xv, 652 p. (Sinauer Associates, Sunderland, Mass., 2007).

302. Kumpornsin, K. *et al.* Origin of Robustness in Generating Drug-Resistant Malaria Parasites. *Mol Biol Evol* **31**, 1649-60 (2014).

303. Burkot, T.R., Williams, J.L. & Schneider, I. Infectivity to mosquitoes of *Plasmodium falciparum* clones grown *in vitro* from the same isolate. *Trans R Soc Trop Med Hyg* **78**, 339-41 (1984).

304. Wongsrichanalai, C., Pickard, A.L., Wernsdorfer, W.H. & Meshnick, S.R. Epidemiology of drug-resistant malaria. *Lancet Infect Dis* **2**, 209-18 (2002).

305. Johnson, D.J. *et al.* Evidence for a central role for PfCRT in conferring *Plasmodium falciparum* resistance to diverse antimalarial agents. *Mol Cell* **15**, 867-77 (2004).

306. Zheng, Q. Mathematical issues arising from the directed mutation controversy. *Genetics* **164**, 373-9 (2003).

307. Bopp, S.E. *et al.* Mitotic evolution of *Plasmodium falciparum* shows a stable core genome but recombination in antigen families. *PLoS Genet* **9**, e1003293 (2013).

308. Claessens, A. *et al.* Generation of antigenic diversity in *Plasmodium falciparum* by structured rearrangement of *var* genes during mitosis. *PLoS Genet* **10**, e1004812 (2014).

309. Brown, T.S. *et al. Plasmodium falciparum* field isolates from areas of repeated emergence of drug resistant malaria show no evidence of hypermutator phenotype. *Infect Genet Evol* **30**, 318-22 (2015).

310. Palmer, A.C. *et al.* Delayed commitment to evolutionary fate in antibiotic resistance fitness landscapes. *Nat Commun* **6**, 7385 (2015).

311. Wellems, T.E. Transporter of a malaria catastrophe. *Nat Med* **10**, 1169-71 (2004).

312. Summers, R.L. *et al.* Diverse mutational pathways converge on saturable chloroquine transport via the malaria parasite's chloroquine resistance transporter. *Proc Natl Acad Sci U S A* **111**, E1759-67 (2014).

313. Wu, E.Y. *et al.* A conservative isoleucine to leucine mutation causes major rearrangements and cold sensitivity in KlenTaq1 DNA polymerase. *Biochemistry* **54**, 881-9 (2015).

314. Cooper, R.A., Hartwig, C.L. & Ferdig, M.T. *pfcrt* is more than the *Plasmodium falciparum* chloroquine resistance gene: a functional and evolutionary perspective. *Acta Trop* **94**, 170-80 (2005).

315. Hastings, I.M., Watkins, W.M. & White, N.J. The evolution of drug-resistant malaria: the role of drug elimination half-life. *Philos Trans R Soc Lond B Biol Sci* **357**, 505-19 (2002).

316. Wellems, T.E. *et al.* Chloroquine resistance not linked to *mdr*-like genes in a *Plasmodium*

falciparum cross. *Nature* **345**, 253-5 (1990).

317. Sanchez, C.P., Dave, A., Stein, W.D. & Lanzer, M. Transporters as mediators of drug resistance in *Plasmodium falciparum*. *Int J Parasitol* **40**, 1109-18 (2010).

318. Mehlotra, R.K. *et al.* Discordant patterns of genetic variation at two chloroquine resistance loci in worldwide populations of the malaria parasite *Plasmodium falciparum*. *Antimicrob Agents Chemother* **52**, 2212-22 (2008).

319. Nagesha, H.S. *et al.* New haplotypes of the *Plasmodium falciparum* chloroquine resistance transporter (*pfcrt*) gene among chloroquine-resistant parasite isolates. *Am J Trop Med Hyg* **68**, 398-402 (2003).

320. Koleala, T. *et al.* Temporal changes in *Plasmodium falciparum* anti-malarial drug sensitivity *in vitro* and resistance-associated genetic mutations in isolates from Papua New Guinea. *Malar J* **14**, 37 (2015).

321. Chauhan, K., Pande, V. & Das, A. DNA sequence polymorphisms of the *pfmdr1* gene and association of mutations with the *pfcrt* gene in Indian *Plasmodium falciparum* isolates. *Infect Genet Evol* **26**, 213-22 (2014).

322. Gama, B.E. *et al. Plasmodium falciparum* isolates from Angola show the StctVMNT haplotype in the *pfcrt* gene. *Malar J* **9**, 174 (2010).

323. Beshir, K. *et al.* Amodiaquine resistance in *Plasmodium falciparum* malaria in Afghanistan is associated with the *pfcrt* SVMNT allele at codons 72 to 76. *Antimicrob Agents Chemother* **54**, 3714-6 (2010).

324. Gustafsson, L.L. *et al.* Disposition of chloroquine in man after single intravenous and oral doses. *Br J Clin Pharmacol* **15**, 471-9 (1983).

325. Miotto, O. *et al.* Multiple populations of artemisinin-resistant *Plasmodium falciparum* in Cambodia. *Nat Genet* **45**, 648-55 (2013).

326. Roper, C. *et al.* Intercontinental spread of pyrimethamine-resistant malaria. *Science* **305**, 1124 (2004).

327. Carter, R. & Mendis, K.N. Evolutionary and historical aspects of the burden of malaria. *Clin Microbiol Rev* **15**, 564-94 (2002).

328. Jones, R.A., Panda, S.S. & Hall, C.D. Quinine conjugates and quinine analogues as potential antimalarial agents. *Eur J Med Chem* **97**, 335-355 (2015).

329. Volkman, S.K., Neafsey, D.E., Schaffner, S.F., Park, D.J. & Wirth, D.F. Harnessing genomics and genome biology to understand malaria biology. *Nat Rev Genet* **13**, 315-28 (2012).

330. Reed, M.B., Saliba, K.J., Caruana, S.R., Kirk, K. & Cowman, A.F. Pgh1 modulates sensitivity and resistance to multiple antimalarials in *Plasmodium falciparum*. *Nature* **403**, 906-9 (2000).

331. Ashley, E.A. *et al.* Spread of artemisinin resistance in *Plasmodium falciparum* malaria. *N Engl J Med* **371**, 411-23 (2014).

332. Frosch, A.E. *et al.* Return of Widespread Chloroquine-Sensitive *Plasmodium falciparum* to Malawi. *J Infect Dis* (2014).

333. Adjalley, S.H. *et al.* Quantitative assessment of *Plasmodium falciparum* sexual development reveals potent transmission-blocking activity by methylene blue. *Proc Natl Acad Sci U S A* **108**, E1214-23 (2011).

334. Combrinck, J.M. *et al.* Optimization of a multi-well colorimetric assay to determine haem species in *Plasmodium falciparum* in the presence of anti-malarials. *Malar J* **14**, 253 (2015).

335. Makler, M.T. *et al.* Parasite lactate dehydrogenase as an assay for *Plasmodium falciparum* drug sensitivity. *Am J Trop Med Hyg* **48**, 739-41 (1993).

336. Baro, N.K., Pooput, C. & Roepe, P.D. Analysis of chloroquine resistance transporter (CRT) isoforms and orthologues in *S. cerevisiae* yeast. *Biochemistry* **50**, 6701-10 (2011).

337. Gligorijevic, B., McAllister, R., Urbach, J.S. & Roepe, P.D. Spinning disk confocal microscopy of live, intraerythrocytic malarial parasites. 1. Quantification of hemozoin development for drug sensitive versus resistant malaria. *Biochemistry* **45**, 12400-10 (2006).

338. Sherlach, K.S. & Roepe, P.D. Determination of the cytostatic and cytocidal activities of antimalarial compounds and their combination interactions. *Curr Protoc Chem Biol* **6**, 237-48 (2014).

339. Dzekunov, S.M., Ursos, L.M. & Roepe, P.D. Digestive vacuolar pH of intact intraerythrocytic *P. falciparum* either sensitive or resistant to chloroquine. *Mol Biochem Parasitol* **110**, 107-24 (2000).

340. Goldberg, D.E. Complex nature of malaria parasite hemoglobin degradation. *Proc Natl Acad Sci U S A* **110**, 5283-4 (2013).

341. Hardie, D.G., Ross, F.A. & Hawley, S.A. AMPK: a nutrient and energy sensor that maintains energy homeostasis. *Nat Rev Mol Cell Biol* **13**, 251-62 (2012).

342. Ke, H. *et al.* Genetic investigation of tricarboxylic acid metabolism during the *Plasmodium falciparum* life cycle. *Cell Rep* **11**, 164-74 (2015).

343. Sandlin, R.D. *et al.* Identification of beta-hematin inhibitors in a high-throughput screening effort reveals scaffolds with *in vitro* antimalarial activity. *Int J Parasitol Drugs Drug Resist* **4**, 316-25 (2014).

344. Schmitt, T.H., Frezzatti, W.A., Jr. & Schreier, S. Hemin-induced lipid membrane disorder and increased permeability: a molecular model for the mechanism of cell lysis. *Arch Biochem Biophys* **307**, 96-103 (1993).

345. Callaghan, P.S., Siriwardana, A., Hassett, M.R. & Roepe, P.D. *Plasmodium falciparum* chloroquine resistance transporter (PfCRT) isoforms PH1 and PH2 perturb vacuolar physiology. *Malar J* **15**, 186 (2016).

346. Famin, O. & Ginsburg, H. Differential effects of 4-aminoquinoline-containing antimalarial drugs on hemoglobin digestion in *Plasmodium falciparum*-infected erythrocytes. *Biochem*

Pharmacol **63**, 393-8 (2002).

347. Roberts, L., Egan, T.J., Joiner, K.A. & Hoppe, H.C. Differential effects of quinoline antimalarials on endocytosis in *Plasmodium falciparum*. *Antimicrob Agents Chemother* **52**, 1840-2 (2008).

348. Elliott, D.A. *et al.* Four distinct pathways of hemoglobin uptake in the malaria parasite *Plasmodium falciparum*. *Proc Natl Acad Sci U S A* **105**, 2463-8 (2008).

349. Ogbunugafor, C.B. & Hartl, D. A pivot mutation impedes reverse evolution across an adaptive landscape for drug resistance in *Plasmodium vivax*. *Malar J* **15**, 40 (2016).

350. Chen, N. *et al. pfcrt* Allelic types with two novel amino acid mutations in chloroquine-resistant *Plasmodium falciparum* isolates from the Philippines. *Antimicrob Agents Chemother* **47**, 3500-5 (2003).

351. Yang, Z. *et al.* Molecular analysis of chloroquine resistance in *Plasmodium falciparum* in Yunnan Province, China. *Trop Med Int Health* **12**, 1051-60 (2007).

352. Jiang, H. *et al.* Genome-wide compensatory changes accompany drug-selected mutations in the *Plasmodium falciparum crt* gene. *PLoS One* **3**, e2484 (2008).

353. Lee, M.C. & Fidock, D.A. CRISPR-mediated genome editing of *Plasmodium falciparum* malaria parasites. *Genome Med* **6**, 63 (2014).

354. Dondorp, A.M. *et al.* Artemisinin resistance in *Plasmodium falciparum* malaria. *N Engl J Med* **361**, 455-67 (2009).

355. Amaratunga, C., Neal, A.T. & Fairhurst, R.M. Flow cytometry-based analysis of artemisinin-resistant *Plasmodium falciparum* in the ring-stage survival assay. *Antimicrob Agents Chemother* (2014).

356. Taylor, S.M. *et al.* Absence of putative artemisinin resistance mutations among *Plasmodium falciparum* in Sub-Saharan Africa: a molecular epidemiologic study. *J Infect Dis* **211**, 680-8 (2015).

357. Kamau, E. *et al.* K13-propeller polymorphisms in *Plasmodium falciparum* parasites from sub-Saharan Africa. *J Infect Dis* **211**, 1352-5 (2015).

358. Chaorattanakawee, S. *et al. Ex vivo* drug susceptibility and molecular profiling of clinical *Plasmodium falciparum* isolates from Cambodia in 2008-2013 suggest emerging piperaquine resistance. *Antimicrob Agents Chemother* (2015).

359. Sisowath, C. *et al.* The role of *pfmdr1* in *Plasmodium falciparum* tolerance to artemether-lumefantrine in Africa. *Trop Med Int Health* **12**, 736-42 (2007).

360. Baraka, V. *et al. In vivo* selection of *Plasmodium falciparum* Pfcrt and Pfmdr1 variants by artemether-lumefantrine and dihydroartemisinin-piperaquine in Burkina Faso. *Antimicrob Agents Chemother* **59**, 734-7 (2015).

361. Hsieh, P.C. & Vaisvila, R. Protein engineering: single or multiple site-directed mutagenesis. *Methods Mol Biol* **978**, 173-86 (2013).

362. WorldWide Antimalarial Resistance Network, *et al.* The effect of dosing strategies on the therapeutic efficacy of artesunate-amodiaquine for uncomplicated malaria: a meta-analysis of individual patient data. *BMC Med* **13**, 66 (2015).

363. Kasozi, D., Mohring, F., Rahlfs, S., Meyer, A.J. & Becker, K. Real-time imaging of the intracellular glutathione redox potential in the malaria parasite *Plasmodium falciparum*. *PLoS Pathog* **9**, e1003782 (2013).

364. Patzewitz, E.M., Wong, E.H. & Muller, S. Dissecting the role of glutathione biosynthesis in *Plasmodium falciparum*. *Mol Microbiol* **83**, 304-18 (2012).

365. Fairhurst, R.M. High Antimalarial Efficacy of Dihydroartemisinin-Piperaquine on the China-Myanmar Border: The Calm Before the Storm. *Am J Trop Med Hyg* **93**, 436-7 (2015).

366. Tarning, J. *et al.* Population pharmacokinetics of piperaquine after two different treatment regimens with dihydroartemisinin-piperaquine in patients with *Plasmodium falciparum* malaria in Thailand. *Antimicrob Agents Chemother* **52**, 1052-61 (2008).

367. White, N.J. Pharmacokinetic and pharmacodynamic considerations in antimalarial dose optimization. *Antimicrob Agents Chemother* **57**, 5792-807 (2013).

368. Adjalley, S.H., Scanfeld, D., Kozlowski, E., Llinas, M. & Fidock, D.A. Genome-wide transcriptome profiling reveals functional networks involving the *Plasmodium falciparum* drug resistance transporters PfCRT and PfMDR1. *BMC Genomics* **16**, 1090 (2015).

369. Antonia, A.L. *et al.* A Cross-Sectional Survey of *Plasmodium falciparum pfcrt* Mutant Haplotypes in the Democratic Republic of Congo. *Am J Trop Med Hyg* (2014).

370. Gbotosho, G.O. *et al.* Different patterns of *pfcrt* and *pfmdr1* polymorphisms in *P. falciparum* isolates from Nigeria and Brazil: the potential role of antimalarial drug selection pressure. *Am J Trop Med Hyg* **86**, 211-3 (2012).

371. Paguio, M.F., Bogle, K.L. & Roepe, P.D. *Plasmodium falciparum* resistance to cytocidal versus cytostatic effects of chloroquine. *Mol Biochem Parasitol* **178**, 1-6 (2011).

372. Zhang, H., Howard, E.M. & Roepe, P.D. Analysis of the antimalarial drug resistance protein PfCRT expressed in yeast. *J Biol Chem* **277**, 49767-75 (2002).

373. Radfar, A., Diez, A. & Bautista, J.M. Chloroquine mediates specific proteome oxidative damage across the erythrocytic cycle of resistant *Plasmodium falciparum*. *Free Radic Biol Med* **44**, 2034-42 (2008).

374. Ginsburg, H. & Golenser, J. Glutathione is involved in the antimalarial action of chloroquine and its modulation affects drug sensitivity of human and murine species of *Plasmodium*. *Redox Rep* **8**, 276-9 (2003).

375. Malhotra, K., Salmon, D., Le Bras, J. & Vilde, J.L. Potentiation of chloroquine activity against *Plasmodium falciparum* by the peroxidase-hydrogen peroxide system. *Antimicrob Agents Chemother* **34**, 1981-5 (1990).

376. Lee, J.W. & Helmann, J.D. Functional specialization within the Fur family of metalloregulators. *Biometals* **20**, 485-99 (2007).

377. Yang, J., Panek, H.R. & O'Brian, M.R. Oxidative stress promotes degradation of the Irr protein to regulate haem biosynthesis in Bradyrhizobium japonicum. *Mol Microbiol* **60**, 209-18 (2006).

378. Lisewski, A.M. *et al.* Supergenomic Network Compression and the Discovery of EXP1 as a Glutathione Transferase Inhibited by Artesunate. *Cell* **158**, 916-28 (2014).

379. Gadalla, N.B. *et al.* Alternatively spliced transcripts and novel pseudogenes of the *Plasmodium falciparum* resistance-associated locus *pfcrt* detected in East African malaria patients. *J Antimicrob Chemother* (2014).

380. Flannery, E.L. *et al.* Next-Generation Sequencing of Patient Samples Shows Evidence of Direct Evolution in Drug-Resistance Genes. *ACS Infect Dis* **1**, 367-379 (2015).

381. Ocholla, H. *et al.* Whole-genome scans provide evidence of adaptive evolution in Malawian *Plasmodium falciparum* isolates. *J Infect Dis* **210**, 1991-2000 (2014).

382. Mwai, L. *et al. In vitro* activities of piperaquine, lumefantrine, and dihydroartemisinin in Kenyan *Plasmodium falciparum* isolates and polymorphisms in *pfcrt* and *pfmdr1*. *Antimicrob Agents Chemother* **53**, 5069-73 (2009).

383. Some, A.F. *et al.* Selection of drug resistance-mediating *Plasmodium falciparum* genetic polymorphisms by seasonal malaria chemoprevention in Burkina Faso. *Antimicrob Agents Chemother* (2014).

384. Smithuis, F. *et al.* Effectiveness of five artemisinin combination regimens with or without primaquine in uncomplicated falciparum malaria: an open-label randomised trial. *Lancet Infect Dis* **10**, 673-81 (2010).

385. Nwaka, S. & Ridley, R.G. Virtual drug discovery and development for neglected diseases through public-private partnerships. *Nat Rev Drug Discov* **2**, 919-28 (2003).

386. Chugh, M. *et al.* Identification and Deconvolution of Cross-Resistance Signals from Antimalarial Compounds Using Multidrug-Resistant *Plasmodium falciparum* Strains. *Antimicrob Agents Chemother* **59**, 1110-8 (2015).

387. Yuan, J. *et al.* Chemical genomic profiling for antimalarial therapies, response signatures, and molecular targets. *Science* **333**, 724-9 (2011).

APPENDIX A: BALANCING DRUG RESISTANCE AND GROWTH RATES VIA COMPENSATORY MUTATIONS IN THE *PLASMODIUM FALCIPARUM* CHLOROQUINE RESISTANCE TRANSPORTER

Ines Petersen,[1,2] **Stanislaw J. Gabryszewski**,[1] Geoffrey L. Johnston,[1,3] Satish K. Dhingra,[1,4] Andrea Ecker,[1,3] Rebecca E. Lewis,[1,3] Mariana Justino de Almeida,[1] Judith Straimer,[1] Philipp P. Henrich,[1] Eugene Palatulan,[1] David J. Johnson,[1] Olivia Coburn-Flynn,[1] Cecilia Sanchez,[1] Adele M. Lehane,[1] Michael Lanzer,[2] David A. Fidock,[1,5]

[1]Department of Microbiology and Immunology, Columbia University Medical Center, New York, NY 10032, USA; [2]Hygiene Institut, Abteilung Parasitologie, Universitätsklinikum Heidelberg, 69120 Heidelberg, Germany; [3]School of International and Public Affairs, Columbia University, New York, NY 10027, USA; [4]Department of Biological Sciences, Binghamton University, Binghamton, NY 13902, USA; [5]Division of Infectious Diseases, Department of Medicine, Columbia University Medical Center, New York, NY 10032, USA.

Author contributions: IP, AML, and DAF conceived and designed the experiments; IP, AE, REL, MJA, JS, EP, DJJ, OCF, CS, and AML performed the experiments; IP, **SJG**, GLJ, AE, SKD, PPH, AML, ML, and DAF analyzed the data; IP, **SJG**, GLJ, AML, and DAF wrote the paper.

Molecular Microbiology (2015) 97(2), 381–395 ■
doi:10.1111/mmi.13035
First published online 20 May 2015

Balancing drug resistance and growth rates via compensatory mutations in the *Plasmodium falciparum* chloroquine resistance transporter

Ines Petersen,[1,2] Stanislaw J. Gabryszewski,[1] Geoffrey L. Johnston,[1,3] Satish K. Dhingra,[1,4] Andrea Ecker,[1] Rebecca E. Lewis,[1] Mariana Justino de Almeida,[1] Judith Straimer,[1] Philipp P. Henrich,[1] Eugene Palatulan,[1] David J. Johnson,[1] Olivia Coburn-Flynn,[1] Cecilia Sanchez,[2] Adele M. Lehane,[1,‡] Michael Lanzer[2] and David A. Fidock[1,5*]

[1]*Department of Microbiology and Immunology, Columbia University Medical Center, New York, NY 10032, USA.*
[2]*Hygiene Institut, Abteilung Parasitologie, Universitätsklinikum Heidelberg, 69120 Heidelberg, Germany.*
[3]*School of International and Public Affairs, Columbia University, New York, NY 10027, USA.*
[4]*Department of Biological Sciences, Binghamton University, Binghamton, NY 13902, USA.*
[5]*Division of Infectious Diseases, Department of Medicine, Columbia University Medical Center, New York, NY 10032, USA*

Summary

The widespread use of chloroquine to treat *Plasmodium falciparum* infections has resulted in the selection and dissemination of variant haplotypes of the primary resistance determinant PfCRT. These haplotypes have encountered drug pressure and within-host competition with wild-type drug-sensitive parasites. To examine these selective forces *in vitro*, we genetically engineered *P. falciparum* to express geographically diverse PfCRT haplotypes. Variant alleles from the Philippines (PH1 and PH2, which differ solely by the C72S mutation) both conferred a moderate gain of chloroquine resistance and a reduction in growth rates *in vitro*. Of the two, PH2 showed higher IC_{50} values, contrasting with reduced growth. Furthermore, a highly mutated *pfcrt* allele from Cambodia (Cam734) conferred moderate chloroquine resistance and enhanced growth rates, when tested against wild-type *pfcrt* in co-culture competition assays. These three alleles mediated cross-resistance to amodiaquine, an antimalarial drug widely used in Africa. Each allele, along with the globally prevalent Dd2 and 7G8 alleles, rendered parasites more susceptible to lumefantrine, the partner drug used in the leading first-line artemisinin-based combination therapy. These data reveal ongoing region-specific evolution of PfCRT that impacts drug susceptibility and relative fitness in settings of mixed infections, and raise important considerations about optimal agents to treat chloroquine-resistant malaria.

Accepted 17 April, 2015. *For correspondence. E-mail df2260@cumc.columbia.edu; Tel. (+1) 212 305 0816; Fax (+1) 212 305 4038. ‡Present address: Research School of Biology, The Australian National University, Canberra, ACT 2601, Australia.

Introduction

In functionally constrained genes, the rise of non-synonymous mutations may decrease an organism's fitness by steering it away from a long-optimized machinery of closely interacting components. Without a specific selective pressure, the more fit wild-type usually predominates at the population level and the less fit variants are either eliminated or persist at low frequencies (Mitchell-Olds *et al.*, 2007). An example of selective pressure is the use of drugs to treat human pathogens. As such, drug-resistant pathogens constitute an ideal group in which to study the balance between surviving drug pressure and remaining competitive with wild-type organisms.

Generally, fitness costs associated with initial resistance-conferring mutations will lead to the attrition of mutants upon the removal of drug pressure, allowing for the reemergence of surviving wild-type organisms (Hastings and Donnelly, 2005). However, prolonged drug exposure can provide pathogens the opportunity to acquire additional mutations, either within the primary resistance determinant or within secondary factors, which compensate for the initial fitness cost (Brown *et al.*, 2010). Competition between mutants carrying those compensatory mutations can then take place, leading to a mutant population with a reduced fitness cost that eventually can successfully compete with wild-type organisms in a drug-free environment (Levin *et al.*, 2000). Fitness costs and the prevalence of initial resistance-conferring mutations can

also be influenced by the use of other drugs to replace the failed therapeutic agent, particularly in instances where their efficacy is impacted by the same resistance determinants.

The malarial parasite *Plasmodium falciparum*, which caused an estimated 198 million clinical cases and 584 000 deaths in 2013 (WHO, 2014), is a prime example of a human pathogen that repeatedly encounters drug pressure and within-host competition among parasite strains. For much of the 20th century, the antimalarial treatment of choice was chloroquine (CQ), a drug characterized by its rapidity of action, safety and low cost. This drug prevents the detoxification of reactive iron-containing heme that is liberated as a result of hemoglobin proteolysis in the acidic digestive vacuole (DV) of intra-erythrocytic parasites (Fitch, 2004). CQ resistance (CQR) emerged slowly, but by the early 1990s had taken hold across virtually all the malaria-endemic world (Wellems and Plowe, 2001). The cellular basis for CQR has been attributed to reduced CQ accumulation in the DV, resulting in diminished access of CQ to its otherwise toxic heme target (Saliba *et al*., 1998).

At the molecular level, CQR has been traced primarily to amino acid changes in the DV transmembrane protein PfCRT (Fidock *et al*., 2000). These include K76T, ubiquitous among CQ-resistant strains and a highly sensitive marker of CQ treatment failure, as well as three to eight additional PfCRT polymorphisms that produce region-specific haplotypes (Ecker *et al*., 2012). These haplotypes reflect a handful of origins of mutant *pfcrt* that disseminated under drug pressure in selective sweeps across the world (Nash *et al*., 2005; Kidgell *et al*., 2006; Mu *et al*., 2010; Park *et al*., 2012). At least 34 different mutant PfCRT haplotypes have been reported, contrasting with a conserved wild-type haplotype in CQ-sensitive parasites (Isozumi *et al*., 2010; Ecker *et al*., 2012; Baro *et al*., 2013). In Malawi, the prevalent African mutant form of PfCRT (CVIET haplotype at positions 72–76, found in strains including Dd2) largely disappeared within several years of CQ withdrawal, presumably due to a fitness cost that rendered this variant less competitive than *pfcrt* wild-type parasites in the absence of drug pressure (Kublin *et al*., 2003; Mita *et al*., 2003; Laufer *et al*., 2010).

The notion that mutation of PfCRT negatively impacts parasite fitness in field settings is supported by recent *in vitro* metabolomic and allelic competition investigations, which revealed a defect in hemoglobin catabolism and reduced relative growth rates *in vitro*, interpreted as a proxy of fitness costs for the CQ-resistant Dd2 and 7G8 PfCRT haplotypes (Lewis *et al*., 2014). Consistent with these findings, a fitness disadvantage was observed for CQ-resistant parasites during the dry season in The Gambia, when drug pressure is transiently removed and transmission is low (Ord *et al*., 2007). This fitness disadvantage was recapitulated in southern Zambia at the level of vectorial selection, whereby the wild-type (K76) form of PfCRT was significantly enriched in the infected *Anopheles arabiensis* mosquitoes compared with its baseline prevalence in the local infected human populations (Mharakurwa *et al*., 2013). Field studies in South America and Asia, however, have documented no or only modest attrition in mutant PfCRT forms, including 7G8 (SVMNT haplotype at positions 72–76), despite the discontinued use of CQ for the treatment of *P. falciparum* malaria for over two decades (Wang *et al*., 2005; Chen *et al*., 2008; Griffing *et al*., 2010). Those studies have led to the suggestion that the fitness cost of parasites harboring the ^{72}SVMNT^{76} haplotype may be less severe than that of parasites carrying the ^{72}CVIET^{76} signature (Sa and Twu, 2010).

Aside from regional differences in the choice of antimalarial drug regimens that may help sustain variant PfCRT haplotypes (Ecker *et al*., 2012), studies of human and murine parasites highlight a potential selective advantage of mutant *pfcrt* alleles in enhancing human to mosquito transmission of parasites following CQ treatment. Among Sudanese parasite isolates bearing the K76T mutation in PfCRT, a higher gametocyte carriage rate was observed as compared with parasites encoding wild-type PfCRT (Osman *et al*., 2007). Furthermore, *P. berghei* parasites engineered to express the *P. falciparum* 7G8 *pfcrt* variant protected early gametocytes against CQ action and were transmitted at higher levels compared with drug-sensitive parasites (Ecker *et al*., 2011). These observations underscore the complexity of factors that collectively determine the fitness of *Plasmodium* parasites, of which relative growth rates in infected erythrocytes is but one component, with others including antimalarial drug susceptibility profiles, the impact of host immunity and transmission dynamics, differences in gametocyte production and infectivity, competition between strains within mosquitoes, and growth differences that could manifest during the liver stages (Walliker *et al*., 2005; Rosenthal, 2013).

Here, we dissect the specific contribution of geographically distinct PfCRT haplotypes to parasite *in vitro* relative growth rates and antimalarial drug susceptibility. Our study includes novel haplotypes that have not been previously assessed in a controlled genetic background, including two closely related PfCRT isoforms from the Philippines (Chen *et al*., 2005), as well as an allele from Cambodia that harbors nine mutations, an exceptionally high number (Durrand *et al*., 2004). These alleles were assessed alongside the geographically widespread Dd2 and 7G8 alleles *in vitro* in drug susceptibility assays as well as mixed-infection competition assays. We also investigated how various mutant PfCRT haplotypes impact CQ accumulation and parasite response to other

Table 1. Transformation status and PfCRT haplotype of recombinant and wild-type lines.

			Functional PfCRT haplotype													
Clone	Parent	Transfection plasmid	72	74	75	76	144	148	160	194	220	271	326	333	356	371
GC03	HB3 × Dd2	–	C	M	N	K	A	L	L	I	A	Q	N	T	I	R
$C1^{GC03}$	GC03	phDHFR-crt-$GC03^{Pf3'}$	C	M	N	K	A	L	L	I	A	Q	N	T	I	R
$C8^{PH1-II}$	$C1^{GC03}$	pBSD-crt-$PH1^{Py3'}$	C	M	N	T	T	L	Y	I	A	Q	D	T	I	R
$C10^{PH2-I,II}$	$C1^{GC03}$	pBSD-crt-$PH2^{Py3'}$	S	M	N	T	T	L	Y	I	A	Q	D	T	I	R
$C12^{Cam734-I,II}$	$C1^{GC03}$	pBSD-crt-$Cam734^{Py3'}$	C	I	D	T	F	I	L	T	S	E	N	S	I	R
$C2^{GC03}$	$C1^{GC03}$	pBSD-crt-$GC03^{Pf3'}$	C	M	N	K	A	L	L	I	A	Q	N	T	I	R
$C4^{Dd2}$	$C1^{GC03}$	pBSD-crt-$Dd2^{Py3'}$	C	I	E	T	A	L	L	I	S	E	S	T	T	I
$C6^{7G8}$	$C1^{GC03}$	pBSD-crt-$7G8^{Py3'}$	S	M	N	T	A	L	L	I	S	Q	D	T	L	R
HB3	–	–	C	M	N	K	A	L	L	I	A	Q	N	T	I	R
Dd2	–	–	C	I	E	T	A	L	L	I	S	E	S	T	T	I
7G8	–	–	S	M	N	T	A	L	L	I	S	Q	D	T	L	R

Plasmids harboring different *pfcrt* allelic sequences were transfected into CQ-sensitive $C1^{GC03}$ parasites to generate the recombinant mutant and control lines. Grey shading indicates residues that differ from the wild-type sequence.

antimalarials in current clinical use. Our results highlight the importance of regional PfCRT haplotypes in contributing to parasite fitness and define a novel allele in Cambodia that appears to have overcome the hurdle of reduced fitness associated with less mutated *pfcrt* forms while still maintaining a moderate degree of CQR.

Results

Generation of isogenic parasite lines expressing Asian pfcrt *alleles from the endogenous locus by allelic exchange*

We engineered the mutant *pfcrt* alleles PH1 and PH2 (from the Philippines) and Cam734 (from Cambodia) into *P. falciparum* CQ-sensitive parasites via allelic exchange. The recipient CQ-sensitive strain $C1^{GC03}$ was genetically modified from the GC03 parasite line, a progeny of the HB3 × Dd2 genetic cross (Su *et al.*, 1997), in a prior round of transfection. Briefly, the highly interrupted endogenous wild-type *pfcrt* gene sequence was replaced with a shortened sequence containing all exons and intron 1, rendering this line more amenable to *pfcrt* allelic exchange (Sidhu *et al.*, 2002). PH1 and PH2 represent two common PfCRT haplotypes in the Philippines (Chen *et al.*, 2003) that differ from one another at position 72 and that are notable for lacking the common A220S mutation but harboring the two novel mutations A144T and L160Y (Table 1). Cam734 comprises ~ 20% of all *pfcrt* alleles in Cambodia and is a highly mutated *pfcrt* allele, differing from the wild-type allele at nine positions (Durrand *et al.*, 2004).

To generate recombinants, $C1^{GC03}$ parasites were electroporated with the plasmids pBSD-crt-$PH1^{Py3'}$, pBSD-crt-$PH2^{Py3'}$ and pBSD-crt-$Cam734^{Py3'}$, containing exons 2–13 of the three Asian *pfcrt* alleles (Fig. 1A). Transfected parasite cultures were obtained following exposure to blasticidin and WR99210 to select for expression of *blasticidin S-deaminase* (*bsd*) from the transfection plasmid and human *dihydrofolate reductase* (*dhfr*) in the $C1^{GC03}$ parental line respectively.

Polymerase chain reaction (PCR) was used to identify transfected lines that had undergone homologous recombination and single-site cross-over into the *pfcrt* locus. Recombinant clones were then obtained by limiting dilution. Clones from each successfully integrated transfection were selected for further characterization and were termed $C8^{PH1-I}$, $C8^{PH1-II}$, $C10^{PH2-I}$, $C10^{PH2-II}$, $C12^{Cam734-I}$ and $C12^{Cam734-II}$. Following our earlier reports (Sidhu *et al.*, 2002), the superscript indicates the *pfcrt* allele, with the Roman numeral indicating the clone. For comparison, we included $C1^{GC03}$, which was generated using the same allelic exchange strategy (Sidhu *et al.*, 2002) and which expresses the canonical wild-type allele (Table 1).

To confirm the clonality of these lines, we performed PCR with primers P1 and P3 that targeted parasites with integrated plasmid and primers P1 and P2 that were specific for the original $C1^{GC03}$ locus (Fig. 1A and B; Table S1). Primers P1 and P3 yielded the expected 1.3 kb band from the clones that had undergone two rounds of recombination, but not from the first-round $C1^{GC03}$ or parental GC03 parasites. PCR with primers P1 and P2 resulted in expected bands of 3.3 kb from the unmodified genomic *pfcrt* locus in GC03 and 1.7 kb from the first round of recombination present in the $C1^{GC03}$ line (Fig. 1B). Southern blot analysis of genomic DNA (gDNA) digested with SalI + ClaI revealed band sizes of ~ 16.3 kb, 8.1 kb, 7.7 kb and 1.2 kb, consistent with plasmid integration into the $C1^{GC03}$ *pfcrt* locus (Fig. 1C). GC03 parasites and linearized plasmid DNA showed the predicted 9.4 kb and 7.7 kb bands respectively.

Sequencing of the functional recombinant *pfcrt* locus amplified from gDNA, which was performed shortly after limiting dilution cloning, confirmed the expected full-length

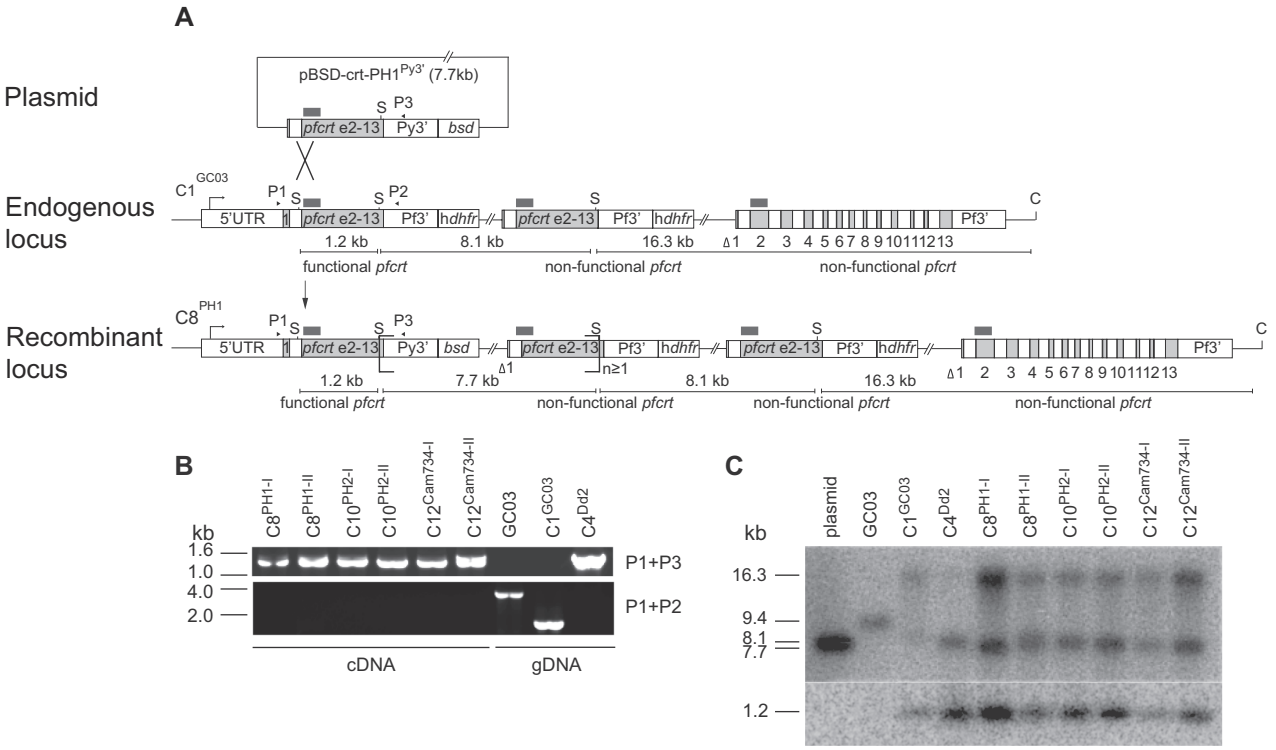

Fig. 1. *pfcrt* allelic exchange strategy and molecular characterization of clones.
A. Schematic representation of single-site cross-over between a pBSD-based *pfcrt* transfection plasmid and the functional *pfcrt* locus of $C1^{GC03}$, leading to expression of a recombinant allele (PH1, PH2, or Cam734; see Table 1) from the endogenous full-length promoter. The diagram illustrates transfection of the CQ-sensitive $C1^{GC03}$ clone with pBSD-crt-$PH1^{Py3'}$. This construct contained a *pfcrt* sequence with a deletion in exon 1, no introns between exons 2–13 and a downstream 0.7 kb 3′ UTR sequence from the *P. yoelii* ortholog *pycrt*. Homologous recombination upstream of codon positions 74–76 resulted in generation of a functional *pfcrt* allele containing all the point mutations from the mutant PH1 allele, under the control of *pfcrt* 5′ UTR and *pycrt* 3′ UTR regulatory elements. Downstream remnant *pfcrt* fragments were truncated in exon 1, had a 5′ in-frame stop codon and lacked a promoter.
B. PCR-based analysis of the recombinant clones and parental lines (primer positions illustrated in A). Parasite strain and primer details are provided in Table 1 and Table S1 respectively.
C. Southern blot hybridization of gDNA digested with SalI and ClaI and subsequently probed with a *pfcrt* fragment from exon 2. The positions of the restriction sites and exon 2-specific probe are indicated in A. B and C include the clone $C8^{PH1-I}$, which was subsequently found to have undergone a spontaneous back mutation in codon 326 and was removed from further analysis.

sequence of *pfcrt* in the individual lines. Amplification of the *pfcrt* locus from cDNA and gDNA and subsequent sequencing of the polymorphic region coding for amino acids 72–76 confirmed the exclusive expression of the integrated allele in the new second-round recombinants (data not shown). Real-time PCR analysis was also performed using two independent preparations of parasite RNA from synchronized ring-stage cultures. These were assayed for *pfcrt* and the housekeeping gene *actin* (PFL2215w) on four to eight independent occasions with each sample tested in triplicate per assay. Kruskal–Wallis tests showed no significant differences in *pfcrt* transcript levels between any *pfcrt*-modified lines (Table S2). The same finding of statistically indistinguishable expression levels was observed by quantitative Western blot analysis of protein extracts from these recombinant lines (Table S2).

Ongoing characterization of these recombinant lines, during the lengthy period of propagation required to complete their phenotypic assessment, revealed a highly unusual event in the $C8^{PH1-I}$ clone. Over time, a subpopulation arose that outgrew the original line. This subpopulation was found to have undergone reversion of the N326D mutation back to the wild-type N326 codon in *pfcrt*, with the other three PH1 mutations being retained (K76T, A144T and L160Y; Table 1). Interestingly, this revertant was found to be CQ sensitive, implicating N326D as an important contributor to CQR, consistent with a previous report (Summers *et al.*, 2014). Nevertheless, the advent of a spontaneous sequence reversion in this line made us cautious about using the $C8^{PH1-I}$ line, and it was excluded from further consideration in this present study. Repeated sequence analysis of other recombinant lines during long-term culture confirmed the genotypes of all other lines

under investigation. Analysis of the PH1 haplotype was therefore confined to the $C8^{PH1\text{-}II}$ clone, whose genotype was closely monitored and remained stable over time.

Mutant Southeast Asian pfcrt *alleles influence susceptibility to locally used drugs*

Using these recombinant isogenic lines, we assayed the impact of different PfCRT haplotypes (Table 1) on parasite susceptibility to CQ as well as other antimalarials. For comparison, we included $C2^{GC03}$, $C4^{Dd2}$ and $C6^{7G8}$, which were generated using the same genetic strategy (Sidhu *et al*., 2002). These encode the wild-type GC03 haplotype, the Dd2 haplotype commonly found in Asia and Africa and the 7G8 haplotype that is widespread in South America and the Pacific region respectively (Sa *et al*., 2009). For reference, we also included the non-recombinant lines GC03, Dd2 and 7G8.

We note that our CQ values, both for resistant and sensitive strains, are lower than earlier reports (Sidhu *et al*., 2002; Lakshmanan *et al*., 2005; Valderramos *et al*., 2010). One important technical difference is that we reduced the HEPES concentration from the earlier 50 mM to the current 25 mM. Our detailed studies have since revealed that this decrease in the HEPES concentration leads to a substantial reduction in half-maximal inhibitory concentration (IC_{50}) values for CQ-sensitive and even more so for CQ-resistant parasites, as detailed in the Supporting Information (Supplemental Text and Figs S2–S4). This is one of the variables that can produce differences in CQ IC_{50} values (others include genetic differences between strains maintained long-term in separate laboratories and the choice of assay). Relative differences between strains in a given dataset are thus recognized to provide the most informative data (Ekland and Fidock, 2008). Consequently, we also discuss below the relative differences between parasite lines expressing distinct *pfcrt* alleles.

For CQ, all recombinant lines expressing mutant *pfcrt* alleles ($C8^{PH1}$, $C10^{PH2}$, $C12^{Cam734}$, $C4^{Dd2}$ and $C6^{7G8}$) had a statistically significant, 2.5- to 4.7-fold increase in mean IC_{50} value relative to the isogenic recombinant $C2^{GC03}$ line expressing the wild-type allele (mean IC_{50} value of 14 nM) (Fig. 2A; Table S3). Of note, $C10^{PH2}$ and $C12^{Cam734}$ yielded CQ IC_{50} values (53–54 nM) that were comparable in these assays to the recombinant $C4^{Dd2}$ and $C6^{7G8}$ parasites expressing the most globally prevalent mutant *pfcrt* alleles (Sidhu *et al*., 2002). We note, however, that $C4^{Dd2}$ and $C6^{7G8}$ are no longer as CQ-resistant as when they were originally generated (in 2002) and characterized by several groups (Sidhu *et al*., 2002; Lakshmanan *et al*., 2005; Gligorijevic *et al*., 2008). This has also been observed in an independent recent study that employed these lines (Hrycyna *et al*., 2014). $C4^{Dd2}$ and $C6^{7G8}$ currently display CQ IC_{50} values that are now 51% and 68% of the parental Dd2 and 7G8 lines respectively (Fig. 2A and Table S3), as compared with the initial report that documented corresponding values of 76% and 90%. These relative levels of CQR are illustrated for the original $C4^{Dd2}$ and $C6^{7G8}$ lines, alongside the now-attenuated lines, in Fig. 2A. Thus, our present data with the more recently generated PH1, PH2 and Cam734 *pfcrt*-expressing lines identify these as only modestly CQR, with relatively low CQ IC_{50} values. Strikingly, the two $C10^{PH2}$ clones demonstrated higher CQ mean IC_{50} values as compared with $C8^{PH1\text{-}II}$ parasites (53–54 nM compared with 35 nM). This finding implicates amino acid 72, which is the only polymorphism that distinguishes the PH2 and PH1 alleles (Table 1), as an important determinant of the degree of CQR.

Similar observations were made with the CQ metabolite monodesethyl-chloroquine (md-CQ), which yields much higher IC_{50} values in CQ-resistant parasites, allowing for greater discrimination between resistant and sensitive lines (Sidhu *et al*., 2002). $C10^{PH2}$ and $C12^{Cam734}$ clones all yielded mean IC_{50} values (267–346 nM) that were comparable with $C4^{Dd2}$ and $C6^{7G8}$ (282 and 262 nM, respectively; Fig. 2B; Table S3). In comparison, the CQ-sensitive lines $C2^{GC03}$ and GC03 showed mean IC_{50} values of 17–22 nM. Of note, the mean md-CQ IC_{50} value (164 nM) of the $C8^{PH1}$ clone was considerably lower than the IC_{50} values of the two $C10^{PH2}$ lines (267 and 305 nM), again supporting a direct role for the C72S mutation in augmenting the degree of CQR.

Prior work has shown that CQ-resistant parasites can be chemosensitized to CQ and md-CQ by the resistance-reversing agent verapamil (VP) (Krogstad *et al*., 1987; Martin *et al*., 1987). The primary determinant of this reversibility trait has been mapped by quantitative trait loci analysis to mutant *pfcrt* (Patel *et al*., 2010) and is more pronounced in the presence of the Dd2 allele as compared with the 7G8 allele (Mehlotra *et al*., 2001; Sidhu *et al*., 2002; Sa *et al*., 2009). To assess VP reversibility in our recombinant lines, we performed drug assays in the presence or absence of 0.8 μM VP and compared IC_{50} values. Results showed a high degree of resistance reversal (74–85%) for $C4^{Dd2}$ and the reference Dd2 line and an intermediate degree (43–56%) for $C6^{7G8}$ and 7G8 parasites (Fig. 2C). These values were significantly different from the CQ-sensitive $C2^{GC03}$ line that along with GC03 showed no reversibility with this concentration of VP. Intriguingly, both $C8^{PH1}$ and $C10^{PH2}$ showed only a slight degree of reversal, which did not attain statistical significance. A similar lack of significant reversal was also observed with the metabolite md-CQ (Table S3). This agrees with an earlier report of Philippine isolates (Chen *et al*., 2003) and is consistent with a recent study that associated PfCRT N75 (present in both haplotypes; Table 1) with minimal VP reversal (Sa *et al*., 2009). We note that $C12^{Cam734}$ parasites,

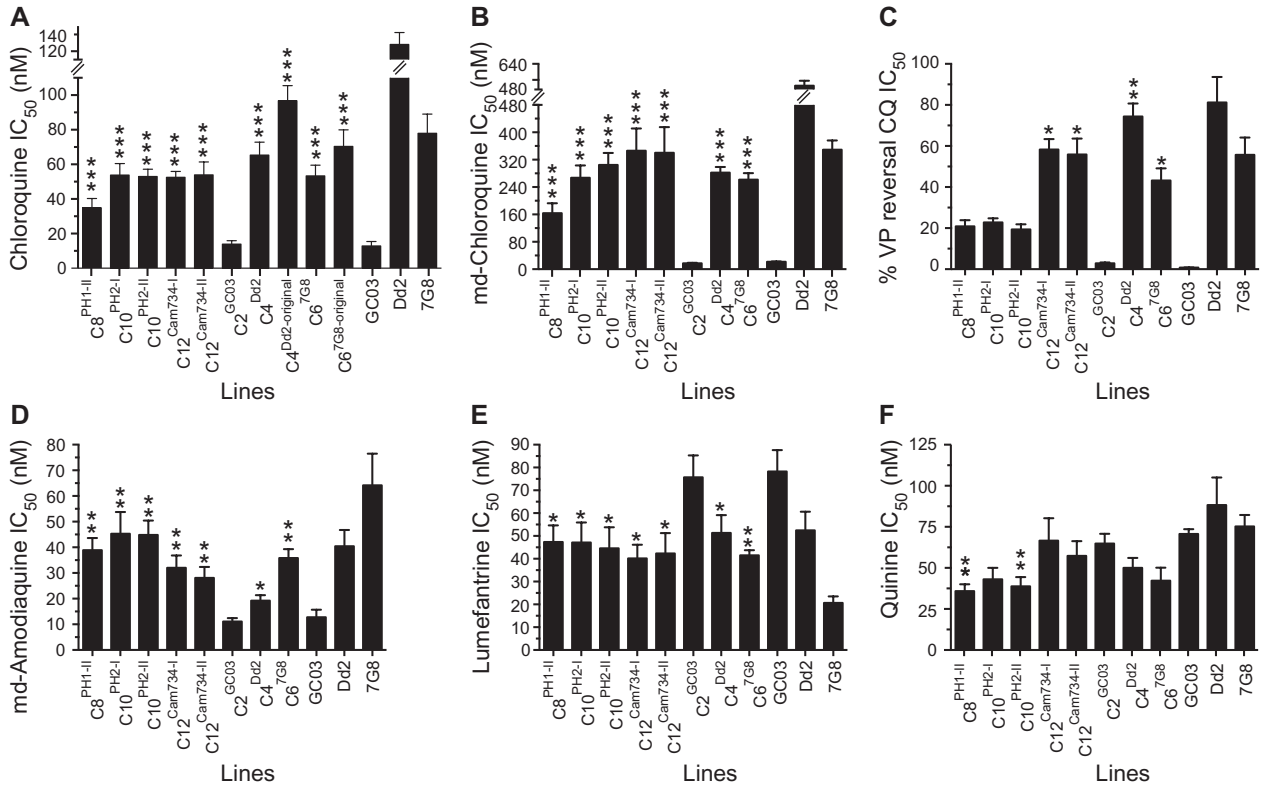

Fig. 2. Susceptibility of *pfcrt*-modified clones to selected antimalarial drugs. Mean IC_{50} values ± SEM for the indicated parasite strains subjected to clinically significant antimalarials, as measured *in vitro* using [^{3}H]-hypoxanthine incorporation assays. We note that the CQ values, both for resistant and sensitive strains, are markedly lower than earlier reports (Sidhu *et al*., 2002; Lakshmanan *et al*., 2005; Valderramos *et al*., 2010), and coincide with our reducing the HEPES concentration from the earlier 50 mM to the current 25 mM (see Supporting information). CQ values for the original $C4^{Dd2}$ and $C6^{7G8}$ lines, presented as a proportion of their IC_{50} values of the reference Dd2 and 7G8 lines, are included to illustrate the attenuation of the CQR phenotypes of these lines over time. The $C4^{Dd2\text{-}original}$ CQ mean ± SEM IC_{50} value of 96.8 ± 8.7 nM is comparable to the values of 91.8 ± 10.7 nM and 100.3 ± 15.5 nM recently reported with two *pfcrt*-modified GC03 clones engineered to express the Dd2 allele (i.e. analogous to $C4^{Dd2}$) using customized zinc-finger nucleases (Straimer *et al*., 2012). VP reversal was calculated as the IC_{50} of CQ + 0.8 μM VP divided by the IC_{50} of CQ. VP reversal values for CQ, md-CQ and md-ADQ are provided in Table S4. Mann–Whitney *U* tests were used to assess for statistically significant differences between a recombinant line expressing mutant *pfcrt* and the CQ-sensitive line $C2^{GC03}$ expressing wild-type *pfcrt*. *$P < 0.05$; **$P < 0.01$; ***$P < 0.001$. IC_{50} and IC_{90} values, numbers of assays and tests for significance are reported in Table S3.

which harbor the novel N75D mutation, were also subject to a significant degree (56–72%) of VP reversal of CQ and md-CQ resistance, at levels intermediate to the Dd2 and 7G8 alleles (Fig. 2C; Table S3).

We extended these studies to monodesethyl-amodiaquine (md-AQ), the clinically relevant metabolite of amodiaquine, a 4-aminoquinoline drug formerly used in monotherapy in many South American, African and Asian countries, including the Philippines (Sa *et al*., 2009). This drug continues to be clinically important because of its incorporation into the widely used amodiaquine–artesunate combination (Wells *et al*., 2009). Our studies reveal a substantial impact of both Philippine *pfcrt* alleles, as well as the Cam734 allele, on md-AQ responses (Fig. 2D), resulting in a 2.5 to fourfold increase in IC_{50} values compared with $C2^{GC03}$. Of all alleles tested, the smallest gain in md-AQ resistance was afforded by expression of the recombinant Dd2 allele that mediates relatively high-level CQR (see $C4^{Dd2}$ responses in Fig. 2A and D). These data implicate an important role for the PfCRT mutations unique to the Philippine and Cambodian alleles in reducing parasite susceptibility to amodiaquine.

Importantly, every mutant *pfcrt* allele significantly increased susceptibility to the arylaminoalcohol drug lumefantrine (LMF; Fig. 2E), the partner drug comprising the most widely used artemisinin-based combination therapy (ACT), artemether-lumefantrine (Wells *et al*., 2009). Mean IC_{50} reductions were 37–47%, as compared with $C2^{GC03}$ (Table S3). It is worth noting that a similar decrease in LMF IC_{50} values in parasites expressing mutant *pfcrt* as compared with isogenic parasites expressing the wild-type allele was earlier found to be associated with a significant reduction in the prevalence of mutant *pfcrt* in field isolates that recrudesced in patients treated with artemether–

lumefantrine (Sisowath *et al.*, 2009). These findings support the therapeutic advantage of using LMF in areas of CQ-resistant malaria.

A similar trend was observed with the arylaminoalcohol mefloquine and the endoperoxide artemisinin. However, the differences in IC_{50} values did not attain statistical significance (Table S3). The PH1 and PH2 *pfcrt* alleles, but not Cam734, also significantly increased parasite susceptibility to quinine (Fig. 2F), a centuries-old drug used to treat severe malaria. Quinine resistance is known to be multifactorial, with quantitative trait loci analyses implicating mutant *pfcrt* and *pfmdr1* as major determinants (Ferdig *et al.*, 2004; Sanchez *et al.*, 2011; 2014). Our data support the hypothesis that the direction and magnitude of the effect of mutant *pfcrt* on quinine response depends on the genetic background and PfCRT haplotype (Cooper *et al.*, 2002; 2007; Sidhu *et al.*, 2002; Lakshmanan *et al.*, 2005). Finally, no differences were observed with piperaquine (Table S3), an ACT partner drug that comprises two CQ 4-aminoquinoline rings tethered together with a spacer (Wells *et al.*, 2009), consistent with this drug being equally potent against parasites expressing wild-type or common mutant variants of *pfcrt* (Pascual *et al.*, 2013).

Reduced chloroquine accumulation alone does not account for differences in the degree of chloroquine resistance

Resistance to CQ has been associated with reduced drug accumulation in the DV and has previously been attributed to mutant PfCRT-mediated efflux of CQ from this acidic organelle (Krogstad *et al.*, 1987; Martin *et al.*, 1987; 2009; Valderramos and Fidock, 2006). To investigate the influence of the Southeast Asian *pfcrt* alleles on CQ accumulation, we measured the kinetics of [^{3}H]-CQ uptake in cultured parasites. The CQ-sensitive control lines GC03 and $C2^{GC03}$ showed a rapid increase in CQ accumulation, as measured by a very high ratio (up to 2300) of total intracellular CQ to extracellular CQ ($[CQ_{in}]/[CQ_{out}]$) (Fig. 3A). In contrast, the four *pfcrt*-variant recombinant lines ($C4^{Dd2}$, $C8^{PH1\text{-}I}$, $C10^{PH2\text{-}I}$ and $C12^{Cam734\text{-}I}$) accumulated minimal levels of CQ ($[CQ_{in}]/[CQ_{out}]$ values of ~ 200–300). Thus, these mutant PfCRT haplotypes, all expressed in the same genetic background, were associated with a very similar reduction of intracellular CQ levels (Fig. 3B), despite marked differences in their CQ IC_{50} values (Fig. 2). These data lead us to suggest that reduced CQ accumulation might represent only one means by which mutant PfCRT dictates the degree of CQR.

PfCRT haplotypes influence parasite growth rates in co-culture in vitro *competition assays*

To measure the extent to which *pfcrt* mutations influence the relative growth rates of asexual blood stage parasites,

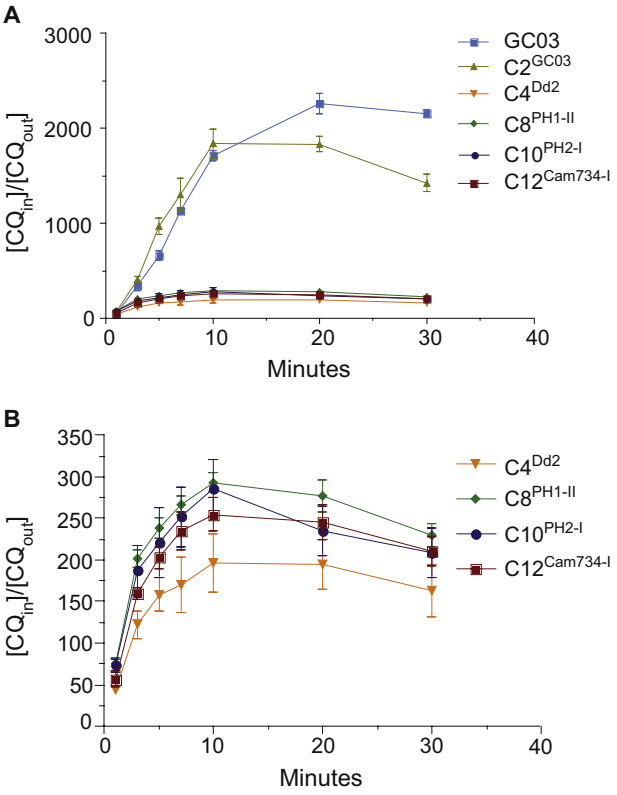

Fig. 3. Chloroquine accumulation of *pfcrt*-modified parasite lines. [^{3}H]-CQ accumulation is represented as the ratio of the total intracellular CQ to extracellular CQ ($[CQ_{in}]/[CQ_{out}]$). Values represent the mean ± SEM determined from three independent experiments performed in duplicate. Data are shown in (A) for the full set of *pfcrt*-modified lines and the CQ-sensitive control GC03, and in (B) exclusively for the lines expressing mutant *pfcrt* (note the reduced *y*-axis scale).

serving as a partial proxy for assessing fitness costs, we performed *in vitro* co-culture competition assays. In these assays, two lines were mixed in 1:1 ratios, and the proportions of the individual *pfcrt* alleles were quantified by pyrosequencing every 4 days, on average, over a two to three month period. Data from these assays were converted using the ratio of the natural logs of the allelic frequencies, based on an assumption of exponential growth, and were subjected to linear regression (Maree *et al.*, 2000; Mita *et al.*, 2004). Linear regression R^2 values were generally high (average 0.64, reflecting an acceptable goodness of fit; Table S5). In total, 34 co-culture assays were followed, yielding 518 measurements of *pfcrt* allelic frequencies over time (Table S5). From these measurements, we computed the mean relative growth rate value for each line, as detailed in the Supporting Information.

Results indicated that the isogenic clones $C8^{PH1\text{-}II}$ and $C10^{PH2\text{-}I}$, expressing the PH1 and PH2 mutant *pfcrt* alleles respectively, each displayed reduced *in vitro* growth when independently co-cultured with $C2^{GC03}$ parasites (Figs 4

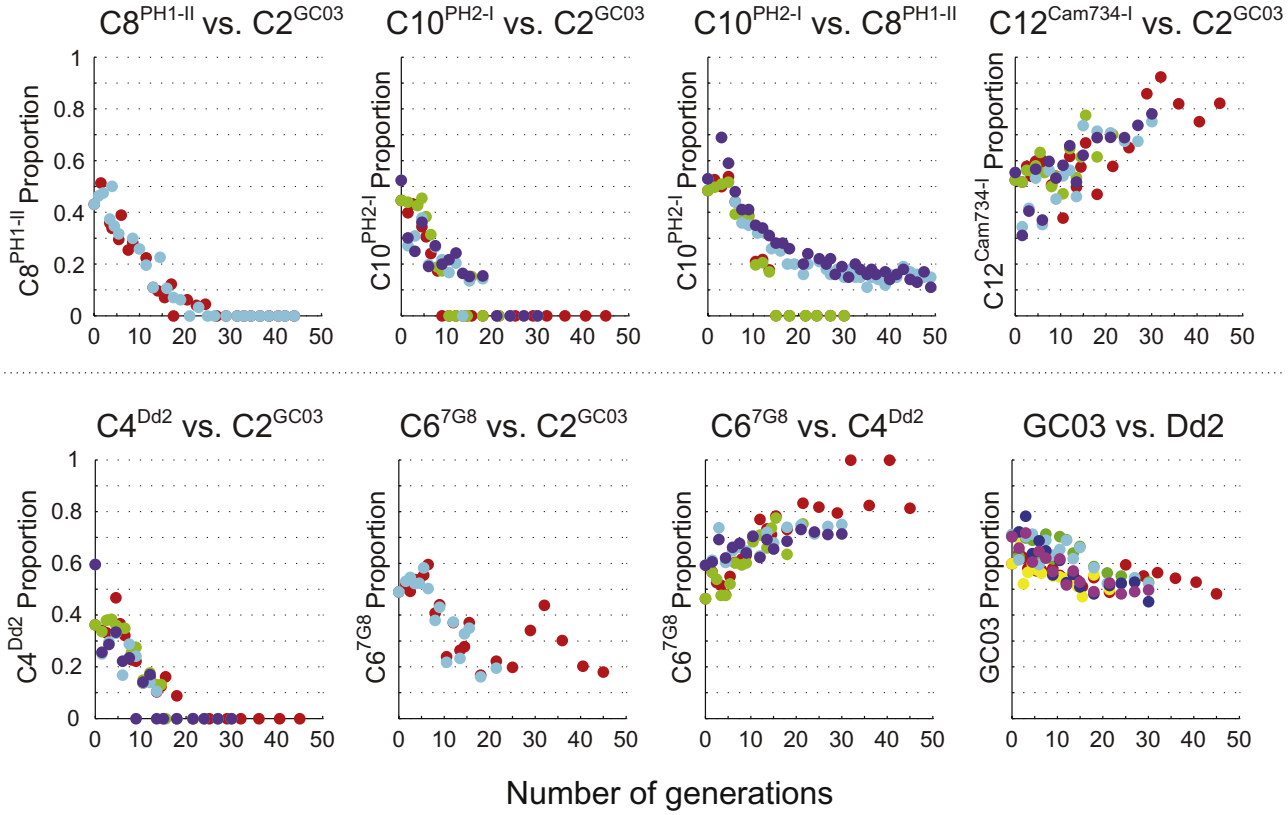

Fig. 4. Relative growth rate plots for mixed competition assays between *pfcrt*-modified lines. Parasite cultures were initiated at ~ 1:1 ratios, and allelic proportions were measured over time for up to 45 generations by pyrosequencing. The *y*-axis illustrates the proportion of the first listed allele comprising the mixed cultures. Each color represents a separate assay. Data are collectively summarized in Fig. 5A and Table S5.

and 5A). Of the two mutant *pfcrt* parasites, $C10^{PH2-I}$ parasites showed the more substantial loss of relative growth rate *in vitro*. This finding was consistent with direct competition assays between $C10^{PH2-I}$ and $C8^{PH1-II}$, which revealed reduced relative growth rates with the former (Table S5). This contrasted with CQ and md-CQ IC_{50} values that were higher for $C10^{PH2-I}$ (Fig. 2; Table S3). These results suggest a state of balanced polymorphisms whereby the PH1 allele could be predicted to fare better than the more unfit PH2 in mixed infections in the absence of CQ drug pressure, whereas the moderately more CQR PH2 allele could be more competitive in the presence of CQ and thus be retained in the population. Intriguingly, parallel studies with the CQ-resistant $C12^{Cam734-I}$ line documented that these parasites were consistently as fit in terms of growth rates, if not slightly more so, when compared with $C2^{GC03}$ *in vitro*. These data suggest that the Cam734 allele, harboring an unusually high number of point mutations (Table 1), has achieved a functional state that might reduce the fitness cost typically observed with mutant *pfcrt* alleles in endemic settings.

In contrast to Cam734, we observed a substantial reduction in relative growth rates associated with the Dd2 *pfcrt* allele when comparing $C4^{Dd2}$ to $C2^{GC03}$, a finding consistent with reports of reduced fitness associated with this allele in African parasite populations (Kublin *et al.*, 2003; Mita *et al.*, 2003; Ord *et al.*, 2007). A more modest reduction in relative growth rates was observed with the 7G8 allele present in $C6^{7G8}$. The reduced relative growth rates of the Dd2 and 7G8 alleles is consistent with a recent report that also assessed these recombinant parasite lines in mixed culture experiments (Lewis *et al.*, 2014). In our studies, $C6^{7G8}$ consistently outcompeted $C4^{Dd2}$ in mixed cultures in four independent experiments (Fig. 4; Table S5). Importantly, when testing non-recombinant lines, we found the Dd2 line to have moderately increased growth rates relative to lines expressing wild-type *pfcrt* (GC03 and HB3), suggesting that Dd2 harbors additional compensatory mutations in its genome that corrected the growth defect associated with expression of its *pfcrt* allele. A summary of the influence of *pfcrt* alleles on *in vitro* growth rates in these co-competition assays is depicted in Fig. 5A. Independent support for these data came from measurements of *in vitro* growth rates for individual lines, which were monitored daily for 7 days in three independent assays per line. Calculated multiplication rates per 48 h revealed that in

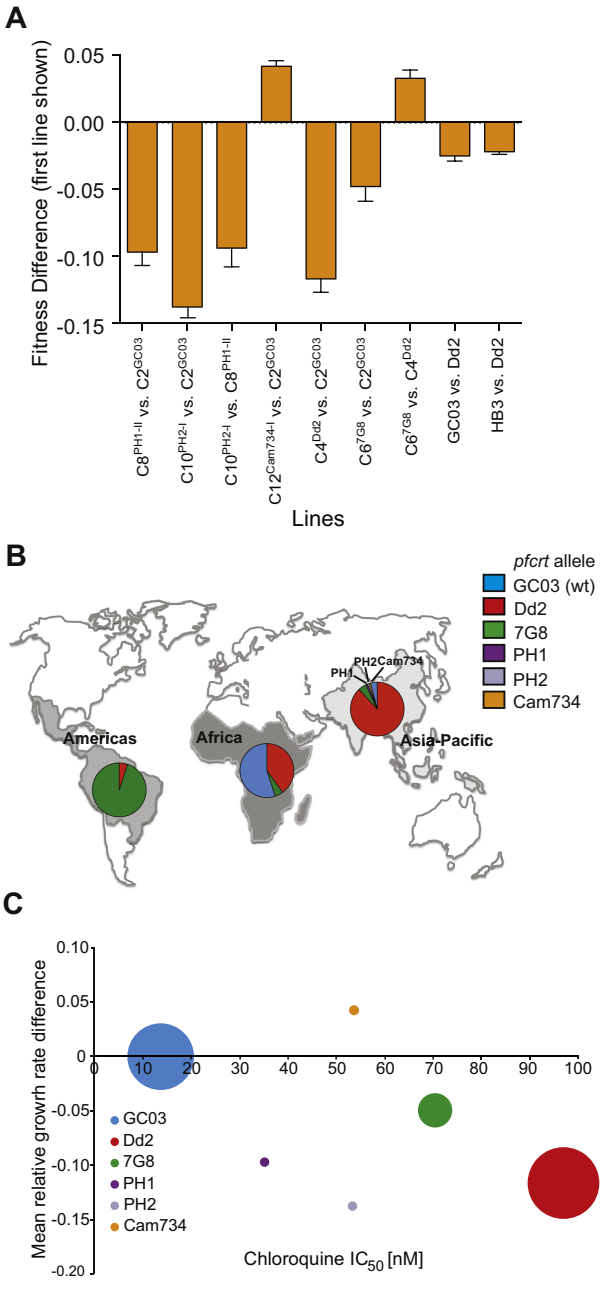

Fig. 5. Influence of *pfcrt* alleles on relative growth rates and chloroquine resistance.
A. Relative growth rate values for the individual *pfcrt*-modified parasite lines were measured following pyrosequencing-based assessment of changes in *pfcrt* allele frequencies in mixed cultures maintained for up to 45 generations. For each combination, 1–6 independent competition assays were performed in duplicate (summarized in Table S5; data plotted in Fig. 4). The histogram depicts the relative growth rate of the first line compared with the second, e.g. for $C8^{PH1\text{-}II}$ vs. $C2^{GC03}$ the negative value reflects the reduced relative growth rate of $C8^{PH1\text{-}II}$.
B. Distribution of various *pfcrt* alleles in the major malaria-endemic regions.
C. Mean relative growth rate differences between wild-type and mutant *pfcrt* alleles (in the GC03 background) presented as a function of the effect of these alleles on CQ IC_{50} values (based on data presented in Tables S3 and S5 and depicted in Figs 2 and 5A). Circle size indicates the estimated worldwide frequency of the *pfcrt* allele, approximated from literature reports and database summaries on the number of clinical cases and the distribution of *pfcrt* alleles (see Table S6).

comparison with parasites expressing the *pfcrt* wild-type GC03 allele, parasites expressing the Cam734 allele showed an equivalent growth rate, whereas parasites expressing the PH2, Dd2 and 7G8 alleles displayed slower rates of growth (Fig. S1).

Discussion

Genome-wide studies of *P. falciparum* populations have demonstrated a remarkable degree of recent evolution in the *pfcrt* coding sequence, beginning with several independent origins of variant alleles. These alleles have spread across malaria-endemic regions as selective sweeps driven by intense drug pressure (Wootton *et al.*, 2002; Kidgell *et al.*, 2006; Volkman *et al.*, 2007; Mu *et al.*, 2010). Primary origins have been localized to South America and Papua New Guinea (independent sources of the 7G8 variant haplotype), the Philippines (PH1 and PH2), the Thai-Cambodian border (Dd2) and most likely Cambodia (Cam734; Fig. 5B) (Ecker *et al.*, 2012). CQR in Africa resulted from the introduction of variant *pfcrt* of Southeast Asian origin (Ariey *et al.*, 2006), whose insidious impact on malaria rates was highlighted by reports from Senegal showing nearly a sixfold increase in malarial deaths following the arrival of resistant strains (Snow *et al.*, 2001; Trape, 2001). Our study of geographically distinct PfCRT haplotypes reveals an intricate balance between CQR and parasite growth rates, which provide an *in vitro* proxy of fitness. Our data also highlight the emergence (in Cambodia) of the Cam734 allele (Durrand *et al.*, 2004), which appears to have succeeded in mediating a moderate degree of resistance while concurrently maintaining *in vitro* growth rates at least as good if not better than wild-type *pfcrt* (Fig. 5C). Notably, Cambodia is a known hotbed of multidrug resistance, beginning with CQ and pyrimethamine-sulfadoxine and more recently with emerging resistance to artemisinin derivatives (Dondorp *et al.*, 2011; Ariey *et al.*, 2014; Straimer *et al.*, 2015). We ascribe the lack of an observable growth rate defect in the Cam734 allele to its complex set of mutations (Table 1), which include the L148I, I194T and T333S mutations not present in other parasites studied herein. We posit that these mutations have evolved to compensate for a loss of fitness bestowed by an initial set of mutations that were sufficient to confer CQR, including but not limited to K76T (Lakshmanan *et al.*, 2005). The ability of *Plasmodium* parasites to acquire a set of mutations simultaneously conferring CQR and enhanced

fitness has previously been documented in murine studies, in which CQ-resistant *P. chabaudi* parasites outgrew their sensitive counterparts, even when mice were inoculated with a ninefold excess of sensitive parasites (Rosario *et al*., 1978). Recent metabolomic studies show that the widespread Dd2 and 7G8 alleles cause increased levels of intracellular peptides in asexual blood stage parasites, presumably stemming from impaired hemoglobin digestion that restricts the supply of amino acids required for parasite proliferation (Lewis *et al*., 2014). These recent findings provide a potential mechanistic explanation for the fitness costs observed with the Dd2 and 7G8 haplotypes. Further studies are required to assess whether the Cam734 allele corrects this abnormal accumulation of hemoglobin-derived peptides.

Our findings also illustrate a singular impact of PfCRT residue 72, which is the sole sequence distinction between the Philippine PH1 allele that mediates marginal CQR and the PH2 allele that is moderately more resistant (Fig. 5C). This residue is also associated with differences in relative growth rates *in vitro* (Figs 4 and 5A). How this single amino acid difference might impact protein conformation, stability or post-translational modifications remains to be determined. During these experiments, we isolated a separate recombinant $C8^{PH1}$ parasite, referred to as $C8^{PH1\text{-}II}$, which underwent a spontaneous loss of the N326D mutation during extended culture. This reversion back to the wild-type residue was associated with an increased rate of parasite propagation and a loss of CQR. The reversion to a CQS phenotype by the N326D mutation is consistent with a recent report that showed a lack of CQ transport in *Xenopus* oocyte-based heterologous expression assays, in contrast to the PH1 PfCRT variant that showed CQ transport behavior (Summers *et al*., 2014). These data highlight a requirement for multiple PfCRT mutations in producing the CQR phenotype, arguing against the notion that CQR results solely from the K76T mutation and that the other mutations in this protein compensate solely for loss of function. This conclusion is supported by transport studies in an oocyte expression system, which provided evidence that the K76T mutation needed to be accompanied by either the N75E (Southeast Asian PfCRT variants) or the N326D mutation (Latin American and oceanic PfCRT variants) to attain a CQ transport function (Summers *et al*., 2014). Although two mutational changes sufficed for a basal CQ transport activity, additional mutations were required for full activity. The order in which these mutations were added was important to avoid reductions in CQ transport activity (Summers *et al*., 2014).

Epidemiological studies have found that some parasites harboring the PfCRT K76T mutation have low to moderate CQ IC_{50} values that do not meet the standard definition of CQR and in some instances are similar to values observed with CQ-sensitive parasites, for example some Cambodian isolates harboring the Cam734 allele (Durrand *et al*., 2004). Studies are ongoing to dissect the role of the PfCRT SNPs that are unique to the Cam734 haplotype. Furthermore, *in vitro* selection studies have shown that parasites harboring the Dd2 *pfcrt* allele acquired a C101F mutation that resulted in a loss of CQR despite the presence of K76T (Eastman *et al*., 2011). Thus, although K76T continues to be an important molecular marker of CQR, recent evidence suggests that additional PfCRT SNPs can substantially modify the CQ response, in some cases causing an attenuation or loss of the resistance phenotype. We also note that while PfCRT is widely recognized to be the primary mediator of CQR, several studies point to a requirement for secondary determinants to augment CQR, including *pfmdr1* (Sidhu *et al*., 2002; Sa *et al*., 2009; Patel *et al*., 2010; Valderramos *et al*., 2010; Gaviria *et al*., 2013).

In our mixed infection studies with isogenic *pfcrt*-modified clones, we also observed that parasites displayed the greatest loss of asexual blood stage growth when expressing the Dd2 allele, consistent with its progressive disappearance from high-transmission African settings in the absence of CQ pressure (Mita *et al*., 2003; Ord *et al*., 2007; Mwai *et al*., 2009; Laufer *et al*., 2010; Frosch *et al*., 2011). This contrasts with the situation in Southeast Asia where the Dd2 allele remains at high frequencies in the absence of CQ pressure. Fewer mixed infections in Asia compared with Africa likely result in less opportunity for competition with the wild-type allele. The lesser fitness cost observed with the 7G8 allele, which is prevalent in South America and the Pacific region, is concordant with studies from these regions showing the continued presence of mutant *pfcrt* despite minimal CQ use in recent decades to treat *P. falciparum* malaria (Mu *et al*., 2010). We note that modest selective pressure on mutant *pfcrt* may also have come from the use of CQ to treat *P. vivax* infections, which are common outside of Africa (Price *et al*., 2007). Overall, our *in vitro* mixed competition relative growth rate data would suggest that the idea of reintroducing CQ into regions where prolonged drug removal has led to the near disappearance of resistant strains (Juliano *et al*., 2007; Laufer *et al*., 2010) is suitable only in areas harboring mutant *pfcrt* alleles such as Dd2 that cause reduced fitness and would be less applicable to regions harboring relatively 'fit' alleles such as Cam734.

The loss of CQ efficacy across the globe, followed by a short-lived dependence on the sulfadoxine-pyrimethamine antifolates, has resulted in recent years in the global adoption of ACTs (White, 2008; Eastman and Fidock, 2009). Notably, our study shows that all mutant *pfcrt* alleles tested herein, including the two that are most prevalent (Dd2 and 7G8), increase parasite susceptibility to lumefantrine. This is particularly significant as this drug, partnered with

artemether (CoArtem®), is globally the most widely used antimalarial (Wells *et al*., 2009). Although the fold change in lumefantrine IC_{50} values is relatively low (≤ 2-fold; Fig. 2E; Table S3), we note that a clinical trial from Tanzania observed significant selection against mutant *pfcrt* parasites harboring the ^{72}CVIET^{76} PfCRT haplotype following artemether–lumefantrine treatment (Sisowath *et al*., 2009).

Amodiaquine–artesunate is another ACT that is often used in Africa (Olliaro and Mussano, 2000). We observed significantly reduced parasite susceptibility to the amodiaquine metabolite md-AQ with every tested mutant *pfcrt* allele. This includes both Philippine alleles, obtained from a country where amodiaquine has been used as an antimalarial treatment for over 40 years (Sa *et al*., 2009). We thus posit that amodiaquine could have been a major contributor to the emergence and/or maintenance of the PH1 and PH2 alleles. An important role for amodiaquine in driving the spread of the ^{72}SVMNT^{76} PfCRT haplotype (present in 7G8) has recently been proposed based on studies of parasites from South America and Asia (Sa *et al*., 2009; Beshir *et al*., 2010), and amodiaquine pressure could conceivably account for the apparent recent spread of this haplotype into Africa and in India (Alifrangis *et al*., 2006; Gama *et al*., 2010; Mixson-Hayden *et al*., 2010). In addition, as with many Asian countries, CQ has continued to be used to treat patients infected with *P. vivax*, thus sustaining local CQ pressure that could influence the course of mixed infections of *P. vivax* and *P. falciparum*. Overall, our data support the use of artemether–lumefantrine in preference to amodiaquine-artesunate to treat CQ-resistant malaria. We also found no evident effect of mutant *pfcrt* alleles studied herein on the efficacy of piperaquine, an ACT partner drug with excellent clinical efficacy and post-treatment prophylactic activity (Wells *et al*., 2009).

Our mechanistic investigations into CQR provide evidence that mutant PfCRT-mediated CQR can be phenotypically distinguished from reduced intracellular CQ accumulation, as also noted by a previous study (Sanchez *et al*., 2011). This was particularly evident with C8^{PH1} parasites that, despite having only a nominal degree of CQR, displayed kinetics of intracellular CQ accumulation that paralleled the other, more CQ-resistant parasites. In contrast, CQ-sensitive parasites showed 7- to 10-fold higher levels of CQ accumulation (Fig. 4). Thus, all mutant PfCRT variants shared an ability to reduce CQ accumulation. This study agrees with recent evidence that reduced CQ accumulation is not the sole cause of CQR (Cabrera *et al*., 2009; Sanchez *et al*., 2011; Baro *et al*., 2013). We posit that mutant PfCRT generally reduces CQ accumulation and that this is an essential feature of CQR but that various PfCRT haplotypes differ in a second respect that further contributes to the CQR phenotype. One possibility is that the higher degree of CQR reflects varying degrees to which PfCRT functions to also reduce the cellular toxicity associated with CQ action, possibly by negating the effect of CQ on preventing the buildup of reactive heme-iron or oxygen species liberated following hemoglobin proteolysis. Another possibility is that the drug competes with a yet to be identified physiological substrate for transport via PfCRT and that this competition impacts on the natural function of the transporter. In this context, it is interesting to note that PfCRT appears capable of simultaneously accepting different substrates at distinct but antagonistically interacting binding sites (Bellanca *et al*., 2014). Binding of two different substrates might result in an inactive transporter or one with substantially reduced activity, depending on the nature of the substrates bound (Bellanca *et al*., 2014). How a geographic PfCRT variant copes with its drug and physiological transport functions is likely determined by its specific amino acid substitutions. Further dissection of the biochemical parameters associated with heme detoxification and CQ action can now be achieved using the series of isogenic *pfcrt*-modified lines described herein.

Experimental procedures

Parasite culture, transfection, and selection and characterization of integrant clones

Parasites were cultured at 37°C in human red blood cells in Albumax-containing culture medium, as described (Fidock *et al*., 1998). Isogenic lines expressing variant *pfcrt* alleles were generated following transfection of the C1^{GC03} clone (Sidhu *et al*., 2002). This clone was previously generated from GC03 (a progeny of the HB3 × Dd2 genetic cross, Wellems *et al*., 1990) and expresses wild-type *pfcrt* from a recombinant locus lacking introns 2–12 (Fig. 1). C1^{GC03} parasites were propagated to ~ 8% ring stage parasitemia and electroporated with 50 µg of plasmid (pBSD-crt-PH1$^{Py3'}$, pBSD-crt-PH2$^{Py3'}$ or pBSD-crt-Cam734$^{Py3'}$; Table 1; Fig. 1). Transformed parasites were selected using 2.5 nM WR99210 (Jacobus Pharmaceuticals, Princeton, NJ, USA) and 2.5 µM Blasticidin HCl (Invitrogen). Successfully transfected parasites were detectable in culture 2–3 weeks post-transfection and cloned by limiting dilution once plasmid integration was detected. Details of plasmid construction, and of the molecular characterization of parasite lines, are provided in the Supporting Information (primers listed in Table S1). *pfcrt*-modified transgenic lines will be made available upon request and are being deposited in the MR4 Malaria Reagent Repository.

In vitro *drug susceptibility assays*

Parasite susceptibilities to antimalarial drugs were assessed *in vitro* as described (Fidock *et al*., 1998) using 72 h [^{3}H]-hypoxanthine assays (see Supporting Information). IC_{50} values were calculated by non-linear extrapolation. Statistical analyses employed Mann–Whitney *U* tests.

In vitro *mixed culture competition assays, pyrosequencing and determination of relative growth rate values*

For growth competition assays, two parasite lines were mixed 1:1 and seeded in duplicate or triplicate at an initial parasitemia of 0.6% ring stage parasites, in drug-free medium. Parasitemias were maintained between 0.3% and 8% to assure optimal growth conditions. Two to six separate competition assays were performed for each drug-free mixture, and each assay was monitored for an average of 66 days (range 43–90; Fig. 4; Table S5). To determine the ratio of both strains in the mixture over time, saponin-lysed parasite pellets of the mixed cultures were collected on average every 4 days (range 2–9), and DNA was extracted using DNeasy Blood & Tissue Kits (Qiagen). The DNA was then used for ratiometric determination of individual allele frequencies in these mixed cultures by pyrosequencing of codon position 72 or 76 (detailed in the Supporting Information). To calculate the relative growth rates of individual parasite lines, the relative proportion of the two distinct *pfcrt* alleles (whose values were always between 0 and 1, inclusive) were natural log-transformed, and linear regression was applied to estimate the relative growth rate value, as detailed in the Supporting Information. These values, along with the calculated SEM and R^2 values, are listed in Table S5.

Chloroquine accumulation assays

These were performed, as previously described (Sanchez *et al.*, 2003), using magnet-purified, sorbitol-synchronized trophozoites (detailed in Supporting Information). The amount of accumulated intracellular [^{3}H]-CQ was calculated as the ratio of [CQ_{in}]/[CQ_{out}], normalized to 1×10^6 infected erythrocytes.

Author contributions

Conceived and designed the experiments: IP, AML and DAF. Performed the experiments: IP, AE, REL, MJA, JS, EP, DJJ, OCF, CS and AML. Analyzed the data: IP, SJG, GLJ, AE, SKD, PPH, AML, ML and DAF. Wrote the paper: IP, SJG, GLJ, AML and DAF.

Acknowledgements

We are grateful to Drs Thierry Fandeur (Centre de Recherche Médicale et Sanitaire, Niamey, Niger) and Qin Cheng (Australian Army Malaria Institute, Enoggera, Queensland, Australia) for their kind gifts of Cam734 and PH1 *pfcrt* cDNA, and Dr. Liyong Deng, Division of Molecular Genetics, Columbia University College of Physicians and Surgeons, New York, for assistance with pyrosequencing. We also thank all members of the Fidock lab for helpful discussions. Funding for this work was provided in part by the NIH (R01 AI50234, to D.A.F.) and an Investigator in Pathogenesis of Infectious Diseases Award from the Burroughs Wellcome Fund (to D.A.F.). Geoffrey Johnston is a recipient of a Graduate Research Fellowship from the National Science Foundation. The funders had no role in study design, data collection and analysis, decision to publish, or preparation of the manuscript. The authors have no conflict of interest to declare.

References

Alifrangis, M., Dalgaard, M.B., Lusingu, J.P., Vestergaard, L.S., Staalsoe, T., Jensen, A.T., *et al.* (2006) Occurrence of the Southeast Asian/South American SVMNT haplotype of the chloroquine-resistance transporter gene in *Plasmodium falciparum* in Tanzania. *J Infect Dis* **193:** 1738–1741.

Ariey, F., Fandeur, T., Durand, R., Randrianarivelojosia, M., Jambou, R., Legrand, E., *et al.* (2006) Invasion of Africa by a single *pfcrt* allele of South East Asian type. *Malar J* **5:** 34.

Ariey, F., Witkowski, B., Amaratunga, C., Beghain, J., Langlois, A.C., Khim, N., *et al.* (2014) A molecular marker of artemisinin-resistant *Plasmodium falciparum* malaria. *Nature* **505:** 50–55.

Baro, N.K., Callaghan, P.S., and Roepe, P.D. (2013) Function of resistance conferring *Plasmodium falciparum* chloroquine resistance transporter isoforms. *Biochemistry* **52:** 4242–4249.

Bellanca, S., Summers, R.L., Meyrath, M., Dave, A., Nash, M.N., Dittmer, M., *et al.* (2014) Multiple drugs compete for transport via the *Plasmodium falciparum* chloroquine resistance transporter at distinct but interdependent sites. *J Biol Chem* **289:** 36336–36351.

Beshir, K., Sutherland, C.J., Merinopoulos, I., Durrani, N., Leslie, T., Rowland, M., and Hallett, R.L. (2010) Amodiaquine resistance in *Plasmodium falciparum* malaria in Afghanistan is associated with the *pfcrt* SVMNT allele at codons 72 to 76. *Antimicrob Agents Chemother* **54:** 3714–3716.

Brown, K.M., Costanzo, M.S., Xu, W., Roy, S., Lozovsky, E.R., and Hartl, D.L. (2010) Compensatory mutations restore fitness during the evolution of dihydrofolate reductase. *Mol Biol Evol* **27:** 2682–2690.

Cabrera, M., Paguio, M.F., Xie, C., and Roepe, P.D. (2009) Reduced digestive vacuolar accumulation of chloroquine is not linked to resistance to chloroquine toxicity. *Biochemistry* **48:** 11152–11154.

Chen, N., Kyle, D.E., Pasay, C., Fowler, E.V., Baker, J., Peters, J.M., and Cheng, Q. (2003) *pfcrt* allelic types with two novel amino acid mutations in chloroquine-resistant *Plasmodium falciparum* isolates from the Philippines. *Antimicrob Agents Chemother* **47:** 3500–3505.

Chen, N., Wilson, D.W., Pasay, C., Bell, D., Martin, L.B., Kyle, D., and Cheng, Q. (2005) Origin and dissemination of chloroquine-resistant *Plasmodium falciparum* with mutant *pfcrt* alleles in the Philippines. *Antimicrob Agents Chemother* **49:** 2102–2105.

Chen, N., Gao, Q., Wang, S., Wang, G., Gatton, M., and Cheng, Q. (2008) No genetic bottleneck in *Plasmodium falciparum* wild-type *pfcrt* alleles reemerging in Hainan Island, China, following high-level chloroquine resistance. *Antimicrob Agents Chemother* **52:** 345–347.

Cooper, R.A., Ferdig, M.T., Su, X.Z., Ursos, L.M., Mu, J., Nomura, T., *et al.* (2002) Alternative mutations at position 76 of the vacuolar transmembrane protein PfCRT are associated with chloroquine resistance and unique stereospecific quinine and quinidine responses in *Plasmodium falciparum*. *Mol Pharmacol* **61:** 35–42.

Cooper, R.A., Lane, K.D., Deng, B., Mu, J., Patel, J.J., Wellems, T.E., *et al*. (2007) Mutations in transmembrane domains 1, 4 and 9 of the *Plasmodium falciparum* chloroquine resistance transporter alter susceptibility to chloroquine, quinine and quinidine. *Mol Microbiol* **63:** 270–282.

Dondorp, A.M., Fairhurst, R.M., Slutsker, L., Macarthur, J.R., Breman, J.G., Guerin, P.J., *et al*. (2011) The threat of artemisinin-resistant malaria. *N Engl J Med* **365:** 1073–1075.

Durrand, V., Berry, A., Sem, R., Glaziou, P., Beaudou, J., and Fandeur, T. (2004) Variations in the sequence and expression of the *Plasmodium falciparum* chloroquine resistance transporter (Pfcrt) and their relationship to chloroquine resistance *in vitro*. *Mol Bochem Parasitol* **136:** 273–285.

Eastman, R.T., and Fidock, D.A. (2009) Artemisinin-based combination therapies: a vital tool in efforts to eliminate malaria. *Nat Rev Microbiol* **7:** 864–874.

Eastman, R.T., Dharia, N.V., Winzeler, E.A., and Fidock, D.A. (2011) Piperaquine resistance is associated with a copy number variation on chromosome 5 in drug-pressured *Plasmodium falciparum* parasites. *Antimicrob Agents Chemother* **55:** 3908–3916.

Ecker, A., Lakshmanan, V., Sinnis, P., Coppens, I., and Fidock, D.A. (2011) Evidence that mutant PfCRT facilitates the transmission to mosquitoes of chloroquine-treated *Plasmodium* gametocytes. *J Infect Dis* **203:** 228–236.

Ecker, A., Lehane, A.M., Clain, J., and Fidock, D.A. (2012) PfCRT and its role in antimalarial drug resistance. *Trends Parasitol* **28:** 504–514.

Ekland, E.H., and Fidock, D.A. (2008) *In vitro* evaluations of antimalarial drugs and their relevance to clinical outcomes. *Int J Parasitol* **38:** 743–747.

Ferdig, M.T., Cooper, R.A., Mu, J., Deng, B., Joy, D., Su, X.Z., and Wellems, T.E. (2004) Dissecting the loci of low-level quinine resistance in malaria parasites. *Mol Microbiol* **52:** 985–997.

Fidock, D.A., Nomura, T., and Wellems, T.E. (1998) Cycloguanil and its parent compound proguanil demonstrate distinct activities against *Plasmodium falciparum* malaria parasites transformed with human dihydrofolate reductase. *Mol Pharmacol* **54:** 1140–1147.

Fidock, D.A., Nomura, T., Talley, A.K., Cooper, R.A., Dzekunov, S.M., Ferdig, M.T., *et al*. (2000) Mutations in the *P. falciparum* digestive vacuole transmembrane protein PfCRT and evidence for their role in chloroquine resistance. *Mol Cell* **6:** 861–871.

Fitch, C.D. (2004) Ferriprotoporphyrin IX, phospholipids, and the antimalarial actions of quinoline drugs. *Life Sci* **74:** 1957–1972.

Frosch, A.E., Venkatesan, M., and Laufer, M.K. (2011) Patterns of chloroquine use and resistance in sub-Saharan Africa: a systematic review of household survey and molecular data. *Malar J* **10:** 116.

Gama, B.E., Pereira-Carvalho, G.A., Lutucuta Kosi, F.J., Almeida de Oliveira, N.K., Fortes, F., Rosenthal, P.J., *et al*. (2010) *Plasmodium falciparum* isolates from Angola show the StctVMNT haplotype in the *pfcrt* gene. *Malar J* **9:** 174.

Gaviria, D., Paguio, M.F., Turnbull, L.B., Tan, A., Siriwardana, A., Ghosh, D., *et al*. (2013) A process similar to autophagy is associated with cytocidal chloroquine resistance in *Plasmodium falciparum*. *PLoS ONE* **8:** e79059.

Gligorijevic, B., Purdy, K., Elliott, D.A., Cooper, R.A., and Roepe, P.D. (2008) Stage independent chloroquine resistance and chloroquine toxicity revealed via spinning disk confocal microscopy. *Mol Biochem Parasitol* **159:** 7–23.

Griffing, S., Syphard, L., Sridaran, S., McCollum, A.M., Mixson-Hayden, T., Vinayak, S., *et al*. (2010) *pfmdr1* amplification and fixation of *pfcrt* chloroquine resistance alleles in *Plasmodium falciparum* in Venezuela. *Antimicrob Agents Chemother* **54:** 1572–1579.

Hastings, I.M., and Donnelly, M.J. (2005) The impact of antimalarial drug resistance mutations on parasite fitness, and its implications for the evolution of resistance. *Drug Resist Updat* **8:** 43–50.

Hrycyna, C.A., Summers, R.L., Lehane, A.M., Pires, M.M., Namanja, H., Bohn, K., *et al*. (2014) Quinine dimers are potent inhibitors of the *Plasmodium falciparum* chloroquine resistance transporter and are active against quinoline-resistant *P. falciparum*. *ACS Chem Biol* **9:** 722–730.

Isozumi, R., Uemura, H., Le, D.D., Truong, V.H., Nguyen, D.G., Ha, V.V., *et al*. (2010) Longitudinal survey of *Plasmodium falciparum* infection in Vietnam: characteristics of antimalarial resistance and their associated factors. *J Clin Microbiol* **48:** 70–77.

Juliano, J.J., Kwiek, J.J., Cappell, K., Mwapasa, V., and Meshnick, S.R. (2007) Minority-variant *pfcrt* K76T mutations and chloroquine resistance, Malawi. *Emerg Infect Dis* **13:** 872–877.

Kidgell, C., Volkman, S.K., Daily, J., Borevitz, J.O., Plouffe, D., Zhou, Y., *et al*. (2006) A systematic map of genetic variation in *Plasmodium falciparum*. *PLoS Pathog* **2:** e57.

Krogstad, D.J., Gluzman, I.Y., Kyle, D.E., Oduola, A.M., Martin, S.K., Milhous, W.K., and Schlesinger, P.H. (1987) Efflux of chloroquine from *Plasmodium falciparum*: mechanism of chloroquine resistance. *Science* **238:** 1283–1285.

Kublin, J.G., Cortese, J.F., Njunju, E.M., Mukadam, R.A., Wirima, J.J., Kazembe, P.N., *et al*. (2003) Reemergence of chloroquine-sensitive *Plasmodium falciparum* malaria after cessation of chloroquine use in Malawi. *J Infect Dis* **187:** 1870–1875.

Lakshmanan, V., Bray, P.G., Verdier-Pinard, D., Johnson, D.J., Horrocks, P., Muhle, R.A., *et al*. (2005) A critical role for PfCRT K76T in *Plasmodium falciparum* verapamil-reversible chloroquine resistance. *EMBO J* **24:** 2294–2305.

Laufer, M.K., Takala-Harrison, S., Dzinjalamala, F.K., Stine, O.C., Taylor, T.E., and Plowe, C.V. (2010) Return of chloroquine-susceptible *falciparum* malaria in Malawi was a reexpansion of diverse susceptible parasites. *J Infect Dis* **202:** 801–808.

Levin, B.R., Perrot, V., and Walker, N. (2000) Compensatory mutations, antibiotic resistance and the population genetics of adaptive evolution in bacteria. *Genetics* **154:** 985.

Lewis, I.A., Wacker, M., Olszewski, K.L., Cobbold, S.A., Baska, K.S., Tan, A., *et al*. (2014) Metabolic QTL analysis links chloroquine resistance in *Plasmodium falciparum* to impaired hemoglobin catabolism. *PLoS Genet* **10:** e1004085.

Maree, A.F., Keulen, W., Boucher, C.A., and De Boer, R.J. (2000) Estimating relative fitness in viral competition experiments. *J Virol* **74:** 11067–11072.

Martin, R.E., Marchetti, R.V., Cowan, A.I., Howitt, S.M.,

Broer, S., and Kirk, K. (2009) Chloroquine transport via the malaria parasite's chloroquine resistance transporter. *Science* **325:** 1680–1682.

Martin, S.K., Oduola, A.M., and Milhous, W.K. (1987) Reversal of chloroquine resistance in *Plasmodium falciparum* by verapamil. *Science* **235:** 899–901.

Mehlotra, R.K., Fujioka, H., Roepe, P.D., Janneh, O., Ursos, L.M., Jacobs-Lorena, V., *et al.* (2001) Evolution of a unique *Plasmodium falciparum* chloroquine-resistance phenotype in association with *pfcrt* polymorphism in Papua New Guinea and South America. *Proc Natl Acad Sci USA* **98:** 12689–12694.

Mharakurwa, S., Sialumano, M., Liu, K., Scott, A., and Thuma, P. (2013) Selection for chloroquine-sensitive *Plasmodium falciparum* by wild *Anopheles arabiensis* in Southern Zambia. *Malar J* **12:** 453.

Mita, T., Kaneko, A., Lum, J.K., Bwijo, B., Takechi, M., Zungu, I., *et al.* (2003) Recovery of chloroquine sensitivity and low prevalence of the *Plasmodium falciparum* chloroquine resistance transporter gene mutation K76T following the discontinuance of chloroquine use in Malawi. *Am J Trop Med Hyg* **68:** 413–415.

Mita, T., Kaneko, A., Lum, J., Zungu, I., Tsukahara, T., Eto, H., *et al.* (2004) Expansion of wild type allele rather than back mutation in *pfcrt* explains the recent recovery of chloroquine sensitivity of *Plasmodium falciparum* in Malawi. *Mol Biochem Parasitol* **135:** 159–163.

Mitchell-Olds, T., Willis, J.H., and Goldstein, D.B. (2007) Which evolutionary processes influence natural genetic variation for phenotypic traits? *Nat Rev Genet* **8:** 845–856.

Mixson-Hayden, T., Jain, V., McCollum, A.M., Poe, A., Nagpal, A.C., Dash, A.P., *et al.* (2010) Evidence of selective sweeps in genes conferring resistance to chloroquine and pyrimethamine in *Plasmodium falciparum* isolates in India. *Antimicrob Agents Chemother* **54:** 997–1006.

Mu, J., Myers, R.A., Jiang, H., Liu, S., Ricklefs, S., Waisberg, M., *et al.* (2010) *Plasmodium falciparum* genome-wide scans for positive selection, recombination hot spots and resistance to antimalarial drugs. *Nat Genet* **42:** 268–271.

Mwai, L., Ochong, E., Abdirahman, A., Kiara, S.M., Ward, S., Kokwaro, G., *et al.* (2009) Chloroquine resistance before and after its withdrawal in Kenya. *Malar J* **8:** 106.

Nash, D., Nair, S., Mayxay, M., Newton, P.N., Guthmann, J.P., Nosten, F., and Anderson, T.J. (2005) Selection strength and hitchhiking around two anti-malarial resistance genes. *Proc Biol Sci* **272:** 1153–1161.

Olliaro, P., and Mussano, P. (2000) Amodiaquine for treating malaria. *Cochrane Database Syst Rev* (2): CD000016.

Ord, R., Alexander, N., Dunyo, S., Hallett, R., Jawara, M., Targett, G., *et al.* (2007) Seasonal carriage of *pfcrt* and *pfmdr1* alleles in Gambian *Plasmodium falciparum* imply reduced fitness of chloroquine-resistant parasites. *J Infect Dis* **196:** 1613–1619.

Osman, M.E., Mockenhaupt, F.P., Bienzle, U., Elbashir, M.I., and Giha, H.A. (2007) Field-based evidence for linkage of mutations associated with chloroquine (*pfcrt/pfmdr1*) and sulfadoxine-pyrimethamine (*pfdhfr/pfdhps*) resistance and for the fitness cost of multiple mutations in *P. falciparum*. *Infect Genet Evol* **7:** 52–59.

Park, D.J., Lukens, A.K., Neafsey, D.E., Schaffner, S.F., Chang, H.H., Valim, C., *et al.* (2012) Sequence-based association and selection scans identify drug resistance loci in the *Plasmodium falciparum* malaria parasite. *Proc Natl Acad Sci USA* **109:** 13052–13057.

Pascual, A., Madamet, M., Bertaux, L., Amalvict, R., Benoit, N., Travers, D., *et al.* (2013) *In vitro* piperaquine susceptibility is not associated with the *Plasmodium falciparum* chloroquine resistance transporter gene. *Malar J* **12:** 431.

Patel, J.J., Thacker, D., Tan, J.C., Pleeter, P., Checkley, L., Gonzales, J.M., *et al.* (2010) Chloroquine susceptibility and reversibility in a *Plasmodium falciparum* genetic cross. *Mol Microbiol* **78:** 770–787.

Price, R.N., Tjitra, E., Guerra, C.A., Yeung, S., White, N.J., and Anstey, N.M. (2007) *Vivax* malaria: neglected and not benign. *Am J Trop Med Hyg* **77:** 79–87.

Rosario, V.E., Hall, R., Walliker, D., and Beale, G.H. (1978) Persistence of drug-resistant malaria parasites. *Lancet* **1:** 185–187.

Rosenthal, P.J. (2013) The interplay between drug resistance and fitness in malaria parasites. *Mol Microbiol* **89:** 1025–1038.

Sa, J.M., and Twu, O. (2010) Protecting the malaria drug arsenal: halting the rise and spread of amodiaquine resistance by monitoring the PfCRT SVMNT type. *Malar J* **9:** 374.

Sa, J.M., Twu, O., Hayton, K., Reyes, S., Fay, M.P., Ringwald, P., and Wellems, T.E. (2009) Geographic patterns of *Plasmodium falciparum* drug resistance distinguished by differential responses to amodiaquine and chloroquine. *Proc Natl Acad Sci USA* **106:** 18883–18889.

Saliba, K.J., Folb, P.I., and Smith, P.J. (1998) Role for the *Plasmodium falciparum* digestive vacuole in chloroquine resistance. *Biochem Pharmacol* **56:** 313–320.

Sanchez, C.P., Stein, W., and Lanzer, M. (2003) Trans stimulation provides evidence for a drug efflux carrier as the mechanism of chloroquine resistance in *Plasmodium falciparum*. *Biochemistry* **42:** 9383–9394.

Sanchez, C.P., Mayer, S., Nurhasanah, A., Stein, W.D., and Lanzer, M. (2011) Genetic linkage analyses redefine the roles of PfCRT and PfMDR1 in drug accumulation and susceptibility in *Plasmodium falciparum*. *Mol Microbiol* **82:** 865–878.

Sanchez, C.P., Liu, C.H., Mayer, S., Nurhasanah, A., Cyrklaff, M., Mu, J., *et al.* (2014) A HECT ubiquitin-protein ligase as a novel candidate gene for altered quinine and quinidine responses in *Plasmodium falciparum*. *PLoS Genet* **10:** e1004382.

Sidhu, A.B., Verdier-Pinard, D., and Fidock, D.A. (2002) Chloroquine resistance in *Plasmodium falciparum* malaria parasites conferred by *pfcrt* mutations. *Science* **298:** 210–213.

Sisowath, C., Petersen, I., Veiga, M.I., Mortensson, A., Premji, Z., Bjorkman, A., *et al.* (2009) *In vivo* selection of *Plasmodium falciparum* parasites carrying the chloroquine-susceptible *pfcrt* K76 allele after treatment with artemether-lumefantrine in Africa. *J Infect Dis* **199:** 750–757.

Snow, R.W., Trape, J.F., and Marsh, K. (2001) The past, present and future of childhood malaria mortality in Africa. *Trends Parasitol* **17:** 593–597.

Straimer, J., Lee, M.C., Lee, A.H., Zeitler, B., Williams, A.E., Pearl, J.R., *et al.* (2012) Site-specific genome editing in

Plasmodium falciparum using engineered zinc-finger nucleases. *Nat Methods* **9:** 993–998.
Straimer, J., Gnadig, N.F., Witkowski, B., Amaratunga, C., Duru, V., Ramadani, A.P., *et al*. (2015) Drug resistance. K13-propeller mutations confer artemisinin resistance in *Plasmodium falciparum* clinical isolates. *Science* **347:** 428–431.
Su, X., Kirkman, L.A., Fujioka, H., and Wellems, T.E. (1997) Complex polymorphisms in an approximately 330 kDa protein are linked to chloroquine-resistant *P. falciparum* in Southeast Asia and Africa. *Cell* **91:** 593–603.
Summers, R.L., Dave, A., Dolstra, T.J., Bellanca, S., Marchetti, R.V., Nash, M.N., *et al*. (2014) Diverse mutational pathways converge on saturable chloroquine transport via the malaria parasite's chloroquine resistance transporter. *Proc Natl Acad Sci USA* **111:** E1759–E1767.
Trape, J.F. (2001) The public health impact of chloroquine resistance in Africa. *Am J Trop Med Hyg* **64:** 12–17.
Valderramos, S.G., and Fidock, D.A. (2006) Transporters involved in resistance to antimalarial drugs. *Trends Pharmacol Sci* **27:** 594–601.
Valderramos, S.G., Valderramos, J.C., Musset, L., Purcell, L.A., Mercereau-Puijalon, O., Legrand, E., and Fidock, D.A. (2010) Identification of a mutant PfCRT-mediated chloroquine tolerance phenotype in *Plasmodium falciparum*. *PLoS Pathog* **6:** e1000887.
Volkman, S., Sabeti, P., Decaprio, D., Neafsey, D., Schaffner, S., Milner, D., *et al*. (2007) A genome-wide map of diversity in *Plasmodium falciparum*. *Nat Genet* **39:** 113–119.
Walliker, D., Hunt, P., and Babiker, H. (2005) Fitness of drug-resistant malaria parasites. *Acta Trop* **94:** 251–259.
Wang, X., Mu, J., Li, G., Chen, P., Guo, X., Fu, L., *et al*. (2005) Decreased prevalence of the *Plasmodium falciparum* chloroquine resistance transporter 76T marker associated with cessation of chloroquine use against *P. falciparum* malaria in Hainan, People's Republic of China. *Am J Trop Med Hyg* **72:** 410–414.
Wellems, T.E., and Plowe, C.V. (2001) Chloroquine-resistant malaria. *J Infect Dis* **184:** 770–776.
Wellems, T.E., Panton, L.J., Gluzman, I.Y., do Rosario, V.E., Gwadz, R.W., Walker-Jonah, A., and Krogstad, D.J. (1990) Chloroquine resistance not linked to *mdr*-like genes in a *Plasmodium falciparum* cross. *Nature* **345:** 253–255.
Wells, T.N., Alonso, P.L., and Gutteridge, W.E. (2009) New medicines to improve control and contribute to the eradication of malaria. *Nat Rev Drug Discov* **8:** 879–891.
White, N.J. (2008) Qinghaosu (artemisinin): the price of success. *Science* **320:** 330–334.
WHO (2014) World Malaria Report 2014. URL http://www.who.int/malaria/publications/world_malaria_report_2014/report/en
Wootton, J.C., Feng, X., Ferdig, M.T., Cooper, R.A., Mu, J., Baruch, D.I., *et al*. (2002) Genetic diversity and chloroquine selective sweeps in *Plasmodium falciparum*. *Nature* **418:** 320–323.

Supporting information

Additional supporting information may be found in the online version of this article at the publisher's web-site.

APPENDIX B: ADAPTIVE EVOLUTION OF MALARIA PARASITES IN FRENCH GUIANA: REVERSAL OF CHLOROQUINE RESISTANCE BY ACQUISITION OF A MUTATION IN *PFCRT*

Stéphane Pelleau,[1] Eli L. Moss,[2] Satish K. Dhingra,[3] Béatrice Volney,[1] Jessica Casteras,[1] **Stanislaw J. Gabryszewski**,[3] Sarah K. Volkman,[4] Dyann F. Wirth,[5] Eric Legrand,[1] David A. Fidock,[6] Daniel E. Neafsey,[2] and Lise Musset[7]

[1]Laboratoire de parasitologie, WHO Collaborating Center for Surveillance of Anti-Malarial Drug Resistance, Centre National de Référence du paludisme, Laboratoire associé pour la région Antilles-Guyane, Institut Pasteur de la Guyane, 97300 Cayenne, French Guiana; [2]Genome Sequencing and Analysis Program, Broad Institute, Cambridge, MA 02142; [3]Department of Microbiology and Immunology, Columbia University College of Physicians and Surgeons, New York, NY 10032; [4]Department of Immunology and Infectious Diseases, Harvard School of Public Health, Boston, MA 02115; Infectious Disease Program, Broad Institute, Cambridge, MA 02142; School of Nursing and Health Sciences, Simmons College, Boston, MA 02115; [5]Department of Immunology and Infectious Diseases, Harvard School of Public Health, Boston, MA 02115; Infectious Disease Program, Broad Institute, Cambridge, MA 02142; [6]Department of Microbiology and Immunology, Columbia University College of Physicians and Surgeons, New York, NY 10032; Division of Infectious Diseases, Department of Medicine, Columbia University College of Physicians and Surgeons, New York, NY 10032; [7]Laboratoire de parasitologie, WHO Collaborating Center for Surveillance of Anti-Malarial Drug Resistance, Centre National de Référence du paludisme, Laboratoire associé pour la région Antilles-Guyane, Institut Pasteur de la Guyane, 97300 Cayenne, French Guiana.

Author contributions: SP, SKV, DAF, DEN, and LM designed research; SP, SKD, BV, JC, **SJG**, DFW, and LM performed research; ELM and DEN contributed new reagents/analytic tools; SP, ELM, SKD, **SJG**, EL, DAF, DEN, and LM analyzed data; SP, **SJG**, DAF, DEN, and LM wrote the paper.

Adaptive evolution of malaria parasites in French Guiana: Reversal of chloroquine resistance by acquisition of a mutation in *pfcrt*

Stéphane Pelleau[a], Eli L. Moss[b], Satish K. Dhingra[c], Béatrice Volney[a], Jessica Casteras[a], Stanislaw J. Gabryszewski[c], Sarah K. Volkman[d,e,f], Dyann F. Wirth[d,e], Eric Legrand[a], David A. Fidock[c,g,1], Daniel E. Neafsey[b,1], and Lise Musset[a,2]

[a]Laboratoire de parasitologie, WHO Collaborating Center for Surveillance of Anti-Malarial Drug Resistance, Centre National de Référence du paludisme, Laboratoire associé pour la région Antilles-Guyane, Institut Pasteur de la Guyane, 97300 Cayenne, French Guiana; [b]Genome Sequencing and Analysis Program, Broad Institute, Cambridge, MA 02142; [c]Department of Microbiology and Immunology, Columbia University College of Physicians and Surgeons, New York, NY 10032; [d]Department of Immunology and Infectious Diseases, Harvard School of Public Health, Boston, MA 02115; [e]Infectious Disease Program, Broad Institute, Cambridge, MA 02142; [f]School of Nursing and Health Sciences, Simmons College, Boston, MA 02115; and [g]Division of Infectious Diseases, Department of Medicine, Columbia University College of Physicians and Surgeons, New York, NY 10032

Edited by Thomas E. Wellems, NIH, Bethesda, MD, and approved July 6, 2015 (received for review April 16, 2015)

In regions with high malaria endemicity, the withdrawal of chloroquine (CQ) as first-line treatment of *Plasmodium falciparum* infections has typically led to the restoration of CQ susceptibility through the reexpansion of the wild-type (WT) allele K76 of the chloroquine resistance transporter gene (*pfcrt*) at the expense of less fit mutant alleles carrying the CQ resistance (CQR) marker K76T. In low-transmission settings, such as South America, drug resistance mutations can attain 100% prevalence, thereby precluding the return of WT parasites after the complete removal of drug pressure. In French Guiana, despite the fixation of the K76T allele, the prevalence of CQR isolates progressively dropped from >90% to <30% during 17 y after CQ withdrawal in 1995. Using a genome-wide association study with CQ-sensitive (CQS) and CQR isolates, we have identified a single mutation in *pfcrt* encoding a C350R substitution that is associated with the restoration of CQ susceptibility. Genome editing of the CQR reference strain 7G8 to incorporate PfCRT C350R caused a complete loss of CQR. A retrospective molecular survey on 580 isolates collected from 1997 to 2012 identified all C350R mutant parasites as being CQS. This mutation emerged in 2002 and rapidly spread throughout the *P. falciparum* population. The C350R allele is also associated with a significant decrease in piperaquine susceptibility in vitro, suggesting that piperaquine pressure in addition to potential fitness costs associated with the 7G8-type CQR *pfcrt* allele may have selected for this mutation. These findings have important implications for understanding the evolutionary dynamics of antimalarial drug resistance.

malaria | drug resistance | evolution | *Plasmodium falciparum* | PfCRT

The emergence of drug-resistant pathogens is a major threat to human health, and *Plasmodium falciparum* has shown its capacity to develop resistance to every drug that has been deployed against it on a large scale. Although Africa carries by far the heaviest burden of malaria, parasite resistance to chloroquine (CQ), sulfadoxine-pyrimethamine (1), and more recently, artemisinins (2) first emerged in southeast Asia and South America (the latter only for CQ and sulfadoxine-pyrimethamine), where transmission intensity is low. This evolving situation underscores the importance of understanding the evolutionary dynamics of antimalarial drug resistance in distinct transmission contexts. In Central or South America, where clonal propagation can occur (3), the population genetic diversity is reduced, with high rates of inbreeding (4). As a consequence, strong drug pressure can ultimately lead to fixation of drug resistance alleles, even if they generate a fitness cost to parasites in the absence of drug pressure. Thus, whereas in high-transmission African settings, changes in drug pressure are known to alter the relative proportions of mutant and WT alleles of drug resistance determinants, less is known about how drug-selective forces operate in low-transmission contexts where resistance alleles are already fixed. Here, we have examined the evolution of *P. falciparum* CQ resistance (CQR) in French Guiana after successive changes in therapeutic policy.

French Guiana is a French overseas territory in South America that is included in the Guiana Shield, a pre-Cambrian geological formation including Guyana, Surinam, French Guiana, and parts of Venezuela, Brazil, and Colombia. The region is endemic for both *P. falciparum* and *Plasmodium vivax* (5). In the past 15 y, this population of ∼250,000 inhabitants has experienced a greater than 75% decrease in annual cases of malaria: ∼4,500 cases in 2000 compared with fewer than 500 cases in 2014. French Guiana is currently in a control phase and on track to soon enter a preelimination phase (fewer than 5% of febrile patients test positive for *Plasmodium*), a situation akin to that in 55 other countries around the world (6). Treatment of uncomplicated *P. falciparum* malaria cases with the former first-line antimalarial CQ was officially abandoned in 1995 because of poor clinical efficacy. Quinine (QN) plus doxycycline became the subsequent treatment of choice until 2007, with sporadic use of halofantrine and mefloquine (MQ). Artemether-lumefantrine, an artemisinin-based combination therapy (ACT), was widely implemented in 2008. Although the artemether–lumefantrine combination has been

Significance

This study addresses the evolutionary dynamics of antimalarial drug resistance after changes in drug use. We show that chloroquine resistance in *Plasmodium falciparum* from French Guiana was lost after sustained drug removal, whereas the resistance marker PfCRT K76T remained fixed in the parasite population. This phenotypic reversion was caused by the acquisition of a single additional C350R substitution in PfCRT. This genetic change also impaired susceptibility to piperaquine, suggesting that piperaquine pressure drove the expansion of this allele. These findings have important implications for understanding drug resistance evolution when standard resistance alleles reach fixation and can lose their utility as markers because of adaptive changes at other amino acid positions or loci in the genome.

Author contributions: S.P., S.K.V., D.A.F., D.E.N., and L.M. designed research; S.P., S.K.D., B.V., J.C., S.J.G., D.F.W., and L.M. performed research; E.L.M. and D.E.N. contributed new reagents/analytic tools; S.P., E.L.M., S.K.D., S.J.G., E.L., D.A.F., D.E.N., and L.M. analyzed data; and S.P., S.J.G., D.A.F., D.E.N., and L.M. wrote the paper.

The authors declare no conflict of interest.

This article is a PNAS Direct Submission.

Freely available online through the PNAS open access option.

See Commentary on page 11432.

[1]D.A.F. and D.E.N. contributed equally to this work.

[2]To whom correspondence should be addressed. Email: lisemusset@gmail.com.

This article contains supporting information online at www.pnas.org/lookup/suppl/doi:10.1073/pnas.1507142112/-/DCSupplemental.

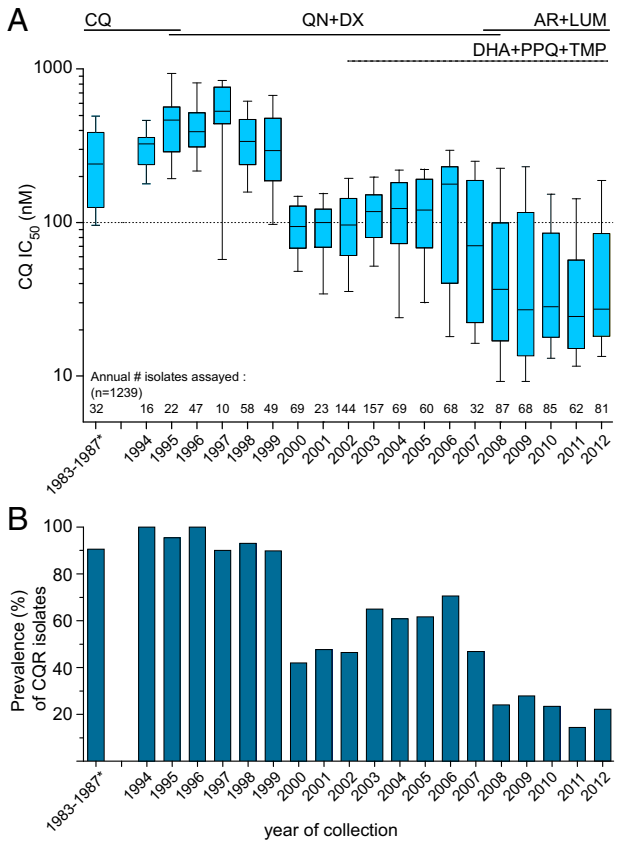

Fig. 1. Evolution of *P. falciparum* in vitro CQ susceptibility in French Guiana from 1983 to 2012. Lines above graphs indicate the successive change in drug recommendations in French Guiana throughout the study period. (*A*) Box and whisker plots showing the distribution of CQ IC_{50} values. Whiskers show the 10th and 90th percentiles, boxes represent interquartile range, and the horizontal line is the median. Isolate numbers per year are listed above the *x* axis. (*B*) Observed percentage of CQR isolates over time defined by an IC_{50} > 100 nM. AR, artemether; DX, doxycycline.*1983–1987 data are from ref. 17.

the official first-line treatment since 2008, illegal gold miners living in the forest are known to self-medicate their fevers with dihydroartemisinin (DHA) -piperaquine (PPQ) -trimethoprim (TMP; DHA + PPQ + TMP; Artecom) tablets.

In South America, the prevalence of the CQR marker K76T in the drug efflux transmembrane protein PfCRT has remained high, despite CQ having been abandoned for the treatment of *P. falciparum* infections (7–9). This situation contrasts with multiple settings in Africa, where the majority of molecular studies (10–13) have documented an increase in the prevalence of WT *pfcrt* after CQ withdrawal. An analysis of the diversity of microsatellites flanking *pfcrt* in Malawi showed that the return to CQ susceptibility was caused by a reexpansion of the WT PfCRT haplotype (11). Such a difference between South America and other endemic regions in response to CQ withdrawal is generally attributed to other amino acid changes in PfCRT and PfMDR1 (both present on the parasite digestive vacuole membrane), which accompany the PfCRT K76T substitution. Specifically, the SVMNT haplotype of South American parasites at PfCRT amino acids 72–76 has been found to be less deleterious than the CVIET haplotype present elsewhere (14, 15). Another explanation for the virtual fixation of CQR alleles in South American parasites is that CQ continues to be used to treat *P. vivax* infections and therefore, may exert a residual pressure. Lastly, it is thought that the earlier campaign of adding low-dose amodiaquine (AQ) to table salt proved highly effective at creating a selective sweep of AQ and CQR-conferring mutant *pfcrt* after it had arisen in the late 1950s and eliminating any vestigial WT *pfcrt*.

We have previously reported that a significant proportion of *P. falciparum* parasites from French Guiana have a CQ IC_{50} below the adopted resistance threshold of 100 nM, despite elevated prevalence of K76T, suggesting a reduced predictive value of this marker, at least in this region of South America (16). In this study, we pursued a genotypic and phenotypic survey, including whole-genome sequencing and gene-editing experiments, which led us to identify a molecular marker of drug susceptibility. These findings have important implications for understanding drug resistance evolution in a low-endemicity context where drug resistance alleles can reach fixation, a scenario that will become increasingly dominant as successful control efforts progressively reduce the burden of malaria.

Results

CQ Susceptibility Has Returned to French Guiana After Drug Withdrawal. We tested the in vitro CQ susceptibility of 1,207 *P. falciparum* isolates collected between 1994 and 2012 and compared these data with those previously reported for the 1983–1987 period (17). The general trend is that CQ susceptibility followed changes in drug policy (Fig. 1) and can be divided into three main periods. It took 5 y after the official CQ withdrawal in 1995 to observe a decrease in the prevalence of in vitro CQR isolates from ∼90% to ∼40% (Fig. 1*B*). Of note, such a high prevalence of CQR at ∼90% in the 1990s was already reported in the mid-1980s. From 2000 to 2006, a consistent but small increase in the prevalence of CQR isolates was observed (up to 70% in 2006), potentially because of an overlap between the mechanisms of drug response to CQ and the first-line therapies used at that time (notably QN). This trend toward a resurgence of CQR, however, reversed concomitantly with the progressive introduction of ACT as first-line therapy in 2007. Within 2 y, the prevalence of CQR isolates dropped and thereafter, remained stable at ∼25% (2008–2012).

Mutant PfCRT and PfMDR1 Haplotypes Are Fixed in the Parasite Population. We genotyped a large panel of patient isolates collected between 1997 and 2012 (Table 1). Of 1,054 isolates genotyped for the *pfcrt* gene, the mutant haplotype SVMNT was present in 97.5%, a far greater proportion than the mean percentage of in vitro CQR parasites (48.6%) observed in the same period. Haplotypes other than SVMNT were very rare (n = 26 of 1,054). For 18 of these 26 patients for whom we had information, 15 had traveled to West Africa (5 CVIET and 10 CVMNK) and 2 had traveled to Haiti (CVMNK) in the previous month, leaving a single patient harboring a CVMNK haplotype that could have been transmitted locally. A similar allelic fixation could be observed for the *pfmdr1* gene, because 86.3% of 861 genotyped isolates displayed the South American resistance-associated NFCDY haplotype (amino acids 86, 184, 1,034, 1,042, and 1,246) (Table 1). Altogether, the sum of PfCRT/PfMDR1 haplotypes SVMNT/NFCDY (7G8-type; n = 688) and SVMNT/NFSDY (n = 108) was present in 99.0% of the

Table 1. Prevalence of PfCRT and PfMDR1 haplotypes of isolates collected in French Guiana (1997–2012)

Haplotype	*n*	Frequency (%)
PfCRT (n = 1,054)		
SVMNT	1,028	97.5
CVMNK	17	1.6
CVIET	9	0.9
PfMDR1 (n = 861)		
NFCDY	743	86.3
NFSDY	113	13.1
NFCDD	2	0.2
NFSND	2	0.2
NYSND	1	0.1

Haplotypes denote amino acids at positions 72–76 for PfCRT and positions 86, 184, 1,034, 1,042, and 1,246 for PfMDR1.

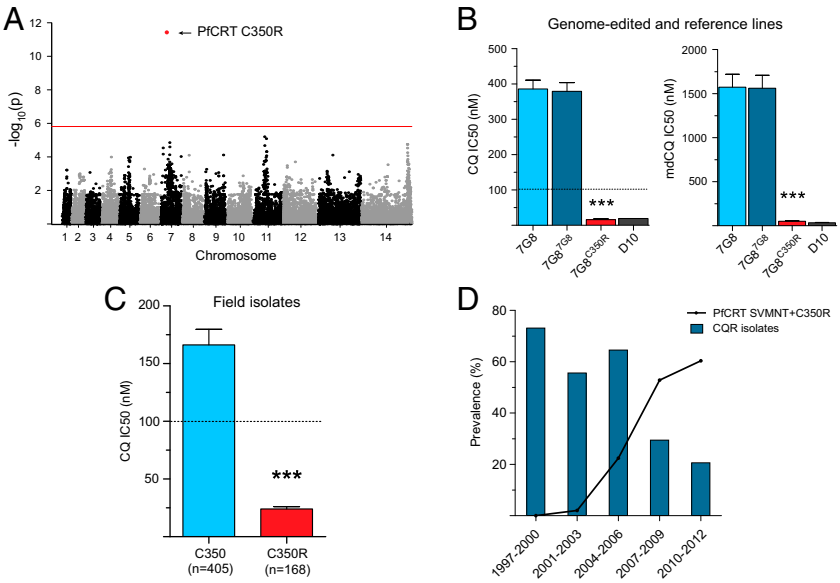

Fig. 2. PfCRT C350R is the determinant of in vitro CQR reversion. (*A*) Signal of SNPs associated with CQ susceptibility. The Manhattan plot shows *P* values for SNPs with minor allele frequencies >10%. The horizontal red line indicates the *P* value significance threshold. After adjusting *P* values for genome-wide inflation (Fig. S2), a single SNP (red dot) on chromosome 7 displayed a highly significant association with CQ susceptibility ($P <$ 1E-11; PfCRT C350R; arrow). (*B*) *pfcrt*-edited clones and control reference lines 7G8 and D10 were assayed for their susceptibilities to CQ and its active in vivo metabolite monodesethyl-CQ (mdCQ). IC_{50} values are represented as means ± SEM. Each line was assayed on at least eight separate occasions in duplicate (Table S1). (*C*) IC_{50} values for *P. falciparum* isolates from French Guiana (means ± SEM). Horizontal dashed lines in *B* and *C* denote the resistance threshold of 100 nM. ***$P <$ 0.0001 relative to (*B*) $7G8^{7G8}$ or (*C*) PfCRT C350 isolates (Student *t* test). (*D*) Decreasing prevalence of CQR isolates from 1997 to 2012 and its inverse relationship with the increasing prevalence of isolates harboring PfCRT C350R (continuous line). Only isolates carrying the PfCRT SVMNT haplotype at amino acids 72–76 were included in the analysis.

isolates sampled during this 16-y period. These results confirmed that the standard molecular markers, notably PfCRT K76T and to a lesser degree, PfMDR1, are no longer predictive of CQR in French Guiana.

Genome-Wide Association Study Identifies PfCRT C350R as the Single Mutation Associated with CQ Susceptibility. To identify the genomic variants associated with the reversion of CQR in mutant isolates harboring PfCRT K76T, we performed whole-genome sequence analysis of 54 culture-adapted isolates obtained from distinct malaria-infected patients in French Guiana between 2009 and 2013. We then performed a genome-wide association study (GWAS) on a final dataset of 35 isolates [18 CQ-sensitive (CQS) and 17 CQR parasites] containing 34,196 SNPs (Figs. S1 and S2). Strikingly, a single locus on chromosome 7 achieved genome-wide significance for association with CQS: a Tgt/Cgt non-synonymous substitution in exon 10 of the *pfcrt* gene that leads to the replacement of a cysteine by an arginine at codon 350 (C350R) (Fig. 2*A*).

Genome Editing and Molecular Surveys Show That PfCRT C350R Is Responsible for a Loss of CQR. To assess the impact of PfCRT C350R, we edited the *pfcrt* gene in the CQR reference strain 7G8. This Brazilian strain carries the canonical South American PfCRT (SVMNT) and PfMDR1 (NFCDY) haplotypes that are shared by the vast majority of isolates from French Guiana. 7G8 parasites that expressed either the recombinant 7G8 allele ($7G8^{7G8}$; transfection control) or the 7G8 variant containing the C350R mutation ($7G8^{C350R}$) were generated using *pfcrt*-specific zinc finger nucleases as previously described (18) (Fig. S3). Recombinant clones were obtained by limiting dilution and validated using PCR and sequencing. Drug assay data showed that the PfCRT C350R mutation caused a 24-fold reduction in the mean CQ IC_{50} values from 380 nM in the reference $7G8^{7G8}$ clone to 16 nM in the $7G8^{C350R}$ variant ($P < 0.0001$, Student *t* test) (Fig. 2*B*). A similar reversal of resistance to monodesethyl-CQ, the active in vivo metabolite of CQ, was observed. Parallel studies with parental 7G8 parasites yielded a mean CQ IC_{50} value of 386 nM, indicating that the expression of the cDNA *pfcrt* locus (lacking most introns) did not itself cause a significant shift in CQ IC_{50} values. Of note, the $7G8^{C350R}$ clone showed a similar mean CQ IC_{50} value as the reference CQS strain D10 (Papua New Guinea; mean IC_{50} of 19 nM) that harbors the PfCRT CVMNK WT sequence.

In parallel, we examined the association of the C350R mutation with CQ susceptibility in PfCRT K76T mutant isolates in a large set of isolates collected between 1997 and 2012. Exons 2 and 10 were sequenced from 580 isolates. Biallelic samples (C350 + 350R; $n = 7$) were excluded from the analysis because of a putatively biased IC_{50} value. All PfCRT C350R mutant isolates ($n = 168$) were found to be CQS, with a mean CQ IC_{50} of 23 nM. This value is significantly lower than the mean CQ IC_{50} value of 160 nM observed with PfCRT C350 parasites ($n = 405$; $P <$ 0.0001) (Fig. 2*C*). Altogether, these results provide compelling evidence that the emergence of the PfCRT C350R mutation is primarily responsible for the recent gain of CQ susceptibility in PfCRT K76T isolates from French Guiana.

PfCRT C350R Emerged in 2002 and Then, Rapidly Spread Throughout the Parasite Population in French Guiana. Only 54% of the CQS isolates with the PfCRT SVMNT sequence harbored the additional C350R mutation in the combined dataset. However, this general picture obscures important temporal disparities. Although it took 5 y after the official withdrawal of CQ to observe a significant decrease of CQR (i.e., in 2000), interestingly, the first PfCRT C350R isolate was not detected until 2 y later in 2002 (Fig. 2*D*). Thereafter, the prevalence of PfCRT C350R in the total parasite population increased rapidly from 2.7% in 2002 up to 58% in 2012. We note that 100% of the CQR isolates harbored K76T and the C350 residue. Among the SVMNT CQS isolates (defined as CQ $IC_{50} < 100$ nM), the prevalence of PfCRT C350R increased from 5% in 2002 to 83% in 2012; the few other CQS C350 isolates nonetheless showed a significantly higher mean CQ IC_{50} than the CQS C350R isolates (62 vs. 23 nM, respectively; $P < 0.001$).

Significant Impact of the PfCRT C350R Mutation on Decreased PPQ Susceptibility. Because PfCRT is known to modulate *P. falciparum* response to diverse antimalarial drugs, we investigated whether the C350R mutation had an impact on other drug susceptibilities in both the 7G8 genome-edited lines and field isolates collected during the 2008–2012 period (Fig. 3). For all tested compounds, the $7G8^{7G8}$ modified clone displayed IC_{50} values similar to the 7G8 parental line, confirming that the *pfcrt* gene editing did not affect drug responses. Introduction of the PfCRT C350R mutation had no effect on pyronaridine response but significantly increased 7G8 susceptibilities to monodesethyl-AQ (mdAQ), QN, MQ, and lumefantrine (LUM) by 2- to 4-fold ($P < 0.001$) and induced a moderate but significant 1.6-fold increase in artesunate susceptibility (3.5 vs. 2.2 nM for $7G8^{7G8}$ and $7G8^{C350R}$, respectively; $P < 0.05$). A significant effect of C350R on PPQ response was also observed, with the $7G8^{C350R}$ clone showing a 1.4-fold decreased

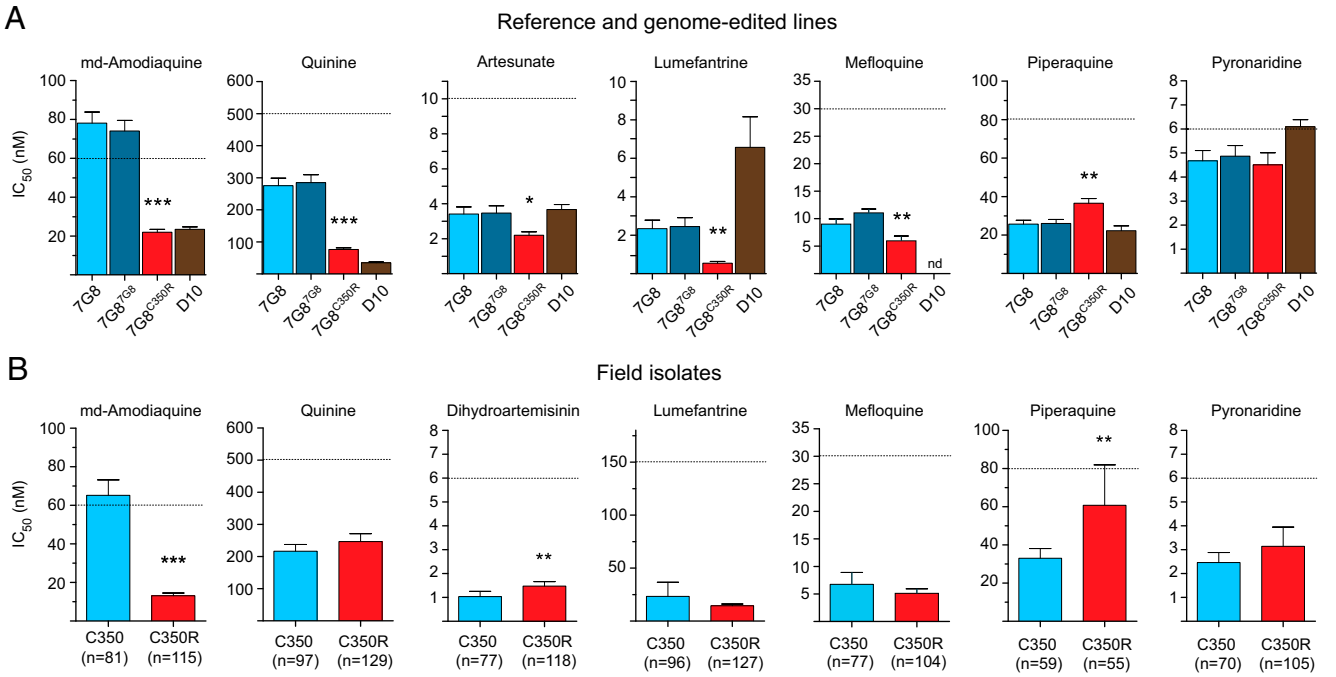

Fig. 3. Impact of PfCRT C350R on antimalarial drug responses (means ± SEM). IC_{50} values are shown for (*A*) genome-edited and reference lines (assayed on four to nine separate occasions in duplicate) (Table S1) and (*B*) French Guianan field isolates from 2008 to 2012. All isolates analyzed in *B* have the PfCRT SVMNT haplotype at amino acids 72–76. Genome-edited lines or field isolates harboring PfCRT C350R show concordant results in their higher susceptibilities to CQ and mdAQ, contrasting with a decreased susceptibility to PPQ. Asterisks denote the significance level of the difference (*A*) between $7G8^{C350R}$ and $7G8^{7G8}$ or (*B*) between PfCRT C350R and C350 isolates (Student *t* test). nd, not determined. $*P < 0.05$; $**P < 0.001$; $***P < 0.0001$.

susceptibility (mean PPQ IC_{50} of 26 vs. 37 nM for $7G8^{7G8}$ and $7G8^{C350R}$, respectively; $P < 0.001$) (Fig. 3*A* and Table S1).

French Guianan isolates showed a quite different pattern of drug susceptibilities (Fig. 3*B*). As expected, C350R mutant isolates were also found to be highly susceptible to mdAQ. Unlike the 7G8 genome-edited lines, no differences in QN, MQ, and LUM susceptibilities were found. However, a moderate but significant association between the presence of the C350R mutation and a decrease in DHA susceptibility was observed (1.0 vs. 1.5 nM for C350 and C350R, respectively; $P < 0.001$). C350R mutant isolates also displayed a significantly lower susceptibility to PPQ compared with WT C350 isolates (mean IC_{50} of 61 vs. 33 nM for C350R and C350, respectively; $P < 0.001$). Overall, both the gene-edited $7G8^{C350R}$ line and field isolates harboring a PfCRT SVMNT + C350R haplotype showed concordant results in their higher susceptibilities to CQ and mdAQ in contrast with their decreased susceptibilities to PPQ.

Discussion

In French Guiana, the prevalence of CQR has decreased significantly after CQ withdrawal, a pattern also noted in many other endemic areas worldwide (10–13). Here, we show that this phenotypic reversion is caused by the acquisition of a single mutation in the *pfcrt* gene that completely abolishes the effect of the K76T resistance mutation as opposed to the alternative scenario of the WT allele reemerging.

Repopulation by an allele is driven by multiple parameters, including initial frequency, population size, and the allele's selective advantage. Our findings clearly show that the WT PfCRT CVMNK haplotype has been purged from the entire population and that the few cases of imported parasites from Africa or Haiti were not sufficient to initiate colonization. The return to CQ susceptibility was not as straightforward as in Malawi, where CQR has completely disappeared, and it has been proposed that CQ treatment could be reintroduced (19). In addition to the fact that an additional mutation had to emerge and then spread in French Guiana, the differential rate of CQR reversal might be related to the clear differences in transmission intensity, population dynamics, and history of drug use between these two settings. In French Guiana, 18 y after CQ withdrawal, 25% of isolates are still CQR in vitro, precluding the reintroduction of CQ as antimalarial treatment.

Two studies have reported the emergence of polymorphisms nearby C350R in PfCRT after in vitro drug selection experiments on CQR strains. Using the $106/1^{76I}$ line, QN single-step selection experiments generated lines with an additional PfCRT Q352K or Q352R mutation that had acquired QN resistance but simultaneously regained CQ susceptibility (20). Separately, in vitro selection for resistance to the IDI-3783 compound that is selectively active against CQR parasites resulted in acquisition of the Q352R mutation in PfCRT (and concomitantly, a loss of CQR), thus providing a conceptual framework for the development of combination therapies that would exploit this evolutionary trap (21). These mutations occur in *pfcrt* exon 10, which corresponds to amino acid substitutions in transmembrane domain 9. This domain is postulated to function in substrate binding and translocation, similar to transmembrane domain 1, which contains the K76T substitution (20, 22–24). The functional hypothesis for the regained in vitro CQ susceptibility by acquisition of mutations in exon 10 is the reintroduction of a positive charge (K and R) that would inhibit the binding of CQ and block its extrusion from the digestive vacuole. Therefore, an important finding of our study is the demonstration that these particular adaptive mechanisms observed in individual strains during in vitro experiments can also be selected in natural parasite populations where drug resistance alleles are fixed.

Examining the temporal changes in PfCRT haplotype diversity, we note that, between 2001 and 2003, the majority of CQS field isolates did not harbor the C350R mutation. By 2012, however, almost all of the susceptible parasites harbored the PfCRT C350R mutation, implying strong selection for this variant. These results suggest the existence of additional determinants accounting for the loss of CQR in the early 2000s. In another study that examined how the parasite genetic background dictates the degree of mutant *pfcrt*-mediated CQR, the WT *pfcrt*

allele in CQS strains was replaced by the mutant 7G8-type *pfcrt* (25). The $3D7^{7G8}$- and $D10^{7G8}$-transfected lines exhibited only a modest increase in their CQ IC_{50} values. Nonetheless, these mutant lines were able to withstand high concentrations of CQ and showed delayed recrudescence in culture after high CQ exposure, indicative of a CQ tolerance phenotype. Interestingly, two CQS isolates from French Guiana with the PfCRT SVMNT haplotype were assayed in the same study. The isolate G224 (exhibiting PfCRT C350) also displayed the characteristics of CQ tolerance, whereas the other isolate, H209 (exhibiting PfCRT C350R), had a more typical CQS phenotype. From these previous results and our own observation that the few CQS isolates with WT PfCRT C350 are significantly less susceptible to CQ than the PfCRT C350R isolates, we can hypothesize that these SVMNT PfCRT C350 isolates with a CQ $IC_{50} < 100$ nM had a CQ-tolerant phenotype, having already lost robust resistance. Acquisition of full CQ susceptibility would, therefore, be a multistep process that proceeds by an accumulation of adaptive changes, including mutations acquired at other loci, with PfCRT C350R being the final step of a complete CQR reversal.

The successive implementation over time of various first-line drugs after the official cessation of CQ use (Fig. 1) has created a complex selection landscape operating on the *pfcrt* gene, which is known to impact the efficacy of multiple antimalarials (20, 26). Our drug profiling data showed a significant loss of mdAQ resistance in field isolates harboring the PfCRT C350R mutation, consistent with earlier reports that highlighted the close correlation between CQ and mdAQ responses of PfCRT SVMNT parasites from South America (14). Our observation that mutant C350R isolates were nominally less susceptible to DHA, however, should be interpreted with caution, notably because in vitro artemisinin susceptibilities, as measured using IC_{50} values, do not correlate with the clinical phenotype of delayed parasite clearance rates in southeast Asia (27, 28).

Our genome-edited $7G8^{C350R}$ line displayed increased susceptibility to multiple drugs, including mdAQ (as noted above for C350R-carrying field isolates), QN, MQ, artesunate, and LUM. This result reveals a pleiotropic role for this recently emerged *pfcrt* allele in modulating parasite susceptibility to clinically important antimalarials. This role differs from what is generally observed in Africa with the PfCRT CVIET haplotype or even the PfCRT SVMNT haplotype in Papua New Guinea (29, 30). This effect of C350R on QN and MQ, however, was not replicated in field isolates, underscoring a complex genetic basis of susceptibility in the field. Another primary determinant of susceptibility to these drugs in *P. falciparum* is the *pfmdr1* gene, which in French Guiana harbors the 86N and 184F residues that are associated with increased LUM susceptibility (31, 32). Of note, all isolates remained highly susceptible to LUM, a finding that argues for maintaining the artemether + LUM combination as first-line therapy in the region.

Finally, our data provide evidence that the *pfcrt* genotype impacts PPQ response. These results suggest that the PPQ pressure exerted by the erratic consumption of Artecom (DHA + PPQ + TMP) by thousands of illegal gold miners in French Guiana since 2002 might be one of the selective forces that drove the expansion of the PfCRT C350R allele during this same period and as a consequence, the return of CQ susceptibility. In fact, miners on the Guiana Shield readily cross borders between Brazil, French Guiana, and Suriname and regularly automedicate with Artecom (33–35). This clue to the putative mechanism of resistance to PPQ is potentially of considerable importance, because PPQ treatment failure is a major and increasing concern in southeast Asia (36–38). Therefore, the association between PfCRT haplotypes and PPQ treatment failure should be further explored in southeast Asia, where polymorphisms in the *pfcrt* gene, notably in exon 10, were found to accompany mutations in the *pfK13* gene associated with artemisinin resistance (39). Given that increased PPQ pressure is likely under mass drug administration campaigns that use DHA–PPQ, it would be also important to monitor parasite changes at the entire *pfcrt* locus that may result in reduced PPQ susceptibility.

In conclusion, this work illustrates a unique evolutionary path taken by the *pfcrt* gene as a consequence of an altered drug policy. In the virtual absence of the competing WT, sensitive *pfcrt* allele, drug susceptibility evolved through the acquisition of an additional amino acid substitution rather than reversion of an existing mutation, such as the critical CQR marker K76T. The extent of this particular mechanism of CQR reversion, described here for the first time to our knowledge, should be further assessed to determine whether it reflects a local evolutionary event or is also happening in other settings or at larger scales. Finally, we provide evidence that, in regions where *P. falciparum* parasite populations are small and malaria elimination efforts will be targeted, the usefulness of standard molecular markers for drug resistance will require periodic phenotypic validation to contend with ongoing parasite evolution.

Materials and Methods

Origin and Collection of French Guianan Isolates. *P. falciparum* isolates were collected between 1994 and 2013 from symptomatic patients diagnosed throughout the network of hospitals, medical laboratories, and health centers in French Guiana. The GWAS samples were collected during 2009–2013. To ensure clonality before whole-genome sequencing, isolates were either assayed with a subset of 15 SNPs from a 24-SNP barcode (40) and confirmed as monoclonal or cloned by limiting dilution.

Drug Assays. The phenotypes of the isolates were determined ex vivo (i.e., directly after patient blood sampling) or in vitro (after parasite multiplication in culture for several days). The ex vivo method was applied if, at the time of starting phenotypic analysis, the isolate exhibited (*i*) a *P. falciparum* infection without concomitant *P. vivax* infection, (*ii*) a parasitemia greater than 0.05%, (*iii*) an interval of less than 4 d between sampling and analysis, and (*iv*) a quantity of blood sufficient to run the method. Parasite growth was determined by incorporation of tritiated hypoxanthine using a 42-h standard 96-well candle jar method (41). French Guianan culture-adapted clones selected for whole-genome sequencing were assayed in a controlled gas atmosphere with 5% (vol/vol) CO_2, 10% (vol/vol) O_2, and 85% (vol/vol) N_2. For 7G8 and D10 clones, in vitro 72-h drug dose–response assays were performed, and parasite growth was determined using flow cytometry with SYBR Green I and MitoTracker Deep Red (42). Mean $IC_{50} \pm$ SEM values and numbers of repeats are listed in Table S1. Statistical significance of differences between mean IC_{50} values was assessed using Student *t* tests.

DNA Extraction and Genotyping. Genomic DNA was prepared using the QIAmp DNA Blood Kit (Qiagen). Conditions for PCR and targeted sequencing of *pfcrt* exon 2 (harboring codons 72–76) and polymorphic regions of *pfmdr1* were previously described (16). A 121-bp fragment encompassing the complete exon 10 of *pfcrt* (harboring codon 350) was PCR-amplified and Sanger-sequenced.

Whole-Genome Sequencing and the GWAS. DNA samples were made into 200-bp Illumina fragment libraries by the Broad Institute Genomics Platform and sequenced with paired-end 101-bp reads on an Illumina HiSeq2000 instrument using V2 chemistry. This design yielded a 70-fold mean coverage, a level sufficient to perform SNP calling. Reads were processed through the Picard sequencing analysis pipeline at the Broad Institute, generating standard sequencing metrics and demultiplexed sample-specific sequencing read BAM (Binary Alignment Map) files. Reads were aligned to the 3D7 reference assembly (PlasmoDB v9.0) using BWA (43), and SNPs were called using the GATK Unified Genotyper (44). Heterozygous SNP calls were discarded along with all calls exhibiting QUAL (quality scores) < Q30. Principal components analysis on called SNPs led to the exclusion of six confounders because of perfect genome identity ($n = 4$; implying clonal infection in different patients) and population stratification ($n = 2$; outliers) to find an unstructured sample of unique individual genomes (Fig. S1). We further filtered the dataset to exclude samples exhibiting either a low fraction of genotypable bases because of low sequencing coverage or SNP sites exhibiting a call rate of less than 50% in the remaining samples and/or a minor allele frequency of less than 10%. Samples were excluded from the GWAS if they exhibited calls for fewer than 90% of the SNP loci matching the criteria just described. The GWAS was performed in PLINK v1.07 (pngu.mgh.harvard.edu/purcell/plink/) (45). To avoid false-positive associations, we applied a genomic control correction to adjust *P* values for genome-wide inflation (Fig. S2).

Generation of *pfcrt*-Edited 7G8 Clones. To generate recombinant isogenic lines differing only at their *pfcrt* locus, we used a previously validated zinc finger nuclease-mediated genome editing strategy (18). A schematic and a description of this approach are shown in Fig. S3.

Ethical Considerations. Analyzed samples were all obtained by blood collections performed as part of the standard medical care for any patient presenting with fever on hospital admission in French Guiana. Specimen collection complied with Article L.1211–2 and related articles of the French Public Health Code, which states that biobanking and secondary use for scientific purpose of remaining human clinical samples are justified with the informed consent of the patient. Moreover, in compliance with French legislation (article L.1243–3 and related articles of the French Public Health Code), samples received at the Malaria NRC (National Reference Center) had been registered for research purposes in the NRC Biobank declared to both the French Ministry for Research and a French Ethics Committee, which both approved and registered this thematic biobank (declaration number DC-2010–1223; collection no. 2). No institutional review board approval is required according to the French legislation.

ACKNOWLEDGMENTS. We thank Denis Blanchet, Bernard Carme, Magalie Demar, Félix Djossou, Claire Grenier, Michel Joubert, and Rachida Boukhari for contributions to the sample collection. This work was supported by European Commission Grant REGPOT-CT-2011-285837-430 STRonGer (to S.P.), Agence Nationale de la Recherche Investissements d'Avenir Grant ANR-10-LABX-25-01 (to S.P. and L.M.), NIH Grants R01AI50234 (to D.A.F.) and R01AI109023 (to D.A.F.), and the Institut de Veille Sanitaire. Sequencing was supported, in part, by National Institute of Allergy and Infectious Diseases, NIH, Department of Health and Human Services Contract HHSN272200900018C.

1. Naidoo I, Roper C (2013) Mapping 'partially resistant', 'fully resistant', and 'super resistant' malaria. *Trends Parasitol* 29(10):505–515.
2. Ashley EA, et al.; Tracking Resistance to Artemisinin Collaboration (TRAC) (2014) Spread of artemisinin resistance in *Plasmodium falciparum* malaria. *N Engl J Med* 371(5):411–423.
3. Obaldia N, 3rd, et al. (2015) Clonal outbreak of *Plasmodium falciparum* infection in eastern Panama. *J Infect Dis* 211(7):1087–1096.
4. Volkman SK, et al. (2007) A genome-wide map of diversity in *Plasmodium falciparum*. *Nat Genet* 39(1):113–119.
5. Musset L, et al. (2014) Malaria on the Guiana Shield: A review of the situation in French Guiana. *Mem Inst Oswaldo Cruz* 109(5):525–533.
6. WHO (2014) *World Malaria Report* (WHO, Geneva).
7. Adhin MR, Labadie-Bracho M, Bretas G (2013) Molecular surveillance as monitoring tool for drug-resistant *Plasmodium falciparum* in Suriname. *Am J Trop Med Hyg* 89(2): 311–316.
8. Griffing S, et al. (2010) *pfmdr1* amplification and fixation of *pfcrt* chloroquine resistance alleles in *Plasmodium falciparum* in Venezuela. *Antimicrob Agents Chemother* 54(4):1572–1579.
9. Vieira PP, et al. (2004) *pfcrt* Polymorphism and the spread of chloroquine resistance in *Plasmodium falciparum* populations across the Amazon Basin. *J Infect Dis* 190(2): 417–424.
10. Mekonnen SK, et al. (2014) Return of chloroquine-sensitive *Plasmodium falciparum* parasites and emergence of chloroquine-resistant *Plasmodium vivax* in Ethiopia. *Malar J* 13:244.
11. Laufer MK, et al. (2010) Return of chloroquine-susceptible *falciparum* malaria in Malawi was a reexpansion of diverse susceptible parasites. *J Infect Dis* 202(5):801–808.
12. Mbogo GW, et al. (2014) Temporal changes in prevalence of molecular markers mediating antimalarial drug resistance in a high malaria transmission setting in Uganda. *Am J Trop Med Hyg* 91(1):54–61.
13. Mohammed A, et al. (2013) Trends in chloroquine resistance marker, Pfcrt-K76T mutation ten years after chloroquine withdrawal in Tanzania. *Malar J* 12:415.
14. Sá JM, et al. (2009) Geographic patterns of *Plasmodium falciparum* drug resistance distinguished by differential responses to amodiaquine and chloroquine. *Proc Natl Acad Sci USA* 106(45):18883–18889.
15. Petersen I, et al. (2015) Balancing drug resistance and growth rates via compensatory mutations in the Plasmodium falciparum chloroquine resistance transporter. *Mol Microbiol* 97(2):381–395.
16. Legrand E, et al. (2012) Discordant temporal evolution of *Pfcrt* and *Pfmdr1* genotypes and *Plasmodium falciparum in vitro* drug susceptibility to 4-aminoquinolines after drug policy change in French Guiana. *Antimicrob Agents Chemother* 56(3): 1382–1389.
17. Dedet JP, Germanetto P, Cordoliani G, Bonnevie O, Le Bras J (1988) *In vitro* activity of various antimalarials (chloroquine, amodiaquine, quinine and mefloquine) against 32 isolates of *Plasmodium falciparum* in French Guiana. *Bull Soc Pathol Exot* 81(1):88–93.
18. Straimer J, et al. (2012) Site-specific genome editing in *Plasmodium falciparum* using engineered zinc-finger nucleases. *Nat Methods* 9(10):993–998.
19. Frosch AE, et al. (2014) Return of widespread chloroquine-sensitive *Plasmodium falciparum* to Malawi. *J Infect Dis* 210(7):1110–1114.
20. Cooper RA, et al. (2007) Mutations in transmembrane domains 1, 4 and 9 of the *Plasmodium falciparum* chloroquine resistance transporter alter susceptibility to chloroquine, quinine and quinidine. *Mol Microbiol* 63(1):270–282.
21. Lukens AK, et al. (2014) Harnessing evolutionary fitness in *Plasmodium falciparum* for drug discovery and suppressing resistance. *Proc Natl Acad Sci USA* 111(2):799–804.
22. Martin RE, Kirk K (2004) The malaria parasite's chloroquine resistance transporter is a member of the drug/metabolite transporter superfamily. *Mol Biol Evol* 21(10): 1938–1949.
23. Bellanca S, et al. (2014) Multiple drugs compete for transport via the *Plasmodium falciparum* chloroquine resistance transporter at distinct but interdependent sites. *J Biol Chem* 289(52):36336–36351.
24. Zhang H, Paguio M, Roepe PD (2004) The antimalarial drug resistance protein *Plasmodium falciparum* chloroquine resistance transporter binds chloroquine. *Biochemistry* 43(26):8290–8296.
25. Valderramos SG, et al. (2010) Identification of a mutant PfCRT-mediated chloroquine tolerance phenotype in *Plasmodium falciparum*. *PLoS Pathog* 6(5):e1000887.
26. Johnson DJ, et al. (2004) Evidence for a central role for PfCRT in conferring *Plasmodium falciparum* resistance to diverse antimalarial agents. *Mol Cell* 15(6):867–877.
27. Witkowski B, et al. (2013) Novel phenotypic assays for the detection of artemisinin-resistant *Plasmodium falciparum* malaria in Cambodia: *In vitro* and *ex vivo* drug-response studies. *Lancet Infect Dis* 13(12):1043–1049.
28. Dondorp AM, et al. (2009) Artemisinin resistance in *Plasmodium falciparum* malaria. *N Engl J Med* 361(5):455–467.
29. Mwai L, et al. (2009) *In vitro* activities of piperaquine, lumefantrine, and dihydroartemisinin in Kenyan *Plasmodium falciparum* isolates and polymorphisms in *pfcrt* and *pfmdr1*. *Antimicrob Agents Chemother* 53(12):5069–5073.
30. Wong RP, et al. (2010) *In vitro* sensitivity of *Plasmodium falciparum* to conventional and novel antimalarial drugs in Papua New Guinea. *Trop Med Int Health* 15(3): 342–349.
31. Sisowath C, et al. (2009) *In vivo* selection of *Plasmodium falciparum* parasites carrying the chloroquine-susceptible *pfcrt* K76 allele after treatment with artemether-lumefantrine in Africa. *J Infect Dis* 199(5):750–757.
32. Conrad MD, et al. (2014) Comparative impacts over 5 years of artemisinin-based combination therapies on *Plasmodium falciparum* polymorphisms that modulate drug sensitivity in Ugandan children. *J Infect Dis* 210(3):344–353.
33. de Theije M, Heemskerk M (2009) Moving frontiers in the Amazon: Brazilian small-scale gold miners in Suriname. *Eur Rev Latin Am Carib* 87:5–25.
34. Evans L, 3rd, et al. (2012) Quality of anti-malarials collected in the private and informal sectors in Guyana and Suriname. *Malar J* 11:203.
35. Nacher M, et al. (2013) Made in Europe: Will artemisinin resistance emerge in French Guiana? *Malar J* 12:152.
36. Saunders DL, Vanachayangkul P, Lon C; US Army Military Malaria Research Program; National Center for Parasitology, Entomology, and Malaria Control (CNM); Royal Cambodian Armed Forces (2014) Dihydroartemisinin-piperaquine failure in Cambodia. *N Engl J Med* 371(5):484–485.
37. Lim P, et al. (2015) Decreasing *pfmdr1* copy number suggests that *Plasmodium falciparum* in Western Cambodia is regaining *in vitro* susceptibility to mefloquine. *Antimicrob Agents Chemother* 59(5):2934–2937.
38. Leang R, et al. (May 26, 2015) Evidence of falciparum malaria multidrug resistance to artemisinin and piperaquine in western Cambodia: Dihydroartemisinin-piperaquine open-label multicenter clinical assessment. *Antimicrob Agents Chemother*, AAC.00835-15.
39. Miotto O, et al. (2015) Genetic architecture of artemisinin-resistant *Plasmodium falciparum*. *Nat Genet* 47(3):226–234.
40. Daniels R, et al. (2008) A general SNP-based molecular barcode for *Plasmodium falciparum* identification and tracking. *Malar J* 7:223.
41. Desjardins RE, Canfield CJ, Haynes JD, Chulay JD (1979) Quantitative assessment of antimalarial activity *in vitro* by a semiautomated microdilution technique. *Antimicrob Agents Chemother* 16(6):710–718.
42. Ekland EH, Schneider J, Fidock DA (2011) Identifying apicoplast-targeting antimalarials using high-throughput compatible approaches. *FASEB J* 25(10):3583–3593.
43. Li H, Durbin R (2009) Fast and accurate short read alignment with Burrows-Wheeler transform. *Bioinformatics* 25(14):1754–1760.
44. McKenna A, et al. (2010) The Genome Analysis Toolkit: A MapReduce framework for analyzing next-generation DNA sequencing data. *Genome Res* 20(9):1297–1303.
45. Purcell S, et al. (2007) PLINK: A tool set for whole-genome association and population-based linkage analyses. *Am J Hum Genet* 81(3):559–575.

Supporting Information

Pelleau et al. 10.1073/pnas.1507142112

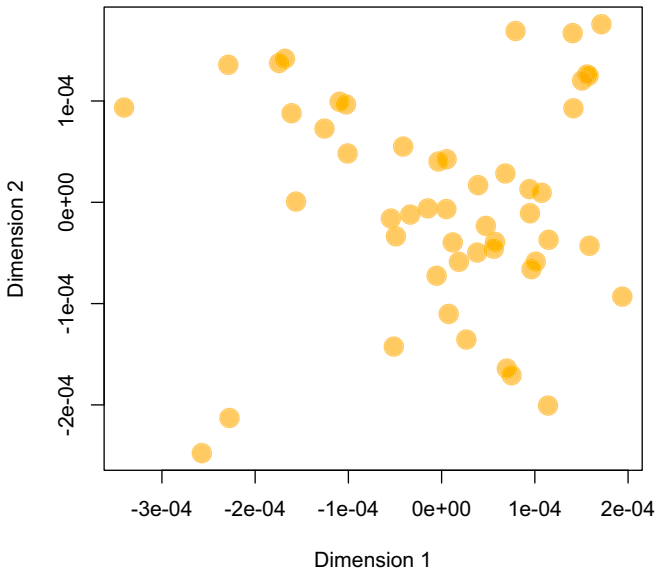

Fig. S1. Principal component analysis of a pairwise distance matrix between the genomes of parasites collected in French Guiana from 2008 to 2012. This two-component graph shows the relatively homogeneous distribution of the parasite genomes included in the study and the absence of population stratification.

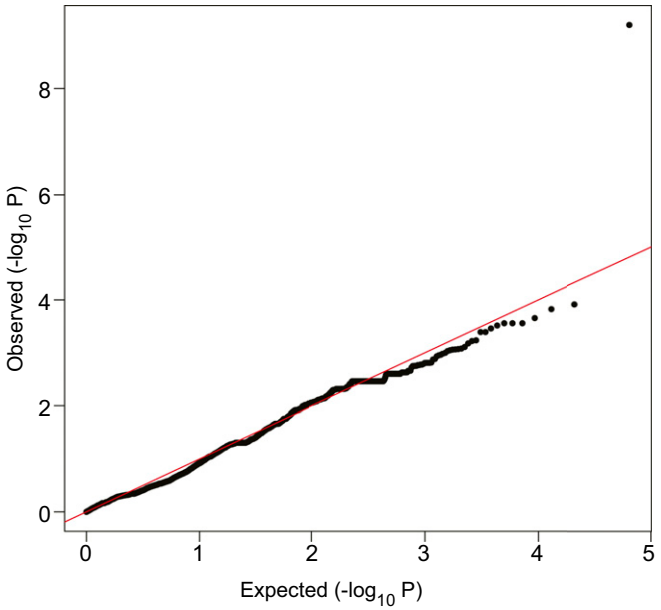

Fig. S2. Quantile–quantile plots of expected vs. observed *P* values of individual SNPs associated with the CQ-susceptible phenotype. This plot was generated after correction for inflated *P* values. The SNP with the most important deviation from the expected *P* value (upper right corner) corresponds to the PfCRT C350R mutation found in CQ-susceptible parasites.

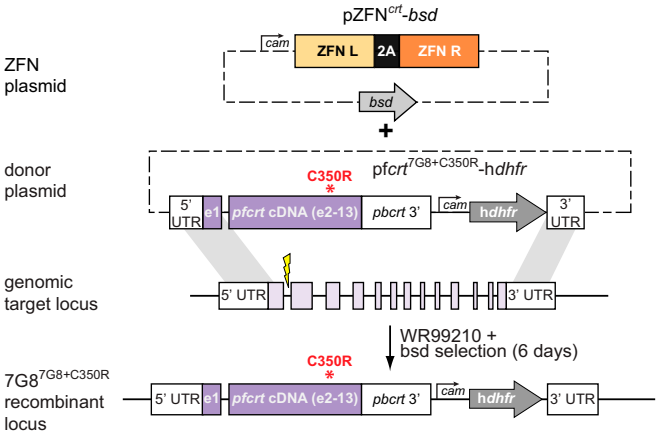

Fig. S3. Site-specific genome editing strategy to introduce *pfcrt* modifications into the 7G8 reference line; 7G8 parasites were electroporated with a donor plasmid (pf*crt*-h*dhfr*) encoding a desired compacted (exons 2–13) *pfcrt* haplotype and pressured with 2.5 nM WR99210. Transformed parasites were subsequently electroporated with a zinc finger nuclease (ZFN) -encoding plasmid (pZFN^{crt}-*bsd*) and pressured for 6 d with 2.5 μg/mL BSD + 2.5 nM WR99210 followed by culture in 2.5 nM WR99210. Our *pfcrt*-specific ZFNs were linked using a viral 2A peptide that permits translation of the two separate ZFNs from a single transcribed mRNA. Binding of these customized DNA binding ZFNs to adjacent sites of intron 1 results in pairing of their split FokI endonucleases, which as an obligate heterodimer form, causes a double-stranded break in intron 1. These events are repaired using the donor template present on the second plasmid that contains 5′ and 3′ regions of homology with DNA resection and donor template strand invasion-dependent DNA repair and resynthesis, thus exchanging the endogenous *pfcrt* allele with the plasmid-borne variant that contains the entire coding sequence that removes all introns except for intron 1. The presence of ZFN binding site mutations on the plasmid sequences ensures that both the plasmid and the subsequently gene-edited locus are refractory to the ZFNs that can only cleave the original genomic copy. Editing of *pfcrt* was assessed by PCR analysis of bulk cultures. Cultures showing editing were cloned by limiting dilution and flow cytometrically assessed for growth after 20 d by SYBR Green I and MitoTracker Deep Red (Invitrogen) staining. Presence of the desired *pfcrt* sequence was validated by PCR and RT-PCR.

Table S1. Detailed antimalarial drug susceptibilities in genome-edited and reference lines

Drug and IC values (nM)	D10	7G8	$7G8^{7G8}$	$7G8^{C350R}$
CQ				
Mean IC_{50} ± SEM	19.5 ± 1.5	386.2 ± 24.8	379.6 ± 24.4	16.2 ± 1.8
Mean IC_{90} ± SEM	35.1 ± 3.8	694.0 ± 67.3	676.9 ± 65.7	46.3 ± 4.4
Nb of assays	8	8	8	8
P value vs. $7G8^{7G8}$				<0.0001
mdCQ				
Mean IC_{50} ± SEM	35.1 ± 3.2	1,571.0 ± 228.0	1,559.5 ± 146.7	53.3 ± 5.7
Mean IC_{90} ± SEM	89.0 ± 10.9	2,273.2 ± 241.1	2,242.1 ± 237.8	179.1 ± 16.5
Nb of assays	8	9	9	9
P value vs. $7G8^{7G8}$				<0.0001
mdAQ				
Mean IC_{50} ± SEM	24.2 ± 1.2	77.9 ± 9.0	73.9 ± 5.5	21.1 ± 1.5
Mean IC_{90} ± SEM	34.8 ± 3.3	122.9 ± 9.2	121.3 ± 9.1	34.6 ± 4.0
Nb of assays	8	8	8	8
P value vs. $7G8^{7G8}$				<0.0001
QN				
Mean IC_{50} ± SEM	35.1 ± 2.2	275.4 ± 23.4	285.1 ± 24.2	76.4 ± 5.1
Mean IC_{90} ± SEM	151.8 ± 39.1	768.0 ± 83.5	847.6 ± 92.2	260.5 ± 19.6
Nb of assays	8	7	7	7
P value vs. $7G8^{7G8}$				<0.0001
LUM				
Mean IC_{50} ± SEM	6.6 ± 1.6	2.3 ± 0.4	2.4 ± 0.5	0.6 ± 0.1
Mean IC_{90} ± SEM	19.8 ± 3.4	9.4 ± 0.9	9.7 ± 0.9	2.7 ± 0.3
Nb of assays	7	4	4	4
P value vs. $7G8^{7G8}$				<0.01
MQ				
Mean IC_{50} ± SEM	nd	9.0 ± 0.9	11.1 ± 0.7	6.0 ± 0.9
Mean IC_{90} ± SEM	nd	27.4 ± 3.8	30.7 ± 3.9	20.4 ± 2.0
Nb of assays	nd	4	4	4
P value vs. $7G8^{7G8}$				<0.01
AS				
Mean IC_{50} ± SEM	3.7 ± 0.3	3.4 ± 0.4	3.5 ± 0.4	2.2 ± 0.2
Mean IC_{90} ± SEM	8.0 ± 1.1	6.3 ± 0.9	6.7 ± 0.9	5.5 ± 0.4
Nb of assays	7	7	7	7
P value vs. $7G8^{7G8}$				<0.05
PPQ				
Mean IC_{50} ± SEM	22.2 ± 2.6	25.6 ± 2.1	26 ± 2.1	36.5 ± 2.4
Mean IC_{90} ± SEM	43.1 ± 5.2	57.4 ± 3.6	60.0 ± 3.7	77.9 ± 7.2
Nb of assays	8	9	9	9
P value vs. $7G8^{7G8}$				<0.001
PND				
Mean IC_{50} ± SEM	6.1 ± 0.3	4.7 ± 0.4	4.9 ± 0.4	4.5 ± 0.5
Mean IC_{90} ± SEM	10.1 ± 1.0	7.6 ± 0.5	8.7 ± 0.5	7.7 ± 0.5
Nb of assays	8	9	9	9
P value vs. $7G8^{7G8}$				ns

Student *t* tests were used to compare $7G8^{7G8}$ with $7G8^{C350R}$ mean IC_{50} values. AS, artesunate; mdCQ, monodesethyl-CQ; Nb, number; nd, not determined; ns, not significant; PND, pyronaridine.